INTERNATIONAL REVIEW OF CYTOLOGY

A SURVEY OF CELL BIOLOGY

Edited by
Kwang W. Jeon

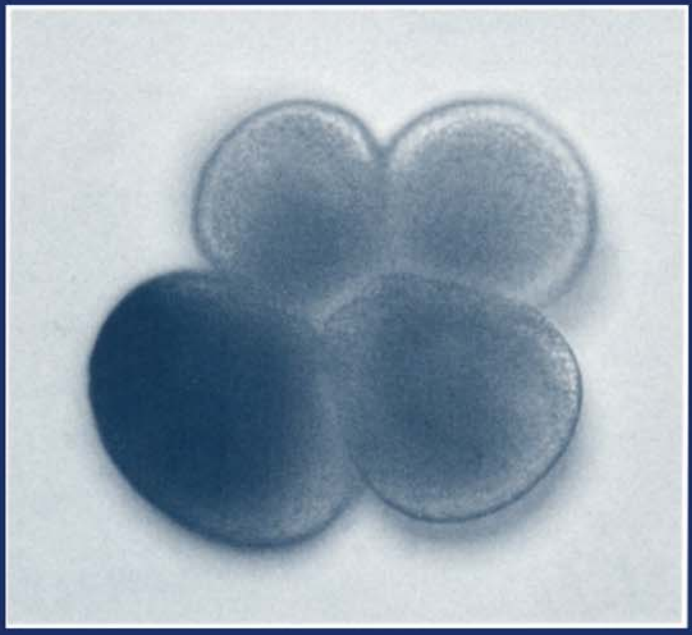

Volume 176

ACADEMIC PRESS

International Review of Cytology

A Survey of Cell Biology

VOLUME 176

SERIES EDITORS

Geoffrey H. Bourne	1949–1988
James F. Danielli	1949–1984
Kwang W. Jeon	1967–
Martin Friedlander	1984–1992
Jonathan Jarvik	1993–1995

EDITORIAL ADVISORY BOARD

Aimee Bakken
Eve Ida Barak
Rosa Beddington
Howard A. Bern
Robert A. Bloodgood
Dean Bok
Stanley Cohen
Rene Couteaux
Marie A. DiBerardino
Charles J. Flickinger
Nicholas Gillham
Elizabeth D. Hay
P. Mark Hogarth
Anthony P. Mahowald
M. Melkonian
Keith E. Mostov
Andreas Oksche
Muriel J. Ord
Vladimir R. Pantić
Thomas D. Pollard
L. Evans Roth
Jozef St. Schell
Manfred Schliwa
Hiroh Shibaoka
Wilfred D. Stein
Ralph M. Steinman
M. Tazawa
Yoshio Watanabe
Donald P. Weeks
Robin Wright
Alexander L. Yudin

International Review of Cytology

A Survey of Cell Biology

Edited by

Kwang W. Jeon
Department of Biochemistry
University of Tennessee
Knoxville, Tennessee

VOLUME 176

ACADEMIC PRESS
San Diego London Boston New York Sydney Tokyo Toronto

Front cover photograph: Strictly restricted distribution of *pem* mRNA in the myoplasm of an 8-cell embryo of *Ciona savigni*. (See Chapter 5 for more details.)

This book is printed on acid-free paper. ♾

Copyright © 1997 by ACADEMIC PRESS

All Rights Reserved.
No part of this publication may be reproduced or transmitted in any form or by any means, electronic or mechanical, including photocopy, recording, or any information storage and retrieval system, without permission in writing from the Publisher.
The appearance of the code at the bottom of the first page of a chapter in this book indicates the Publisher's consent that copies of the chapter may be made for personal or internal use of specific clients. This consent is given on the condition, however, that the copier pay the stated per copy fee through the Copyright Clearance Center, Inc. (222 Rosewood Drive, Danvers, Massachusetts 01923), for copying beyond that permitted by Sections 107 or 108 of the U.S. Copyright Law. This consent does not extend to other kinds of copying, such as copying for general distribution, for advertising or promotional purposes, for creating new collective works, or for resale. Copy fees for pre-1997 chapters are as shown on the title pages, if no fee code appears on the title page, the copy fee is the same as for current chapters.
0074-7696/97 $25.00

Academic Press
a division of Harcourt Brace & Company
525 B Street, Suite 1900, San Diego, California 92101-4495, USA
http://www.apnet.com

Academic Press Limited
24-28 Oval Road, London NW1 7DX, UK
http://www.hbuk.co.uk/ap/

International Standard Book Number: 0-12-364580-8

PRINTED IN THE UNITED STATES OF AMERICA
97 98 99 00 01 02 EB 9 8 7 6 5 4 3 2 1

CONTENTS

Functional Interactions among Cytoskeleton, Membranes, and Cell Wall in the Pollen Tube of Flowering Plants

Yi-Qin Li, Alessandra Moscatelli, Giampiero Cai, and Mauro Cresti

Biology of the Postsynaptic Glycine Receptor

Christian Vannier and Antoine Triller

Cell Fate Specification by Localized Cytoplasmic Determinants and Cell Interactions in Ascidian Embryos

Hiroki Nishida

Distribution of Na^+,K^+-ATPase in Photoreceptor Cells of Insects

Otto Baumann

This Page Intentionally Left Blank

CONTRIBUTORS

Numbers in parentheses indicate the pages on which the authors' contributions appear.

A. Ros Barceló (87), *Department of Plant Biology, University of Murcia, Spain*

Otto Baumann (307), *Institut für Zoophysiologie und Zellbiologie, Universität Potsdam, D-14471 Potsdam, Germany*

Giampiero Cai (133), *Dipartimento di Biologia Ambientale, Università degli Studi di Siena, 53100 Siena, Italy*

Mauro Cresti (133), *Dipartimento di Biologia Ambientale, Università degli Studi di Siena, 53100 Siena, Italy*

Yi-Qin Li (133), *Department of Biological Science and Biotechnology, Tsinghua University, 100084-Beijing, China*

Alessandra Moscatelli (133), *Dipartimento di Biologia Ambientale, Università degli Studi di Siena, 53100 Siena, Italy*

Hiroki Nishida (245), *Department of Life Science, Tokyo Institute of Technology, Nagatsuta, Midoriku, Yokohama 226, Japan*

Vesa Olkkonen (1), *Department of Biochemistry, National Health Institute, FIN-00300 Helsinki, Finland*

Harald Stenmark (1), *Department of Biochemistry, The Norwegian Radium Hospital, Montebello, N-0130 Oslo, Norway*

Antoine Triller (201), *Laboratoire de Biologie Cellulare de la Synapse, INSERM CJF 94-10, Ecole Normale Supérieure, 75005 Paris, France*

Christian Vannier (201), *Laboratoire de Biologie Cellulare de la Synapse, INSERM CJF 94-10, Ecole Normale Supérieure, 75005 Paris, France*

This Page Intentionally Left Blank

Role of Rab GTPases in Membrane Traffic

Vesa M. Olkkonen* and Harald Stenmark†
*National Public Health Institute, FIN-00300, Helsinki, Finland; and † The Norwegian Radium Hospital, N-0310, Oslo, Norway

Small GTPases of the Rab subfamily have been known to be key regulators of intracellular membrane traffic since the late 1980s. Today this protein group amounts to more than 40 members in mammalian cells which localize to distinct membrane compartments and exert functions in different trafficking steps on the biosynthetic and endocytic pathways. Recent studies indicate that cycles of GTP binding and hydrolysis by the Rab proteins are linked to the recruitment of specific effector molecules on cellular membranes, which in turn impact on membrane docking/fusion processes. Different Rabs may, nevertheless, have slightly different principles of action. Studies performed in yeast suggest that connections between the Rabs and the SNARE machinery play a central role in membrane docking/fusion. Further elucidation of this linkage is required in order to fully understand the functional mechanisms of Rab GTPases in membrane traffic.

KEY WORDS: Rab, Ypt, Small GTPase, Membrane traffic, Vesicle transport.

I. Introduction

The eukaryotic cells have an elaborate network of membrane-bounded organelles with distinct protein and lipid compositions (Fig. 1). The unique characteristics of the organelles are maintained despite continuous intercompartmental transport of membrane and soluble components. This exchange of material is thought to take place mainly via vesicular carriers budding off one compartment and fusing with another one (Palade, 1975). Furthermore, the cell is capable of major membrane organelle rearrangements, such as mitotic fragmentation and subsequent reassembly of the nuclear membrane, the endoplasmic reticulum (ER), and the Golgi apparatus (Denesvre and Malhotra, 1996; Warren and Wickner, 1996). The molec-

International Review of Cytology, Vol. 176
0074-7696/97 $25.00

Copyright © 1997 by Academic Press.
All rights of reproduction in any form reserved.

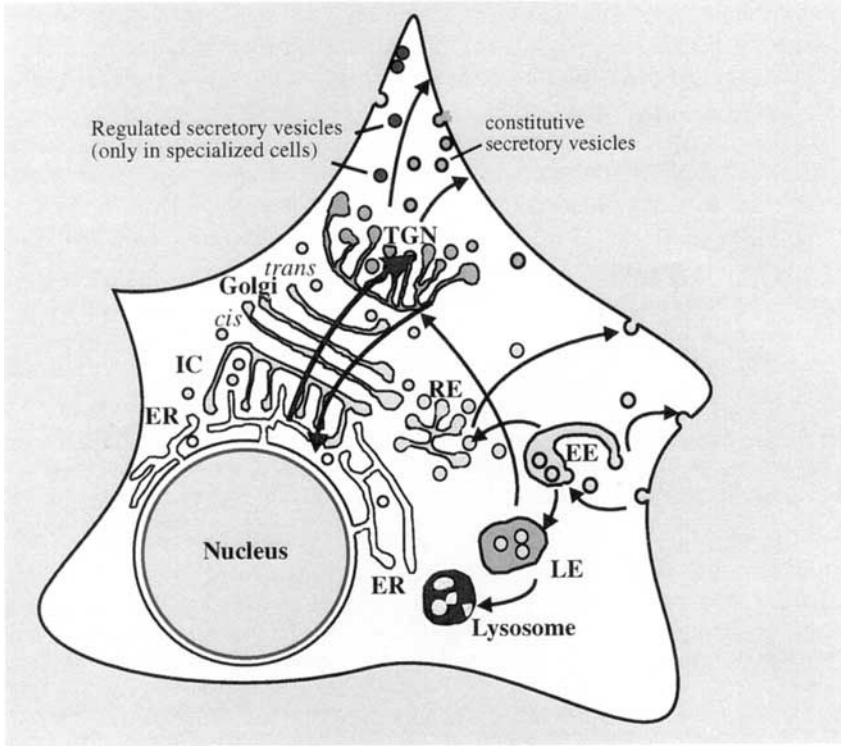

FIG. 1 A schematic view of a eukaryotic cell with the intracellular membrane transport pathways indicated. Secreted and membrane proteins are synthesized in the endoplasmic reticulum (ER) and routed to the ER–Golgi intermediate compartment (IC), which is responsible for sorting ER resident proteins from those transported further to the Golgi apparatus. In the Golgi, maturation and sorting of proteins to their final destinations takes place. The distal sorting station of the Golgi is called the *trans*-Golgi network (TGN). Here, lysosomal constituent proteins are sorted to the endocytic route, and secreted as well as plasma membrane components are routed for transport to the cell surface. The cells take up material from the external milieu via endocytic processes, delivering the material first to early endosomes (EE). Recycling of endocytosed material to the cell surface can occur from the EE or via recycling endosomes (RE). Alternatively, molecules can be sorted to (or EE may "mature" into) late endosomes (LE). From LE, material is delivered to the TGN or to lysosomes, which form an apparatus responsible for degradation processes.

ular machineries regulating the contact and fusion of biological membranes are among the most intensively studied areas of current cell biology. In the past few years spectacular progress has been made in the elucidation of the machineries involved, one of the key events being introduction of the soluble *N*-ethylmaleimide-sensitive fusion attachment protein receptor (SNARE) hypothesis of vesicle transport (Söllner *et al.*, 1993b; Rothman,

1994; see Section V,A). Data produced in several independent areas of cell biology have merged to form a picture in which the striking evolutionary conservation of the machineries responsible for the intracellular membrane dynamics has become evident (Bennett and Scheller, 1993; Ferro-Novick and Jahn, 1994) and a number of key principles governing vesicle traffic have started to crystallize (Rothman, 1996). We have gained insight into the mechanistic principles of transport vesicle formation with the aid of proteinaceous coats (Kreis *et al.,* 1995; Schekman and Orci, 1996) and obtained clues regarding the cargo sorting events taking place upon vesicle formation (Pelham, 1995; Rothman and Wieland, 1996; Simons and Ikonen, 1997). The molecular interactions leading to docking of vesicles on the correct target membranes and subsequent bilayer fusion are currently under debate. The SNAREs and the general components involved, *N*-ethylmaleimide-sensitive fusion (NSF) and NSF attachment (SNAP) proteins (Whiteheart and Kubalek, 1995; Morgan and Burgoyne, 1995), unquestionably play central roles in these events, and a number of other classes of molecules involved in the communication of membranes are being characterized. With regard to this end of a vesicle's "life cycle," however, many questions remain unanswered. One of these is how the small Ras-related Rab GTPases, known for a decade to be key regulators of membrane trafficking, exert their function.

Cycles of GTP binding and hydrolysis by specific proteins, together with kinase/phosphatase cycles, form a major mechanism by which diverse cellular functions are regulated (Bourne *et al.,* 1990). The idea of Ras-related GTPases being involved in membrane trafficking was initially based on the findings that conditional lethal mutations in the *Saccharomyces cerevisiae SEC4* and *YPT1* genes led to defects in the secretory process. The Sec4 GTPase was localized on the cytoplasmic surface of secretory vesicles and the plasma membrane, and *sec4* mutations led to accumulation of *post*-Golgi vesicles (Salminen and Novick, 1987; Goud *et al.,* 1988), whereas the related Ypt1p was demonstrated to function in an earlier transport step between the ER and the Golgi apparatus (Schmitt *et al.,* 1988; Segev *et al.,* 1988). Furthermore, Melancon *et al.* (1987) had shown that a reconstituted *in vitro* intra-Golgi transport assay was inhibited by a nonhydrolyzable GTP analog, GTPγS (the same observation was later made in several other *in vitro* transport assays). Inspired by these findings, Bourne (1988) developed a model in which the GTPases, by a functional principle analogous to that of the protein synthesis elongation factor Tu, would act as molecular switches mediating the vectorial transport of vesicles between two membrane compartments. In this scheme the GTPase would bind to a hypothetical recognition protein on vesicles budding off a donor membrane, and this complex in turn would recognize a docking protein on the specific acceptor membrane, followed by GTP hydrolysis, fusion of the

membranes, and recycling of the GDP-bound form of the GTPase back to the donor membrane. The model has had a remarkably long life span and forms the core of schemes describing the functional cycle of Rab GTPases (Fig. 2), even though its detailed sequence of events cannot be taken as a general paradigm for Rab function.

According to the model depicted previously, each distinct membrane fusion event in the eukaryotic cell should require a specific Rab GTPase, necessitating the presence of a remarkably high number of different Rab proteins with distinct localizations on the intracellular membrane compartments. The first mammalian homologs of the *S.cerevisiae* Sec4p and Ypt1p, Rab1–4, were identified by the groups of Gallwitz and Tavitian (Haubruck *et al.*, 1987; Touchot *et al.*, 1987). Moreover, the Bourne (1988) hypothesis was supported by the first studies on the intracellular distribution of the mammalian Rab GTPases, which demonstrated specific localizations of

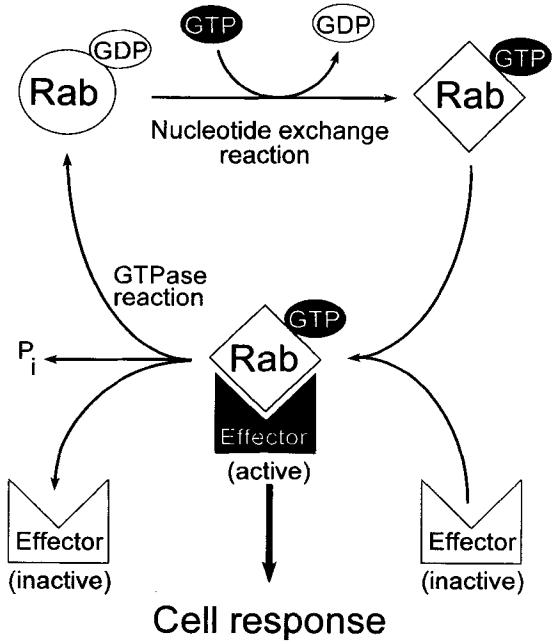

FIG. 2 The GTPase cycle of Rab proteins. Upon exchange of a bound GDP for GTP, the protein undergoes a conformational change. The GTP-bound form binds and activates specific effector molecules, which induce a cellular response (membrane docking/fusion). The effector dissociates upon GTP hydrolysis, and the Rab protein returns to its "inactive" GDP conformation. By alternating between the GDP and GTP conformations, the Rab thus acts as a molecular switch regulating intracellular transport.

these proteins along the endocytic and biosynthetic transport pathways (Chavrier *et al.,* 1990a; Goud *et al.,* 1990). Since then, the cloning efforts of these and other groups have revealed a large family of Rab GTPases in mammalian cells, consisting at the moment of more than 40 members (Table I). During the 1990s we have seen the identification and basic characterization of an increasing number of Rab proteins in a variety of organisms. The Rab proteins characterized are widely used as specific subcellular markers in morphological and biochemical studies. Assuming that one or more Rab GTPases are involved in each specific membrane fusion event, thorough characterization of an increasing number of these proteins can help us to form a more comprehensive picture of the organization of the intracellular transport pathways. However, the most important task at the moment is to elucidate the precise function(s) of the Rab GTPases in the communication of biological membranes. In this chapter we will create a synopsis of the data available on the localization and function of mammalian Rab proteins in the context of the other known components involved in membrane dynamics. We will also discuss in detail work on the yeast proteins (Table II) that provides invaluable data on the function of this GTPase subfamily.

II. General Characteristics of the Rab GTPase Subfamily

A. Sequence Characteristics

1. Motifs Involved in Nucleotide Binding and Hydrolysis

The Rab proteins belong to the superfamily of small (21–25 kDa) Ras-related GTPases that consists of three major subfamilies, the Ras, Rho, and Rab proteins, as well as the smaller ARF, Sar, and Ran groups. The degree of amino acid identity between members of the different subfamilies is approximately 30% (Valencia *et al.,* 1991; Sander and Valencia, 1995). The highest degree of sequence conservation is observed in regions that are directly involved in guanine nucleotide binding and hydrolysis (Fig. 3). These conserved sequence motifs are found in all Ras-related proteins, although subfamily specific features can be detected even in these regions; e.g., the presence of tryptophan (W) in the beginning of the third phosphate/Mg^{2+}-binding domain (PM3) is typical of the Rho and Rab subfamilies. The Rab and Rho GTPases can be readily distinguished by the occurrence of a 10- to 13-amino acid insertion in loop 8 of the latter proteins (Valencia *et al.,* 1991). The conserved GTP-binding regions have been

TABLE I

Mammalian Rab Proteins

Name	Expression pattern	Localization	Function	Reference
Rabla	U[a]	ER–Golgi intermediate compartment, *cis*-Golgi, ER?	ER–Golgi transport	Sections II,D,1, III,B,1
Rablb	U	ER–Golgi intermediate compartment, *cis*-Golgi, ER?	ER–Golgi transport	Sections II,D,1, III,B,1
Rab2	U	ER–Golgi intermediate compartment	Retrograde transport from Golgi to ER?	Sections II,D,1, III,B,1
Rab3a	Neurons, endo- and exocrine cells, adipocytes	Synaptic vesicles, secretory granules	Docking/fusion in regulated secretory events, GTPase activity required for fusion?	Sections II,C,2, II,D,1, III,B,4
Rab3b	Epithelial cells, adipocytes, neurons and neuroendocrine cells, platelets	Tight junction region of epith. cells	Regulated exocytosis in pituitary cells	Sections II,C,2, II,D,1, III,B,4
Rab3c	Neurons and neuroendocrine cells, testis, heart, adipose tissue	Synaptic vesicles	ND[d]	Sections II,C,2, II,D,1, III,B,4
Rab3d/ Rab16	Several nonneuronal tissues, adipocytes, exocrine cells	Pancreatic acinar cell secretory granules, gastric chief cell zymogen granules	ND	Sections II,C,2, II,D,1; Elferink *et al.* (1992)
Rab4a	U	Early endosomes	Early endosome–plasma membrane recycling	Sections II,D,2, III,B,6
Rab4b	ND	ND	ND	Chavrier *et al.* (1990b)
Rab5a	U	Plasma membrane, clathrin-coated vesicles, early endosomes, synaptic vesicles	Plasma membrane–early endosome transport, homotypic fusion of early endosomes	Sections II,D,2, III,B,6
Rab5b	U	Early endosomes	Plasma membrane–early endosome transport	Sections II,D,2, III,B,6; Wilson and Wilson (1992)
Rab5c	U	Early endosomes	Plasma membrane–early endosome transport	Sections II,D,2, III,B,6

Rab6	U	Medial Golgi–TGN, post-Golgi vesicles, platelet α-granules	Intra-Golgi (retrograde?) transport	Sections II,D,1, III,B,2
Rab 7	U	Late endosomes	Early to late endosome and/or late endosome–lysosome transport	Sections II,D,2, III,B,8
Rab8a	U	TGN, post-Golgi exocytic vesicles, tight junction region in epithelial cells, platelet α-granules	Golgi–basolateral/ somatodendritic plasma membrane transport in epithelial cells/neurons	Sections II,D,1, III,B,5
Rab8b	U, abundant in the brain	Plasma membrane, vesicles	ND	Sections II,D,1, III,B,5
Rab9	U	Late endosomes, TGN	Transport from late endosomes to TGN	Sections II,D,2, III,B,3
Rab10	U	Golgi complex, TGN?	ND	Section II,D,1
Rab11a	U	TGN, secretory vesicles/ granules, apical vesicle structures in epithelia, recycling endosomes	Recycling of proteins through the recycling endosome	Sections II,D,2, III,B,7
Rab11b	U	Not distinguished from Rab11a in localization studies	ND	Lai *et al.* (1994), Zhu *et al.* (1994)
Rab12	U	Golgi complex, secretory granules in atrial myocytes	ND	Section II,D,1
Rab13	U	Tight junction region in epithelia	ND	Sections II,D,1, III,E
Rab14	U	ND	ND	Elferink *et al.* (1992)
Rab15	Central nervous system	ND	ND	Elferink *et al.* (1992)
Rab17	Kidney, intestine, liver	Apical dense tubules and basolateral plasma membrane in kidney epithelial cells	ND	Sections II,C,2, II,D,2, III,E
Rab18	U	Apical dense tubules in kidney epithelial cells, apical and basolateral domains of intestinal cells	ND	Sections II,C,1, II,D,2
Rab19	Kidney, intestine, lung, spleen	ND	ND	Section II,C,2

(*continued*)

TABLE I (*continued*)

Name	Expression pattern	Localization	Function	Reference
Rab20	U	Apical dense tubules in kidney epithelial cells	ND	Sections II,C,1, II,D,2
Rab21	MDCK and BHK cells, tissue distribution ND	ND	ND	Chavrier (1995)
Rab22a	U	Plasma membrane, endosomes	ND	Section II,D,2
Rab22b	U	ND	ND	Chen *et al.* (1996)
Rab23	Brain, low levels in other tissues	ND	ND	Olkkonen *et al.* (1994)
Rab24	U	ER, intermediate compartment, late endosomes?	ND	Section II,D,1
Rab25	Kidney, lung gastrointestinal mucosa	ND	ND	Section II,C,2
Rab26	High level in kidney, also detected in other tissues	ND	ND	Wagner *et al.* (1995)
Rab27/Ram	Eye retinal pigment epithelium and choriocapillaries, intestine, lung, pancreas, and spleen	ND	ND	Section IV,A,1; Nagata *et al.* (1990)
Rab28	U	ND	ND	Brauers *et al.* (1996)
Rab30	U	ND	ND	Chen *et al.* (1996)
H-ray	U	ND	ND	Zhu *et al.* (1994)
Rah1	HT4 neural cell line, tissue distribution ND	ND	ND	Morimoto *et al.* (1991)
S10	Lymphoid cell lines, tissue distribution ND	ND	ND	Koda and Kakinuma (1993)

[a] U, ubiquitous.
[b] ND, not determined.

exploited in the molecular cloning of a number of Ras-related proteins, including many of the Rab GTPases (Touchot *et al.,* 1987; Chavrier *et al.,* 1990b, 1992; Ngsee *et al.,* 1991; Drivas *et al.,* 1991; Yu *et al.,* 1993; Koda and Kakinuma, 1993; Goldenring *et al.,* 1993).

One of the key approaches to Rab function has been the mutagenesis of specific amino acid residues essential for guanine nucleotide binding or GTP hydrolysis by the proteins (Table III). The effects of expression of the mutant proteins have been determined morphologically and/or biochemically. The choice of amino acids to be mutagenized is based on well-characterized mutations described in other GTPases, mainly the Ras oncoproteins. Mutations equivalent to the Q61L (in the PM3 conserved motif) mutation in Ras decrease the GTPase activity 10- to 100-fold, which stabilizes the GTP-bound, "active" conformation of the protein (Der *et al.,* 1986; Adari *et al.,* 1988; Stenmark *et al.,* 1994b; Hoffenberg *et al.,* 1995). The steady-state GTP hydrolysis rate by the mutant proteins may, however, be somewhat less affected because the mutation also slows down dissociation of GDP from the protein, which is the rate-limiting step in the GTPase cycle (Hoffenberg *et al.,* 1995). Furthermore, cellular GTPase activating proteins may to some extent stimulate the GTPase activity of these mutant proteins (Walworth *et al.,* 1992; Stenmark *et al.,* 1994b). The defect in GTP hydrolysis leads to increased transforming activity of the Ras proteins (Der *et al.,* 1986; Adari *et al.,* 1988). Similarly, stimulation of endosomal membrane fusion was detected in studies on the corresponding mutant of Rab5 (Stenmark *et al.,* 1994b; Barbieri *et al.,* 1996). Also, several other substitutions in this position have a similar effect (Der *et al.,* 1986; T. Mayer, *et al.,* 1996).

In contrast, mutants equivalent to the S17N (in the PM1 conserved motif) mutation of Ras display lower affinity for GTP than for GDP, leading to a dominant inhibitory effect (Feig and Cooper, 1988; Ridley *et al.,* 1992; Burstein *et al.,* 1992; Medema *et al.,* 1993). The GTPases bind nucleotides as their Mg^{2+} complexes, and the serine at position 17 is implicated in Mg^{2+} coordination in the active site (Pai *et al.,* 1989, 1990). The affinity of the Ras S17A mutant for both GTP and GDP was found to be greatly decreased, the residual affinity for GDP, however, was 30-fold higher than that for GTP (John *et al.,* 1993). Although the GDP off-rate of the wild-type GTPases shows a strong dependence on Mg^{2+} ion concentration, the GDP off-rate of the serine 17 mutants appears to be independent of the ions (John *et al.,* 1993; Riederer *et al.,* 1994). It seems that the dominant inhibitory effects of the serine 17 mutants may be due to the ability of the proteins to sequester upstream regulatory proteins, as shown for Rab3a T36N and the Rab3a guanine nucleotide exchange factor (Burstein *et al.,* 1992).

Other commonly used types of mutations are those corresponding to the transforming Ras mutation N116I in the second guanine base binding motif (G2) which lowers the affinity of the proteins for the guanine nucleotides

TABLE II
Yeast Ypt/Rab Proteins

Name (*species*)	Mammalian homolog	Effect of gene disruption	Function	Reference
Ypt1p (*S. cerevisiae*)	Rab1	Lethal	Fusion of post-ER vesicles with the Golgi	Sections II,A,1, V,B
Ypt1p (*S. pombe*)	Rab1	Lethal	ER–Golgi transport	Section III,A,3
Sec4p (*S. cerevisiae*)	Rab8	Lethal	Fusion of post-Golgi vesicles with the plasma membrane	Sections III,A,1, V,B, V,C
Ypt2p (*S. pombe*)	Rab8	Lethal	Fusion of post-golgi vesicles with the plasma membrane	Section III,A,3
Ypt31p (*S. cerevisiae*)	Rab11	Deletion no phenotype, double deletion *ypt31ypt32* lethal	Intra-Golgi and/or post-Golgi transport	Section III,A,1
Ypt32p (*S. cerevisiae*)	Rab11	Deletion no phenotype, double deletion *ypt31ypt32* lethal	Intra-Golgi and/or post-Golgi transport	Section III,A,1
Ypt3p (*S. pombe*)	Rab11	Lethal	ND[a]	Miyake and Yamamoto (1990)
Ypt4p (*S. pombe*)	?	Increased size/reduced number of vacuoles	Trafficking to or from the vacuole?	Armstrong *et al.* (1994)

Ypt51p/Vps21p (*S. cerevisiae*)	Rab5	*ypt51* deletion and double/triple mutants (*ypt51ypt52, ypt51ypt53, ypt51ypt52ypt53*) ts,[b] defective vacuolar protein sorting	Transport from early to late endocytic compartments and/or from Golgi to the prevacuolar compartment	Section III,A,2
Ypt52p (*S. cerevisiae*)	Rab5	*ypt51* deletion and double/triple mutants *ypt51ypt52, ypt51ypt53, ypt51ypt52ypt53)* ts, defective vacuolar protein sorting	Transport from early to late endocytic compartments and/or from Golgi to the prevacuolar compartment	Section III,A,2
Ypt53p (*S. cerevisiae*)	Rab5	*ypt51* deletion and double/triple mutants *ypt51ypt52, ypt51ypt53, ypt51ypt52ypt53)* ts, defective vacuolar protein sorting	Transport from early to late endocytic compartments and/or from Golgi to the prevacuolar compartment	Section III,A,2
Ypt5p (*S. pombe*)	Rab5	Accumulation of vesicles, no growth in minimal media	Endocytic transport	Section III,A,3
Ypt6p (*S. cerevisiae*)	Rab6	ts	ER–Golgi and/or intra-Golgi transport	Section III,A,1
Ryh1p (*S. pombe*)	Rab6	ts	ND	Hengst *et al.* (1990)
Ypt7p (*S. cerevisiae*)	Rab7	Fragmentation of vacuoles	Transport from endosomes to vacuole, homotypic fusion of vacuoles	Sections III,A,2, III,D, V,D

[a] ND, not determined.
[b] ts, temperature sensitive.

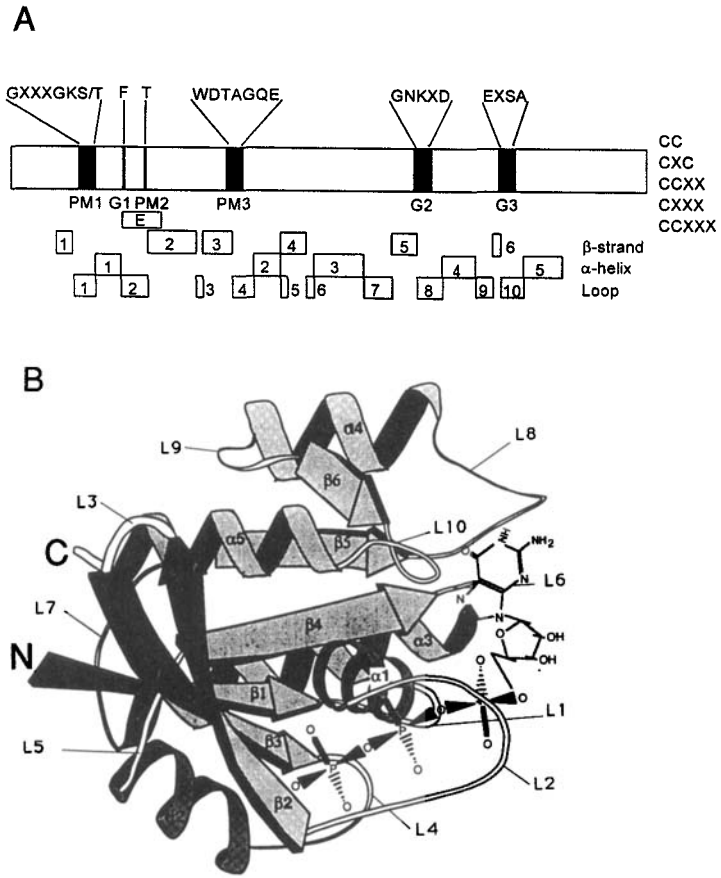

FIG. 3 The structure of Rab GTPases. (A) Linear presentation. The conserved motifs involved in nucleotide binding and hydrolysis are indicated in black. PM1–3 represent the phosphate/Mg^{2+}-binding motifs and G1–3 the guanine base-binding motifs. The highly conserved amino acid residues (in one-letter code) in these motifs are shown above the diagram. The box marked E denotes the "effector" region. The five alternative C-terminal isoprenylation signals are indicated on the right: C, cysteine; X, any amino acid. (B) The three-dimensional fold of the GTPase domain of Ras with a bound GTP molecule (Reprinted with permission from *Biochemistry,* 1991, **30,** 4637–4648. Copyright 1991 American Chemical Society), which has been used as a framework in the molecular modeling of Rab structures.

(Walter *et al.,* 1986; Hoffenberg *et al.,* 1995; Jones *et al.,* 1995). The effects of this mutation in the Rab subfamily were first studied by Schmitt *et al.* (1986), who mutagenized the *S.cerevisiae* Ypt1p, leading to a dominant lethal phenotype. Walworth *et al.* (1989) generated a similar mutation in Sec4p and found that the mutant allele induced a dominant secretory defect.

TABLE III

Rab Mutations Affecting the GTP/GDP Cycle of the Proteins

Corresponding Ras mutation	Biochemical properties	Ras phenotype	Rab phenotype
S17N	Preferential binding of GDP	Inhibitory	Inhibitory
Q61L	Reduced GTPase activity	Strongly activating	Stimulatory on vesicle docking, effect on fusion varies between the Rabs
N116I	Low affinity for GTP/GDP	Weakly activating	Inhibitory
D119N	Low affinity for GTP/GDP, high affinity for XTP/XDP[b]	ND[a]	Inhibitory in the absence of XTP

[a] ND, not determined.

[b] XTP/XDP, xanthosine 5′-tri/diphosphate.

The mutant protein is predicted to display a very rapid nucleotide exchange rate, and because GTP is present in the cytosol in a much larger amount than GDP, a major proportion of the protein would at a given time be associated with GTP. This would explain the transforming activity of the mutant Ras protein; in the case of Rabs the normal GTPase cycle would be blocked, leading to nonproductive binding and sequestration of downstream effector molecules (Hoffenberg *et al.*, 1995). Alternatively, the mutant protein may sequester an upstream guanine nucleotide exchange factor (Jones *et al.*, 1995). Inhibitory effects of the corresponding mutations in different vesicle transport assay setups have been reported for numerous Rab proteins (see Section III).

New types of mutants used to delineate the Rab GTPase cycle are those that preferentially bind xanthosine 5′-triphosphate (XTP) and have a low affinity for guanine nucleotides. Rab5 D136N (Rybin *et al.*, 1996) and Ypt1 D124N (Jones *et al.*, 1995) were found to display inhibitory effects in the absence of XTP, whereas they acted in a stimulatory fashion in the presence of the nucleotide. These mutants may act in an inhibitory fashion analogously to the N116I-type mutants (see above), and binding and hydrolysis of XTP could release the block of the functional cycle (see Section IV).

2. Effector Region

A sequence domain clearly differing between the member groups of the Ras superfamily is the so-called effector region localizing to loop 2 and the beginning of β-strand 2 around the PM2 conserved motif (Fig. 3). In the Rab group the consensus sequence TIG(I/V/A)(D/E)F(K/G/L) is found here. The structure is called the effector region in analogy with the corresponding stretch in the Ras proteins where it mediates interaction with GTPase activating proteins and functions in Ras downstream signaling (M.S. Marshall, 1993, 1995; C.J. Marshall, 1996). In the case of the Rab subfamily, the role of the effector region in the interaction with Rab GAPs (see Section IV,B,3) or other putative Rab downstream effector molecules (see Section IV,C) is not fully characterized. However, it is clear that this sequence feature is highly sensitive to alteration. The effector region is involved in determining the functional specificity of the different GTPases (Brennwald and Novick, 1993; Dunn *et al.*, 1993), and it has been reported to affect the interaction of the proteins with accessory factors regulating the GTP hydrolysis and GDP/GTP exchange (Becker *et al.*, 1991; Burstein *et al.*, 1992). The work of Schalk *et al.* (1996) suggests that the effector region also plays a role in the interaction of Rabs with the GDP-dissociation inhibitor protein (see Section IV,B,1). Furthermore, Beranger *et al.* (1994b) reported that the Rab6 effector region is required for the specific Golgi localization of this GTPase. Whether the region is crucial for the C-terminal

isoprenyl modification of the proteins is under debate: Wilson and Maltese (1993) showed that mutations in the effector domain of Rab1b impaired the efficiency of its isoprenyl modification. However, replacement of the entire Rab6 effector region with a totally different one originating from Ras did not affect the geranylgeranyl modification of the protein (Beranger *et al.*, 1994a). Additionally, synthetic peptides corresponding to the Rab3a effector region are, in numerous investigations, reported to affect transport reactions in assays reconstituting constitutive (Plutner *et al.*, 1990) or regulated secretory events (e.g., Oberhauser *et al.*, 1992; Padfield *et al.*, 1992; Senyshyn *et al.*, 1992; Richmond and Haydon, 1993; Davidson *et al.*, 1993). These results, however, must be interpreted with caution because the commonly used 16-amino acid Rab3AL peptide (Plutner *et al.*, 1990) differs in 2 amino acids from the actual Rab3a effector domain sequence, and it seems that the peptide may affect membrane fusion by mechanisms not necessarily related to the function of Rab3 (Piiper *et al.*, 1993, 1994; Law *et al.*, 1993; MacLean *et al.*, 1993).

3. Variable N and C Termini

The most divergent parts of the Rab amino acid sequence are the N- and C-terminal regions. The C termini of all subfamily members carry a cysteine-containing motif subject to hydrophobic isoprenyl (geranylgeranyl) modification, which is an absolute prerequisite for the membrane association of the proteins (see Section IV,A,1). The C-terminal hypervariable region contains information for the correct targeting of the Rab proteins to their specific locations within the cell, as shown for Rab2, Rab5a, and Rab7 (Chavrier *et al.*, 1991) as well as the *S.cerevisiae* Ypt1p and Sec4p (Brennwald and Novick, 1993). Targeting dictated by the C-terminal hypervariable region, however, is not sufficient to confer a chimeric protein functionality in the new location (Brennwald and Novick, 1993; Stenmark *et al.*, 1994a). The functional significance of the C-terminal sequences is further corroborated by studies in which synthetic peptides corresponding to Rab C termini are demonstrated to inhibit specific exocytic events (Perez *et al.*, 1994; Shibata *et al.*, 1996). The length of the C-terminal region (as calculated from the conserved phenylalanine located 10 amino acids after the G3 motif; Fig. 3A) varies from 36 to 75 amino acid residues within the Rab subfamily, with the shortest known sequence being found in Rab9 (Chavrier *et al.*, 1990b) and the longest in Rab23 (Olkkonen *et al.*, 1994).

The Rab subfamily GTPases display, on the average, longer N-terminal variable regions than the other Ras-related proteins. The longest N-terminal extension is found in Rab3c (31 amino acids before the conserved lysine at position -5 from the PM1 domain; Matsui *et al.*, 1988). The functional role of the variable N terminus of the Rab GTPases has been addressed

in studies on Rab5a, a regulator of early endocytic events (see Section III,B,6). In an *in vitro* early endosome fusion assay tryptic digestion removing four amino acids from Rab5 N terminus abolished fusion. Addition of a synthetic peptide corresponding to the Rab5a N terminus had a similar effect (Steele-Mortimer *et al.*, 1994). Stenmark *et al.* (1994a) showed that this region, together with the helix2/loop5, helix3/loop7, and C-terminal domains, was required for the *in vivo* activity of Rab5/Rab6 chimeras as enhancers of endocytosis. One reason for the importance of the N-terminal sequence may be that it is involved in dictating the prenylation of the C-terminal cysteine motif of Rab5a (Sanford *et al.*, 1995a).

B. Structure of the Rab GTPases

1. Molecular Switch Principle

The structural models for the Rab GTPases are based on the crystal structures determined for Ras (Pai *et al.*, 1989, 1990; Milburn *et al.*, 1990), bacterial elongation factor Tu (Jurnak, 1985; LaCour *et al.*, 1985; Berchtold *et al.*, 1993), and transducin-α (Noel *et al.*, 1993). These studies revealed a highly conserved fold of the GTP-binding domain (Fig. 3B), where the nucleotide binding elements are located in five loops connecting β-strands and α-helices. The structure consists of two subdomains: The N-terminal has four β-strands and two α-helices and contains the loops with the phosphate/Mg^{2+}-binding motifs PM1, -2, and -3 as well as the guanine base-binding motif G1. The C-terminal subdomain consists of two β-strands, two α-helices, and loops containing the G2 and G3 guanine base binding regions. The conserved GTP-binding domain structure has been used as the basis for molecular modeling of other members of the Ras superfamily.

The main regions in Ras undergoing nucleotide-dependent conformational changes are loop2 in the effector region and loop4/helix2/loop5, also called the switch I and switch II regions, respectively (Milburn *et al.*, 1990; Schlichting *et al.*, 1990). In addition, the helix3/loop7 region is predicted to show marked flexibility (Dykes *et al.*, 1993). The activity of the GTPases is controlled by local conformational differences between the GDP- and GTP-bound forms of the proteins, leading to different functional interactions with other cellular components. This principle is called the molecular switch mechanism (Milburn *et al.*, 1990; Bourne *et al.*, 1990; Stouten *et al.*, 1993; Fig. 2). The GTPase in its GDP-bound form is thought to be recruited on a donor membrane or a transport vesicle in a process linked to the exchange of bound GDP for GTP. On the transport vesicle the GTPase may be involved in modulating the activity of the SNARE proteins present (see Section V,B). On the vesicle the Rab may undergo futile cycles of

nucleotide binding and hydrolysis, functioning as a "molecular timer" regulating the subsequent docking/fusion event (see Section III,B,6). During a successful docking event, the GTP-bound Rab recruits a critical density of effector molecules. Proteins acting downstream of the GTPases are predicted to recognize only one of their nucleotide-bound forms (see Section IV,C). After GTP hydrolysis by the Rab the GDP-bound protein can be detached from the acceptor membrane and recycled to the donor membrane. The cyclical molecular switch model is supported by numerous studies on mutant Rab proteins with low affinity for GTP or with reduced GTPase activity, demonstrating inhibition of transport events both *in vivo* and *in vitro* (see Section III).

2. Structural Features Determining the Functional Specificity of Rabs

It is conceivable that the flexible regions in the GTP-binding domain structure should contain elements essential for the functional specificity of the different Rab proteins. This question was first approached experimentally in two studies in which chimeras of the *S. cerevisiae* Ypt1 and Sec4 GTPases (see Section III,A,1) were generated and their function analyzed. Dunn *et al.* (1993) showed that a nine-residue segment of theYpt1p loop7 region substituted for that of Sec4p allowed the chimeric protein to perform the minimal functions of both proteins. If a segment of the effector region was additionally substituted, the Sec4p was transformed into a fully functional Ypt1p without residual Sec4p function. The simultaneous study of Brennwald and Novick (1993) confirmed the role of the effector region, the loop7, and the C-terminal hypervariable region as key features determining the functional specificity of the yeast Rab proteins. These studies demonstrate (i) that the organelle specificity conferred by the Rab C termini is not absolute, and (ii) that Rab proteins by themselves do not act as "address tags" that specify correct vesicle delivery.

In the mammalian system a similar approach was taken by Stenmark *et al.* (1994a) who substituted sequence domains of the endosomal Rab5a (Chavrier *et al.*, 1990a) for those of the Golgi complex GTPase Rab6 (Goud *et al.*, 1990). The intracellular localization and the ability of the chimeric proteins to enhance the rate of endocytosis (see Section III,B,6) were determined. The C-terminal hypervariable region of Rab5a was sufficient to target Rab6 to the location of Rab5a, the plasma membrane, and early endosomes, but did not confer Rab5-like stimulation of endocytosis. Further replacement of the N terminus, the helix2/loop5, and helix3/loop7 regions was required to functionally convert Rab5a to Rab6. However, additional replacement of the effector loop2 impaired the Rab5-like function of the

chimera. This suggests that loop2 of Rab5a necessitates the presence of an additional unknown sequence element of the protein.

In agreement with the studies discussed previously, Moore *et al.* (1995) identified in a sequence comparison study the loop2 and helix3/loop7 regions as the main portions where subclass-specific motifs are found within the Rab GTPase subfamily, indicating interactions with similar auxiliary molecules. To conclude, it is clear that several sequence elements contribute to distinguish the different Rab proteins functionally. This is not surprising when one considers the variety of proteins that are thought to interract with specific Rab GTPases (see Section IV).

C. Tissue and Cell Type-Specific Expression Patterns

1. The Ubiquitous Rab Proteins

A majority of the Rab proteins (Table I) are expressed ubiquitously at the tissue level, as determined by Northern analysis or Western blotting. This is to be expected with regard to the Bourne (1988) hypothesis, due to the large number of intracellular membrane trafficking events common to all mammalian cells. Even though most Rabs appear ubiquitous, this does not mean that they are expressed at equal levels in the various cell types. When studied at a higher resolution by *in situ* hybridization or immunofluorescence/electron microscopy, many of these mRNAs/proteins display marked cell type-specific differences in their expression levels, as exemplified by Rab18 and Rab20 (Lütcke *et al.*, 1994). Detailed analysis of these proteins, which appeared to be present ubiquitously, revealed distinct cell type-specific expression patterns in sections of mouse kidney and intestine. Therefore, it is dangerous to classify a protein as ubiquitous before its distribution has been scrutinized at a higher resolution. However, if one wants to list Rab GTPases that are present in all tissues inspected, this group will undoubtedly include both of the Rab1 isoforms, Rab2, Rab4a, all three Rab5 isoforms, Rab6, Rab7, both Rab8 isoforms, Rab9, Rab10, both Rab11 isoforms, Rab12, Rab13, Rab14, Rab18, Rab20, both Rab22 isoforms, Rab24, Rab28, Rab30, and H-ray (see Table I).

2. Rab Proteins with Distinct, Nonubiquitous Expression Patterns

Cell types with specialized transport functions, such as epithelial cells, neurons, as well as endo- and exocrine cells, are predicted to express specific membrane transport machineries entirely absent or present only at low levels in other cell types. More generally, the functional specialization of

cell types leads to qualitative and quantitative differences in the transport machinery components present in the cells and thus also in the tissues with different cell type constitutions. The Rab3 subgroup members Rab3a, -b, -c, and -d (containing 77–85% identical amino acid residues) are characteristic components of cells with regulated secretory functions. Rab3a originally cloned from rat (Touchot *et al.,* 1987) and bovine (Matsui *et al.,* 1988) brain has been immunologically detected in endo- and exocrine cells of the pancreas, exocrine cells of the submaxillary gland, and adrenal chromaffin cells in addition to the central nervous system (Mizoguchi *et al.,* 1989; Darchen *et al.,* 1990). Rab3a was recently reported to be present in the insulin-secreting β-cells of rat pancreatic islets (Regazzi *et al.,* 1996). Furthermore, Rab3a is also reported to be present in mouse adipocytes and in the 3T3-L1 cell line, in which it is upregulated during differentiation into adipocytes (Baldini *et al.,* 1995). The expression pattern of Rab3a in the different regions of the the brain has been addressed in detail by Moya *et al.* (1992). Like Rab3a, the Rab3b isoform can be detected in neuronal and neuroendocrine tissues (Matsui *et al.,* 1988; Lledo *et al.,* 1993; Regazzi *et al.,* 1996) but is predominantly expressed in epithelial cells (Weber *et al.,* 1994) as well as in adipocytes (Cormont *et al.,* 1993). It has also been detected in platelets (Karniguian *et al.,* 1993). The Rab3a and -b mRNAs display overlapping but not identical distributions in the brain, indicating specialized functions in different neuronal and neuroendocrine cell populations (Lledo *et al.,* 1993; Stettler *et al.,* 1995). Also, the third isoform, Rab3c, is detected in neurons, where it colocalizes with Rab3a on synaptic vesicles (Fischer von Mollard *et al.,* 1994a) and in neuroendocrine tissues, but also in several other tissues such as testis, heart, and adipose tissue (Su *et al.,* 1994; Regazzi *et al.,* 1996). In contrast to the first three isoforms, the Rab3d mRNA is present only at a low level in the brain. It is, however, prominent in a variety of nonneuronal tissues and is enriched in adipocytes (Baldini *et al.,* 1992). Rab3d has also been detected in pancreatic acinar cells (Valentijn *et al.,* 1996) and β-cells (Regazzi *et al.,* 1996), gastric chief cells (Raffaniello *et al.,* 1996; Tang *et al.,* 1996), enterochromaffin-like cells in the stomach, acinar cells in the lacrimal and parotid gland (Ohnishi *et al.,* 1996), and the AtT-20 neuroendocrine cell line (Martelli *et al.,* 1995). Other less well-characterized Rab proteins expressed exclusively or predominantly in the central nervous system are Rab15 (Elferink *et al.,* 1992) and Rab23 (Olkkonen *et al.,* 1994).

Epithelial cells represent another functionally polarized cell type having specialized transport functions (see Section III,E). It has therefore been of interest to search for Rab GTPases predominantly expressed in such cells. Rab17 was identified as the first epithelial-specific member of the GTPase subfamily (Lütcke *et al.,* 1993). The Rab17 mRNA was detected in the kidney, intestine, and liver—tissues with prominent epithelial struc-

tures. Furthermore, by *in situ* hybridization it was shown to be restricted to kidney epithelial cells and to be induced upon differentation of mouse metanephric mesenchyme into epithelium. Other predominantly epithelial GTPases are Rab11a, detected in epithelia of the gastrointestinal tract, liver, exocrine pancreas, prostate, and kidney (Goldenring *et al.,* 1996), Rab25, the mRNA of which is expressed throughout the gastrointestinal mucosa as well as in the lung and the kidney (Goldenring *et al.,* 1993), and Rab3b, which is detected in several epithelial cell lines and a number of epithelial tissues, liver, small intestine, colon, and distal nephron, in addition to the central nervous system (Weber *et al.,* 1994). Furthermore, according to Northern analysis Rab19 (Lütcke *et al.,* 1995) displays a highly tissue-specific expression pattern, the mRNA being detected in kidney, intestine, lung, and spleen, which may indicate predominant expression in epithelial cells and lymphocytes.

D. Intracellular Localization of Rab GTPases

One of the hallmark properties of the Rab GTPases is localization on distinct membrane compartments along the biosynthetic and endocytic pathways of eukaryotic cells. Most of the Rabs are detected not only on one compartment but also at two or more different locations, which is in agreement with the current models for Rab function. Moreover, several GTPases can typically be found on the same membrane compartments. This is explained by the existence of multiple trafficking routes that connect the intracellular organelles and by division of the organelles into functional subdomains. In addition, it is possible that several closely related isoforms of a given Rab may have redundant functions.

1. Proteins Associated with the Biosynthetic Route

a. Endoplasmic Reticulum and Golgi Apparatus Mammalian cells contain two isoforms of Rab1, a functional counterpart of the *S.cerevisiae* Ypt1p (Touchot *et al.,* 1987; Zahraoui *et al.,* 1989; Haubruck *et al.,* 1989; Vielh *et al.,* 1989). Rab1b was localized by immunofluorescence microscopy and subcellular fractionation to the smooth ER and Golgi complex in several cultured cell lines and in rat liver membrane fractions (Plutner *et al.,* 1991). Additionally, low amounts of the protein were detected in the cytosolic, nuclear, and rough ER fractions. The localization of Rab1 (an antibody detecting both isoforms was used) was studied further by Saraste *et al.* (1995), who detected the protein by immunoelectron microscopy on vacuolar and tubulovesicular membranes in the *cis*-Golgi region, also denoted as the ER–Golgi intermediate compartment (IC) (Hauri and

Schweizer, 1992; Saraste and Kuismanen, 1992), as well as on the first one or two cisternae of the Golgi. The immunostaining extensively colocalized with that of the IC marker p58, and labeling of the ER and the nuclear envelope in the cell types used was negligible. The Rab2 protein (Touchot *et al.*, 1987; Zahraoui *et al.*, 1989) was localized in several cell lines to the same membranes as Rab1, the tubulovesicular IC and the *cis*-most cisternum of the Golgi stack (Chavrier *et al.*, 1990a). However, Rab2 appears to be more strictly limited to the IC than Rab1, whose localization seems to extend deeper into the Golgi stack than that of Rab2. On the other hand, Rab2 has been reported to localize on the tubulovesicle membranes of rabbit gastric parietal cells (Tang *et al.*, 1992). These membranes represent a gastric acid storage organelle that fuses with the canalicular plasma membrane upon appropriate stimulus. The finding is somewhat puzzling because there is no obvious functional connection between the IC and the parietal cell tubulovesicle compartments. The fourth protein detected on the early secretory pathway membranes is Rab24 (Olkkonen *et al.*, 1993), which was localized by an epitope tagging/overexpression approach to ER and *cis*-Golgi. However, some of the protein was also detected on late endosomal structures.

Rab6 was the first small GTPase localized to the actual Golgi stack: Using immunofluorescence and immunoelectron microscopy, it was detected on the entire surface of the Golgi *medial* and *trans* cisternae (Goud *et al.*, 1990). Later, this localization was extended to the *trans*-Golgi network (TGN)(Antony *et al.*, 1992), the sorting site of material exiting the Golgi complex (Griffiths and Simons, 1986; Mellman and Simons, 1992). Interestingly, aside from its Golgi localization, Rab6 was reported to associate with regulated secretory organelles, the platelet α-granules, and the plasma membrane in this cell type (Karniguian *et al.*, 1993). Moreover, a close homolog of Rab6 in *Torpedo marmorata* electrocytes was localized to *post*-Golgi vesicles located at the cytoplasmic face of the innervated membrane of the electrocyte (Jasmin *et al.*, 1992). Olkkonen *et al.* (1993) reported localization of Rab12 in the Golgi complex of baby hamster kidney (BHK) cells. Analogously with the situation of Rab6 discussed previously, Rab12 is also reported to reside on secretory granules in atrial myocytes (Iida *et al.*, 1996).

b. Constitutive Post-Golgi Transport Intermediates Rab8 and Rab10 are closely related GTPases that show more homology to *S.cerevisiae* Sec4p than to any other mammalian proteins (Chavrier *et al.*, 1990b). Using immunofluorescence and electron microscopy, Rab8 was localized to the Golgi region, cytoplasmic vesicular structures, and the plasma membrane of the Madin–Darby canine kidney (MDCK) epithelial cell line (Huber *et al.*, 1993b). In filter-grown fully polarized MDCK cells the protein was seen

on the basolateral plasma membranes, concentrated near the junctional complexes and structures at the basal bottom of the cells. Furthermore, the protein was found enriched in immuno-isolated basolateral *post*-Golgi transport vesicles. In cultured rat hippocampal neurons the protein was detected predominantly on the somatodendritic plasma membrane (Huber *et al.*, 1993a), which seems to correspond to the basolateral membrane domain of epithelial cells (Simons *et al.*, 1992). The peripheral localization of Rab8a was independently reported by Chen *et al.* (1993), who used stably transfected Swiss 3T3 or Chinese hamster ovary (CHO) cells expressing an epitope-tagged version of the human Rab8a. The protein seemed to concentrate on membrane ruffles and blebs on the cell surface. With the same approach the authors studied the localization of rat Rab10 and found the protein at a perinuclear location, the staining overlapping with that of the Golgi marker β-COP. The rat Rab8b isotype was identified by Armstrong *et al.* (1996) in a basophilic leukemia cell line, RBL.2H3. In RBL.2H3 and PC12 cells, transiently expressed epitope-tagged protein displayed a localization similar to that of the Rab8a isotype (see above). Like Rab6, Rab8a was also reported to be present on platelet α-granules and plasma membrane (Karniguian *et al.*, 1993), and a protein with Rab8 immunoreactivity was identified as one of the small GTPases present on the rhodopsin-containing *post*-Golgi membranes in frog retinal photoreceptor cells (Deretic *et al.*, 1995).

Rab13 (Elferink *et al.*, 1992; Zahraoui *et al.*, 1994) and Rab3b (Weber *et al.*, 1994) display a distribution reminiscent of that of Rab8a, localizing at the tight junction regions near the apical pole of polarized epithelial cells. In nonpolarized cells Rab13 is distributed in cytoplasmic vesicles of unknown function. Concentration of several Rab GTPases at the junctional complexes of epithelia may indicate a central role of these regions in the polarized membrane trafficking occurring in these cells. On the other hand, the maintenance of these structures may require active transport coordinated by the GTPases.

*c. **Regulated Exocytic Vesicles*** The Rab3 GTPases form a protein group predominantly found on the secretory vesicles/granules fusing with the plasma membrane by a calcium-triggered mechanism (Burgess and Kelly, 1987; De Camilli and Jahn, 1990; Südhof *et al.*, 1993). Rab3a was detected on synaptic vesicles that store and release neurotransmitters (Fischer von Mollard *et al.*, 1990; Mizoguchi *et al.*, 1990). Moreover, the protein was found in the endocrine adrenal medulla chromaffin cells, on microvesicles with similarity to neuronal synaptic vesicles (Fischer von Mollard *et al.*, 1990), and on chromaffin granules responsible for catecholamine secretion (Darchen *et al.*, 1990, 1995). In pancreatic β-cells Rab3a was detected mainly in the cytosolic and secretory granule fractions but not in those

containing synaptic-like microvesicles (Regazzi *et al.,* 1996). Weber *et al.* (1996) expressed the Rab3a and -b isoforms stably in the neuroendocrine PC12 cells. Both proteins were targeted to the norepinephrine-containing large dense core vesicles. The Rab3c isotype localizes together with Rab3a on synaptic vesicles (Fischer von Mollard *et al.,* 1994a), whereas Rab3d has been identified as a component of gastric chief cell zymogen granules (Tang *et al.,* 1996) and secretory granules of pancreatic acinar cells (Valentijn *et al.,* 1996; Ohnishi *et al.,* 1996). Even though Rab3d was first identified in adipocytes (Baldini *et al.,* 1992) it remains to be demonstrated whether the protein is present on the GLUT4 vesicles (containing the glucose transporter protein; James *et al.,* 1994) in these cells. However, the endosomal GTPase Rab4 (see Sections II,D,2 and III,B,6) was reported to be present on the GLUT4 vesicles in rat adipocytes (Cormont *et al.,* 1993), a finding supported by the recent functional data of Shibata *et al.* (1996). The results may imply an endosomal origin of these regulated secretory vesicles. Additionally, in certain cases several other GTPases have been found in purified regulated secretory vesicle preparations, including Rab5 on synaptic vesicles (see Section II,D,2), Rab11 on PC12 cell secretory granules (Urbe *et al.,* 1993), its homolog Ora3 in marine ray cholinergic synaptic vesicles (Volknandt *et al.,* 1993), as well as Rab6 and Rab8a on platelet α-granules (Karniguian *et al.,* 1993).

2. Rab Proteins Associated with Endocytic Compartments

a. Early Endosomal Rab Proteins Chavrier *et al.* (1990a) localized Rab5a in BHK and MDCK cells on the plasma membrane, on a fine tubular network in cell periphery, and on small vesicular structures throughout the cytoplasm. By immunofluorescence and electron microscopy, the intracellular structures were confirmed to represent early endosomes. Occasionally, labeling was also seen on coated pits. No label was seen on late endosomes or lysosomes. When the protein was overexpressed, increased labeling of the plasma membrane and early endosomes was observed. The other two Rab5 isoforms, Rab5b and Rab5c, display a localization similar to that of Rab5a (Bucci *et al.,* 1995). Interestingly, Rab5 is also detected on synaptic vesicles (Fischer von Mollard *et al.,* 1994b; de Hoop *et al.,* 1994), which is in agreement with the suggested recycling of these secretory structures through endocytic intermediates (De Camilli, 1995). Using cell fractionation techniques and specific antibodies, van der Sluijs *et al.* (1991) showed that a majority of the Rab4 protein in CHO cells localized on early endosomes and endocytic vesicles containing internalized ^{125}I-labeled transferrin. The localization was confirmed by expression studies in HeLa and CHO cells (van der Sluijs *et al.,* 1991, 1992b). The distribution of Rab4a was further dissected in a recent study in which Daro *et al.* (1996) demonstrated that the

GTPase resides on the early endosomal population to which the internalized transferrin is initially delivered. The recycling endosomal structures close to the microtubule organizing center (Yamashiro *et al.,* 1984; Hopkins *et al.,* 1994) were devoid of Rab4a. These structures, however, were recently reported to contain Rab11a (Ullrich *et al.,* 1996), which was previously suggested to localize on the TGN and *post*-Golgi secretory vesicles (Urbe *et al.,* 1993). Whether there is a discrepancy between these data cannot currently be stated because the detailed organization of the route from recycling endosomes to cell surface is still unclear.

Recent cloning and characterization efforts have revealed several novel GTPases associating with early endosomes. Rab17 was localized to the basolateral plasma membranes and tubular structures below the apical plasma membrane of kidney proximal tubule epithelial cells, indicating a possible role in transcytosis (Lütcke *et al.,* 1993). Also, Rab18 and Rab20 were detected on the apical dense tubules (Lütcke *et al.,* 1994), endocytic structures underlying the apical plasma membrane of kidney tubule epithelial cells (Christensen and Nielsen, 1991; Cui and Christensen, 1993). Finally, using an epitope tagging approach Rab22 was localized mainly to large perinuclear vesicle-like structures, the size of which increased upon increasing expression time periods (Olkkonen *et al.,* 1993). The Rab22-positive structures showed a significant overlap with transferrin internalized for 5 min, thus representing at least partially an early endosomal compartment. The staining was clearly distinct from, but overlapping with, that of endogenous Rab7, a late endosomal marker. Additionally, the protein was detected on the plasma membrane. The number of Rab GTPases associating with early endosomal membranes is striking but not surprising if one considers the complex sorting tasks these organelles perform (Hopkins, 1992; Gruenberg and Maxfield, 1995).

b. Proteins on Late Endocytic Compartments Antibodies against a C-terminal peptide of the Rab7 GTPase (Bucci *et al.,* 1988) were shown to stain the endogenous protein on large perinuclear vesicular structures in several cultured cell lines (Chavrier *et al.,* 1990a). The structures coincided with bovine serum albumin (BSA)–gold internalized under conditions in which late endosomes are labeled. Furthermore, Rab7 was shown to colocalize with the cation-independent mannose-6-phosphate receptor (CI-MPR). However, lysosomes were devoid of Rab7 immunostaining. In a recent study, Meresse *et al.* (1995) investigated the localization of endogenous Rab7 and an epitope-tagged version in HeLa cells. The protein was present on a vesicular–tubular compartment extending from the perinuclear region to the cell periphery and colocalized only partially with CI-MPR, which showed a more restricted perinuclear distribution. The localization of the Q67L mutant form of Rab7 was strikingly different from that of the wild-

type protein: In addition to the extensive reticular pattern the protein was detected on large vesicular structures throughout the cytoplasm, most probably representing lysosomes. Redistribution of Rab7 to lysosome-like structures was also seen upon disruption of microtubules by nocodazole. The implications of this finding in terms of the function of Rab7 are under debate (Feng *et al.,* 1995; see Section III,B,8).

The second GTPase associated with late endosomes is Rab9 (Chavrier *et al.,* 1990b), which was colocalized with the CI-MPR in the perinuclear region of BHK cells. Preliminary electron microscopic analysis revealed a minor fraction of the protein on the TGN (Lombardi *et al.,* 1993). Furthermore, Rab9 was found to associate *in vitro* with CI-MPR-enriched late endosomal preparations (Soldati *et al.,* 1994). Its function in the recycling of CI-MPR from late endosomes to the TGN is discussed in detail in Section III,B,3.

III. Experimental Evidence for Rab Function in Membrane Trafficking

A. Yeast GTPases

1. The Function of Rab GTPases in the Secretory Pathway of *S. cerevisiae*

The concept of GTPases as regulators of vesicular transport is founded on the identification of the *sec4* mutants, originally isolated in a screen for temperature-sensitive *S. cerevisiae* mutants defective in protein secretion (Novick *et al.,* 1980). These mutants display a temperature-dependent block in transport from the Golgi apparatus to the plasma membrane, and sequencing of the *SEC4* gene revealed that it encodes a protein with 32% identity to Ras, a GTPase implicated in signal transduction (Salminen and Novick, 1987). Sec4p was found to reside in three pools: a small cytoplasmic pool, a pool associated with secretory vesicles, and a pool associated with the plasma membrane (Goud *et al.,* 1988). At the restrictive temperature, a large amount of secretory vesicles was found to accumulate in the *sec4-8* mutant (Salminen and Novick, 1987). This, together with the intracellular localization of Sec4p and its requirement for secretion, indicated a role for Sec4p in the docking or fusion of secretory vesicles with the plasma membrane. The finding that a GTPase-deficient mutant of Sec4p exhibited a loss-of-function phenotype (Walworth *et al.,* 1992) provided a clue that a functional GTPase cycle is required for the biological activity of Sec4p, and

similar conclusions have thereafter been made for several other members of the Rab GTPase subfamily.

The essential *ypt1* gene was identified in 1983 as the open reading frame adjacent to the actin gene (Gallwitz *et al.,* 1983), with similarity to the human Ras protooncogene. The function of Ypt1p remained obscure until it was observed that the *ypt1-1* mutant secretes an underglycosylated form of invertase (Segev *et al.,* 1988). This particular form of invertase had previously been found in yeast mutants with a block in ER to Golgi transport (Novick *et al.,* 1981), thus providing a hint that Ypt1p might be involved in this transport step. Consistent with this, Ypt1p has been localized to ER- and Golgi-derived vesicles (Segev, 1991; Segev *et al.,* 1988). The first evidence for the direct involvement of Ypt1p in intracellular traffic was the finding that *ypt1* mutant fractions were unable to support ER–Golgi transport in an *in vitro* assay (Bacon *et al.,* 1989). Subsequently, anti-Ypt1p antibodies were found to block ER–Golgi transport in this assay (Baker *et al.,* 1990), and under such conditions small vesicles accumulated that contained core-glycosylated α-factor (Segev, 1991). Because the oligosaccharides on α-factor transported to the Golgi would have been further processed, these vesicles appeared to be ER derived. Similar vesicles were also observed, but at lower abundance, when normal Ypt1p function was allowed, indicating that they are not artefactual structures formed when Ypt1p function is blocked. Consistent with these *in vitro* data, electron microscopy of yeast cells showed that the small vesicles were more abundant in *ypt1* mutant cells than in wild-type cells (Schmitt *et al.,* 1988; Segev *et al.,* 1988). These results thus indicate that Ypt1p, like Sec4p, is not required for vesicle formation but rather for a later step in vesicular traffic, such as vesicle docking or fusion. The early studies on *ypt1* did not pinpoint exactly at which transport step Ypt1p is required (ER to Golgi or *cis* to medial Golgi). This problem was addressed using a novel mutant, *ypt1-A136D,* displaying a faster and tighter transport block at the restrictive temperature than the previously studied *ypt1* mutants (Jedd *et al.,* 1995). This mutant allowed pulse-chase studies of different secretory markers to dissect the transport step(s) requiring Ypt1p. The studies indicated that Ypt1p is required both for ER to Golgi and *cis* to medial Golgi transport. This finding is in line with the current view that Rab GTPases can regulate several consecutive transport steps and do not function as primary specificity determinants in vesicular traffic.

A mutant allele of *YPT6* was identified in a screen for temperature-sensitive *S. cerevisiae* mutants defective for the transcription of ribosomal genes (Li and Warner, 1996). For reasons that are still not clear, ribosome biosynthesis requires a functional secretory pathway. At the restrictive temperature, the *ypt6* mutant strain displayed a partial block in ER–Golgi or *cis* -to *medial* Golgi transport, as evidenced by the accumulation

of a core-glycosylated form of invertase and reduced maturation of the vacuolar protein carboxypeptidase Y. Ypt6p thus appears to be required at an early stage in the yeast secretory pathway. On the other hand, disruption of *YPT6* leads to the missorting of the vacuolar enzyme carboxypeptidase Y, suggesting that Ypt6p may also play a role in transport between the Golgi and the prevacuolar endocytic compartment (Tsukada and Gallwitz, 1996). Therefore, it cannot be excluded that Ypt6p, like Ypt1p, regulates several consecutive transport steps in the secretory pathway.

Recently, the group of Gallwitz (Benli *et al.*, 1996) isolated and characterized a pair of related GTPase genes, *YPT31* and *YPT32*. Disruption of either one of these genes had no phenotypic effect, whereas the double disruption was lethal. In experiments in which Ypt31p was depleted in a controlled manner in *ypt32* background, accumulation of Golgi-like membranes, inhibition of invertase secretion, and defective processing of vacuolar hydrolases were observed. Both fully and underglycosylated forms of invertase accumulated in the cells under these conditions. In accordance with these results, by cell fractionation and immunofluorescence microscopy Ypt31p was localized to Golgi-like structures. It thus seems likely that the Ypt31/Ypt32 proteins are involved in intra-Golgi transport or formation of transport vesicles at the most distal Golgi compartment of yeast cells.

2. Rab GTPases Regulating Endocytosis and Vacuolar Protein Sorting in *S. cerevisiae*

The endocytic pathway in yeast is less well characterized than the secretory pathway, but during the past few years a number of yeast mutants with defects in endocytosis have been identified, and biochemical characterization of the yeast endocytic pathway has been initiated (Munn and Riezman, 1994; Stack and Emr, 1993). Also, the isolation and characterization of *vps* mutants defective in sorting of proteins from the secretory pathway to the lysosome-like vacuole has contributed significantly to our understanding of the yeast endocytic pathway because such proteins appear to be sorted via endosome-like organelles (Horazdovsky *et al.*, 1995). Ypt7p was identified in a PCR cloning approach for new Rab proteins in *S. cerevisiae* (Wichmann *et al.*, 1992). Its similarity (63% identity) to mammalian Rab7, which is associated with late endosomes (see Section II,D,2), suggested that Ypt7 might play a role in the endocytic pathway. Disruption of the *YPT7* gene does not impair cell growth, even at elevated or reduced temperatures; however, *ypt7* null mutants do show phenotypic changes—they contain highly fragmented vacuoles, a defect also characteristic of certain classes of *vps* mutants. Furthermore, the degradation of endocytosed α-factor is reduced in the *ypt7* null mutant cells, although the endocytosis step itself is not affected (Wichmann *et al.*, 1992). Subcellular fractionation

suggested that the internalized α-factor accumulates in a late endocytic compartment in *ypt7* null mutants, indicating that Ypt7p regulates transport from late endocytic compartments to the vacuole (Schimmöller and Riezman, 1993). In a cell-free assay, Ypt7p has also been shown to be required for the homotypic fusion between vacuolar membranes (see Section III,D).

In mammalian cells, Rab5 regulates fusion events in the early endocytic pathway (see Section III,B,6), and by PCR cloning two Rab5-like genes, *YPT51* and *YPT53,* were identified in *S. cerevisiae.* In addition, a third gene, *YPT52,* was identified during the yeast genome sequencing project (Singer-Krüger *et al.,* 1994). Ypt51p, Ypt52p, and Ypt53p share 52–54% identity with mammalian Rab5, and the high degree of similarity with Rab5 in their "switch" regions (see Section II,B) suggested that they may perform a function related to that of Rab5. The sequence of the entire *S. cerevisiae* genome is now available, and it is clear that *YPT51, YPT52,* and *YPT53* are the only Rab5-like genes present. Gene disruptions showed that none of the three Rab5-like genes is essential, and even a null mutant disrupted for all three genes is viable in rich medium. However, individual disruptions of the three Rab5-like genes resulted in impaired growth at 37°C, with *ypt51* showing the strongest effect, and a triple disruption of all three genes resulted in an even stronger growth defect. Furthermore, degradation of α-factor was reduced in the individual mutants and further aggravated in the triple disruptant. Thus, the phenotype of *ypt51/ypt52/ypt53* null mutants resembles that of *ypt7,* but cell fractionation experiments suggest that Ypt51p regulates an earlier endocytic transport step than Ypt7p (Singer-Krüger *et al.,* 1995). Consistent with this, Ypt51p expressed in mammalian cells appears to be associated with early endosomes, and Ypt51p mutants affect endocytic traffic in mammalian cells in a similar way as the corresponding Rab5 mutants (see Section III,B,6). The Ypt51p-containing compartment in yeast has been visualized by confocal immunofluorescence microscopy (Singer-Krüger *et al.,* 1995). Ypt51p is present on vesicular compartments that are expanded upon the expression of a GTPase-deficient mutant, an observation similar to that made in mammalian cells in the presence of the corresponding Rab5 mutant (see Section III,B,6). The vesicular structures are positive for an endocytic marker, the α-factor receptor, as well as for a protein sorted to the vacuole, carboxypeptidase Y. This provides evidence that the endocytic and vacuolar protein sorting pathways converge at (or prior to) the Ypt51p-positive compartment. Indeed, *YPT51* has been identified independently as *VPS21* (Horazdovsky *et al.,* 1994). Electron microscopy of cells with disrupted *VPS21/YPT51* showed that they contain a single vacuole, in contrast to *ypt7* cells, but that they accumulate a number of small (40–60 nm) vesicles of unknown origin. This suggests that Vps21p/Ypt51p, like Ypt1p and Sec4p, may function in vesicle docking or fusion (Singer-Krüger *et al.,* 1994; Horazdovsky *et al.,* 1994).

3. The *Schizosaccharomyces pombe* Rab Proteins

The fission yeast *S. pombe* may in some respects offer a model closer to the mammalian system than does *S. cerevisiae.* Because *S. pombe,* like *S. cerevisiae,* is readily amenable to genetic manipulations, studies of Rab function is this organism provide an important complement to studies of Rab proteins in mammals and *S. cerevisiae.* Six different Rab GTPases have been identified in *S. pombe* to date: Ypt1p, Ypt2p, Ypt3p, Ypt4p, Rhy1p, and Ypt5p. Ypt3p and Rhy1p are putative homologs of mammalian Rab11 and Rab6, respectively, but limited functional data are available on these proteins. *Schizosaccharomyces pombe* Ypt1p is 72% identical to *S. cerevisiae* Ypt1p and 80% identical to mammalian Rab1. Like *YPT1* in *S. cerevisiae, S. pombe ypt1* is essential for growth, and moderate expression of *S. pombe* Ypt1p complements the lack of the homologous GTPase in *S. cerevisiae ypt1* null mutants (Miyake and Yamamoto, 1990). Electron microscopy of a temperature-sensitive *ypt1* mutant of *S. pombe* revealed that its Golgi complex is disassembled at the restrictive temperature (Armstrong, 1995). This indicates that Ypt1p is required for the maintenance of the Golgi complex in *S. pombe,* consistent with a function in ER to Golgi (or *cis* to medial Golgi) traffic, as found with its homologs in *S. cerevisiae* (see Section III,A,1) and mammals (see Section III,B,1).

Ypt2p of *S. pombe* shares 55% sequence identity with *S. cerevisiae* Sec4p and 63% identity with canine Rab8 (Craighead *et al.,* 1993). Like *S. cerevisiae SEC4, S. pombe ypt2* is an essential gene, and it can functionally complement a conditional-lethal *sec4* mutation (Haubruck *et al.,* 1990). On the other hand, a temperature-sensitive *ypt2* mutation can be complemented by Rab8 expression (Craighead *et al.,* 1993), indicating that Ypt2p is a functional homolog of both *S. cerevisiae* Sec4p and mammalian Rab8. At the restrictive temperature, the temperature-sensitive *ypt2* mutant accumulates a fully processed form of acid phosphatase, a normally secreted enzyme. Furthermore, electron microscopy revealed the accumulation of vesicles between 130 and 170 nm in diameter. Thus, like *S. cerevisiae* Sec4p, *S. pombe* Ypt2p appears to regulate transport between the Golgi and the plasma membrane, presumably at the vesicle docking/fusion stage.

Although three Rab5-like genes are present in *S. cerevisiae,* only one, *ypt5,* has been found in *S. pombe.* Ypt5p is 63% identical to canine Rab5 and 55% identical to *S. cerevisiae* Ypt51p. Like the *S. cerevisiae YPT51/YPT52/YPT53* genes, *ypt5* is not essential for viability in rich medium (Armstrong *et al.,* 1993). However, it is essential for growth in minimal media, and even in rich medium *ypt5* null mutants grow slowly and accumulate heterogeneous vesicles of 200–300 nm. Canine Rab5 can functionally substitute for Ypt5p and restore *S. pombe* growth and viability (Armstrong *et al.,* 1993). Like *S. cerevisiae* Ypt51p, *S. pombe* Ypt5p colocalizes with

the transferrin receptor when expressed in mammalian cells, indicative of a localization in early endosomes. All available data are thus consistent with the idea that Ypt5p is a functional homolog of Rab5, involved in fusion events in the early endocytic pathway of *S. pombe.*

B. Functional Studies on the Mammalian Rab Proteins

1. Rab1 and Rab2 Regulate the ER–Golgi Interface Trafficking Events

Rab1 and Rab2 both localize in the ER–Golgi area (see Section II,D,1) and function at an early stage of the secretory pathway. Two isoforms (92% identical) of Rab1 have been identified, Rab1a (Touchot *et al.,* 1987) and Rab1b (Vielh *et al.,* 1989). The fact that Rab1a is 71% identical to *S. cerevisiae* Ypt1p and can functionally complement the loss of Ypt1p in yeast (Haubruck *et al.,* 1989) initially suggested that Rab1 might function in ER to Golgi and/or *cis-* to medial Golgi traffic, like its yeast counterpart. ER–Golgi transport in mammalian cells can be assayed by monitoring the trimming of the high mannose residues of a temperature-sensitive mutant of vesicular stomatitis virus G protein (VSV-G), an event that occurs in the Golgi apparatus. Furthermore, it is possible to distinguish between the *cis-* and medial Golgi forms of VSV-G because the oligosaccharide chains of the latter acquire endoglycosidase H resistance. The temperature-sensitive VSV-G mutant accumulates in the ER at the restrictive temperature, whereas it is efficiently transported through the Golgi at the permissive temperature, thus making it a useful probe for ER–Golgi traffic. When the traffic of VSV-G was reconstituted in semi-intact cells (Plutner *et al.,* 1991), monoclonal antibodies against Rab1b were observed to inhibit ER–Golgi and *cis-* to medial Golgi traffic, thus implying a role for Rab1b in these processes. The data are consistent with the findings that the yeast homolog of Rab1, Ypt1p, is required for both ER–Golgi and *cis-* to medial Golgi traffic (see Section III,A,1). In intact transfected cells, a number of point mutants of Rab1a and Rab1b were investigated for their ability to inhibit ER–Golgi transport (Tisdale *et al.,* 1992; Pind *et al.,* 1994; Nuoffer *et al.,* 1994). Rab1b S22N and Rab1a S25N, mutants with higher affinity for GDP than for GTP, and Rab1b N121I and Rab1a N124I, which have a low affinity for both nucleotides, inhibited this transport step. In contrast, Rab1b Q67L, which is predicted to have a reduced GTPase activity, did not. Furthermore, Rab1a N124I appears to inhibit vesicle docking because this mutant protein caused accumulation of VSV-G in apparently undocked vesicles in permeabilized cells, as evidenced by immunoelectron microscopy (Pind *et al.,* 1994). The accumulated vesicles and putative *pre-*Golgi interme-

diates contained Rab1 and the coatomer component, β-COP. Surprisingly, however, fluorescence microscopy of transfected cells suggested that Rab1a S25N could inhibit protein export from the ER and *cis*-Golgi (Nuoffer *et al.,* 1994). This implied a role for Rab1 not only in vesicle docking/fusion but also in vesicle budding, an issue that will be discussed in Section III,C. Overexpression of Rab1a S25N also led to the disassembly of the Golgi apparatus, indicating that Rab1 function is required for the proper assembly of the Golgi apparatus (Wilson *et al.,* 1994). The latter conclusion is consistent with the finding that a temperature-sensitive mutation in the *S. pombe* Rab1 homolog, *ypt1,* led to the disappearance of the Golgi complex at the restrictive temperature (see Section III,A,3).

Compared with Rab1, little is known about the function of Rab2. Recombinant Rab2 loaded into cultured neurons was found to enhance neurite outgrowth and cell adhesion (Ayala *et al.,* 1990), but the mechanism behind these effects is not known. Although the presumably GDP-bound Rab2 S20N mutant did not inhibit ER-Golgi traffic, the putatively GTPase-deficient Rab2 Q65L did. These two Rab2 mutants thus behaved in an opposite manner to their Rab1 counterparts (Tisdale *et al.,* 1992), suggesting that Rab2 may regulate a transport step(s) different from those regulated by Rab1, perhaps retrograde transport from the Golgi to the ER.

2. Role of Rab6 in Intra-Golgi Transport

The wide distribution of Rab6 in the Golgi and TGN (see Section II,D,1) suggests that, like Rab1, it regulates several transport steps. Its function has been studied both in intact cells and in cell-free assays. Rab6 was found in a complex with a 62-kDa protein and TGN38/41 (Jones *et al.,* 1993). This complex has been implicated in vesicle budding from the TGN (Salamero *et al.,* 1990), thus suggesting a role for Rab6 in this process, although direct evidence is lacking (see Section III,C). The function of Rab6 was more directly addressed in a study with transiently transfected cells (Martinez *et al.,* 1994). Overexpression of wild-type Rab6 as well as the GTPase-deficient Rab6 Q72L and the GDP-bound Rab6 T27N mutants was found to inhibit the transport between α-mannosidase II positive (*cis*-/medial Golgi) and sialyl transferase-positive *(trans*-Golgi) compartments. Transport from the ER to the Golgi was not affected and neither was transport from the TGN to the plasma membrane. Confocal microscopy showed that expression of Rab6 Q72L resulted in an apparent fragmentation of the Golgi apparatus and the TGN, whereas little change was observed when wild-type Rab6 was overexpressed (Martinez *et al.,* 1994). On the other hand, expression of Rab6 T27N resulted in an apparent enlargement of the Golgi and the TGN. Because the latter mutant is likely to give a loss-of-function phenotype (see Section II,A,1), Rab6 function, unlike that of Rab1, does not

appear to be required for the assembly or integrity of the Golgi apparatus. Together, these data indicate that Rab6 may either be a negative regulator of anterograde intra-Golgi traffic or a positive regulator of retrograde intra-Golgi transport (Martinez *et al.*, 1994).

An *in vitro* assay for measuring transport between the *cis*- and the *medial* cisternae of the Golgi has identified crucial components of the intracellular transport machinery, such as NSF and SNAPs (Rothman, 1994), although it is still debated how faithfully this assay reconstitutes vesicular transport from the *cis* to the medial Golgi cisternae (Mellman and Simons, 1992). The assay is based on a donor Golgi fraction containing VSV-G but lacking the medial Golgi marker *N*-acetylglucosaminyl transferase, and an acceptor Golgi fraction lacking VSV-G but containing the enzyme. Transport from the donor to the acceptor Golgi fraction is detected as the *N*-acetylglucosamination of VSV-G when the two fractions are incubated together in the presence of ATP and cytosol. Recombinant Rab6 N126I, as well as antibodies against Rab6, potently inhibits transport of VSV-G in this assay, thus suggesting a role for Rab6 at this early step in intra-Golgi traffic. This result is not in direct disagreement with the previous results that implied a role for Rab6 in later intra-Golgi transport steps, but rather suggests that Rab6 may control several consecutive transport steps. The same Rab6 mutant was previously shown not to affect the transport of VSV-G from the ER to a compartment containing α-mannosidase II (*cis*-Golgi) (Tisdale *et al.*, 1992). In the intra-Golgi transport assay, uncoupled (not involving vesicular transport) fusion between the two Golgi fractions can be observed when coat proteins are removed by incubation with high salt. Such uncoupled fusion requires Rab6 (T. Mayer, *et al.*, 1996), and this indicates that Rab6 serves to regulate membrane docking or fusion.

3. Function of Rab9 in the Communication between Endosomes and the Golgi Complex

The function of Rab9 was first addressed using a cell-free assay that reconstitutes the transport of the CI-MPR from late endosomes to the TGN, measured as the sialylation of endosome-derived CI-MPR in the presence of Golgi-enriched fractions. Antibodies against Rab9 inhibited the transport of CI-MPR in this assay by 50%, whereas antibodies against another late endosomal GTPase, Rab7, were without effect (Lombardi *et al.*, 1993). Moreover, *in vitro* prenylated recombinant Rab9 stimulated the transport reaction 2.5-fold, whereas Rab4b and Rab7 showed no effect. Likewise, in intact cells stably transfected with a Rab9 mutant with preferential affinity for GDP, Rab9 S21N, recycling of CI-MPR from late endosomes to the TGN was inhibited (Riederer *et al.*, 1994), whereas fluid-phase endocytosis was unaffected. Consistent with a depletion of CI-MPR from the TGN

in these cells, delivery of newly synthesized lysosomal enzymes to late endosomes/lysosomes was strongly inhibited. On the other hand, the transfected cells appeared to compensate for the inefficient delivery of lysosomal enzymes to lysosomes by upregulating their synthesis. Because confocal immunofluorescence microscopy indicated that the expression of Rab9 S21N did not significantly change the localization of CI-MPR, it was concluded that this mutant inhibits the budding of TGN-destined transport vesicles from late endosomes (Pfeffer, 1994; Riederer *et al.,* 1994), an interpretation similar to that made from the apparent inhibition of the formation of ER-derived vesicles upon expression of the equivalent Rab1 mutant (see Sections III,B,1 and III,C).

4. Rab3 Group GTPases Play a Central Role in Regulated Secretion

The Rab3 group of small GTPases consists of four members (a–d) sharing 77–85% amino acid sequence identity. Common to all four isoforms is that they are implicated in regulated secretion, although they operate in different cell types (see Section II,C,2). Functional studies have been carried out on Rab3a–c. In experiments with isolated nerve terminals (synaptosomes), Rab3a was shown to disappear from the synaptic vesicle membranes during Ca^{2+}-stimulated exocytosis (Fischer von Mollard *et al.,* 1991), unlike another GTPase found on synaptic vesicles, Rab5. When exocytosis was blocked with a clostridial neurotoxin that cleaves vesicle SNARE (v-SNARE) proteins, the dissociation of Rab3a from the membranes was inhibited (Stahl *et al.,* 1996). This indicates that the release of Rab3a is strictly coupled to membrane fusion, although it is still not clear if it is a prerequisite for or a result of the fusion event. The most likely explanation for the disappearance of Rab3a from the synaptic vesicle membranes is that it is removed by Rab–GDI, the recycling factor for Rab GTPases (see Section IV,B,1). Because GDI binds Rab GTPases in their GDP-bound form only, this implies that Rab3a must have hydrolyzed its GTP accompanying membrane fusion. In agreement with this interpretation, in synaptosomes Rab3a was found predominantly in its GTP-bound form, and incubation with α-latrotoxin, which stimulates neurotransmitter release, converted the GTPase to the GDP-bound form (Stahl *et al.,* 1994).

Surprisingly, mice homozygous for a null mutation of Rab3a were reported to be perfectly viable and behave normally (Geppert *et al.,* 1994). Moreover, most aspects of synaptic transmission were found to be normal in the Rab3a-deficient mice. The only anomality detected was a significant increase in synaptic depression after short pulses of repetitive nerve stimulation. The number of repeated stimuli after which the increased synaptic depression in the mutant mice becomes evident correlates with the point

when all the docked vesicles in resting nerve terminal have fused. Because the Rab3a-deficient phenotype is evident only after docked vesicles have been exhausted, Rab3a may thus play a role in the docking of synaptic vesicles on the plasma membrane. When the levels of synaptic proteins in the mutant mice were analyzed, it was observed that the level of the Rab3a effector, Rabphilin-3a, was decreased by 70%, whereas the levels of 20 other synaptic proteins were unchanged. Presumably, the lack of Rab3a leads to an increased degradation of Rabphilin-3a. In contrast to the studies with null mutant mice, membrane capacitance measurements indicated that neuroendocrine PC12 cells microinjected with Rab3a antisense oligonucleotides exhibited an increased ability to exocytose in response to repetitive stimulation (Johannes *et al.,* 1994). The reason for the apparent discrepancy between the data obtained with hippocampal slices from the knockout mice and the PC12 cells is not clear, but both of these studies imply that Rab3a is not essential for exocytosis.

In PC12 cells transiently transfected or microinjected with the GTPase-deficient Rab3a Q81L mutant, nicotinic agonist-stimulated growth hormone release and Ca^{2+}-dependent exocytosis were inhibited. In contrast, Rab3a T36N, which has a preferential affinity for GDP, was without effect (Johannes *et al.,* 1994; Holz *et al.,* 1994). Taken together with the data obtained with null mutant mice and antisense oligonucleotides, these results indicate that Rab3a in its GTP-bound form may inhibit exocytosis. Presumably, Rab3a–GTP functions as a fusion clamp that stabilizes a prefusion complex. Only upon GTP hydrolysis is the fusion reaction allowed to proceed. This model resembles that originally proposed for Rab function (Bourne, 1988), but differs from that proposed for certain other Rab GTPases, which are able to stimulate membrane fusion in the absence of GTP hydrolysis.

One possible explanation for the lack of phenotype upon the elimination of Rab3a is that another protein may share some of its functions. In fact, the less abundant Rab3c isoform partially colocalizes with Rab3a in the brain, and, like Rab3a, Rab3c is removed from synaptosome membranes upon the stimulation of exocytosis (Fischer von Mollard *et al.,* 1994a). Rab3a and Rab3c appear to be heterogeneously distributed between synapses, and analysis of Rab3a-deficient mice indicates that nerve terminals expressing Rab3c contain Rabphilin-3a, whereas this protein is absent from nerve terminals lacking both Rab3a and Rab3c (C. Li, *et al.,* 1994). Because Rabphilin-3a is likely to transmit (some of) the functions of Rab3a in membrane docking/fusion, it is thus possible that Rab3c can substitute for Rab3a in some synapses.

In contrast to Rab3a and Rab3c, Rab3b is mainly expressed in nonneuronal and nonneuroendocrine tissues and is particularly abundant in epithelial tissues, in which it localizes to the apical pole, close to tight junctions (see Sections II,C,2 and II,D,1). Thus, like its neuronal relatives, Rab3b

shows a polarized distribution, and it has been speculated that the epithelial junctional complex may share functional properties with nerve terminals (Weber *et al.,* 1994). When cell–cell contacts are disrupted by lowering the intracellular Ca^{2+} concentration, Rab3b redistributes from the cell periphery to a more cytoplasmic location. It is thus possible that Rab3b may function in the generation of epithelial cell polarity by targeting protein complexes to the junctional complex and the apical membrane domain (see Section III,E). On the other hand, it is tempting to speculate that Rab3b, like its neuronal counterparts, may function in secretion, and in this regard it is interesting to note that pathways of Ca^{2+}-regulated secretion have recently been identified even in fibroblasts (Coorssen *et al.,* 1996). It should be noted, however, that the region near the junctional complex where Rab3b localizes is normally not very abundant with secretory vesicles. That Rab3b does serve to regulate secretion at least in some cases was suggested by studies on anterior pituitary gland cells, in which Rab3b is the dominating Rab3 isoform: Rab3b antisense oligonucleotides introduced into rat pituitary cells by whole cell patch clamping were found to inhibit Ca^{2+}-dependent exocytosis (Lledo *et al.,* 1993). Thus, although Rab3a is dispensable for exocytosis in neurons, Rab3b appears to be required for the secretion in pituitary gland cells.

5. Rab8a Is Involved in Constitutive Exocytosis

Although mammalian Rab8a does not complement the lack of Sec4p in *S. cerevisiae,* it does complement the lack of *S. pombe* Ypt2p, which in turn is capable of substituting for Sec4p in *S.cerevisiae* (see Sections III,A,1 and III,A,3). Rab8a is therefore the likely mammalian homolog of Sec4p, which is involved in transport between the Golgi and the plasma membrane. Its intracellular localization (see Section II,D,1) is consistent with a role in TGN to plasma membrane transport. However, its preferential localization to the basolateral plasma membrane and basolateral transport vesicles indicates that, in polarized epithelial cells, Rab8a may be involved in the transport to this membrane domain only. This idea is supported by experiments employing permeabilized cell assays of polarized transport of the VSV-G and influenza HA glycoproteins. In these assays, a peptide derived from the hypervariable C terminus of Rab8a was found to inhibit transport of VSV-G to the basolateral plasma membrane but not that of HA to the apical side (Huber *et al.,* 1993b). In neurons, the axonal plasma membrane shows functional similarities with the apical membrane of epithelial cells, whereas the somatodendritic plasma membrane is regarded as an equivalent of the basolateral plasma membrane (Dotti and Simons, 1990). In accordance with this notion, Rab8a was found preferentially on the somatodendritic plasma membrane domain in polarized hippocampal neurons in cul-

ture, and antisense oligonucleotides against Rab8a inhibited the transport of a dendritically destined protein (Semliki Forest Virus glycoprotein E2) but not of an axonally targeted protein (HA) (Huber *et al.,* 1993a). Furthermore, the antisense oligonucleotides inhibited the *in vitro* maturation of neurons, and the number of vesicles undergoing anterograde transport was significantly reduced in the antisense-treated cells (Huber *et al.,* 1995). Surprisingly, Northern blotting experiments indicate that Rab8a is found only at low abundance in the brain, whereas an isoform with a highly divergent C terminus, Rab8b, is abundant in this tissue (Armstrong *et al.,* 1996). Because the antisense oligonucleotides in the Huber *et al.* (1995) study were directed against regions in which the two Rab isoforms are highly similar, it is possible that (some of) the observed effects in the antisense studies were due to the downregulation of Rab8b. This, however, does not change the view that Rab8a is involved in transport from the TGN to the basolateral/somatodendritic plasma membrane of polarized cells.

Rab8a is expressed in nonpolarized cells as well as in polarized ones, and its overexpression (or expression of a GTPase-deficient mutant) in fibroblasts leads to a surprising change in cell morphology (Peränen *et al.,* 1996): In the transfected cells, both actin filaments and microtubules reorganize to form plasma membrane processes that appear to contain Rab8a. VSV-G, a basolateral marker in polarized epithelial cells, is preferentially sorted to the actin-containing protrusions, whereas this is not the case with the apical marker, HA. These findings indicate that Rab8a is involved not only in the regulation of polarized membrane traffic but also that of the cytoskeletal organization. In this respect Rab8a may share functional similarity with members of the Rho subfamily of small GTPases. In fact, both Rab8a and Cdc42 (a Rho protein) have been shown to regulate neurite outgrowth during neuronal development (Huber *et al.,* 1995; Luo *et al.,* 1994). In this context, it is interesting to note that Rab8a, in its GTP-bound form, binds a protein kinase, Rab8ip (see Section IV,C,3); on the other hand, protein kinases have been implicated as effectors of the Rho GTPases (Leung *et al.,* 1995; Manser *et al.,* 1993, 1994). It is not known if Rab8a exerts its effects via Rab8ip or through, e.g., actin-binding proteins, but these functional studies clearly implicate Rab8a as a potential link between the basolateral trafficking machinery and the cytoskeleton.

6. Rab5 and Rab4 Regulate Early Endocytic Events

Several Rab proteins are localized to the early endocytic pathway (see Section II,D,2). Among these, the function of the ubiquitously expressed Rab4 and Rab5 proteins has been studied most extensively. Three Rab5 isoforms (a–c), sharing >87% sequence identity, have been isolated. The first clue about the function of Rab5a came from a system that measures the

homotypic fusion between early endosomes. When one endosome fraction containing internalized avidin is mixed with another one containing biotinylated horseradish peroxidase (HRP), fusion in this assay can be measured as the formation of avidin–biotin–HRP complexes. Such fusion requires ATP and cytosol and is strongly inhibited by antibodies against Rab5 (Gorvel *et al.,* 1991). Similarly, cytosol containing the Rab5a N133I mutant form (Gorvel *et al.,* 1991), which has a low affinity for guanine nucleotides, or Rab5a S34N (Stenmark *et al.,* 1994b), which preferentially binds GDP, inhibits early endosome fusion. In contrast, the addition of cytosol from cells overexpressing wild-type Rab5a (Gorvel *et al.,* 1991) or the GTPase-deficient Rab5a Q79L mutant (Stenmark *et al.,* 1994b) stimulates early endosome fusion. These results implicate Rab5a in the fusion between early endosomes, and the finding that a GTPase-deficient mutant stimulates fusion suggests that such fusion requires Rab5–GTP rather than Rab5a-catalyzed GTP hydrolysis. Rab5a thus seems to regulate fusion in a different manner than Rab3a, which appears to allow membrane fusion only after GTP hydrolysis (see Section III,B,4). This interpretation is strongly supported by elegant experiments employing Rab5a D136N, a mutant that binds and hydrolyzses XTP instead of GTP (Rybin *et al.,* 1996). XTP does not bind to endogenous cellular proteins, and the Rab5a D136N mutant can therefore be specifically labeled *in situ* with [α-^{32}P]XTP. Thus, only membranes containing Rab5a D136N bind [α-^{32}P]XTP in a time-dependent manner. Rab5a D136N was found to stimulate early endosome fusion *in vitro* in an XTP-dependent fashion. Interestingly, the slowly hydrolyzable analog, XTPγS, had an even stronger stimulatory effect than XTP, confirming that fusion does not require XTP (GTP) hydrolysis. Surprisingly, the rate of XTP hydrolysis by Rab5a D136N on the endosomal membranes is faster than that of early endosome fusion. This indicates that Rab5a undergoes futile cycles of GTP (XTP) binding and hydrolysis, uncoupled from fusion. Conceivably, Rab5a acts as a timer that sets the frequency of membrane docking/fusion events by promoting transient membrane interactions in its GTP-bound "active" form only. A high frequency of such contacts presumably results in fusion (Rybin *et al.,* 1996).

Even though cell-free assays of early endosome fusion have proved useful in identifying key molecular components of the endocytic pathway, it is not entirely clear how important homotypic early endosome fusion is *in vivo.* It is therefore important to also study the function of Rab5 in intact cells. Transfection experiments showed that overexpressed Rab5a increases the rate of fluid-phase and receptor-mediated endocytosis (Bucci *et al.,* 1992). Conversely, Rab5a N133I and Rab5a S34N were found to inhibit endocytosis (Bucci *et al.,* 1992; Stenmark *et al.,* 1994b). Rab5a Q79L stimulated endocytosis, like wild-type Rab5, but this mutant also caused inhibition of transferrin recycling from early endosomes, in contrast to the wild-

type protein (Stenmark *et al.*, 1994b). Endocytosis starts with the budding of vesicles from the plasma membrane. Does the stimulatory effect of Rab5a on endocytosis imply that Rab5a regulates such vesicle budding? Probably not, because the treatment of semi-intact cells with Rab–GDI, which extracts Rab GTPases from membranes, does not inhibit endocytosis (Lamaze *et al.*, 1996). The effect of Rab5a overexpression on endocytosis is more likely to be a consequence of an increased fusion between endocytic vesicles and early endosomes: An increased rate of such fusion in the presence of excess Rab5a may lead to the release of rate-limiting components needed for the formation of new endocytic vesicles (Bucci *et al.*, 1992). Involvement of Rab5a in increased endocytic membrane fusion even in intact cells is indicated by the observation that overexpression of Rab5a and, to an even greater extent, Rab5a Q79L, causes expansion of early endosomes (Bucci *et al.*, 1992; Stenmark *et al.*, 1994b). Such endosome expansion depends on intact microtubules (D'Arrigo *et al.*, 1997), and video microscopy shows that Rab5a Q79L overexpression leads to homotypic endosome fusion at the cell periphery and subsequent movement of endocytic structures toward the nucleus (Murphy *et al.*, 1996). In contrast, Rab5a S34N and Rab5a N133I cause an apparent fragmentation of early endosomes into small vesicles and tubules. Thus, there is a good correlation between the properties of Rab5a mutants in intact cells and in the early endosome fusion assay: Mutants that inhibit homotypic early endosome fusion *in vitro* induce the appearance of fragmented endosomes and an inhibition of endocytosis in intact cells, whereas Rab5 variants that stimulate endosome fusion cause an increased size of early endosomes and stimulate the rate of endocytosis. The function of the two other Rab5 isoforms, Rab5b and Rab5c, has not been studied in detail. However, the overexpression of wild-type or mutant versions of these molecules evokes morphological and biochemical effects similar to those of the equivalent forms of Rab5a (Bucci *et al.*, 1995).

Two Rab4 isoforms, Rab4a and -b, have been identified, but only Rab4a has been studied in functional terms. Even though Rab4a localizes to early endosomes, as does Rab5a (see Section II,D,2), its overexpression in stable CHO transfectants has consequences highly different from that of Rab5a: Fluid-phase endocytosis is decreased, and transferrin receptors are redistributed from endosomes to the plasma membrane. Furthermore, the discharge of iron from transferrin is prevented, apparently due to a mistargeting of internalized transferrin to a population of nonacidic tubules and tubule clusters. Similar, although less striking, results are obtained upon expression of Rab4a N121I (van der Sluijs *et al.*, 1992b). Therefore, although Rab5 regulates anterograde endocytic transport, Rab4a appears to regulate endocytic recycling. At least in some cell types (particularly well-defined in CHO cells), endocytic recycling occurs via a recycling endosome compart-

ment (RE) located close to the centriole (Fig. 1). It is possible that part of the recycling may occur directly from early (sorting) endosomes to the plasma membrane, whereas some occurs via the RE. Interestingly, Rab4a is not found on the RE, in contrast to Rab11 and the v-SNARE cellubrevin (Daro *et al.*, 1996; Ullrich *et al.*, 1996). It is still possible that Rab4a may regulate the transport to this compartment, without accumulating on it; more likely, however, it regulates transport occurring directly between the sorting early endosome and the plasma membrane (Daro *et al.*, 1996).

7. Rab11 Is Involved in the Function of Recycling Endosomes

The intracellular localization of Rab11 has been examined in several cell types (see Section II,D,1), but its function has so far been studied only in CHO and BHK cells (Ullrich *et al.*, 1996). In these cells, Rab11 is mainly localized to the pericentriolar recycling endosome compartment, but it also partially colocalizes with the early endosomal GTPase Rab5. The expression of Rab11 S25N does not affect endocytosis, but the transport of internalized transferrin from the RE to the plasma membrane is inhibited. Furthermore, the expression of this Rab11 mutant leads to a scattering of the RE into small vesicles and tubules. In contrast, expression of the GTPase-deficient Rab11 Q70L mutant leads to a compacting of the RE, but this mutant also inhibits transferrin recycling. These results are most consistent with a role of Rab11 in the transport from (sorting) early endosomes to the RE. The phenotype of cells expressing Rab11 S25N might thus result from an inefficient docking of early endosome-derived vesicles on the RE. It has been suggested that the moderate reduction in transferrin recycling observed in cells expressing Rab11 Q70L may be due to a shift in recycling from a short (early endosome to plasma membrane) to a long (early endosome to RE to plasma membrane) route (Ullrich *et al.*, 1996). In support of this model, expression of Rab5 Q79L, which traps endocytosed transferrin in expanded (sorting) early endosomes, prevents transport of transferrin to the Rab11-positive compartment, showing that Rab5 acts before Rab11 in the endocytic pathway. Altogether, this suggests the following sequential action of Rab GTPases in the endocytic pathway: Rab5 regulates transport from the plasma membrane to sorting early endosomes; Rab4 regulates the "short" recycling route from sorting early endosomes to the plasma membrane; Rab11 regulates the "long" recycling route from early endosomes to the plasma membrane via the RE; and conceivably, a fourth Rab may regulate the transport between the RE and the plasma membrane.

8. Function of Rab7 in the Late Endocytic Pathway

Like Rab9, Rab7 is specifically associated with late endosomes (see Section II,D,2). However, there is no evidence that Rab7 would regulate mem-

brane traffic between late endosomes and the TGN. Instead, this GTPase appears to regulate membrane traffic between early and late endosomes and/or between late endosomes and lysosomes (Feng *et al.*, 1995; Meresse *et al.*, 1995). In cells transfected with the inhibitory Rab7 N125I or Rab7 T22N mutants, internalized VSV-G appeared to be trapped in early endocytic (transferrin receptor positive) compartments. Furthermore, overexpression of these mutants partially inhibited the cleavage of paramyxovirus SV5 hemagglutinin neuraminidase, a process believed to take place in late endosomes (Feng *et al.*, 1995). These experiments thus argue for a role for Rab7 in early to late endosomal trafficking. On the other hand, the yeast homolog of Rab7, Ypt7p, regulates the transport between endosomes and the lysosome-like vacuole, as well as the homotypic fusion between vacuoles (see Section III,A,2), and immunofluorescence microscopy and subcellular fractionation indicate that a GTPase-deficient Rab7 mutant, Rab7 Q67L, is partially localized to lysosomes (Meresse *et al.*, 1995). Like Rab1 and Rab6, Rab7 may thus regulate several distinct transport steps, one occurring between early and late endosomes and the other between late endosomes and lysosomes.

C. Are Rab Proteins also Involved in the Formation of Transport Vesicles?

Multiple evidence implicates Rab proteins as regulators of membrane docking or fusion (see Sections III,A and III,B), whereas the small ARF and Sar GTPases are known to play central roles in the formation of transport vesicles (Donaldson and Klausner, 1994; Schekman and Orci, 1996; Rothman, 1996). In general, the lack of a specific Rab function in yeast leads to the cytoplasmic accumulation of more or less well-defined vesicles, indicating that vesicle docking is inhibited. Furthermore, Ypt7p, Rab5, and Rab6 have been shown to be required for membrane fusion in cell-free assays, and the lack of Rab3a is associated with an inefficient recruitment of synaptic vesicles to the presynaptic terminal. On the other hand, the incubation of permeabilized cells with Rab–GDI, which efficiently removes Rab GTPases from membranes, does not affect the budding of clathrin-coated vesicles, indicating that Rabs are not involved in this process (Lamaze *et al.*, 1996). However, some reports do argue for an involvement of Rab proteins in vesicle budding. First, yeast cells lacking Ypt31p/Ypt32p function fail to accumulate vesicles, but instead accumulate enlarged Golgi-like cisternae (Benli *et al.*, 1996). Howell and co-workers (Jones *et al.*, 1993) have established an assay that reconstitutes vesicle budding from the Golgi. Here, a stacked Golgi fraction is immobilized on magnetic beads and the vesicles formed in the presence of cytosol are analyzed. In this assay,

an antiserum against Rab6 was found to reduce vesicle formation to the background level, thus implicating Rab6 in budding from the Golgi or the TGN (Jones *et al.*, 1993). In two further studies, the GDP-bound Rab mutants, Rab1a S25N and Rab9 S21N, were found to inhibit budding from the ER and late endosomes, respectively (Nuoffer *et al.*, 1994; Riederer *et al.*, 1994), as evidenced by immunofluorescence microscopy of cargo proteins, which apparently became trapped in the donor compartment in the presence of the Rab mutants. The result with the Rab1a mutant is perhaps most surprising because the yeast homolog of Rab1a, Ypt1p, does not seem to be required for budding. Antibodies against Ypt1p inhibit ER–Golgi transport without inhibiting vesicle formation, and a temperature-sensitive *ypt1* mutant shows an accumulation of vesicles, indicating that vesicle budding is allowed in the absence of Ypt1p function (see Section III,A,1). Moreover, Rab1a is almost completely absent from the ER at least in some cell types (Saraste *et al.*, 1995), suggesting that membrane recruitment of Rab1 is a post-ER event. Altogether, the evidence for Rab function in vesicle budding is much more circumstantial than that implying a role in docking/fusion, but it is possible that some Rab proteins do function at this stage of the transport process.

D. Rab Proteins and Homotypic Membrane Fusion

Although the intracellular membrane transport events involve the fusion of two membranes with distinct compositions (heterotypic fusion), fusion between "like" membranes (homotypic fusion) does occur. For instance, endosomes are capable of fusing with similar endosomes and lysosomes with each other, and both ER and Golgi fragments undergo homotypic fusion as these organelles reassemble during the telophase of mitosis. Apart from the organelle reassembly after mitosis, homotypic fusion has been postulated to compensate for the loss of membrane upon vesicle budding (Rothman and Warren, 1994). With few exceptions, homotypic fusion is generally dependent on the SNARE and Rab proteins, and the mechanism of homotypic membrane fusion is probably similar to that occurring between transport vesicles and their cognate target membranes (Rothman and Warren, 1994). In yeast, an *in vitro* assay that reconstitutes the homotypic fusion between vacuoles has been established (Conradt *et al.*, 1994). In intact yeast cells, such fusion occurs during the late stage of vacuole inheritance, when vesicles derived from the mother vacuole fuse in the bud tip. Vacuole fusion *in vitro* is dependent on ATP, cytosol, and the NSF/SNAP homologs and is sensitive to GTPγS. The latter requirement indicates a role for a GTPase in this reaction. Indeed, removal of Ypt7p from vacuolar membranes with the yeast GDI homolog, Gdi1, abolishes vacuole fusion,

and so does treatment with anti-Ypt7p antibodies (Haas *et al.,* 1995). The requirement of Ypt7p for vacuole fusion *in vitro* is coherent with the fact that *ypt7* null mutants contain highly fragmented vacuoles (Wichmann *et al.,* 1992; Haas *et al.,* 1995). Importantly, vacuoles from *ypt7* null mutant cells do not fuse with those of wild-type cells (Haas *et al.,* 1995). This shows that Ypt7p is required on *both* membranes for homotypic fusion to occur, and the presence of the same Rab protein on both membranes may turn out to be a general requirement in Rab-dependent homotypic fusion. Furthermore, this result raises the possiblity that a given Rab GTPase could be required on both membranes even in heterotypic fusion events.

In mammalian cells, the requirement of Rab5 for homotypic fusion between early endosomes is well documented (Gorvel *et al.,* 1991; G. Li, *et al.,* 1994). Like other intracellular fusion events, homotypic early endosome fusion is ATP and cytosol dependent. It requires NSF, implying that the SNARE model of membrane fusion also applies to homotypic early endosome fusion (Colombo *et al.,* 1996). The fusion is strongly inhibited by anti-Rab5 antibodies and by dominant-negative Rab5 mutants, whereas it is stimulated by wild-type Rab5 and by a GTPase-deficient Rab5 mutant (see Section III,B,6). In agreement with this, cells expressing inhibitory Rab5 mutants contain fragmented early endosomes, whereas cells overexpressing wild-type or GTPase-deficient Rab5 contain abnormally large early endosomes. This effect is particularly prominent in cells expressing the GTPase-deficient Rab5 Q79L mutant, and by video microscopy it is possible to appreciate how this mutant protein enhances the fusion between endocytic structures of intact cells (Murphy *et al.,* 1996). In the case of Rab5, a cytosolic downstream effector protein, Rabaptin-5, has been identified (see Section IV,C,2), and immunodepletion of Rabaptin-5 from cytosol strongly inhibits Rab5-dependent membrane fusion (Stenmark *et al.,* 1995). With both the Rab and its effector at hand, it should now be possible to study in more detail the mechanism of homotypic early endosome fusion. One major task in the future is the identification of SNAREs involved in this process and the linkage of Rab5 function with these proteins.

E. Rab Proteins and Cell Polarity

Many cell types in the body display a polarized organization. The plasma membrane of epithelial cells is divided into an apical (facing the exterior) and a basolateral (facing the basement membrane and the blood supply) domain. These two domains are separated by tight junctions, which also function to form an impermeable connection between neighboring cells in the epithelial cell sheet. Analogously to epithelial cells, neurons are also polarized. In many respects, their axonal plasma membrane resembles the

apical one of epithelial cells, whereas their somatodendritic plasma membrane corresponds to the basolateral one (Dotti and Simons, 1990). The existence of functionally distinct plasma membrane domains complicates the pattern of intracellular traffic: Polarized cells target membrane proteins and lipids to the distinct apical and basolateral plasma membrane domains, secrete proteins in a polarized manner, and transcytose material from one plasma membrane domain to the other (Rodriguez-Boulan and Powell, 1992; Matter and Mellman, 1994; Mostov, 1995). Given their putative role in the specificity of intracellular trafficking, Rab proteins have been considered candidates for molecules that could distinguish between apical and basolateral transport pathways (Simons and Zerial, 1993). For example, Rab3a functions in neurons in the axonal nerve terminals (see Section III,B,4). Moreover, Rab8a has been found to regulate transport between the TGN and the somatodendritic plasma membrane domain in neurons without affecting apical or axonal trafficking. In epithelial cells, this protein is involved in traffic between the TGN and the basolateral plasma membrane (see Section III,B,5). The ability to distinguish between the two membrane domains of polarized cells is, however, not universally shared among Rab GTPases. This is illustrated by the findings that Rab5a regulates both apical and basolateral endocytosis in epithelial cells (Bucci *et al.,* 1994) and both axonal and somatodendritic endocytosis in neurons (de Hoop *et al.,* 1994). When overexpressed in fibroblasts, Rab8 affects not only intracellular traffic in a "polarized" fashion but also alters the distribution of microtubules and actin filaments (see Section III,B,5). Rab8 could possibly regulate intracellular traffic to polarized domains of the plasma membrane by recruiting actin- or microtubule-binding proteins to the membrane in a GTP-dependent manner (Peränen *et al.,* 1996).

The only epithelial-specific Rab GTPase identified to date is Rab17 (Lütcke et al., 1993). The function of this GTPase is not known, but its localization in kidney tubule epithelia to the basolateral plasma membrane and apical dense tubules has suggested that it may play a role in transcytosis, the transport between the apical and basolateral membrane domains. In the developing kidney, Rab17 is absent from the mesenchymal precursors, but its expression is induced during their differentiation into epithelial cells. Thus, it is possible that Rab17 participates in the generation of epithelial polarity, although there may be other reasons for the temporal correlation between epithelialization and Rab17 expression. Furthermore, Rab3b is predominantly found in epithelial cells, although this protein is also present in neurons, neuroendocrine cells, and platelets. In cultured epithelial cells, Rab3b is localized to the apical pole, close to tight junctions, and a reduction in the intracellular Ca^{2+} concentration leads to a redistribution of Rab3b. Its localization in polarized epithelial cells suggests that Rab3b may regulate apical or junctional protein traffic (Weber *et al.,* 1994). It might play a role

in apical secretion because the inhibition of Rab3b expression inhibits the Ca^{2+}-stimulated exocytosis in anterior pituitary cells (see Section III,B,4). Similarly to Rab3b, Rab13 also localizes in the tight junction region of epithelia (Zahraoui *et al.,* 1994). It colocalizes with the tight junction marker ZO-1 and, like Rab3b, is redistributed to cytoplasmic vesicles when tight junctions are disassembled at low Ca^{2+} concentrations. It has been speculated that Rab13 may participate in formation of tight junctions by being involved in the targeting of integral membrane proteins to the junctional area (Zahraoui *et al.,* 1994).

To date, it has been puzzling that certain Rab proteins, such as Rab8a, are found basolaterally in epithelial cells, whereas others, such as Rab11, Rab18, and Rab20, show a mainly apical distribution in these cells, and yet all these Rabs are also expressed in nonpolarized cells (Lütcke *et al.,* 1994; Goldenring *et al.,* 1996). A possible explanation to this apparent paradox has emerged: It was discovered that even *bona fide* nonpolarized cells, such as BHK and CHO cells, contain cognate "apical" and "basolateral" transport routes for proteins exported from the TGN (Yoshimori *et al.,* 1996). This means that nonpolarized cells contain more complex patterns of intracellular transport routes than previously surmised and may explain why so many distinct Rab GTPases are expressed in even these cells.

IV. Membrane Association and GTPase Cycle of Rab Proteins

A. Posttranslational Modifications and Membrane Association of the Rab GTPases

1. Isoprenylation of Rab C Termini

The reversible association of Rab GTPases with specific membranes is essential for their function. Thus, it has been shown that Rabs permanently attached to membranes by transmembrane anchors show reduced ability to support intracellular transport (Ossig *et al.,* 1995). How is the reversible binding accomplished? All Rab proteins contain one or two cysteine residues near their C termini. Like the cysteine in the C-terminal "CAAX box" of Ras, these residues are subject to isoprenylation,which is required for the membrane association and function of Rab GTPases (Walworth *et al.,* 1989; Chavrier *et al.,* 1990a; Gorvel *et al.,* 1991; Johnston *et al.,* 1991; Khosravi-Far *et al.,* 1991; Peter *et al.,* 1992; Kinsella and Maltese, 1991). The C-terminal cysteine residue of Rab proteins terminating in

CXC is additionally carboxyl methylated, but this modification is not essential for their membrane association (Farnsworth *et al.,* 1991; C. Newman, *et al.,* 1992; Musha *et al.,* 1992; Smeland *et al.,* 1994). The enzyme responsible for the isoprenylation reaction is called Rab geranylgeranyl transferase (GGTase), and it attaches 20 carbon geranylgeranyl groups to C-terminal cysteines in a sequential manner (Shen and Seabra, 1996). The Rab GGTase consists of two tightly bound chains, α (60 kDa) and β (38 kDa), both of which are related to those of the farnesyl transferase that modifies Ras (Andres *et al.,* 1993). However, whereas the C-terminal CAAX motif of Ras is sufficient to specify its prenylation by farnesyl transferase, the C-terminal cysteines of Rab proteins are not recognized as such by the Rab GGTase. Also, upstream regions are needed for Rab isoprenylation, and this process requires a 73-kDa accessory protein called Rab escort protein (REP; Seabra *et al.,* 1992a,b; Andres *et al.,* 1993; Cremers *et al.,* 1994) in addition to the GGTase. Two related REPs, REP-1 and REP-2, have been identified to date, and mutations in REP-1 have been found to give rise to choroideremia, a retinal degeneration disease (Seabra *et al.,* 1993). *In vitro,* REP-2 can assist in the prenylation of most Rab proteins as efficiently as REP-1. An exception is Rab27, which is prenylated with a threefold higher efficiency in the presence of REP-1 than REP-2. Rab27 is expressed in the retinal cell layers that are first degenerated during choroideremia, and it is possibly the inefficient geranylgeranylation of this Rab (due to a malfunctioning of REP-1) that causes the disease (Seabra *et al.,* 1995).

What is the precise role of REP in the isoprenylation reaction? This protein shares sequence similarity with GDP dissociation inhibitor (GDI; see Section IV,B,1), a protein that binds preferentially to the GDP form of Rab GTPases and inhibits GDP release under low Mg^{2+} conditions. REP shares the ability of GDI to recognize the GDP-bound form and inhibit GDP release from Rab proteins (Alexandrov *et al.,* 1994; Seabra, 1996). In contrast to GDI, REP can bind to unprenylated Rab proteins, and the prenylation of a Rab begins with formation of a complex with REP (Fig. 4). This complex is subsequently recognized by the Rab GGTase, which attaches geranylgeranyl groups to the C-terminal cysteines via thioether bonds. Most Rabs contain two C-terminal cysteines and are double geranylgeranylated. Mutational studies indicate that the N-terminal cysteine is isoprenylated first, and the monogeranylgeranylated protein remains stably associated (resistant to removal by detergents or phospholipids) with REP, thus allowing a second round of geranylgeranylation by the GGTase (Shen and Seabra, 1996). It appears that the prenylation leads to a shift in the stoichiometry of the REP–Rab complex from 1:1 to 2:1 or 2:2 (Shen and Seabra, 1996). There does not appear to be a stable complex formed between the REP–Rab and the GGTase, and prenylation also occurs effi-

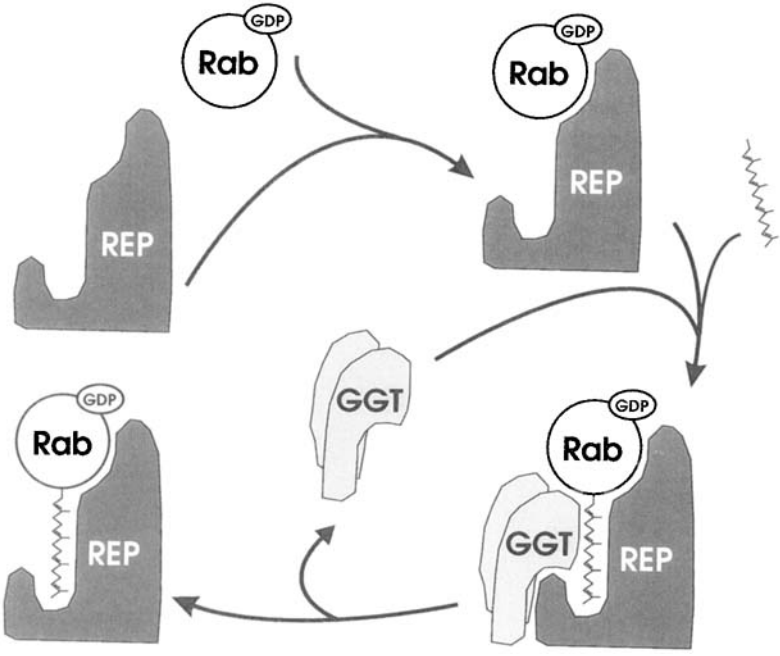

FIG. 4 Isoprenylation of a Rab protein. The newly synthesized GTPase (in its GDP form) is bound by the Rab escort protein, REP, which introduces it to the Rab geranylgeranyl transferase (GGT). This enzyme attaches one or two geranylgeranyl groups on C-terminal cysteine residues of the GTPase. After isoprenylation, the Rab remains associated with REP.

ciently when the GGTase is present at substoichiometric amounts. The double geranylgeranylated Rab protein also remains stably complexed to REP (Alexandrov *et al.,* 1994; Seabra, 1996), and the REP–Rab complex is subsequently targeted to specific membranes (Alexandrov *et al.,* 1994). Here, the complex is first bound to (unknown) receptor molecules, REP is then released, and the Rab protein becomes converted from its GDP-bound form to the GTP-bound form through the action of a guanine nucleotide exchange factor (GEF, see Section IV,B,2). The association of REP–Rab with membranes is very similar to that of GDI–Rab (see Section IV,B,1; Fig. 5A); it has been speculated that GDI may capture the Rab from the REP–Rab complex immediately after prenylation, and that it is actually GDI that serves to deliver newly prenylated Rab GTPases to membranes. In support of this view, GDI forms a complex with Rab5 isoprenylated in a reticulocyte lysate system (Sanford *et al.,* 1995b). However, in such a system, plenty of time is allowed for GDI to capture the

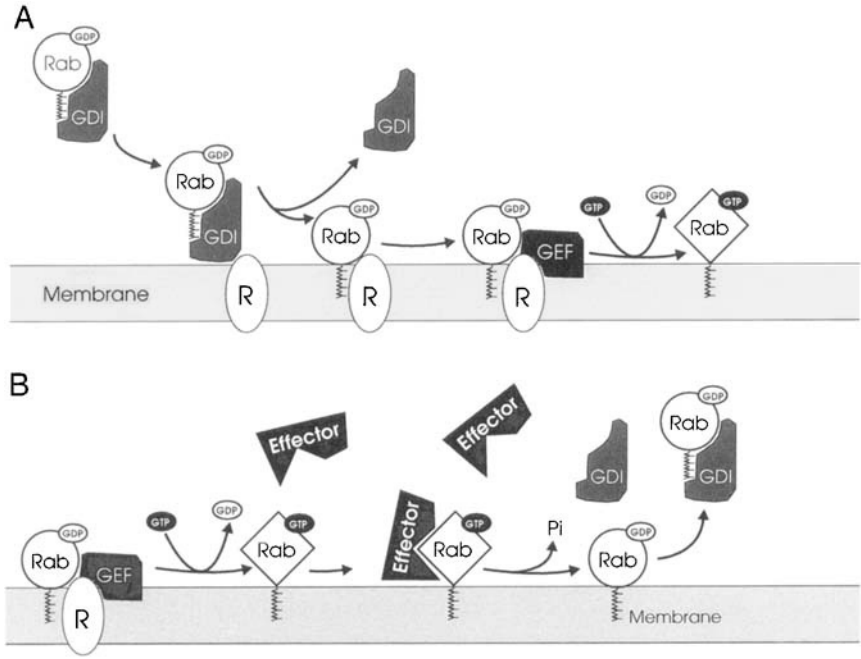

FIG. 5 (A) The membrane association and activation of a Rab GTPase. In the cytosol, a GDP-bound Rab is found as a soluble complex with the GDP dissociation inhibitor, GDI (or in the case of a newly synthesized Rab, with REP). This protein is capable of presenting a Rab to a specific membrane. The Rab–GDI complex binds to a receptor (R), and GDI is subsequently released. Thereafter, the bound GDP is exchanged for GTP in a reaction catalyzed by a guanine nucleotide exchange factor (GEF). It is not known if the receptor and the GEF are identical. (B) Membrane recruitment of a cytosolic effector protein by the activated Rab. The GTP-bound form of a Rab recruits a cytosolic effector to the membrane, thus facilitating a downstream docking/fusion event. The effector remains bound until GTP is hydrolyzed in a reaction catalyzed by a GTPase activating protein. The resulting Rab–GDP is subsequently translocated to the cytosol by GDI and can now undergo a new round of membrane association (see A).

Rab protein from the REP–Rab complex, whereas in cells, prenylated proteins rapidly associate with membranes (Ullrich *et al.*, 1994; Soldati *et al.*, 1994). Furthermore, a Rab1b mutant incapable of interacting with GDI exhibits efficient isoprenylation and membrane association, indicating that GDI is not required for these processes (Wilson *et al.*, 1996). REP is therefore most likely responsible for the first targeting of the newly isoprenylated Rab to membranes, whereas GDI serves as a recycling factor that allows the Rab to perform multiple cycles between membranes and cytosol (see Section IV,B,1).

2. Phosphorylation

A number of Rab proteins, including Rab1a, Rab4a, Rab3b, Rab6, and Rab8a, are phosphorylated under specific conditions (Bailly *et al.*, 1991; van der Sluijs *et al.*, 1992a; Karniguian *et al.*, 1993). Most strikingly, Rab1a and Rab4a are phosphorylated during mitosis by $p34^{cdc2}$ kinase (Bailly *et al.*, 1991). The phosphorylation of these proteins occurs at serine/threonine residues located in their hypervariable C termini, which are probably involved in their targeting to specific membranes (see Section II,A,3). Interestingly, the subcellular distribution of Rab1a and Rab4a changes during mitosis: Rab1a appears to translocate from the cytosol to membranes, whereas Rab4b redistributes from membranes to cytosol (Bailly *et al.*, 1991). A mutation of Ser196 within the consensus recognition site for $p34^{cdc2}$ kinase in Rab4a (Ser196-Pro-Arg-Arg) to glutamine prevented its phosphorylation during mitosis and also its translocation to the cytosol (van der Sluijs *et al.*, 1992a), demonstrating that the phosphorylation indeed regulates the subcellular distribution of Rab4a. The exact mechanism of the phosphorylation-induced translocation of Rab4a during mitosis is not known, but neither geranylgeranylation nor C-terminal carboxymethylation is affected. Because geranylgeranylated Rab proteins can be removed from membranes by GDI (see Section IV,B,1), it is reasonable to assume that this protein is involved in the cytosolic translocation of Rab4a. One possibility would be that phosphorylation of Rab4a by $p34^{cdc2}$ may contribute to its conversion to the GDP-bound state, which is preferentially recognized by GDI. Another alternative is that the phosphorylation may prevent binding of Rab4a to membrane receptors. Apart from being redistributed to the cytosol during mitosis, Rab4a has also been found to translocate to the cytosol upon treatment of cells with okadaic acid (a phosphatase inhibitor) or insulin (Cormont *et al.*, 1993, 1994). Insulin stimulation activates the protein kinase ERK1, which is able to phosphorylate Rab4a *in vitro,* probably at the same serine residue as that phosphorylated by $p34^{cdc2}$ kinase. Also, the membrane association of other Rab proteins appears to be regulated by phosphorylation: In neutrophils, treatment with PMA, a stimulator of protein kinase C and an activator of this cell type, leads to the translocation of Rab5a from cytosol to membranes (Vita *et al.*, 1996).

It is well established that both endocytic and biosynthetic membrane traffic ceases during mitosis (Warren, 1993). The phosphorylation of Rab proteins, such as Rab1a and Rab4a, by $p34^{cdc2}$ kinase could be one mechanism to modulate membrane traffic during cell division. During interphase, the phosphorylation of Rab proteins by ERK1 and other growth factor-regulated kinases may provide a means of regulating intracellular membrane traffic as a response to external stimuli. Integrating membrane receptor signaling with intracellular traffic remains an important challenge to

current cell biology, and the study of Rab proteins in this context promises to yield clarifying results.

B. Auxiliary Factors Regulating Rab Membrane Association and GTPase Cycle

1. GDP Dissociation Inhibitors

Rab GDP dissociation inhibitors constitute a small family consisting of at least three highly related proteins (Pfeffer *et al.,* 1995). Functional differences between the GDI isoforms have not yet been detected, but to date most studies have been carried out on GDI-α. This protein was originally isolated from bovine brain cytosol as a factor inhibiting the release of GDP from Rab3a (Sasaki *et al.,* 1990). Subsequently, it was realized that GDI-α has the ability to regulate the membrane association of Rab3a (Araki *et al.,* 1990) as well as that of all other Rab proteins tested (Ullrich *et al.,* 1993). This is probably the most important biological function of GDI because the rate of GDP release from Rab proteins is slow at physiological Mg^{2+} concentrations. GDI-α shows a strong preference for the GDP-bound form of Rab proteins, and its interactions with the GTPases require their C-terminal geranylgeranylation (Sasaki *et al.,* 1990). The farnesyl group does not appear to be able to substitute for geranylgeranyl groups in Rab–GDI interactions (Ullrich *et al.,* 1993). Addition of excess GDI-α leads to the removal of Rab proteins from internal membranes (Ullrich *et al.,* 1993; Soldati *et al.,* 1993), and in cytosol GDI can be found complexed to a number of Rab proteins (Regazzi *et al.,* 1992). Although the K_D for the complex of GDI-α and prenylated, GDP-bound Rab9 (Shapiro and Pfeffer, 1995) is in the low nanomolar range (increasing in the presence of detergent), the cytosolic concentration of GDI-α has been estimated to be 1.2 μM in MDCK cells (Ullrich *et al.,* 1993) and 0.17 μM in CHO cells (Shapiro and Pfeffer, 1995). This explains why cytosolic, isoprenylated Rab proteins are found almost exclusively complexed with GDI (Regazzi *et al.,* 1992). According to the current view, GDI serves to remove GDP-bound Rabs from membranes and thereby acts as a recycling factor (Fig. 5B). In fact, in the absence of GDI, isoprenylated Rab GTPases are hydrophobic and tend to stick unspecifically to various surfaces (Araki *et al.,* 1990). The essential role of GDI is illustrated by the fact that yeast cells lacking the GDI homolog Gdi1p fail to grow and display multiple defects in intracellular transport. Moreover, *GDI1* is allelic to *sec19-1,* a temperature-sensitive mutant that exhibits a block in both biosynthetic and endocytic membrane traffic at the restrictive temperature (Garrett *et al.,* 1994).

The crystal structure of GDI-α has been determined (Schalk *et al.*, 1996). It shows a two-domain structure with a large complex multisheet domain I and a smaller α-helical domain II. Together, these two major domains form a "V" structure. Unexpectedly, the organization of domain I is related to that of FAD-containing oxidases and monooxygenases. GDI-α does not, however, appear to bind FAD, and the significance of its similarity to FAD-containing enzymes remains enigmatic. The two most conserved regions, located at the apex of the V, are involved in Rab binding because mutations in critical residues here impair the binding (Schalk *et al.*, 1996). These regions also show similarity with REP (see Section IV,A,1), a protein with many of the same properties as those of GDI, indicating that these proteins interact with Rab proteins in a similar fashion. The preferential binding of GDI to the GDP-bound form of Rab proteins implies that it must recognize regions involved in nucleotide-dependent conformational changes, and mutagenesis studies suggest that GDI-α interacts with the "effector" loop of Rab3a (Schalk *et al.*, 1996).

Because Rab proteins are found complexed with GDI in the cytosol, one might expect that they are also delivered to specific membranes as GDI complexes (Fig. 5A). Indeed, such membrane delivery has been demonstrated in the cases of Rab5–GDI and Rab9–GDI (Ullrich *et al.*, 1994; Soldati *et al.*, 1994). These complexes are targeted to membranes enriched in early and late endosomes, respectively, and transiently associate with these membranes. Subsequently, GDI is released, and the Rab protein is converted from its GDP form to the GTP form through nucleotide exchange (Fig. 5A). Both the rate and the extent of the association of Rab proteins with membranes are saturable, indicating the presence of membrane receptors that recognize the Rab–GDI complex. The fact that different Rab GTPases are recruited to distinct membranes indicates the presence of specific receptors, and even two Rab proteins recruited to the same organelle appear to use distinct receptors (Soldati *et al.*, 1995). The receptor could be identical to or associated with a guanine nucleotide exchange factor (GEF) that catalyzes nucleotide exchange (see Section IV,B,2). Based on kinetic differences in nucleotide exchange between membrane-associating and free Rab9 it has also been speculated that the membrane recruitment of Rabs may involve a GDI displacement factor that would accelerate the rate of GDI release upon membrane binding (Soldati *et al.*, 1994). The membrane association of Rab5–GDI and Rab9–GDI occurs in the absence of cytosol, indicating that GDI is the only cytosolic factor required for the process. Which part of the Rab–GDI complex is recognized by the membrane receptor? Clearly, the Rab portion must be recognized in order to give specificity, but also GDI seems essential for the specific targeting: Delipidated albumin can substitute for GDI in the solubilization of isoprenylated Rab proteins, but, unlike Rab–GDI complexes, Rab–albumin

complexes associate with membranes in a nonspecific manner (Dirac-Svejstrup *et al.,* 1994).

If GDI serves both in the delivery to and capture of Rab proteins from membranes, what prevents the immediate membrane reassociation of a Rab that has just been taken off the membrane by GDI? One clue may come from the observation that cytosolic GDI is phosphorylated, whereas the small pool of GDI that is membrane associated appears to be unphosphorylated (Steele-Mortimer *et al.,* 1993). Thus, it is possible that phosphorylation of GDI upon retrieval of the Rab from the membrane may keep the Rab–GDI complex cytosolic. The phosphorylation of Rho GDI stabilizes its association with RhoA (Bourmeyster and Vignais, 1996), and perhaps complexes between Rab GDI and Rab GTPases are stabilized in a similar manner. Because GDI release appears to precede the stable association of Rab proteins with membranes, a stabilization of the Rab–GDI complex by phosphorylation may contribute to keeping the proteins cytosolic.

2. Guanine Nucleotide Exchange Factors

As evident from Section III, the GDP/GTP cycle is essential for the function of Rab GTPases in membrane traffic. At least in the cases of Rab5 and Rab9, membrane association of the Rab protein is accompanied by the exchange of GDP with GTP (see Section IV,B,1; Fig. 5A). Most Rab GTPases exchange bound GDP for GTP only very slowly *in vitro,* but the exchange rates are significantly accelerated by cellular proteins called GEFs. The following two functional mechanisms have been proposed for the GEFs: (i) They may function by stimulating GDP release, thus allowing binding of GTP, which is typically present in cytosol at a 20-fold excess over GDP; and (ii) GEFs may stabilize the intermediate nucleotide-free state, thus allowing GTP to enter (Quilliam *et al.,* 1995). Three Rab GEFs have been molecularly identified to date. Dss4p was identified as a dominant suppressor of *sec4-8* and was found to possess GEF activity on Sec4p (Moya *et al.,* 1993). Subsequently, a mammalian suppressor of *dss4,* Mss4, was identified (Burton *et al.,* 1993). Mss4 is a small cytosolic protein with local sequence similarities to Dss4p but not to the GEFs of other small GTPases. Like Dss4p, it aids Sec4p function when expressed in yeast. In gel overlay experiments, Mss4 was found to interact not only with Sec4p but also with Ypt1p, Rab1a, Rab3a, Rab8, and Rab10. On the other hand, Mss4 did not interact with Rab2, Rab4a, Rab5, Rab6, Rab9, or Rab11 (Burton *et al.,* 1993, 1994; Miyazaki *et al.,* 1994). It is interesting that all the Rab proteins interacting with Mss4 function in the exocytic pathway, and microinjection of the Mss4 protein into squid giant nerve terminals led to an enhancement of neurotransmitter release. Mss4 may thus play a role in the regulation of a specific subset of Rab proteins acting along the secretory pathway. It

binds a Zn^{2+} ion (Yu and Schreiber, 1995a), and its structure has been solved by multidimensional NMR (Yu and Schreiber, 1995b). Mutations in one of its Zn^{2+}-binding loops inhibit the GEF activity. This region is conserved between Mss4 and Dss4 and may represent the Rab-interacting interface of Mss4 (Yu and Schreiber, 1995b). Mss4 stimulates GDP release of those proteins it interacts with in gel overlay experiments, but the stimulation is weak compared with that evoked by other GEFs on their substrate GTPases. Thus, at an 8-fold molar excess over Rab3a, Mss4 only stimulates GDP release 6-fold (Burton *et al.*, 1993). Mss4 binds both isoprenylated and nonisoprenylated proteins, but its GEF activity has only been investigated with the latter. The stimulation of GDP/GTP exchange on Rab GTPases by Mss4 under physiological conditions remains to be determined.

One of the largest proteins known to date, p619, contains a region with similarity to RCC1, a GEF for the small GTPase Ran. p619 is localized to the Golgi apparatus and cytosol, and its RCC1-like region possesses GEF activity on Arf1 (Rosa *et al.*, 1996). Surprisingly, it also stimulates the release of GDP (but not of Ran and TC21) from Rab3a and Rab5, suggesting that p619 may function as a GEF for a number of GTPases. However, its potential role in Rab function has not been investigated.

Although the Rab GEFs that have been cloned show a limited specificity, seemingly more specific GEFs have been partially purified. Rab3a GEF (not active on Rab2, Rab5, Rab11, or Ras) is a cytosolic protein of approximately 300 kDa (Burstein and Macara, 1992; Miyazaki *et al.*, 1994), whereas clathrin-coated vesicle membranes contain an exchange activity for Rab5, which does not act on Rab7 (Soldati *et al.*, 1994). The Rab3a GEF is most active on isoprenylated Rab3a, whereas the Rab5 GEF stimulates GDP release equally well from isoprenylated or nonisoprenylated Rab5. However, maximal stimulation of GDP dissociation requires the presence of a low concentration of GDI, suggesting that the Rab5 GEF recognizes the Rab5–GDI complex. This is consistent with the finding that Rab5 associates with membranes as a complex with GDI, and that this association is accompanied by nucleotide exchange.

In summary, a number of proteins with highly different properties possess Rab GEF activity. Their importance in Rab function will only become clear when the purified GEFs can be introduced into functional assays for specific Rab GTPases.

3. GTPase Activating Proteins

GTP hydrolysis probably occurs at two stages in the life cycle of a Rab protein. First, because GTP is in excess of GDP in cytosol, newly synthesized Rab proteins are likely to contain bound GTP. REP, which presents the newly synthesized Rab to the geranylgeranyl transferase, binds preferen-

tially to the GDP bound form (Seabra, 1996), implying that a GTP hydrolysis step must occur before REP binding and isoprenylation. Second, in its membrane-bound form, the Rab protein hydrolyzes GTP, either to terminate vesicle/target interactions (e.g., Rab5) or to release a fusion clamp (e.g., Rab3a). Like the nucleotide exchange rate, the intrinsic GTPase activity of most Rab GTPases is low, and cellular GTPase activating proteins (GAPs) are required to stimulate this activity. The only Rab GAP cloned to date is Gyp6p, which activates the GTPase activity of *S.cerevisiae* Ypt6p more than 100-fold *in vitro* (Strom *et al.,* 1993). Gyp6p is an ~50-kDa cytosolic GAP specific for Ypt6p: It shows only weak activity on Ypt7p and no activity on Ypt1p, Sec4p, Ypt31p, Ras, or Rab2. Gyp6p has no sequence similarity to other GAPs. *ypt6* deletion mutants exhibit temperature sensitivity of growth, but neither the gene disruption nor the overexpression of Gyp6p results in any scoreable phenotype. This means either that the intrinsic GTPase activity is sufficient for Ypt6p function or, more likely, that yeast cells contain additional GAPs that are active on Ypt6p.

Several Rab GAPs have been partially purified. Two GAPs of ~30 and ~100 kDa were purified from porcine liver cytosol. They stimulate the GTPase activity of Ypt1p and Rab1 as well as (weakly) that of *S. pombe* Ypt6p, but not of Rab2 or Ras (Tan *et al.,* 1991). From yeast, an ~40-kDa cytosolic GAP was partially purified that stimulates the GTPase activity of Ypt1p and Rab1, but not that of Ras nor that of Ypt1p with a mutation in the effector domain (Tan *et al.,* 1991). Similarly, an ~300-kDa GAP active on Rab3a, but not on Ras or Rab2, has been partially purified from rat brain cytosol (Burstein and Macara, 1992). Thus, most Rab GAPs characterized to date are cytosolic, but a membrane associated GAP activity for Ypt1p has also been described (Jena *et al.,* 1992). To date, little is known about the biological function of the Rab GAPs, and it is not known whether they stimulate only one or both of the two GTPase steps described previously.

C. Putative Rab Effector Proteins

1. Rabphilin-3a

In order to understand how Rab proteins function, it is essential to identify the molecules (effectors) that are controlled by their GTPase cycle. Rabphilin-3a (Shirataki *et al.,* 1993), a 78-kDa protein purified from bovine brain membranes, was identified in cross-linking experiments as a protein binding to the GTP-bound form of Rab3a (Shirataki *et al.,* 1992). In addition to binding Rab3a, Rabphilin-3a also binds the structurally and functionally

related Rab3c isoform, but not a number of other Rab GTPases (C. Li *et al.*, 1994; Shirataki *et al.*, 1992). Even though its primary structure predicts a hydrophilic protein, Rabphilin-3a is found almost exclusively localized to the membranes of synaptic vesicles and chromaffin granules (Mizoguchi *et al.*, 1994; McKiernan *et al.*, 1996). The Rab3a-binding domain of Rabphilin-3a is located at the Zn^{2+}-containing N terminus, whereas the C terminus contains two C2 domains similar to those found in synaptotagmin, protein kinase C, and phospholipase A2. These domains are known to bind phospholipids in a Ca^{2+}-dependent manner (Yamaguchi *et al.*, 1993; McKiernan *et al.*, 1996). The colocalization of Rab3a and Rabphilin-3a raises the question of whether one of the two proteins functions as a "receptor" for the other one on the vesicle membrane. Rabphilin-3a does not appear to function as a membrane acceptor for Rab3a because (i) removal of Rabphilin-3a from synaptic vesicles by salt wash does not lead to a reduction in the amount of Rab3a and (ii) a Rab3a mutant unable to bind Rabphilin-3a colocalizes with a green fluorescent protein–Rabphilin-3a fusion protein on the membrane of neuroendocrine secretory vesicles (Shirataki *et al.*, 1994; McKiernan *et al.*, 1996). On the other hand, conflicting results have emerged regarding the role of Rab3a in recruiting Rabphilin-3a to membranes. Shirataki *et al.* (1994) found that the removal of Rab3a from synaptic vesicle membranes by GDI was not accompanied by a removal of Rabphilin-3a , whereas Stahl *et al.* (1996) did find a reduced level of vesicle-associated Rabphilin-3a under such conditions. Moreover, Rabphilin-3a, like Rab3a, disappears from synaptosome membranes upon the stimulation of exocytosis, and Rabphilin-3a is found mainly in the cell body of neurons devoid of both Rab3a and Rab3c. Consistent with this, mutations that interfere with zinc binding abolish the ability of Rabphilin-3a to bind Rab3a (C. Li, *et al.*, 1994). The latter result was confirmed by McKiernan *et al.* (1996), but these authors concluded that such mutations do not reduce the membrane association of Rabphilin-3a. They also found that a deletion of the C2 domains of Rabphilin-3a led to a strong decrease in the membrane association, although a fraction still appeared to be correctly localized to chromaffin secretory granules. Taken together, the data suggest that Rab3a may play a role in the correct targeting of Rabphilin-3a to synaptic vesicles/chromaffin granules, but that additional molecules also contribute to its membrane association.

What is the function of Rabphilin-3a? Overexpresssion of Rabphilin-3a enhances the induced secretion of growth hormone in chromaffin cells, and Rabphilin-3a antisense oligonucleotides inhibit such exocytosis. Moreover, the expression of the Rab3a-binding domain of Rabphilin-3a, which should compete for Rab3a association with the endogenous, full-length Rabphilin-3a, inhibits exocytosis (Komuro *et al.*, 1996; Chung *et al.*, 1995). These results implicate Rabphilin-3A as a positive regulator of exocytosis. The

paradox is that the presumed upstream regulator of Rabphilin-3A, Rab3A, is regarded as a *negative* regulator of exocytosis (see Section III,B,4). It cannot be excluded that Rabphilin-3a may serve as a regulatory factor rather than as an effector of Rab3a because it has been shown to display GEF activity on Rab3a as well as to inhibit the activity of Rab3a GAP (Fujita *et al.,* 1994; Kishida *et al.,* 1993). Concerning the functional mechanism of Rabphilin-3a, it is of interest that its C2 domains are similar to those of synaptotagmin, a synaptic membrane protein that binds target membrane SNAREs (t-SNAREs) (Südhof and Rizo, 1996). To date, however, no association between Rabphilin-3a and SNAREs has been detected. Rabphilin-3a binds to phospholipids in the presence of Ca^{2+}, and this ability places Rabphilin-3a as a candidate protein for a Ca^{2+} sensor in Ca^{2+}-stimulated secretion (Yamaguchi *et al.,* 1993). Its activity may be further modulated by phosphorylation because Rabphilin-3a is a substrate for both cyclic AMP-dependent protein kinase and Ca^{2+}/calmodulin-dependent kinase II (Fykse *et al.,* 1995; Kato *et al.,* 1994; Numata *et al.,* 1994).

2. Rabaptin-5

In order to gain insight into the mechanisms by which Rab5 stimulates endocytic membrane fusion, the GTPase-deficient Rab5 Q79L mutant was used as a bait in a two-hybrid screen (Stenmark *et al.,* 1995). This screening led to the identification of Rabaptin-5, a 100-kDa protein with putative coiled-coil regions at the N and C termini. The C-terminal part binds specifically to Rab5 but not to a number of other Rab GTPases. Like Rabphilin-3a, Rabaptin-5 binds its Rab target preferentially in its GTP-bound form, but in contrast to Rabphilin-3a, Rabaptin-5 is found mainly in the cytosol. However, it is recruited to early endosome-enriched membranes in a Rab5- and GTP-dependent manner, reminiscent of the way the protein kinase Raf is recruited to the plasma membrane by Ras–GTP (Vojtek *et al.,* 1993). Immunodepletion of Rabaptin-5 from cytosol strongly inhibits Rab5-dependent early endosome fusion *in vitro,* and its overexpression leads to expanded early endosomes, reminiscent of the result of Rab5 overexpression (Stenmark *et al.,* 1995). Although Rabaptin-5 weakly inhibits the GTPase activity of Rab5, possibly by interfering with a GAP interaction (Rybin *et al.,* 1996), it is unlikely that its action as a GTPase inhibitory protein is sufficient to explain its essential function in Rab5-dependent early endosome fusion. Most likely, Rabaptin-5 functions as an effector for Rab5, conveying Rab5 regulation to the membrane docking and fusion apparatus. How does this occur? Preliminary data indicate that Rabaptin-5 is complexed with at least one other protein in the cytosol and, conceivably, this protein complex is recruited to endocytic membranes by Rab5–GTP. Here, the Rabaptin-5 complex may play an essential role in membrane

docking, possibly by interacting with other coiled-coil containing proteins such as SNAREs (Chapman *et al.,* 1994), TAP/p115 (Barroso *et al.,* 1995; Sapperstein *et al.,* 1995), or mammalian homologs of Sec6 and Sec8 (TerBush and Novick, 1995; Ting *et al.,* 1995). The long coiled-coil regions of Rabaptin-5 are predicted to have a rod-like conformation, and one can envision that the protein could function as a spacer between two membranes. Membrane-bound Rab5 continously hydrolyzes GTP independently of membrane fusion, and it is conceivable that a transient membrane docking induced by recruitment of the Rabaptin-5 complex may increase the probability of membrane fusion (Fig. 6). Further knowledge about this process requires identification of the proteins on the membrane (other than Rab5) that interact with Rabaptin-5. No Rabaptin-5 homologs have been identified in yeast, but Vps9p, which is involved in vacuolar protein sorting, has been proposed as a candidate for such a homolog. This protein contains a binding site for a small GTPase, possibly Ypt51p, and, like Rabaptin-5, is a cytosolic coiled-coil protein (Burd *et al.,* 1996).

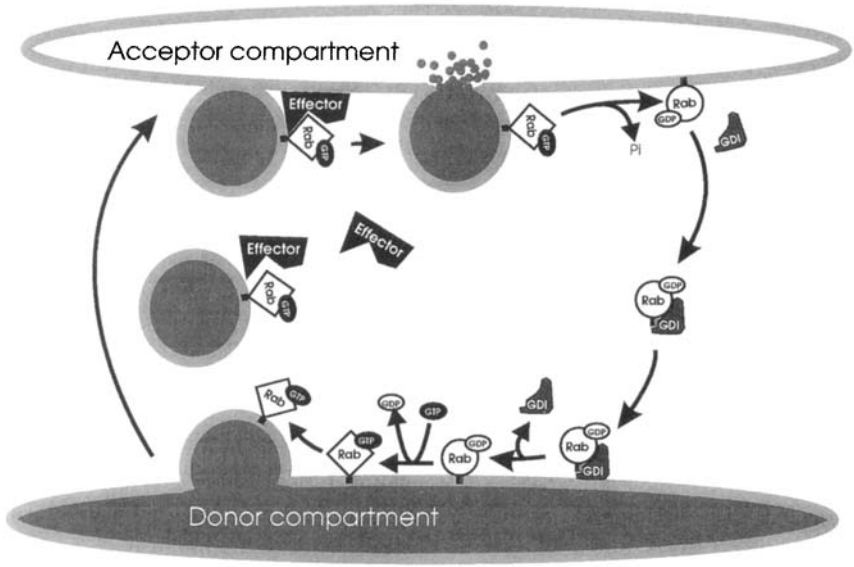

FIG. 6 The GTPase cycle of a Rab protein regulates membrane docking and fusion. A cytosolic effector becomes membrane associated upon binding to a GTP-bound Rab. This results in docking of two membranes, which facilitates the fusion of the bilayers. After GTP hydrolysis the Rab and its effector can be recycled and used in a new round of membrane transport. The Rab may associate either with the donor compartment or directly with a transport vesicle. In some cases hydrolysis of GTP by the Rab appears to be a prerequisite for bilayer fusion.

3. Other Newly Identified Effector Candidates

In addition to Rabaptin-5, to date two other putative Rab effectors have emerged from two-hybrid screens, and others are likely to follow. Rabin3, a 50-kDa cytosolic protein, interacts with Rab3a and Rab3d but not with Rab2 or Rab3c (Brondyk *et al.,* 1995). It interacts with wild-type Rab3a as well as the putatively GDP-bound T36N mutant. In this respect, Rabin3 differs from the other putative Rab3a effector, Rabphilin-3a. Rabin3 does not influence regulated secretion when overexpressed, and it has no effect on the GTPase activity and nucleotide exchange rate of Rab3a. Currently, the significance of the binding between Rabin3 and Rab3a remains unclear, but some structural features of Rabin3 are interesting: It contains an N-terminal coiled-coil region, like Rabaptin-5, and two short segments that show similarity to Sec2p, a cytosolic yeast protein that interacts genetically with Sec4p (Nair *et al.,* 1990). Although Rabin3 is unable to complement the lack of Sec2p in yeast, the possibility still remains that these two proteins have related functions.

Both Ras and Rho GTPases interact with specific protein kinases in their active forms, and the GTP-bound form of Rab8 has also now been found to bind to a kinase, Rab8ip (Ren *et al.,* 1996). Rab8ip is 93% identical to GC kinase, a threonine/serine kinase, and it has been shown to possess this type of kinase activity. According to cell fractionation and immunofluorescence microscopy studies, Rab8ip is present in the cytosol, on membranes in the Golgi area, and at the basolateral plasma membrane of polarized MDCK cells. The localization of Rab8ip is thus reminiscent of that of Rab8, consistent with the idea that Rab8ip could be an effector of Rab8. Although functional data to support this are still lacking, it is tempting to speculate that Rab8ip may be recruited to Golgi membranes or *post*-Golgi vesicles by Rab8–GTP and thereafter catalyze the phosphorylation of SNARE proteins or other molecules involved in vesicle docking and fusion.

Apart from the putative Rab effectors identified biochemically or by two-hybrid screening, a number of possible Rab effectors have emerged from genetic studies in yeast, although biochemical evidence for their direct interaction with Rab proteins is lacking. Such molecules are discussed in the following section.

V. Linkages of Rab GTPases to Other Components of the Membrane Transport Machinery

A. SNARE Hypothesis of Vesicle Transport

Association of the NSF required for most of the intracellular membrane fusion events depends on the SNAPs (Whiteheart and Kubalek, 1995;

Rothman, 1996). The search for the integral membrane receptor proteins for SNAPs led to the identification of the brain SNARE proteins (Söllner *et al.,* 1993b), which turned out to be previously known components of the nerve terminal: the synaptic vesicle VAMP/synaptobrevin 1 and 2 proteins, and syntaxin as well as the SNAP-25 protein (synaptosomal-associated protein of 25 kDa) mainly localizing to the presynaptic plasma membrane (Südhof *et al.,* 1993; Bajjalieh and Scheller, 1995). According to the hypothesis put forward by Rothman (1994, 1996), complex formation between specific pairs of v-SNAREs and t-SNAREs plays a key role in determining the specificity of membrane docking/fusion events; the complex then functions as a core on which the general fusion machinery (SNAPs and NSF) is assembled. As predicted by this hypothesis, homologs of the neuronal SNAREs have been identified in a variety of nonneuronal mammalian cells as well as in lower eukaryotes. Furthermore, they are found involved in the different transport steps of the yeast exocytic pathway and on different membrane compartments of mammalian cells (Bennett and Scheller, 1993; Ferro-Novick and Jahn, 1994; Söllner, 1995). Currently, however, it seems that the SNARE proteins are not the sole components responsible for docking of transport vesicles on the correct target membrane, but rather the docking/fusion events may require several "layers" of protein–protein interactions (Broadie *et al.,* 1995; Barroso *et al.,* 1995; Galli *et al.,* 1995; Sapperstein *et al.,* 1995, 1996). It has been suggested that the SNARE complexes could actually exert their function in the bilayer fusion event (Hayashi *et al.,* 1994). The simple idea of specificity and directionality of transport events being determined by nonsymmetrical distributions of v- and t-SNAREs has been undermined to some extent by the findings that synaptic vesicles and secretory granules contain both types of SNAREs (Koh *et al.,* 1993; Schulze *et al.,* 1995; Walch-Solimena *et al.,* 1995; Tagaya *et al.,* 1995, 1996). Also, there are findings suggesting that in specific transport events such as apical exocytosis in epithelial cells the SNARE/NSF/SNAP might be substituted by a totally unrelated protein machinery (Ikonen *et al.,* 1995). Furthermore, the precise stage in which the NSF and SNAP proteins are acting is under debate (Morgan and Burgoyne, 1995; A. Mayer *et al.,* 1996). Nevertheless, because an increasing mass of experimental evidence supports the basic outline of the SNARE hypothesis—the role of these proteins as core components of the vesicle docking/fusion machinery—several groups are attempting to experimentally link the function of the Rab GTPases to that of the SNAREs. One can see how this thinking parallels the original model for Rab function presented by Bourne (1988): the SNAREs correspond to the hypothetical recognition molecules suggested to reside on the transport vesicle and target membranes.

B. Interactions of Rabs and the SNARE Machinery in *S.cerevisiae*

1. Genetic Interactions

A major advantage of the yeast system is the potential of classical genetic analysis this unicellular eukaryote offers (Pryer *et al.,* 1992; Schekman, 1992). Various screens and selection schemes have been devised for the isolation of mutants defective in intercompartmental transport. Null or conditional lethal mutants have been widely used to search for suppressors of the phenotypic alterations observed. Typically, this approach has been employed to screen for genes that, when present in multiple copies, can suppress the defect in a mutant strain. On the other hand, interactions of genes/gene products have been approached by so-called synthetic lethality experiments. Here, a combination of two mutations, neither of which is lethal alone in given circumstances, may turn out lethal, which is usually considered to be stronger proof for relatedness of functions than suppression in a multicopy situation.

Suppressor screens of the lethal yeast *ypt1* deletion (Dascher *et al.,* 1991; Ossig *et al.,* 1991) revealed a group of *SLY* (*s*uppressor of *l*oss of *YPT1*) genes, two of which (multicopy suppressors *SLY2* and *SLY12*) were found to encode proteins sharing a similar domain structure and limited homology with the VAMP/synaptobrevin proteins. The gene products were shown to function in ER to Golgi transport. *SLY2* is identical to *SEC22* (Novick *et al.,* 1980; A. P. Newman *et al.,* 1992b) and *SLY12* is the same as *BET1* (Newman and Ferro-Novick, 1987; A. P. Newman *et al.,* 1992a) encoding another SNARE-type membrane protein. Both Sec22p and Bet1p have been demonstrated to be components of a tentative ER to Golgi transport vesicle docking/fusion complex (Søgaard *et al.,* 1994). Moreover, a third ER–Golgi interface SNARE protein is linked to these genetic interactions. Although overexpression of the Sly2p/Sec22p yields only very weak suppression of Ypt1p loss, it is potentiated by coexpression of Bos1p (Lian *et al.,* 1994), a further v-SNARE protein involved in ER to Golgi trafficking in yeast (Shim *et al.,* 1991; Lian and Ferro-Novick, 1993). Furthermore, Dascher *et al.* (1990) isolated a mutant form of a gene, called *SLY1,* as a single copy suppressor of *ypt1* deletion. *SLY1* encodes an essential protein belonging to the family of Sec1-related proteins that bind to syntaxin-type t-SNAREs and thereby regulate SNARE complex assembly (Aalto *et al.,* 1992; Halachmi and Lev, 1996). The gain-of-function mutant allele identified, *sly1-20,* could possibly encode a protein that is permanently in an "active" conformation that is normally induced (directly or indirectly) by Ypt1p, thus bypassing the requirement for the GTPase.

In the late secretory step from the Golgi to the yeast plasma membrane, the *SEC9* gene encoding a yeast homolog of the neuronal SNAP-25

t-SNARE protein was found to effectively suppress a cold-sensitive effector domain mutation in the late secretory Rab gene *SEC4* (Brennwald *et al.*, 1994), indicating that Sec9p is situated downstream on the effector pathway of the small GTPase. The authors, however, were unable to detect direct physical interaction between Sec4p and Sec9p. As shown for *YPT1* and *SLY1* in the ER to Golgi transport step (see above), a genetic interaction, although weak, was also reported between *SEC4* and *SEC1:* Twofold overexpression of Sec4p was found to partially suppress the *sec1-1* mutation (Salminen and Novick, 1987). These genetic findings clearly indicate that the functions of Rab GTPases are at least indirectly linked to that of the SNARE complexes in vesicle docking/fusion.

Data by Sapperstein *et al.* (1996) suggest that Ypt1p functions in the SNARE regulatory pathway downstream of or in conjunction with Uso1p (Nakajima *et al.*, 1991), a *S.cerevisiae* homolog of the mammalian p115/TAP protein demonstrated to be required for the docking stage of several membrane transport events (Waters *et al.*, 1992; Sapperstein *et al.*, 1995; Barroso *et al.*, 1995). The nature of the relationship between Ypt1p and Uso1p, however, is not known. Whether Uso1p might have GAP or GEF (see Section IV,B) activities on Ypt1p has not been investigated; the interaction between the proteins could be indirect via an as yet undiscovered factor(s). Alternatively, the two proteins could act in a "parallel" fashion to facilitate v-SNARE/t-SNARE complex formation. Sapperstein *et al.* (1996) present two possible (not mutually exclusive) models for the Ypt1p regulation of SNAREs (Fig. 7). The GTPase could either facilitate the assembly of the v-SNARE/t-SNARE complex directly by activating v-SNAREs (Lian *et al.*, 1994) or impact on Sly1p to relieve an inhibitory effect of this Sec1 homolog on the SNARE complex assembly (Pevsner *et al.*, 1994; Schulze *et al.*, 1994). The latter model depicts a stimulating scheme in which the effect of Rab GTPases on SNARE complex assembly would be mediated through displacement of a Sec1-related protein from syntaxin, allowing binding of the other SNAREs and activation of the recognition/fusion complex.

2. Role of Ypt1p as a Regulator of SNARE Complex Formation in ER to Golgi Transport

In addition to the genetic interaction data summarized in the previous section, more direct biochemical evidence for functional linkages between Rabs and SNARE proteins has been reported during the past few years. These reports deal with the role of *S.cerevisiae* Ypt1p in formation of a complex between the v-SNAREs functioning in ER to Golgi transport (Lian *et al.*, 1994) and with the assembly of a tentative multimeric docking complex on the Golgi membranes (Søgaard *et al.*, 1994). Lian *et al.* (1994)

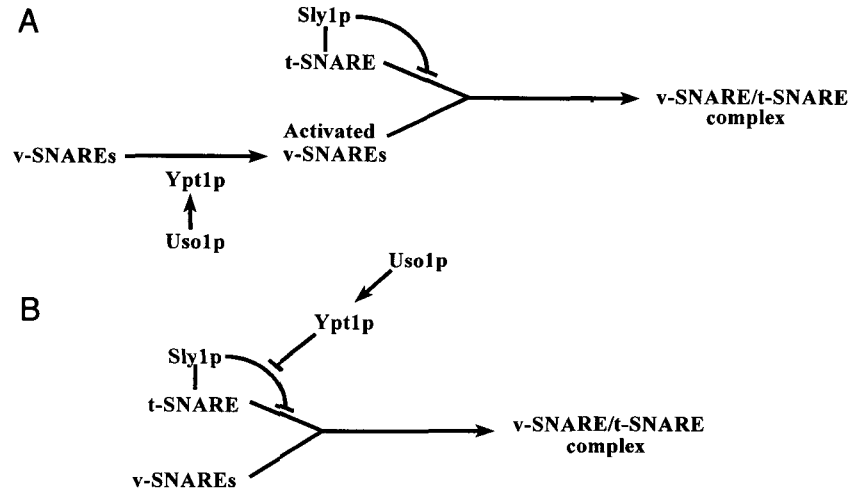

FIG. 7 Potential modes of action for Ypt1p in the assembly of ER to Golgi SNARE complexes (redrawn from *The Journal of Cell Biology,* 1996, **132,** 755–767, by copyright permission of The Rockefeller University Press). (A) Ypt1p may activate v-SNAREs by affecting their conformation or oligomeric status. Uso1p may be an upstream regulator of Ypt1p or act in parallel with the GTPase in this process. (B) Ypt1p may relieve the inhibitory effect that the Sec1-related Sly1p imparts on formation of a v-SNARE/t-SNARE complex.

convincingly demonstrated that a complex of the v-SNAREs Bos1p and Sec22p failed to form on the transport vesicles in a *ypt1*^{ts} mutant strain at the restrictive temperature, suggesting that Rabs may regulate the oligomerization of the v-SNARE on the vesicles, a process that could be necessary for the SNARE function. No direct interaction between Ypt1p and the SNAREs, however, was detected, indicating that the effect of the GTPase may be indirect or very transient. Søgaard *et al.* (1994) identified a multimeric protein assembly that was suggested to represent a vesicle docking complex in yeast cells in which ER to Golgi vesicle transport was blocked by a *sec18*^{ts} mutation (*SEC18* encodes a yeast homolog of the mammalian NSF). This complex consisted of the v-SNAREs Bos1p, Sec22p, and Ykt6p, the Golgi t-SNARE Sed5p, and five other proteins including the Sec1 homolog Sly1p, and Sec17p, a yeast counterpart of the mammalian α-SNAP. The complex could not be detected in *ypt1*^{ts} mutant strains incubated at the restrictive temperature, leading to the interpretation that Ypt1p controls the multimeric interactions between SNARE proteins required for vesicle targeting. The conclusion, however, is somewhat blurred by the fact that the authors were unable to construct a *sec18 ypt1* double mutant. Nevertheless, these studies support the idea that Ypt1p functions as a

regulator of SNARE complex assembly in the yeast ER to Golgi vesicle trafficking.

C. 19.5S Complex and the Rab GTPases

A strong genetic interaction between the *S. cerevisiae SEC4* and *SEC15* genes affecting the late secretory step was first observed by Salminen and Novick (1987). The *SEC15* gene was found to encode a hydrophilic protein associated with a yeast microsomal fraction by ionic interactions (Salminen and Novick, 1989). Overproduction of the protein resulted in disturbance of the secretion process and accumulation of secretory vesicle clusters. This effect was inhibited in a *sec4*^{ts} strain, indicating that Sec15p lies downstream of Sec4p in the regulatory pathway or that Sec15p may even be the target or part of the target of the small GTPase. Later, Sec15p was found to be a component of a large (19.5S) multisubunit complex consisting of at least eight polypeptides including the *SEC6* and *SEC8* gene products (Bowser *et al.*, 1992; TerBush and Novick, 1995). The complex was found to localize to small bud tips, the sites of exocytosis in yeast. In addition to the interactions with *SEC4,* the genes encoding its components display interactions with the yeast late secretory SNARE genes *SSO1, SSO2* (Aalto *et al.*, 1993), and *SEC9* (Brennwald *et al.*, 1994). This may indicate that the 19.5S complex lies in the docking/fusion pathway between the Sec4 GTPase and the SNAREs. Furthermore, Salminen and Novick (1987) observed a genetic interaction between *SEC4* and *SEC2,* another gene affecting the intracellular localization of Sec15p. Additionally, *sec4*^{ts} mutations were found to display synthetic lethality with mutant alleles of several genes encoding components of the 19.5S complex, further corroborating the notion that the functions of the GTPase and the multisubunit complex are interconnected. The sequence of Sec8p may offer a clue regarding a possible functional interaction between the complex and Sec4p. A 202-amino acid domain near the Sec8p N terminus shares 25% identity with the yeast adenylate cyclase. This specific region of the adenylate cyclase is known as the Ras-responsive element and may represent a site of direct contact with the Ras GTPase. The N-terminal region of Sec8p could, by analogy, interact with Sec4p, which through this interaction could control the function of the 19.5S complex (Bowser *et al.*, 1992).

Given the similarities observed between the docking/fusion machineries throughout the eukaryotic kingdom (Bennett and Scheller, 1993; Ferro-Novick and Jahn, 1994), an equivalent of the 19.5S complex should also be found in mammals. Indeed, this is the case: Ting *et al.* (1995) reported the identification of mammalian Sec6 and Sec8 (rSec6 and rSec8) homolog proteins expressed ubiquitously in rat tissues. rSec8 was found to be part

of a 17S complex in the brain and colocalized in transfected COS cells with Rab3a and syntaxin 1A at patches along the plasma membrane. However, it is not known whether the 17S complex interacts with the Rab GTPases. In yeast no counterpart of the 19.5S complex has been found to be involved in the other intracellular transport events besides the post-Golgi exocytic step. This may indicate that the 19.5S/17S complex could be confined to the late secretory function.

D. Studies on Yeast Vacuole Fusion: New Ideas on the Sequence of Events during the Docking/Fusion Process

As judged from the data reviewed earlier in this section, it seems that the Rab GTPases should have a function upstream of the SNAREs and, according to the original SNARE hypothesis, also the general fusion proteins, NSF and SNAPs. Kinetic studies on regulated secretory events indicate that the ATPase activity of NSF is required in a priming step necessary for maintenance of fusion competence but not for the actual Ca^{2+}-triggered fusion event (Morgan and Burgoyne, 1995). On the other hand, the ability of NSF to dissociate the synaptic SNARE complexes *in vitro* in the presence of SNAPs and Mg^{2+}-ATP is well established (Wilson *et al.,* 1992; Söllner *et al.,* 1993a; Hayashi *et al.,* 1995; Schiavo *et al.,* 1995). Wickner and coworkers (A. Mayer *et al.,* 1996) using an *S. cerevisiae* vacuole *in vitro* fusion assay, have achieved results that imply a very early role for NSF and SNAPs in the docking/fusion process, which significantly deviates from that postulated by the SNARE hypothesis: The actions of Sec17p (yeast α-SNAP) and Sec18p (yeast NSF) seem to precede the step requiring the Rab GTPase Ypt7p (A. Mayer *et al.,* 1996). Release of Sec17p from the vacuole membranes driven by the Sec18p ATPase activity seems to be crucial for fusion in this assay, and this can even precede vacuole docking because it can occur prior to mixing of the vacuoles. This result could imply that NSF is required for dissociation of "used" SNARE complexes and thus reactivation of the SNAREs for the next functional cycle. In addition, the SNAPs, which are capable of binding individual, undocked t-SNAREs (Söllner *et al.,* 1993a; Hayashi *et al.,* 1995), could shield the t-SNAREs from binding of their cognate v-SNAREs. In this case, the activity of NSF would be required for making the t-SNAREs accessible again for docking complex formation. Furthermore, a third possible function of NSF and SNAPs could be to facilitate exchange of binding partners of the SNAREs, which are also known to bind several other protein classes (Edelmann *et al.,* 1995; McMahon *et al.,* 1995; Halachmi and Lev, 1996). A. Mayer *et al.* (1996) show that the Rab GTPase Ypt7p can function only in vacuole fusion after Sec17p and Sec18p have acted on the (unknown) SNAREs involved, leaving

them in a distinct conformation or oligomeric assembly. Ypt7p could then act either to enhance the specificity of the reaction or to set the stage for the assembly of other components.

VI. Perspectives

Since their first appearance on the scene of intracellular trafficking in 1987, Rab GTPases have rapidly established themselves as principal actors in membrane docking and fusion processes. A multitude of different Rabs have been identified and localized to distinct compartments in yeast and mammals, and many of them have been demonstrated to regulate specific transport processes. However, a number of questions remain to be addressed before we can fully appreciate the beauty of the Rab regulatory cycle.

First, do all Rab GTPases function principally in the same way? The limited sequence identity between distinct Rab GTPases (typically 30–40 %) actually suggests that distinct members of the Rab family may function in different ways. This is substantiated by the fact that the putative Rab effectors identified to date are highly divergent: Rabphilin-3a (interacting with Rab3a and Rab3c) is a Zn^{2+}-binding protein with Ca^{2+}/phospholipid-binding C2 domains, Rabaptin-5 (interacting with Rab5) contains long coiled-coil regions, whereas Rab8ip (interacting with Rab8a) is a protein kinase. Ras and Rho GTPases bind multiple putative effectors in their GTP-bound state, and further studies will probably reveal that this also applies to the Rab GTPases. Moreover, overexpression of Rab8 leads to alterations in both microtubules and the actin cytoskeleton, whereas such effects have not been observed with other Rab GTPases. The consensus for Rab function thus appears to be that they act to recruit effector proteins to specific membranes in a GTP-dependent manner, and that this recruitment plays a role in membrane docking and fusion. However, although Rab3a–GTP inhibits membrane fusion, Rab5–GTP stimulates the process. It has therefore been proposed that the Rab GTPase subfamily could be divided into "inhibitory" and "stimulatory" subgroups (Lledo *et al.*, 1994). Nevertheless, Rab proteins might have a common functional principle of promoting membrane docking, a prerequisite for fusion. The difference may be that some Rabs, such as Rab5, may display the single property of promoting membrane docking in their GTP-bound form, whereas others, such as Rab3a, may possess a dual activity (i) to promote vesicle docking in their GTP-bound form and (ii) to function as fusion clamps until the bound GTP is hydrolyzed. The ongoing identification of new Rab effectors and regulators will contribute to the clarification of this issue.

Second, how is the Rab regulatory function on the membrane docking/fusion apparatus implemented? Indirect evidence suggests that Rab proteins serve to regulate the pairing of v- and t-SNAREs, thus perhaps acting to determine the directionality of vesicle delivery. One may speculate whether Rab effectors could serve as regulators of SNARE function. Evidence for a functional link between Rab3a and the SNARE complex has recently come from *Aplysia* neurons: The preinjection of a GTPase-deficient Rab3a mutant protein into these cells was found to protect them against tetanus and botulinum A neurotoxins, which cleave uncomplexed SNAREs. This suggests that Rab3a–GTP may stabilize the synaptic SNARE complex (Johannes *et al.*, 1996). In theory, the three Rab effector candidates identified to date could regulate SNAREs in three different ways: Rabphilin-3a binds phospholipids in a Ca^{2+}-dependent manner and displays similarity to the SNARE-interacting protein synaptotagmin. This protein could thus confer calcium regulation on the function of the SNAREs. Rabaptin-5 contains N- and C-terminal coiled-coil regions. Such regions are also found in v- and t-SNAREs (Rothman, 1996), and one can envision that Rabaptin-5 may function to bring the v- and t-SNARE together by interacting with their respective coiled-coil regions. Rab8ip is a protein kinase, and it is very possible that a membrane-targeted kinase could control the action of SNAREs by phosphorylating them or other components involved in SNARE regulation. However, one cannot exclude the possibility that Rab GTPases and their effectors may operate independently of the SNAREs. For instance, Rab proteins and their effectors may cause weak or transient membrane–membrane interactions. Such interactions may kinetically favor the formation of SNARE complexes, even if there is no contact between Rabs or their effectors and the SNARE proteins. The identification of molecules interacting with Rab effectors during membrane docking/fusion should contribute to clarify the current vague picture of the Rab–SNARE relationships.

Third, which molecules are acting upstream of the Rab proteins? It is already evident that the membrane association and presumably the function of some of the Rab GTPases is modulated by cell cycle-specific kinases during mitosis and by growth factor activated kinases during interphase. Perhaps phosphorylation is a general way of modulating the activity of Rab GTPases according to the specific needs of the cell. Such phosphorylation might explain the occurrence of seemingly redundant Rab isoforms. For instance, Rab4a contains a phosphorylation site for $p32^{cdc2}$ kinase, whereas its isoform Rab4b lacks this site. This opens the possibility for a differential regulation of the two proteins during the cell cycle, and differences in phosphorylation between Rab isoforms could offer a general means of fine-tuning Rab function at specific developmental or metabolic stages. In the case of Ras, it is well established that its GTP/GDP cycle and hence its

function can be modulated by external factors, such as growth factors and hormones. Could the same apply to Rab proteins? This is not unlikely because external factors do affect intracellular transport processes (Sato *et al.,* 1996). Future studies will reveal if the GTPase activity or nucleotide exchange rates of Rabs are affected by the binding of external signaling molecules to their receptors and if there is indeed such a tie between signal transduction and the machinery of membrane traffic.

Fourth, will the study of Rab GTPases lead to the discovery of even more intricate routes of intracellular traffic than those known to date? It has been amazing to see how the number of different mammalian Rabs has increased, currently amounting to more than 40 members. The high number of different Rabs most probably reflects the high number of intracellular trafficking events taking place in the cell. It is becoming evident that compartments such as the Golgi complex and the early endosome in fact consist of several functional subdomains (Rothman and Warren, 1994; Hopkins, 1992; Gruenberg and Maxfield, 1995), and multiple Rabs may be required to ensure specific vesicle delivery between such subdomains. Adding to the complexity of intracellular trafficking routes is the new discovery of cognate apical and basolateral pathways in even nonpolarized cells (Yoshimori *et al.,* 1996). Therefore, although at first glance it may seem confusing that early endosomes contain several distinct Rabs, such as Rab4, Rab5, Rab18, Rab20, and Rab22, their existence may give us a clue to a functional subcompartmentalization of this organelle.

Fifth, what is the importance of Rab GTPases in development and physiology? To date, almost all functional studies on Rab proteins have been carried out on cells in culture. However, given the essential role of Rab GTPases in membrane traffic, and the crucial role of membrane traffic in cell shape, polarity, and migration (Eaton and Simons, 1995; Simons, 1993), one would expect Rab GTPases to be fundamental regulators of developmental and physiological processes. In order to study this, it is obviously necessary to extend from cell culture experiments to those involving multicellular organisms. The use of organisms readily amenable to genetic manipulation, such as *Caenorhabditis elegans* and *Drosophila melanogaster,* will undoubtedly shed light on Rab function in development. Unfortunately, the only mammalian Rab gene knockout, that of Rab3a, resulted in no striking phenotypic alterations (see Section III,B,4).This result, combined with the fact that many Rab GTPases have isoforms that may be functionally redundant, may discourage researchers from initiating new labor-consuming gene knockout experiments. On the other hand, gene knockouts in yeast show that some, but not all, Rabs are essential, and with increased experience from cell culture experiments it should be possible to design knockout experiments that have a good chance of yielding a scoreable phenotype. Moreover, the expression of dominant interfering Rab mutants

in transgenic mice at specific developmental stages and the application of antisense technology should help us to further delineate the function of Rab GTPases in the living animal.

Acknowledgments

We are grateful to Dr. Sirkka Keränen for critical reading of the manuscript. V. M. O. is recipient of a grant from the Genome Research Programme of the Academy of Finland and H. S. is a fellow of the Norwegian Cancer Society. This work was supported by the European Union TMR Programme Grant No. ERBFMRXCT960020.

References

Aalto, M. K., Keränen, S., and Ronne, H. (1992). A family of proteins involved in intracellular transport. *Cell* **68,** 181–182.

Aalto, M. K., Ronne, H., and Keränen, S. (1993). Yeast syntaxins Sso1p and Sso2p belong to a family of related membrane proteins that function in vesicular transport. *EMBO J.* **12,** 4095–4104.

Adari, H., Lowy, D. R., Willumsen, B. M., Der, C. J., and McCormick, F. (1988). *Science* **240,** 518–521.

Alexandrov, K., Horiuchi, H., Steele-Mortimer, O., Seabra, M. C., and Zerial, M. (1994). Rab escort protein-1 is a multifunctional protein that accompanies newly prenylated rab proteins to their target membranes. *EMBO J.* **13,** 5262–5273.

Andres, D. A., Seabra, M. C., Brown, M. S., Armstrong, S. A., Smeland, T. E., Cremers, F. P., and Goldstein, J. L. (1993). cDNA cloning of component A of Rab geranylgeranyl transferase and demonstration of its role as a Rab escort protein. *Cell* **73,** 1091–1099.

Antony, C., Cibert, C., Geraud, G., Santa Maria, A., Maro, B., Mayau, V., and Goud, B. (1992). The small GTP-binding protein rab6p is distributed from medial Golgi to the trans-Golgi network as determined by a confocal microscopic approach. *J. Cell Sci.* **103,** 785–796.

Araki, S., Kikuchi, A., Hata, Y., Isomura, M., and Takai, Y. (1990). Regulation of reversible binding of smg p25A, a ras p21-like GTP-binding protein, to synaptic plasma membranes and vesicles by its specific regulatory protein, GDP dissociation inhibitor. *J. Biol. Chem.* **265,** 13007–13015.

Armstrong, J. (1995). Ypt1 (Scizosaccharomyces pombe). *In* "Guidebook to the Small GTPases" (M. Zerial and L. A. Huber, Eds), pp. 418–419. Oxford Univ. Press, London.

Armstrong, J., Craighead, M. W., Watson, R., Ponnambalam, S., and Bowden, S. (1993). Schizosaccharomyces pombe ypt5: A homologue of the rab5 endosome fusion regulator. *Mol. Biol. Cell.* **4,** 583–592.

Armstrong, J., Pidoux, A., Bowden, S., Craighead, M., Bone, N., and Robinson, E. (1994). The ypt proteins of Scizosaccharomyces pombe. *Biochem. Soc. Trans.* **22,** 460–463.

Armstrong, J., Thompson, N., Squire, J. H., Smith, J., Hayes, B., and Solari, R. (1996). Identification of a novel member of the Rab8 family from the rat basophilic leukemia cell line, RBL.2H3. *J. Cell Sci.* **109,** 1265–1274.

Ayala, J., Touchot, N., Zahraoui, A., Tavitian, A., and Prochiantz, A. (1990). The product of rab2, a small GTP binding protein, increases neuronal adhesion, and neurite growth in vitro. *Neuron* **4,** 797–805.

Bacon, R. A., Salminen, A., Ruohola, H., Novick, P., and Ferro-Novick, S. (1989). The GTP-binding protein Ypt1 is required for transport in vitro: The Golgi apparatus is defective in ypt1 mutants. *J. Cell Biol.* **109,** 1015–1022.

Bailly, E., McCaffrey, M., Touchot, N., Zahraoui, A., Goud, B., and Bornens, M. (1991). Phosphorylation of two small GTP-binding proteins of the Rab family by $p34^{cdc2}$. *Nature (London)* **350,** 715–718.

Bajjalieh, S. M., and Scheller, R. H. (1995). The biochemistry of neurotransmitter secretion. *J. Biol. Chem.* **270,** 1971–1974.

Baker, D., Wuestehube, L., Schekman, R., Botstein, D., and Segev, N. (1990). GTP-binding Ypt1 protein and Ca2+ function independently in a cell-free protein transport reaction. *Proc. Natl. Acad. Sci. USA* **87,** 355–359.

Baldini, G., Hohl, T., Lin, H. Y., and Lodish, H. F. (1992). Cloning of a Rab3 isotype predominantly expressed in adipocytes. *Proc. Natl. Acad. Sci. USA* **89,** 5049–5052.

Baldini, G., Scherer, P. E., and Lodish, H. F. (1995). Nonneuronal expression of Rab3A: Induction during adipogenesis and association with different intracellular membranes than Rab3D. *Proc. Natl. Acad. Sci. USA* **92,** 4284–4288.

Barbieri, M. A., Li, G., Mayorga, L. S., and Stahl, P. D. (1996). Characterization of Rab5:Q79L-stimulated endosome fusion. *Arch. Biochem. Biophys.* **326,** 64–72.

Barroso, M., Nelson, D. S., and Sztul, E. (1995). Transcytosis-associated protein (TAP)/p115 is a general fusion factor required for binding of vesicles to acceptor membranes. *Proc. Natl. Acad. Sci. USA* **92,** 527–531.

Becker, J., Tan, T. J., Trepte, H.-H., and Gallwitz, D. (1991). Mutational analysis of the putative effector domain of the GTP-binding Ypt1 protein in yeast suggests specific regulation by a novel GAP activity. *EMBO J.* **10,** 785–792.

Benli, M., Döring, F., Robinson, D. G., Yang, X., and Gallwitz, D. (1996). Two GTPase isoforms, Ypt31p and Ypt32p, are essential for Golgi function in yeast. *EMBO J.* **15,** 6460–6475.

Bennett, M. K., and Scheller, R. H. (1993). The molecular machinery for secretion is conserved from yeast to neurons. *Proc. Natl. Acad. Sci. USA* **90,** 2559–2563.

Beranger, F., Cadwallader, K., Porfiri, E., Powers, S., Evans, T., de Gunzburg, J., and Hancock, J. F. (1994a). Determination of structural requirements for the interaction of Rab6 with RabGDI and Rab geranylgeranyltransferase. *J. Biol. Chem.* **269,** 13637–13643.

Beranger, F., Paterson, H., Powers, S., de Gunzburg, J., and Hancock, J. F. (1994b). The effector domain of Rab6, plus a hydrophobic C terminus, is required for Golgi apparatus localization. *Mol. Cell. Biol.* **14,** 744–758.

Berchtold, H., Reshetnikova, L., Reiser, C. O. A., Schirmer, N. K., Sprinzl, M., and Hilgenfeld, R. (1993). Crystal structure of active elongation factor Tu reveals major domain rearrangements. *Nature (London)* **365,** 126–132.

Bourmeyster, N., and Vignais, P. V. (1996). Phosphorylation of Rho GDI stabilizes the Rho A-Rho GDI complex in neutrophil cytosol. *Biochem. Biophys. Res. Commun.* **218,** 54–60.

Bourne, H. R. (1988). Do GTPases direct membrane traffic in secretion? *Cell* **53,** 669–671.

Bourne, H. R., Sanders, D. A., McCormick, F. (1990). The GTPase superfamily: A conserved switch for diverse cell functions. *Nature (London)* **348,** 125–132.

Bowser, R., Müller, H., Govindan, B., and Novick, P. (1992). Sec8p and Sec15p are components of a plasma membrane-associated 19.5S particle that may function downstream of Sec4p to control exocytosis. *J. Cell. Biol.* **118,** 1041–1056.

Brauers, A., Schürmann, A., Massman, S., MMühl-Zürbes P., Becker, W., Kainulainen, H., Lie, C., and Joost, H.-G. (1996). Alternative mRNA splicing of the novel GTPase Rab28 generates isoforms with different C-termini. *Eur. J. Biochem.* 237, 833–840.

Brennwald, P., and Novick, P. (1993). Interactions of three domains distinguishing the Ras-related GTP-binding proteins Ypt1p and Sec4p. *Nature (London)* **365,** 560–563.

Brennwald, P., Kearns, B., Champion, K., Keränen, S., Bankaitis, V., and Novick, P. (1994). Sec9 is a SNAP-25-like component of a yeast SNARE complex that may be the effector of Sec4 function in exocytosis. *Cell* **79,** 245–258.

Broadie, K., Prokop, A., Bellen, H. J., O'Kane, C. J., Schulze, K. L., and Sweeney, S. T. (1995). *Neuron* **15,** 663–673.

Brondyk, W. H., McKiernan, C. J., Fortner, K. A., Stabila, P., Holz, R. W., and Macara, I. G. (1995). Interaction cloning of Rabin3, a novel protein that associates with the Ras-like GTPase Rab3A. *Mol Cell Biol.***15,** 1137–1143.

Bucci, C., Frunzio, R., Chiarotti, R., Brown, L., Rechler, M. M., and Bruni, C. B. (1988). A new member of the ras gene superfamily identified in a rat liver cell line. *Nucleic Acids Res.* **16,** 9979–9993.

Bucci, C., Parton, R. G., Mather, I. H., Stunnenberg, H., Simons, K., Hoflack, B., and Zerial, M. (1992). The small GTPase rab5 functions as a regulatory factor in the early endocytic pathway. *Cell***70,** 715–728.

Bucci, C., Wandinger-Ness, A., Lütcke, A., Chiariello, M., Bruni, C. B., and Zerial, M. (1994). Rab5a is a common component of the apical and basolateral endocytic machinery in polarized epithelial cells. *Proc. Natl. Acad. Sci. USA* **91,** 5061–5065.

Bucci, C., Lütcke, A., Steele-Mortimer, O., Olkkonen, V. M., Dupree, P., Chiariello, M., Bruni, C. B., Simons, K., and Zerial, M. (1995). Co-operative regulation of endocytosis by three Rab5 isoforms. *FEBS Lett.* **366,** 65–71.

Burd, C. G., Mustol, P. A., Schu, P. V., and Emr, S. D. (1996). A yeast protein related to a mammalian ras-binding protein, Vps9p, is required for localization of vacuolar proteins. *Mol. Cell. Biol.* **16,** 2369–2377.

Burgess, T. L., and Kelly, R. B. (1987). Constitutive and regulated secretion of proteins. *Annu. Rev. Cell Biol.* **3,** 243–293.

Burstein, E. S., and Macara, I. G. (1992). Characterization of a guanine nucleotide-releasing factor and a GTPase-activating protein that are specific for the ras-related protein p25rab3A. *Proc. Natl. Acad. Sci. USA* **89,** 1154–1158.

Burstein, E. S., Brondyk, W. H., and Macara, I. G. (1992). Amino acid residues in the Ras-like GTPase Rab3A that specify sensitivity to factors that regulate the GTP/GDP cycling of Rab3A. *J. Biol. Chem.* **267,** 22715–22718.

Burton, J., Roberts, D., Montaldi, M., Novick, P., and De Camilli, P. (1993). A mammalian guanine-nucleotide-releasing protein enhances function of yeast secretory protein Sec4. *Nature* (*London*) **361,** 464–467.

Burton, J. L., Burns, M. E., Gatti, E., Augustine, G. J., and De Camilli, P. (1994). Specific interactions of Mss4 with members of the Rab GTPase subfamily. *EMBO J.* **13,** 5547–5558.

Chapman, E. R., An, S., Barton, N., and Jahn, R. (1994). SNAP-25, a t-SNARE which binds to both syntaxin and synaptobrevin via domains that may form coiled coils. *J. Biol. Chem.* **269,** 27427–27432.

Chavrier, P. (1995). Rab21. *In* "Guidebook to the Small GTPases" (M. Zerial and L. A. Huber, Eds.), pp. 365–366. Oxford Univ. Press, London.

Chavrier, P., Parton, R. G., Hauri, H. P., Simons, K., and Zerial, M. (1990a). Localization of low molecular weight GTP binding proteins to exocytic and endocytic compartments. *Cell* **62,** 317–329.

Chavrier, P., Vingron, M., Sander, C., Simons, K., and Zerial, M. (1990b). Molecular cloning of YPT1/SEC4-related cDNAs from an epithelial cell line. *Mol. Cell. Biol.* **10,** 6578–6585.

Chavrier, P., Gorvel, J-P., Stelzer, E. Simons, K., Gruenberg, J., and Zerial, M. (1991). Hypervariable C-terminal domain of rab proteins acts as a targeting signal. *Nature* (*London*) 353, 769–772.

Chavrier, P., Simons, K., and Zerial, M. (1992). The complexity of the Rab and Rho GTP-binding protein subfamilies revealed by a PCR cloning approach. *Gene* **112,** 261–264.

Chen, D., Guo, J., Miki, T., Tachibana, M., and Gahl, A. W. (1996). Molecular cloning of two novel rab genes from human melanocytes. *Gene* **174,** 129–134.

Chen, Y-T., Holcomb, C., and Moore, H-P. P. (1993). Expression and localization of two low molecular weight GTP-binding proteins, Rab8 and Rab 10, by epitope tag. *Proc. Natl. Acad. Sci. USA* **90,** 6508- 6512.

Christensen, E. I., and Nielsen, S. (1991). Structural and functional analysis of protein handling in the kidney proximal tubule. *Semin. Nephrol.* 11, 414–439.

Chung, S. H., Takai, Y., and Holz, R. W. (1995). Evidence that the Rab3a-binding protein, rabphilin3a, enhances regulated secretion. Studies in adrenal chromaffin cells. *J. Biol. Chem.* **270,** 16714–16718.

Colombo, M. I., Taddese, M., Whiteheart, S. W., and Stahl, P. D. (1996). A possible predocking attachment site for N-ethylmaleimide-sensitive fusion protein—Insights from in vitro endosome fusion. *J. Biol. Chem.* **271,** 18810-18816.

Conradt, B., Haas, A., and Wickner, W. (1994). Determination of four biochemically distinct, sequential stages during vacuole inheritance in vitro. *J. Cell Biol.* **126,** 99–110.

Coorssen, J. R., Schmitt, H., and Almers, W. (1996). Ca^{2+}-triggers massive exocytosis in Chinese hamster ovary cells. *EMBO J.* **15,** 3787–3791.

Cormont, M., Tanti, J.-F., Zahraoui, A., Van Obberghen, E., Tavitian, A., and Le Marchand-Brustel, Y. (1993). Insulin and okadaic acid induce Rab4 redistribution in adipocytes. *J. Biol. Chem.* **268,** 19491–19497.

Cormont, M., Tanti, J.-F., Zahraoui, A., Van Obberghen, E., and Le Marchand-Brustel, Y. (1994). Rab4 is phosphorylated by the insulin-activated extracellular-signal-regulated kinase ERK1. *Eur. J. Biochem.* **219,**1081-1085.

Craighead, M. W., Bowden, S., Watson, R., and Armstrong, J. (1993). Function of the ypt2 gene in the exocytic pathway of Schizosaccharomyces pombe. *Mol. Biol. Cell.* **4,** 1069–1076.

Cremers, F. P. M., Armstrong, S. A., Seabra, M. C., Brown, M. S., and Goldstein, J. L. (1994). REP-2, a rab escort protein encoded by the choroideremia-like gene. *J. Biol. Chem.* **269,** 2111–2117.

Cui, S., and Christensen, E. I. (1993). Three-dimensional organization of the vacuolar apparatus involved in endocytosis and membrane recycling of rat kidney proximal tubule cells. *Exp. Nephrol.* **21,** 175–184.

Darchen, F., Zahraoui, A., Hammel, F., Minteils, M-P., Tavitian, A., and Scherman, D. (1990). Association of the GTP-binding protein Rab3A with bovine adrenal chromaffin granules. *Proc. Natl. Acad. Sci. USA* **87,** 5692–5696.

Darchen, F., Senyshyn, J., Brondyk, W. H., Taatjes, D. J., Holz, R. W., Henry, J-P., Denizot, J-P., and Macara, I. G. (1995). The GTPase Rab3 is associated with large dense core vesicles in bovine chromaffin cells and rat PC12 cells. *J. Cell. Sci.* **108,** 1639–1649.

Daro, E., van der Sluijs, P., Galli, T., and Mellman, I. (1996). Rab4 and cellubrevin define different early endosome populations on the pathway of transferrin receptor recycling. *Proc. Natl. Acad. Sci. USA* **93,** 9559–9564.

D'Arrigo, A., Bucci, C., Toh, B.-H., and Stenmark, H. (1997). Microtubules are involved in Bafilomycin A1 induced tubulation and Rab5 dependent vacuolation of early endosomes. *Eur. J. Cell Biol.* **72,** 95–103.

Dascher, C., Ossig, R., Gallwitz, D., and Schmitt, H. D. (1990). Identification and structure of four yeast genes (SLY) that are able to suppress the functional loss of YPT1, a member of the RAS superfamily. *Mol. Cell. Biol.* **11,** 872–885.

Davidson, J. S., Eales, A., Roeske, R. W., and Millar, R. P. (1993). Inhibition of pituitary hormone exocytosis by a synthetic peptide related to the rab effector domain. *FEBS Lett.* **326,** 219–221.

De Camilli, P. (1995). Molecular mechanism in synaptic vesicle recycling. *FEBS Lett.* **369,** 3–12.

De Camilli, P., and Jahn, R. (1990). Pathways to regulated exocytosis in neurons. *Annu. Rev. Physiol.* **52,** 625–645.

de Hoop, M. J., Huber, L. A., Stenmark, H., Williamson, E., Zerial, M., Parton, R. G., and Dotti, C. G. (1994). The involvement of the small GTP-binding protein Rab5a in neuronal endocytosis. *Neuron* **13,** 11–22.

Denesvre, C., and Malhotra, V. (1996). Membrane fusion in organelle biogenesis. *Curr. Opin. Cell Biol.* **8,** 519–523.

Der, C. J., Finkel, T., and Cooper, G. M. (1986). Biological and biochemical properties of human ras^H genes mutated at codon 61. *Cell* **44,** 167–176.

Deretic, D., Huber, L. A., Ransom, N., Mancini, M., Simons, K., and Papermaster, D. S. (1995). Rab8 in retinal photoreceptors may participate in rhodopsin transport and in rod outer segment disk morphogenesis. *J. Cell Sci.* **108,** 215–224.

Dirac-Svejstrup, A. B., Soldati, T., Shapiro, A. D., and Pfeffer, S. R. (1994). Rab-GDI presents functional Rab9 to the intracellular transport machinery and contributes selectivity to Rab9 membrane recruitment. *J. Biol. Chem.* **269,** 15427–15430.

Donaldson, J. G., and Klausner, R. D. (1994). ARF: A key regulatory switch in membrane traffic and organelle structure. *Curr. Opin. Cell Biol.* **6,** 527–532.

Dotti, C. G., and Simons, K. (1990). Polarized sorting of viral glycoproteins to the axon and dendrites of hippocampal neurons in culture. *Cell* **62,** 63–72.

Drivas, G. T., Shih, A., Coutavas, E. E., D'Eustachio, P., and Rush, M. G. (1991). Identification and characterization of a human homolog of the Schizosaccharomyces pombe ras-like gene YPT-3. *Oncogene* **6,** 3–9.

Dunn, B., Stearns, T., and Botstein, D. (1993). Specificity domains distinguish the Ras-related GTPases Ypt1 and Sec4. *Nature (London)* **362,** 563–565.

Dykes, D. C., Friedman, F. K., Dykes, S. L., Murphy, R. B., Brandt-Rauf, P. W., and Pincus, M. R. (1993). Molecular dynamics of the H-ras gene-encoded p21 protein; Identification of flexible regions and possible effector domains. *J. Biomol. Struct. Dynamics.* **11,** 443–458.

Eaton, S., and Simons, K. (1995). Apical, basal, and lateral cues for epithelial polarization. *Cell.* **82,** 5–8.

Edelmann, L., Hanson, P. I., Chapman, E. R., and Jahn, R. (1995). Synaptobrevin binding to synaptophysin: A potential mechanism for controlling the exocytic fusion machine. *EMBO J.* **14,** 224–231.

Elferink, L. A., Anzai, K., and Scheller, R. H. (1992). Rab15, a novel low molecular weight GTP-binding protein specifically expressed in rat brain. *J. Biol. Chem.* **267,** 5768–5775.

Farnsworth, C. C., Kawata, M., Yoshida, Y., Takai, Y., Gelb, M. H., and Glomset, J. A. (1991). C terminus of the small GTP-binding protein smg p25A contains two geranylgeranylated residues and a methyl ester. *Proc. Natl. Acad. Sci. USA* **88,** 6196–6200.

Feig, L. A., and Cooper, G. M. (1988). Inhibition of NIH 3T3 cell proliferation by a mutant ras protein with preferential affinity for GDP. *Mol. Cell. Biol.* **8,** 3235–3243.

Feng, Y., Press, B., and Wandinger-Ness, A. (1995). Rab7: An important regulator of late endocytic membrane traffic. *J. Cell Biol.* **131,** 1435–1452.

Ferro-Novick, S., and Jahn, R. (1994). Vesicle fusion from yeast to man. *Nature (London)* **370,** 191–193.

Fischer von Mollard, G., Mignery, G. A., Baumert, M., Perin, M. S., Hanson, T. J., Burger, P. M., Jahn, R., and Südhof, T. C. (1990). Rab3 is a small GTP-binding protein exclusively localized to synaptic vesicles. *Proc. Natl. Acad. Sci. USA* **87,** 1988–1992.

Fischer von Mollard, G., Südhof, T. C., and Jahn, R. (1991). A small GTP-binding protein dissociates from synaptic vesicles during exocytosis. *Nature (London)* **349,** 79–81.

Fischer von Mollard, G., Stahl, B., Khokhlatchev, A., Südhof, T. C., and Jahn, R. (1994a). Rab3C is a synaptic vesicle protein that dissociates from synaptic vesicles after stimulation of exocytosis. *J. Biol. Chem.* **269,** 10971–10974.

Fischer von Mollard, G., Stahl, B., Walch-Solimena, C., Takei, K., Daniels, L., Khoklatchev, A., De Camilli, P., Südhof, T. C., and Jahn, R. (1994b). Localization of Rab5 to synaptic

vesicles identifies endosomal intermediate in synaptic vesicle recycling pathway. *Eur. J. Cell Biol.* **65,** 319–326.

Fujita, Y., Sasaki, T., Araki, K., Takahashi, K., Imazumi, K., Kato, M., Matsuura, Y., and Takai, Y. (1994). GDP/GTP exchange reaction-stimulating activity of Rabphilin-3A for Rab3A small GTP-binding protein. *FEBS Lett.* **353,** 67–70.

Fykse, E. M., Li, C., and Sudhof, T. C. (1995). Phosphorylation of rabphilin-3A by Ca^{2+}/calmodulin- and cAMP-dependent protein kinases in vitro. *J. Neurosci.* **15,** 2385–2395.

Galli, T., Garcia, E. P., Mundigl, O., Chilcote, T. J., and De Camilli, P. (1995). v- and t.SNAREs in neuronal exocytosis: A need for additional components to define sites of release. *Neuropharmacolog* **34,** 1351–1360.

Gallwitz, D., Donrath, C., and Sander, C. (1983). A yeast oncogene encoding a protein homologous to the human c-has/bas proto-oncogene product. *Nature (London)* **306,** 704–709.

Garrett, M. D., Zahner, J. E., Cheney, C. M., and Novick, P. J. (1994). *GDI1* encodes a GDP dissociation inhibitor that plays an essential role in the yeast secretory pathway. *EMBO J.* **13,** 1718–1728.

Geppert, M., Bolshakov, V. Y., Siegelbaum, S. A., Takei, K., De Camilli, P., Hammer, R. E., and Sudhof, T. C. (1994). The role of Rab3A in neurotransmitter release. *Nature (London)* **369,** 493–497.

Goldenring, J. R., Shen, K. R., Vaughan, H. D., and Modlin, I. M. (1993). Identification of a small GTP-binding protein, Rab25, expressed in the gastrointestinal mucosa, kidney, and lung. *J. Biol. Chem.* **268,** 18419–18422.

Goldenring, J. R., Smith, J., Vaughan, H. D., Cameron, P., Hawkins, W., and Navarre, J. (1996). Rab11 is an apically located small GTP-binding protein in epithelial tissues. *Am. J. Physiol.* **270,** G515–G525.

Gorvel, J. P., Chavrier, P., Zerial, M., and Gruenberg, J. (1991). rab5 controls early endosome fusion in vitro. *Cell* **64,** 915–925.

Goud, B., Salminen, A., Walworth, N. C., and Novick, P. J. (1988). A GTP-binding protein required for secretion rapidly associates with secretory vesicles and the plasma membrane in yeast. *Cell* **53,** 753–768.

Goud, B., Zahraoui, A., Tavitian, A., and Saraste, J. (1990). Small GTP-binding protein associated with Golgi cisternae. *Nature (London)* **345,** 553–556.

Griffiths, G., and Simons, K. (1986). The trans Golgi network: Sorting at the exit site of the Golgi complex. *Science* **234,** 438–443.

Gruenberg, J,. and Maxfield, F. R. (1995). Membrane transport in the endocytic pathway. *Curr. Opin. Cell Biol.* **7,** 552–563.

Haas, A., Scheglmann, D., Lazar, T., Gallwitz, D., and Wickner, W. (1995). The GTPase Ypt7p of Saccharomyces cerevisiae is required on both partner vacuoles for the homotypic fusion step of vacuole inheritance. *EMBO J.* **14,** 5258–5270.

Halachmi, N., and Lev, Z. (1996). The Sec1 family: A novel family of proteins involved in synaptic transmission and general secretion. *J. Neurochem.* **66,** 889–897.

Haubruck, H., Disela, C., Wagner, P., and Gallwitz, D. (1987). The ras-related ypt protein is an ubiquitous eukaryotic protein: Isolation and sequence analysis of mouse cDNA clones highly homologous to the yeast YPT1 gene. *EMBO J.* **6,** 4049–4053.

Haubruck, H., Prange, R., Vorgias, C., and Gallwitz, D. (1989). The ras-related mouse ypt1 protein can functionally replace the YPT1 gene product in yeast. *EMBO J.* **8,** 1427–1432.

Haubruck, H., Engelke, U., Mertins, P., and Gallwitz, D. (1990). Structural and functional analysis of ypt2, an essential ras-related gene in the fission yeast Schizosaccharomyces pombe encoding a Sec4 protein homologue. *EMBO J.* **9,** 1957–1962.

Hauri, H.-P., and Schweizer, A. (1992). The endoplasmic reticulum–Golgi intermediate compartment. *Curr. Opin. Cell Biol.* **4,** 600–608.

Hayashi, T., McMahon, H., Yamasaki, S., Binz, T., Hata, Y., Südhof, T. C., and Niemann, H. (1994). Synaptic vesicle membrane fusion complex: Action of clostridial neurotoxins on assembly. *EMBO J.* **13,** 5051–5061.

Hayashi, T., Yamasaki, S., Nauenburg, S., Binz, T., and Niemann, H. (1995). Disassembly of the reconstituted synaptic vesicle membrane fusion complex in vitro. *EMBO J.* **14,** 2317–2325.

Hengst, L., Lehmeier, T., and Gallwitz, D. (1990). The *ryh1* gene in fission yeast *Schizosaccharomyces pombe* encoding a GTP-binding protein related to ras, rho, and ypt: structure, expression, and identification of its human homologue. *EMBO J.* **9,** 1949–1955.

Hoffenberg, S., Sanford, J. C., Liu, S., Daniel, D. S., Tuvin, M., Knoll, B. J., Wessling-Resnick, M., and Dickey, B. F. (1995). Biochemical and functional characterization of a recombinant GTPase, Rab5, and two of its mutants. *J. Biol. Chem.* **270.** 5048–5056.

Holz, R. W., Brondyk, W. H., Senter, R. A., Kuizon, L., and Macara, I. G. (1994). Evidence for the involvement of Rab3A in Ca^{2+}-dependent exocytosis from adrenal chromaffin cells. *J. Biol. Chem.* **269,** 10229–10234.

Hopkins, C. R. (1992). Selective membrane protein trafficking: Vectorial flow and filter. *Trends Biochem. Sci.* **17,** 27–32.

Hopkins, C. R., Gibson, A., Shipman, M., Strickland, D. K., and Trowbridge, I. S. (1994). In migrating fibroblasts, recycling receptors are concentrated in narrow tubules in the pericentriolar area, and then routed to the plasma membrane of the leading lamella. *J. Cell Biol.* **125,** 1265–1274.

Horazdovsky, B. F., Busch, G. R., and Emr, S. D. (1994). VPS21 encodes a rab5-like GTP binding protein that is required for the sorting of yeast vacuolar proteins. *EMBO J.* **13,** 1297–1309.

Horazdovsky, B. F., DeWald, D. B., and Emr, S. D. (1995). Protein transport to the yeast vacuole. *Curr. Opin. Cell Biol.* **7,** 544–551.

Huber, L. A., de Hoop, M. J., Dupree, P., Zerial, M., Simons, K., and Dotti, C. (1993a). Protein transport to the dendritic plasma membrane of cultured neurons is regulated by rab8p. *J. Cell Biol.* **123,** 47–55.

Huber, L. A., Pimplikar, S., Parton, R. G., Virta, H., Zerial, M., and Simons, K. (1993b). Rab8, a small GTPase involved in vesicular traffic between the TGN and the basolateral plasma membrane. *J. Cell Biol.* **123,** 35–45.

Huber, L. A., Dupree, P., and Dotti, C. G. (1995). A deficiency of the small GTPase rab8 inhibits membrane traffic in developing neurons. *Mol. Cell. Biol.* **15,** 918–924.

Iida, H., Wang, L., Nishii, K., Ookuma, A., and Shibata, Y. (1996). Identification of Rab12 as a secretory granule-associated small GTP-binding protein in atrial myocytes. *Circ. Res.* **78,** 343–347.

Ikonen, E., Tagaya, M., Ullrich, O., Montecucco, C., and Simons, K. (1995). Different requirements for NSF, SNAP, and Rab proteins in apical and basolateral transport in MDCK cells. *Cell* **81,** 571–580.

James, D. E., Piper, R. C., and Slot, J. W. (1994). Insulin stimulation of GLUT-4 translocation: A model for regulated recycling. *Trends Cell Biol.* **4,** 120–126.

Jasmin, B. J., Goud, B., Camus, G., and Cartaud, J. (1992). The low molecular weight guanosine triphosphate-binding protein Rab6p associates with distinct post-Golgi vesicles in Torpedo marmorata electrocytes. *Neuroscience* **49,** 849–855.

Jedd, G., Richardson, C., Litt, R., and Segev, N. (1995). The Ypt1 GTPase is essential for the first two steps of the yeast secretory pathway. *J. Cell Biol.* **131,** 583–590.

Jena, B. P., Brennwald, P., Garrett, M. D., Novick, P., and Jamieson, J. D. (1992). Distinct and specific GAP activities in rat pancreas act on the yeast GTP-binding proteins Ypt1 and Sec4. *FEBS Lett.* **309,** 5–9.

Johannes, L., Lledo, P. M., Roa, M., Vincent, J. D., Henry, J. P., and Darchen, F. (1994). The GTPase Rab3a negatively controls calcium-dependent exocytosis in neuroendocrine cells. *EMBO J.* **13,** 2029-2037.

Johannes, L., Dossau, F., Clabecq, A., Henry, J.-P., Darchen, F., and Poulain, B. (1996). Evidence for a functional link between rab3 and the SNARE complex. *J. Cell Sci.* **109,** 2875–2884.

John, J., Rensland, H., Schlichting, I., Vetter, I., Borasio, G. D., Goody, R. S., and Wittinghofer, A. (1993). Kinetic and structural analysis of the Mg^{2+}-binding site of the guanine nucleotide-binding protein $p21^{H\text{-}ras}$. *J. Biol. Chem.* **268,** 923–929.

Johnston, P. A., Archer, B. T., III, Robinson, K., Mignery, G. A., Jahn, R., and Südhof, T. C. (1991). Rab3A attachment to the synaptic vesicle membrane mediated by a conserved polyiosprenylated carboxy-terminal sequence. *Neuron* **7,** 101–109.

Jones, S., Litt, R. J., Richardson, C. J., and Segev, N. (1995). Requirement of nucleotide exchange factor for Ypt1 GTPase mediated protein transport. *J. Cell Biol.* **130,** 1051–1061.

Jones, S. M., Crosby, J. R., Salamero, J., and Howell, K. E. (1993). A cytosolic complex of p62 and rab6 associates with TGN38/41 and is involved in budding of exocytic vesicles from the trans-Golgi network. *J. Cell Biol.* **122,** 775–788.

Jurnak, F. (1985). Structure of the GDP domain of EF-Tu and location of the amino acids homologous to ras oncogene proteins. *Science* **230,** 32–36.

Karniguian, A., Zahraoui, A., and Tavitian, A. (1993). Identification of small GTP-binding rab proteins in human platelets: Thrombin-induced phosphorylation of rab3B, rab6, and rab8 proteins. *Proc. Natl. Acad. Sci. USA* **90,** 7647–7651.

Kato, M., Sasaki, T., Imazumi, K., Takahashi, K., Araki, K., Shirataki, H., Matsuura, Y., Ishida, A., Fujisawa, H., and Takai, Y. (1994). Phosphorylation of Rabphilin-3A by calmodulin-dependent protein kinase II. *Biochem. Biophys. Res. Commun.* **205,** 1776–1784.

Khosravi-Far, R., Lutz, R. J., Cox, A. D., Conroy, L., Bourne, J. R., Sinensky, M., Balch, W. E., Buss, J. E., and Der, C. J. (1991). Isoprenoid modification of rab proteins terminating in CC or CXC motifs. *Proc. Natl. Acad. Sci. USA* **88,** 6264–6268.

Kinsella, B. T., and Maltese, W. A. (1991). Rab GTP-binding proteins implicated in vesicular transport are isoprenylated in vitro at cysteines within a novel carboxyl-terminal motif. *J. Biol. Chem.* **266,** 8540–8544.

Kishida, S., Shirataki, H., Sasaki, T., Kato, M., Kaibuchi, K., and Takai, Y. (1993). Rab3A GTPase-activating protein-inhibiting activity of Rabphilin-3A, a putative Rab3A target protein. *J. Biol. Chem.* **268,** 22259–22261.

Koda, T., and Kakinuma, M. (1993). Molecular cloning of a cDNA encoding a novel small GTP-binding protein.*FEBS Lett.* **328,** 21–24.

Koh, S., Yamamoto, A., Inoue, A., Inoue, Y., Akagawa, K., Kawamura, Y., Kawamoto, K., and Tashiro, Y. (1993). Immunoelectron microscopic localization of the HPC-1 antigen in rat cerebellum. *J. Neurocytol.* **22,** 995–1005.

Komuro, R., Sasaki, T., Orita, S., Maeda, M., and Takai, Y. (1996). Involvement of rabphilin-3A in Ca^{2+}-dependent exocytosis from PC12 cells. *Biochem. Biophys. Res. Commun.* **219,** 435–440.

Kreis, T. E., Lowe, M., and Pepperkok, R. (1995). COPs regulating membrane traffic. *Annu. Rev. Cell Dev. Biol.* **11,** 677–706.

LaCour, T. F. M., Nyborg, J., Thirup, S., and Clark, B. F. C. (1985). Structural details of the binding of guanosine diphosphate to elongation factor Tu from E. coli as studied by X-ray crystallography. *EMBO J.* **4,** 2385–2388.

Lai, F., Stubbs, L., and Artzt, K. (1994). Molecular analysis of mouse Rab11b: A new type of mammalian YPT/Rab protein. *Genomics* **22,** 610–616.

Lamaze, C., Chuang, T. H., Terlecky, L. J., Bokoch, G. M., and Schmid, S. L. (1996). Regulation of receptor-mediated endocytosis by Rho and Rac. *Nature* (*London*) **382,** 177–179.

Law, G. J., Northrop, A. J., and Mason, W. T. (1993). Rab3-peptide stimulates exocytosis from mast cells via a pertussis toxin-sensitive mechanism. *FEBS Lett.* **333,** 56–60.

Leung, T., Manser, E., Tan, L., and Lim, L. (1995). A novel serine/threonine kinase binding the Ras-related RhoA GTPase which translocates the kinase to peripheral membranes. *J. Biol. Chem.* **270,** 29051–29054.

Li, B. J., and Warner, J. R. (1996). Mutation of the Rab6 homologue of Saccharomyces cerevisiae, YPT6, inhibits both early Golgi function and ribosome biosynthesis. *J. Biol. Chem.* **271,** 16813–16819.

Li, C., Takei, K., Geppert, M., Daniell, L., Stenius, K., Chapman, E. R., Jahn, R., De Camilli, P., and Südhof, T. C. (1994). Synaptic targeting of rabphilin-3A, a synaptic vesicle Ca2+/phospholipid-binding protein, depends on rab3A/3C. *Neuron* **13,** 885–898.

Li, G., Barbieri, M. A., Colombo, M. I., and Stahl, P. D. (1994). Structural features of the GTP-binding defective Rab5 mutants required for their inhibitory activity on endocytosis. *J. Biol. Chem.* **269,** 14631–14635.

Lian, J. P., and Ferro-Novick, S. (1993). Bos1p, an integral membrane protein of the endoplasmic reticulum to Golgi transport vesicles, is required for their fusion competence. *Cell* **73,** 735–745.

Lian, J. P., Stone, S., Jiang, Y., Lyons, P., and Ferro-Novick, S. (1994). Ypt1p implicated in v-SNARE activation. *Nature* (*London*) **372,** 698–701.

Lledo, P. M., Vernier, P., Vincent, J. D., Mason, W. T., and Zorec, R. (1993). Inhibition of Rab3B expression attenuates Ca(2+)-dependent exocytosis in rat anterior pituitary cells. *Nature* (*London*) **364,** 540–544.

Lledo, P. M., Johannes, L., Vernier, P., Zorec, R., Darchen, F., Vincent, J. D., Henry, J. P., and Mason, W. T. (1994). Rab3 proteins: Key players in the control of exocytosis. *Trends Neurosci.* **17,** 426–432.

Lombardi, D., Soldati, T., Riederer, M. A., Goda, Y., Zerial, M., and Pfeffer, S. R. (1993). Rab9 functions in transport between late endosomes and the trans Golgi network. *EMBO J.* **12,** 677–682.

Luo, L., Liao, Y. J., Jan, L. Y., and Jan, Y. N. (1994). Distinct morphogenetic functions of similar small GTPases: Drosophila Drac1 is involved in axonal outgrowth and myoblast fusion. *Genes Dev.* **8,** 1787–1802.

Lütcke, A., Jansson, S., Parton, R. G., Chavrier, P., Valencia, A., Huber, L. A., Lehtonen, E., and Zerial, M. (1993). Rab17, a novel small GTPase, is specific for epithelial cells and is induced during cell polarization. *J. Cell Biol.* **121,** 553–564.

Lütcke, A., Parton, R. G., Murphy, C., Olkkonen, V. M., Dupree, P., Valencia, A., Simons, K., and Zerial, M. (1994). Cloning and subcellular localization of novel rab proteins reveals polarized and cell type-specific expression. *J. Cell Sci.* **107,** 3437–3448.

Lütcke, A., Olkkonen, V. M., Dupree, P., Lütcke, H., Simons, K., and Zerial, M. (1995). Isolation of a murine cDNA cDNA clone encoding Rab19, a novel tissue-specific small GTPase. *Gene* **155,** 257–260.

MacLean, C. M., Law, G. J., and Edwardson, J. M. (1993). Stimulation of exocytotic membrane fusion by modified peptides of the rab3 effector domain: Re-evaluation of the role of rab3 in regulated exocytosis. *Biochem. J.* **294,** 325–328.

Manser, E., Leung, T., Salihuddin, H., Tan, L., and Lim, L. (1993). A non-receptor tyrosine kinase that inhibits the GTPase activity of $p21^{cdc42}$. *Nature* (*London*) **363,** 364–367.

Manser, E., Leung, T., Salihuddin, H., Zhao, Z.-S., and Lim, L. (1994). A brain serine/threonine protein kinase activated by cdc42 and Rac1. *Nature* (*London*) **367,** 40–46.

Marshall, C. J. (1996). Ras effectors. *Curr. Opin. Cell Biol.* **8,** 197–204.

Marshall, M. S. (1993). The effector interactions of $p21^{ras}$. *Trends Biochem. Sci.* **18,** 250–254.

Marshall, M. S. (1995). Ras target proteins in eukaryotic cells. *FASEB J.* **9,** 1311–1318.

Martelli, A. M., Bareggi, R., Baldini, G., Scherer, P. E., Lodish, H. F., and Baldini, G. (1995). Diffuse vesicular distribution of Rab3D in the polarized neuroendocrine cell line AtT-20. *FEBS Lett.* **368,** 271– 275.

Martinez, O., Schmidt, A., Salamero, J., Hoflack, B., Roa, M., and Goud, B. (1994). The small GTP-binding protein rab6 functions in intra-Golgi transport. *J. Cell Biol.* **127,** 1575–1588.

Matsui, Y., Kikuchi, A., Kondo, J., Hishida, T., Teranishi, Y., and Takai, Y. (1988). Nucleotide and deduced amino acid sequences of a GTP-binding protein family with molecular weights of 25,000 from bovine brain. *J. Biol. Chem.* **263,** 11071–11074.

Matter, K., and Mellman, I. (1994). Mechanisms of cell polarity: Sorting and transport in epithelial cells. *Curr. Opin. Cell Biol.* **6,** 545–554.

Mayer, A., Wickner, W., and Haas, A. (1996). Sec18p (NSF)-driven release of Sec17p (α-SNAP) can precede docking and fusion of yeast vacuoles. *Cell* **85,** 83–94.

Mayer, T., Touchot, N., and Elazar, Z. (1996). Transport between cis and medial Golgi cisternae requires the function of the Ras-related protein Rab6. *J. Biol. Chem.* **271,** 16097–16103.

McKiernan, C. J., Stabila, P. F., and Macara, I. G. (1996). Role of the Rab3A-binding domain in targeting of Rabphilin-3A to vesicle membranes of PC12 cells. *Mol. Cell. Biol.* **16,** 4985–4995.

McMahon, H. T., Missler, M., Li, C., and Südhof, T. C. (1995). Complexins: Cytosolic proteins that regulate SNAP receptor function. *Cell* **83,** 111–119.

Medema, R. H., de Vries-Smits, A. M. M., van der Zon, G. C. M., Maassen, J. A., and Bos, J. L. (1993). Ras activation by insulin and epidermal growth factor through enhanced exchange of guanine nucleotides on $p21^{ras}$. *Mol. Cell. Biol.* **13,** 155–162.

Melancon, P., Glick, B. S., Malhotra, V., Weidman, P. J., Serafini, T., Gleason, M. L., Orci, L., and Rothman, J. E. (1987). Involvement of GTP-binding "G" proteins in transport through the Golgi stack. *Cell* **51,** 1053–1062.

Mellman, I., and Simons, K. (1992). The Golgi complex: In vitro veritas? *Cell* **68,** 829–840.

Meresse, S., Gorvel, J.-P., and Chavrier, P. (1995). The rab7 GTPase resides on a vesicular compartment connected to lysosomes. *J. Cell Sci.* **108,** 3349–3358.

Milburn, M. V., Tong, L., deVos, A. M., Brünger, A., Yamaizumi, Z., Nishimura, S., and Kim, S.-H. (1990). Molecular switch for signal transduction: Structural differences between active and inactive forms of protooncogenic ras proteins. *Science* **247,** 939–945.

Miyake, S., and Yamamoto, M. (1990). Identification of ras-related, YPT family genes in Schizosaccharomyces pombe. *EMBO J.* **9,** 1417–1422.

Miyazaki, A., Sasaki, T., Araki, K., Ueno, N., Imazumi, K., Nagano, F., Takahashi, K., and Takai, Y. (1994). Comparison of kinetic properties between MSS4 and Rab3A GRF GDP/GTP exchange proteins. *FEBS Lett.* **350,** 333–336.

Mizoguchi, A., Kim, S., Ueda, T., and Takai, Y. (1989). Tissue distribution of smg p25A, a ras p21-like GTP-binding protein, studied by use of a specific monoclonal antibody. *Biochem. Biophys. Res. Commun.* **162,** 1438–1445.

Mizoguchi, A., Kim, S., Ueda, T., Kikuchi, A., Yorifuji, H., Hirokawa, N., and Takai, Y. (1990). Localization and subcellular distribution of smg p25A, a ras p21-like GTP-binding protein, in rat brain. *J. Biol. Chem.* **265,** 11872–11879.

Mizoguchi, A., Yano, Y., Hamaguchi, H., Yanagida, H., Ide, C., Zahraoui, A., Shirataki, H., Sasaki, T., and Takai, Y. (1994). Localization of Rabphilin-3A on the synaptic vesicle. *Biochem. Biophys. Res. Commun.* **202,** 1235–1243.

Moore, I., Schell, J., and Palme, K. (1995). Subclass-specific sequence motifs identified in Rab GTPases. *Trends Biochem. Sci.* **20,** 10–12.

Morgan, A., and Burgoyne, R. D. (1995). Is NSF a fusion protein? *Trends Cell Biol.* **5,** 335–339.

Morimoto, B. H., Chuang, C.-C., and Koshland, D. E., Jr. (1991). Molecular cloning of a member of a new class of low-molecular-weight GTP-binding proteins. *Genes Dev.* **5,** 2386–2391.

Mostov, K. E. (1995). Regulation of protein traffic in polarized epithelial cells. *Histol. Histopathol.* **10,** 423–431.

Moya, K. L., Tavitian, B., Zahraoui, A., and Tavitian, A. (1992). Localization of the ras-like rab3A protein in the adult rat brain. *Brain Res.* **590,** 118–127.

Moya, M., Roberts, D., and Novick, P. (1993). DSS4-1 is a dominant suppressor of sec4-8 that encodes a nucleotide exchange protein that aids Sec4p function. *Nature (London)* **361,** 460–463.

Munn, A. L., and Riezman, H. (1994). Endocytosis is required for the growth of vacuolar H(+)-ATPase-defective yeast: Identification of six new END genes. *J. Cell Biol.* **127,** 373–386.

Murphy, C., Saffrich, R., Grummt, M., Gournier, H., Rybin, V., Rubino, M., Auvinen, P., Lütcke, A., Parton, R. G., and Zerial, M. (1996). Endosome dynamics regulated by a Rho protein. *Nature (London)* **384,** 427–432.

Musha, T., Kawata, M., and Takai, Y. (1992). The geranylgeranyl moiety but not the methyl moiety of the smg-25A/rab3A protein is essential for the interactions with membrane and its inhibitory GDP/GTP exchange protein. *J. Biol. Chem.* **267,** 9821–9825.

Nagata, K., Satoh, T., Itoh, H., Kozasa, T., Okano, Y., Doi, T., Kaziro, Y., and Nozawa, Y. (1990). The ram: A novel low molecular weight GTP-binding protein cDNA from a rat megakaryocyte library. *FEBS Lett.* **275,** 29–32.

Nair, J., Muller, H., Peterson, M., and Novick, P. (1990). Sec2 protein contains a coiled-coil domain essential for vesicular transport and a dispensable carboxy terminal domain. *J. Cell Biol.* **110,** 1897–1909.

Nakajima, H., Hirata, A., Ogawa, Y., Yonehara, T., Yoda, K., and Yamasaki, M. (1991). A cytoskeletal-related gene, USO1, is required for intracellular protein transport in Saccharomyces cerevisiae. *J. Cell Biol.* **113,** 245–260.

Newman, A. P., and Ferro-Novick, S. (1987). Characterization of new mutants in the early part of the yeast secretory pathway isolated by a [^{3}H]mannose suicide selection. *J. Cell Biol.* **105,** 1587–1594.

Newman, A. P., Groesch, M. E., and Ferro-Novick, S. (1992a). Bos1p, a membrane protein required for ER to Golgi transport in yeast, co-purifies with the carrier vesicles and with Bet1p and the ER membrane. *EMBO J.* **11,** 3609–3617.

Newman, A. P., Graf, J., Mancini, P., Rossi, G., Lian, J. P., and Ferro-Novick, S. (1992b). SEC22 and SLY2 are identical. *Mol. Cell. Biol.* **12,** 3663–3664.

Newman, C. M. H., Giannakouros, T., Hancock, J. F., Fawell, E. H., Armstrong, J., and Magee, A. I. (1992). Post-translational processing of Scizosaccharomyces pombe YPT proteins. *J. Biol. Chem.* **267,** 11329–11336.

Ngsee, J. K., Elferink, L. A., and Scheller, R. H. (1991). A family of ras-like GTP-binding proteins expressed in electromotor neurons. *J. Biol. Chem.* **266,** 2675–2680.

Noel, J. P., Hamm, H. E., and Sigler, P. B. (1993). The 2.2 Å crystal structure of transducin-α complexed with GTPS. *Nature (London)* **366,** 654–663.

Novick, P., Field, C., and Schekman, R. (1980). Identification of 23 complementation groups required for post-translational events in the yeast secretory pathway. *Cell* **21,** 205–215.

Novick, P., Ferro, S., and Schekman, R. (1981). Order of events in the yeast secretory pathway. *Cell* **25,** 461–469.

Numata, S., Shirataki, H., Hagi, S., Yamamoto, T., and Takai, Y. (1994). Phosphorylation of Rabphilin-3A, a putative target protein for Rab3A, by cyclic AMP-dependent protein kinase. *Biochem. Biophys. Res. Commun.* **203,** 1927–1934.

Nuoffer, C., Davidson, H. W., Matteson, J., Meinkoth, J., and Balch, W. E. (1994). A GDP-bound rab1 inhibits protein export from the endoplasmic reticulum and transport between Golgi compartments. *J. Cell Biol.* **125,** 225–237.

Oberhauser, A. F., Monck, J. R., Balch, W. E., and Fernandez, J. M. (1992). Exocytotic fucion is activated by Rab3a peptides. *Nature (London)* **360,** 270–273.

Ohnishi, H., Ernst, S. A., Wys, N., McNiven, M., and Williams, J. A. (1996). Rab3D localizes to zymogen granules in rat pancreatic acini and other exocrine glands. *Am. J. Physiol.* **271,** G531–G538.

Olkkonen, V. M., Dupree, P., Killisch, I., Lütcke, A., Zerial, M., and Simons, K. (1993). Molecular cloning and subcellular localization of three GTP-binding proteins of the rab subfamily. *J. Cell Sci.* **106,** 1249–1261.

Olkkonen, V. M., Peterson, J. R., Dupree, P., Lütcke, A., Zerial, M., and Simons, K. (1994). Isolation of a mouse cDNA encoding Rab23, a small novel GTPase expressed predominantly in the brain. *Gene* **138,** 207–211.

Ossig, R., Dascher, C., Trepte, H.-H., Schmitt, H. D., and Gallwitz, D. (1991). The yeast SLY gene products, suppressors of defects in the essential GTP-binding Ypt1 protein, may act in endoplasmic reticulum-to-Golgi transport. *Mol. Cell. Biol.* **11,** 2980–2993.

Ossig, R., Laufer, W., Schmitt, H. D., and Gallwitz, D. (1995). Functionality and specific membrane localization of transport GTPases carrying C-terminal membrane anchors of synaptobrevin-like proteins. *EMBO J.* **14,** 3645–3653.

Padfield, P. J., Balch, W. E., and Jamieson, J. D. (1992). A synthetic peptide of the rab3a effector domain stimulates amylase release from permeabilized pancreatic acini. *Proc. Natl. Acad. Sci. USA* **89,** 1656–1660.

Pai, E. F., Kabsch, W., Krengel, U., Holmes, K. C., John, J., and Wittinghofer, A. (1989). Structure of the guanine-nucleotide-binding domain of the Ha-ras oncogene product p21 in the triphosphate conformation. *Nature (London)* **341,** 209–214.

Pai, E. F., Krengel, U., Petsko, G. A., Goody, R. S., Kabsch, W., and Wittinghofer, A. (1990). Refined crytal structure of the triphosphate conformation of H-ras p21 at 1.35 Å resolution: Implications for the mechanism of GTP hydrolysis. *EMBO J.* **9,** 2351–2359.

Palade, G. (1975). Intracellular aspects of the process of protein synthesis. *Science* **189,** 347–358.

Pelham, H. R. B. (1995). Sorting and retrieval between the endoplasmic reticulum and Golgi apparatus. *Curr. Opin. Cell Biol.* **7,** 530–535.

Peränen, J., Auvinen, P., Virta, H., Wepf, R., and Simons, K. (1996). Rab8 promotes polarized membrane transport through reorganization of actin and microtubules in fibroblasts. *J. Cell Biol.* **135,** 153–167.

Perez, F., Lledo, P. M., Karagogeos, D., Vincent, J. D., Prochiantz, A., and Ayala, J. (1994). Rab3A and Rab3B carboxy-terminal peptides are both potent and specific inhibitors of prolactin release by rat cultured anterior pituitary cells. *Mol. Endocrinol.* **8,** 1278–1287.

Peter, M., Chavrier, P., Nigg, E. A., and Zerial, M. (1992). Isoprenylation of rab proteins with structurally distinct cysteine motifs. *J. Cell Sci.* **102,** 857-865.

Pevsner, J., Hsu, S.-C., Braun, J. E. A., Calakos, N., Ting, A. E., Bennett, M. K., and Scheller, R. H. (1994). Specificity and regulation of a synaptic vesicle docking complex. *Neuron* **13,** 353–361.

Pfeffer, S. R. (1994). Rab GTPases: Master regulators of membrane trafficking. *Curr. Opin. Cell Biol.* **6,** 522–526.

Pfeffer, S. R., Dirac-Svejstrup, A. B., and Soldati, T. (1995). Rab GDP dissociation inhibitor: Putting Rab GTPases in the right place. *J. Biol. Chem.* **270,** 17057–17059.

Piiper, A., Stryjek-Kaminska, D., Stein, J., Caspary, W. F., and Zeuzem, S. (1993). A synthetic peptide of the effector domain of rab3A stimulates inositol 1,4,5-trisphosphate production in digitonin-permeabilized pancreatic acini. *Biochem. Biophys. Res. Commun.* **192,** 1030–1036.

Piiper, A., Stryjek-Kaminska, D., and Zeuzem, S. (1994). Synthetic Rab3A effector domain peptide stimulates inositol 1,4,5-trisphosphate production in various permeabilized cells. *Biochem. Biophys. Res. Commun.* **203,** 756–762.

Pind, S. N., Nuoffer, C., McCaffery, J. M., Plutner, H., Davidson, H. W., Farquhar, M. G., and Balch, W. E. (1994). Rab1 and Ca^{2+} are required for the fusion of carrier vesicles mediating endoplasmic reticulum to Golgi transport. *J. Cell Biol.* **125,** 239–252.

Plutner, H., Schwaninger, R., Pind, S., and Balch, W. E. (1990). Synthetic peptides of the Rab effector domain inhibit vesicular transport through the secretory pathway. *EMBO J.* **9,** 2375–2383.

Plutner, H., Cox, A. D., Pind, S., Khosravi-Far, R., Bourne, J. R., Schwaninger, R., Der, C. J., and Balch, W. E. (1991). Rab1b regulates vesicular transport between the endoplasmic reticulum and successive Golgi compartments. *J. Cell Biol.* **115,** 31–43.

Pryer, N. K., Wuestehube, L. J., and Schekman, R. (1992). Vesicle-mediated protein sorting. *Annu. Rev. Biochem.* **61,** 471–516.

Quilliam, L. A., Khosravi-Far, R., Huff, S. Y., and Der, C. J. (1995). Guanine nucleotide exchange factors: Activators of the Ras superfamily of proteins. *BioEssays* **17,** 395–404.

Raffaniello, R. D., Lin, J., Wang, F., and Raufman, J.-P. (1996). Expression of Rab3D in dispersed chief cells from guinea pig stomach. *Biochim. Biophys. Acta* **1311,** 11–116.

Regazzi, R., Kikuchi, A., Takai, Y., and Wollheim, C. B. (1992). The small GTP-binding proteins in the cytosol of insulin-secreting cells are complexed to GDP dissociation inhibitor proteins. *J. Biol. Chem.* **267,** 17512–17519.

Regazzi, R., Ravazzola, M., Iezzi, M., Lang, J., Zahraoui, A., Andereggen, E., Morel, P., Takai, Y., and Wollheim, C. B. (1996). Expression, localization and functional role of small GTPases of the Rab3 family in insulin-secreting cells. *J. Cell Sci.* **109,** 2265–2273.

Ren, M., Zeng, J., De Lemos-Chiarandini, C., Rosenfeld, M., Adesnik, M., and Sabatini, D. D. (1996). In its active form, the GTP-binding protein rab8 interacts with a stress-activated protein kinase. *Proc. Natl. Acad. Sci. USA* **93,** 5151–5155.

Richmond, J., and Haydon, P. G. (1993). Rab effector domain peptides stimulate the release of neurotransmitter from cell cultured synapses. *FEBS Lett.* **326,** 124–130.

Ridley, A. J., Paterson, H. F., Johnston, C. L., Diekmann, D., and Hall, A. (1992). The small GTP-binding protein rac regulates growth factor-induced membrane ruffling. *Cell* **70,** 401–410.

Riederer, M. A., Soldati, T., Shapiro, A. D., Lin, J., and Pfeffer, S. R. (1994). Lysosome biogenesis requires Rab9 function and receptor recycling from endosomes to the trans-Golgi network. *J. Cell Biol.* **125,** 573–582.

Rodriguez-Boulan, E., and Powell, S. K. (1992). Polarity of epithelial and neuronal cells. *Annu. Rev. Cell Biol.* **8,** 395–427.

Rosa, J. L., Casaroli-Marano, R. P., Buckler, A. J., Vilaró, S., and Barbacid, M. (1996). p619, a giant protein related to the chromosome condensation regulator RCC1, stimulates guanine nucleotide exchange on ARF1 and Rab proteins. *EMBO J.* **15,** 4262–4273.

Rothman, J. E. (1994). Mechanisms of intracellular protein transport. *Nature* (*London*) **372,** 55–63.

Rothman, J. E. (1996). The protein machinery of vesicle budding and fusion. *Protein Sci.* **5,** 185–194.

Rothman, J. E., and Warren, G. (1994). Implications of the SNARE hypothesis for intracellular membrane topology and dynamics. *Curr. Biol.* **4,** 220–233.

Rothman, J. E., and Wieland, F. T. (1996). Protein sorting by transport vesicles. *Science* **272,** 227–234.

Rybin, V., Ullrich, O., Rubino, M., Alexandrov, K., Simon, I., Seabra, M. C., Goody, R., and Zerial, M. (1996). GTPase activity of Rab5 acts as a timer for endocytic membrane fusion. *Nature* (*London*) **383,** 266–269.

Salamero, J., Sztul, E. S., and Howell, K. E. (1990). Exocytic transport vesicles generated in vitro from the trans-Golgi network carry secretory and plasma membrane proteins. *Proc. Natl. Acad. Sci. USA* **87,** 7717–7721.

Salminen, A., and Novick, P. J. (1987). A ras-like protein is required for a post-Golgi event in yeast secretion. *Cell* **49,** 527–538.

Salminen, A., and Novick, P. (1989). The Sec15 protein responds to the function of the GTP binding protein, Sec4, to control vesicular traffic in yeast. *J. Cell Biol.* **109,** 1023–1036.

Sander, C., and Valencia, A. (1995). The Ras superfamily. *In* "Guidebook to the Small GTPases" (M. Zerial and L.A. Huber, Eds.), pp. 12–20. Oxford Univ. Press, London.

Sanford, J. C., Pan, Y., and Wessling-Resnick, M. (1995a). Properties of Rab5 N-terminal domain dictate prenylation of C-terminal cysteines. *Mol. Biol. Cell* **6,** 71–85.

Sanford, J. C., Yu, J. M., Pan, J. Y., and Wessling-Resnick, M. (1995b). GDP dissociation inhibitor serves as a cytosolic acceptor for newly synthesized and prenylated Rab5. *J. Biol. Chem.* **270,** 26904–26909.

Sapperstein, S. K., Walter, D. M., Grosvenor, A. R., Heuser, J. E., and Waters, M. G. (1995). p115 is a general vesicular transport factor related to the yeast endoplasmic reticulum to Golgi transport factor Uso1p. *Proc. Natl. Acad. Sci. USA* **92,** 522–526.

Sapperstein, S. K., Lupashin, V. V., Schmitt, H. D., and Waters, M. G. (1996). Assembly of the ER to Golgi SNARE complex requires Uso1p. *J. Cell Biol.* **132,** 755–767.

Saraste, J., and Kuismanen, E. (1992). Pathways of protein sorting and membrane traffic between the rough endoplasmic reticulum and the Golgi complex. *Semin. Cell Biol.* **3,** 343–355.

Saraste, J., Lahtinen, U., and Goud, B. (1995). Localization of the small GTP-binding protein rab1p to early compartments of the secretory pathway. *J. Cell Sci.* **108,** 1541–1552.

Sasaki, T., Kikuchi, A., Araki, S., Hata, Y., Isomura, M., Kuroda, S., and Takai, Y. (1990). Purification and characterization from bovine brain cytosol of a protein that inhibits the dissociation of GDP from and the subsequent binding of GTP to smg p25A, a ras p21-like GTP-binding protein. *J. Biol. Chem.* **265,** 2333–2337.

Sato, H., Sugiyama, Y., Tsuji, A., and Horikoshi, I. (1996). Importance of receptor-mediated endocytosis in peptide delivery and targeting: Kinetic aspects. *Adv. Drug Delivery Rev.* **19,** 445–467.

Schalk, I., Zeng, K., Wu, S. K., Stura, E. A., Matteson, J., Huang, M. D., Tandon, A., Wilson, I. A., and Balch, W. E. (1996). Structure and mutational analysis of Rab GDP-dissociation inhibitor. *Nature (London)* **381,** 42–48.

Schekman, R. (1992). Genetic and biochemical analysis of vesicular traffic in yeast. *Curr. Opin. Cell Biol.* **4,** 587–592.

Schekman, R., and Orci, L. (1996). Coat proteins and vesicle budding. *Science* **271,** 1526–1533.

Schiavo, G., Gmachi, M. J. S., Stenbeck, G., Söllner, T. H., and Rothman, J. E. (1995). A possible docking and fusion particle for synaptic transmission. *Nature (London)* **378,** 733–736.

Schimmöller, F., and Riezman, H. (1993). Involvement of Ypt7p, a small GTPase, in traffic from late endosome to the vacuole in yeast. *J. Cell Sci.* **106,** 823–830.

Schlichting, I., Almo, S. C., Rapp, G., Wilson, K., Petratos, K., Lentfer, A., Wittinghofer, A., Kabsch, W., Pai, E. F., Petsko, G. A., and Goody, R. S. (1990). Time-resolved X-ray crystallographic study of the conformational change in Ha-Ras p21 protein on GTP hydrolysis. *Nature (London)* **345,** 309–315.

Schmitt, H. D., Wagner, P., Pfaff, E., and Gallwitz, D. (1986). The ras-related YPT1 gene product in yeast: A GTP-binding protein that might be involved in microtubule organization. *Cell* **47,** 401–412.

Schmitt, H. D., Puzicha, M., and Gallwitz, D. (1988). Study of a temperature-sensitive mutant of the ras-related YPT1 gene product in yeast suggests a role in the regulation of intracellular calcium. *Cell* **53,** 635–647.

Schulze, K. L., Littleton, J. T., Salzberg, A., Halachmi, N., Stern, M., Lev, Z., and Bellen, H. J. (1994). Rop, a Drosophila homolog of yeast Sec1 and vertebrate n-Sec1/Munc-18 proteins, is a negative regulator of neurotransmitter release in vivo. *Neuron* **13,** 1099–1108.

Schulze, K. L., Broadie, K., Perin, M. S., and Bellen, H. J. (1995). Genetic and electrophysiological studies of Drosophila syntaxin-1A demonstrate its role in nonneuronal secretion and neurotransmission. *Cell* **80,** 311–320.

Seabra, M. C. (1996). Nucleotide dependence of Rab geranylgeranylation—Rab escort protein interacts preferentially with GDP-bound Rab. *J. Biol. Chem.* **271,** 14398–14404.

Seabra, M. C., Brown, M. S., Slaughter, C. A., Südhof, T. C., and Goldstein, J. L. (1992a). Purification of component A of Rab geranylgeranyl transferase: Possible identity with the choroideremia gene product. *Cell* **70,** 1049–1057.

Seabra, M. C., Goldstein, J. L., Südhof, T. C., and Brown, M. S. (1992b). Rab geranylgeranyl transferase, a multisubunit enzyme that prenylates GTP-binding proteins terminating in Cys-X-Cys or Cys-Cys. *J. Biol. Chem.* **267,** 14497–14503.

Seabra, M. C., Brown, M. S., and Goldstein, J. L. (1993). Retinal degeneration in choroideremia: Deficiency of rab geranylgeranyl transferase. *Science* **259,** 377–381.

Seabra, M. C., Ho, Y. K., and Anant, J. S. (1995). Deficient geranylgeranylation of Ram/Rab27 in choroideremia. *J. Biol. Chem.* **270,** 24420–24427.

Segev, N. (1991). Mediation of the attachment or fusion step in vesicular transport by the GTP-binding Ypt1 protein. *Science* **252,** 1553–1556.

Segev, N., Mulholland, J., and Botstein, D. (1988). The yeast GTP-binding YPT1 protein and a mammalian counterpart are associated with the secretion machinery. *Cell* **52,** 915–924.

Senyshyn, J., Balch, W. E., and Holz, R. W. (1992). Synthetic peptides of the effector-binding domain of rab enhance secretion from digitonin-permeabilized chromaffin cells. *FEBS Lett.* **309,** 41–46.

Shapiro, A. D., and Pfeffer, S. R. (1995). Quantitative analysis of the interactions between prenyl Rab9, GDP dissociation inhibitor-α, and guanine nucleotides. *J. Biol. Chem.* **270,** 11085–11090.

Shen, F., and Seabra, M. C. (1996). Mechanism of digeranylgeranylation of rab proteins—Formation of a complex between monogeranylgeranyl-rab and rab escort protein. *J. Biol. Chem.* **271,** 3692–3698.

Shibata, H., Omata, W., Suzuki, Y., Tanaka, S., and Kojima, I. (1996). A synthetic peptide corresponding to the Rab4 hypervariable carboxyl-terminal domain inhibits insulin action on glucose transport in rat adipocytes. *J. Biol. Chem.* **271,** 9704–9709.

Shim, J., Newman, A. P., and Ferro-Novick, S. (1991). The BOS1 gene encodes an essential 27-kD putative membrane protein that is required for vesicular transport from the ER to the Golgi complex in yeast. *J. Cell Biol.* **113,** 55–64.

Shirataki, H., Kaibuchi, K., Yamaguchi, T., Wada, K., Horiuchi, H., and Takai, Y. (1992). A possible target protein for smg-25A/rab3A small GTP-binding protein. *J Biol Chem.* **267,** 10946–10949.

Shirataki, H., Kaibuchi, K., Sakoda, T., Kishida, S., Yamaguchi, T., Wada, K., Miyazaki, M., and Takai, Y. (1993). Rabphilin-3A, a putative target protein for smg p25A/rab3A p25 small GTP-binding protein related to synaptotagmin. *Mol. Cell. Biol.* **13,** 2061–2068.

Shirataki, H., Yamamoto, T., Hagi, S., Miura, H., Oishi, H., Jin-no, Y., Senbonmatsu, T., and Takai, Y. (1994). Rabphilin-3A is associated with synaptic vesicles through a vesicle protein in a manner independent of Rab3A. *J. Biol. Chem.* **269,** 32717–32720.

Simons, K. (1993). Biogenesis of epithelial cell surface polarity. *Harvey Lect.* **89,** 125–146.

Simons, K., and Ikonen, E. (1997). Sphingolipid-cholesterol rafts in membrane trafficking and signalling. *Nature,* in press.

Simons, K., and Zerial, M. (1993). Rab proteins and the road maps for intracellular transport. *Neuron* **11,** 789–799.

Simons, K., Dupree, P., Fiedler, K., Huber, L. A., Kobayashi, T., Kurzchalia, T., Olkkonen, V., Pimplikar, S., Parton, R., and Dotti, C. (1992). Biogenesis of cell-surface polarity in epithelial cells and neurons. *Cold Spring Harbor Symp. Quant. Biol.* **LVII,** 611–619.

Singer-Krüger, B., Stenmark, H., Düsterhöft, A., Philippsen, P., Yoo, J. S., Gallwitz, D., and Zerial, M. (1994). Role of three rab5-like GTPases, Ypt51p, Ypt52p, and Ypt53p, in the endocytic and vacuolar protein sorting pathways of yeast. *J. Cell Biol.* **125,** 283–298.

Singer-Krüger, B., Stenmark, H., and Zerial, M. (1995). Yeast Ypt51p and mammalian Rab5: Counterparts with similar function in the early endocytic pathway. *J. Cell Sci.* **108,** 3509–3521.

Smeland, T. E., Seabra, M. C., Goldstein, J. L., and Brown, M. S. (1994). Geranylgeranylated Rab proteins terminating in Cys-Ala-Cys, but not Cys-Cys, are carboxyl-methylated by bovine brain membranes in vitro. *Proc. Natl. Acad. Sci. USA* **91,** 10712–10716.

Søgaard, M., Tani, K., Ye, R. R., Geromanos, S., Tempst, P., Kirchhausen, T., Rothman, J. E., and Söllber, T. (1994). A Rab protein is required for the assembly of SNARE complexes in the docking of transport vesicles. *Cell* **78,** 937–948.

Soldati, T., Riederer, M. A., and Pfeffer, S. R. (1993). Rab GDI: A solubilizing and recycling factor for rab9 protein. *Mol. Biol. Cell* **4,** 425–434.

Soldati, T., Shapiro, A. D., Svejstrup, A. B., and Pfeffer, S. R. (1994). Membrane targeting of the small GTPase Rab9 is accompanied by nucleotide exchange [see comments]. *Nature* **369,** 76–78.

Soldati, T., Rancano, C., Geissler, H., and Pfeffer, S. R. (1995). Rab7 and Rab9 are recruited onto late endosomes by biochemically distinguishable processes. *J Biol Chem.* **270,** 25541–25548.

Söllner, T. (1995). SNAREs and targeted membrane fusion. *FEBS Lett.* **369,** 80–83.

Söllner, T., Bennett, M. K., Whiteheart, S. W., Scheller, R. H., and Rothman, J. E. (1993a). A protein assembly–disassembly pathway in vitro that may correspond to sequential steps of synaptic vesicle docking, activation, and fusion. *Cell* **75,** 409–418.

Söllner, T., Whiteheart, S. W., Brunner, M., Erdjument-Bromage, H., Geromanos, S., Tempst, P., and Rothman, J. E. (1993b). SNAP receptors implicated in vesicle targeting and fusion. *Nature* (*London*) **362,** 318–324.

Stack, J. H., and Emr, S. D. (1993). Genetic and biochemical studies of protein sorting to the yeast vacuole. *Curr. Opin. Cell Biol.* **5,** 641–646.

Stahl, B., von Mollard, G. F., Walch-Solimena, C., and Jahn, R. (1994). GTP cleavage by the small GTP-binding protein Rab3A is associated with exocytosis of synaptic vesicles induced by alpha-latrotoxin. *J. Biol. Chem.* **269,** 24770–24776.

Stahl, B., Chou, J. H., Li, C., Südhof, T. C., and Jahn, R. (1996). Rab3 reversibly recruits rabphilin to synaptic vesicles by a mechanism analogous to raf recruitment by ras. *EMBO J.* **15,** 1799–1809.

Steele-Mortimer, O., Gruenberg, J., and Clague, M. J. (1993). Phosphorylation of GDI and membrane cycling of rab proteins. *FEBS Lett.* **329,** 313–318.

Steele-Mortimer, O., Clague, M. J., Huber, L. A., Chavrier, P., Gruenberg, J., and Gorvel, J.-P. (1994). The N-terminal domain of a rab protein is involved in membrane–membrane recognition and/or fusion. *EMBO J.* **13,** 34–41.

Stenmark, H., Valencia, A., Martinez, O., Ullrich, O., Goud, B., and Zerial, M. (1994a). Distinct structural elements of rab5 define its functional specificity. *EMBO J.* **13,** 575–583.

Stenmark, H., Parton, R. G., Steele-Mortimer, O., Lütcke, A., Gruenberg, J., and Zerial, M. (1994b). Inhibition of rab5 GTPase activity stimulates membrane fusion in endocytosis. *EMBO J.* **13,** 1287–1296.

Stenmark, H., Vitale, G., Ullrich, O., and Zerial, M. (1995). Rabaptin-5 is a direct effector of the small GTPase Rab5 in endocytic membrane fusion. *Cell* **83,** 423–432.

Stettler, O., Nothias, F., Tavitian, B., and Vernier, P. (1995). Double in situ hybridization reveals overlapping neuronal populations expressing the low molecular weight GTPases Rab3a and Rab3b in rat brain. *Eur. J. Neurosci.* **7,** 702–713.

Stouten, P. F. W., Sander, C., Wittinghofer, A., and Valencia, A. (1993). How does the switch II region of G-domains work? *FEBS Lett.* **320,** 1–6.

Strom, M., Vollmer, P., Tan, T. J., and Gallwitz, D. (1993). A yeast GTPase-activating protein that interacts specifically with a member of the Ypt/Rab family. *Nature* (*London*) **361,** 736–739.

Su, Y.-C., Kao, L.-S., Chu, Y.-Y., Liang, Y., Tsai, M.-H., and Chern, Y. (1994). Distribution and regulation of Rab3c, a small molecular weight GTP-binding protein. *Biochem. Biophys. Res. Commun.* **200,** 1257–1263.

Südhof, T. C., and Rizo, J. (1996). Synaptotagmins: C_2-domain proteins that regulate membrane traffic. *Neuron* **17,** 379–388.

Südhof, T. C., De Camilli, P., Niemann, H., and Jahn, R. (1993). Membrane fusion machinery: Insights from synaptic proteins. *Cell* **75,** 1–4.

Tagaya, M., Toyonaga, S., Takahashi, M., Yamamoto, A., Fujiwara, T., Akagawa, K., Moriyama, Y., and Mizushima, S. (1995). Syntaxin 1 (HPC-1) is associated with chromaffin granules. *J. Biol. Chem.* **270,** 15930–15933.

Tagaya, M., Genma, T., Yamamoto, A., Kozaki, S., and Mizushima, S. (1996). SNAP-25 is present on chromaffin granules and acts as a SNAP receptor. *FEBS Lett.* **394,** 83–86.

Tan, T. J., Vollmer, P., and Gallwitz, D. (1991). Identification and partial purification of GTPase-activating proteins from yeast and mammalian cells that preferentially act on Ypt1/rab1 proteins. *FEBS Lett.* **291,** 322–326.

Tang, L. H., Stoch, S. A., Modlin, I. M., and Goldenring, J. R. (1992). Identification of rab2 as a tubulovesicle-membrane-associated protein is gastric parietal cells. *Biochem. J.* **285,** 715–719.

Tang, L. H., Gumkowski, F. D., Sengupta, D., and Modlin, I. M. (1996). Rab3D protein is a specific marker for zymogen granules in gastric chief cells of rats and rabbits. *Gastroenterology* **110,** 809–820.

TerBush, D. R., and Novick, P. (1995). Sec6, Sec8, and Sec15 are components of a multisubunit complex which localizes to small bud tips in Saccharomyces cerevisiae. *J. Cell Biol.* **130,** 299–312.

Ting, A. E., Hazuka, C. D., Hsu, S. C., Kirk, M. D., Bean, A. J., and Scheller, R. H. (1995). rSec6 and rSec8, mammalian homologs of yeast proteins essential for secretion. *Proc. Natl. Acad. Sci. USA* **92,** 9613–9617.

Tisdale, E. J., Bourne, J. R., Khosravi-Far, R., Der, C. J., and Balch, W. E. (1992). GTP-binding mutants of rab1 and rab2 are potent inhibitors of vesicular transport from the endoplasmic reticulum to the Golgi complex. *J. Cell Biol.* **119,** 749–761.

Touchot, N., Chardin, P., and Tavitian, A. (1987). Four additional members of the ras gene superfamily isolated by an oligonucleotide strategy: Molecular cloning of YPT-related cDNAs from a rat brain library. *Proc. Natl. Acad. Sci. USA* **84,** 8210–8214.

Tsukada, M., and Gallwitz, D. (1996). Isolation and characterization of SYS genes from yeast, multicopy suppressors of the functional loss of the transport GTPase Ypt6p. *J. Cell Sci.* **109,** 2471–2481.

Ullrich, O., Stenmark, H., Alexandrov, K., Huber, L. A., Kaibuchi, K., Sasaki, T., Takai, Y., and Zerial, M. (1993). Rab GDP dissociation inhibitor as a general regulator for the membrane association of rab proteins. *J. Biol. Chem.* **268,** 18143–18150.

Ullrich, O., Horiuchi, H., Bucci, C., and Zerial, M. (1994). Membrane association of Rab5 mediated by GDP-dissociation inhibitor and accompanied by GDP/GTP exchange. *Nature (London)* **368,** 157–160.

Ullrich, O., Reinsch, S., Urbe, S., Zerial, M., and Parton, R. G. (1996). Rab11 regulates recycling through the pericentriolar recycling endosome. *J. Cell Biol.* **135,** 913–924.

Urbe, S., Huber, L. A., Zerial, M., Tooze, S. A., and Parton, R. G. (1993). Rab11, a small GTPase associated with both constitutive and regulated secretory pathways in PC12 cells. *FEBS Lett.* **334,** 175–182.

Valencia, A., Chardin, P., Wittinghofer, A., and Sander, C. (1991). The ras protein family: Evolutionary tree and role of conserved amino acids. *Biochemistry* **30,** 4639–4648.

Valentijn, J. A., Sengupta, D., Gumkowski, F. D., Tang, L. H., Konieczko, E. M., and Jamieson, J. D. (1996). Rab3D localizes to secretory granules in rat pancreatic acinar cells. *Eur. J. Cell Biol.* **70,** 33–41.

van der Sluijs, P., Hull, M., Zahraoui, A., Tavitian, A., Goud, B., and Mellman, I. (1991). The small GTP-binding protein rab4 is associated with early endosomes. *Proc. Natl. Acad. Sci. USA* **88,** 6313–6317.

van der Sluijs, P., Hull, M., Huber, L. A., Mâle, P., Goud, B., and Mellman, I. (1992a). Reversible phosphorylation—Dephosphorylation determines the localization of rab4 during the cell cycle. *EMBO J.* **11,** 4379–4389.

van der Sluijs, P., Hull, M., Webster, P., Male, P., Goud, B., and Mellman, I. (1992b). The small GTP-binding protein rab4 controls an early sorting event on the endocytic pathway. *Cell* **70,** 729–740.

Vielh, E., Touchot, N., Zahraoui, A., and Tavitian, A. (1989). Nucleotide sequence of a rat cDNA: rab1B, encoding a rab1-YPT related protein. *Nucleic Acids Res.* **17,** 1770.

Vita, F., Soranzo, M. R., Borelli, V., Bertoncin, P., and Zabucchi, G. (1996). Subcellular localization of the small GTPase Rab5a in resting and stimulated human neutrophils. *Exp. Cell Res.* **227,** 367–373.

Vojtek, A. B., Hollenberg, S. M., and Cooper, J. A. (1993). Mammalian Ras interacts directly with the serine/threonine kinase Raf. *Cell* **74,** 205–214.

Volknandt, W., Pevsner, J., Elferink, L. A., and Scheller, R. H. (1993). Association of three small GTP-binding proteins with cholinergic synaptic vesicles. *FEBS Lett.* **317,** 53–56.

Wagner, A. C. C., Strowski, M. Z., Göke, B., and Williams, J. A. (1995). Molecular cloning of a new member of the Rab protein family, Rab26, from rat pancreas. *Biochem. Biophys. Res. Commun.* **207,** 950–956.

Walch-Solimena, C., Blasi, J., Edelmann, L., Chapman, E. R., Fischer von Mollard, G., and Jahn, R. (1995). The t-SNAREs syntaxin 1 and SNAP-25 are present on organelles that participate in synaptic vesicle recycling. *J. Cell Biol.* **128,** 637–645.

Walter, M., Clark, S. G., and Levinson, A. D. (1986). The oncogenic activation of human $p21^{ras}$ by a novel mechanism. *Science* **233,** 649–652.

Walworth, N. C., Goud, B., Kabcenell, A. K., and Novick, P. J. (1989). Mutational analysis of SEC4 suggests a cyclical mechanism for the regulation of vesicular traffic. *EMBO J.* **8,** 1685–1693.

Walworth, N. C., Brennwald, P., Kabcenell, A. K., Garrett, M., and Novick, P. (1992). Hydrolysis of GTP by Sec4 protein plays an important role in vesicular transport and is stimulated by a GTPase-activating protein in Saccharomyces cerevisiae. *Mol. Cell. Biol.* **12,** 2017–2028.

Warren, G. (1993). Membrane partitioning during cell division. *Annu. Rev. Biochem.* **62,** 323–348.

Warren, G., and Wickner, W. (1996). Organelle inheritance. *Cell* **84,** 395–400.

Waters, M. G., Clary, D. O., and Rothman, J. E. (1992). A novel 115-kD peripheral membrane protein is required for intercisternal transport in the Golgi stack. *J. Cell Biol.* **118,** 1015–1026.

Weber, E., Berta, G., Tousson, A., St. John, P., Green, M. W., Gopalokrishnan, U., Jilling, T., Sorscher, E. J., Elton, T. S., Abrahamson, D. R., *et al.* (1994). Expression and polarized targeting of a rab3 isoform in epithelial cells. *J. Cell Biol.* **125,** 583–594.

Weber, E., Jilling, T., and Kirk, K. L. (1996). Distinct functional properties of Rab3A and Rab3B in PC12 neuroendocrine cells. *J. Biol. Chem.* **271,** 6963–6971.

Whiteheart, S. W., and Kubalek, E. W. (1995). SNAPs and NSF: General members of the fusion apparatus. *Trends Cell Biol.* **5,** 64–68.

Wichmann, H., Hengst, L., and Gallwitz, D. (1992). Endocytosis in yeast: Evidence for the involvement of a small GTP-binding protein (Ypt7p). *Cell* **71,** 1131–1142.

Wilson, A. L., and Maltese, W. A. (1993). Isoprenylation of Rab1B is impaired by mutations in its effector domain. *J. Biol. Chem.* **268,** 14561–14564.

Wilson, A. L., Erdman, R. A., and Maltese, W. A. (1996). Association of Rab1B with GDP-dissociation inhibitor (GDI) is required for recycling but not initial membrane targeting of the Rab protein. *J. Biol. Chem.* **271,** 10932–10940.

Wilson, B. S., Nuoffer, C., Meinkoth, J. L., McCaffery, M., Feramisco, J. R., Balch, W. E., and Farquhar, M. G. (1994). A Rab1 mutant affecting guanine nucleotide exchange promotes disassembly of the Golgi apparatus. *J. Cell Biol.* **125,** 557–571.

Wilson, D. B., and Wilson, M. P. (1992). Identification and subcellular localization of human Rab5b, a new member of the Ras-related superfamily of GTPases. *J. Clin. Invest.* **89,** 996–1005.

Wilson, D. W., Whiteheart, S. W., Wiedmann, M., Brunner, M., and Rothman, J. E. (1992). A multisubunit particle implicated in membrane fusion. *J. Cell Biol.* **117,** 531–538.

Yamaguchi, T., Shirataki, H., Kishida, S., Miyazaki, M., Nishikawa, J., Wada, K., Numata, S., Kaibuchi, K., and Takai, Y. (1993). Two functionally different domains of rabphilin-

3A, Rab3A p25/smg p25A-binding and phospholipid- and Ca(2+)-binding domains. *J. Biol. Chem.* **268,** 27164–27170.

Yamashiro, D. J., Tycko, B., Fluss, S. R., and Maxfield, F. R. (1984). Segregation of transferrin to a mildly acidic (pH 6.5) para-Golgi compartment in the recycling pathway. *Cell* **37,** 789–800.

Yoshimori, T., Keller, P., Roth, M. G., and Simons, K. (1996). Different biosynthetic transport routes to the plasma membrane in BHK and CHO cells. *J. Cell Biol.* **133,** 247–256.

Yu, H., and Schreiber, S. L. (1995a). Cloning, Zn^{2+} binding, and structural characterization of the guanine nucleotide exchange factor human Mss4. *Biochemistry* **34,** 9103–9110.

Yu, H., and Schreiber, S. L. (1995b). Structure of guanine-nucleotide-exchange factor human Mss4 and identification of its Rab-interacting surface. *Nature (London)* **376,** 788–791.

Yu, H., Leaf, D. S., and Moore, H.-P. H. (1993). Gene cloning and characterization of a GTP-binding Rab protein from mouse pituitary AtT-20 cells. *Gene* **132,** 273–278.

Zahraoui, A., Touchot, N., Chardin, P., and Tavitian, A. (1989). The human Rab genes encode a family of GTP-binding proteins related to yeast YPT1 and SEC4 products involved in secretion. *J. Biol. Chem.* **264,** 12394–12401.

Zahraoui, A., Joberty, G., Arpin, M., Fontaine, J. J., Hellio, R., Tavitian, A., and Louvard, D. (1994). A small rab GTPase is distributed in cytoplasmic vesicles in nonpolarized cells but colocalizes with the tight junction marker ZO-1 in polarized epithelial cells. *J. Cell Biol.* **124,** 101–115.

Zhu, A. X., Zhao, Y., and Flier, J. S. (1994). Molecular cloning of two small GTP-binding proteins from human skeletal muscle. *Biochem. Biophys. Res. Commun.* **205,** 1875–1882.

This Page Intentionally Left Blank

Lignification in Plant Cell Walls

A. Ros Barceló
Department of Plant Biology, University of Murcia, E-30100 Murcia, Spain

Cell wall lignification is a complex process occurring exclusively in higher plants; its main function is to strengthen the plant vascular body. This process involves the deposition of ill-defined phenolic polymers, the so-called lignins, on the extracellular polysaccharidic matrix. These polymers arise from the oxidative coupling of three cinnamyl alcohols in a nonrandom reaction, in which cell wall polysaccharides appear to influence the freedom of cinnamyl alcohol radicals, giving rise to a highly orchestrated process. This review is focused on the most recent advances in the chemical, biochemical, cytological, physiological, and evolutive aspects of cell wall lignification. As we shall see throughout this review, there are still some open questions to be answered which may serve as the basis of future endeavors.

KEY WORDS: Cell walls, Lignins, Lignification, Gymnosperms, Angiosperms.

I. Introduction

Lignins (from the Latin *lignum:* wood) are complex cell wall phenolic heteropolymers covalently associated with both polysaccharides and proteins. Lignins have been identified in pteridophytes, widely considered to be the first vascular plants, and are likely to have played a key role in the colonization of the terrestrial landscape by plants in the early Devonian period, 400 to 450 million years ago (Lewis and Davin, 1994; Wallace and Fry, 1994). The deposition of lignins in the cell walls of higher terrestrial plants provides rigidity and structural support to the aerial axis. In xylem vessels, lignins contribute to resistance of the tensile forces of the water columns they contain, also imparting water impermeability. However, the impact of lignin quantity and quality on the chemical, physical, and mechanical properties of the cell wall remains to be evaluated.

Copyright © 1997 by Academic Press.
All rights of reproduction in any form reserved.

The ability to synthesize lignins is also considered to be a mechanism of disease resistance (Vance *et al.,* 1980) and has often been proposed as a possible initial selection pressure in favor of plants with lignified structures during the evolution of land flora. Likewise, it has also been suggested (Trenck and Sandermann, 1981) that the copolymerization of toxic xenobiotics with lignins may be an effective form for inactivating (and/or immobilizing) these dangerous metabolites. Thus, in all senses, the acquisition of lignified cell walls by land plants must be considered a major step in their evolution and adaptation to the earth.

Lignins represent the second most abundant organic compound on the earth's surface after cellulose and account for about 25% of the plant biomass (Higuchi, 1990). They occur in greatest quantity in the secondary cell walls of particular cells which form parts of woody tissues, such as fibers, xylem vessels, and tracheids. In smaller quantities, lignins are also located in the peridermal/endodermal cell layers, where they play a protective role, forming part of the suberin. However, there is a strong contrast between the abundance of these phenolic polymers and what we really know about them.

Lignins are amorphous and apparently optically inactive heteropolymers which result from the oxidative coupling of the three cinnamyl alcohols (Fig. 1), *p*-coumaryl, coniferyl, and sinapyl alcohol, giving rise within the lignin polymer to H (hydroxyphenyl), G (guaiacyl), and S (syringyl) units, respectively. Lignins exhibit a high degree of structural variability, which depends not only on the species and tissue but also on the cell type. This heterogeneity mainly concerns the relative proportion of the three constituent monomers, different types of interunit linkages, and the occurrence of nonconventional phenolic units within the polymer (Lapierre, 1993; Monties, 1985).

There are several unanswered questions concerning the lignification process and the metabolic pathway which leads from primary metabolism to lignins. In fact, many of the uncertainties in the order and mechanisms of

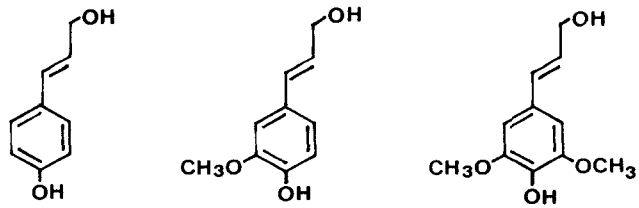

FIG. 1 Structure of *p*-coumaryl alcohol (**1**), coniferyl alcohol (**2**), and sinapyl alcohol (**3**).

the pathway discussed by Neish (1968) still exist today. At this point, it is necessary to remember the observation made by Sederoff *et al.* (1994), who emphasized that there is no single tissue or single plant species in which the entire pathway of lignin biosynthesis has been completely characterized. Rather, our actual knowledge has been inferred from studies of specific steps in evolutionarily diverse plant species.

Nevertheless, this knowledge has been sufficient to allow the characterization of several genes involved in the biosynthesis of lignins. This situation has stimulated several research programs aimed at modifying the lignin profiles of cultivated plants through genetic engineering, since lignins hinder efficient use of the plant biomass in the pulp and paper industry, and in animal husbandry, where crops are used as forage. Some of the corresponding strategies, which principally involve the down-regulation of specific genes which seem to control the quality or quantity of lignins, have been reviewed by Dean and Eriksson (1992), Boudet *et al.* (1996), and Boudet and Grima-Pettenati (1995).

It is the intent of this review to summarize some of the most recent data and to revise some basic concepts to help understand the recent progress made in several areas of cell wall lignification. Since extensive reviews have recently been published on various aspects of cell wall lignification (Higuchi, 1990; Lewis and Yamamoto, 1990; Whetten and Sederoff, 1995; Boudet *et al.*, 1995; Douglas, 1996), this review will confine itself to highlighting some of the most up-to-date results which are particularly significant and which may represent the basis for future endeavors.

II. Nature, Composition, and Distribution of Lignins

One of the main problems in studying the nature of lignins is the difficulty derived from their chemical analysis. In contrast to other polymers found in plant cell walls, a complete analysis of lignin structure has not been carried out. This is due to the fact that there is no existing analytical method which can provide a complete picture of the structure and, as mentioned by Boudet *et al.* (1996), it is unlikely that such an analytical method will be available in the near future. Our actual knowledge of lignin structure comes from introspection using many methods based on very different principles, which will be briefly described below (see III).

Lignins occur in cell walls of true vascular plants, ferns, and probably in club mosses, although there is some controversy in the last case (Lewis and Yamamoto, 1990). However, they are absent in those mosses, algae, and microorganisms which have no tracheids (Wardrop, 1971; Lewis and Yamamoto, 1990). From the botanical standpoint, the phenomenon of lignifica-

tion is essentially associated with development of the vascular system in the plant body.

Lignins are a complex hydrophobic network of phenylpropanoid units resulting from the oxidative coupling of one or more of the three types of cinnamyl alcohols (Fig. 1). Phenylpropane units are interconnected in lignins by a series of ether and carbon–carbon linkages, in various bonding patterns (Higuchi, 1990), leading to the following main substructures (Fig. 2): guaiacylglycerol-β-aryl ether, phenylcoumaran, diarylpropane, resinol, biphenyl, and diphenyl ether, as well as others of minor importance.

The most frequent inter-unit bonds, β-*O*-4, are present in guaiacylglycerol-β-aryl ether substructures and are the targets of most lignin depolymerization processes. In contrast, other bonds, such as β-5 (in phenylcoumaran), β-1 (in diarylpropane), β-β (in resinol), 5-5 (in biphenyl), and 5-*O*-4 (in diphenyl ether) interunit bonds, are very resistant toward degradation. Besides these main inter-unit linkages, there are minor ones, such as the β-6 bonds of phenylisochroman structures, or the noncyclic benzyl ether bonds, α-*O*-4 (Lapierre *et al.*, 1995). It is noteworthy that controversy still exists as to whether β-1 bonds and the noncyclic α-*O*-4 benzyl-aryl ethers

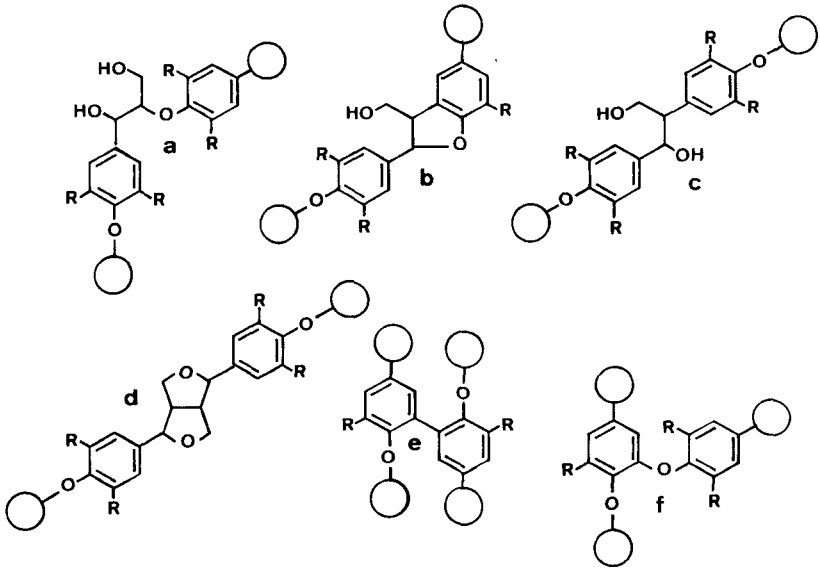

FIG. 2 Principal bonding patterns between the phenolic units in native lignins: guaiacylglycerol-β-aryl ether (**a**), phenylcoumaran (**b**), diarylpropane (**c**), resinol (**d**), biphenyl (**e**), and diphenyl ether (**f**). The pino-, medio-, and syringa-resinol structures involve 2G, 1G/1S, and 2S units. R: H or OCH_3.

are inter-unit linkages that are present in substantial or trace amounts in lignins. The prevailing idea is that both β-1 and α-*O*-4 substructures are mainly artifacts of isolation procedures (Ede and Brunow, 1990).

On the other hand, the fact that the three-monomer constituents of lignins differ as to the extent of their methoxylation (Fig. 1) means that a variety of substructures may be formed during polymerization. Thus, at the chemical level, lignins are ill-defined polymers whose monomeric composition is strongly variable as is the nature of their inter-unit linkages. This means that the expression "lignins" is preferable to the use of "lignin," since a great diversity of chemical structures probably exists within natural lignins (Boudet *et al.*, 1995).

By far, the greatest proportion of lignins found in vascular plants is deposited in cell walls of a limited number of cell types, such as tracheids, vessel elements, xylem and phloem fibers, and sclereids, with the nature of lignins differing according to cell type. For example, guaiacyl lignins predominate in the xylem of *Arabidopsis* stems, while adjacent, heavily lignified sclerenchyma cells contain mainly syringyl lignins (Chapple *et al.*, 1992).

Lignins may also vary within a given cell wall. In fact, lignin heterogeneity is regulated during secondary cell wall deposition to form layers of lignins that can differ both in the amount and in the average monomer composition. Thus, in xylem cell walls from conifers (Donaldson, 1985b), the lignin concentration in the secondary thickening is 16–27% (v/v), while the cell corner and middle lamella have a lignin content of 38–88% (v/v). Furthermore, lignins deposited in the middle lamella and the cell corners are rich in H units, while G lignins, which are the predominant type, are deposited in both the middle lamella and the secondary thickening (Terashima and Fukushima, 1989).

A. Differences between Gymnosperms and Angiosperms

The most distinctive variation in lignin content and lignin monomer composition in vascular plants is that found between the two main subphyla of spermatophyta. Thus, in gymnosperms, lignins are typically composed of G units with a minor proportion of H units, while in angiosperms lignin is mainly composed of G-S units (Higuchi, 1990). However, caution should be exercised in defining lignin composition as a function of taxonomy. For example, there are some gymnosperms in which S moieties predominate and some angiosperms in which lignins are principally of the G type (Lewis and Yamamoto, 1990).

In the case of Gramineae, Ralph *et al.* (1994a) have detected the presence of significant amounts of esterified *p*-coumaric acid in lignins. These data

suggesting the existence of possible ester and ether linkages of *p*-coumaric acid in gramineae lignins led Billa *et al.* (1996) to propose the occurrence of a G-S core in straw lignins, analogous to standard angiosperm lignins, onto which H derivative units are grafted in structures which are characterized by their differing susceptibility to degradation. Thus, during the course of evolution the chemical complexity of lignins may have increased from pteridophyte and gymnosperm lignins to grasses, the most developed plants, whose lignins appear to show the most complex composition.

Angiosperm and gymnosperm lignins not only differ in the relative amount of S/G units, but also in the abundance of the inter-unit bonds within the core lignin network. Thus, using thioacidolysis, Lapierre *et al.* (1995) have elegantly shown that lignins of woody angiosperms analyzed so far differ in the proportion of lineal lignin fragments linked through *β-O*-4 bonds from those found in woody gymnosperms and grass straws. Thus, whereas 60–65% of the C_6C_3 building blocks are essentially represented by *β-O*-4 bonds in woody angiosperm lignins, only 30% are so represented in gymnosperm lignins, and the percentage is even lower in grass lignins. Therefore, woody gymnosperm lignins are more highly branched through carbon–carbon inter-unit linkages than woody angiosperm lignins.

The determination of lignin-derived dimers in conifer lignins revealed that they were representative of the 5-5, *β*-5, *β*-1, and 4-*O*-5 bonds, whereas pinoresinol-derived dimers (*β-β*) were present in negligible amounts (Lapierre *et al.,* 1991). In the case of angiosperm lignins, the dimers recovered were principally representative of the *β*-1 and syringaresinol (*β-β*) structures (Nimz, 1974; Lapierre, 1993). Results obtained for native grass lignins have revealed (Lapierre, 1993) that the relative frequencies of the various recovered dimers are similar to the frequencies shown by angiosperm lignins, the most abundant dimers being representative of the *β*-1 and syringaresinol bonding patterns, followed by *β*-5 dimers and those arising from 4-*O*-5 and 5-5 bonds.

With regard to the terminal phenolic building blocks, it has been observed (Lapierre *et al.,* 1995) that H, G, and S units are not evenly distributed at the periphery or inside the core lignin network. In fact, among the uncondensed lignin structures, it has been found that about 90% of the H units in grass and compression wood lignins are terminal units with free phenolic groups. These results are in accordance with those described by Nose *et al.* (1995), who demonstrated that the incorporation of H units into the growing lignin polymer in *Pinus taeda* suspension cell cultures occurs later.

Finally, all these structural features of native lignins point to a highly controlled polymerization process. This process apparently gives rise to a structurally ordered polymer, predominantly composed of lineal *β-O*-4

linked fragments, and with a nonrandom distribution of the H, G, and S building blocks (Lapierre *et al.,* 1995).

B. Lignan and Other Lignin-like Compounds

Lignans and neolignans [(neo)lignans] are products which result from the oxidative coupling of two cinnamyl alcohols (and/or cinnamic acids), although other oligomeric forms can also exist (Lewis and Davin, 1994). Typically, they are found *in planta* as single enantiomeric forms, but racemic products are also encountered. Lignans are usually defined as phenylpropanoid units interconnected via β-β carbon–carbon linkages and, in this bonding pattern, they differ from neolignans, which are interconnected via linkages other than β-β (e.g., β-3, β-1, β-*O*-4, β-5, 3-*O*-4, etc.).

Some of the simplest and most abundant (neo)lignans (dehydrodiconiferyl alcohol, pinoresinol, syringaresinol, and guaiacylglycerol-β-*O*-coniferyl alcohol ether; Fig. 3) have structures found as building blocks in natural lignins, and there is no clear line of demarcation, in terms of either molecular size or structure, between oligomeric (neo)lignans and lignins (Lewis and Davin, 1994). This situation is accentuated by the fact that certain lignans (e.g., pinoresinol), and neolignans (e.g., dehydrodiconiferyl alcohol), are formed by the action of either laccase or peroxidase on coniferyl alcohol, although other uncharacterized cell wall oxidases (Davin *et al.,* 1992; Savidge and Udagama-Randeniya, 1992; McDougall *et al.,* 1994b) have also been reported as being involved in this process. It is worth noting that, in cases where the optical nature of products of the peroxidase (or laccase)-mediated reactions has been characterized, these products consti-

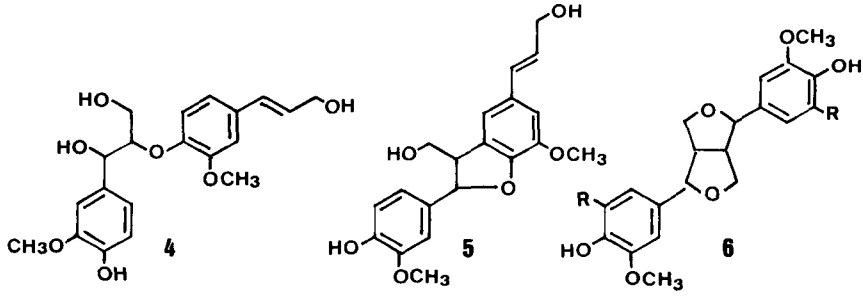

FIG. 3 Structures of the lignan guaiacylglycerol-β-*O*-coniferyl alcohol ether (**4**) and of the neolignans dehydrodiconiferyl alcohol (**5**), pinoresinol (**6**; R: H), and syringaresinol (**6**; R: OCH_3).

tute a mixture of 50% of each enantioisomer. In other words, they are racemic.

In spite of the fact that lignins are generally considered to be racemic, whereas (neo)lignans are generally optically active, (neo)lignans, such as pinoresinol, dehydrodiconiferyl alcohol, guaiacylglycerol-β-*O*-coniferyl alcohol, and syringaresinol, are often viewed as intermediaries, coupling forms of cinnamyl (coniferyl and syringyl) alcohols, which may undergo further polymerization by peroxidases to give lignins. Thus, it is worth noting that in *P. taeda* suspension cell cultures (SCCs) (Nose *et al.,* 1995), the scavenging of H_2O_2 blocks the formation of (neo)lignans (dehydrodiconiferyl alcohol, guaiacylglycerol-β-*O*-coniferyl alcohol, and pinoresinol, among others), and the simultaneous deposition of cell wall lignins, without affecting laccase activities or the level of the precursor (i.e., coniferyl alcohol). These results suggest that the formation of these (neo)lignans (and therefore of lignins) is exclusively mediated by a H_2O_2-consuming reaction and that these compounds may be used as building blocks for the synthesis of lignins.

Other specific types of (neo)lignans are those derived from dehydrodiferulic acid, particularly those arising from β-5, β-β, β-*O*-4, 4-*O*-5, and 5-5 radical coupling. These have been identified in grasses (Ralph *et al.,* 1994b) and conifers (Sánchez *et al.,* 1996) and appear to be involved in the cross-linking of hemicelluloses and pectins through ester bonds. It is worth noting that these products, similar to those derived from cinnamyl alcohols, are products typical of peroxidase-catalyzed reactions (Frías *et al.,* 1991; Wallace and Fry, 1994). It has been hypothesized (Lewis and Yammamoto, 1990) that these dehydrodimers, together with ester-bound single cinnamic acids, may act as anchoring sites for lignins in the cell wall polysaccharide matrix.

III. Lignin Detection and Analysis

Lignin analysis is generally an arduous labor due to the size, insolubility, and multiplicity of the functional groups and bonding patterns occurring in natural lignins. This means that, in order to unravel lignin structure, several analytical techniques must be used in combination. Obviously, the lack of a single analytical tool providing a complete and unequivocal picture of lignins makes the synergistic combination of such methods the only realistic approach to detect and to unravel the complex and heterogeneous nature of the lignin network.

On the other hand, because of the intractable nature of cell wall lignins, much of our actual knowledge of lignin structure comes from the character-

ization of lignin-derived monomeric, dimeric, and trimeric fragments released during solubilization procedures. It must be admitted, therefore, that although various pieces of the puzzle are known, they do not yet make up a clear picture of cell wall lignins although, from the plethora of products identified, various tentative schemes for lignin structure(s) have been proposed (Lewis and Yamamoto, 1990).

A. Histochemical and Cytochemical Probes in Lignin Detection

Since lignins have an extraordinarily high number of chemical functional groups they react with many different histochemical reagents to produce a vast array of colored products. The most commonly used histochemical tests are the toluidine blue O test, Wiesner's test (specific for cinnamaldehyde groups), and Mäule's reaction (specific for syringyl groups) (Strivastava, 1966). The most commonly used cytochemical probes for lignin detection are the stain with $KMnO_4$ and Coppick and Fowler's reaction (Czaninski, 1979).

B. Lignin Determination

Quantitative determinations of lignins may be achieved by various direct and indirect methods. The most widely used direct chemical methods include the preparations of "Klason lignins" and "thioglycolate lignins" (Effland, 1977). Spectrophotometric methods, such as the acetyl-bromide method (Johnson *et al.,* 1961; Iiyama and Wallis, 1988), which consists of the solubilization of lignins with acetyl bromide in glacial acetic acid, are only valuable with lignified cell walls of tissues (such as those derived from legumes and brassicas) that do not contain significant amounts of ester-bound cinnamic acids. Nevertheless, some protocols designed to avoid this interference when using grasses have been described (Morrison and Stewart, 1995).

The quantitative determination of lignins may also be made *in situ* by microscopy. The techniques most commonly used include UV microscopy (Scott *et al.,* 1969), which is based on the blue autofluorescence of lignins when they are illuminated with UV light, interference microscopy (Donaldson, 1985a), and bromination in conjunction with energy-dispersive X-ray analysis (Saka *et al.,* 1978). These techniques have the advantage over conventional microchemical methods in that not only the lignin content but also variations in lignin deposition may be studied through the primary

and through several layers of the secondary cell wall, something that can hardly be done by microchemical analysis.

C. Determination of the Lignin Monomer Composition

Methods to ascertain both the nature and the monomer composition of lignins include chemical and physical methods. The best method for ascertaining the presence of lignins in isolated cell walls, and their monomer composition, is chemical degradation. This can be achieved by nitrobenzene oxidation (Iiyama and Lam, 1990), permanganate oxidation (Erikson *et al.*, 1973), acidolysis (Lundquist and Kirk, 1971), and thioacidolysis (Lapierre, 1993) and provides a relatively easy and reliable procedure for qualitatively determining both the monomer composition and the inter-unit bonds. Chemical degradation of lignins results in products of low molecular weight, and from their amount and nature, one may obtain structural information about the units which make up the polymer. However, the main disadvantage of chemical degradation is that it only allows us to characterize the less condensed regions of lignins.

Alkaline nitrobenzene oxidation was introduced by Freudenberg *et al.* (1940) and represents a reference method which is still one of the most frequently used for the characterization of the monomer composition of lignins. It consists of treating lignified cell walls with nitrobenzene in a NaOH solution. H, G, and S units of lignins are released as *p*-hydroxybenzaldehyde, vanillin, and syringaldehyde, respectively. The production of these aldehydes is a good indicator that lignin is present, and they can be easily identified and quantified by HPLC (Billa *et al.*, 1996). The main problem associated with this method is that other cell wall phenolics, such as *p*-coumaric acid and ferulic acid, which are especially important in the cell walls of Gramineae, may interfere, since they are also oxidized to benzaldehydes. Likewise, alkaline nitrobenzene oxidation causes the shortening of lignin side chains and thus fails to provide information on their functionality and interconnections.

The best method for determining lignin monomer composition and the nature of most C-C and C-O-C bonds is thiacidolysis (Lapierre, 1993). This method consists of solvolysis of lignins in dioxane/ethanethiol, the target being the H, G, and S lignin units bound by labile β-*O*-4 bonds. Thus, only lignin units of the arylglycerol-β-aryl ether type are susceptible to thioacidolysis cleavage, and they afford C_6C_3 phenylpropane monomers with thioethylated side chains. These units, which are the structures most typical of native lignins, give rise to thioethylated H, G, and S monomers, with a high reaction yield.

Compared to alkaline oxidation, thioacidolysis provides more information on the core lignin structure, without interference from other cell wall phenolics. However, the monomer yield from alkaline nitrobenzene oxidation is higher than that from thiacidolysis. In fact, in the former case, monomers originate not only from β-*O*-4 uncondensed C_6C_3 units, but also partly from those involved in β-5, β-1, and β-β inter-unit bonds (Iiyama and Lam, 1990).

Recent developments of thioacidolysis involve methylation of lignin-free phenolic groups prior to thioacidolysis, which is performed to specifically characterize the terminal β-*O*-4 linked units that contain free-phenolic groups (Lapierre, 1993), and a further desulfurization step after the depolymerization step (Lapierre, 1993), through which a series of lignin-derived dimers, representative of the main condensed bonding patterns of native lignins, may be recovered and identified. This monomer and dimer analysis enables about 50–70% of native lignins to be characterized (Lapierre, 1993). Thioacidolysis has often been successfully used to estimate H and G units in grass lignins in which, due to the interference of *p*-coumaric and ferulic acid units, other methods (such as ^{13}C-NMR, analytical pyrolysis, and nitrobenzene oxidation) have failed.

Physical methods, such as analytical pyrolysis (Py), for ascertaining the presence of lignins and their monomer composition in isolated cell walls, are based on the thermal flash degradation of nonvolatile lignin material into a volatile degradation mixture in which, after separation by gas chromatography (GC), the individual components may be identified by mass spectrometry (MS) (Lapierre, 1993). The on-line Py–GC–MS profiles are molecular fingerprints of the lignin sample. To interpret these spectra, diagnostic ion markers of lignin units and components have been identified (Ralph and Hatfield, 1991).

D. Probing Lignin Structure *in Situ*

For most of the analytical techniques used to probe lignin structure, an indispensable preliminary step is the solubilization of lignins or of their fragments from cell walls. However, no method is capable of isolating lignins in their intact state. Most soluble lignin preparations, such as milled wood, dioxane, and kraft lignins, can only be obtained by vigorous cell wall treatment and, for this reason, they cannot be considered either qualitatively or quantitatively as representative of native lignins.

To date, the only available nondisruptive methods for investigating lignin structure are those involving the use of spectroscopy: NMR and Raman spectroscopy. These techniques may be used with soluble lignins and, potentially, with native lignins, since information may also be recovered from

the solid state (i.e., native lignified cell walls). This is the case with Raman spectroscopy (Atalla and Agarwal, 1985). Nevertheless, although this technique arose from the need to explore the molecular cell wall architecture, its usefulness for studying lignin structure *in situ* has lessened with time. This may be due to the fact that the main problem in using these techniques is that the information recovered from the spectra is restricted by the inherent broad signals and by the overlapping of a great number of peaks. In the case of NMR spectroscopy, the joint use of one-dimensional and two-dimensional multipulse techniques partly avoids the problem of peak overlap and simplifies spectral assignment (Ede and Brunow, 1990).

MR spectroscopy, and particularly ^{13}C-NMR spectroscopy, of lignins may be performed both in solution (Lüdemann and Nimz, 1973) and in solid state (Maciel *et al.*, 1985). ^{13}C-NMR spectroscopy constitutes a valuable tool in determining the type and amount of monomer building lignin units, the type of key functional groups, as well as for tracing the main C-C (or C-O-C) bonds (Lapierre, 1993).

One limitation of the technique is its low sensitivity, since it requires a large amount of sample, which in most cases hinders its solubility in NMR solvents. However, the rapid advances made in NMR instrumentation and sample preparation have permitted the creation of new NMR strategies for unraveling the complex spectra of lignins. This is the case in ^{31}P-NMR spectroscopy, both in solution and in solid state (Argyropoulos, 1995), in which lignins are phosphitylated with 1,3,2-dioxaphospholanyl chloride before the ^{31}P signal is analyzed.

IV. Model Systems for Studying Cell Wall Lignification

One of the most attractive models for studying cell wall lignification, as well as the metabolic and cytological changes associated with it, is to follow the pattern of vascular differentiation in stems and roots (Gahan, 1981). In these organs vascular development involves, in the first instance, the formation of procambium and, second, the overt cytodifferentiation of these procambial cells into lignifying xylem elements (vessels and fibers), and phloem elements (Fukuda, 1996). In axillary shoots, procambium and xylem elements are thought to differentiate acropetally, while the direction is basipetal in adventitious buds (Shininger, 1979). In the case of roots, the formation of lignifying tracheary elements (TEs) always follows a continuous acropetal sequence, and its advantage over the use of shoots is that there are no complications with terminal appendages. Therefore, roots are geometrically simple organs which show, in a true linear sequence, progressive stages of xylem element differentiation and lignin deposition,

so that TEs which differ as to the extent of cell wall lignification are arranged linearly from the meristem to the mature root region.

The biosynthesis of lignins is developmentally activated in specific tissues and cell types, such as xylem elements during vascular development (see above), but can also be activated in response to many environmental factors such as pathogen infection of cells that normally do not accumulate lignins (Vance *et al.*, 1980; Nicholson and Hammerschmidt, 1992). From this point of view, lignin genes which are transcriptionally silenced in certain cell types may be activated in response to fungal and bacterial elicitors, so that this system constitutes a special and valuable model for studying the nature of lignin-gene transcription regulating factors.

To date, the role of lignins in defense mechanisms has been considered to be of less importance than the role that they play in mechanical support and conduction. However, the synthesis of lignin-like compounds in response to microbial attack in charophycean green algae (Delwiche *et al.*, 1989), the presumed predecessors of land plants, suggests that the original role of lignins may indeed have been a defense-type reaction.

The chemical nature, regulation of spatial deposition, and the molecular mechanism involved in gene activation of disease-induced lignins are, at present, poorly understood. However, it appears evident that disease-induced lignins differ from constitutive lignins in their monomeric composition, which is also dependent upon an individual plant/pathogen interaction. Thus, whereas resistance in cucurbit leaves is associated with the deposition of enriched H lignins (Hammerschmidt *et al.*, 1985), resistance in wheat leaves is associated with the deposition of enriched S lignins (Southerton and Deverall, 1990).

Suberization, whether induced or not, of certain plant tissues may also be considered a model system for studying some aspect of cell wall lignification. Thus, detailed morphological and histochemical studies (see Kolattukudy, 1984) point to the existence of a lignin network within the suberin layer constitutive present in endodermal cells or formed in response either to mechanical wounding or to pathogen infection.

Suberin is a complex heteropolymer composed of aromatic and aliphatic domains (Kolattukudy, 1984). Although the phenolic (aromatic) core in suberized tissues resembles lignins with regard to histochemical staining and oxidation products, the structure of the phenolic core has remained obscure until recently. In 1984, Kolattukudy proposed a tentative model for the aromatic moiety of suberin in which H, G, and S units were interconnected by typical β-*O*-4 bonds. However, recent results suggest that although G and S units in suberin are involved in β-*O*-4 bonds, no H homologous compounds may be detected (Borg-Olivier and Monties, 1993; Lapierre *et al.*, 1996). Furthermore, when the nature of lignin-derived dimers involving G and S units was studied, it was concluded that the rel-

ative proportion was different from that observed in angiosperm lignins. Thus, the yield in the β-*O*-4 linked G and S units was about one-tenth of that obtained from xylem lignins (Lapierre *et al.*, 1996), whereas the yield of 4-*O*-5 (G-G and G-S) and 5-5 (G-G) interlinked units was somewhat greater (Lapierre *et al.*, 1996). These results suggest that the aromatic (lignin-like) domain of suberin shows a higher degree of cross-linking than that of wood lignins.

Studies on inducible lignification in SCCs have provided new insights into our knowledge of lignin biosynthesis. Thus, SCCs can be induced by a variety of stimuli to proceed through temporally controlled metabolic and developmental programs that conclude in the formation of single-cell-derived vascular TEs. The best characterized cell culture system used to study lignification is that derived from isolated *Zinnia* mesophyll cells. *Zinnia* mesophyll cultured cells can be induced to differentiate into cells resembling TEs in a medium containing suitable auxin and cytokinin levels (Church, 1993).

Cytological, ultrastructural, and biochemical changes associated with TE differentiation have recently been reviewed by Church (1993) and Fukuda (1996). In this system, the lignification of secondary cell wall thickening is a late event which occurs several hours after the initiation of cellulose deposition. Thus, during the course of TE differentiation, several enzymes of the lignin biosynthetic pathway are induced concomitantly with the lignification of the tracheary cell wall (Fukuda, 1996; Church, 1993; Taylor *et al.*, 1992; Ye *et al.*, 1994).

TE differentiation in SCCs represents a unique and interesting model system, in which secondary cell wall deposition, lignin biosynthesis, and programmed cell death may be studied (Fukuda, 1996), and where the interrelationship among these unique cellular events may be explored.

Lignification in certain SCCs may also be induced with no accompanying TE differentiation by lowering the levels of plant growth regulators. Lignins produced by these SCCs are either produced as an integral part of the cell wall or released into the nutrient medium. Analysis of the structure of these soluble (released) lignins has offered new insights into understanding the effect of the polysaccharidic matrix on lignin nature.

Eberhardt *et al.* (1993) have recently characterized the structure of lignins in the cell walls of *P. taeda* SCCs. These authors found that the major linkages involving the side chains were β-*O*-4 linkages, immediately followed by β-β resinol bonds. In contrast, β-5 and β-1 linkages seemed to participate to a lesser extent.

On the other hand, analysis of the lignins released to the medium by SCCs of *Picea abies* (Brunow *et al.*, 1990; Simola *et al.*, 1992) showed that β-β (resinol) structures were more abundant than those in wood lignins, while β-1 substructures were found in significantly smaller proportions.

These results suggest that extracellular lignins from *P. abies* do not resemble lignins isolated so far from spruce wood.

Thus, guaiacyl lignins which have been polymerized outside the cell wall matrix seem to be characterized by a high content of β-β resinol structures and a low β-1 bond content, two features which are also common to peroxidase-mediated synthetic G lignins (Boudet *et al.*, 1995). However, when SCC released lignins are compared with peroxidase-mediated synthetic G lignins (Boudet *et al.*, 1995) differences remain as regards the quantity of β-5 inter-unit linkages, which are greater in synthetic G lignins, while 5-5 inter-unit linkages are more abundant in lignins released by SCCs.

Lignification may also be induced in SCCs by fungal-derived elicitors, the induced-metabolic mechanisms resembling those observed in *Zinnia* cell cultures (Campbell and Ellis, 1992). Analysis of these lignins shows that, for example, elicitor-induced spruce cell culture lignins contain a higher level of H units (approximately 20-fold higher) than native spruce wood lignins (Lange *et al.*, 1995). This is not surprising since a comparison of lignins from different gymnosperm SCCs indicated a high level of H units in both elicited and nonelicited cells (Lange *et al.*, 1995). At this point, it is necessary to remember that high proportions of H units are also characteristic of the early lignification of the middle lamella (Fukushima and Terashima, 1990) and gymnosperm compression wood. These results suggest that the nonpredisposition to elaborate a secondary wall in the plant cell may precondition the nature of the deposited lignins and are only examples of the great heterogeneity that is found when exploring the nature and structural features of natural lignins.

V. Lignin Biosynthetic Pathways

The biosynthesis of lignins proceeds through a long sequence of reactions which involve (i) the shikimate pathway, which provides phenylalanine and tyrosine, (ii) the common phenylpropanoid pathway from phenylalanine (and/or tyrosine) to the cinnamoyl CoAs, and (iii) the lignin-specific pathway, which channels the cinnamoyl CoAs toward the synthesis of cinnamyl alcohols (Whetten and Sederoff, 1995).

The entry point into the shikimate pathway from both the glycolytic (phosphoenol piruvate) and the pentose phosphate pathway (erythrose-4-phosphate) intermediates is catalyzed by the enzyme 3-deoxy-D-arabino-heptulosonate-7-phosphate synthase (DAHP synthase, EC 4.1.2.15). This pathway leads, via chrorismate, to the biosynthesis of the amino acids phenylalanine, tyrosine, and tryptophan (Herrmann, 1995). Plants are the only living organisms capable of channeling carbon from the primary metab-

olism toward lignin biosynthesis, with the evolutionary acquisition (gain) of the phenylpropanoid pathway having played a key role in the ability of plants to colonize land, not only because one of its products (lignin) serves to strengthen the aerial organs of the plant, but also because other products (flavonoids) act as protectors against dangerous UV radiation passing through the atmosphere.

To integrate this novel evolutionary pathway and the general aromatic amino acid biosynthesis pathway in an efficient metabolic highway, the activities of the enzymes of the shikimate pathway are closely coordinated in vascular plants with the activities of the enzymes of the phenylpropanoid pathway (see VII.A).

A. The Common Phenylpropanoid Pathway

The enzymes involved in the phenylpropanoid pathway are phenylalanine ammonia-lyase (PAL), cinnamate-4-hydroxylase (C4H), *p*-coumarate-3-hydroxylase (C3H), *O*-methyltransferase (OMT), ferulate-5-hydroxylase (F5H), and hydroxycinnamate CoA ligase (4CL). The end products of this pathway, the hydroxycinnamoyl CoAs, are the precursors of lignins but also of other phenolic compounds which accumulate in great amounts in plant tissues, such as flavonoids and tannins.

The enzyme PAL (EC 4.3.1.5) catalyzes the first metabolic step from primary metabolism into phenylpropanoid metabolism, which is the deamination of phenylalanine to produce cinnamic acid. This enzyme is encoded in angiosperms by a multigene family and apparently by a single gene in gymnosperms (Boudet *et al.,* 1995). Cinnamic acid is further modified by the consecutive action of the hydroxylases C4H, C3H, and F5H and OMTs to lead to *p*-coumaric acid ferulic acid, and sinapic acid (Fig. 4). Although C4H [*trans*-cinnamate, NADH: oxygen oxidoreductase (4-hydroxylating), EC 1.14.13.11] and F5H are known plant cytochrome P-450 monooxygenases (Schuler, 1996), the precise nature of C3H is still unknown. Following these steps, the enzyme 4CL (*p*-coumarate: CoA ligase, EC 6.2.1.12) catalyzes the formation of hydroxycinnamic acid CoA esters, and these activated intermediates are then reduced to cinnamyl alcohols via the cinnamyl aldehydes (Fig. 4). 4CL also represents the branching point within the general phenylpropanoid metabolism toward the synthesis of either flavonoids or lignins.

This sequence of reactions, frequently known as the classical pathway, is subject to revision with new available data. A good example is what occurs in grasses, in which the enzyme tyrosine ammonia-lyase catalyzes the deamination of L-tyrosine to *p*-coumaric (Higuchi, 1990). Another example is C3H. Our present knowledge of this enzyme is very limited and,

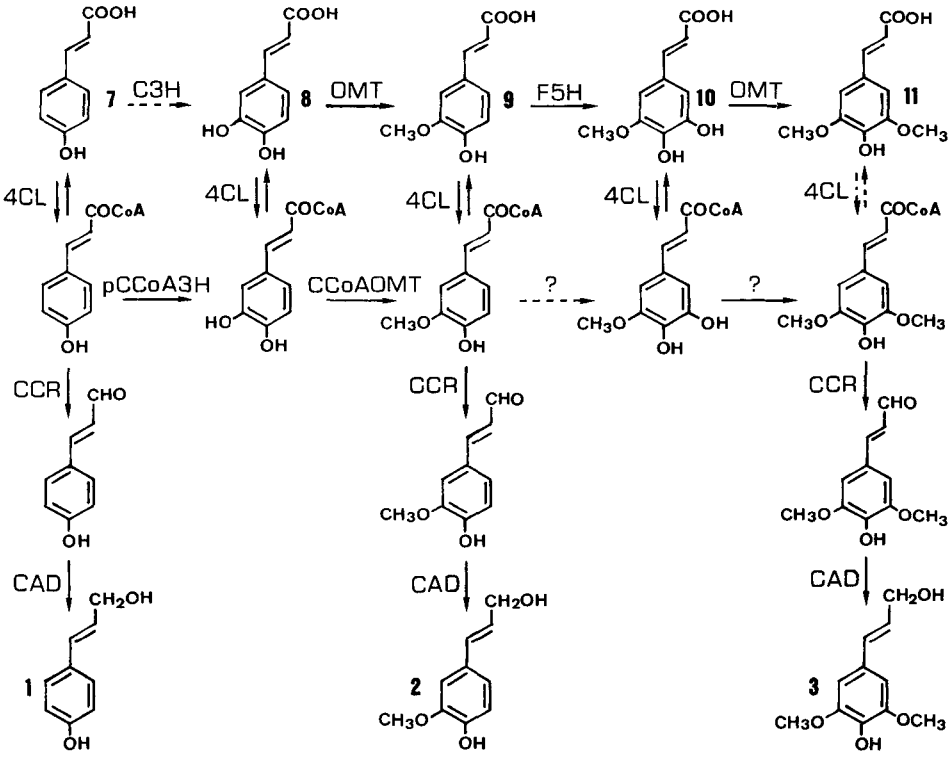

FIG. 4 Possible pathways for the biosynthesis of *p*-coumaryl (**1**), coniferyl (**2**), and sinapyl (**3**) alcohols from *p*-coumaric acid (**7**), caffeic acid (**8**), ferulic acid (**9**), 5-hydroxyferulic acid (**10**), and sinapic acid (**11**) and their corresponding cinnamoyl-CoAs. Dashed arrows show steps in which evidence for the enzymatic activity is lacking although it has been inferred by feeding studies.

to date, it is not known whether an unspecific phenoloxidase (EC 1.10.3.1 and 1.14.18.1), or a specific *p*-coumaryl-CoA hydroxylase (Matern *et al.*, 1995), is the real enzyme which catalyzes 3-hydroxylation. If the latter was the case, feruloyl-CoA could arise from the hydroxylation of *p*-coumaryl-CoA into caffeoyl-CoA, with the subsequent methylation of the latter by a caffeoyl-CoA 3-*O*-methyltransferase (CCoAOMT; see Fig. 4) (Matern *et al.*, 1995).

Similarly, an alternative pathway for sinapyl alcohol synthesis has recently been proposed by Higuchi (1990), based on the low affinity of 4CL for sinapic acid in angiosperms and some gymnosperms. This pathway involves the hydroxylation of ferulate by F5H and subsequent activation of 5-hydroxyferulate to the corresponding CoA thioester (see Fig. 4).

Recently, it has also been reported that some of the lignin precursors may not be methylated at the level of cinnamic acids, but later at the level of activated cinnamoyl CoA esters (Fig. 4) (Ye *et al.*, 1994) or even of cinnamyl alcohols or cinnamyl aldehydes (Matsui *et al.*, 1994).

In the appraisal of these new insights, specific gene down-regulation has proved to be a useful tool both to corroborate/discriminate the individual enzymatic steps (as well as the order of the enzymatic steps) of the classical pathway and to investigate new control points in lignin metabolism, such as the extent of functional redundancy in the lignin biosynthetic pathway (Boudet and Grima-Pettenati, 1995). As an example of the benefits to be gained from the use of gene down-regulation in the clarification of the lignin biosynthetic pathway, we describe below the most revealing findings obtained from the use of OMT down-regulated transgenic plants.

Until recently, it has been assumed that methylations in the phenylpropanoid pathway are performed by OMTs (*S*-adenosyl-L-methionine: caffeic acid 3-*O*-methyltransferase, EC 2.1.1.6), which control the production of ferulic acid in gymnosperms and ferns or of both ferulic acid and sinapic acid in angiosperms. In fact, angiosperm OMTs have been reported to catalyze the methylation both of caffeic acid to ferulic acid and of 5-hydroxyferulic acid to sinapic acid. Gymnosperms, on the other hand, have monospecific OMT, which uses only caffeic acid as substrate (Higuchi *et al.*, 1977). Owing to their specific enzymatic activity, OMTs have received special attention since they could potentially be responsible for the different monomeric compositions of angiosperm and gymnosperm lignins (Boudet *et al.*, 1995).

However, transformation of tobacco (Dwivedi *et al.*, 1994; Atanassova *et al.*, 1995) and poplar (Van Doorsselaere *et al.*, 1995) with an antisense OMT construct revealed a decrease in the S/G ratio in transgenic plants in which OMT was dramatically depleted. Moreover, an unusual monomeric unit, the 5-hydroxyguaiacyl, was identified in lignins of both transformed plants (Atanassova *et al.*, 1995; Van Doorsselaere *et al.*, 1995). The latter authors provided evidence that 5-hydroxyferulic acid may be channeled into the cinnamyl alcohol biosynthetic pathway, where it is converted to 5-hydroxyconiferyl alcohol prior to its incorporation into lignins.

These data are in apparent disagreement with previous data obtained from the biochemical characterization of angiosperm OMTs, which suggested that this enzyme can methylate both caffeic and 5-hydroxyferulic acid. Rather, the down-regulation of OMTs suggests that methylation at C5 of 5-hydroxyferulic acid is the preferential reaction performed by the enzyme *in planta,* since only levels of S moieties are affected by down-regulation of this supposedly bifunctional enzyme.

These results, and those obtained by Varner's group (Ye *et al.*, 1994; Ye and Varner, 1995) using *Zinnia* single-cell cultures, have contributed

to the recent proposition of an alternative pathway for the methylation of caffeic acid (see Fig. 4). In this novel pathway, a likely candidate is the enzyme CCoAOMT (*S*-adenosyl-L-methionine: caffeoyl-CoA 3-*O*-methyltransferase, EC 2.1.1.104), which catalyzes the methylation of caffeoyl-CoA into feruloyl-CoA (Ye *et al.*, 1994). This methylation pathway is dominant in *Zinnia* cell cultures (Ye *et al.*, 1994) and apparently also in transgenic tobacco (Atanassova *et al.*, 1995) and poplar (Van Doorsselaere *et al.*, 1995). Suggestions have been made that CCoAOMT is specific (monofunctional) for the methylation of caffeoyl-CoA ester in both tobacco (Atanassova *et al.*, 1995) and poplar (Van Doorsselaere *et al.*, 1995). From the above-described results, one may conclude that the OMTs described as unspecific have, paradoxically, a preferential and perhaps exclusive role in the methylation of 5-hydroxyferulic acid in angiosperms.

In the form of cinnamoyl-CoA, cinnamic acids may be channeled for further reduction to cinnamyl alcohols through the lignin-specific pathway or may be used for the synthesis of cinnamate esters, which are later mainly stored in vacuoles, probably until metabolic mobilization (Hahlbrock and Grisebach, 1979). A typical representative form of this class of storage compound is chlorogenic acid (an ester of caffeic acid and quinic acid). This ester is formed (Hahlbrock and Grisebach, 1979) by specific transferases (hydroxycinnamoyl-CoA: quinate hydroxycinnamoyl transferase), which catalyze reversible reactions and, consequently, the quinate esters of cinnamic acids may be considered to be storage forms of cinnamoyl-CoA, which can be channeled on demand for the biosynthesis of lignins (Aerts and Baumann, 1994).

B. The Lignin-Specific Pathway

This pathway involves two reductive steps which convert the hydroxycinnamoyl-CoA esters into hydroxycinnamyl alcohols. These two consecutive steps are catalyzed by the enzymes cinnamoyl-CoA reductase (CCR) and cinnamyl alcohol dehydrogenase (CAD) and are often considered to be specific to the lignification pathway.

CCR (EC 1.2.1.44) catalyzes the conversion of hydroxycinnamoyl-CoA esters to their corresponding aldehydes (Fig. 4), this being the first step in the lignin specific pathway. In this respect, CCR is thought to be an important control point regulating the flux of phenylpropanoid metabolites toward the biosynthesis of lignins, although data to support the nature and/or extent of this control are not available.

CAD (EC 1.1.1.195, hydroxycinnamyl aldehyde: NADPH oxidoreductase) appears as a polymorphic enzyme in angiosperms and is apparently encoded by one single gene in gymnosperms. Available biochemical data

suggest that gymnosperm CADs exhibit a very low affinity for sinapaldehyde, whereas angiosperm CADs use all three aldehydes with roughly identical affinities (Boudet and Grima-Pettenati, 1995).

The first CAD down-regulated plants were obtained by Halpin *et al.* (1994), through ectopic expression in tobacco of a homologous CAD cDNA antisense construct. It is worth noting that these plants showed a red-brown pigmentation in the xylem, which recalls that observed in maize and sorghum brown-midrib mutants (Boudet *et al.*, 1995). Analysis of the lignin monomeric composition of transformant plants with suppressed CAD activity indicated an increase in both coniferyl and sinapyl aldehydes in the lignin polymer (Halpin *et al.*, 1994; Hibino *et al.*, 1995), with the inclusion of the cinnamyl aldehydes in place of the corresponding alcohols resulting in a lignin polymer with altered intermolecular bonding and modified chemical reactivity. This is not surprising since Higuchi *et al.* (1994) have demonstrated that coniferyl aldehyde may be oxidized by peroxidase to a dark wine-red lignin-like polymer. These results strongly suggest that the red-brown coloration of transgenic plants with reduced CAD activity could be ascribed to abnormal lignins with increased cinnamaldehyde groups, and this is the other example, together with the inclusion of 5-hydroxyguaiacyl units in the case of OMT-suppressed plants, that illustrates the potential metabolic adaptation of plants and the chemical flexibility of lignins.

1. Storage Forms of Cinnamyl Alcohols

Once they are synthesized, cinnamyl alcohols may be glycosylate by specific transferases (UDP-glucose: coniferyl alcohol glucosyl transferase, EC 2.4.1.111) to yield the β-D-glucosides of *p*-hydroxycinnamyl, coniferyl (coniferin), and syringyl (syringin) alcohol. These glucosides are found in great amounts in gymnosperms but seem to be largely absent from angiosperms (Marcinowski and Grisebach, 1978).

To cast light on the role which cinnamyl alcohol glucosides may play in lignification, we should recall the recent observation of Dharmawardhana *et al.* (1995), who suggested that these glucosides may function as storage forms of cinnamyl alcohols, at least in conifers. In this sense, these authors have demonstrated that coniferin β-glucosidase (EC 3.2.1.126) is located in differentiating xylem, the most active site for lignin biosynthesis in woody plant species, and where coniferin concentration is reported to be highest (Savidge, 1989), and that this β-glucosidase shows a similar distribution to that shown by peroxidase and lignins (Dharmawardhana *et al.*, 1995).

From these results, it can be speculated that cinnamyl alcohol glucosides are synthesized by tracheary elements during their early stages of differentiation and that these glucosides are targeted and stored in vacuoles of living tracheary elements. Upon lysis of the protoplast, which occurs at the later

stages of differentiation, cinnamyl alcohol glucosides are liberated, and once in contact with the cell wall, they are hydrolyzed to their corresponding aglycones by specific xylem element cell wall β-glucosidases. The subsequent action of xylem cell wall oxidases on cinnamyl alcohols would allow polymerization in the cell wall of enucleated xylem elements.

This hypothesis is supported by the observation that these glucosides are stored in vacuoles of xylem elements (Savidge, 1989) and by the fact that a continuous deposition of tritiated lignins in the secondary thickening of xylem vessels may be observed even after their enucleation and cell death (Pickett-Heaps, 1968), probably due to the existence of a peroxidase activity that remains active in primary cell walls and secondary thickenings (Ros Barceló, 1995). Taken together, these results suggest that cell wall lignification may take place after tracheids have died and point to the existence of a residual but active peroxidase in these apparently inert cell wall structures, which may polymerize cinnamyl alcohols after the death of xylem vessels.

2. Subcellular Localization of Enzymes

The study of subcellular localization of enzymes of lignin biosynthesis is important if we wish to understand the regulation by compartmentalization of this pathway and how phenylpropanoid precursors may be modified along the transport pathway which finishes with the secretion of cinnamyl alcohols to the cell wall. Thus, while studies on reporter-gene expression can give considerable information concerning the control of the accumulation pattern of transcripts, complementary studies on enzyme localization are necessary to underline the subcellular fate of translation products. Thus, coupled with our knowledge of enzyme properties, the complexities of the factors governing the accumulation of phenylpropanoid skeletons will only be appreciated when we know all the details concerning the different levels of regulation.

However, there have been very few conclusive studies on the subcellular localization of the enzymes of the phenylpropanoid pathway and of the lignin-specific pathway, and such studies mainly concern the localization of PAL and 4CH. Similar studies for other enzymes of the pathway, such as C3H, F5H, OMT, CCoAOMT, CCR, and CAD, have not been made. For other enzymes (e.g., β-glycosidase, laccase, and peroxidase), their localization in the cell wall is beyond doubt (Hosel *et al.*, 1982; Dharmawardhana *et al.*, 1995; Driouich *et al.*, 1992; Ros Barceló *et al.*, 1997).

Studies on the subcellular localization of PAL in xylem parenchyma cells are consistent with a cytosolic localization (Smith *et al.*, 1994), and little evidence is found for a major association of the enzyme with any membrane structure. Although a membrane localization for PAL has often been postulated (Hahlbrock and Grisebach, 1979), this may not be the case since

membranes are really permeable to cinnamic acid. In fact, the scavenging of cinnamic acid within the endomembrane secretory system would prevent it from functioning as a down-regulator of the phenylpropanoid pathway, either directly or as a metabolite (Bolwell, 1993).

Unlike to the cytoplasmic soluble nature of PAL, C4H is clearly associated with ER membranes in xylem parenchyma cells (Smith *et al.,* 1994), which is in accordance with the subcellular localization of the plant cytochrome P-450 family. This may also be the case for F5H, although data for this enzyme are not available. Smith *et al.* (1994) also reported C4H in Golgi stacks, which is consistent not only with the glycosylated nature of plant C4H (Schuler, 1996), but also with its role in the synthesis and secretion of hydroxycinnamyl alcohols. In this sense, the localization of C4H in Golgi stacks could trace the route for a secretion coupled with metabolic maturation (hydroxylations and methylations) for the precursors of cinnamyl alcohols.

C. Cell-to-Cell Cooperation during Lignin Biosynthesis

As early as 1965, Freudenberg proposed that cinnamyl alcohols, or their glycosides, might be exported from the sites where they are synthesized toward the site where they are polymerized. He introduced the idea of possible cell cooperation during lignin synthesis in which living xylem parenchymatous cells would provide monomeric precursors which are then polymerized in the cell walls of enucleated vessels and tracheids. However, due to the lack of hard experimental evidence, this hypothesis fell on barren ground, and the concept of cell autonomy for lignin biosynthesis was favored (Wardrop, 1971).

Recently, based on several pieces of evidence obtained in different laboratories, the concept of cell-to-cell cooperation during lignin biosynthesis has reemerged. The first report that reclaimed Freudenberg's hypothesis was that of Bevan *et al.* (1989), who showed a tissue and cell-specific activity of a PAL promoter in ray cells. These results were confirmed by Hauffe *et al.* (1991), who reported the localization of a reported gene under the control of the 4CL promoter in xylem parenchyma cells, and by Smith *et al.* (1994), who confirmed the accumulation of PAL and 4CL in cells adjacent to metaxylem. However, since PAL and 4CL are enzymes of the general phenylpropanoid pathway, the role of xylem parenchyma cells in providing cinnamyl glucosides to adjacent vessel elements for lignin biosynthesis has been questioned until very recently.

This is not, however, the case for CAD, an enzyme specific for the lignin biosynthetic pathway. Feuillet *et al.* (1995) have recently reported, for the first time, that the transcriptional activity of a CAD gene takes place in

xylem parenchyma cells, providing firm evidence about the role played by these metabolically active cells in the lignification of adjacent enucleated vessels. Thus, it seems likely that ray cells could provide precursors for lignin biosynthesis to the adjacent xylem vessels.

As suggested by Feuillet *et al.* (1995), several pieces of evidence support the role of ray cells in contributing to the supply of cinnamoyl alcohol precursors, and of other cell wall components, for the lignification of the adjacent xylem elements. First, Ryser and Keller (1992) presented evidence that a structural glycine-rich protein was mainly synthesized in xylem parenchyma cells and then exported to the cell walls of adjacent mature protoxylem after the death of protoxylem cells. Second, Leinhos and Savidge (1993) reported that xylem ray cells are able to synthesize coniferin, a well-established lignin precursor in conifers. And third, it is also interesting to note that differentiating suspension cultures of *Zinnia elegans* have not been able to induce more than 70% of the living cells to differentiate in TEs (Roberts *et al.,* 1992), so that it is therefore possible that the whole culture is involved in differentiating and that the undifferentiated cells have the special task of providing lignin precursors for the lignification of the enucleated cells which have differentiated to TEs.

However, as has been pointed out by Boudet *et al.* (1996), it should be kept in mind that the lack of gene expression in mature xylem elements is to be expected since these cells contain no living protoplasts. In addition, parenchyma (ray) cells are themselves partially lignified, so that it cannot be determined, at the present time, to what extent mature xylem elements provide their own precursors while they remain metabolically active or receive them from living neighboring cells after lysis.

VI. The Polymerization Step

The last step in the process of lignin biosynthesis from cinnamyl alcohols involves their oxidation to 4-*O*-phenoxy radicals, which spontaneously polymerize to give oligomers and, in subsequent steps, a growing lignin polymer (Higuchi, 1990; and Hapiot *et al.,* 1994). These 4-*O* radicals are in equilibrium with at least two mesomeric forms, which may couple among themselves and that determine the different bonding patterns found in natural lignins (Fig. 5).

Until very recently, peroxidase had been considered to be the principal enzyme responsible for this reaction, since it appeared to play a key role in the timing and extent of cell wall lignification. However, during the last 5 years, several observations have resurrected a potential role for laccase in the polymerization process (O'Malley *et al.,* 1993; Dean and Eriksson, 1994).

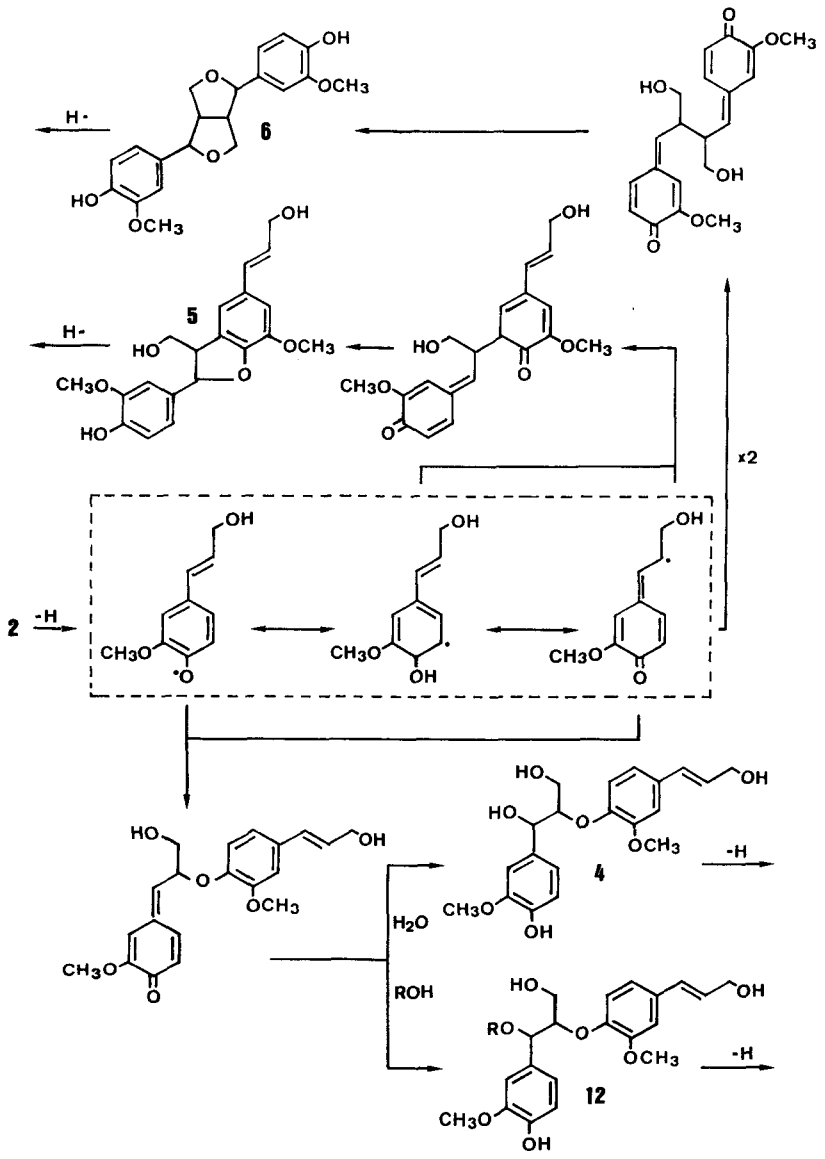

FIG. 5 Phenoxy radical formed by oxidation of coniferyl alcohol (**2**) by peroxidases/laccases and formation of the dimers guaiacylglycerol-*β*-*O*-coniferyl alcohol ether (**4**), dehydrodiconiferyl alcohol (**5**), and pinoresinol (**6**) via quinone methides. This figure also shows how quinone methides may react with the hydroxyl groups of polysaccharides (ROH) to lead to anchoring points for lignins in the cell wall polysaccharide matrix (**12**).

Lewis and Yamamoto (1990) established four criteria to establish whether an enzyme was really involved in lignification: substrate specificity, primary structure, subcellular localization, and a temporal correlation with active lignification. To these four criteria, we take the liberty of adding two new criteria: a widespread distribution throughout vascular (lignified) plant species, and a special affinity for oxidizing cinnamyl alcohols to highly polymeric lignin-like compounds.

It is worth noting that neither of the above-described enzymes satisfies all these criteria: laccase, because of its low affinity for cinnamyl alcohols, its inability to form highly polymeric lignin-like compounds, its distribution being restricted to a few plant species, and the absence of quantitative correlations between laccase levels and lignification (Alba *et al.,* 1996); and peroxidase, because it is difficult to imagine that one single peroxidase isoenzyme may be exclusively involved in the complex and orchestrated process of cell wall lignification. However, peroxidase has the following in its favor: (i) it has a high affinity for oxidizing cinnamyl alcohols to highly polymeric lignin-like compounds, (ii) its levels are quantitatively correlated with cell wall lignification, and (iii) it is found in high levels in all the vascular tissues, as are lignins.

A. Laccases

Laccase (*p*-diphenol: O_2 oxidoreductase, EC 1.10.3.2) is a copper-containing protein which catalyzes the oxidation of phenolics at the expenses of O_2. It was the first enzyme shown to be involved in the polymerization of cinnamyl alcohols (Freudenberg *et al.,* 1958) although, after these initial studies, its role in lignification was partially discredited since, on one hand, conflicting results were obtained for the ability of purified plant laccase to form synthetic lignins (Nakamura, 1967) and, on the other hand, because evidence was presented in favor of an exclusive participation of peroxidase in this process (Harkin and Obst, 1973). This situation was apparently aggravated by the intrinsic difficulty involved in solubilizing cell wall-bound H_2O_2-independent phenoloxidases (McDougall *et al.,* 1994a) and due to the vast excess of peroxidase compared to phenoloxidases present in the cell walls of lignifying tissues. Likewise, the sensitivity of laccase to freezing (Dean and Eriksson, 1994) may explain why in some cases (Harkin and Obst, 1973) laccase-like activities have not been detected in some plant materials, making the actual picture on laccase research rather confusing.

Plant laccases belong to the blue copper oxidase (BCO) group, in which L-ascorbate oxidase (EC 1.10.3.3) is also included. Both laccases and ascorbate oxidases are cell wall associated glycosylated enzymes (Lin and Varner,

1991; O'Malley *et al.*, 1993), similar in size and in copper content, and capable of indistinctly oxidizing ascorbic acid and phenolics (Bao *et al.*, 1993). Thus, the physical and catalytic properties of laccase and ascorbate oxidase do not appear to provide a reliable basis for distinguishing among these BCOs. This situation is further complicated by the observation that three different BCO cDNA sequences, which have been isolated from a loblolly pine xylem cDNa library, in which a laccase involved in lignification has been documented (Bao *et al.*, 1993), show an identity percentage between 51.8 and 53.5 with *Cucumis* ascorbate oxidase (O'Malley *et al.*, 1993).

Another problem when working with plant laccases is that they are easily confused with other phenoloxidases. Thus, true laccases may be differentiated from catecholase (*o*-diphenol: O_2 oxidoreductase, EC 1.10.3.1) on the basis of their substrate specificity and specific inhibitors (Mayer, 1987), although in some cases the difference between both enzymes is not clear. In this sense, Chabanet *et al.* (1994) have recently reported the localization by immunolabeling of a phenoloxidase in the secondary thickening of xylem vessels from mung bean hypocotyls that, like *o*-diphenoloxidases, was unable to oxidize *p*-diphenols, but which showed cross-reactivity with an anti-laccase antiserum, and whose activity, like that of laccase, was inhibited by cationic detergents but not by ferulic acid.

Nevertheless, that laccase plays a role of greater or lesser importance in lignin biosynthesis in vascular plants is hardly questionable. Thus, laccase has been detected by immunocytochemical methods in the secondary thickening of lignifying xylem vessels of sycamore maple (Driouich *et al.*, 1992), and by direct histochemical methods in lignifying vascular tissues of both *Zinnia* stems (Liu *et al.*, 1994) and loblolly pine (Bao *et al.*, 1993). Furthermore, it is now apparent that purified plant laccases retain the ability to oxidize cinnamyl alcohols (Sterjiades *et al.*, 1992, 1993; Bao *et al.*, 1993) and that the down-regulation of laccase using antisense laccase constructs results in a 10% loss of lignin (see Carpita *et al.*, 1996), although there are contradictory results concerning the ability of purified laccases to produce dehydrogenation polymers (DHPs) *in vitro* (Bao *et al.*, 1993; Okusa *et al.*, 1996).

However, some direct histochemical methods have possibly overevaluated the importance of laccase in lignifying tissues (De Pinto and Ros Barceló, 1997). Furthermore, there is apparent disagreement between data reporting the presence of laccase in the vascular body of certain plants (Bao *et al.*, 1993; Liu *et al.*, 1994) and those found in their respective lignifying cell cultures (Nose *et al.*, 1995; Sato *et al.*, 1995).

To circumvent these apparent difficulties in defining a clear role for laccase in lignification, Sterjiades *et al.* (1993) have recently suggested that laccases may be primarily responsible for the initial polymerization of cinnamyl alcohols into dimers and trimers, while peroxidases are more

likely required to catalyze the reactions leading from these compounds to highly condensed polymerization products. This proposal is in agreement with the recent report of Okusa *et al.* (1996), which showed that although laccase is capable of forming coniferyl alcohol dimers, it is unable to form DHPs. However, Sterjiades *et al.* (1992, 1993), do not report K_m values in order to know the affinity of laccases for cinnamyl alcohols. To the best of our knowledge, the only K_m available for a plant laccase is that reported by Bao *et al.* (1993), who gave K_m values for coniferyl alcohol and sinapyl alcohols of 12 and 25 m*M*, respectively. With these high K_m values, it is difficult to imagine what concentration of cinnamyl alcohol it would be necessary to reach in lignifying cell walls to saturate laccase during the oxidation of cinnamyl alcohols to lignin-like compounds.

At the present, various research groups are known to have obtained partial or complete cDNA sequences for plant laccases (Boudet *et al.*, 1995; LaFayette *et al.*, 1995). However, it is interesting to observe that sycamore and poplar laccase cDNA coding sequences do not cross-hybridize with RNA or DNA from other plant species (Boudet *et al.*, 1995). This is not surprising since laccase-like activities are not significantly detectable in lignifying cells of *P. contorta* (Dharmawardhana *et al.*, 1995), *P. taeda* (Nose *et al.*, 1995), *Lupinus albus* (Ros Barceló, 1995), or *Z. elegans* (Sato *et al.*, 1995). It should be remembered here that as long ago as 1959 Higuchi argued that the limited distribution of laccases in higher plants made it an unlikely candidate to be the agent of cinnamyl alcohol polymerization in lignifying vascular tissues.

In fact, laccases are considered to be largely absent from monocotyledons (Lewis and Davin, 1994), which are considered the most evolved plants. This observation would suggest that the presence of laccase in gymnosperms and dicotyledon angiosperms is the result of a reminiscent and/or recalcitrant evolutive residue. At this point, it is interesting to remember that, first, laccases are widely distributed in fungi (Mayer, 1987) and that their importance decreases from gymnosperms to monocotyledons, from which they are considered absent. Second, in fungi, laccases appear to play a key role in the synthesis of melanins (Mayer, 1987), a polymer that plays a role in fungi similar to that performed by lignins in higher plants. Third, these fungal melanins are especially abundant in rhizomorphs (Dean and Eriksson, 1994), which are specialized organs whose function is to translocate water and nutrients to distal portions of the fungus, and which probably constitute the primitive model from which the vascular structure of land plants evolved.

Thus, it can be speculated that during the course of evolution of land flora, the acquisition of the lignin biosynthesis pathway preceded the acquisition of secretory peroxidases and that laccases, which were probably largely present in the predecessors of higher vascular plants, from which

secretory peroxidases were absent, originally played a key role in the oxidation of cinnamyl alcohols to low-molecular-weight lignin-like compounds. However, during the evolution of vascular plants, laccases were probably displaced from performing their original function by the evolutionary advance of the more efficient lignin-synthesizing enzymes, the secretory peroxidases, which are capable of forming highly condensed lignin structures, and which could contribute to vigorously strengthening the aerial parts of primitive water-emerging plants.

Following this argument, laccases in their present form might be considered to be representing an evolutive residue, which have probably degenerated into intermediate enzyme forms, which maintain only some of their original properties. This hypothesis concerning the degenerative evolution of plant laccases is supported by the identification in higher plants of several cell wall phenoloxidases (Savidge and Udagama-Randeniya, 1992; McDougall *et al.*, 1994a; Chabanet *et al.*, 1994), which retain some of the original properties of laccases, although they cannot be considered true laccases *in sensu stricto.*

B. Peroxidases

1. General Properties

Peroxidases (EC 1.11.1.7, hydrogen donor: H_2O_2 oxidoreductase) are well-defined plant enzymes which contain Fe(III)-protoporphyrin IX as the prosthetic group and which are capable of oxidizing phenolics at the expense of H_2O_2. Unlike laccase, peroxidases have been detected in all vascular (lignifying) plants so far studied.

Secretory (vacuolar and cell wall located) plant peroxidases are easily distinguishable from other heme-containing enzymes by their subcellular localization, antigenic properties, and substrate specificity. Secretory plant peroxidases are glycoproteins that may be classified into two main groups according to their pI (Ros Barceló *et al.*, 1997): acidic and basic. While basic peroxidases are simultaneously located in the cell wall and vacuoles, acidic peroxidases are normally restricted to the cell wall. Acidic peroxidases have a greater affinity and reactivity for cinnamyl alcohols than basic peroxidases (Ros Barceló *et al.*, 1997).

That peroxidases may play a certain role in the polymerization of cinnamyl alcohols is supported by the following observations. Peroxidase gene promotors and peroxidase transcripts are expressed in lignifying tissues of tobacco (Lagrimini *et al.*, 1987), tomato (Mohan *et al.*, 1993), and *Populus kitakamiensis* (Osakabe *et al.*, 1994). Besides, histochemical (Ferrer and Ros Barceló, 1994), cytochemical (Hepler *et al.*, 1972; Czaninski, 1978; Ros

Barceló, 1995), and immunocytochemical (Kim *et al.,* 1988; Smith *et al.,* 1994) studies have revealed that peroxidase is located in lignifying cell walls mainly at the level of cell corners and middle lamella, and, in the case of xylem elements, at the level of secondary thickening.

Peroxidases oxidize the three cinnamyl alcohols (Sterjiades *et al.,* 1993; Dean *et al.,* 1994; Takahama, 1995) to give highly cross-linked DHPs (Weymouth *et al.,* 1993; Okusa *et al.,* 1996; Saake *et al.,* 1996). Furthermore, when the complexity of the polymerization conditions is increased in order to mimic more closely the process *in muro,* it has been found that the DHPs take on a greater resemblance to natural lignins (Tollier *et al.,* 1991; Terashima *et al.,* 1995, 1996; Grabber *et al.,* 1996). This is not surprising since there are several physico–chemical parameters, such as pH, the supply of substrata, the relative concentration of phenolic monomers and oligomers, the occurrence of radical scavengers, and the nature of the carbohydrate matrix, among others, which may control the polymerization of phenolic radicals and their channeling to specific lignin substructures (Terashima, 1990). This is probably the reason why synthetic lignins, prepared by peroxidative polymerization of cinnamyl alcohols, only approximate the structure of native lignins (Terashima, 1990).

Furthermore, the affinities (K_m) for cinnamyl alcohols (e.g., coniferyl alcohol) shown by several peroxidases isolated from lignifying tissues are in the order of 10-400 μM (Takahama, 1993; Ros Barceló *et al.,* 1997), always below the values shown by plant laccases (12,000 μM) (Bao *et al.,* 1993), but in the same order (5–500 μM) of those shown by their preceding enzymes in the lignin biosynthetic pathway, i.e., CCR, CAD, and β-glucosidases (Grisebach, 1981; Dharmawardhana *et al.,* 1995). It must not be forgotten at this stage that peroxidase K_m values for coniferyl alcohol vary greatly with H_2O_2 concentration and that they are proportionally lower at low H_2O_2 concentrations (Ros Barceló *et al.,* 1997). On the other hand, the H_2O_2 concentration in lignifying vessels cannot be expected to be very high (Schopfer, 1994). Indeed, the K_m values for H_2O_2 shown by most peroxidases when using coniferyl alcohol range between 30 and 160 μM (Takahama, 1993; Ros Barceló *et al.,* 1997), suggesting that they are well adapted to working at low H_2O_2 concentrations.

Nevertheless, for peroxidases to really participate in cell wall lignification, they must not only be located in the specific areas of the cell wall which lignify, but also remain active. For this, it is preferable, although not indispensable (Ferrer *et al.,* 1990), that these lignifying areas show H_2O_2 production. However, the results arising from the study of the cyto/histochemical localization of H_2O_2 cannot easily be interpreted. This difficulty and variability was shown by Schopfer (1994), who studied H_2O_2 localization in several plant tissues using a tissue-printing assay. In spite of this, it is worth noting that direct cytochemical (Czaninski *et al.,* 1993) or histochemical

(Olson and Varner, 1993) methods have revealed high levels of H_2O_2 in lignifying xylem tissues, supporting the previous conclusion that peroxidase, H_2O_2, and lignification are closely correlated (Catesson et al., 1978). At this point, it is necessary to mention a recent report by Nose *et al.* (1995), which described how H_2O_2 scavengers abolish lignification of *P. taeda* SCCs, lignin deposition being totally dependent on H_2O_2 production, and strongly implied, therefore, a regulatory role for H_2O_2.

However, the observations made with several transgenic tobacco lines that show a significant down-regulation of the acidic peroxidase isoenzyme (Lagrimini, 1991) cast some doubts on the exclusive participation of peroxidase in the polymerization process. Indeed, some transformed plants with up to 20 times less acidic peroxidase do not have smaller amounts of lignins than wild-type plants (Chabbert *et al.,* 1992). Similarly, when antisense experiments were performed to eliminate the expression of an acidic peroxidase isoenzyme involved in suberin biosynthesis, no corresponding changes were detected in the phenolic domain of suberin (Sherf *et al.,* 1993).

Quantitative correlations between peroxidase activity and lignification have frequently been reported in the literature. Suffice it to mention such different model systems as lignifying peach fruit endocarp (Abeles and Biles, 1991), lignifying flax fibers (McDougall, 1992), lignifying poplar tissues (Baier *et al.,* 1993), lignifying needles from Norway spruce (Polle *et al.,* 1994), lignifying lupin hypocotyls (Ros Barceló *et al.,* 1994), or lignifying *Zinnia* tracheary elements (Sato *et al.,* 1993, 1995), in all of which a close correlation between peroxidase activity and lignification has been observed. However, in no case was a specific peroxidase, basic or acidic, exclusively involved in these correlations. From all these studies emerged the idea that more than one individual peroxidase isoenzyme may participate in lignification. This observation, perhaps, may explain why specific down-regulation of a particular peroxidase isoenzyme is not accompanied by a specific reduction in cell wall lignification.

Moreover, this apparent redundancy in their biological function found for peroxidase isoenzymes could be one of the causes of lignin microheterogeneity between the different areas of a lignifying cell wall, since it is well known that peroxidase isoenzymes may show a certain specificity and strong differences in their reactivity toward cinnamyl alcohols (Ros Barceló *et al.,* 1997), as well as a specific cell wall localization, either in primary cell walls or in secondary thickening (see Ros Barceló *et al.,* 1997). Thus, among the factors which may affect this specific localization of different peroxidase isoenzymes in the several cell wall domains, one may point to pectins (Ros Barceló *et al.,* 1988). In fact, while secreted basic peroxidases may be retained by electrostatic interactions with pectins (Ferrer *et al.,* 1992) and thus concentrated in cell corners and middle lamella, acidic peroxidases may diffuse through the different (primary and secondary) cell wall layers, and even move freely in the xylem sap. In this sense, the exclusive presence

of acidic peroxidases in the xylem sap reported by some authors (Biles and Abeles, 1991; Polle and Glavac, 1993) supports this unrestricted diffusion of acidic peroxidases through the primary and the secondary cell wall of xylem vessels.

Finally, all these results suggest that, as our knowledge of cell wall peroxidases increases, several fascinating questions concerning cell wall lignification may be answered, such as the reasons why lignins are not uniformly deposited through the cell wall and, possibly, why lignin structure is intrinsically so heterogeneous.

2. The Origin of Hydrogen Peroxide

If there is an enigma in our knowledge of cell wall lignification, it is that of the origin of H_2O_2, which is necessary for activating peroxidases during oxidation of cinnamyl alcohols. The existence of several H_2O_2-generating systems has been proposed at the cell wall level as well as at the plasma membrane level. However, direct evidence that they may be functional in lignifying cells is to date lacking.

The first hypothesis as regards the existence of an H_2O_2-generating system in the cell wall was put forward by Elstner and Heupel in 1976. These authors suggested that cell wall peroxidases could generate H_2O_2 during the oxidation of NADH and that this H_2O_2 could be later used by peroxidases to oxidize cinnamyl alcohols. Although this hypothesis received further experimental support (Halliwell, 1978; Mäder *et al.*, 1980; Goldberg *et al.*, 1985), the very low amounts, if any, of NADH which may be expected in cell walls mean that caution must be exercised. Similar arguments may be put forward for other proposed H_2O_2-generating systems, such as those which involve di(poly)amine oxidases (Angelini and Federico, 1989) and oxalate oxidases (Zhang *et al.*, 1995), enzymatic systems which, in some cases (see Liu et al., 1995), show little, if any, association with lignifying vascular tissues.

Recently, the idea that a H_2O_2-generating system may be located at the level of the plasma membrane has been reinforced (Bolwell *et al.*, 1995). This H_2O_2-generating system would involve a NAD(P)H oxidase similar to that in animal blood neutrophils, which utilizes cytoplasmic NADPH, and which appears to be responsible for producing H_2O_2 during plant defense responses (Auh and Murphy, 1995; Desikan *et al.*, 1996). However, further research is necessary to elucidate whether this mechanism of H_2O_2 production is associated with cell wall lignification in elicited SCCs and whether it is present in lignifying vascular tissues.

C. Some Aspects of Lignin Deposition in the Cell Wall

The process of lignin deposition in the plant cell wall is a highly organized process in which cell wall phenolics, cell wall polysaccharides, and cell

wall proteins appear to play a role as scaffolding or template for lignin polymerization. The first direct evidence to support this was obtained by Atalla and Agarwal (1985) who, by means of Raman spectrometry, showed that the aromatic rings of lignins are parallel to the surface of the cell wall, suggesting that polysaccharides may act as matrices for the orientation of newly synthesized lignins. Furthermore, Houtman and Atalla (1995) have recently reported that cellulose microfibrils appear to have a net attractive interaction with lignin models, this interaction being sufficient to restrict the motion of coniferyl alcohol and to orient the phenyl ring parallel to the surface. This would provide a rationalization of the experimental observation (Terashima *et al.*, 1995, 1996) that polysaccharides can change the course of cinnamyl alcohol polymerization and influence their freedom to participate in a random polymerization process.

The interaction between cell wall polysaccharides and lignins may also be performed through covalent bonds. Thus, Iiyama *et al.* (1994) have recently suggested that several potential cross-links, of an ether or ester nature, may exist between lignins and other cell wall polysaccharides. Furthermore, in grasses, it is possible to detect linkages between polysaccharides and lignins through hydroxycinnamic acid ester–ether bridges (Ralph *et al.*, 1994a), the cinnamic acids being esterified to polysaccharides and etherified to lignins.

Similarly, there is evidence that lignins may be associated with cell wall proteins such as hydroxyproline and glycine-rich proteins (Iiyama *et al.*, 1993). However, although cross-links between lignins and both polysaccharides (Ohnishi *et al.*, 1992) and proteins (McDougall *et al.*, 1996) have been known for some time, there is no direct evidence to date of the chemical fragment involved in these covalent linkages.

The above-described interactions between cell wall polymers for determining the final architecture of the mature and lignified plant cell wall may be studied using chemical inhibitors of the synthesis of cell wall components. For example, using L-α-aminooxy-β-phenylpropionic (AOPP), a potent inhibitor of PAL, Ingold *et al.* (1990) have shown that the inhibition of lignin biosynthesis has no effect on the synthesis of cell wall polysaccharides, although the deposition of cellulose microfibrils in xylem cell walls may indeed be affected (Smart and Amrhein, 1985). In fact, cellulose microfibrils of unlignified secondary thickening are separated from one another and lie disorganized in the lumen of mature xylem vessels (Smart and Amrhein, 1985).

Similar results were obtained when using 2,6-dichlorobenzonitrile, an inhibitor of cellulose synthesis. Using this inhibitor probe, Taylor *et al.* (1992) found that cellulose-depleted cell wall thickening contained dispersed lignins. This dispersion of lignins when cellulose synthesis was inhibited provides the first evidence that the location of cellulose in the secondary

cell wall directly or indirectly mediates the patterns of lignin deposition, this interaction between cell wall components being reciprocal.

Further support for the existence of a strong relationship, both spatial and temporal, between cell wall components during the elaboration of the final architecture of lignified cell walls, was provided by Terashima *et al.* (1993) during their study of the growth process of the protolignin macromolecule in specific layers (domains) of the secondary plant cell wall. These authors described how the process of cell wall lignification proceeded through three clearly differentiated phases. The first phase of lignin deposition occurs at the level of cell corners and middle lamella after pectic substance deposition has finished and the formation of the S1 layer has started. The second phase is a slow lignification stage associated with cellulose microfibrils and manan and xylan deposition in the S2 layer, whereas the main lignification occurs in the third stage when the deposition of cellulose microfibrils in the S3 layer has started.

VII. Factors Determining the Amount and Nature of Lignins

As may be expected from the high contribution which lignins make to the plant biomass, woody plant species channel a large proportion of their photosynthetically assimilated carbon to lignin biosynthesis. The amount varies among species probably due to differential carbon partitioning among lignins and other carbon sinks. Once the battery of genes required for lignification is activated, what factors control the overall carbon flux for lignin biosynthesis? Since the deposition of lignins does not seem to be limited by end-product-mediated types of feedback control (Jensen, 1994), it might reasonably be expected that flux into the pathway is probably determined by the levels of entry-point enzymes, whereas flux through the pathway is probably conditioned by both the levels and the substrate specificity of branching enzymes in the pathway which determine the metabolic channeling of substrates, products, and by-products.

A. Regulation of Carbon Flow

Control of carbon flux through the lignin biosynthetic pathway is performed on the first enzyme of the aromatic acid biosynthesis pathway, DAHP synthase. Recent results underscore the close coordination existing between the biosynthesis of aromatic amino acids and phenylpropanoids. In *Solanum,* the repression of DAHP synthase activity by the introduction of a

DNA antisense construct reduced lignin deposition by up to 65% (Jones *et al.*, 1995).

Carbon flux through the lignin biosynthetic pathway is not only controlled by the levels of DAHP synthase, but also by the levels of the end product of this pathway, phenylalanine. In this respect, when Yao *et al.* (1995) created a metabolic sink for tryptophan by overexpressing the enzyme tryptophan decarboxylase in potato, phenylalanine pools were reduced by about 50% and lignin levels were 30–50% lower in the tubers. These results provide evidence that carbon flow into the lignin biosynthetic pathway depends on a pool of phenylalanine generated by the pathway of aromatic amino acid biosynthesis and indicate that the series of enzymatic steps from DAHP to CAD may be considered to be a single and continuous highway that funnels the carbon skeletons into lignin biosynthesis.

Inhibition of PAL by chemical compounds (Amrhein *et al.*, 1983) or genetic engineering (PAL down-regulation) (Elkind *et al.*, 1990; Bate *et al.*, 1994) is generally associated with a reduction in lignin content. Increases in PAL activity during lignification are generally rapid and transient. Thus, in elicited jack pine SCCs, for example, PAL activity is rapidly induced to levels 10 times greater than that observed in controls, but decreases to control levels within 48 h (Campbell and Ellis, 1992; Campbell and Sederoff, 1996). These results suggest that high levels of PAL activity are needed for lignification, probably so that phenylalanine pools may be channeled toward the biosynthesis of phenylpropanoids. In this sense, the spatial and temporal regulation of PAL activity appears to be important in redirecting the flux of aromatic metabolites toward the lignin biosynthetic pathway.

The situation, however, is somewhat confusing in the case of OMTs. Thus, although transformation of tobacco with an OMT antisense heterologous construct led to a significant reduction in lignin content (Dwivedi *et al.*, 1994; Ni *et al.*, 1994), two recent reports dealing with homologous OMT constructs in tobacco (Atanassova *et al.*, 1995) and poplar (Van Doorsselaere et al., 1995) revealed that the total amount of lignins, when assessed by different methods, remained unchanged even in transgenic plants in which OMT was dramatically depleted.

Other important regulatory enzymes that might control flux through the lignin biosynthesis pathway are CCR and CAD. CCR catalyzes the conversion of hydroxycinnamoyl-CoA esters into the corresponding aldehydes and thus channels metabolites from the general phenylpropanoid pathway to the lignin-specific pathway. However, no data on the effect of CCR down-regulation on lignin levels in transgenic plants are available.

In the case of CAD, it has been found that plants in which CAD was down-regulated exhibit no changes in the lignin content with regards to wild-type plants (Halpin *et al.*, 1994; Hibino *et al.*, 1995). It is interesting to note that when CAD activity was reduced to 10% of the levels observed

in wild-type plants (Halpin *et al.*, 1994), there was no effect on the quantity of lignins deposited in cell walls, while the reduction of PAL activity to 20% affected the deposition of lignin in tobacco. Thus, although CAD catalyzes a terminal step in cinnamyl alcohol biosynthesis, the enzyme does not appear to exert any control on the supply rate of precursors, unlike PAL, when suppressed to the same level.

As regards peroxidase, transgenic tobacco, which overexpressed an anionic peroxidase believed to be involved in lignification (Lagrimini *et al.*, 1990), lignified sooner than control plants in response to a wound, although the final levels of lignins was the same in both plants (Lagrimini, 1991). These results suggest that in tobacco homologous constructs, peroxidase limits the rate rather than the amount of lignin deposition. Similar results were found in the case of tomato heterologous constructs overexpressing the tobacco anionic peroxidase gene (Lagrimini *et al.*, 1993). Experiments involving the down-regulation of peroxidase and laccase, and their relation with the amount of lignin deposited, have already been described in a previous section (see VI).

Judging by the bulk of data concerning the regulation of enzymes of lignin biosynthesis, one may conclude that a key regulatory event is the transcriptional activation of these genes (Hahlbrock and Scheel, 1989; Dixon and Paiva, 1995). However, although transcription factors of the Myb and Myc classes appear to play a key role in the regulation of flavonoid biosynthesis (Holton and Cornish, 1995), analogous transcription factors that could specify temporal and spatial expression of enzymes of phenylpropanoid metabolism, including the specific lignin biosynthetic pathway, have not yet been identified. The evidence supporting the existence of such transcription factors has been reviewed by Douglas (1996) and Campbell and Sederoff (1996).

Consistent with the existence of these factors is the recent observation that the accumulation of several mRNAs specific to several shikimate pathway genes and the PAL mRNA are jointly activated in elicitor-treated tomato cells (Gorlach *et al.*, 1995). Moreover, when carbon flow into the phenylpropanoid pathway was blocked by the use of specific PAL inhibitors, no effect on transcript accumulation was observed. These studies indicate that genes in the shikimate–aromatic amino acid biosynthetic pathway are transcriptionally regulated jointly with genes of the phenylpropanoid metabolism but that this transcriptional control is independent of the carbon flow through the phenylpropanoid pathway (Herrmann, 1995).

Likewise, Christensen *et al.* (1996) have recently noted that in transgenic poplar plants with reduced CAD activity, a group of acidic peroxidases showed reduced activity compared to the levels observed in wild-type plants. All these recent results together suggest that the genes of the lignin biosynthetic pathway are transcriptionally coregulated. Undoubtedly, this complex

regulation network opens new perspectives in the control of metabolic flux through the lignin biosynthetic pathway.

B. Regulation of the Monomeric Composition of Lignins

The most plausible hypothesis to explain lignin heterogeneity in plant species, as well as in the tissues of the same plant species, is based on the differential substrate specificity of the enzyme which dictates (e.g., 4CL) which of the different methoxylated cinnamoyl-CoA esters is to be made. However, several studies which have attempted to establish the role of 4CL in controlling lignin heterogeneity in the tissues of the same plant species, as well as in tissues of different plant species, reached no conclusive results (Boudet *et al.,* 1995). Another key regulatory enzyme might be C3H, which would regulate the H/G ratio in native lignins. Unfortunately, no such data for C3H are available, reflecting our poor knowledge of this enzyme.

The most distinctive variation in lignin composition is that occurring between gymnosperms and angiosperms. Several hypotheses to account for the differences observed in the monomer composition of their lignins have been proposed (Campbell and Sederoff, 1996). Among the most probable is that involving F5H as the branching point for determining the different quantities of the various monomers to be synthesized.

A possible confirmation of this hypothesis may be found in *Erythrina cristagalli* and in the *fah 1* mutant of *Arabidopsis thaliana.* Thus, *E. cristagalli* is an angiosperm that produces only G lignins (gymnosperm type) but which has typical angiosperm lignin biosynthetic enzymes, such as a 4CL which uses sinapate, an OMT which uses 5-hydroxyferulic acid, and a CAD which can reduce sinapaldehyde (Higuchi, 1990). However, *E. cristagalli* lacks F5H activity, suggesting that the absence of S units in conifer lignins might be due to the absence of this enzyme. Further support for this hypothesis was given by Chapple *et al.* (1992), who isolated an *A. thaliana* F5H mutant (*fah 1*), in which F5H is not functional, and which is also unable to produce both sinapyl alcohol and S lignins. Thus, while wild-type *Arabidopsis* contains active F5H activity and produces the G-S lignins typical of angiosperms, the *fah 1* mutant produced only G lignin. The *Arabidopsis fah1* mutant supports the hypothesis that the difference between angiosperm and gymnosperm lignins may be related to the absence of F5H in gymnosperms.

VIII. Concluding Remarks

From the volume of recent publications on cell wall lignification and from the numerous efforts that are being made in several laboratories (Carpita

et al., 1996), it seems that we are on the threshold of great advances in understanding several aspects of cell wall lignification. Although some recent progress in this field has been made possible by the introduction of molecular biology techniques, all the different events which lead to cell wall lignification will only be elucidated in the coming years through an interdisciplinary approximation, in which chemists, biochemists, molecular biologists, cytologists, and physiologists work together toward an identical goal. Only through such cooperation will we find an answer to the fascinating questions that the complex process of cell wall lignification poses and which still remain unresolved.

Acknowledgments

I thank all members of my laboratory, past and present, for their support.

References

Abeles, F. B., and Biles, C. L. (1991). Characterization of peroxidases in lignifying peach fruit endocarp. *Plant Physiol.* **95,** 269–273.

Aerts, R. J., and Baumann, T. W. (1994). Distribution and utilization of chlorogenic acid in *Coffea* seedlings. *J. Exp. Bot.* **45,** 497–503.

Alba, C. M., de Forchetti, S. M., and Tigier, H. A. (1996). Peroxidase and phenoloxidase activities in peach endocarp. *In* "Plant Peroxidases: Biochemistry and Physiology" (C. Obinger, U Burner, R. Ebermann, C. Penel, and H. Greppin, eds.), pp. 243–246. University of Geneva, Geneva.

Amrhein, N., Franck, G., Lemm, G., and Luhman, H. B. (1983). Inhibition of lignin formation by L-α-aminooxy-β-phenylpropionic acid an inhibitor of phenylalanine ammonia-lyase. *Eur. J. Cell Biol.* **9,** 139–144.

Angelini, R., and Federico, R. (1989). Histochemical evidence of polyamine oxidation and generation of hydrogen peroxide in the cell wall. *J. Plant Physiol.* **135,** 212–217.

Argyropoulos, D. S. (1995). ^{31}PNMR in wood chemistry: A review of recent progress. *Res. Chem. Intermed.* **21,** 373–395.

Atalla, R. H., and Agarwall, U. P. (1985). Raman microprobe evidence for lignin orientation in the cell walls of native woody tissue. *Science* **227,** 636–638.

Atanassova, R., Favet, N., Martz, F., Chabbert, B., Tollier, M. T., Monties, V. B., Fritig, B., and Legrand, M. (1995). Altered lignin composition in transgenic tobacco expressing *O*-methyltransferase sequences in sense and antisense orientation. *Plant J.* **8,** 465–477.

Auh, C. K., and Murphy, T. M. (1995). Plasma membrane redox enzyme is involved in the synthesis of O_2^- and H_2O_2 by *Phytophthora* elicitor-stimulated rose cells. *Plant Physiol.* **107,** 1241–1247.

Baier, M., Goldberg, R., Catesson, A. M., Francesch, C., and Rolando, C. (1993). Seasonal changes of isoperoxidases from poplar bark tissues. *Phytochemistry* **32,** 789–793.

Bao, W., O'Malley, D. M., Whetten, R., and Sederoff, R. R. (1993). A laccase associated with lignification in loblolly pine xylem. *Science* **260,** 672–674.

Bate, N. J., Orr, J., Ni, W., Meromi, A., Nadler-Hassar, T., Doerner, P. W., Dixon, R. A., Lamb, C. J., and Elkind, Y. (1994). Quantitative relationship between phenylalanine ammonia-lyase levels and phenylpropanoid accumulation in transgenic tobacco identifies a rate-determining step in natural product synthesis. *Proc. Natl. Acad. Sci. USA* **91,** 7608–7612.

Bevan, M., Shufflebottom, D., Edwards, K., Jefferson, R., and Schuch, W. (1989). Tissue and cell-specific activity of a phenylalanine ammonia-lyase promoter in transgenic plants. *EMBO J.* **8,** 1899–1906.

Biles, C. L., and Abeles, F. B. (1991). Xylem sap proteins. *Plant Physiol.* **96,** 597–601.

Billa, E., Tollier, M. T., and Monties, B. (1996). Characterization of the monomeric composition of *in situ* wheat straw lignins by alkaline nitrobenzene oxidation: Effect of temperature and reaction time. *J. Sci. Food Agric.* **72,** 250–256.

Bolwell, G. P. (1993). Dynamic aspects of the plant extracellular matrix. *Int. Rev. Cytol* **146,** 261–323.

Bolwell, G. P., Butt, V. S., Davies, D. R., and Zimmerlin, A. (1995). The origin of the oxidative burst in plants. *Free Rad. Res.* **23,** 517–532.

Borg-Olivier, O., and Monties, B. (1993). Lignin, suberin, phenolic acids and tyramine in the suberized wound-induced potato periderm. *Phytochemistry* **32,** 601–606.

Boudet, A. M., and Grima-Pettenati, J. (1995). Lignin genetic engineering. *Mol. Breed.* **2,** 23–39.

Boudet, A. M., Lapierre, C., and Grima-Pettenati, J. (1995). Biochemistry and molecular biology of lignification. *New Phytol.* **129,** 203–236.

Boudet, A. M., Goffner, D. P., and Grima-Pettenati, J. (1996). Lignins and lignification: Recent biochemical and biotechnological developments. *C.R. Acad. Sci. Paris* (*Life Sci.*) **319,** 317–331.

Brunow, G., Ede, R. M., Simola, L. K., and Lemmetyinen, J. (1990). Lignin released from *Picea abies* suspension cultures—true native spruce lignins? *Phytochemistry* **29,** 2535–2538.

Campbell, M. M., and Ellis, B. E. (1992). Fungal-elicitor mediated responses in pine cell cultures. I. Induction of phenylpropanoid metabolism. *Planta* **186,** 409-417.

Campbell, M. M., and Sederoff, R. R. (1996). Variation in lignin content and composition: Mechanism of control and implications for the genetic improvement of plants. *Plant Physiol.* **110,** 3–13.

Carpita, N., McCann, M., and Griffing, L. R. (1996). The plant extracellular matrix: New from the cell's frontier. *Plant Cell* **8,** 1451–1463.

Catesson, A. M., Czaninski, Y., and Monties, B. (1978). Caracteres histochimiques des peroxydases parietales dans les cellules en cours de lignification. *C.R. Acad. Sci. Paris* **286,** 1787–1790.

Chabanet, A., Goldberg, R., Catesson, A. M., Quinet-Szely, M., Delaunay, A. M., and Faye, L. (1994). Characterization and localization of a phenoloxidase in mung bean hypocotyl cell walls. *Plant Physiol.* **106,** 1095-1102.

Chabbert, B., Monties, B., Liu, Y. T., and Lagrimini, M. (1992). Lignin content and composition in transgenic tobacco plants with altered peroxidase activity. *In* "Proceedings 5th International Conference on Biotechnology in Pulp and Paper Industry" (M. Kuwahara and M. Shimada, eds.), pp. 481–485. Uni Publishers Co., Tokyo.

Chapple, C. C. S., Vogt, T., Ellis, B. E., and Somerville, C. R. (1992). An *Arabidopsis* mutant defective in the general phenylpropanoid pathway. *Plant Cell* **4,** 1413-1424.

Christensen, J. H., Bauw, G., Van Montagu, M., and Boerjan, W. (1996). Towards the identification of lignin specific peroxidases in poplar. *In* "Plant Peroxidases: Biochemistry and Physiology" (C. Obinger, U. Burner, R. Ebermann, C. Penel, and H. Greppin, eds.), pp. 113–117. University of Geneva, Geneva.

Church, D. L. (1993). Tracheary element differentiation in *Zinnia* mesophyll cell cultures. *Plant Growth Regul.* **12,** 179–188.

Czaninski, Y. (1978). Localisation ultrastructurale d'activites peroxydasiques dans les parois du xyleme du ble pendant leur differentiation. *C.R. Acad. Sci. Paris* **286,** 957–959.

Czaninski, Y. (1979). Cytochimie ultrastructurale des parois du xyleme secondaire. *Biol. Cell.* 35, 97-102.

Czaninski, Y., Sachot, R. M., and Catesson, A. M. (1993). Cytochemical localization of hydrogen peroxide in lignifying cell wall. *Ann. Bot.* **72,** 547–550.

Davin, L. B., Bedgar, D. L., Katayama, T., and Lewis, N. G. (1992). On the stereoselective synthesis of (+)-pinoresinol in *Forsythia suspensa* from its achiral precursor, coniferyl alcohol. *Phytochemistry* **31,** 3869–3874.

Dean, J. F. D., and Eriksson, K. E. L. (1992). Biotechnological modification of lignin structure and composition in forest trees. *Holzforschung* **46,** 135–147.

Dean, J. F. D., and Eriksson, K. E. L. (1994). Laccase and the deposition of lignin in vascular plants. *Holzforschung* **48,** 21-33.

Dean, J. F. D., Sterjiades, R., and Eriksson, K. E. L. (1994). Purification and characterization of an anionic peroxidase from sycamore maple (*Acer pseudoplatanus*) cell suspension cultures. *Physiol. Plant.* **92,** 233–240.

Delwiche, C. F., Graham, L. E., and Thomson, N. (1989). Lignin-like compounds and sporopollenin in *Coleachaete,* an algae model for land plant ancestry. *Sci. Rep.* **245,** 399–401.

De Pinto, M. C., and Ros Barceló, A. (1997). Cytochemical localization of phenol-oxidizing enzymes in lignifying *Coleus blumei* stems. *Eur. J. Histochem.* **41,** 17–22.

Desikan, R., Hancock, J. T., Coffey, M. J., and Neill, S. J. (1996). Generation of active oxigen in elicited cells of *Arabidopsis thaliana* is mediated by a NADPH oxidase-like enzyme. *FEBS Lett.* **382,** 213–217.

Dharmawardhana, D. P., Ellis, B. E., and Carlson, J. E. (1995). A β-glucosidase from lodgepole pine xylem specific for the lignin precursor coniferin. *Plant Physiol.* **107,** 331–339.

Dixon, R. A., and Paiva, N. L. (1995). Stress-induced phenylpropanoid metabolism. *Plant Cell* **7,** 1085–1097.

Donaldson, L. A. (1985a). Critical assessment of interference microscopy as a technique for measuring lignin distribution in cell walls. *N.Z. J. For. Sci.* **15,** 349–360.

Donaldson, L. A. (1985b). Within- and between-tree variation in lignin concentration in the tracheid cell wall of *Pinus radiata. N.Z. J. For. Sci.* **15,** 361–369.

Douglas, C. J. (1996). Phenylpropanoid metabolism and lignin biosynthesis: From weeds to trees. *Trends Plant Sci.* **1,** 171–178.

Driouich, A., Laine, A. C., Vian, B., and Faye, L. (1992). Characterization and localization of laccase forms in stem and cell cultures of sycamore. *Plant J.* **2,** 13–24.

Dwivedi, U. N., Campbell, W. H., Yu, J., Datla, R. S. S., Bugos, R. C., Chiang, V. L., and Podila, G. K. (1994). Modification of lignin biosynthesis in transgenic tobacco through expression of an antisense *O*-methyltransferase gene from *Populus. Plant Mol. Biol.* **26,** 61–71.

Eberhardt, T. L., Bernards, M. A., He, L., Davin, L. B., Wooten, J. B., and Lewis, N. G. (1993). Lignification in cell suspension cultures of *Pinus taeda. J. Biol. Chem.* **28,** 21088–21096.

Ede, R. M., and Brunow, G. (1990). Two-dimensional ^{1}H-^{1}H chemical shift correlation and J-resolved NMR studies on isolated and synthetic lignins. *Holzforschung* **44,** 95–101.

Effland, M. J. (1977). Modified procedure to determine acid-insoluble lignin in wood and pulp. *Tappi* **60,** 143–144.

Elkind, Y., Edwards, R., Mavandad, M., Hedrick, S. A., Ribak, O., Dixon, R. A., and Lamb, C. J. (1990). Abnormal plant development and down-regulation of phenylpropanoid biosynthesis in transgenic tobacco containing a heterologous phenylalanine ammonia-lyase gene. *Proc. Natl. Acad. Sci. USA* **87,** 9057–9061.

Elstner, E. F., and Heupel, A. (1976). Formation of hydrogen peroxide by isolated cell walls from horseradish (*Armoracia lapathifolia* Gilib.). *Planta* **130,** 175–180.

Erickson, M., Larsson, S., and Miksche, G. E. (1973). Gaschromatograpische analyse von lignin-oxydationsprodukten. VII. Ein verbessertes verfahren zur charakterisierung von ligninen durch oxydativen abbau. *Acta Chem. Scand.* **27,** 127–140.

Ferrer, M. A., and Ros Barceló, A. (1994). Control of the lignification in *Lupinus* by genistein acting as superoxide scavenger and inhibitor of the peroxidase-catalyzed oxidation of coniferyl alcohol. *J. Plant Physiol.* **144,** 64–67.

Ferrer, M. A., Pedreño, M. A., Muñoz, R., and Ros Barceló, A. (1990). Oxidation of coniferyl alcohol by cell wall peroxidases at the expense of indole-3-acetic acid and O_2. A model for the lignification of plant cell walls in the absence of H_2O_2. *FEBS Lett.* **276,** 127–130.

Ferrer, M. A., Pedreño, M. A., Ros Barceló, A., and Muñoz, R. (1992). The cell wall localization of two strongly basic isoperoxidases in etiolated *Lupinus albus* hypocotyls and its significance in coniferyl alcohol oxidation and indole-3-acetic acid catabolism. *J. Plant Physiol.* **139,** 611–616.

Feuillet, C., Lauvergeat, V., Deswarte, C., Pilate, G., Boudet, A., and Grima-Pettenati, J. (1995). Tissue and cell-specific expression of a cinnamyl alcohol dehydrogenase promoter in transgenic poplar plants. *Plant Mol. Biol.* **27,** 651–667.

Freudenberg, K. (1959). Biosynthesis and constitution of lignin. *Nature* **183,** 1152–1155.

Freudenberg, K. (1965). Lignin: Its constitution and formation from *p*-hydroxycinnamyl alcohols. *Science* **148,** 595–600.

Freudenberg, K., Lautsch, W., and Engler, K. (1940). Die bildung von vanillin aus fichtenlignin. *Ber. Dtsch. Chem. Gesells.* **73,** 167–173.

Freudenberg, K., Harkin, J. M., Reichert, M., and Fukuzumi, T. (1958). Die an der verholzung beteiligten enzyme. Die dehydrierung des sinapinalkohols. *Chem. Ber.* **91,** 581–590.

Frías, I., Siverio, J. M., González, C., Trujillo, J. M., and Perez, J. A. (1991). Purification of a new peroxidase catalysing the formation of lignan-type compounds. *Biochem. J.* **273,** 109–113.

Fukuda, H. (1996). Xylogenesis: Initiation, progression and cell death. *Annu. Rev. Plant Physiol. Plant Mol. Biol.* **47,** 299–325.

Fukushima, K., and Terashima, N. (1990). Heterogeneity in formation of lignin. XIII. Formation of *p*-hydroxyphenyl lignin in various hardwood visualized by microautoradiography. *J. Wood Chem. Technol.* **10,** 413–433.

Gahan, P. B. (1981). Biochemical changes during xylem element differentiation. *In* "Xylem Cell Development" (J. R. Barnett, ed.), pp. 168–191. Castle House, Kent.

Goldberg, R., Le, T., and Catesson, A. M. (1985). Localization and properties of cell wall enzyme activities related to the final stages of lignin biosynthesis. *J. Exp. Bot.* **36,** 503–510.

Gorlach, J., Raesecke, H., Rentsch, D., Regenass, M., Roy, P., Zala, M., Keel, C., Boller, T., Amrheim, N., and Schmid, J. (1995). Temporally distinct accumulation of transcripts encoding enzymes of the prechorismate pathway in elicitor-treated cultured tomato cells. *Proc. Natl. Acad. Sci. USA* **92,** 3166–3170.

Grabber, J. H., Ralph, J., Hatfield, R. D., Quideau, S., Kuster, T., and Pell, A. N. (1996). Dehydrogenation polymer–cell wall complexes as a model for lignified grass walls. *J. Agric. Food Chem.* **44,** 1453–1459.

Grisebach, H. (1981). Lignins. *In* "The Biochemistry of Plants" (E. E. Conn, ed.), Vol. 7, pp. 457–478. Academic Press, New York.

Hahlbrock, K., and Grisebach, H. (1979). Enzymic control in the biosynthesis of lignin and flavonoids. *Annu. Rev. Plant Physiol.* **30,** 105–130.

Hahlbrock, K., and Scheel, D. (1989). Physiology and molecular biology of phenylpropanoid metabolism. *Annu. Rev. Plant Physiol. Plant Mol. Biol.* **40,** 347–369.

Halliwell, B. (1978). Lignin synthesis: The generation of hydrogen peroxide and superoxide by horseradish peroxidase and its stimulation by manganese (II) and phenols. *Planta* **140,** 81–88.

Halpin, C., Knight, M. E., Foxon, G. A., Campbell, M. M., Boudet, A. M., Boon, J. J., Chabbert, B., Tollier, M. T., and Schuch, W. (1994). Manipulation of lignin quality by down-regulation of cinnamyl alcohol dehydrogenase. *Plant J.* **6,** 339–350.

Hammerschmidt, R., Bonnen, A. M., Bergstrom, G. C., and Baker, K. (1985). Association of epidermal lignification with non-host resistance of cucurbits to fungi. *Can. J. Bot.* **63,** 2393–2398.

Hapiot, P., Pinson, J., Neta, P., Francesch, C., Mhamdi, F., Rolando, C., and Schneider, S. (1994). Mechanism of oxidative coupling of coniferyl alcohol. *Phytochemistry* **36,** 1013–1020.

Harkin, J. M., and Obst, T. R. (1973). Lignification in trees: Indication of exclusive peroxidase participation. *Science* **180,** 296–297.

Hauffe, K. D., Paszkowski, U., Schulze-Lefert, P., Halbrock, K., Dangl, J. L., and Douglas, C. J. (1991). A parsley 4CL-1 promoter fragment specifies complex expression patterns in transgenic tobacco. *Plant Cell* **3,** 435–443.

Hepler, P. K., Rice, R. M., and Terranova, W. A. (1972). Cytochemical localization of peroxidase in wound vessel members of *Coleus*. *Can. J. Bot.* **50,** 977–983.

Herrmann, K. M. (1995). The shikimate pathway: Early steps in the biosynthesis of aromatic compounds. *Plant Cell* **7,** 907–919.

Hibino, T., Takabe, K., Kawazu, T., Shibata, D., and Higuchi, T. (1995). Increase of cinnamaldehyde groups in lignin of transgenic tobacco plants carrying an antisense gene for cinnamyl alcohol dehydrogenase. *Biosci. Biotechnol. Biochem.* **59,** 929–931.

Higuchi, T. (1959). Studies on the biosynthesis of lignins. *In* "Biochemistry of Wood" (K. Kratzl and G. Billek, eds.), pp. 161–168. Pergammon, New York.

Higuchi, T. (1990). Lignin biochemistry: Biosynthesis and biodegradation. *Wood Sci. Technol.* **24,** 23–63.

Higuchi, T., Shimada, M., Nakatsubo, F., and Tanahashi, M. (1977). Differences in biosynthesis of guaiacyl and syringyl lignins in woods. *Wood Sci. Technol.* **11,** 153–167.

Higuchi, T., Ito, T., Umezawa, T., Hibino, T., and Shibata, D. (1994). Red-brown color of lignified tissues of transgenic plants with antisense CAD gene: Wine-red lignin from coniferyl aldehyde. *J. Biotechnol.* **37,** 151–158.

Holton, T. A., and Cornish, E. C. (1995). Genetics and biochemistry of anthocyanin biosynthesis. *Plant Cell* **7,** 1071–1083.

Hosel, W., Fiedler-Preiss, A., and Borgmann, E. (1982). Relationship of coniferin β-glucosidase to lignification in various plant cell suspension cultures. *Plant Cell Tissue Org. Cult.* **1,** 137–148.

Houtman, C. J., and Atalla, R. H. (1995). Cellulose–lignin interactions. *Plant Physiol.* **107,** 977–984.

Iiyama, K., and Lam, T. (1990). Lignin in wheat internodes. Part 1: The reactivities of lignin units during alkaline nitrobenzene oxidation. *J. Sci. Food Agric.* **51,** 481–491.

Iiyama, K., and Wallis, A. F. A. (1988). An improved acetyl bromide procedure for determining lignin in woods and wood pulps. *Wood Sci. Technol.* **22,** 271–280.

Iiyama, K., and Lam, T., Meikle, P. J., Ng, K., Rhodes, D., and Stone, B. A. (1993). Cell wall biosynthesis and its regulation. *In* "Forage Cell Wall Structure and Digestibility" (H. Jung, D. Buxton, J. Hatfield, and J. Ralph, eds.), pp. 621–683. American Society of Agronomy, Madison, WI.

Iiyama, K., and Lam, T., and Stone, B. A. (1994). Covalent cross-links in the cell wall. *Plant Physiol.* **104,** 315–320.

Ingold, E., Sugiyama, M., and Komamine, A. (1990). L-α-Aminoxy-β-phenylpropionic acid inhibits lignification but not the differentiation to tracheary elements on isolated mesophyll cells of *Zinnia elegans*. *Physiol. Plant.* **78,** 67–74.

Jensen, R. A. (1994). Does subcellular compartmentation channel metabolite flow to lignin?. *In* "DOE Lignin Workshop: Research Needs in Lignin Biosynthesis and Biodegradation," pp. 29–30. Asilomar, U.S.A.

Johnson, D. B., Moore, W. E., and Zank, L. C. (1961). The spectrophotometric determination of lignin in small wood samples. *Tappi* **44,** 793–798.

Jones, J. D., Henstrand, J. M., Handa, A. K., Herrmann, K. M., and Weller, S. C. (1995). Impaired wound induction of 3-deoxy-D-arabino-heptulosonate-7-phosphate (DAHP) synthase and altered stem development in transgenic potato plants expressing a DAHP synthase antisense construct. *Plant Physiol.* **108,** 1413–1421.

Kim, S. H., Terry, M. E., Hoops, P., Dauwalder, M., and Roux, S. J. (1988). Production and characterization of monoclonal antibodies to wall-localized peroxidases from corn seedlings. *Plant Physiol.* **88,** 1446–1453.

Kolattukudy, P. E. (1984). Biochemistry and function of cutin and suberin. *Can. J. Bot.* **62,** 2918–2933.

LaFayette, P. R., Eriksson, K. E. L., and Dean, J. F. D. (1995). Nucleotide sequence of a cDNA clone encoding an acidic laccase from sycamore mapple (*Acer pseudoplatanus* L.). *Plant Physiol.* **107,** 667–668.

Lagrimini, L. M. (1991). Wound-induced deposition of polyphenols in transgenic plants overexpressing peroxidase. *Plant Physiol.* **96,** 577–583.

Lagrimini, L. M., Burkhart, W., Moyer, M., and Rothstein, S. (1987). Molecular cloning of complementary DNA encoding the lignin-forming peroxidase from tobacco: Molecular analysis and tissue-specific expression. *Proc. Natl. Acad. Sci. U.S.A.* **84,** 7542–7546.

Lagrimini, L. M., Bradford, S., and Rothstein, S. (1990). Peroxidase-induced wilting in transgenic tobacco plants. *Plant Cell* **2,** 7–18.

Lagrimini, L. M., Vaughn, J., Erb, A., and Miller, S. A. (1993). Peroxidase overproduction in tomato: Wound induced polyphenol deposition and disease resistance. *HortScience* **28,** 218–221.

Lange, B. M., Lapierre, C., and Sandermann, M. (1995). Elicitor-induced spruce stress lignin. *Plant Physiol.* **108,** 1277–1287.

Lapierre, C. (1993). Applications of new methods for the investigation of lignin structure. *In* "Forage Cell Wall Structure and Digestibility" (H. G. Jung, D. R. Buxton, R. D. Hatfield, and J. Ralph, eds.), pp. 133–166. American Society of Agronomy, Madison, WI.

Lapierre, C., Pollet, B., Monties, B., and Rolando, C. (1991). Thioacidolysis of spruce lignins: GC-MS analysis of the main dimers recovered after Raney nickel desulphuration. *Holzforschung* **45,** 61–68.

Lapierre, C., Pollet, B., and Rolando, C. (1995). New insights into the molecular architecture of hardwood lignins by chemical degradative methods. *Res. Chem. Intermed.* **21,** 397–412.

Lapierre, C., Pollet, B., and Negrel, J. (1996). The phenolic domain of potato suberin: structural comparison with lignins. *Phytochemistry* **42,** 949–953.

Leinhos, V., and Savidge, R. A. (1993). Isolation of protoplasts from developing xylem of *Pinus banksiana* and *Pinus strobus*. *Can. J. For. Res.* **23,** 343–348.

Lewis, N. G., and Davin, L. B. (1994). Evolution of lignan and neolignan biochemical pathways. *In* "Evolution of Natural Products" (D. Nes, ed.), ACS Symp. Series, Vol. 562, pp. 202–246. Am. Chem. Soc., Washington, DC.

Lewis, N. G., and Yamamoto, E. (1990). Lignin: Occurrence, biogenesis and biodegradation. *Annu. Rev. Plant Physiol. Plant Mol. Biol.* **41,** 455–496.

Lin, L. S., and Varner, J. E. (1991). Expression of ascorbic acid oxidase in zucchini squash (*Cucurbita pepo* L.). *Plant Physiol.* **96,** 159–165.

Liu, L., Dean, J. F. D., Friedman, W. E., and Eriksson, K. E. L. (1994). A laccase-like phenoloxidase is correlated with lignin biosynthesis in *Zinnia elegans* stem tissues. *Plant J.* **6,** 213–224.

Liu, L., Eriksson, K. E. L., and Dean, J. F. D. (1995). Localization of hydrogen peroxide production in *Pisum sativum* L. using epi-polarization microscopy to follow cerium perhydroxide deposition. *Plant Physiol.* **107,** 501–506.

Lüdemann, H. D., and Nimz, H. H. (1973). Carbon-13 nuclear magnetic resonance spectra of lignins. *Biochem. Biophys. Res. Commun.* **52,** 1162–1169.

Lundquist, K., and Kirk, T. K. (1971). Acid degradation of lignin. IV. Analysis of lignin acidolysis products by gas chromatography using trimethylsilyl derivatives. *Acta Chem. Scand.* **25,** 889–894.

Maciel, G. E., Haw, J. F., Smith, D. H., Gabrielson, B. C., and Hatfield, G. R. (1985). Carbon-13 nuclear magnetic resonance of herbaceous plants and their components, using cross polarization and magic angle spinning. *J. Agric. Biol. Chem.* **33,** 185–191.

Mäder, M., Ungemach, J., and Schloβ, P. (1980). The role of peroxidase isoenzyme groups of *Nicotiana tabacum* in hydrogen peroxide formation. *Planta* **147,** 467–470.

Marcinowski, S., and Grisebach, H. (1978). Enzymology of lignification. Cell wall-bound β-glucosidase for coniferin from spruce (*Picea abies*) seedlings. *Eur. J. Biochem.* **87,** 37–44.

Matern, U., Grimming, B., and Kneusel, R. E. (1995). Plant cell wall reinforcement in the disease-resistance response: Molecular composition and regulation. *Can. J. Bot.* **73S,** S511–S517.

Matsui, N., Fukushima, K., Yasuda, S., and Terashima, N. (1994). On the behavior of monolignol glucosides in lignin biosynthesis. II. Synthesis of monolignol glucosides labeled with ^3H at the hydroxymethyl group of side chain and incorporation of the label into magnolia and ginkgo lignin. *Holzforschung* **48,** 375–380.

Mayer, A. M. (1987). Polyphenol oxidases in plants. Recent progress. *Phytochemistry* **26,** 11–20.

McDougall, G. J. (1992). Changes in cell wall associated peroxidases during the lignification of flax fibers. *Phytochemistry* **31,** 3385–3389.

McDougall, G. J., Stewart, D., and Morrison, I. M. (1994a). Cell wall-bound oxidases from tobacco (*Nicotiana tabacum*) xylem participate in lignin formation. *Planta* **194,** 9–14.

McDougall, G. J., Stewart, D., and Morrison, I. M. (1994b). Oxidation of coniferyl alcohol to lignin-like products by tobacco xylem cell walls. *Phytochemistry* **37,** 683–688.

McDougall, G. J., Stewart, D., and Morrison, I. M. (1996). Tyrosine residues enhance cross-linking of synthetic proteins into lignin-like dehydrogenation products. *Phytochemistry* **41,** 43–47.

Mohan, R., Bajar, A. M., and Kolattukudy, P. E. (1993). Induction of a tomato anionic peroxidase gene (*tap1*) by wounding in transgenic tobacco and activation of *tap1*/GUS and *tap2*/GUS chimeric gene fusions in transgenic tobacco by wounding and pathogen attack. *Plant Mol. Biol.* **21,** 341–354.

Monties, B. (1985). Recent advances in lignin inhomogeneity. *In* "The Biochemistry of Plant Phenolics" (C. F. Van Sumere and P. J. Lea, eds.), Annual Proceedings of the Phytochemical Society of Europe, Vol. 25, pp. 161–181. Clarendon, Oxford.

Morrison, I. M., and Stewart, D. (1995). Determination of lignin in the presence of ester-bound substituted cinnamic acids by a modified acetyl bromide procedure. *J. Sci. Food Agric.* **69,** 151–157.

Nakamura, W. (1967). Studies on the biosynthesis of lignins. I. Disproof against the catalytic activity of laccase in the oxidation of coniferyl alcohol. *J. Biochem.* **62,** 54–61.

Neish, A. C. (1968). Monomeric intermediates in the biosynthesis of lignin. *In* "Constitution and Biosynthesis of Lignin" (K. Freudenberg and A. C. Neish, eds.), pp. 3–43. Springer-Verlag, New York.

Ni, W. T., Paiva, N. L., and Dixon, R. A. (1994). Reduced lignin in transgenic plants containing a caffeic acid *O*-methyltransferase antisense gene. *Transgen. Res.* **3,** 120–126.

Nicholson, R. L., and Hammerschmidt, R. (1992). Phenolic compounds and their role in disease resistance. *Annu. Rev. Phytopathol.* **30,** 369–389.

Nimz, H. H. (1974). Beech lignin: Proposal of a constitutional scheme. *Angew. Chem. Int. Ed.* **13,** 313–321.

Nose, M., Bernards, M. A., Furlan, M., Zajicek, J., Eberhardt, T. L., and Lewis, N. G. (1995). Evidence for sequential biosynthetic steps during lignin polymerization. *Phytochemistry* **39,** 71–79.

Ohnishi, J., Watanabe, T., and Koshijama, T. (1992). Synthesis of dehydrogenation polymer–polyose complexes by peroxidase. *Phytochemistry* **31,** 1185–1190.

Okusa, K., Miyakoshi, T., and Chen, C. L. (1996). Comparative studies on dehydrogenative polymerization of coniferyl alcohol by laccases and peroxidases. Part 1. Preliminary results. *Holzforschung* **50,** 15–23.

Olson, P. D., and Varner, J. E. (1993). Hydrogen peroxide and lignification. *Plant J.* **4,** 887–892.

O'Malley, D. M., Whetten, R., Bao, W., Chen, C. L., and Sederoff, R. R. (1993). The role of laccase in lignification. *Plant J.* **4,** 751–757.

Osakabe, K., Koyama, H., Kawai, S., Katayama, Y., and Morohoshi, N. (1994). Molecular cloning and the nucleotide sequences of two novel cDNAs that encode anionic peroxidases of *Populus kitakammiensis. Plant Sci.* **103,** 167–175.

Pickett-Heaps, J. D. (1968). Xylem wall deposition: Radioautographic investigations using lignin precursors. *Protoplasma* **65,** 181–205.

Polle, A., and Glavac, V. (1993). Seasonal changes in the axial distribution of peroxidase activity in the xylem sap of beech (*Fagus sylvatica* L.) tress. *Tree Physiol.* **13,** 409–413.

Polle, A., Otter, T., and Seifert, F. (1994). Apoplastic peroxidases and lignification in needles of Norway spruce (*Picea abies* L.). *Plant Physiol.* **106,** 53–60.

Ralph, J., and Hatfield, R. D. (1991). Pyrolysis-GC-MS characterization of forage materials. *J. Agric. Food Chem.* **39,** 1426–1437.

Ralph, J., Hatfield, R. D., Quideae, S., Helm, R. F., Grabber, J. H., and Jung, H. J. G. (1994a). Pathway of *p*-coumaric acid incorporation into maize lignin as revealed by NMR. *J. Am. Chem. Soc.* **116,** 9448–9456.

Ralph, J., Quideae, S., Grabber, and Hatfield, R. D. (1994b). Identification and synthesis of new ferulic acid dehydrodimers present in grass cell walls. *J. Chem. Soc. Perkin Trans.* **I,** 3485–3498.

Roberts, A. W., Koonce, L. T., and Haigler, C. H. (1992). A simplified method for *in vitro* tracheary element differentiation in mesophyll suspension cultures of *Zinnia elegans* L. *Plant Cell Tissue Org. Cult.* **28,** 27–35.

Ros Barceló, A. (1995). Peroxidase and not laccase is the enzyme responsible for cell wall lignification in the secondary thickening of xylem vessels in *Lupinus. Protoplasma* **186,** 41–44.

Ros Barceló, A., Pedreño, M. A., Muñoz, R., and Sabater, F. (1988). Lupin peroxidases. II. Binding of acidic isoperoxidases to cell walls. *Physiol. Plant.* **73,** 238–244.

Ros Barceló, A., Ferrer, M. A., and Pedreño, M. A. (1994). Oxidase and peroxidase activities of cell wall acidic peroxidase isoenzymes are correlated with cell wall lignification in *Lupinus. Plant Physiol.* (*Life Sci. Adv.*) **13,** 335–339.

Ros Barceló, A., Morales, M., and Pedreño, M. A. (1997). Specific compartmentalization of peroxidase isoenzymes in relation with lignin biosynthesis in the plant cell. *In* "Lignin and Lignan Biosynthesis" (N. G. Lewis and S. Sarkanen, eds.), ACS Symp. Series, in press. Am. Chem. Soc., Washington, DC.

Ryser, U., and Keller, B. (1992). Ultrastructural localization of a bean glycine-rich protein in unlignified primary walls of protoxylem cells. *Plant Cell* **4,** 773–783.

Saake, B., Argyropoulos, D. S., Beinhoff, O., and Faiz, O. (1996). A comparison of lignin polymer models (DHPs) and lignins by ^{31}PNMR spectroscopy. *Phytochemistry* **43,** 499–507.

Saka, S., Thomas, R. J., and Gratzl, J. S. (1978). Lignin distribution determination be energy-dispersive analysis of X-rays. *Tappi* **61,** 73–76.

Sánchez, M., Peña, M. J., Revilla, G., and Zarra, I. (1996). Changes in dehydrodiferulic acids and peroxidase activity against ferulic acid associated with cell walls during growth of *Pinus pinaster* hypocotyl. *Plant Physiol.* **111,** 941–946.

Sato, Y., Sugiyama, M., Gorecki, R. J., Fukuda, H., and Komamine, A. (1993). Interrelationship between lignin deposition and the activities of peroxidase isoenzymes in differentiating tracheary elements of *Zinnia.* Analysis using L-α-aminooxy-β-phenylpropionic acid and 2-aminoindan-2-phosphonic acid. *Planta* **189,** 584–589.

Sato, Y., Sugiyama, M., Komamine, A., and Fukuda, H. (1995). Separation and characterization of the isoenzymes of wall-bound peroxidase from cultured *Zinnia* cells during tracheary element differentiation. *Planta* **196,** 141–147.

Savidge, R. A. (1989). Coniferin, a biochemical indicator of commitment to tracheid differentiation in conifers. *Can. J. Bot.* **67,** 2663–2668.

Savidge, R. A., and Udagama-Randeniya, P. (1992). Cell wall bound coniferyl alcohol oxidase associated with lignification in conifers. *Phytochemistry* **31,** 2959–2966.

Schopfer, P. (1994). Histological demonstration and localization of H_2O_2 in organs of higher plants by tissue printing on nitrocellulose paper. *Plant Physiol.* **104,** 1269–1275.

Schuler, M. A. (1996). Plant cytochrome P450 monooxygenases. *Crit. Rev. Plant Sci.* **15,** 235–284.

Scott, J. A. N., Procter, A. R., Fergus, B. J., and Goring, D. A. (1969). The application of UV microscopy to the distribution of lignin in wood; description and validity of the technique. *Wood Sci. Technol.* **3,** 73–92.

Sederoff, R., Campbell, M., O'Malley, D., and Whetten, R. (1994). Genetic regulation of lignin biosynthesis and the potential modification of wood by genetic engineering in loblolly pine. *In* "Genetic Engineering of Plant Secondary Metabolism" (B. E. Ellis, ed.), pp. 313–355. Plenum, New York.

Sherf, B. A., Bajar, A. M., and Kolattukudy, P. E. (1993). Abolition of an inducible highly anionic peroxidase activity in transgenic tomato. *Plant Physiol.* **101,** 201–208.

Shininger, T. L. (1979). The control of vascular development. *Annu. Rev. Plant Physiol.* **30,** 313–337.

Simola, L. K., Lemmetyinen, J., and Santannen, A. (1992). Lignin release and photomixotrophism in suspension cultures of *Picea abies*. *Physiol. Plant.* **84,** 374–379.

Smart, C. C., and Amrhein, N. (1985). The influence of lignification on the development of vascular tissue in *Vigna radiata* L. *Protoplasma* **124,** 87–95.

Smith C. G., Rodgers, M. W., Zimmerlin, A., Fernandino, D., and Bolwell, G. P. (1994). Tissue and subcellular immunolocalisation of enzymes of lignin synthesis in differentiating and wounded hypocotyl tissue of french bean (*Phaseolus vulgaris* L.). *Planta* **192,** 155–164.

Southerton, S. G., and Deverall, B. J. (1990). Histochemical and chemical evidence for lignin accumulation during the expression of resistance to leaf rust fungi in wheat. *Physiol. Mol. Plant Pathol.* **36,** 483–494.

Sterjiades, R., Dean, J. F. D., and Eriksson, K. E. L. (1992). Laccase from sycamore maple (*Acer pseudoplatanus*) polymerizes monolignols. *Plant Physiol.* **99,** 1162–1168.

Sterjiades, R., Dean, J. F. D., Gamble, G., Himmelsbach, D. S., and Eriksson, K. E. L. (1993). Extracellular laccases and peroxidases from sycamore maple (*Acer pseudoplatanus*) cell suspension cultures. Reactions with monolignols and lignin model compounds. *Planta* **190,** 75–87.

Strivastava, L. M. (1966). Histochemical studies on lignin. *Tappi* **49,** 173–183.

Takahama, U. (1993). Regulation of peroxidase-dependent oxidation of phenolics by ascorbic acid: Different effects of ascorbic acid on the oxidation of coniferyl alcohol by the apoplastic soluble and cell wall-bound peroxidases from epicotyls of *Vigna angularis*. *Plant Cell Physiol.* **34,** 809–817.

Takahama, U. (1995). Oxidation of hydroxycinnamic acid and hydroxycinnamyl alcohol derivatives by laccase and peroxidase. Interactions among *p*-hydroxyphenyl, guaiacyl and syringyl groups during the oxidation reactions. *Physiol. Plant.* **93,** 61–68.

Taylor, J. G., Owen, T. P., Koonce, L. T., and Haigler, C. H. (1992). Dispersed lignin in tracheary elements treated with cellulose synthesis inhibitors provides evidence that molecules of the secondary cell wall mediate wall patterning. *Plant J.* **2,** 959–970.

Terashima, N. (1990). A new mechanism for formation of a structurally ordered protolignin macromolecule in the cell wall of tree xylem. *J. Pulp Paper Sci.* **16,** 150–155.

Terashima, N., and Fukushima, K. (1989). Biogenesis and structure of macromolecular lignin in cell wall of tree xylem as studied by microautoradiography. *In* "Plant Cell Wall Polymers: Biogenesis and Biodegradation" (N. G. Lewis and M. G. Paice, eds.), ACS Symp. Series, Vol. 399, pp. 160–168. Am. Chem. Soc., Washington, DC.

Terashima, N., Fukushima, K., He, L. F., and Takabe, K. (1993). Comprehensive model of the lignified plant cell wall. *In* "Forage Cell Wall Structure and Digestibility" (H. G. Jung, D. R. Buxton, R. D. Hatfield, and J. Ralph, eds.), pp. 247–269. American Society of Agronomy, Madison, WI.

Terashima, N., Atalla, R. H., Ralph, S. A., Landucci, L. L., Lapierre, C., and Monties, B. (1995). New preparations of lignin polymer models under conditions that approximate cell wall lignification. I. Synthesis of novel lignin polymer models and their structural characterization by ^{13}CNMR. *Holzforschung* **49,** 521–527.

Terashima, N., Atalla, R. H., Ralph, S. A., Landucci, L. L., Lapierre, C., and Monties, B. (1996). New preparations of lignin polymer models under conditions that approximate cell wall lignification. II. Structural characterization of the models by thioacidolysis. *Holzforschung* **50,** 9–14.

Tollier, M. T., Lapierre, C., Monties, B., Francesch, C., and Rolando, C. (1991). Structural variations in synthetic lignins (DHPs) according to the conditions of their preparation. *In* "Proc. Int. Symp. Wood Pulping Chem., Parkville, Victoria," pp. 35–40.

Trenck, Th., and Sandermann, H. (1981). Incorporation of benzo[α]pyrene quinones into lignin. *FEBS Lett.* **125,** 72–76.

Vance, C. P., Kirk, T. K., and Sherwood, R. T. (1980). Lignification as mechanism of disease resistance. *Annu. Rev. Phytopathol.* **18,** 259–288.

Van Doorsselaere, J., Baucher, M., Chognot, E., Chabbert, B., Tollier, M. T., Petit-Conil, M., Leplé, J. M., Pilate, G., Cornu, D., Monties, B., Van Montagu, M., Inzé, D., Boerjan, W., and Jouanin, L. (1995). A novel lignin in poplar trees with a reduced *O*-methyltransferase activity. *Plant J.* **8,** 855–864.

Wallace, G., and Fry, S. C. (1994). Phenolic components of the plant cell wall. *Int. Rev. Cytol.* **151,** 229–267.

Wardrop, A. B. (1971). Lignins: Occurrence and formation in plants. *In* "Lignins: Occurrence, Formation, Structure and Reactions" (K. V. Sarkanen and G. H. Ludwig, eds.), pp. 19–41. Wiley–Interscience, New York.

Weymouth, N., Dean, J. F. D., Eriksson, K. E. L. (1993). Synthesis and spectroscopic characterization of *p*-hydroxypphenyl, guaiacyl and syringyl lignin polymer models (DHPs). *Nord. Pulp Paper Res. J.* **8,** 344–349.

Whetten, R., and Sederoff, R. (1995). Lignin biosynthesis. *Plant Cell* **7,** 1001–1013.

Yao, K., De Luca, V., and Brisson, N. (1995). Creation of a metabolic sink for tryptophan alters the phenylpropanoid pathway and susceptibility of potato to *Phytophthora infestans*. *Plant Cell* **7,** 1787–1799.

Ye, Z. H., and Varner, J. E. (1995). Differential expression of two *O*-methyltransferases in lignin biosynthesis in *Zinnia elegans*. *Plant Physiol.* **108,** 459–467.

Ye, Z. H., Kneusel, R. E., Matern, U., and Varner, J. E. (1994). An alternative methylation pathway in lignin biosynthesis in *Zinnia*. *Plant Cell* **6,** 1427–1439.

Zhang, Z., Collinge, D. B., and Thordal-Christiansen, H. (1995). Germin-like oxalate oxidase, a H_2O_2-producing enzyme, accumulates in barley attacked by the powdery mildew fungus. *Plant J.* **8,** 139–145.

Functional Interactions among Cytoskeleton, Membranes, and Cell Wall in the Pollen Tube of Flowering Plants

Yi-Qin Li,[1] Alessandra Moscatelli, Giampiero Cai, and Mauro Cresti[2]
Dipartimento Biologia Ambientale, Università di Siena, 53100 Siena, Italy

The pollen tube is a cellular system that plays a fundamental role during the process of fertilization in higher plants. Because it is so important, the pollen tube has been subjected to intensive studies with the aim of understanding its biology. The pollen tube represents a fascinating model for studying interactions between the internal cytoskeletal machinery, the membrane system, and the cell wall. These compartments, often studied as independent units, show several molecular interactions and can influence the structure and organization of each other. The way the cell wall is constructed, the dynamics of the endomembrane system, and functions of the cytoskeleton suggest that these compartments are a molecular "continuum," which represents a link between the extracellular environment and the pollen tube cytoplasm. Several experimental approaches have been used to understand how these interactions may translate the pollen–pistil interactions into differential processes of pollen tube growth.
KEY WORDS: Calcium gradient, Cell wall, Cytoplasmic streaming, Cytoskeleton, Cytoskeleton–membrane interaction, Exocytosis, Pollen tube.

I. Introduction

A. Scope and Organization of This Review

Sexual reproduction in plants means an alternating diploid sporophytic and haploid gamethophytic generation. In seed plants the mature gametophyte

[1] Current address: Department of Biological Science and Biotechnology, Tsinghua University, 100084 Bejing, China.
[2] To whom correspondence should be addressed. Fax: 39-577-298860. E-mail: cresti@unisi.it.

Copyright © 1997 by Academic Press.
All rights of reproduction in any form reserved.

generation is reduced to a single vegetative cell forming one or two sperm cells. The male gametophyte develops from the sporigenous tissue inside the anthers (Golberg *et al.*, 1993). The vegetative and generative cells are formed after meiotic division of the pollen mother cell and subsequent mitotic division. In nature, at the anthesis, the ripe pollen grains are dried and released from the anthers to be transported by different vectors (such as insects, birds, wind, and water) on the stigma surface. After pollination the mission of the male gamete is only partially completed because it is concerned with conveying the two sperm cells or their progenitor, the generative cell, to the female gametophyte. The pollen tube serves as a guide and a pathway for the sperm cells on their course to the embryo sac to complete the double fertilization. For such reasons the pollen tube emission and growth represent one key step in the fertilization process of flowering plants (Cresti *et al.*, 1992). Pollen germination and pollen tube growth were first described by an Italian scientist, GiovanBattista Amici (Amici, 1824; see also Battaglia, 1987, and references therein). Since then an unbelievable amount of research has been done on the morphology, physiology, biochemistry, and molecular biology of pollen, tube emission, and its growth (Stanley and Linskens, 1974; Heslop-Harrison, 1987; Pierson and Cresti, 1992; Derksen *et al.*, 1995b; Ylstra, 1995). The scope of this review is to give a critical evaluation on the functional role of the cytoskeleton during growth and cell wall formation in a very peculiar cell, such as the pollen tube of flowering plants. The interactions between the cytoskeleton and membranes (especially those involved in secretion), the process of exocytosis, and the pattern of cell wall formation are discussed. Mechanisms of pollen tube elongation and factors affecting this activity are also presented.

The review is divided into eight sections. Section II provides information on the endomembrane pollen tube organization involved in the tip growth process. The third part of this review is a summary of the current state of morphology and biochemistry of the cytoskeleton (microtubules (MTs), actin filaments (AFs), and others cytoskeletal proteins), and its role in pollen tube growth. In section IV the cytological and biochemical evidence of the connection between the cytoskeleton, the plasma membrane, and the cell wall is described. Particular emphasis is given to the description of peculiar proteins such as spectrin and integrin, not very familiar in plant tissues. The construction of the pollen tube wall is reported in section V, where the more recent results on the structure and function of the pollen tube cell wall are reviewed. Section VI reports recent insights into the process of synthesis and transport of cell wall precursors. Particularly, the processes of exocytosis and endocytosis are discussed here. Section VII reports information on processes such as cell polarity and signal transduction; the regulation of growth rate and fluctuation is also discussed. Closing

comments on the state of the art in the "cytoskeleton–membrane–cell wall" research in the pollen tube and a perspective on the future are expounded in section VIII.

B. Pollen Germination and Pollen Tube Growth

The process of pollen germination begins after pollination, immediately or soon after the pollen reaches the stigma surface. Pollen grains generally shrink due to dehydration after the anthesis stage and once grains are placed on the stigma or an artificial medium, they swell due to water absorption or hydration. At the beginning of hydration, the pollen cell membranes are not biologically functional, so the chemical components (including sugars, amino acids, and enzymes) are excreted from the cell. Simultaneously, large molecular substances enter from the stigma exudate or from the artificial medium. Gradually, the membrane recovers its biological functions and becomes semipermeable, allowing water to pass through the membrane but preventing substances other than water from entering. Consequently, turgor pressure inside the pollen increases, enabling the tube of the pollen cell to elongate (Iwanami *et al.,* 1988). The duration between the end of water absorption and tube emission varies among species: it can be a few minutes in *Impatiens* and 20 hr in red pine. During pollen hydration and activation many morphological changes occur in the vegetative and generative cell: restoration of bilayer organization of membrane lipids, aggregation of ribosomes to form polysomes, formation of new lamellae and starch grains in the plastids, dilatation of the rough endoplasmic reticulum (RER), an increase of the secretory activity of Golgi bodies, and the subsequent accumulation of vesicles near the germination pore, the enlargement in volume of the vegetative nucleus and generative cell, and a decrease in the number of nuclear pores (Pierson and Cresti, 1992). These changes are accompanied by the beginning of a rotational movement of the organelles in the pollen cytoplasm (Iwanami, 1956). At the start of germination, the intine protrudes through the exine, a kind of hinge is formed resembling a porthole door, and the tube finally outgrows (Cresti *et al.,* 1977; Cresti and Keijzer, 1985; Heslop-Harrison, 1987). In many species the pollen can grow not only in the stigma of a pistil, but also in an artificial medium by allowing the pollen grains to imbibe water in a moist chamber (Gilissen, 1977). The incubation medium generally contains boric acid, calcium nitrate, and an osmoticum, such as sucrose or polyethylene glycol (Shivanna and Rangaswami, 1992).

Additional substances such as lipids, fatty acids, flavonols, amino acids, and probably also trace elements like metals, plant hormones, and steroids are necessary (Brewbaker and Kwack, 1963; Ylstra *et al.,* 1992, 1994a, 1995a;

Dickinson, 1995). In the mature pollen grains these compounds are either intracellularly located or they are present in the exine. Compounds in the exine are synthesized during maturation by a specialized tissue within the anther: the tapetum. The bulk of the nutrients required for tube growth has to be absorbed from the pistil. The stigma has to offer an exudate with exactly the right fluidity and chemical composition as a landing base for the pollen (Dickinson, 1995; Kandasamy *et al.,* 1993). When the pollen is cultured in a medium (e.g., solid or liquid medium), various patterns of tube growth can be obtained, depending on the culture condition. Frequently, pollens can grow more vigorously when they are sowed thickly (positive density effect). On the other hand, there are other species that show a negative density effect in artificial pollen culturing. Pollen tubes grow at their apex by fusion of wall vesicles with the cell membrane. The precise localization of this growing point on the tube apex determines the direction of tube growth. The delivery of constructive material for rapid polar wall synthesis is sustained by a flow of organelles and the Golgi vesicle-forming wall (Mascarenhas, 1993; Derksen *et al.,* 1995b). The movement of organelles and vesicles occurs on a dynamic cytoskeletal matrix and is driven by active acto-myosin interactions (Pierson and Cresti, 1992; Cai *et al.,* 1996a, and references therein). Specific mechanisms regulate constant synthesis, degradation, and the assemblage of cytoskeletal elements to maintain the delivery of wall vesicles at the apex. Despite the enormous cellular enlargement due to pollen tube growth, the total amount of cytoplasm remains almost constant. When the pollen tube elongates to a certain extent, plugs (which consist of callose, a β-1-3-glucanepolysaccharide) are formed inside it at almost regular lengths (Cresti and Van Went, 1976). The first plug is generated at the basal part of the tube, and several plugs are then formed one by one toward the central part of the tube. The synthesis of callose plugs behind the cytoplasmic section results in the development of a living apical tip apart from a dead remnant skeleton. The remnant wall skeleton, which is mainly composed by callose and pecto-cellulosic walls, is lost for further participation in the tube growth process (Ylstra *et al.,* 1995b). From the early study in *Lilium* (Rosen *et al.,* 1964) and *Petunia* (Sassen, 1964) on the ultrastructure of the pollen tube, it is known that these cells contain an enormous quantity of organelles; however, their distribution is not uniform over the length of the pollen tube. Starting from the pollen tube apex four cytological or functional zones can be distinguished (Cresti *et al.,* 1976, 1977): (1) an apical zone (also called the cap-block or hyaline zone; Steer, 1990; Steer and Steer, 1989) populated by many vesicles; (2) a subapical zone rich in organelles, mainly Golgi bodies, mitochondria, and ER; (3) a nuclear zone, containing the generative cell and vegetative nucleus; and (4) a zone with large vacuoles and a thin layer of cortical cytoplasm, separated from the more apical part of the tube

by callose plugs. This kind of zonation is a common characteristic of the pollen tubes of many species, but it is not universal. For example, in grasses or in *Pinus sylvestris* the zonation is not completely clear or does not exist (Heslop-Harrison, 1979; De Win *et al.,* 1996). The polar organization of the cytoplasm reflects the unipolar growth of the pollen tubes, which is restricted to the very tip region (Pierson and Cresti, 1992). Briefly, the Golgi bodies produce a large amount of secretory vesicles (SVs) that is transferred by an intense reverse fountain-like streaming pattern in the direction of the plasma membrane at the tube tip where the growth takes place. The vesicles provide new membrane and cell wall materials that are indispensable for extension. The pollen tube growth can be considered a highly specialized example of secretory activity because the growth rate is very fast, in many species it can be more than 2–3 mm/hr.

II. Organization of the Endomembrane System in the Pollen Tube

Pollen tubes exhibit a vigorous cytoplasmic streaming that usually appears as a central stream directed toward the tip with return streams along the cortex, the so-called reverse fountain-like streaming (Iwanami, 1956), which does not extend into the tip. When observed by light microscopy, the cytoplasm of the tip region appears to be clear, which suggests the absence of larger organelles (Pierson *et al.,* 1990). Ultrastructural observations presented by Rosen *et al.* (1964) and Sassen (1964) showed that the tip region is the site of accumulation for SVs, whereas other organelles were not distributed uniformly along the tube. The term "zonation" was introduced by Cresti *et al.* (1977) and referred to a functional distribution of organelles. The four zones described in *in vitro* grown *Lycopersicon* tubes were (a) an apical or growth zone with SVs, (b) a subapical zone rich in organelles, (c) the nuclear zone containing both the vegetative nucleus and the generative cell, and (d) the vacuolization and callose plug formation zone. This general description is applicable to most if not all angiosperm pollen tubes.

A. The Plasma Membrane

It has been shown that the plasma membrane and the wall material needed for tube growth are provided by the fusion of SVs with the plasma membrane in the tip. The membrane flow toward the pollen tube surface is more than the immediate requirement for growth (Steer and Steer, 1989), and the excess plasma membrane may be removed. Whether endocytosis

can account for this return flow remains a question. Part of the plasma membrane may also be removed by direct enzymatic degradation or by lipid transfer (Arondel and Kader, 1990). The plasma membrane and the other organelle membranes contain a specific set of resident integral membrane proteins that provide each membrane with its unique characteristics. A variety of plant ion channels has been found in the plasma membrane of pollen tubes (Hedrich and Schroeder, 1989; Tester, 1990; see below). The pollen tube plasma membrane contains channels that regulate ion influxes in the pollen tube during tip growth, as for Ca^{2+} and K^+ (Weisenseel and Jaffe, 1976; Kuhtreiber and Jaffe, 1990; see section VII for further discussion).

B. The Secretory System

1. Endoplasmic Reticulum

Exocytosis consists of the fusion of the vesicle membrane with the plasma membrane, allowing secretory material to be reversed outside the cell. Products to be secreted are initially synthesized in the ER, and then they pass through the Golgi apparatus and travel either to the plasma membrane or to the vacuole. Each step is vesicle-mediated and involves membrane fusion events. The structure and distribution of the RER, as well as of the Golgi and SVs, were recently investigated in cryofixed and freeze-substituted *Nicotiana tabacum* pollen tubes (Derksen *et al.*, 1995a). The RER appeared to consist of flat sheets with a diameter around 27 nm. Tubular RER was occasionally seen near the sheets. The latter may represent intermediate stages between cisternal RER and smooth ER since the two forms of ER are highly dynamic and may easily convert into each other (Quader and Schnepf, 1986; Quader *et al.*, 1989; Knebel *et al.*, 1990). The RER was almost completely absent from the extreme tip, but it was abundantly present 10 μm behind the apex in *N. tabacum* pollen tubes. A distinct zone of accumulation for the RER was not seen, but each pollen tube contained local aggregations of RER randomly dispersed within the cytoplasm. The RER was observed to run parallel to the pollen tube axis, with the exception of a region 5–10 μm behind the apex, where the streaming is reversed. The accumulation of RER near the tip was often reported in the pollen tube, inducing us to hypothesize that it may accomplish this for the requirement of proteins in the growing apex (Derksen *et al.*, 1995a).

The smooth ER consisted of tubular structures, especially abundant behind the tip region where SVs accumulated. In tobacco pollen tubes, smooth ER was not observed within the apex, whereas elements of smooth ER were seen between SVs in cryofixed freeze-substituted lily pollen tubes

(Lancelle and Hepler, 1992). Sheets of ER were seen in association with other organelles such as mitochondria, microbodies, and plastids. Elements of ER were also present near the plasma membrane and they were sometimes observed in the vicinity of or all around the vacuole (Derksen *et al.*, 1995a). It was proposed that smooth ER may function in the regulation of Ca^{2+} concentration (Evans *et al.*, 1991).

2. Golgi Apparatus

The Golgi apparatus is a highly polar organelle consisting of stark flattened cisternae. The Golgi apparatus in most animal cells consists of many stacks interconnected by tubular elements (Mellman and Simons, 1992), whereas the Golgi apparatus of higher plant cells usually appears as distinct organelles defined as Golgi bodies or dictyosomes (Robinson, 1980; Morrè, 1990). The Golgi apparatus of plant cells serves two major synthetic functions: it assembles and processes the oligosaccharide side chains of glycoproteins and proteoglicans and it synthesizes the complex polysaccharides of the cell wall matrix (Zhang and Staehelin, 1992). During pollen tube growth, the Golgi systems produce a large amount of SVs that accumulate in the tip region and fuse with the plasma membrane, reversing their content of polysaccharides outside the tube (Derksen *et al.*, 1995a). With the exception of the very tip, Golgi bodies were found throughout the pollen tube. Golgi bodies appeared to contain four to six cisternae (Cresti *et al.*, 1977; Picton and Steer, 1983; Noguchi, 1990), showing a distinct *cis–trans* polarity as determined by the decreasing width of the cisternal lumina.

The walls of tip growing cells, like pollen tubes, are mainly derived from the contents of the secretory vesicles and, simultaneously, the membrane of vesicles contributes to the extension of the plasma membrane in the tip region (Steer and Steer, 1989). The pollen tube Golgi apparatus shows the classic form in which all cisternae (*cis,* medial, and *trans*) are present. A fourth type of cisterna was identified as a *trans* Golgi network (TGN) (Griffith and Simons, 1986). The TGN was described as a reticulated structure characterized by budding coated vesicles (CVs) (Novikoff, 1976). The TGN was also known as the partially coated reticulum in plant cells (Pesacreta and Lucas, 1985) and is often connected with the *trans* site of the Golgi (Hilmer *et al.*, 1988; Juniper *et al.*, 1982). The TGN was observed in the tobacco pollen tubes as intimately linked to the Golgi (Rutten, 1993). In most plant cells, SVs are reported to arise from the swollen margins of the cisternae (Kristen, 1978; Staehelin, 1988). Sometimes intact cisternae are released as single vesicles (Domozych, 1991). In tobacco pollen tubes, SVs appeared to originate from the TGN through the formation of various intermediate stages between intact TGN, vesicle clusters, and vesicles. A prerequisite for the maintenance of the Golgi is a constant supply of mem-

brane material to counterbalance the loss caused by the continuous production of SVs. In tobacco pollen tubes, about 10% of the membrane material delivered to the plasma membrane is needed for tube growth (Derksen *et al.,* 1995a). The remainder is probably retrieved by endocytosis (Pearse and Bretscher, 1981).

3. Secretory Vesicles

Mature SVs were observed to be connected to the *trans* site of the Golgi apparatus. SVs in the extreme tip do not show any directional motion but are often described as a trembling mass (Herth, 1989; Pierson *et al.,* 1990). Quantitative measurements of SVs in freeze-substituted tobacco pollen tubes revealed that their concentration is very high in the very tip but declines behind the apex. The Golgi bodies are usually accompanied by CVs, which distribution was found to be identical to that of the Golgi (Derksen *et al.,* 1995a). From the size and smoothness of their coating, the CVs near the Golgi bodies seem nonclathrin-coated (Orci *et al.,* 1986). It is not clear whether these vesicles are only involved in an intra-Golgi transport (Orci *et al.,* 1986) or they represent a second vesicle transport route from or to the Golgi (Lodish, 1988; Mellman and Simons, 1992). The distribution analysis of the nonclathrin CVs (which appears identical to that of Golgi bodies) supports the first hypothesis. The presence of nonclathrin CVs near the *cis* phase of Golgi bodies may also suggest a transport toward the Golgi. It has been reported that a large portion of membranes supplied to Golgi bodies derives from membrane recycling, and it is represented by small nonclathrin CVs near the Golgi (Tanchak *et al.,* 1988). Consequently, endocytosed membrane material may be not transported directly to the Golgi but may first enter another cell compartment, such as the ER (Kappler *et al.,* 1986). The recent identification of clathrin-like molecules in the tip region of growing pollen tubes supports the evidence that an endocytotic process is active and responsible for membrane recycling in pollen tubes (Blackbourn and Jackson, 1996).

III. The Cytoskeleton of Pollen Tubes

The pollen tube reveals a cytoskeletal apparatus characterized by the presence of two threadlike systems: AFs and MTs. Both of them have been observed in the vegetative cytoplasm of angiosperm pollen tubes by ultrastructural observations and fluorescence microscopy, making use of specific markers for their main constituent proteins, actin and tubulin, respectively.

A. Biochemical Characteristics of Actin and Tubulin

The actomyosin system has an important role in several plant cell functions, such as the maintenance of the cell shape and cell motility processes like cytokinesis, mitosis, cytoplasmic streaming, and organelle movement (Emons *et al.*, 1991; Pierson and Cresti, 1992).

The backbone protein of AFs is formed by actin, which has a molecular weight of 42 kDa. In the filaments, actin molecules are filed up in such a way that they form a double-stranded twisted polymer. In animal as in plant cells, individual AFs have a diameter of 5–7 nm and show a distinct polarity (Vahey *et al.*, 1982; Ma and Yen, 1989; Tang *et al.*, 1989a; Villanueva *et al.*, 1990). Actin in plant cells is present in a dynamic state: it undergoes polymerization into AFs and depolymerization into actin monomers (Hennessey *et al.*, 1993). During cell growth (as in the pollen tube), actin monomers are polymerized into AFs, the latter representing essential elements for the cytoplasmic streaming that carries SVs to the growing tube tip (Pierson and Cresti, 1992).

A method for purifying actin from maize pollen has been developed that allowed us to obtain biologically active actin (Liu and Yen, 1992). The actin was electrophoretically homogeneous: only one band of 42 kDa was seen. When compared with rabbit muscle actin, pollen actin comigrated and appeared to be related by immunological methods and amino acid composition (Liu and Yen, 1992). Maize pollen actin displayed biological properties such as polymerization ability and activation of myosin ATPase activity. The polymerization property of pollen actin was much lower than that of muscle actin observed under the same conditions. The *in vitro* reconstituted AFs were analyzed by electron microscopy. The diameter of a single filament was about 7 nm (Yen *et al.*, 1995), very similar to that of other nonmuscle AFs (Koffer and Dickens, 1989). Reconstitued AFs also exhibited the same sensitivity to the AF-affecting drug Cytochalasin B.

MTs, the second component of the pollen tube cytoskeleton, appear as filamentous hollows highly variable in length and with a diameter of approximately 24 nm. MTs are primarily composed of the heterodimeric protein tubulin, which has a molecular mass of 100 kDa. The tubulin heterodimer is formed by the noncovalent interactions of α-and β-tubulin subunits, each with molecular masses near 50 kDa. Tubulin heterodimers polymerize in a "head-to-tail" fashion to form linear protofilaments. Typically, MTs contain 13 protofilaments that associate laterally to form the MT wall (Fosket and Morejohn, 1992). The conventional purification methods applied to obtain MT proteins from animal cells are successful when the homogenate contains tubulin levels higher than the critical dimer concentration. These methods are of limited value for plant cells since the low protein

concentration in plant tissues does not allow direct MT assembly from a crude supernatant.

In higher plants, tubulin properties and MT architecture have not been deeply investigated until recently, when tubulin isolation methods from a plant supernatant were designed. These methods are based on anion exchange chromatography strategies (Morejohn and Fosket, 1982; Morejohn *et al.,* 1984) or on herbicide-affinity chromatography (Mizuno *et al.,* 1981; Akashi *et al.,* 1988). Tubulin from a variety of plants shows distinct biochemical and immunological characteristics when compared with animal tubulin. In particular, plant α-tubulin shows distinctive peptide mapping patterns and electrophoretic mobility (Morejohn and Fosket, 1982; Hussey and Gull, 1985). In pollen tubes, the α subunit was shown to migrate faster than the β-subunit (Raudaskoski *et al.,* 1987). Furthermore, plant tubulins are also different from animal and fungi tubulin in immunological and pharmacological features (Morejohn *et al.,* 1984). In this view, the antigenic determinants were shared largely among more β than α subunits. Moreover, higher plant tubulins showed a lower affinity to the anti-MT drug colchicine than bovine brain tubulin under identical conditions (Morejohn *et al.,* 1984; Morejohn and Fosket, 1991).

Tubulin subunits are encoded by multigenic families consisting of three subclasses: the α- and β-tubulins, which form heterodimers and assemble in MTs, and the more recently identified γ-tubulin, which is primarily associated with MT poles (Oakley and Oakley, 1989). Several α- and β-tubulin genes are expressed in most plant tissues (Fosket, 1989; Siflow *et al.,* 1987). Two-dimensional gel electrophoresis has shown that plant α- and β-tubulins exhibit heterogeneity (isoforms) (Hussey *et al.,* 1987, 1988), possibly due to different gene products and/or posttranslational modifications. Posttranslational modifications of α-tubulin, such as tyrosination/detyrosination or acetylation, are well known. Dynamic MTs are usually tyrosinated, while those that are more stable are detyrosinated, acetylated, or both (Bulinski and Gundersen, 1991; Gelfand and Bershadsky, 1991, Piperno *et al.,* 1987; Webster and Borisy, 1989). Posttranslational modifications are less well known in plant cells than in animal cells. α-Tubulin has been reported to be tyrosinated in meristematic root cells of *Allium* (Wehland *et al.,* 1984) and in suspension cells of daucus (Dawson and Lloyd, 1987). Tyrosinated (-tubulin was identified in pollen tubes grown *in vitro* by Western blotting and then localized in growing tobacco pollen tubes by immunofluorescence techniques (Del Casino *et al.,* 1993). The acetylated α-tubulin was not seen in pollen tubes grown until 3 hr (Del Casino *et al.,* 1993), whereas it was observed within the generative, but not vegetative, cytoplasm of pollen tubes grown for longer times in Taxol-containing culture medium (Åström, 1992). γ-Tubulin in the pollen tube has

been localized by immunofluorescence, but it has not been yet biochemically characterized (Palevitz *et al.*, 1994).

Plant tubulin can polymerize *in vitro* into MTs by the addition of assembly-enhancing components like glycerol (Morejohn and Fosket, 1982), DMSO (Akashi *et al.*, 1988), and Taxol (Morejohn and Fosket, 1982; Morejohn *et al.*, 1984; Dawson and Lloyd, 1987; Falconer and Seagull, 1985). Ultrastructural observations of Taxol-induced structures from pollen tube supernatant revealed some peculiar characteristics. Pollen tubulin does not polymerize into single MTs, as is observed for other plant cell tubulin, but forms wide filaments (80–370 nm) interpreted as MT bundles (Tiezzi *et al.*, 1987). The bundling process is mostly characteristic of plant cells (such as in maize root tip Taxol-derived structures), whereas animal MTs polymerized under the same experimental conditions are individually distributed (Tiezzi *et al.*, 1988). A complex system of thin filaments and debris-like material is also associated with Taxol-derived MTs in *Nicotiana* pollen tubes. The ultrastructure and biochemistry of these Taxol-induced aggregates have been investigated, showing that the filamentous component was predominantly formed by actin (Tiezzi *et al.*, 1987; Moscatelli *et al.*, 1991). The formation of MT bundles and the presence of putative AFs in the pollen tube of Taxol-induced structures represented a distinctive feature of the cytoskeletal apparatus. It also suggests that specific tubulin isoforms could be present and responsible for the Taxol-induced structures described above. Studies on the gene expression of tubulin in *Arabidopsis* showed that a gene encoding for an α-tubulin isoform (TUA1) was primarily expressed in pollen, whereas most tubulin genes were expressed in many plant tissues (Carpenter *et al.*, 1992). The correlation between the timing of TUA1 expression and the assembly of extensive MT arrays in the pollen tube cytoplasm suggested that the TUA1 isotype is used in the vegetative cell but it does not play a role in sperm cell MTs. This circumstance could support the hypothesis of specialized MTs in pollen tubes with respect to those of other plant tissues.

B. Actin-Binding Proteins and Microtubule-Associated Proteins

The actin cytoskeleton of eukaryotic cells undergoes rapid and dynamic rearrangements in response to external stimuli during the cell cycle. The reorganization of the actin cytoskeleton is highly regulated temporally and spatially by a spectrum of actin binding proteins (Pollard and Cooper, 1986). Actin binding proteins can organize AFs into a loose network or tight bundles, capping the end or blocking the sides of filaments or even sequestering actin monomers. Specific interactions of actin binding proteins

with monomeric or polymeric actin can control the three-dimensional organization of the actin cytoskeleton.

Profilin is an actin monomer binding protein with low molecular mass (12–15 kDa) (Pollard and Cooper, 1986; Haarer and Brown, 1990), which has been identified in animal as well as in plant tissues. Profilin appears to be a multifunctional protein, which plays both a positive and a negative effect on actin polymerization (Theriot and Mitchison, 1993). Profilin binds to actin monomers, forming a 1:1 profilin:actin complex that sequesters actin monomers and prevents their polymerization. On the other hand, profilin also catalyzes the exchange of ATP for ADP on recycled monomeric actin, thus promoting actin polymerization. Profilin was first isolated from calf spleen (Carlsoon et al., 1977) and homologues have been subsequently found in many organisms including plants (Magdolen *et al.,* 1988; Binette *et al.,* 1990; Haugwitz *et al.,* 1991; Cooley *et al.,* 1992; Machesky and Pollard, 1993; Staiger *et al.,* 1993; Mittermann *et al.,* 1995; Vidali *et al.,* 1995). Plant profilins were originally discovered as allergens (Valenta *et al.,* 1991, 1993; Vallier *et al.,* 1992) and were subsequently described as actin binding proteins (Staiger *et al.,* 1993; Valenta *et al.,* 1993). cDNAs encoding for profilins were shown to be very similar in different plants, such as birch, maize, timoty grass, tobacco, and wheat (Valenta *et al.,* 1991, 1994; Staiger *et al.,* 1993; Mittermann *et al.,* 1995). Experiments of profilin microinjection into *Tradescantia blossfeldiana* stamen hair cells confirmed that profilin induces a rapid and irreversible depolymerization of AFs, causing inhibition of cytoplasmic streaming (Staiger *et al.,* 1994). Evidence that profilins have a prominent role during pollen maturation, pollen tube growth, and sexual reproduction of plants came from the observation that profilin expression is high in mature and germinated pollen (Mittermann *et al.,* 1995). A correct formation of AFs is required for maintaining cytoplasmic streaming and pollen tube growth (Pierson and Cresti, 1992; Derksen *et al.,* 1995b). In this view, the role of profilin in controlling actin polymerization could be critical during pollen maturation and tube growth. Approaches to identifying multiple profilin isoforms were carried out by both two-dimensional electrophoresis and cDNA library screening. The finding that large amounts of profilins are present in mature pollen compared to the lower levels in somatic plant tissues suggested that profilins play an important role in pollen biology (Mittermann *et al.,* 1995). cDNAs encoding for three tobacco profilin isoforms showed high sequence conservation (Staiger *et al.,* 1993). This suggests that different profilin isoforms may be functionally equivalent and may protect the pollen against a loss of profilin activity. Profilins could promote actin polymerization and stabilize dynamic actin structures during pollen germination.

MTs are polymers made of tubulins and MT-associated proteins (MAPs). The latter bind the tubulin subunits during MT polymerization and protrude from the polymer surface. In plant and animal cells, the MT activity is thought to depend on their spatial organization, on the ability to polymerize/depolymerize, to link each other, and to bind other cytoskeletal elements and/or organelles. The modulation of MT function involves the regulation of both tubulin and MAP properties. Although much information is available on these proteins in animal and especially neuronal cells (Kreis and Vale, 1993), little is known about MAPs in plants.

A fundamental question about MTs is how these polymers with highly conserved structures can have a wide range of activities (Lloyd, 1991). From recent data obtained in animal cells (Matus, 1990), it is proposed that the different properties of MTs during the cell cycle and/or differentiation may be regulated by selective MAPs. Different MAPs can mediate the interactions of MTs, control the rate of tubulin assembly by lowering the critical tubulin concentration, and regulate the stability of MTs (Olmsted, 1996). Generally, MAPs are divided into two main classes: structural MAPs and energy transducing MAPs (motor proteins) like kinesin, dynein, or dynamin (Vale and Goldstein, 1990). Only structural MAPs will be considered in this paragraph. In higher plants, MAPs were identified in carrot (Cyr and Palevitz, 1989; Cyr, 1991) and cotton (Seagull *et al.,* 1990). More recently a set of proteins were identified in BY-2 (Jiang and Sonobe, 1993) and maize cultured cells. In the latter, one of these proteins shows an immunological relationship to the neuronal τ proteins (Vantard *et al.,* 1991). All these proteins displayed typical MAP properties of promoting purified animal and plant tubulin to coassemble with both animal and plant MTs (Schellembaum *et al.,* 1993). Plant cell MAPs have also been hypothesized to play a role in regulating cell morphogenesis. A 100-kDa MAP from maize suspension culture cells (Vantard *et al.,* 1994) was shown to modulate the activity of cortical MTs during cell elongation (Nick *et al.,* 1995).

Since the pollen tube is a rapidly elongating structure, the control of cell morphogenesis is important for maintaining proper growth. A role of MTs in regulating the pollen tube morphogenesis has been proposed after observing that MT-affecting drugs altered pollen tube diameter and influenced growth polarity (Derksen *et al.,* 1995b). Furthermore, pollen tube MTs appeared to establish physical connections with other cytoplasmic structures such as the plasma membrane, AFs, and ER to form a complex cortical network (Lancelle *et al.,* 1987). All these circumstances led us to hypothesize the requirements of MT-binding proteins that regulate the MT dynamic and connect them with other cellular structures. However, structural MAPs have not been yet identified in pollen tubes.

C. Distribution of Actin Filaments and Microtubules and Their Concerted Actions

Early electron-microscopical studies provided some evidence of AFs in the pollen tube (Franke *et al.,* 1972). However, the first demonstration of actin in pollen tubes was given by Condeelis (1974), which showed that fibrils from disrupted pollen tubes and pollen tube protoplasts of *Amaryllis belladonna* could bind to rabbit muscle meromyosin. Furthermore, the composition of AFs was confirmed by immunogold labeling (Lancelle and Hepler, 1989, 1991). The spatial organization of these elements has been investigated by fluorescence microscopy after staining with anti-actin antibodies or fluorescent phalloidin (Perdue and Parthasarathy, 1985; Pierson *et al.,* 1986; Tang *et al.,* 1989a). The distribution of AFs during pollen hydration and germination was investigated after both chemical fixation (Heslop-Harrison *et al.,* 1986) and permeabilization with DMSO in several angiosperms (Pierson, 1988).

Phalloidin-binding bodies were observed throughout the cytoplasm of the vegetative cell in ungerminated pollen (Heslop-Harrison *et al.,* 1986). These putative actin storage bodies undergo a rapid dissociation during pollen activation and germination, since they are no longer present when the tube emerges (Heslop-Harrison *et al.,* 1986; Tiwari and Polito, 1990a). A complex of attenuated filaments appeared, converging toward the germination aperture as the cytoplasm is leaving the grain and the cytoplasmic streaming starts (Heslop-Harrison *et al.,* 1986; Tiwari and Polito, 1990a). A clearer image of AF organization was observed in lily and tobacco pollen grains and tubes permeabilized by DMSO. In this case, a three-dimensional network of actin bundles was visualized in the entire vegetative cytoplasm (Pierson, 1988; Heslop-Harrison and Heslop-Harrison, 1991). The integrity of the actin cytoskeleton was revealed to be crucial in determining pollen germination and growth in *Pyrus communis,* since pollen grains treated with the AF-affecting drug Cytochalasin D failed to germinate (Tiwari and Polito, 1990a). During pollen tube elongation, AFs are axially oriented and extended over the whole tube length (Fig. 1). Studies on the distribution of AFs within the vegetative cell showed that they are distributed more in the cytoplasmic area than in the tube cortex (Pierson *et al.,* 1986; Pierson, 1988; Tang *et al.,* 1989a). It has also been frequently reported that arrays of AF bundles occur in the tube apex of different species (Perdue and Parthasarathy, 1985; Pierson *et al.,* 1986; Pierson, 1988). The presence of a dense AF network in the tube tip led to the development of a model of pollen tube growth in which the structure of the tube tip was controlled by AFs (Steer, 1990; Mascarenhas, 1993; Derksen *et al.,* 1995b). Other studies at the electron microscope after rapid freeze fixation and substitution failed to show AFs in the apex (Lancelle and Hepler, 1992), suggesting

that previous observations might be artifacts due to the chemical fixation methods. Microinjection experiments of fluorescence-labeled phalloidin allowed to localize AF bundles throughout growing pollen tubes, with the exception of the tip region (Miller *et al.,* 1996). A colocalization of AFs and MTs was observed in the cortical region of pollen tubes by both fluorescence microscopy (Pierson *et al.,* 1989) and ultrastructural observations after rapid freeze fixation and substitution (Lancelle and Hepler, 1991). The presence of structures connecting AFs and MTs to each other, and with both the ER and the plasma membrane, suggested functional relationships between those components and that both MTs and AFs contribute to the organization of the cortical cytoplasm.

Immunofluorescence techniques using antibodies to α- and β-tubulin subunits did not usually allow detection of MTs within ungerminated pollen grain, with the exception of *P. communis,* where a MT network was shown in hydrated pollen (Tiwari and Polito, 1990b). Generally, the MT cytoskeleton of pollen tubes mainly consists of cortical MTs with either helicoid or axial orientation (Derksen *et al.,* 1985; Tiezzi *et al.,* 1986; Raudaskoski *et al.,* 1987). Both cortical and cytoplasmic MTs are individually distributed in the vegetative cytoplasm (Fig. 1), whereas they are organized in bundles within the generative cell cytoplasm (Derksen *et al.,* 1985; Tiezzi *et al.,* 1986; Lancelle and Hepler, 1991). More recently, the MT distribution was investigated during pollen tube elongation in *N. tabacum.* Bundles of MTs with both cortical and cytoplasmic distribution were shown to extend from one-third to one-half of the pollen tube length, whereas only a few short MTs were found in the apical part. As the elongation proceeds, an intricate network of MTs normally extends into the apical zone, while the labeling intensity decreases in the oldest parts of the tube (Del Casino *et al.,* 1993). The lack of MTs in the apex of young pollen tubes suggested that they are not directly related to the growth process. The use of anti-tyrosinated tubulin antibodies on *Nicotiana* pollen tubes at different elongation stages suggested that tyrosinated MTs were mostly localized in the cortex of emerging tubes during early stages of growth. After further tube development, the labeling was also detected in the cytoplasm, especially in the apical and subapical zones. The tyrosinated form is always present in both the cortex and the cytoplasm of the apex. In animal cells, tyrosinated (-tubulin seems to be involved in dynamic processes. In that sense, the presence of tyrosinated (-tubulin may be related to tube growth (Del Casino *et al.,* 1993). Experiments with the MT-disrupting agent colchicine showed that MTs do not play a role in active tube growth, but in controlling tube diameter (Heslop-Harrison *et al.,* 1988). Recent data obtained with more specific anti-MT drugs (such as carbetamide, propham, and oryzalin) both *in vitro* and *in vivo* suggested that *Nicotiana* pollen tube MTs contribute to maintaining the internal cytoplasmic organization (Joos *et al.,* 1994,

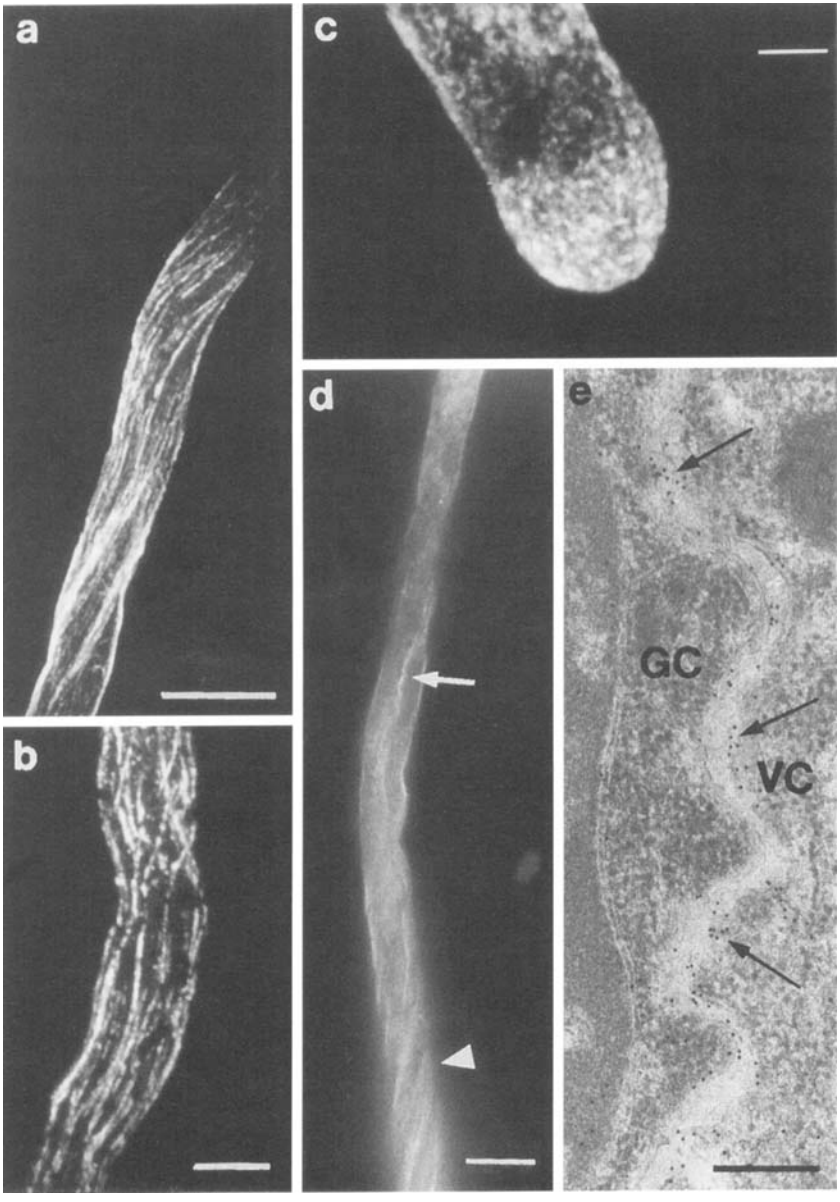
a
b
c
d
e
GC
VC

1995) and to regulating the timing of generative cell and vegetative nucleus entrance into the tube (Åström *et al.,* 1995).

Although the pattern of MTs in pollen tubes is known, few data are available on the localization of MT-nucleating sites. When pollen tube MTs were disrupted by cold treatment, tubulin was immunologically detected only in specific areas associated with the plasma membrane (Åström *et al.,* 1991). In *Lilium auratum,* the subapical region of the pollen tube was supposed to contain putative MT-generating sites (Heslop-Harrison and Heslop-Harrison, 1988). This is consistent with observations that short MTs are present in the apex of *Nicotiana* pollen tubes (Del Casino *et al.,* 1993). Recently, a pericentriolar immunoreactive homologue (p77) was found in association with a plasma membrane fraction from pollen tubes. Immunofluorescence observations showed the antigen to be located in the apical part in association with the cortical tube area (Cai *et al.,* 1996b). The only other component of MT-organizing centers found in pollen tubes is a γ-tubulin related antigen (Palevitz *et al.,* 1994). Since it showed a wide cytoplasmic pattern, it is differentially distributed with respect to p77. The different spatial arrangement of the two components could be related to the diverse functions they play in the pollen tube.

FIG. 1 Localization of cytoskeletal structures in the pollen tube. (a) Microtubules can be visualized using indirect immunofluorescence techniques with specific antitubulin antibodies. In this picture, a two hours-grown pollen tube of *Nicotiana tabacum* was chemically fixed and processed for immunofluorescence with an anti-α-tubulin antibody. Bundles of microtubules can be seen along the main axis of the pollen tube, running in a helicoidal manner. At this stage of pollen tube growth, microtubules are only partially visible in the tube apex (top right). The image was obtained with a confocal microscope. Bar, 20 μm. (b) Microtubules are sometimes observed to form a criss-cross pattern in the cortex of tobacco pollen tubes. The image was obtained with a confocal microscope. Bar, 10 μm. (Micrograph courtesy of C. Del Casino.) (c) Distribution of the pollen kinesin homolog as revealed by the k7ls23 monoclonal antikinesin antibody. A punctuate pattern is observed in the pollen tube apex, and also in the cortical region behind the tip. Spots are presumed to represent kinesin-related molecules bound to membrane-bound structures, probably vesicles not directly involved in the process of secretion. Bar, 5 μm. (Micrograph courtesy of C. Del Casino.) (d) The actin filament skeleton of pollen tubes as shown by staining with rhodamine-phalloidine. Actin filaments can be seen in the two typical organization pattern, as longitudinal bundles running in the cytoplasm (arrow) and as helicoidal fibers in the pollen tube cortex (arrowheads). The image was obtained with an optical microscope after chemical fixation. Bar, 20 μm. (e) Immuno-gold labelling with an antimyosin antibody in the cytoplasm on the *Nicotiana tabacum* pollen tube. In this particular image, clusters of gold particles (arrows) are observed on the surface of the generative cell (GC), in contact with the vegetative cytoplasm (VC). Myosin molecules are suggested to interact with the actin filaments, thus promoting the translocation of the generative cell through the pollen tube. Bar, 200 nm. (Micrograph courtesy of C. Faleri.)

IV. Connections of Cytoskeleton and Membranes

A. Transmembrane Linkage Proteins and Matrix Proteins

The pollen tube is a finger-like cellular protuberance produced by the pollen grain and naturally growing through the stigma and style. During its growth, the pollen tube is in communication with stigma and stylar components, which can be called the extracellular matrix (ECM). The ECM is considered very important in controlling the elongation of pollen tubes. The following sections will describe what is known on the membrane-associated skeleton, on transmembrane connecting proteins, and on ECM components interacting with the pollen tube.

1. Spectrin

Membrane proteins are not generally allowed to diffuse freely in the membrane sheet, but they are restricted to some specific areas, where their functions are required. To achieve such a limitation, some structural elements of the cytoskeletal apparatus are involved. Moreover, a membrane-associated cytoskeleton is also required to limit the alteration in shape or dimension of a cell (Cowin and Burke, 1996). Among the membrane-associated cytoskeletal molecules, spectrins are a pertinent example. Spectrin is a cytoskeletal protein associated with the cytoplasmic side of the plasma membrane. In red blood cells, spectrin is a heterodimeric molecule, composed by two 220- to 240-kDa polypeptidic chains (α and β) linked in a noncovalent way. The role of spectrins in red blood cells is to build a cytoskeletal structure on the cytoplasmic side of the plasma membrane, enabling red blood cells to offer resistance to tensions on their membranes. Spectrin molecules are linked together into a network by molecular complexes in which even actin takes part. All this intricate cytoplasmic side-associated cytoskeleton is bound to the plasma membrane by transmembrane proteins (Bennett and Gilligan, 1993).

Plant cells can sustain the tension exerted on their plasma membrane by the presence of a rigid cell wall (Showalter, 1993). However, the existence of further internal support may occasionally be useful. The apex of pollen tubes is a good example, since it is the place where tube growth occurs. The thickness and physical resistance of the cell wall in the tip are thought to be lower, when compared to other parts of the pollen tube (Derksen *et al.,* 1995b). On the contrary, the apex cell wall must be quite flexible to guarantee that tube elongation occurs. Immunorelated homologues of spectrins were identified in plant cells (De Ruijter and Emons, 1993) and also in pollen tubes, where they are localized in association with the tip

area (Derksen *et al.*, 1995b). Spectrins in the tip may participate in the construction of a cytoplasmic side cytoskeleton, which in turn may have a double function: (a) to serve as a membrane skeleton, allowing the tip membrane to withstand turgor pressure, and (b) to limit the mobility of membrane proteins in the apical membrane. Concerning the second possibility, a role for spectrin in limiting the lateral mobility of integral membrane proteins has already been shown in other cell types (Dahl *et al.*, 1994). Membrane proteins are probably also differentially distributed in the plasma membrane of pollen tubes; examples are the 100-kDa H^+-ATPase of the plasma membrane (Obermeyer *et al.*, 1992), the K^+ channels (Feijo *et al.*, 1995), the 77-kDa centrosome-related polypeptide (Cai *et al.*, 1996b), and polypeptides belonging to the Rho GTPase family (Lin *et al.*, 1996). All this evidence supports the idea that proteins in the plasma membrane of pollen tubes are actively maintained in precise positions.

Other speculative functions may be attributed to the spectrin homologues in pollen tubes. For example, α-spectrin contains a C-terminal domain structurally related to calmodulin (CaM) (Trave *et al.*, 1995b), whereas Ca^{2+} can induce a conformational change of spectrin, which is probably involved in regulating its binding to actin (Trave *et al.*, 1995a). Consequently, spectrin in the tube tip may bind to short AFs in a Ca^{2+}-dependent manner. While the association of actin to the plasma membrane of plant cells is already proven (Sonesson and Widell, 1993), we do not have corresponding evidence in the pollen tube. Spectrin has also been shown to contain a PH domain, which is a binding site for phosphatidyl-inositol 4,5-bisposphate, a polyphosphoinositide important for cell signaling (Hyvonen *et al.*, 1995). Spectrin in the tube tip may consequently participate in the pathway of signal transduction, but no data are available to support this hypothesis.

2. Integrins

Considering that some stylar components can attract the growing pollen tube and speed up its growth rate (Cheung *et al.*, 1995), the ECM is suggested to play a crucial role in directing pollen tube growth. In eucaryotes, integrins are the main receptors used by cells to bind to the ECM (Clark and Brugge, 1995). Integrins are a large family of homologous transmembrane proteins, generally formed by two 100- to 140-kDa polypeptidic chains (α and β) held together by noncovalent bonds. While the extracellular N-terminal domains bind to ECM molecules, the cytoplasmic C-terminal domains can interact with the cytoskeletal apparatus. Integrins do not bind directly to actin molecules, but the presence of auxiliary attachment proteins (such as talin, tensin, vinculin, and α-actinin) is required.

Immunologically related integrin molecules were also identified in plant cells. For example, the brown alga *Fucus* contains a homologous polypeptide of 92 kDa (Quatrano *et al.,* 1991), whereas a 120-kDa polypeptide was identified in the fungus *Saprolegnia* (Kaminskyj and Heath, 1995). Both polypeptides were detected using antibodies to the β1-integrin, which cytoplasmic domain is highly conserved in vertebrates, invertebrates, and fungi (Marcantonio and Hynes, 1988). In *Saprolegnia,* the antibody was found to label membrane spots in the tip region by immunofluorescence microscopy. After plasmolysis, the polypeptide remained attached to the cell wall, suggesting a strong interaction. Moreover, a 70- to 72-kDa vitronectin receptor-like polypeptide (such as integrins) was identified in soybean root cells by affinity chromatography and an immunological reaction against a polyclonal antibody to the human β3-integrin (Schindler *et al.,* 1989). The role of integrins in plant cells is related to the attachment process between the cytoskeleton and the cell wall. Integrin molecules may be involved in processes such as organelle motility, tip morphogenesis, and apex-directed contraction (Wyatt and Carpita, 1993).

Integrin molecules have not been yet identified in pollen tubes; therefore, only speculations can be made. AFs in pollen tubes are sometimes observed to focus in definite areas, which are hypothesized to act as putative "AF organizing sites" or "focal adhesions" (Pierson *et al.,* 1986). Although the precise subcellular localization of those actin foci has not been found, they are detected in pollen tubes grown in *in vivo* systems, but not under *in vitro* conditions. This evidence allows the speculation that the ECM may have a role in controlling the assembly of AFs within the growing pollen tube; the formation of ECM–cytoskeleton interactions may require the presence of transmembrane proteins with integrin-like characteristics.

The role of the tube plasma membrane (especially the tip area) in modulating the actin cytoskeleton has recently been made less mysterious by the identification of polypeptides immunologically related to Rho-GTPase (Lin *et al.,* 1996). In animal cells, Rho proteins participate in the pathway leading to the assembly of stress fibers (Nobes and Hall, 1995) following activation of cell-surface receptors. Current models on the assembly of focal adhesions involve the ECM-mediated aggregation of integrin molecules, a process also reliant on the activation of Rho proteins (Parsons, 1996). Rho-related GTP-binding proteins were also characterized in plant cells (Yang and Watson, 1993). The localization of Rho-related polypeptides in the tube tip plasma membrane (Lin *et al.,* 1996) suggests that the pollen tube apex is involved in the assembly of AFs as a response to external signals or interactions with the ECM.

3. Vitronectin- and Fibronectin-like Proteins

By definition, the ECM comprises several adhesive proteins having multiple domains, each with specific binding sites for both other ECM molecules

and receptors on the cell surface. Fibronectin is a large glycoprotein found in vertebrates that consists of two subunits connected by disulfide bonds (Mosher, 1988). The cell binding domain of fibronectin is characterized by the presence of a specific tripeptide sequence (Arg–Gly–Asp) that is an essential element for the binding of fibronectin to integrin molecules. Plant cells contain immunologically related fibronectin-like proteins, which were identified in the walls of NaCl-adapted cells using polyclonal antibodies against human fibronectin. The reactive polypeptide was not observed in NaCl-unadapted cells (Zhu *et al.,* 1993).

Vitronectin is a glycoprotein that was originally discovered as a cell attachment factor and is present in the ECM of many mammalian cells (Preissner, 1991). The adhesion mechanism is based on the attachment of the cytoskeleton to vitronectin molecules by transmembrane proteins, such as integrins. Although the activity of vitronectin is similar to that of fibronectin, the two molecules are biochemically and immunologically different (Preissner, 1991).

Vitronectin-like proteins were also identified in plant cells, like in the brown alga *Fucus* (Quatrano *et al.,* 1991), and in some species of flowering plants (Sanders *et al.,* 1991; Zhu *et al.,* 1993). These polypeptides were detected using polyclonal antibodies to vertebrate vitronectins, but they were not examined for specific functions. A 55-kDa vitronectin-like protein was isolated from NaCl-adapted cells and shown to bind to glass surfaces and heparin (Zhu *et al.,* 1994). Sequencing of this plant adhesion molecule revealed a strong identity with the translational elongation factor 1α, but almost no similarity to vitronectin. Immunogold localization suggested that the vitronectin-like protein is present in the inner wall of transmitting tissue cells in pollinated mature tobacco styles, and in the external wall of the cortical tissue cells within intercellular spaces. This specific localization allows the supposition that the novel vitronectin-like protein may be involved in some features of pollen tube extension. Two other classes related to vitronectin proteins were identified in *Lilium longiforum* using different preparations of human vitronectin antisera (Wang *et al.,* 1994). Compared with the vitronectin-like protein from NaCl-adapted cells (Zhu *et al.,* 1993), sequence analysis of one vitronectin-like polypeptide from *Lilium* revealed a strong similarity to human vitronectin (Wang *et al.,* 1994). Vitronectin-like proteins in plant cells are suggested to participate in various processes, such as cell adaptation to stress (Zhu *et al.,* 1993), the attachment of infecting bacteria to host cells (Wagner and Matthysse, 1992), and pollen tube guidance (Sanders *et al.,* 1991).

Concerning the involvement of ECM molecules in guiding pollen tube growth, the pollen tube tip may behave like a migrating cell, interacting with ECM components in the stylar transmitting tissue (Sanders *et al.,* 1991). This hypothesis was worked out by observing that latex beads put on the stigma translocate to the ovary at rates corresponding to the growth

speed of pollen tubes (Sanders and Lord, 1989). As support of this theory, vitronectin-like proteins were localized by immunological approaches on the surface of the transmitting tissue in the style (Sanders *et al.,* 1991).

ECM molecules may be important either in guiding the pollen tubes through the transmitting tissue of styles or in establishing the proper interactions between pollen tubes and pistil. The vitronectin-mediated interactions may induce some cytological modifications within the pollen tube, such as a different arrangement of the cytoskeleton. The actin foci of pollen tubes described above (Pierson *et al.,* 1986) may be interpreted as being induced by contacts with ECM molecules, since they are observed in *in vivo* systems, but not in *in vitro* ones.

B. The Movement of Membrane-Bounded Organelles along the Cytoskeleton

When a growing pollen tube is observed under the light microscope, it is easy to discern the movement of its cytoplasmic components (Pierson *et al.,* 1990). Under normal growth conditions, two separate directions of movement can be distinguished: from the grain to the tip and contrariwise. This translocation activity represents the way by which the growing pollen tube is continuously filled by the cytoplasm. After the onset of germination (depending on the plant species), it may also be possible to observe the generative cell/sperm cells while getting into the pollen tube and moving toward the tip. All movements in the pollen tube are likely to depend on the presence and activity of the cyoskeletal apparatus.

1. Cytoskeleton-Based Motor Proteins

In eucaryotes, the organelles within cells are not stationary, but they are actively organized and displaced according to the particular physiological condition of the cell. The approaches made in many laboratories during the last 10 years clearly showed that cells use their own cytoskeletal apparatus to move organelles (Langford, 1995). A particular kind of cytoskeletal protein—known as the cytoplasmic molecular motor—is the dynamic linkage between the track-like cytoskeletal fibrils (MTs and AFs) and the organelles to be moved. The cytoplasmic motor group includes three main protein categories: myosin (an AF-based motor), kinesin, and dynein (MT-based motors). Members of all three classes have been identified in the pollen tube system.

a. Myosin Heavy Chain Polypeptides The term myosin includes all the AF motor proteins identified to date. All myosins can hydrolize ATP in

the presence of AFs. This feature represents, with *in vitro* motility assays (Chaen *et al.,* 1993) and gene sequence analysis (Moepps *et al.,* 1993), the main criterion for the identification of new myosin polypeptides. The skeletal muscle myosin belongs to the myosin-II subfamily, which is formed by two polypeptides (the heavy chains) forming two heads and a rod-like structure (Titus, 1993). The heads carry the actin-binding and the ATP-hydrolyzing sites, whereas the rod is formed by the dimerization of the long α-helical tail domains of each heavy chain. Nonmuscle cells contain a different type of myosin, known as myosin I, characterized by a single head domain with the same functions as the myosin II heads, and by a rod-like tail highly divergent in structure and function from the myosin II class (Pollard *et al.,* 1991). Genetic analyses allowed the classification of all myosins into distinct classes (Cheney *et al.,* 1993).

In plant cells, the actomyosin system has been considered the main force-generating mechanism of cytoplasmic streaming. Information on such a role can be found in recent reviews on the subject (Shimmen and Yokota, 1994). As for other plant cells, AFs are suggested to be the main factor responsible for the active streaming of organelles in living pollen tubes (Heslop-Harrison and Heslop-Harrison, 1989a). The first indirect evidence for myosin polypeptides came from the observation that isolated pollen organelles move along Characean actin bundles in a Ca^{2+}-dependent manner (Khono and Shimmen, 1988). These results clearly show that polypeptides functionally related to myosins might exist in pollen tubes and that their activity was regulated by Ca^{2+}. In 1989, an immunoreactive polypeptide of 175 kDa was identified in extracts from pollen tubes of *Nicotiana alata* (Tang *et al.,* 1989b). The polypeptide is recognized by commercial antibodies to the head and tail domains of skeletal myosin. Both antibodies produce a similar type of staining when applied in fluorescence microscopy. Putative organelles and/or vesicles are stained but, while the anti-myosin head antibody gives a more uniform staining pattern along the tube, the anti-myosin tail antibody prevalently stains the apical region of pollen tubes. A more important difference is found in relation to the generative cell/vegetative nucleus staining. The anti-myosin head antibody produces a punctate uniform staining of both organelles, whereas the anti-myosin tail antibody does not yield any kind of staining. Subsequently, a different type of commercial anti-skeletal myosin antibody was used to label isolated pollen organelles, including the generative cell (Heslop-Harrison and Heslop-Harrison, 1989b). This preliminary evidence suggests the association of myosin polypeptides with pollen tube organelles and reinforces the hypothesis that the actomyosin system is the main mechanism for the movement of organelles and vesicles.

Biochemical analysis of the *in vitro* translocation activity of the pollen organelle revealed that the characteristics of the putative translocator are

very similar to those of conventional myosins (Khono *et al.*, 1990). Furthermore, a pollen tube extract was shown to contain a molecular component able to translocate fluorescently labeled chicken muscle AFs (Khono *et al.*, 1991). A 120-kDa polypeptide was subsequently purified from lily pollen tubes on the basis of its ability to translocate AFs in an *in vitro* motility assay (Khono *et al.*, 1992). The polypeptide binds to AFs and has an AF-activated ATPase activity. The 120-kDa myosin polypeptide was subsequently shown to be one fragment of a larger polypeptide of 170 kDa, which is particularly susceptible to proteolysis during purification (Yokota and Shimmen, 1994). Since the isolated 170-kDa polypeptide translocates AFs and has an AF-activated ATPase activity, it represents the first functional myosin polypeptide isolated from pollen tubes. The pollen myosin does not cross-react with an anti-pan myosin antibody and an antiserum raised to the pollen myosin does not label skeletal muscle myosin, suggesting that the pollen myosin is not immunologically related to conventional skeletal muscle myosins. These results distinguish the 170-kDa pollen myosin from the 175-kDa myosin polypeptide identified in *N. alata* (Tang *et al.*, 1989b), which is, on the contrary, labeled by anti-skeletal muscle myosin antibodies. A remarkable difference is also observed when the antiserum to the 170-kDa polypeptide is used in immunofluorescence microscopy. In tobacco and lily, the antiserum stains the apical and subapical regions of pollen tubes with a punctate staining pattern, which appears like the organelle distribution (Yokota *et al.*, 1995). Against previous results, the antiserum does not recognize any epitope associated with the surface of generative cell or vegetative nucleus.

Further observations were obtained with antibodies to specific myosin subfamilies. In particular, three different classes of myosin were identified in the pollen tubes of *N. alata* and *L. longiflorum* using heterologous antibodies directed against myosins I, II and V (Miller *et al.*, 1995). Antibodies to myosins IA and IB identify a main polypeptide of 125 kDa, which is essentially associated with the vegetative cell plasma membrane, larger organelles, and the surface of both the generative cell and the vegetative nucleus. This evidence suggests that myosin I may be the primary molecular motor involved in the translocation activity of the male germ unit. Antibodies to myosin V bind to a 190-kDa polypeptide, which is localized in association with smaller organelles, such as vesicles, suggesting a direct participation of myosin V polypeptides in the movement of SVs. On the other hand, antibodies to myosin II (against both the head and the tail domains) bind to a 205-kDa polypeptide in *Nicotiana* and *Lilium* pollen tubes. The putative myosin II is localized in association with larger organelles, such as plastids, mitochondria, and dyctiosomes. Since the 205-kDa myosin II polypeptide is only infrequently observed in association with the generative cell surface, its localization does not appear like that of the 175-kDa myosin. However,

these new results on myosins show that different pollen organelles may be moved by diverse translocators and suggest that the various organelle categories may be subjected to different types of regulation.

The association of myosins with the male germ unit surface is further supported by the identification of a 174-kDa myosin-related polypeptide on the generative cell surface. This result was obtained with a commercial antibody to skeletal muscle myosin in immunogold electron microscopy on chemically fixed material (Tirlapur *et al.,* 1995, 1996) (Fig. 1). This result was already shown in a previous work using the same antibody in immunofluorescence microscopy (Heslop-Harrison and Heslop-Harrison, 1989b). Although the physical fixation techniques, such as rapid fixation and freeze substitution, may yield a better preservation level of cellular structures than chemical fixation, the presence of myosin-II-related polypeptides in association with the generative cell surface must be considered. From these results, we can speculate either that only one myosin class is not sufficient for the translocation of the generative cell or that different myosins can have overlapping functions, or, otherwise, that some myosins may simply be redundant.

b. Kinesin-like Proteins The kinesin superfamily consists of MT-based motor proteins that play an active role in the translocation of organelles toward the plus end of MTs (Langford, 1995). Kinesins are involved in the MT-mediated translocation of membrane-bounded organelles (such as vesicles, ER, and mitocondria) and chromosomes (Hoyt, 1994). Kinesins were first discovered in nerve cells (Vale *et al.,* 1985) and shown to be heteropolymers of heavy and light chains (Bloom *et al.,* 1988). The kinesin heavy chains (KHCs) are characterized by a highly conserved motor domain of 350–400 amino acids, which carries both the MT- and the ATP-binding sites (Goldstein, 1993; Sablin *et al.,* 1996). Polypeptides whose gene sequence is significantly homologous only to the motor domain of KHCs (Hall and Hedgecock, 1991) were identified in many eucaryotic cells and are known as kinesin-like polypeptides (KLPs). Gene analyses showed that some KLPs might be involved in processes related to cell division (Wang and Adler, 1995; Wordeman and Mitchison, 1995). Frequently, the direction of translocation is determined by the position of the motor domain within the polypeptidic chain (Goodson *et al.,* 1994).

The presence of MT-based motor proteins in plant cells has been always controversial, since almost all the cytoplasmic movements that occur in plant cells were known to depend on the actomyosin system (Williamson, 1993). The identification of a GTP-dependent translocator in the phragmoplast of dividing BY-2 cells represented the first evidence for putative MT-based motor proteins in plant cells (Asada *et al.,* 1991). Neuronal tissues have been the first source for kinesin motors and purified KHCs were often

used as antigen to raise antibodies. Using a monoclonal antibody (k71s23) to the KHC from bovine brain, two immunoreactive polypeptides of 100–108 kDa were identified in cytoplasmic extracts from tobacco pollen tubes and shown to copellet with MTs in binding assays (Tiezzi *et al.,* 1992). Analysis by immunofluorescence microscopy with the anti-kinesin antibody provided a punctate staining in the apex of pollen tubes (Tiezzi *et al.,* 1992) (Fig. 2). These results suggested that the pollen kinesin homologues (PKHs) might be associated with vesicles and possibly involved in their translocation in the tube apex. This hypothesis was not supported by both the poor presence of MTs in the pollen tube apex (Derksen *et al.,* 1985; Del Casino *et al.,* 1993) and the evidence that KHCs from animal cells sometimes colocalize with cytoplasmic MTs (Hollenbeck, 1989). Subsequent works allowed us to obtain major insights into the function and structure of PKHs. The purified 100-kDa PKH has a MT-dependent ATPase activity and an ATP-sensitive MT-binding capacity (Cai *et al.,* 1993). These results suggested that the PKH is similar in biochemical properties to conventional KHCs. A deeper investigation by indirect immunofluorescence microscopy revealed two further characteristics. First, the PKH was detected along the cortex in growing pollen tubes and not only in the apical region. Second, double immunofluorescence studies showed that the PKH colocalizes with short MTs in the apex of tobacco pollen tubes (Cai *et al.,* 1993). Furthermore, immunological techniques showed that the k71s23 antibody binds to an antigenic polypeptide of 100 kDa (p100) on the surface of around 80-nm Golgi-derived vesicles (Liu *et al.,* 1994). The p100-containing Golgi-derived vesicles always copelleted with MTs in ATP-free binding assays. After treatment with high salt concentrations, p100 is detached from membranes and shows a MT-dependent ATPase activity (Liu *et al.,* 1994). This evidence shows that p100 is not an integral membrane protein, but instead a peripheral protein, which probably interacts with membranes by hypothetical receptors.

Kinesin-like gene sequences were also identified in plant cells. Five sequences related to the KHC motor domain (katA-E) were discovered in the genome of *Arabidopsis thaliana* (Mitsui *et al.,* 1993, 1994). All sequences contain the motor domain at the C terminus, suggesting that they codify for minus-end-directed motors. Antibodies directed to *in vitro* expressed fragments of katB-C identify an 85-kDa polypeptide in BY-2 cells, which level increases during cell division with a maximum of relative concentration at the M phase (Mitsui *et al.,* 1996). This information suggests that katB-C, like many KLPs of animals cells, might play a role during cell division. A plus-end-directed motor was also identified in BY-2 cells by *in vitro* motility assays and purified by MT-binding techniques (Asada and Shibaoka, 1994).

An antibody raised to a common peptide sequence in katA-B-C identifies a single polypeptide around 140 kDa in extracts from *A. thaliana* (Liu *et al.,* 1996). The polypeptide (named katAp) is localized by immunofluorescence studies in association with the mitotic apparatus of dividing cells. The same antibody was also used to identify antigenic polypeptides of 102–110 kDa in pollen tubes, which mainly associate with the MT cytoskeleton of the generative cell (Liu and Palevitz, 1996). A variable punctate staining is also observed in the vegetative cytoplasm, suggesting that other kinesin-related polypeptides may be present in pollen tubes beyond that previously identified.

Recently, other KLPs have been identified in plant cells by screening of expression libraries with biotinylated CaM (Reddy *et al.,* 1996a,b; Wang *et al.,* 1996). The biological activity of these KLPs is likely mediated by the formation of a Ca^{2+}/CaM complex. No evidence of such a KLP is found in the pollen tube.

c. Dynein-like Proteins Dyneins are MT-based motor proteins usually composed of several polypeptides and broadly subdivided into two main categories: axonemal and cytoplasmic dyneins (Holzbaur and Vallee, 1994). A polypeptidic chain around 400–500 kDa (known as the heavy chain and present in two to three copies per molecule) is the dynein component that binds to MTs in an ATP-dependent manner. Dynein heavy chains, like those of kinesins, can convert the chemical energy of ATP hydrolysis into a mechanical movement. While kinesin molecules can usually move toward the plus end of MTs, dynein molecules, on the contrary, can translocate toward the minus end of MTs (Schroer *et al.,* 1989). Dyneins were first identified as the molecular motors that boost axoneme bending and, consequently, the beating of axoneme-containing structures, such as cilia and flagella (Goodenough and Heuser, 1985). A homologue of axonemal dyneins with MT-dependent ATPase activity, ATP-dependent MT binding, and minus-end-directed motion (Paschal *et al.,* 1987) was identified in nerve cells and named cytoplasmic dynein. Subsequently, cytoplasmic dyneins were identified in many eucaryotic cells, again using genetic approaches (Andrews *et al.,* 1996). Cytoplasmic dyneins are also localized in association with kinetochores (Pfarr *et al.,* 1990), which suggests a further role in the minus-end-directed motion of chromosomes.

In higher plants, the only evidence for dynein concerned its presence in flagellated cells, like the sperms of primitive gymnosperms (for example, *Gingko biloba* and cycads). All published dynein sequences contain four P loop consensus sequences corresponding to the ATP-binding sites, which are highly conserved among dyneins from phylogenetically divergent species (Vallee, 1993). A peptide antibody raised to the conserved sequence of the first P loop can label two high-molecular-weight polypeptides in

extracts from tobacco pollen tubes. Consequently, this higher plant cell type is the first one where homologues of dynein heavy chains have been identified (Moscatelli *et al.,* 1995). The two polypeptides show an apparent molecular weight near that of axonemal and cytoplasmic dynein heavy chains and, most important, have a MT-activated ATPase activity and an ATP-dependent MT-binding ability (Moscatelli *et al.,* 1995). Since the two dynein polypeptides can be separated by zonal centrifugation in two distinct fractions sedimenting at 22 S and 12 S, respectively, they are probably not part of the same molecular complex. Although *in vitro* motility assays have not yet been performed, results suggest that the two dynein-related polypeptides may have a function in some kind of intracytoplasmic movement within pollen tubes. It is reported that *G. biloba* pollen also contains a dynein-related polypeptide (Moscatelli *et al.,* 1996), which has characteristics similar but not identical to those of the dynein doublet of tobacco pollen tubes. The finding of dynein-related polypeptides in *Gingko* pollen may be related either to MT-based cytoplasmic events (if the dynein polypeptide belongs to the cytoplasmic class) or to precursors of axonemal dyneins. Further ultrastructural and biochemical information are needed to clarify this question.

In animal cells, cytoplasmic dynein molecules are located in association with organelles and are involved in the vesicular traffic between the internal membrane compartments (Hirokawa *et al.,* 1990). New results have recently been obtained for the dynein-related polypeptides in pollen tubes, which show that they bind to organelles and are probably related to their transportation (Moscatelli *et al.,* manuscript in preparation). These results will be introduced and discussed below.

2. Proposed Mechanism of Interrelations among Motor Proteins

As previously described, polypeptides related to both AF- and MT-based motors are present in the vegetative cytoplasm of pollen tubes and probably involved in the organelle translocation activity. This section mainly describes possible models of interaction between AF- and MT-based motors.

As reported (Miller *et al.,* 1995), distinct organelles may be moved by different myosins. This evidence suggests that individual organelles have specific receptors for each myosin class, so that myosin I can bind to the male germ unit but not to SVs. This differentiation may be useful for α separately regulating the movement of various organelles, according to the particular growth condition of the pollen tube. Most larger organelles exhibit a bidirectional movement within the pollen tube (Pierson and Cresti, 1992). Organelles are translocated to the apex and after that moved back toward the grain (Steer and Steer, 1989); amyloplasts and lipid globuli are

observed to move to the proximity of the tip (around 20 μm from it) and then return (Heslop-Harrison and Heslop-Harrison, 1989a). This bidirectional movement is suggested to depend on the occurrence of AFs with both orientations along the tube and on the Ca^{2+}-induced fragmentation of AFs in the tip (Khono and Shimmen, 1987). Ca^{2+} may also exert a regulatory function on myosin activities in pollen tubes, thus preventing organelles from penetrating further into the apical region and favoring their movement back to the grain. Although MTs may play a role under particular conditions, such as in very old pollen tubes (Joos *et al.,* 1994), the incapacity for larger organelles to reach the apical region seems unrelated to MTs (Heslop-Harrison *et al.,* 1988).

The role of MTs in organelle translocation along the pollen tube is uncertain. The PKH is apparently located in the apical region (Tiezzi *et al.,* 1992) and, consequently, it is unlikely to control the movement of cytoplasmic organelles. On the other hand, the pollen dynein-related polypeptides could participate in such a process. Pollen dyneins were initially characterized as soluble components, but different extraction procedures have subsequently shown that they may be associated with the membrane fraction of pollen tubes (Moscatelli *et al.,* manuscript in preparation). Membrane-associated dynein-related polypeptides can be extracted only by treatment with detergents, suggesting a strong association with membranes. Immunoelectron microscopy reveals that the membrane-associated dynein-related polypeptides are restricted to defined organelles, such as small vacuoles, Golgi stacks, and other vesicular structures. Immunofluorescence microscopy shows that dynein-containing organelles are distributed along the pollen tube, following the same pattern of tube length-dependent distribution of MTs, as described in tobacco pollen tubes (Del Casino *et al.,* 1993). Although the dynein-related polypeptides are characterized by a MT-activated ATPase activity, no information on MT-dependent motility is available to date. Animal cells contain some clear examples of cooperation between the two motility systems, such as the Myo2p/Smy1p model in yeast (see below). Two other cases of interrelationship are found in nerve and epithelial cells, respectively. In the former, organelles move toward the synaptic terminal and back. Although kinesin and dynein molecules are the principal motors responsible for such bidirectional translocation activity (Hirokawa *et al.,* 1990, 1991), the actomyosin system is also found to participate in the movement of organelles along the axon (Kuznetsov *et al.,* 1992). Another example of a functional interrelationship between AFs and MTs is found in epithelial cells, where Golgi membranes possess both myosin I and cytoplasmic dynein molecules (Fath *et al.,* 1994). These examples suggest that eucaryotic cells can control the precise delivery of membrane-bounded organelles using both motor systems. The discovery of similar mechanisms in pollen tubes is an intriguing challenge.

The apex of pollen tubes is usually described as a "clear zone" to indicate the nonoccurrence of larger organelles and the presence of small vesicles deriving from the activity of dyctiosomes (Lancelle and Hepler, 1992). After vesicles are released into the apex, they are probably subjected to continuous random motions, which convey them to fuse with the apical plasma membrane. It is uncertain whether myosin polypeptides play a role in the tip region of pollen tubes. The main doubt concerns the low abundance of an actin network in the tip (Miller *et al.,* 1996), which is not apparently able to support the translocation of SVs onto the tip membrane. The problem is further complicated by opposite results on the presence of myosins in the tip region. Myosin-related polypeptides are observed in the tube tip in relation to the specific type of antibody used for labeling. Presently, myosin polypeptides in the 170- to 175-kDa range are detected in the apex and related to the movement of SVs (Tang *et al.,* 1989b; Yokota *et al.,* 1995). Myosins I, II, and V are not (or rarely) found in the apex (Miller *et al.,* 1995). We hypothesize that the 170- to 175-kDa myosins may be involved in the translocation of vesicles to the apex, but, when vesicles get to the tip, myosins are no longer essential for their translocation activity. The inactivation of myosin may be dependent on the higher Ca^{2+} concentration in the tip, since Ca^{2+} can inhibit vesicle translocation in *in vitro* systems (Khono and Shimmen, 1988). Another interpretation for the tip-located myosins may concern the organization of AFs. Although an elaborate actin network is not found in the apex (Miller *et al.,* 1996), the tip should represent the region where AFs are nucleated or elongated. Assuming the validity of the "nucleation-release model" (Theriot and Mitchison, 1992), short AFs could be incorporated or aligned to preexisting longer AFs in the subapical region. Myosins in the tip could be important in favoring and controlling the process of actin organization. In support of the opinion that the tip domain may control the growth of AFs, polypeptides related to Rho-GTPases have been identified in the pollen tube apex (Lin *et al.,* 1996). In animals, members of the Rho family participate in the cascade pathway, leading to the assembly of stress fibers in motile cells (Nobes and Hall, 1995).

Are MTs important in translocation events occurring in the pollen tube apex? Since the depolymerization of MTs does not alter the tube growth process (suggesting that the fusion rate of SVs is not modified), the answer is apparently negative. The only exceptions are found in special cases, such as very old pollen tubes (Joos *et al.,* 1994) or, more curiously, under *in vivo* conditions (Joos *et al.,* 1995). Depolymerization of MTs can also temporarily alter the pulsatory growth of pollen tubes, without affecting their elongation rate (Geitmann *et al.,* 1995b). In light of this evidence, it was unexpected to find an immunoreactive homologue of kinesin in the pollen tube apex (Tiezzi *et al.,* 1992), where MTs are not as abundant as in distal regions. Currently, the only way to find a possible function for the

PKH is to compare the pollen tube system with other cell types with polarized growth. In yeast, for example, a peculiar kind of cooperation between AF- and MT-based motors is found (Lillie and Brown, 1994). Myo2p is an unconventional yeast myosin that participates in polarized growth by conveying SVs. Myo2p mutants can be restored by another protein with motor activity, Smy1p, which is a KLP. Both proteins colocalize in the same cellular areas, suggesting that they may cooperate to control the delivery of SVs to precise places. The PKH may be a functional analogue of the yeast Smy1p.

Movement of the generative cell and vegetative nucleus in the pollen tube is probably dependent upon both AFs and MTs. Although AFs have the motive function, MTs are likely to lend support to the actin network. This subordinate activity is mainly derived from observations after oryzalin treatment, which selectively removes the MT cytoskeleton (Åström *et al.*, 1995). The movement of the male germ unit is not halted, but it is slowed. Presently, a direct involvement of MT-based motor proteins in the translocation of the male germ unit is not convincing. Neither the PKH nor the dynein-related polypeptides are detected in association with the generative cell or the vegetative nucleus (Tiezzi *et al.*, 1992; Moscatelli *et al.*, manuscript in preparation). On the other hand, disruption of the actin skeleton can efficiently block the translocation activity of the male germ unit (Heslop-Harrison *et al.*, 1988). Many data suggest the presence of myosin polypeptides in association with the surface of both the generative cell and the vegetative nucleus (Tang *et al.*, 1989b; Heslop-Harrison and Heslop-Harrison, 1989b; Tirlapur *et al.*, 1995, 1996). Ultrastructural evidence showed the presence of strip-shaped projections on the outer membrane of the generative cell (Bohdanowicz *et al.*, 1995), which are interpreted as myosin heads. Current models propose that the actin skeleton of the pollen tube may serve as tracks along which the generative cell and vegetative nucleus can move. MTs may help in the correct placement of AFs around the male germ unit to favor their proper interaction with myosins. Although protein links between MTs and AFs have not been identified, electron micrographs often showed that AFs and MTs align in the pollen tube cortex (Lancelle and Hepler, 1991).

A formal picture representing the role of motor proteins in the pollen tube is shown in Figure 2.

V. Structure of the Cell Wall of the Pollen Tube

The plant cell wall is generally constructed with three coextensive polymer networks: a network formed by cellulose microfibrils coated by an array

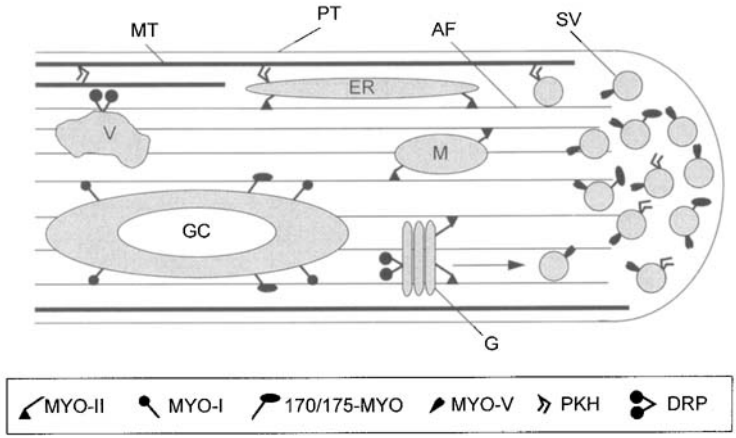

FIG. 2 The role of motor proteins in the growing pollen tube (PT). Organelles, such as mitochondria (M), endoplasmic reticulum (ER), and Golgi apparatus (G), are likely to be transported along the actin filament system (AF) by myosin molecules, expressly of the myosin-II class (MYO-II). The generative cell (GC) and the vegetative nucleus (not included in the picture) are probably translocated by myosin-I molecules (MYO-I). It is likely that 170/175-kDa myosins (170/175-MYO) can also be involved in this process. The accumulation of secretory vesicles (SV) in the tip region is probably dependent on the interactions of myosin-V (MYO-V) and 170/175-kDa myosins with the actin filaments. The role of microtubule (MT)-motor proteins during the tube growth is more uncertain. The pollen kinesin homolog (PKH) is suggested to be involved in the accumulation of vesicles in the tip, but other functions (such as the organization of the endoplasmic reticulum or the microtubular cytoskeleton) may be supposed. Dynein-related polypeptides (DRP) are probably associated with organelles, such as the Golgi apparatus and small vacuoles (V), and may be involved in their positioning.

of hemicelluloses (of which the major component is xyloglucans), a network formed by various pectins, and a minor network formed by structural proteins, such as extensins and expansin (Carpita and Gibeaut, 1993; McCann and Roberts, 1994). The cell wall of pollen tubes, which are rapidly tip-growing cells, exhibits a distinctive structure characterized as an outer pectocellulosic layer and an inner callosic lining.

A. Outer Pectocellulosic Layer

1. Differentiated Distribution of Esterified and Acidic Pectins

Pectins have been characterized by defining structural domains of carbohydrates in plant cell walls. The most common domain, homogalacturonan, is composed of linear chains of α-1,4-linked D-galacturonate, named acidic pectin. These chains may self-associate to form dimers (egg-box structure)

and further aggregate to form a rigid gel by a Ca^{2+}-mediated bridge. The carboxyl group of galacturonans are often partially methyl-esterified, known as esterified pectins that do not aggregate through Ca^{2+} binding and remain in a nonrigid form (Van Cutsem and Messiaen, 1994). The localization of acidic and esterified pectins in the wall of pollen tubes was shown by using MAbs JIM 5 and JIM 7 in confocal laser scanning microscopy (CLSM) and electron microscopy (Fig. 3). The important aspects of pectin distribution in the pollen tube wall are summarized as follows.

A periodic annular deposition of acidic pectins was found to coat the cell walls of pollen tubes in the species possessing solid styles (having transmitting tissue cells). A more even pectin sheath in the cell wall of pollen tubes in the species having hollow styles (with a stylar canal) or very short styles (Li *et al.*, 1994; Geitmann *et al.*, 1995a) was observed. The distinct pectin localization patterns were also shown in the *in vivo* grown pollen tubes of two representative species, *Petunia hybrida* (Li *et al.*, 1995a) and *L. longiflorum* (Li *et al.*, 1995a; Jauh and Lord, 1996). The pectic and cellulosic part of the cell wall, stained with Calcofluor white, also showed bands of the wall thickening in *Gasteria* pollen tubes (Plyushch *et al.*, 1995). Furthermore, it is likely that primitive species have a hollow style and a moderately uniform pectin sheath in the pollen tube wall. Advanced species have a solid style and periodic ring-like structure in the pectin layer of the pollen tube wall. This might suggest evolutionary adaptation of the pollen tube wall to its growth environment. However, this premature presumption should be proved by a complete investigation in flowering plants (Li *et al.*, 1995a). The tip extension of the pollen tube essentially requires both mechanical strength and the extensibility of the cell wall at the apex. Acidic pectins localized at apex provide mechanical strength to the tip wall by Ca^{2+}-induced gelification of pectate. Esterified pectins, deposited predominantly at the apex wall, caused "wall loosening" (Li *et al.*, 1994, 1995b). Esterified pectins were also detected in the mid- and *trans*-Golgi cestae and its derived vesicles, suggesting that they were primarily synthesized and transported to the growing tip. Pectin deesterification, catalyzed by pectin methyl-esterase (PME), occurred during pollen tube elongation, which leads to a more rigid form of pectins in the mature pollen tube wall (Li *et al.*, 1994, 1995b; Geitmann *et al.*, 1995a).

2. Distribution and Orientation of Cellulose Microfibrils

Cellulose microfibrils (CMF) were shown as wall texture in S and Z helices at 45° to the longitudinal axis of *Petunia* (Sassen, 1964) pollen tubes. On the other hand, CMF seemed "randomly" oriented at the tip. Recently, a lenticular thickened wall region has been observed at the extreme tip of lily (Lancelle and Hepler, 1992) and tobacco (Van Amstel, 1994; Derksen

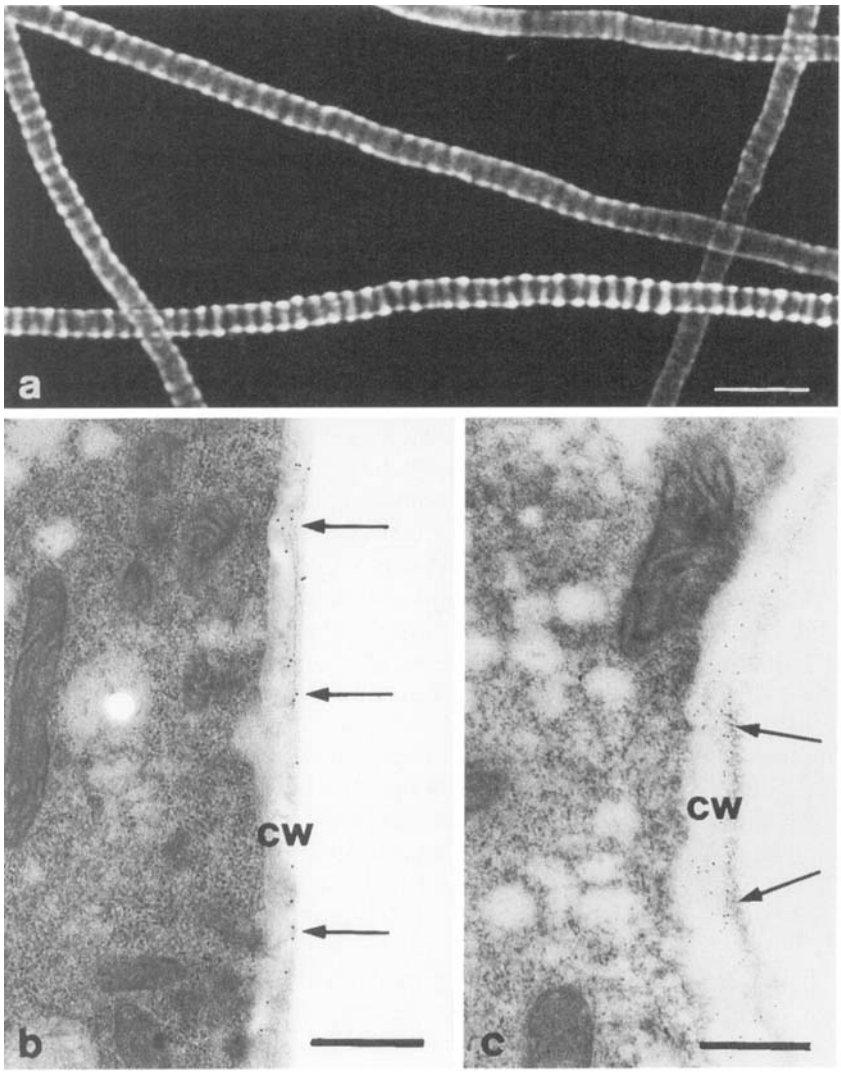

FIG. 3 Distribution of unesterified pectins in the growing pollen tube. (a) Confocal Laser Scanning Microscopy of *Petunia hybrida* pollen tubes cultured in PEG (polyethylene glycol) medium at 22-23° for 24 hr, and labelled with the monoclonal antibody JIM5. Relatively unesterified pectin rings are periodically deposited in the walls pollen tubes. Bar, 40 μm. (b) Immunogold labelling of unesterified pectins in the pollen tube of *Petunia hybrida*. Gold particles (arrows) are mainly distributed in the cortical region of the pollen tube, in association with the cell wall (CW). Bar, 300 nm. (Micrograph courtesy of C. Faleri.) (c) Same as in (b). Bar, 250 nm. (Micrograph courtesy of C. Faleri.)

et al., 1995a) pollen tubes. The pectic layer and cellulose layer appeared under a merged condition in the thickened wall region. Using cryofixation techniques instead of chemical ones, Van Amstel (1994) described that the cellulosic layer contained five to seven strata of CMF in the cell wall of tobacco, lily, and *Petunia* pollen tubes. The tube tip showed a texture similar to that in the rest part of the tube, which suggests that no reorientation occurs during pollen tube elongation. The very thin CMF network gradually thickened toward the base of the pollen tube. In most primary walls of plant cells, cellulose exists as elementary fibrils that form a complex with hemicellulose, mainly composed of xyloglucan (Levy and Staehelin, 1992). However, the presence of hemicellulose in the pollen tube wall is still obscure. The pollen tube wall of *Camellia japonica* was fractionated into hemicellulose, cellulose and pectic substance (Nakamura and Suzuki, 1981), and callose (Nakamura and Suzuki, 1983). The analysis of the fraction, called "hemicellulose fractions," showed that the polysaccharide is a linear β-1,3-D-glucan, not a 1-4 (-glucan backbone. Apparently, further chemical analysis and the application of MAb against xyloglucan might be necessary to discover whether the hemicellulose is present in pollen tube walls.

B. Inner Callosic Lining

1. Deposition of Callose in the Cell Wall

The cell wall of pollen tubes consists of an unusually large amount of callose compared to that of other plant cells. Seventy-five to eighty-eight percent of the wall polysaccharides in cultured tobacco pollen tubes are callose (Rae *et al.,* 1985; Read *et al.,* 1996). The deposition of callose in pollen tube walls is characterized by an increasing intensity of Aniline blue fluorescence from the subapical region toward the pollen grain. The tip of growing pollen tubes is always lacking callose, and if growth ceases or under an incompatible growth condition, callose gradually forms in the entire tip (Rae *et al.,* 1985; Van Amstel, 1994; Geitmann *et al.,* 1995a). The thickness of the callosic layer is variable in tobacco pollen tubes grown *in vitro* (Van Amstel, 1994), also in *Petunia* pollen tubes grown *in vivo* (Herrero and Dickinson, 1981). Using α(1-3)-β-glucan-specific MAb, Meikle *et al.* (1991) have ultrastructurally shown that callose is localized in the inner wall layer of *N. alata* pollen tubes grown *in vivo.* In lily and tobacco pollen tube walls callose is shown as a granular, reticulate manner and sometimes in fibrillar form (Van Amstel, 1994). The inner wall of pollen tubes contains not only callose, but also microfibril cellulose and pectin-like microfibrils (Cresti and Van Went, 1976; Kroh and Knuiman, 1982; Vennigerholz *et al.,* 1992). Inclusions in the callosic wall contain arabinogalactan proteins (AGPs) and

pectins, however, the way of their linking remains unclear (Anderson *et al.,* 1987; Li *et al.,* 1992, 1995b).

2. Callosic Wall Thickening and Callose Plug Formation

The formation of callose plugs, initiated by the locale thickening of the callose wall, is a precisely controlled process. The first plug is always formed at a distance of about 170 μm away from the pollen grain in tobacco pollen tubes grown *in vitro.* The other plugs are regularly spaced, having morphology similar to that of the pollen tubes growing through compatibly pollinated styles (Read *et al.,* 1996; Van Amstel, 1994). It is noteworthy that the plugs do not appear to shut the pollen tubes, at least in many observed tobacco and lily pollen tubes. So in 24-h-cultured lily pollen tubes organelle movement can be found even in the region that is close to the pollen grain (Van Amstel, 1994; Li *et al.,* unpublished data). Callose is not the only component of the plugs. The plugs contain microfibrils of cellulose (Kroh and Knuiman, 1982; Nakamura and Suzuki, 1983) and pectin-like microfibrils (Kroh and Knuiman, 1982). Plugs are presumably formed by the fusion of so-called "callose grains" with the plasma membrane (Cresti and Van Went, 1976). As SVs occur in excess in the tip, several SVs will never fuse there and may relocate down the tube. Plug formation may then be a way to dispose of the excess SVs at locations where the excess SVs are disposed of and, consequently, callose plugs are formed (Van Amstel, 1994).

C. Cell Wall-Bound Proteins

1. Wall-Bound Glycoproteins

The level of cell wall-bound proteins varies according to the plant species and the growth condition of pollen tubes. A much higher protein content was found in the cell wall of lily pollen tubes grown *in vivo* than *in vitro* (Li and Linskens, 1983; Li *et al.,* 1983; Rae *et al.,* 1985). There are two kinds of wall proteins: loosely bound and tightly bound (assumed to be covalently bound). The major part, including hydroxyproline-containing proteins, is covalently bound to the cell wall. During pollen tube elongation some proteins decreased in quantity and many new proteins, most of which were glycoproteins, were incorporated into the cell wall. Some wall-bound proteins were shown to be related to gametophytic self-incompatibility (Li and Linskens, 1983; Li *et al.,* 1983; Li and Tsao, 1985). In tobacco pollen tubes a 69-kDa glycoprotein was synthesized during pollen germination and pollen tube growth and became

the most abundant protein in the cell wall. In tobacco pollen grain, the pollen-specific gene NTP 303 encodes a pollen tube-specific glycoprotein with a molecular mass of 69 kDa exclusively in the insoluble fraction of the germinated pollen (Wittink *et al.,* 1996).

The growth of *Malus domestica* pollen tubes was associated with newly synthesized glycoproteins, and actinomycin D strongly modified the glycoprotein composition in the pollen tube wall (Calzoni and Speranza, 1989). The growth of lily and tobacco pollen tubes was markedly interrupted by tunicamycin, an inhibitor of N-linked protein glycosilation on the RER (Li *et al.,* 1986; Capkova *et al.,* 1994). It is likely that the glycoproteins might play an important role in pollen tube wall construction and thus pollen tube growth.

2. Arabinofuranosyl Residue and Arabinogalactan Proteins

AGPs are ubiquitous glycoproteins found in plant cells. By using a MAb PCBC3, an L-arabinofuranosyl residue was detected in the outer fibrillar layer of the *N. alata* pollen tube wall. Some pollen tubes showed a pronounced banding of the fluorescence along the length of the pollen tube (Anderson *et al.,* 1987; Harris *et al.,* 1987). The MAbs MAC 207 and JIM 8, recognizing AGPs, were used to localize the corresponding antigenic sites in pollen tubes of *N. tabacum* grown *in vitro* and semi *in vivo.* Most of the pollen tubes were labeled along their length, except the tip region, in a ring-like pattern with remarkable periodicity (Li *et al.,* 1992). At the ultrastructural level, AGPs were colocalized with pectins in the pollen intine, preferably close to the plasma membrane (Pennell *et al.,* 1989; Van Aelst and Van Went 1992; Li *et al.,* 1995b). In pollen tubes, AGPs were found in the outer and middle layers of the cell wall. The density of the epitopes showed alterations along the tube length and lacks at the tip. AGPs were also detected in Golgi vesicles, and in the generative cell wall (Li *et al.,* 1995b). In *L. longiflorum* pollen tubes grown *in vitro* and *in vivo,* AGPs were localized in the tube tip by MAb JIM 13 immunofluorescence labeling. At the transmission electron microscope level, AGPs were mainly found on the plasma membrane and vesicle membranes of *in vivo* grown pollen tubes (Jauh and Lord, 1996).

3. Extensin-like Glycoproteins

Although the structure and function of extensin in plant cell walls have been thoroughly studied, the data on extensin in pollen tube walls are still not found. A maize pollen-specific gene (pex-1) was currently discovered to encode a protein with an extensin-like domain. The pex-1 proteins are tissue-specific glycoproteins located in the intine of the mature pollen and

tightly associated with the pollen tube inner wall. As in many aspects the movement of the pollen tube resembles the movement of animal cells during development (Lord and Sanders, 1992; Sanders and Lord, 1992), the pex-1 protein was proposed to play a role of cell adhesion that is necessary for the pollen tube to find its path through the transmitting tissue to the ovary (Rubinstein *et al.,* 1995a,b).

VI. Exocytosis and Cell Wall Formation

Exocytosis is very important for the growth of pollen tubes. In this dynamic process, SVs deliver polysaccharide precursors, membrane materials, and soluble and membrane-associated proteins by fusion with plasma membrane to form new plasma membrane and cell wall. Transport of vesicles from the Golgi apparatus to the plasma membrane is accompanied by marked changes in their contents and in the activity of membrane-associated proteins (Blackbourn and Battey, 1993). The cell wall construction is directed by sophisticated mechanisms that ensure the correct delivery of all the materials to the precise location at the appropriate time (Battey *et al.,* 1996).

A. Biosynthesis and Transport of Cell Wall Precursors

1. Pectins

The synthesis of pectins in pollen tubes was studied early by Helsper *et al.* (1986). The incorporation of myo-2-3-H-inositol into phospholipids and pectic cell wall polysaccharides showed that, when pollen tube growth begins, at 2 h the demand for newly synthesized pectic polysaccharides and phospholipid biosynthesis or turnover greatly increased. Concanavalin A (Con A) interfered with phospholipid turnover and biosynthesis of pectic polysaccharides in germinating pollen and growing pollen tubes. Con A also affected the incorporation of polysaccharide precursors in the cell wall, after their release from SVs, by interference with the appropriated glycosyltransferase (Helsper and Pierson, 1986). Pectins were thought to be synthesized and transported in their esterified form. In *N. tabacum* pollen tubes, esterified pectins were immunocytochemically detected over medial and *trans*-Golgi cisternae, and SVs, by which the esterified pectins were transported to the pollen tube tip. Esterified pectins undergo deesterification (demethylation) when they are inside the cell wall of pollen tubes

(Li *et al.,* 1995b; Geitmann *et al.,* 1995a), as reported in other plant cells (Zhang and Staehelin, 1992; Bordenave, 1996).

The pectin-demethylation reaction is catalyzed by PME. Immunocytochemical localization suggested that PMEs were mainly present in the middle lamella and in the cell junctions of mung been hypocotyl (Goldberg *et al.,* 1992). Properties of PME relied on many factors. Divalent cations (Ca^{2+} and Mg^{2+}) were more potent activators of PME than monovalent cations (K^+ and Na^+). Ca^{2+} in a concentration higher than 50 m*M* was inhibitory. The sensibility of PME to Ca^{2+} and Mg^{2+} was pH dependent: at acid pH (from 5.6 up to 7.0) Ca^{2+} was the most potent activator, while above pH 7.5 Mg^{2+} was more effective (Goldberg, 1984). Now few reports on PME in pollen and pollen tubes are available. The Bp 19 gene shows sequence similarity to pectin esterase and is highly expressed during *Brassica napus* microspore development. The accumulation of Bp 19 mRNA starts in uninucleate microspores and increases during development, reaching a peak in the late stage, but declines considerably in mature pollen (Albani *et al.,* 1991). In the pollen tube of *P. hybrida,* cDNA clones encoding a protein, PPE1, which exhibits sequence similarity with plant, bacterial, and fungal pectinesterase, were isolated. PPE1 mRNA was first detected in anthers containing uninucleate microspores; it reached the highest level in mature pollen and persisted at a high level in *in vitro* germinated pollen tubes (Mu *et al.,* 1994). The immunoultrastructural localization of PME in tobacco pollen tubes reveals its pathway via vesicle to plasma membrane and cell wall (Li *et al.,* unpublished data).

2. Cellulose

Cellulose biosynthesis is a very important but poorly understood process in plant cells. A hypothetical model of a cellulose synthase complex in the plasma membrane was illustrated by Delmer and Amor (1995). The cellulose synthase complex is composed of many subunits. These complexes, particularly the rosette-like structures found in the plasma membrane, were exceedingly labile. The activity of the synthase complex was dependent on their location and orientation in the membrane and was directly related to membrane potential (Delmer *et al.,* 1993; Delmer and Amor, 1995). The data on the cellulose synthase in pollen tubes are very limited. According to the deposition of cellulose in the pollen tube wall, as revealed by both the determination of ^{3}H-UDPG incorporation and the ultrastructural observation, it is assumed that the cellulose synthase complex initially produced CMF in the tip and switched to callose formation in the tubular part (Van Amstel, 1994). Phthoxazolin, a specific inhibitor of cellulose biosynthesis, significantly inhibited pollen

germination and pollen tube growth, and also callose deposition in the tube. It seemed to agree with the hypothesis that the *trans*-membrane cellulose-synthase is alternatively able to produce cellulose or callose under a certain condition (Van Amstel, 1994).

There are different models to propose how MTs might direct the movement of cellulose synthase complexes within the plasma membrane. One model supposes that there is a direct connection between cellulose synthase and cytoskeleton via accessory proteins. The more recent model suggests that MTs serve as "fences" between which the complexes are constrained to move without any direct interaction (Giddings and Staehelin, 1990). The relationship between MT and microfibril orientation has been discussed for decades. MTs and microfibrils have been supposed to be oriented by separate mechanisms (Preston, 1988). In tobacco pollen tubes the secondary wall had a random texture (Kroh and Knuiman, 1982), whereas the MTs were longitudinal (Derksen *et al.*, 1985). The nonparallel alignment of MTs and CMFs was in the nongrowing tube and not in the growing tip, where both structures were distributed in all directions (Emons, 1989). The observation on the local wall thickening suggested that MTs helped in leading the Golgi vesicles to a particular place and/or in inserting them in the plasma membrane. MTs may determine the site of the wall deposition rather than the orientation of the CMF (Emons *et al.*, 1992). However, tubulin microinjection has recently illustrated that MTs in plant cells were surprisingly dynamic, which leads to the speculation that MTs have the properties required of a changeable, three-dimensionally complex template for cellulose biosynthesis (Wymer and Lloyd, 1996).

3. Callose

Since tobacco pollen grains contained no detectable callose, pollen germination apparently involved highly regulated activation of callose synthesis. The rate of callose synthesis by pollen tube membranes was comparable to the rate of callose deposition in actively growing pollen tubes (Read *et al.*, 1995). Callose synthase was located on the membrane layer facing cytoplasm in the pollen tubes. Membranes prepared from cultured *N. alata* pollen tubes contained a stable and highly active callose synthase whose activity was not stimulated by Ca^{2+} or other cations (Schlupmann *et al.*, 1993; Read *et al.*, 1996). On the other hand, the activity of the callose synthase was stimulated by various detergents, in different mechanisms, either by permeabilizing outside-out membrane vesicles or by a super-activating action that resembled activation by trypsin treatment (Li *et al.*, 1996a).

B. Regulation of the Fusion of Secretory Vesicles with Plasma Membrane

1. Secretory Vesicle Pathway

In plant cells the current studies on the regulation of the SV pathway have revealed that budding of ER vesicles is driven by ATP, whereas transfer between the *trans*-Golgi apparatus membranes and the plasma membrane is supported by a reduced pyridine nucleotide. For the ER to Golgi transfer, two of the involved proteins (a 100-kDa ATPase and a 38-kDa protein) have been identified. In the elongating pollen tubes the source of new membrane and cell wall appears very much dependent upon a vesicular pathway (Morrè, 1994). Growing tobacco pollen tubes were labeled with [^{3}H]leucine and fractionated into constituent membranes by preparative free-flow electrophoresis. The results suggested that tube elongation is accompanied by a steady-state flow of membranes from the ER to the cell surface via the Golgi apparatus. With respect to other cells and tissues, the membrane flow in pollen tubes was insensitive to interruption by low temperature (Kappler *et al.*, 1986; Noguchi and Morrè, 1991). Recently, Derksen *et al.* (1995b) and Van Amstel (1994) declared that in tobacco pollen tubes SVs originated from the TGN and that different secretory products were carried in a single type of vesicle.

2. Secretory Vesicle Aggregation

The fusion of SVs with plasma membrane is proposed to follow precise events initiated by the vesicle movement near the plasma membrane, with a conformational change in membrane-associated protein(s). In animal secretory cells, a class of Ca^{2+}-dependent phospholipid binding proteins (annexins) were proved to induce membrane aggregation, to form voltage-gated Ca^{2+} channels, and to promote membrane fusion. The plant annexins can bind to the SVs and are effective at aggregating plant SVs (Blackbourn and Battey, 1993). Annexin-like proteins have been immunolocalized to lily pollen tube tips, where cytosolic free Ca^{2+} was concentrated (Blackbourn *et al.*, 1992). This is consistent for an involvement of annexin-like proteins in SV aggregation.

Syntaxins are integral membrane proteins, thought to act as receptors for transport vesicles arriving at and fusing with the membrane, with the bulk of the protein facing the cytosol. Upon docking of a vesicle with its target membrane, syntaxin interacts with many proteins, both in the vesicle membrane and in the cytosol, to form a docking complex. Different isoforms of syntaxin have been proposed to reside on different cellular membranes

and to provide specificity for the docking and fusion reaction (Bassham and Raikhel, 1996). Whether docking and fusion of pollen tube SVs are associated with syntaxins might be an interesting topic to study.

VII. Polarized Growth of Pollen Tubes

A. Characteristics of Polarized Growth of Pollen Tubes: Oscillatory and Pulsatory Growth

The fluctuation in growth rate has been currently described in polarized tip-growing plant cells, such as pollen tubes and fungal hyphae. The fluctuated growth can be classified into two distinct patterns: oscillatory growth and pulsatory growth. The oscillatory growth, found in fugal hyphae (Lopez-Franco *et al.,* 1994; and in some species of pollen tubes, e.g., *Aleo zebrida* (Tang *et al.,* 1992), *Campanula sarmatica,* and *L. longiflorum* (Pierson *et al.,* 1995, 1996), was characterized by weak alterations in the growth rate. For example, lily pollen tubes which were in a certain range of length, showed growth-rate oscillations with a regular period (23 s) and over a 3-fold change in amplitude (Pierson *et al.,* 1996). On the other hand, the pulsatory growth of *P. hybrida* and *N. tabacum* (Pierson *et al.,* 1995) displayed two differentiated growth phases, a period of very slow and even paused growth, which extended for several minutes, and a sudden rapid growth, which lasted for less than 20 s. The increase of growth rate could be about 12-fold. On the contrary, *Gasteria verrucosa* pollen tubes exhibited higher pulsing frequency, as the slow growth phase is shorter (Pierson *et al.,* 1995; Plyushch *et al.,* 1995). The growth pulses occurred periodically in both cases.

B. Factors Affecting the Fluctuated Tip Growth

The continuous discussion on the mechanism of plant cell growth is argued on the process that initiates cell expansion/extension, or water uptake, or relaxation of wall stress. Growth of plant cells results from the interaction between turgor pressure and stress–relaxation of the cell wall. Relaxation of wall stress will lower turgor and thus the water potential that leads to water uptake. The influx of water into the cell results in an increase of cell volume, which rebuilds up the turgor and therefore wall stress. It is likely acceptable that the relaxation of wall stress initiates cell growth (Cosgrove, 1993). Distinctively, the regulatory mechanism of fluctuated growth found

in pollen tubes becomes even more mysterious. The recent findings about the factors affecting tip growth may shed new light on the subject.

1. Calcium as a Secondary Messenger

Calcium is known as secondary messenger similarly to cAMP. The crucial role of calcium in regulating pollen tube growth has been thoroughly documented (Heslop-Harrison, 1987; Steer and Steer, 1989; Derksen *et al.*, 1995b; Hepler *et al.*, 1994). Here we cover some recent findings that show the crucial role of Ca^{2+} in regulation of the fluctuated growth of pollen tubes.

a. Intracellular Free Calcium Concentration in the Pollen Tube In lily pollen tubes the extracellular Ca^{2+} influx, detected by using an ion-selective vibrating electrode, was restricted to a small area of plasma membrane at the extreme apex of the tube dome. The tip-localized calcium entry fluctuated during pollen tube growth. The intensity of Ca^{2+} influx was related to tube length. The tubes longer than 700 μm exhibit oscillations with a period of 23 s, while the shorter tubes display erratic fluctuations that can be more than threefold (Pierson *et al.*, 1994, 1996).

Fluorescence ratiometric imaging of growing pollen tubes of *L. longiflorum, Nicotiana sylvestris,* and *Tradescantia virginiana,* which were loaded with Fura-2 dextran, has revealed a distinct elevation of the free intracellular Ca^{2+} concentration at the extreme tip. The tip-focused Ca^{2+} gradient is restricted to the 10–20 μm next to the tube tip. The location of the highest Ca^{2+} domain within the tip region defines the point from which normal cylindrical elongation will go on. The osmotic challenge and treatment with caffeine, and also other agents that block growth, rapidly dissipate the intracellular tip-focused Ca^{2+} gradient and eliminate the tip-localized Ca^{2+} influx (Miller *et al.*, 1992; Pierson *et al.*, 1994, 1996; Li *et al.*, 1996b).

Very recent studies show correlation of the tip-focused Ca^{2+} gradient and the distribution of AFs at the apex of growing pollen tubes that were loaded with fluorescently labeled phalloidin. The apical region was essentially lacking AF bundles (Miller *et al.*, 1996), which demonstrated that the elevated Ca^{2+} concentration at the tip fragments the AFs (Kohno and Shimmen, 1987). The consequence is to prevent cytoplasmic streaming that helps exocytosis and causes the growth phase. When the Ca^{2+} gradient is dissipated, AFs extend into the apical zone and become competent to transport larger organelles close to the tip, leading to a pause in growth (Pierson *et al.*, 1994; Miller *et al.*, 1996).

b. Active Calcium Transport In growing pollen tubes the tip-localized Ca^{2+} influx and the steep tip-focused Ca^{2+} gradient imply the existence of

an active Ca^{2+} transport that dramatically decreases the Ca^{2+} concentration behind the tip. Cytoplasmic organelles, such as mitochondria and chloroplasts, appear to provide only limited Ca^{2+} storage capacity and may function for peak loads and for short times only. Since the pollen tubes exhibit active exocytosis, the long-term Ca^{2+} transport may be important in a final extrusion of the Ca^{2+} accumulated in the ER. The massive amount of ER, seen in the flanks of the apex of tobacco pollen tubes (Derksen *et al.,* 1995a) and between SVs in lily pollen tubes (Lancelle and Hepler, 1992), might represent a vast sink of Ca^{2+} (Derksen *et al.,* 1995b). Recently a cDNA (LCA), exhibiting high homology to ER Ca^{2+}-dependent ATPases, was isolated from tomato root cells (Ferrol and Bennett, 1996). It seems meaningful to detect the gene encoding ER Ca^{2+}-dependent ATPases in pollen tubes to understand the role of the ER in active Ca^{2+} transport.

c. Calcium Channels The presence of Ca^{2+} channels in pollen tubes has been indirectly proven by various techniques. Reiss and Herth (1985) reported that after the addition of nifedipine, a Ca^{2+}-channel blocker, normal tip growth of cultured lily pollen tubes stopped in 10 min. However, cytoplasmic streaming continued until 15 h. Obermeyer and Kolb (1993) considered that the inhibition in pollen tubes by nifedipine could be an effect of K^+ channels. The addition of another Ca^{2+} channel blocker, La^{3+}, caused a decrease of the intracellular free Ca^{2+} maximum in the tube tip, showing a heterogeneous distribution of Ca^{2+} channels along the plasma membrane of pollen tubes (Obermeyer and Weisenseel, 1991). The effect of a weak electric field on elevating cytoplasmic free Ca^{2+} can also be inhibited by the Ca^{2+} channel blocker lanthanum chloride (Malhò *et al.,* 1994). The mechanisms of action for the Ca^{2+} channel blockers, such as nifedipine, verapamil, and diltiazem, were proposed to be the following: (i) perturbations of membrane permeability by interference with one or more of the cell's Ca^{2+} transport systems, or (ii) a more indirect mechanism affecting vesicle transport via the AF system (Wacker and Schnepf, 1990). Ca^{2+} channel activity was measured by adding extracellular Mn^{2+} to quench the fluorescence of intercellular indo-1 at its Ca^{2+}-insensitive wavelength. In nongrowing pollen tubes, Ca^{2+} channel activity was very low and cytoplasmic free Ca^{2+} gradients were absent. When the growth reorienting treatment (electrical fields and ionophoretic microinjection) induced a depolarization of the plasma membrane, the voltage-gated Ca^{2+} channel might be activated (Malhò *et al.,* 1995).

Recently, a new system, combined with CLSM, was set up for fast photoactivation and immediate imaging. Using an aperture system that confines UV light to an area of about 80 μm^2 and enables caged Ca^{2+} release in discreet regions of the cell it has been found that increasing Ca^{2+} in one side of the pollen tube apex induced reorientation of the growth axis toward

that side. The activation of Ca^{2+} channels in the tip region is critical for polarized growth (Malhò *et al.,* 1996).

d. Ca^{2+} Binding Proteins Ca^{2+} may be actively pumped out of the cytosol by Ca^{2+}-ATPase. The regulation of the Ca^{2+} pump in the plasma membrane is controlled by the level of Ca^{2+} through the mediation of CaM. CaM was extracted and partially characterized from *Brassica campestris* pollen, *Pinus yunnanensis* pollen, and *Corylus avellana* pollen (Liu and Du, 1989; Gong *et al.,* 1993; Scali *et al.,* 1994). Using MAb anti-CaM, it has been detected that CaM is in association with the plasma membrane in the tip region of tobacco pollen tubes (Tirlapur *et al.,* 1994). It was also suggested that Ca^{2+}-ATPases, mainly located in the zone up to 20 μm behind the pollen tube tip, may be involved in the generation of the steady-state Ca^{2+} gradient as a Ca^{2+} sink. After addition of the ATPase inhibitor vanadate and the CaM antagonist C48/80 to the medium, the free Ca^{2+} increased. This suggested an involvement of a CaM-dependent Ca^{2+} pump in the generation of the Ca^{2+} gradient in lily pollen tubes (Obermeyer and Weisenseel, 1991).

Annexins (including calpactins, synnexins, and calcimedins in mammalian systems) are a major group of Ca^{2+}-dependent membrane-binding proteins. Some of these proteins can catalyze membrane fusion (Pollard *et al.,* 1990). Little is known about annexins in pollen tubes (see section VI).

2. Properties of the Cell Wall

During elongation or expansion of the cells, the cell wall architecture must be modified to allow incorporation of new material. Modification of the cell wall architecture influences several properties, particularly the extensibility.

a. Cell Wall Porosity Pollen tube walls have porosity similar to that of other cell types such as stigma papillae, root hairs, cotton fibers, and callus cells. The actual pore size of the cell walls of *Gladiolus gandavensis* pollen tubes grown *in vitro* is 3.5–4.5 nm, as measured by the solute exclusion technique, which estimates the size of molecules that might pass through cell walls (Hoggart and Clarke, 1984). Fluorescent dextrans varying in size were added to the pollen tube growth medium at different times after the onset of incubation to measure the porosity of cell walls. Permeability of the walls varies in pollen tubes of *T. virginiana* and *N. tabacum* and is not uniform along the pollen tube length, being limited to 5 nm for *T. Virginiana* and 7 nm for *N. tabacum* in the tip region. The cell walls of pollen tubes grown *in vitro* are able to support the transport of macromolecules up to about 10 kDa in size, but are only slowly permeable to larger molecules. The pectic network, not cellulose and xyloglucan, plays a major role in determining wall porosity (O'Driscoll *et al.,* 1993). It is found that a tobacco

transmitting tissue glycoprotein promotes pollen tube growth and is incorporated into pollen tube walls (Wu *et al.,* 1995). Obviously wall porosity is related to pollen tube elongation through the stylar transmitting tissue. It is also possible that the self- incompatibility-related glycoproteins, found in the *N. alata* style, might gain entry through the pollen tube tip walls. However, until now there have been no data to show that cell wall porosity is involved in the regulation of fluctuated pollen tube growth.

b. Cell Wall Extensibility The changes in wall extensibility will control cell growth (Cosgrove, 1993). The rate of wall loosening and the rate of deposition of new polymers must be tightly coupled with feedback mechanisms from wall to cell. One way of coupling these two rates is to synthesize wall components that produce an architecture that is extensible, and one part of this might be the synthesis of highly esterified pectins that may alter the rheology of the pectic network (McCann and Roberts, 1994). A recent finding suggests that the pollen tube apical wall consists largely of methyl-esterified pectins. Factors, such as the activity of PME, Ca^{2+} concentration, and pH at the tip region, would be expected to change the tensile properties of this wall. Therefore, pollen tube growth fluctuation might result from endogenous oscillation of these competing factors/processes that changes the cell wall extensibility (Li *et al.,* 1996b).

3. Turgor Pressure

The water potential of a walled plant cell has been expressed as the sum of two major components: hydrostatic (turgor) and osmotic potentials. The plant cells subjected to variation in external water potential often respond by altering the number of osmotically active particles per cell, with the consequent restoration of turgor pressure to a value close to the original level. Turgor pressure is thought to be the driving force of pollen tube tip growth. It was proposed that changes in turgor pressure might be the underlying cause of fluctuations in the growth rate of pollen tubes, and in extreme cases cause pulsatory growth (Pierson *et al.,* 1995).

To evaluate this hypothesis, lily pollen tubes have been forced to grow in a marked fluctuation manner by modulating the medium osmolarity. The results, consistent with the previous observations, showed that pollen tube growth is turgor-dependent/sensitive (Van Aelst and Van Went, 1992; Pierson *et al.,* 1994; Li *et al.,* 1996b). However, a non-turgor means, such as treatment with growth inhibitor caffeine, can induce marked growth fluctuations of lily pollen tubes, similar to that found by osmotic challenge. This questions the idea that growth fluctuation is naturally regulated by corresponding turgor changes (Li *et al.,* 1996b) and is supported by the

opinion that turgor pressure is not a condition sufficient for cell expansion (McCann and Roberts, 1994).

4. pH, K^+, and Plasma Membrane H^+-ATPase

Cytosolic pH is thought to be a factor associated with the formation of polarity in the cell. In polarized tip-growing cells the data on the effect of cytosolic pH on cell growth are very limited, and the reports about the presence of a pH gradient in the cells are not consistent. In root hair tips of *Spinapis alba* the cytosolic pH is statistically not different from values measured in the base (Herrmann and Felle, 1995). In apically growing rhizoids of *Pelvetia* embryos, the pH gradient was spatially superimposed on the cytosolic Ca^{2+} gradient, and inhibition of calcium fluxes abolished the pH gradient (Gibbon and Kropf, 1994). In pollen tubes, the occurrence of a pH gradient remains uncertain, although a steep tip-focused Ca^{2+} gradient is evident.

Loaded with the H^+-specific dye BCECF, growing *Agapanthus umbellatus* pollen tubes showed a pH gradient decreasing toward the tip (Malhò *et al.,* 1992). However, confocal ratio imaging of another H^+-specific dye, SNARF-1, revealed that some growing pollen tubes did not present a pH gradient (Malhò *et al.,* unpublished data).

The proton translocating ATPase (H^+-ATPase) is the primary active transport system at the plasma membrane. H^+-ATPase couples ATP hydrolysis to the transport of protons from cytosol across the plasma membrane (Bassham and Raikhel, 1996). Immunolocalization data suggest that H^+-ATPases are heterogeneously distributed, to create H^+ efflux behind the lily pollen tube tip (Obermeyer *et al.,* 1992).

The polar distribution of H^+-ATPases was found in the plasma membrane of *A. umbellatus* pollen tubes (Feijo *et al.,* 1992). At present, the relationship between cytosolic pH and pollen tube growth is far from clear. It is mostly expected that cytosolic pH plays a role in the regulation of pollen tube fluctuated growth, since various events are pH-dependent (e.g., the activity of PME, which affects elasticity of the pectic layer in the wall, is highly dependent on cytosolic pH).

5. Boron

Boron is an essential element for living cells of plants. However, the physiological role of boron remained an enigma for decades. Recently, some findings showed that the essentiality of B is directly associated with cell wall extensibility and consequently cell growth. The cell walls of cultured tobacco cells grown in B-deficient media are thicker than those of control cells. In these cells Golgi bodies were accompanied by more SVs than those

in the control cells (Matoh *et al.,* 1992). In squash tissue cells most of the B is associated with pectins within the cell wall. Physical analysis of B-deficient tissue suggests that cell wall extensibility was greatly reduced (Hu and Brown, 1994). Extensin and pectin were decreased in bean nodules grown in B-deficient nutrient solution (Cassab, 1995). The current study reveals that B links two rhamnogalacturonan II chains to form the boron–polysaccharide complex cross-linked by B-diol ester bound (Kobayashi *et al.,* 1996). This linkage would allow pH-controlled cell expansion (Ghanadan *et al.,* 1995). A pronounced interaction between Ca^{2+}, Mg^{2+}, and B was found in cultured pine cells. An acceptor molecule is thought to be activated only by binding both Ca^{2+} and B at separate sites. Mg^{2+} competitively displaces Ca^{2+} to inactivate the acceptor (Teasdale and Richards, 1990). The mode of action of B in the growth of pollen tubes is much less understood. Jackson (1989) has reported a B involvement in movement of proteins into the extending pollen tube membrane from SVs. A recent study showed the occurrence of B–rhamnogalacturonan II complexes in growing lily pollen tube walls (Matoh, 1996, personal communication). Based on the finding that B plays roles in association with cell wall extensibility and on the coeffect with Ca^{2+} during plant cell extension, it is tempting to speculate that B may contribute to the regulation of fluctuated pollen tube growth.

6. Currently Emerging Factors

a. Flavonols: A Candidate for Regulating Pollen Tube Growth Flavonols are secondary plant products that are involved in pollination. Its biosynthesis is initiated by chalcone synthase, followed by the synthesis of flavonols by chalcone isomerase. Flavonol-containing dispersal from mature pollen of *N. tabacum* and *P. hybrida* strongly promoted pollen germination and pollen tube growth. Flavonols were localized throughout the pollen tube, but not in the exine and the cell wall of growing tubes of *P. hybrida.* This might be the result of accumulation of highly hydrophobic flavonols in the many cytoplasmic membranes. Flavonols are suggested to play a structural role in the membranes of male gametophytes. The absence of flavonols might change the fluidity of the membranes that are involved in tip growth. Alternatively, this structural role may be more indirect, via interference with factors regulating tube growth, such as Ca^{2+}, B, or hydrogen (Ylstra *et al.,* 1994b).

b. Oligosaccharides as Signals It has recently been found that a few selected oligosaccharides can, at very low concentrations, exert "signaling" effects on plant tissues. Such oligosaccharides are termed "oligosaccharins" (Fry *et al.,* 1993). Glycoproteins are implicated as sources of oligosaccharins.

The influence of pectic oligosaccharins on plant growth is shown to evoke rapid changes in ion fluxes, including a K^+ efflux concomitant with membrane depolarization, acidification of the cytoplasm, and an influx of Ca^{2+} (LoSchiavo *et al.,* 1991; Fry *et al.,* 1993). The rapid membrane effects produced by oligogalacturonides initiate a signal cascade, leading to regulation of physiological and developmental processes (Mathieu *et al.,* 1991; Van Cutsem and Messiaen, 1994). It was reported that fructose-containing oligosaccharides strongly promote pollen tube growth (Nakamura and Suzuki, 1983). Van Amstel (1994) has recently shown that along the pollen tube the pectic layer can be partially or completely dissolved. Pollen tubes can shed their pectic layer in a follicular manner. The dissolution of the pectic layer in lily, tobacco, and *Petunia* pollen tubes might be involved in the signal cascade.

The mode of action of pectic fragments is hypothesized as a phosphoinositide signal-transducing system. Pectic fragments under a proper conformation induced by Ca^{2+} bind to plasmalemma receptors. The membrane depolarizes and inositol-(1,4,5)-triphosphate is simultaneously hydrolyzed from plasmalemma phospholipids. The cytosolic Ca^{2+} activity increases due to the opening of Ca^{2+} channels, and Ca^{2+} binds to CaM. Then, protein phosphorylation occurs, and the plasmalemma permeability to ions changes. This leads to cytosolic acidification, and specific genes are finally transcribed and translated (Van Cutsem and Messiaen, 1994).

VIII. Concluding Remarks

Although several data on the physiology, biochemistry, and molecular biology of the pollen tube have been accumulated during the last years, details of the pollen tube growth process are still unclear and constitute an intriguing challenge for the future. For example, it is not known whether extracellular signals can determine the rate and direction of pollen tube growth by exerting an influence upon the cytoskeleton. Many research approaches showed that the pollen tube tip can play a fundamental role in tube growth by controlling the fusion rate of SVs and the arrangement of the cytoskeleton. The identification of polypeptides correlated with Rho-GTPases in the pollen tube tip has been interpreted as the first information on the role played by the apex in controlling the assembly of AFs, probably in response to external signals. The finding of transmitting tissue-specific arabinogalactan proteins, which attract pollen tubes and change their growth *in vitro* after binding to the apex, gives rise to new exciting prospects for studying the regulation of pollen tube growth by external compounds. Whether and how these molecules can influence the cytoskeletal apparatus and/or the

Ca^{2+} gradient are not yet known. In migrating cells, proteins such as integrins are a major component of the system involved in the ECM-mediated assembly of the cytoskeleton. The identification of integrin-like polypeptides and their relationship with the cytoskeleton in the pollen tube will help to puzzle out problem of pollen–pistil interactions.

Ca^{2+} is really an essential component regulating pollen tube growth. In collaboration with Ca^{2+}-activated phospholipid-binding proteins, it regulates the site and rate of vesicle fusion with the apical plasma membrane. Ca^{2+} is also supposed to influence the assembly of AFs in the tube apex and, consequently, to participate in the maintenance of the polar distribution of organelles in the pollen tube. Also, the process of signal transduction, which involves several molecules and a biochemical pathway similar to that observed in animal systems, seems related to the ordered flow of Ca^{2+}. The finding of kinesin-like polypeptides with calmodulin-binding domains suggests that Ca^{2+} can modulate the activity of MT-based motors in plant cells. Although this kind of motor has not been yet identified in pollen tubes, preliminary results on the influence of Ca^{2+} on myosin activity suggest that Ca^{2+} may have additional functions. This and other recent results on the role played by Ca^{2+} during pollen tube growth suggest that the relationships among the cytoskeletal dynamic, the Ca^{2+} gradient, and the cell wall formation pattern are very important.

As described in this review, little is known about the role of MTs in controlling the deposition of the cell wall during pollen tube growth. MTs are described as extremely dynamic structures in the cortex of plant cells. Presently, similar evidence is lacking in the pollen tube system, as well as data on motor proteins that could coordinate this activity. The localization of putative MT-organizing sites in pollen tubes does not provide further indications. Both identification of cellulose synthase complexes and information on their relationships with MTs will be important steps to solve the question of whether MTs control the deposition of cellulose microfibrils.

This review has been organized having the intracellular substance traffic as it occurs in cells in mind. Proteins and other molecules move from one intracellular compartment to another by several means of transport. Molecules to be excreted are normally synthesized on membranes (such as the ER), driven to the Golgi apparatus for further modifications, and then transported to the cell surface. All these movements normally rely on the transport of material-containing vesicles along the cytoskeletal apparatus. The deposition of particular wall components in plant cells is likely to occur in the same way and the elongation activity of the pollen tube is a good example of such a process. The main force propelling pollen tube growth depends on cytoplasmic streaming, which is based on the dynamic properties of the cytoskeletal apparatus. The pollen tube has been in a certain sense compared to a secretory cell because of the secretion activity

that occurs at the apex. On the other hand, some researchers have drawn a comparison between the pollen tube and a migrating cell, because of the directional growth exhibited by pollen tubes through stigma and style. Like migrating cells, the direction of pollen tube growth is likely to be controlled by signals from the extracellular matrix. It is becoming more certain that the elongation of pollen tubes within the pistil is strictly dependent on the interactions between the female tissue cells and the pollen tube itself. These interactions are likely to influence the growth orientation of the pollen tube by being translated into signals for the intracytoplasmic compartments. Schematically, it is possible to affirm that two "opposite flows" exist in the pollen tube: (i) a flow of substances from the cytoplasm to the exterior, and (ii) a reverse flow of signals/substances from the extracellular matrix into the pollen tube. This is an oversimplification of a process that is more complicated. However, we speculate that the two "flows" can influence each other, producing a kind of "feedback regulation" of pollen tube growth. Apparently, the interactions among the cytoskeleton, the membrane system, and the cell wall in pollen tubes are becoming very important research topics for further understanding the regulatory mechanism of pollen tube growth.

References

Akashi, T., Izumi, K., Nagano, E., Enomot, M., Mizuno, K., and Shibaoka, H. (1988). Effects propyzamide on tobacco cell microtubules *in vivo* and *in vitro*. *Plant Cell Physiol.* **29,** 1053–1062.

Albani, D., Altosaar, I., Arnison, P. G., and Fabijanski, S. F. (1991). A gene showing similarity to pectin esterase is specifically expressed in developing pollen of *Brassica napus*. Sequences in its 5′ flanking region are in other pollen-specific promoters. *Plant Mol. Biol.* **16,** 501–513.

Amici, G. B. (1824). Observations microscopiques sur diverses espèces de plantes. *Ann. Sci. Nat. Bot.* **2,** 41–70.

Anderson, M. A., Harris, P. J., Boning, I., and Clarke, A. E. (1987). Immuno-gold localization of a-L-arabinofuranosyl residues in pollen tubes of *Nicotiana alata* Link et Otto. *Planta* **171,** 438–442.

Andrews, K. L., Nettesheim, P., Asai, D. J., and Ostrowski, L. E. (1996). Identification of seven rat axonemal dynein heavy chain genes: Expression during ciliated cell differentiation. *Mol. Biol. Cell* **7,** 71–79.

Arondel, V., and Kader, J.-C. (1990). Lipid transfer in plants. *Experientia* **46,** 579–585.

Asada, T., and Shibaoka, H. (1994). Isolation of polypeptides with microtubule-translocating activity from phragmoplasts of tobacco BY-2 cells. *J. Cell Sci.* **107,** 2249–2257.

Asada, T., Seonobe, S., and Shibaoka, H. (1991). Microtubule translocation in the cytokinetic apparatus of cultured tobacco cells. *Nature* **350,** 238–241.

Åström, H. (1992). Acetylated α-tubulin in the pollen tube MTs. *Cell Biol. Int. Rep.* **16,** 871–881.

Åström, H., Virtanen, L., and Raudaskoski, M. (1991). Cold-stability in the pollen tube cytoskeleton. *Protoplasma* **160,** 99–107.

Åström, H., Sorri, O., and Raudaskoski, M. (1995). Role of microtubules in the movement of the vegetative nucleus and generative cell in tobacco pollen tubes. *Sex. Plant Reprod.* **8,** 61–69.

Bassham, D. C., and Raikhel, N. (1996). Transport proteins in the plasma membrane and the secretory system. *Trends Plant Sci.* **1,** 15–20.

Battaglia, E. (1987). *In* "Pollen Embryology: The Tuscan Contribution" (F. Garbari and E. Pacini, eds.), pp. 53–125. Atti Soc. Tosc. Sci. Nat. Mem. Ser. B 94.

Battey, N., Carroll, A., Van Kesteren, P., Taylor, A., and Brownlee, C. (1996). The measurement of exocytosis in plant cells. *J. Exp. Bot.* **47,** 717–728.

Bennett, V., and Gilligan, D. M. (1993). The spectrin-based membrane structure and micron-scale organization of the plasma membrane. *Annu. Rev. Cell Biol.* **8,** 27–66.

Binette, F., Bernard, M., Laroche, A., Pierron, G., and Pallotta, D. (1990). Cell-specific expression of a profilin gene family. *DNA Cell Biol.* **9,** 323–334.

Blackbourn, H. D., and Battey, N. H. (1993). Annexin-mediated secretory vesicle aggregation in plants. *Physiol. Plant.* **89,** 27–32.

Blackbourn, H. D., and Jackson, A. P. (1996). Plant clathrin heavy chain: Sequence analysis and restricted localisation in growing pollen tubes. *J. Cell Sci.* **109,** 777–786.

Blackbourn, H. D., Barker, P. J., Huskisson, N. S., and Battey, N. H. (1992). Properties and partial protein sequence of plant annexins. *Plant Physiol.* **99,** 864–871.

Bloom, G. S., Wagner, M. C., Pfister, K. K., and Brady, S. T. (1988). Native structure and physical properties of bovine brain kinesin and identification of the ATP-binding polypeptide. *Biochemistry* **27,** 3409–3416.

Bohdanowicz, J., Ciampolini, F., and Cresti, M. (1995). Striped projections of the outer membrane of the generative cell in *Convallaria majalis*. *Sex. Plant Reprod.* **8,** 223–227.

Bornenave, M. (1996). Analysis of pectin methyl esterase. *In* "Plant Cell Wall Analysis, Modern method of plant analysis" (H. F. Linskens and Jackson, eds.), Vol. 17, pp. 165–180. Springer-Verlag, Berlin/New York.

Brewbaker, J. L., and Kwack, B. H. (1963). The essential role of calcium ion in pollen germination and pollen tube growth. *Am. J. Bot.* **50,** 859–865.

Bulinski, J. C., and Gundersen, G. G. (1991). Stabilization and post-translational modification of microtubules during cellular morphogenesis. *BioEssays* **13,** 285–293.

Cai, G., Bartalesi, A., Del Casino, C., Moscatelli, A., Tiezzi, A., and Cresti, M. (1993). The kinesin-immunoreactive homologue from *Nicotiana tabacum* pollen tube: Biochemical properties and subcellular localization. *Planta* **191,** 496–506.

Cai, G., Moscatelli, A., Del Casino, C., and Cresti, M. (1996a). Cytoplasmic motors and pollen tube growth. *Sex. Plant Reprod.* **9,** 59–64.

Cai, G., Moscatelli, A., del Casino, C., Chevrier, V., Mazzi, M., Tiezzi, A., and Cresti, M. (1996b). The anti-centrosome mAb 6C6 reacts with a plasma membrane-associated polypeptide of 77-kDa from the *Nicotiana tabacum* pollen tubes. *Protoplasma* **190,** 68–78.

Calzoni, G. L., and Speranza, A. (1989). Glycoprotiens in germinating apple pollen. *Plant Physiol. Biochem.* **27,** 219–225.

Capkova, V., Zbrozek, J., and Tupy, J. (1994). Protein synthesis in tobacco pollen tubes: Preferential synthesis of cell-wall 69-kDa and 66-kDa glycoproteins. *Sex. Plant Reprod.* **7,** 57–66.

Carlsoon, L., Nystrom, L.-E., Sundkvist, I., Markey, F., and Lindberg, U. (1977). Actin polymerizability is influenced by profilin, a low molecular weight protein in non-muscle cells. *J. Mol. Biol.* **115,** 465–483.

Carpenter, J. L., Ploense, S E., Snustad, D. P., and Siflow, C. D. (1992). Preferential expression of an α-tubulin gene of *Arabidopsis* in pollen. *Plant Cell* **4,** 557–571.

Carpita, N. C., and Gibeaut, D. M. (1993). Structural models of primary cell walls in flowering plants: Consistency of molecular structure with the physical properties of the walls during growth. *Plant J.* **3,** 1–30.

Cassab, G. L. (1995). Abnormal cell form due to the absence of extensin in cell wall of boron deficient bean nodules. *In* "Abstract of the 7th Cell Wall Meeting" (I. Zarra and G. Revilla, eds.), p. 57. Santiago de Compostela, Spain.

Chaen, S., Oiwa, K., Kobayashi, T., Gross, T., Kamitsubo, E., Shimmen, T., and Sugi, H. (1993). Kinetic properties of the ATP-dependent actin-myosin sliding as revealed by the force-movement assay system with a centrifuge microscope. *In* "Mechanism of Myofilament Sliding in Muscle Contraction" (H. Sugi and G. H. Pollack, eds.), pp. 351–360. Plenum, New York.

Cheney, R. E., Riley, M. A., and Mooseker, M. S. (1993). Phylogenetic analysis of the myosin superfamily. *Cell Motil. Cytoskeleton* **24,** 215–223.

Cheung, A. Y., Wang, H., and Wu, H. (1995). A floral transmitting tissue-specific glycoprotein attracts pollen tubes and stimulates their growth. *Cell* **82,** 383–393.

Clark, E. A., and Brugge, J. S. (1995). Integrins and signal transduction pathways: The road taken. *Science* **268,** 233–239.

Condeelis, J. S. (1974). The identification of F-actin in the pollen tube and protoplast of *Amaryllis belladonna*. *Exp. Cell Res.* **88,** 434–439.

Cooley, L. E., Verheyen, E., and Ayers, K. (1992). Chickadee encodes a profilin required for intracellular cytoplasm transport during *Drosophila* oogenesis. *Cell* **69,** 173–184.

Cosgrove, D. J. (1993). Wall extensibility: Its nature, measurment and relationship to plant cell growth. *New Cytol.* **124,** 1–23.

Cowin, P., and Burke, B. (1996). Cytoskeleton–membrane interactions. *Curr. Opin. Cell Biol.* **8,** 56–65.

Cresti, M., and Keijzer, C. J. (1985). The structure of the endoplasmic reticulum in pollen grains and pollen tubes, after osmium tetroxide-potassium ferricyanide staining. *J. Submicrosc. Cytol.* **17,** 615–620.

Cresti, M., and Van Went, J. L. (1976). Callose deposition and plug formation in *Petunia* pollen tubes in situ. *Planta* **133,** 35–40.

Cresti, M., VanWent, J. L., Willemse, M. T. M., and Pacini, E. (1976). Fibrous masses and cell and nucleus movement in the pollen tube of *Petunia hybrida*. *Acta Bot. Neerl.* **25,** 381–383.

Cresti, M., Pacini, E., Ciampolini, F., and Sarfatti, G. (1977). Germination and early tube development *in vitro* of *Lycopersiecum peruvianum* pollen: Ultrastrucutral features. *Planta* **136,** 239–247.

Cresti, M., Blackmore, S., and Van Went, J. L. (1992). "Atlas of Sexual Reproduction in Flowering Plants." Springer-Verlag, Berlin/Heidelberg/New York.

Cyr, R. J. (1991). Microtubule-associated proteins in higher plants. *In* "The Cytoskeletal Basis of Plant Growth and Form" (C. W., Lloyd, ed.), pp. 57–67. Academic Press, London.

Cyr, R. J., and Palevitz, B. A. (1989). Microtubule-binding proteins from carrot. Initial characterization and microtubule bundling. *Planta* **177,** 254–260.

Dahl, S. C., Geib, R. W., Fox, M. T., Edidin, M., and Branton, D. (1994). Rapid capping in α-spectrin-deficient MEL cells from mice afflicted with hereditary hemolytic anemia. *J. Cell Biol.* **125,** 1057–1065.

Dawson, P. J., and Lloyd, C. W. (1987). Comparative biochemistry of plant and animal tubulins. *In* "The Biochemistry of Plants" (D. D. Davies, ed.), Vol. 12, pp. 3–47. Academic Press, San Diego.

Del Casino, C., Li, Y., Moscatelli, A., Scali, M., Tiezzi, A., and Cresti, M. (1993). Distribution of microtubules during the growth of tobacco pollen tubes. *Biol. Cell.* **79,** 125–132.

Delmer, D., and Amor, Y. (1995). Cellulose biosynthesis. *Plant Cell* **7,** 987–1000.

Delmer, D. P., Ohana, P., Gonen, L., and Benziman, M. (1993). In vitro synthesis of cellulose in plants: Still a long way to go. *Plant Physiol.* **103,** 307–308.

Derksen, J., Pierson, E. S., and Traas, J. A. (1985). Microtubules in vegetative and generative cells of pollen tubes. *Eur. J. Cell Biol.* **38,** 142–148.

Derksen, J., Rutten, T. L., Lichtscheidel, I. K., De Win, A. H. N., Pierson, E. S., and Rongen, G., M. (1995a). Organelle distribution, exocytosis and endocytosis in tobacco pollen tubes. *Protoplasma* **188,** 267–276.

Derksen, J., Rutten, T., van Amstel, T., de Win, A., Doris, F., and Steer, M. (1995b). Regulation of pollen tube growth. *Acta Bot. Neerl.* **44,** 93–119.

De Ruijter, N. J., and Emons, A. M. C. (1993). Immunodetection of spectrin antigens in plant cells. *Cell Biol. Int.* **17,** 169–182.

De Win, A. H. N., Knuiman, B., Pierson, E. S., Geurts, H., Kengen, H. M. P., and Derksen, J. (1996). Development and cellular organization of *Pinus sylvestris* pollen tubes. *Sex. Plant Reprod.* **9,** 93–101.

Dickinson, H. G. (1995). Dry stigmas, water and self-incompatibility in *Brassica. Sex. Plant Reprod.* **8,** 1–10.

Domozych, D. S. (1991). The Golgi apparatus and membrane trafficking in green algae. *Int. Rev. Cytol.* **131,** 213–253.

Emons, A. M. (1989). Helicoidal microfibril depositionin a tip-growing cell and microtubule alignment during tip morphogenesis: A dry-cleaving and freeze-substitution study. *Can. J. Bot.* **67,** 2401–2408.

Emons, A. M. C., Pierson, E. S., and Derksen, J. (1991). Cytoskeleton and intracellular movements. *In* "Biotechnology Current Progress" (P. N. Cheramisinoff and L. M. Ferante, eds.), Vol.1, pp. 311–355. Technomic, Basel.

Emons, A. M. C., Derksen, J., and Sassen, M. M. A. (1992). Do microtubules orient plant cell microfibrils? *Physiol. Plant.* **84,** 486–493.

Evans, D. E., Briars, S.-A., and Williams, L. E. (1991). Active calcium transport by plant cell membranes. *J. Exp. Bot.* **42,** 285–303.

Falconer, M. M., and Seagull, R. W. (1985). Xylogenesis in tissue culture: Taxol effects on microtubule reorientation and lateral association in differentiating cells. *Protoplasma* **128,** 157–166.

Fath, K. R., Trimbur, G. M., and Burgess, D. R. (1994). Molecular motors are differentially distributed on Golgi membranes from polarized epithelial cells. *J. Cell Biol.* **126,** 661–675.

Feijo, J.A., Malhò, R., and Pais, M.S. (1992). A cytochemical study on the role of ATPases during pollen germination in *Agapathus umbellatus* L. *Sex. Plant Reprod.* **5,** 138–145.

Feijo, J. A., Malho, R., and Obermeyer, G. (1995). Ion dynamics and its possible role during *in vitro* pollen germination and tube growth. *Protoplasma* **187,** 155–167.

Ferrol, N., and Bennet, A. B. (1996). A single gene may encode differentially localized Ca^{2+}-ATPases in plant cells. *Plant Cell* **8,** 1159–1169.

Fosket, D. E. (1989). Cytoskeletal proteins and their genes in higher plants. *In* "Biochemistry of Plants" (P. K. Sumpf and E. D. Conn, eds.), Vol.15, pp. 393–454. Cambridge Univ. Press, Cambridge, UK.

Fosket, D. E., and Morejohn, L. C. (1992). Structural and functional organization of tubulin. *Annu. Rev. Plant Mol. Biol.* **43,** 201–240.

Franke, W. W., Herth, H., Van Der Woude, W. J., and Morrè, D. J. (1972). Tubular and filamentous structures in pollen tubes: Possible involvement as guide elements in protoplasmic streaming and vectorial migration of secretory vesicles. *Planta* **105,** 317–341.

Fry, S., Aldington, S., Hetherington, P. R., and Aitken, J. (1993). Oligosaccharides as signals and substrates in the plant cell wall. *Plant Physiol.* **103,** 1–5.

Geitmann, A., Hudèk, J., Vennigerholz, F., and Walles, B. (1995a). Immunogold localization of pectin and callose in pollen grain and pollen tubes of *Brugmensia susveolens*—Implication for the self-imcompatibility reaction. *J. Plant Physiol.* **147,** 225–235.

Geitmann, A., Li, Y. Q., and Cresti, M. (1995b). The role of cytoskeleton and dictyosome activity in the pulsatory growth of *Nicotiana tabacum* and *Petunia hybrida* pollen tubes. *Bot. Acta* **109,** 102–109.

Gelfand, V. I., and Bershadsky, A. D. (1991). Microtubule dynamics: Mechanism, regulation and function. *Annu. Rev. Cell Biol.* **7,** 93–116.

Ghanadan, H., Loomis, W. D., and Durst, R. W. (1995). A possible borate–apiose cross-link in plant cell walls. *In* "Abstract of the 7th Cell Wall Meeting" (I. Zarra and G. Revilla, eds.), p. 2. Santiago de Compostela, Spain.

Gibbon, B. C., and Kropf, D. L. (1994). Cytosolic pH gradients associated with tip growth. *Science* **263,** 1419–1421.

Giddings, T.H., and Staehelin, L.A. (1990). Microtubule-mediated control of microfibril deposition: A re-examination of the hypothesis. *In* "The Cytoskeletal Basis of Plant Growth and Development" (C. W. Lloyd, ed.), pp. 85–99. Academic Press, London.

Gilissen, L. J. W. (1977). The influence of relative humidity on the swelling of pollen grains *in vitro. Planta* **137,** 299–302.

Goldberg, R. (1984). Changes in the properties of cell wall pectin methylesterase along the *Vigna radiata* hypocotyl. *Physiol. Plant.* **61,** 58–63.

Goldberg, R., Bordenave, M., Pierron, M., Prat, R., and Mutaftschiev, S. (1992). Enzymatic processes in growing cell walls, possible control by pectinmethylesterase. *In* "Plant Cell Walls as Biopolymers with Physiological Functions" (Y. Masuda, ed.), pp. 269–274. Yamada Science Foundation, Osaka.

Goldberg, R. B., Beals, T. P., and Sanders, P. M. (1993). Anther development: Basic principles and practical applications. *Plant Cell* **5,** 1217–1229.

Goldstein, L. S. B. (1993). With apologies to Scheherazade: Tails of 1001 kinesin motors. *Annu. Rev. Genet.* **27,** 319–351.

Gong, M., Yang, Z.H., and Tsao, T.H. (1993). Isolation and characterization of calmodulin and a novel calcium-binding protein calpollenin from *Pinus yunnanensis* pollen. *Plant Sci.* **89,** 5–12.

Goodenough, U. W., and Heuser, J. E. (1985). Outer and inner dynein arms of cilia and flagella. *Cell* **41,** 341–342.

Goodson, H. V., Kang, S. J., and Endow, S. A. (1994). Molecular phylogeny of the kinesin family of microtubule motor proteins. *J. Cell Sci.* **107,** 1875–1884.

Griffith, G., and Simons, K. (1986). The trans-Golgi network: Sorting at the exit of the Golgi complex. *Science* **234,** 438–443.

Haarer, B. K., and Brown, S. S. (1990). Structure and function of profilin. *Cell Motil. Cytoskeleton.* **17,** 71–74.

Hall, D. H., and Hedgecock, E. M. (1991). Kinesin-related gene unc-104 is required for axonal transport if synaptic vesicles in *C. elegans. Cell* **65,** 837–847.

Harris, P. J., Freed, K., Anderson, M. A., Weinhandl, J. A., and Clarke, A. E. (1987). An enzyme-linked immunosorbent assay (ELISA) for in vitro pollen tube growth based on binding of a monoclonal antibody to the pollen tube surface. *Plant Physiol.* **84,** 851–855.

Haugwitz, M., Noegel, A. A., and Rieger, D. (1991). *Dictyostelium discoideum* contains two profilin isoforms that differ in structure and function. *J. Cell Sci.* **100,** 481–489.

Hedrich, R., and Schroeder, J. I. (1989). The physiology of ion channels and electrogenic pumps in higher plants. *Annu. Rev. Plant Physiol.* **40,** 539–569.

Helsper, J. P. F. G., and Pierson, E. S. (1986). The effects of lectins on germinating pollen of *Lilium longiflorum* II. Effect of concanavalin A on phospholipid turnover and on biosynthesis of pectic polysaccharides. *Acta Bot. Neerl.* **35,** 257–263.

Helsper, J. P. F. G., Groot, P. F., Linskens, H. F., and Jackson, J. F. (1986). Phosphatidylinositol monophosphate in *Lilium* pollen and turnover of phospholipid during pollen tube extension. *Phytochemistry* 25, 2193–2199.

Hennessey, E. S., Drummond, D. R., and Sparrow, J. C. (1993). Molecular genetic and actin function. *Biochem. J.* **282,** 657–671.

Hepler, P. K., Miller, D. D., Pierson, E. S., and Callaham, D. A. (1994). Calcium and pollen tube growth. *In* "Pollen–Pistil Interaction and Pollen Tube Growth" (A. G. Stephenson and D. H. Kao, eds.), pp. 111–123. American Society of Plant Physiologists, Rockville, MD.

Herrero, M., and Dickinson, H. G. (1981). Pollen tube development in *Petunia hybrida* following compatible and incompatibile intraspecific matings. *J. Cell Sci.* **47,** 365–383.

Herrmann, A., and Felle, H. H. (1995). Tip growth in root hair cells of *Spinapis alba* L.: Significance of internal and external Ca^{2+} and pH. *New Phytol.* **129,** 523–533.

Herth, W. (1989). The pollen tube tip region in video microscopy. *Eur. J. Cell Biol.* **48 (Suppl. 26),** 89.

Heslop-Harrison, J. (1979). Aspects of the structure, cytochemistry and germination of the pollen of rye (*Secale cereale* L.). *Ann. Bot.* **Suppl. 1,** 1–47.

Heslop-Harrison, J. (1987). Pollen germination and pollen tube growth. *Int. Rev. Cytol.* **107,** 1–78.

Heslop-Harrison, J., and Heslop-Harrison, Y. (1988). Sites of origin of the peripheral microtubule system of the vegetative cell of the Angiosperm pollen tube. *Ann. Bot.* **62,** 455–461.

Heslop-Harrison, J., and Heslop-Harrison, Y. (1989a). Actomyosin and movement in the angiosperm pollen tube: An interpretation of some recent results. *Sex. Plant Reprod.* **2,** 199–207.

Heslop-Harrison, J., and Heslop-Harrison, Y. (1989b). Myosin associated with the surface of organelles, vegetative nuclei and generative cells in angiosperm pollen grains and tubes. *J. Cell Sci.* **94,** 319–325.

Heslop-Harrison, J., and Heslop-Harrison, Y. (1991). The actin cytoskeleton in unfixed pollen tubes following microwave-accelerated DMSO permeabilization and TRITC-phalloidin staining. *Sex. Plant Reprod.* **4,** 6–11.

Heslop-Harrison, J., Heslop-Harrison, Y., Cresti, M., Tiezzi, A., and Ciampolini, F. (1986). Actin during pollen germination. *J. Cell Sci.* **86,** 1–8.

Heslop-Harrison, J., Heslop-Harrison, Y., Cresti, M., Tiezzi, A., and Moscatelli, A. (1988). Cytoskeletal elements, cell shaping and movement in the angiosperm pollen tube. *J. Cell Sci.* **91,** 49–60.

Hilmer, S., Freundt, H., and Robinson, D. G. (1988). The partially coated reticulum and its relationship to the Golgi apparatus in higher plants. *Eur. J. Cell Biol.* **47,** 206–212.

Hirokawa, N., Sato-Yoshitake, R., Yoshida, T., and Kawashima, T. (1990). Brain dynein (MAP1C) localizes on both anterogradely and retrogradely transported membranous organelles *in vivo*. *J. Cell Biol.* **111,** 1027–1037.

Hirokawa, N., Sato-Yoshitake, R., Kobayashi, N., Pfister, K. K., Bloom, G. S., and Brady, S. T. (1991). Kinesin associates with anterogradely transported membranous organelles *in vivo*. *J. Cell Biol.* **114,** 295–302.

Hoggart, R. M., and Clarke, A. E. (1984). Porosity of *Gladiolus* stigmatic papillae and pollen tube walls. *Ann. Bot.* **53,** 271–277.

Hollenbeck, P. J. (1989). The distribution, abundance and subcellular localization of kinesin. *J. Cell Biol.* **108,** 2335–2342.

Holzbaur, E. L. F., and Vallee, R. B. (1994). Dyneins: Molecular structure and cellular function. *Annu. Rev. Cell Biol.* **10,** 339–372.

Hoyt, M. A. (1994). Cellular roles of kinesin and related proteins. *Curr. Opin. Cell Biol.* **6,** 63–68.

Hu, H., and Brown, P. (1994). Localization of boron in cell walls of squash and tobacco and its association with pectin. Evidence for a structural role of boron in the cell wall. *Plant Physiol.* **105,** 681–689 .

Hussey, P. J., and Gull, K. (1985). Multiple isotypes of α and β tubulin in the plant *Phaseolus vulgaris*. *FEBS Lett.* **181,** 113–118.

Hussey, P. J., Traas, J. A., Gull, K., and Lloyd, C. (1987). Isolation of cytoskeletons from synchronized cells: The interphase microtubulue array utilizes multiple tubulin isotypes. *J. Cell Sci.* **88,** 225–230.

Hussey, P. J., Lloyd, C. W., and Gull, K. (1988). Differential and developmental expression of β-tubulins in higher plant cell. *J. Biol. Chem.* **263,** 5474–5479.

Hyvonen, M., Macias, M. J., Nilges, M., Oschkinat, H., Saraste, M., and Wilmanns, M. (1995). Structure of the binding site for inositol phosphates in a PH domain. *EMBO J.* **14,** 4676–4685.

Iwanami, Y., Sasakuma, T., and Yamada, Y. (1988). "Pollen: Illustration and Scanning Electronmicrographs." Springer-Verlag, Berlin/Heidelberg.

Iwanami, Y. (1956). Protoplasmic movement in pollen grains and tubes. *Phytomorphology* **6,** 288–295.

Jackson, J. F. (1989). Borate control of protein secretion from *Petunia* pollen exhibits critical temperature discontinuities. *Sex. Plant Reprod.* **2,** 11–14.

Jauh, G. Y., and Lord, E. M. (1996). Localization of pectins and arabinogalactan-proteins in lily (*Lilium longiflorum* L.) pollen tube and style, and their possible roles in pollination. *Planta* **199,** 251–261.

Jiang, C.-J., and Sonobe, S. (1993). Identification and preliminary characterization of a 65 kDa higher-plant MT-associated protein. *J. Cell Sci.* **105,** 891–901.

Joos, U., van Aken, J., and Kristen, U. (1994). Microtubules are involved in maintaining the cellular polarity in pollen tubes of *Nicotiana sylvestris*. *Protoplasma* **179,** 5–15.

Joos, U., van Aken, J., and Kristen, U. (1995). The anti-microtubule drug carbetamide stops *Nicotiana sylvestris* pollen tube growth in the style. *Protoplasma* **187,** 182–191.

Juniper, B. E., Hawes, C. R., and Horne, J. C. (1982). The relationship between dictyosomes and the forms of endoplasmic reticulum in plant cells with different export programs. *Bot. Gaz.* **143,** 135–145.

Kaminskyj, S. G. W., and Heath, I. B. (1995). Integrin and spectrin homologues, and cytoplasm-wall adhesion in tip growth. *J. Cell Sci.* **108,** 849–856.

Kandasami, K. K., Thorsness, M. K., Rundle, S. L., Goldberg, M. L., Nasrallah, J. B., Nasrallah, M. E. (1993). Ablation of papillar cell function in *Brassica* flowers results in the loss of stigma receptivity to polination. *Plant Cell* **5,** 263–275.

Kappler, R., Kristen, U., and Morrè, D.J. (1986). Membrane flow in plants: Fractionation of growing pollen tubes of tobacco by preparative free-flow electrophoresis and kinetics of labeling of endoplasmic reticulum and Golgi apparatus with [^{3}H]leucine. *Protoplasma* **132,** 38–50.

Khono, T., and Shimmen, T. (1987). Ca^{2+}-induced fragmentation of actin filaments in pollen tubes. *Protoplasma* **141,** 177–179.

Khono, T., and Shimmen, T. (1988). Accelerated sliding of pollen tube organelles along *Characeae* actin bundles regulated by Ca^{2+}. *J. Cell Biol.* **106,** 1539–1543.

Khono, T., Chaen, S., and Shimmen, T. (1990). Characterization of the translocator associated with pollen tube organelles. *Protoplasma* **154,** 179–183.

Khono, T., Okagaki, T., Kohama, K., and Shimmen, T. (1991). Pollen tube extract supports the movement of actin filaments *in vitro*. *Protoplasma* **161,** 75–77.

Khono, T., Ishikawa, R., Nagata, T., Kohama, K., and Shimmen, T. (1992). Partial purification of myosin from lily pollen tubes by monitoring with *in vitro* motility assay. *Protoplasma* **170,** 77–85.

Knebel, W., Quader, H., and Schnepf, E. (1990). Mobile and immobile endoplasmic reticulum in onion bulb epidermis cells: Short- and long-term observations with a confocal laser scanning microscope. *Eur. J. Cell Biol.* **52,** 328–340.

Kobayashi, M., Matoh, T., and Azuma, J. (1996). Two chains of rhamnogalacturonan II are cross-linked by borate-diol ester bounds in higher plant cell walls. *Plant Physiol.* **110,** 1017–1020.

Koffer, A., and Dickens, J. J. (1989). Isolation and characterization of actin from BHK cells. *J. Muscle Res. Cell Motil.* **8,** 397–406.

Kreis, T., and Vale, R. (1993). "Guidebook to the Cytoskeletal and Motor Proteins." Oxford Univ. Press, Oxford.

Kristen, U. (1978). Ultrastructure and possible function of the intercisterna elements in dictyosomes. *Planta* **138,** 29–33.

Kroh, M., and Knuiman, B. (1982). Ultrastructure of cell wall and plugs of tobacco pollen tubes after chemical extraction of polysaccharides. *Planta* **154,** 241–250.

Kuhtreiber, W. M., and Jaffe, L. F. (1990). Detection of extracellular calcium gradients with a calcium-specific vibrating electrode. *J. Cell Biol.* **110,** 1565–1573.

Kuznetsov, S. A., Langford, G. M., and Weiss, D. G. (1992). Actin-dependent organelle movement in squid axoplasm. *Nature* **356,** 722–725.

Lancelle, S. A., and Hepler, P. K.(1989). Immunogold labelling of actin on sections of freeze-substituted plant cells. *Protoplasma* **150,** 72–74.

Lancelle, S. A., and Hepler, P. K. (1991). Association of actin with cortical microtubules revealed by immunogold localization in *Nicotiana* pollen tubes. *Protoplasma* **165,** 167–172.

Lancelle, S. A., and Hepler, P. K. (1992). Ultrastructure of freeze-substituted pollen tubes of *Lilium longiflorum. Protoplasma* **167,** 215–230.

Lancelle, S. A., Cresti, M., and Hepler, P. K. (1987). Ultrastructure of the cytoskeleton in freeze-substituted pollen tubes of *Nicotiana alata. Protoplasma* **140,** 141–150.

Langford, G. M. (1995). Actin- and microtubule-dependent organelle motors: Interrelationships between the two motility system. *Curr. Opin. Cell Biol.* **7,** 82–88.

Levy, S., and Staehelin, L. A. (1992). Synthesis, assembly and function of plant cell wall macromolecules. *Curr. Opin. Cell Biol.* **4,** 856–862.

Li, H., Turner, A., Doblin, M., Read, S. M., and Bacic, A. (1996a). Developmental regulation and partial purification of callose synthase from pollen tubes of *Nicotiana alata. In* "Abstrcts of 14th International Congress of Sexual Plant Reproduction," p. 98. Lorne, Australia.

Li, Y.-Q., and Linskens, H. F. (1983). Wall-bound proteins of pollen tubes after self- and cross-pollination in *Lilium longiflorum. Theor. Appl. Genet.* **67,** 11–16.

Li, Y.-Q., and Tsao, T. H. (1985). Covalently bound wall proteins of pollen grains and pollen tubes grown in vitro and in styles after self- and cross-pollination in *Lilium longiflorum. Theor. Appl. Genet.* **71,** 11–16.

Li, Y.-Q., Croes, A. F., and Linskens, H. F. (1983). Cell-wall proteins in pollen and roots of *Lilium longiflorum:* Extraction and partial characterization. *Planta* **158,** 422–427.

Li, Y.-Q., Tsao, T. H., and Linskens, H. F. (1986). Dependence of *Lilium* pollen germination and tube growth on protein synthesis and glycosylation after inhibitor treatments. *Proc. Kon. Ned. Akad. Wet. Amsterdam* **89,** 61–73.

Li, Y.-Q., Bruun, L., Pierson, E. S., and Cresti, M. (1992). Periodic deposition of arabinogalactan epitopes in the cell wall of pollen tubes of *Nicotiana tabacum* L. *Planta* **188,** 532–538.

Li, Y.-Q., Chen F., Linskens, H. F., and Cresti, M. (1994). Distribution of unesterified and esterified pectins in cell walls of pollen tubes of flowering plants. *Sex. Plant Reprod.* **7,** 145–152.

Li, Y.-Q., Cen, F., Faleri, C., Ciampolini, F., Linskens, H. F., and Cresti, M. (1995a). Presumed phylogenetic basis of the correlation of pectin deposition patter in pollen tube walls and the stylar atructure of angiosperms. *Proc. Kon. Ned. Akad. Wet. Amsterdam* **98,** 39–44.

Li, Y.-Q., Faleri, C., Geitmann, A., Zhang, H.-Q., and Cresti, M. (1995b). Immunogold localization of arabinogalactan proteins, unesterified and esterified pectins in pollen grains and pollen tubes of *Nicotiana tabacum* L. *Protoplasma* **189,** 26–36.

Li, Y.-Q., Zhang, H.-Q., Pierson, E. S., Huang, F.-Y., Linskens, H. F., Hepler, P. K., and Cresti, M. (1996b). Enforced growth-rate fluctuation causes pectin ring formation in the cell wall of *Lilium longiflorum* pollen tubes. *Planta* **200,** 41–49.

Lillie, S. H., and Brown, S. S. (1994). Immunofluorescence localization of the unconventional myosin, Myo2p, and the putative kinesin-related protein, Smy1p, to the same region of polarized growth in *Saccharomyces cerevisiae. J. Cell Biol.* **125,** 825–842.

Lin, Y., Wang, Y., Zhu, J., and Yang, Z. (1996). Localization of a Rho GTPase implies a role in tip growth and movement of the generative cell in pollen tubes. *Plant Cell* **8,** 293–303.

Liu, B., and Du, J. Z. (1989). Purification and some physicochemical properties of calmodulin in *Brassica campestris* pollen. *Acta Biochem. Biophys. Sin.* **21,** 477–483.

Liu, B., and Palevitz, B. A. (1996). Localization of a kinesin-like protein in the generative cells of tobacco. *Protoplasma* **195,** 78–89.

Liu, B., Cyr, R. J., and Palevitz, B. A. (1996). A kinesin-like protein, katAp, in the cells of *Arabidopsis* and other plants. *Plant Cell* **8,** 119–132.

Liu, G. Q., Cai, G., del Casino, C., Tiezzi, A., and Cresti, M. (1994). Kinesin-related polypeptide is associated with vesicles from *Corylus avellana* pollen. *Cell Motil. Cytoskeleton* **29,** 155–166.

Liu, X., and Yen, L. F. (1992). Purification and characterization of actin from maize pollen. *Plant Physiol.* **99,** 1151–1155.

Lloyd, C. W. (1991). Probing the plant cytoskeleton. *Nature* **350,** 189–190.

Lodish, H. F. (1988). Transport of secretory and membrane glycoproteins from the rough endoplasmic reticulum to the Golgi. *J. Biol. Chem.* **262,** 2107–2110.

Lopez-Franco, R., Bartnicki-Garcia, S., and Bracker, C. A. (1994). Pulsed growth of fungal hyphal tips. *Proc. Natl. Acad. Sci. USA* **91,** 12228–12232.

Lord, E.M., and Sanders, L.C. (1992). Roles for the extracellular matrix in plant development and pollination: A special case of cell movement in plants. *Dev. Biol.* **153,** 16–28.

LoSchiavo, F., Filippini, F., Cozzani, F., Vallone, D., and Terzi, M. (1991). Modulation of auxin-binding proteins in cell suspensions. I. Differential responses of carrot embryo culture. *Plant Physiol.* **97,** 60–64.

Ma, Y. Z., and Yen, L. F. (1989). Actin and myosin in pea tendrils. *Plant Physiol.* **89,** 586–589.

Machesky, L. M., and Pollard, T. D. (1993). Profilin as a potential mediator of membrane–cytoskeleton communication. *Trends Cell Biol.* **3,** 381–385.

Magdolen, V., Oechsner, G., Muller, G., and Bandlow, W. (1988). The intron containing gene for yeast profilin (PFY) encodes a vital function. *Mol. Cell. Biol.* **8,** 5108–5115.

Malhò, R., Feijo, J. A., and Pais, M. S. (1992). Effect of electric fields and external ionic currents on pollen tube orientation. *Sex. Plant Reprod.* **5,** 57–63.

Malhò, R., Read, N.D., Pais, M.S., and Trewavas, A.J. (1994). Role of cytosolic free calcium in the reorientation of pollen tube growth. *Plant J.* **5,** 331–341.

Malhò, R., Read, N. D., Trewavas, A. J., and Pais, M. S. (1995). Calcium channel activity during pollen tube growth and reorientation. *Plant Cell* **7,** 1173–1184.

Malhò, R., and Trewavas, A. J. (1996). Localized apical increases of cytosolic free calcium control pollen tube orientation. *Plant Cell* **8,** 1935–1949.

Marcantonio, E. E., and Hynes, R. O. (1988). Anibodies to the conserved cytoplasmic domain of the integrin (1 subunit react with proteins in vertebrates, invertebrates, and fungi. *J. Cell Biol.* **106,** 1765–1772.

Mascarenhas, J. P. (1993). Molecular mechanisms of pollen tube growth and differentiation. *Plant Cell* **5,** 1303–1314.

Mathieu, Y., Kurkdjian, A., Xia, H., Guern, J., Koller, A., Spiro, M. D., O'Neill, M., Albersheim, P., and Darvill, A. (1991). Membrane responses induced by ologogalacturonides in suspension-cultured tobacco cells. *Plant J.* **1,** 333–343.

Matoh, T., Ishigaki, K., Mizutani, M., Matsunaga, W., and Takabe, K. (1992). Boron nutrition of cultured tobacco BY-2 cells. I. Requirement for and intracellular localization of boron and selection of cells that tolerate low levels of boron. *Plant Cell Physiol.* **33,** 1135–1141.

Matus, A. (1990). MT-associated proteins. *Curr. Opin. Cell Biol.* **21,** 10–14.

McCann, M. C., and Roberts, K. (1994). Changes in cell wall architecture during cell elongation. *J. Exp. Bot.* **45,** 1683–1691.

Meikle, P. J., Bonig, I., Hoogenraad, N. J., Clarke, A. E., and Stone, B. A. (1991). The location of (1-3)-β-glucans in the walls of pollen tubes of *Nicotiana alata* using a (1-3)-β-glucan-specific monoclonal antibody. *Planta* **185,** 1–8.

Mellman, I., and Simons, K. (1992). The Golgi complex: *In vitro* veritas? *Cell* **68,** 829–840.

Miller, D. D., Callaham, D. A.,Gross, D. J., and Hepler, P. K. (1992). Free Ca^{2+} gradient in growing pollen tubes of *Lilium*. *J. Cell Sci.* **101,** 7–12.

Miller, D. D., Scordilis, S. P., and Hepler, P. K. (1995). Identification and localization of three classes of myosins in pollen tubes of *Lilium longiflorum* and *Nicotiana alata*. *J. Cell Sci.* **108,** 2549–2563.

Miller, D. D., Lancelle, S. A., and Hepler, P. K. (1996). Actin filaments do not form a dense mehwork in *Lilium longiflorum* pollen tube tips. *Protoplasma* **195,** 123–132.

Mitsui, H., Yamaguchi-Shinozaki, K., Shinozaki, K., Nishikawa, K., and Takahashi, H. (1993). Identification of a gene family (kat) encoding kinesin-like proteins in *Arabidopsis thaliana* and the characterization of secondary structure of KatA. *Mol. Gen. Genet.* **238,** 362–368.

Mitsui, H., Nakatani, K., Yamaguchi-Shinozaki, K., Shinozaki, K., Nishikawa, K., and Takahashi, H. (1994). Sequencing and characterization of the kinesin-related genes katB and katC of *Arabidopsis thaliana*. *Plant Mol. Biol.* **25,** 865–876.

Mitsui, H., Hasezawa, S., Nagata, T., and Takahashi, H. (1996). Cell cycle-dependent accumulation of a kinesin-like protein, KatB/C, in synchronized tobacco BY-2 cells. *Plant Mol. Biol.* **30,** 177–181.

Mittermann, I., Swoboda, I., Pierson, E., Eller, N., Kraft, D., Valenta, R., and Heberle-Bors, E. (1995). Molecular cloning and characterization of profilin from tobacco (*Nicotiana tabacum*) increased profilin expression during pollen maturation. *Plant Mol. Biol.* **14,** 513–526.

Mizuno, K., Koyama, M., and Shibaoka, H. (1981). Isolation of tubulin from Azuki bean epicotyls by ethyl N-phenyl-carbamate-sepharose affinity chromatography. *J. Biochem.* **89,** 329–332.

Moepps, B., Conrad, S., and Schraudolf, H. (1993). PCR-dependent amplification and sequence characterization of partial cDNAs encoding myosin-like proteins in *Anemia phyllitidis* (L.) Sw. and *Arabidopsis thaliana* (L.) Heynh. *Plant Mol. Biol.* **21,** 1077–1083.

Morejohn, L. C., and Fosket, D. E. (1982). Higher plant tubulin identified by self-assembly in vitro. *Nature* **297,** 426–428.

Morejohn, L. C., and Fosket, D. E. (1984). Taxol-induced rose microtubule polymerization in vitro and its inhibition by colchicine. *J. Cell Biol.* **99,** 141–147.

Morejohn, L. C., and Fosket, D. E. (1991). The biochemistry of compounds with anti-microtubule activity in plant cells. *Pharmacol. Ther.* **51,** 217–230.

Morejohn, L. C., Bureau, E. T., Tocchi, L. P., and Fosket, D. E. (1984). Tubulins from different higher plant species are immnunologically nonidentical and bind colchicine differentially. *Proc. Natl. Acad. Sci. USA* **81,** 1440–1444.

Morrè, D. J. (1990). Endomembrane system of plants and fungi. *In* "Tip Growth in Plant and Fungal Cells" (I. B. Heath, ed.), pp. 183–210. Academic Press, San Diego.

Morrè, D. J. (1994). Physical membrane displacement: Reconstitution in a cell-free system and relationship to cell growth. *Protoplasma* **180,** 3–13.

Moscatelli, A., Tiezzi, A., Cai, G., and Cresti, M. (1991). Biochemical characterization of Taxol-induced structures from Nicotiana pollen tubes. *In* "Recent Advances in Plant Biology" (C. P. Malik and Y. P. Abrol, eds.), pp. 39–46. Narendra Publishing House, Delhi.

Moscatelli, A., Del Casino, C., Lozzi, L., Cai, G., Scali, M., Tiezzi, A., and Cresti, M. (1995). High molecular weight polypeptides related to dynein heavy chains in *Nicotiana tabacum* pollen tubes. *J. Cell Sci.* **108,** 1117–1125.

Moscatelli, A., Cai, G., Liu, G. Q., Tiezzi, A., and Cresti, M. (1996). Dynein-related polypeptides in pollen and pollen tubes. *Sex. Plant Reprod.* **9,** 312–317.

Mosher, D. R. (1988). "Fibronectin." Academic Press, New York.

Mu, J. H., Stains, J. P., and Kao, T.-H. (1994). Characterization of a pollen-expressed gene encoding a putative pectin esterase of *Petunia inflata*. *Plant Mol. Biol.* **25,** 539–544.

Nakamura, N., and Suzuki, H. (1981). Sugar composition of pollen grain and pollen tube cell walls. Phytochemistry **20,** 981–984.

Nakamura, N., and Suzuki, H. (1983). Cellulose and callose of the pollen tube wall of *Camellia japonica*. *Phytochemistry* **22,** 2517–2519.

Nick, P., Lambert, A.-M., and Vantard, M. (1995). A microtubule-associated protein in maize is expressed during phytochrome-induced cell elongation. *Plant J.* **8,** 835–844.

Nobes, C. D., and Hall, A. (1995). Rho, Rac, and Cdc42 GTPases regulate the assembly of multimolecular focal complexes associated with actin stress fibers, lamellipodia, and filopodia. *Cell* **81,** 53–62.

Noguchi, T. (1990). Consumption of lipid granules and formation of vacuoles in the pollen tube of *Tradescantia reflexa. Protoplasma* **156,** 19–28.

Noguchi, T., and Morrè, D. J. (1991). Membrane flow in plants: Preporation and kinetics of labelling of plasma membranes from growing pollen tubes of tobacco. *Protoplasma* **163,** 34–42.

Novikoff, A. B. (1976). The endoplasmic reticulum: A cytochemist's view (a review). *Proc. Natl. Acad. Sci. USA* **73,** 2781–2787.

Oakley, C. E., and Oakley, B. R. (1989). Identification of γ-tubulin, a new member of the tubulin superfamily encoded by *mipA* gene of *Aspergillus nidulans. Nature* **338,** 662–664.

Obermeyer, G., and Kolb, H.-A. (1993). K^+ channels in the plasma membrane of lily pollen protoplasts. *Bot. Acta* **106,** 26–31.

Obermeyer, G., and Weisenseel, M. (1991). Calcium channel blocker and calmodulin antagonists affect the gradient of free calcium ions in lily pollen tubes. *Eur. J. Cell Biol.* **56,** 319–327.

Obermeyer, G., Lützelschwab, M., Heumann, H. G., and Weisenseel, M. W. (1992). Immunolocalization of H^+-ATPases in the plasma membrane of pollen grains and pollen tubes of *Lilium longiflorum. Protoplasma* **171,** 55–63.

O'Driscoll, D., Read, S. M., and Steer, M. W. (1993). Determination of cell wall porosity by microscopy: Walls of cultured cells and pollen tubes. *Acta Bot. Neerl.* **42,** 237–244.

Olmsted, J. (1986). Microtubule-associated proteins. *Annu. Rev. Cell Biol.* **2,** 421–457.

Orci, L., Glick, B. S., and Rothman, J. E. (1986). A new type of coated vesicular carrier that appears not to contain clathrin: Its possible role in protein transport within the Golgi. *Cell* **46,** 171–184.

Palevitz, B. A., Liu, B., and Joshi, C. (1994). γ-Tubulin in tobacco pollen tubes: Association with generative cell and vegetative MTs. *Sex. Plant Reprod.* **7,** 209–214.

Parsons, J. T. (1996). Integrin-mediated signalling: Regulation by protein tyrosine kinase and small GTP-binding proteins. *Curr. Opin. Cell Biol.* **8,** 146–152.

Paschal, B. M., Shpetner, H. S., and Vallee, R. B. (1987). MAP1C is a microtubule-activated ATPase which translocates microtubules *in vitro* and has dynein-like properties. *J. Cell Biol.* **105,** 1273–1282.

Pearse, B. M. F., and Bretscher, M. S. (1981). Membrane recycling by coated vesicles. *Annu. Rev. Biochem.* **50,** 85–101.

Pennell, R. I., Knox, J. P., Scofield, G. N., Selvendran, R. R., and Roberts, K. (1989). A family of abundant plasma membraneassociated glycoproteins related to the arabinogalactan proteins in unique to flowering plants. *J. Cell Biol.* **108,** 1967–1977.

Perdue, T. D., and Parthasarathy, M. W. (1985). *In situ* localization of F-actin in pollen tubes. *Eur. J. Cell Biol.* **39,** 13–20.

Pesacreta, T. C., and Lucas, W. J. (1985). Presence of a partially coated reticulum in angiosperms. *Protoplasma* **125,** 173–184.

Pfarr, C. M., Coue, M., Grissom, P. M., Hays, T. S., Porter, M. E., and McIntosh, J. R. (1990). Cytoplasmic dynein is localized to kinetochores during mitosis. *Nature* **345,** 263–265.

Picton, J. M., and Steer, M. W. (1983). Membrane recycling an the control of secretory activity in pollen tubes. *J. Cell Sci.* **63,** 303–310.

Pierson, E. S. (1988). Rhodamine-phalloidin staining of F-actin in pollen after dimethylsulphoxide permeabilization. *Sex. Plant Reprod.* **1,** 83–87.

Pierson, E. S., and Cresti, M. (1992). Cytoskeleton and cytoplasmic organization of pollen and pollen tubes. *Int. Rev. Cytol.* **140,** 73–125.

Pierson, E. S., Derksen, J., and Traas, J. A. (1986). Organization of microfilaments and microtubules in pollen tubes grown *in vitro* or *in vivo* in various angiosperms. *Eur. J. Cell Biol.* **41,** 14–18.

Pierson, E. S., Kengen, H. M. P., and Derksen, J. (1989). MTs and actin filaments co-localize in pollen tubes of *Nicotiana tabacum* L. and *Lilium longiflorum* Thumb. *Protoplasma* **150,** 75–77.

Pierson, E. S., Lichtscheidl, I. L., and Derksen, J. (1990). Structure and behaviour of organelles in living pollen tubes of *Lilium longiflorum. J. Exp. Bot.* **41,** 1461–1468.

Pierson, E. S., Miller, D. D, Callaham, D. A., Shipley, A. M., Rivers, B. A., Cresti, M., and Hepler, P. K. (1994). Pollen tube growth is coupled to the extracellular calcium ion flux and the intracellular calcium gradient: Effect of BAPTA-type buffer and hypertonic media. *Plant Cell* **6,** 1815–1828.

Pierson, E. S., Li, Y.-Q., Zhang, H.-Q., Willemse, M. T. M., Linskens, H. F., and Cresti, M. (1995). Pulsatory growth of pollen tubes: Investigation of a possible relationship with the periodic distribution of cell wall components. *Acta Bot. Neerl.* **44,** 121–128.

Pierson, E. S., Miller, D. D., Callaham, D. A., Van Aken, J., Heckett, G., and Hepler, P. K. (1996). Tip-localized calcium entry fluctuates during pollen tube growth. *Dev. Biol.* **174,** 160–173.

Piperno, G., LeDizet, M., and Chang, X. (1987). Microtubules containing acetylated α-tubulin in mammalian cells in culture. *J. Cell Biol.* **104,** 289–302.

Plyushch, T. A., Willemse, M. T. M., Franssen-Verheijen, M. A. W., and Reinders, M. C. (1995). Structural aspects of pollen tube growth and micropylar penetration in vitro in *Gasteria verrucosa* (Mill) H. Duval and *Lilium longiflorum* Thumb. *Protoplasma* **187,** 13–21.

Pollard, H. B., Birns, A .L., and Rojas, E. (1990). Synexin, a new member of the annexin gene family, is a calcium channel and membrane fusion protein. *Prog. Lin. Biol. Res.* **349,** 159–172.

Pollard, T. D., and Cooper, J. A. (1986). Actin and actin binding proteins. A critical evaluation of mechanisms and functions. *Annu. Rev. Biochem.* **55,** 987–1035.

Pollard, T. D., Doberstein, S. K., and Zot, H. G. (1991). Myosin-I. *Annu. Rev. Plant Physiol. Plant Mol. Biol.* **53,** 653–681.

Preissner, K. T. (1991). Structure and biological role of vitronectin. *Annu. Rev. Cell Biol.* **7,** 275–310.

Preston, R. D. (1988). Cellulose-microfibril-orientating mechanisms in plant cell wall. *Planta* **174,** 67–74.

Quader, H., and Schnepf, E. (1986). Endoplasmic reticulum and cytoplasmic streaming: Fluorescence microscopical observations in adaxial epidermis cells of onion bulb scales. *Protoplasma* **131,** 250–252.

Quader, H., Hofman, A., and Schnepf, E. (1989). Reorganization of the endoplasmic reticulum in epidermal cells of onion bulb scales after cold stress: Involvement of cytoskeletal elements. *Planta* **177,** 273–280.

Quatrano, R. S., Brian, L., Aldridge, J., and Schultz, T. (1991). Polar axis fixation in *Fucus* zygotes: Component of the cytoskeleton and extracellular matrix. *Development Suppl.* **1,** 11–16.

Rae, A. L., Harris, A., Bacic, A., and Clarke, A. E. (1985). Composition of the cell wall of *Nicotiana alata* Link et Otto pollen tubes. *Planta* **166,** 128–133.

Raudaskoski, M., Åström, H., Perttila, K., Virtanen, I., and Louhelainen, J. (1987). Role of MT cytoskeleton in pollen tubes: An immunocytochemical and ultrastructural approach. *Biol. Cell* **61,** 177–188.

Read, S. M., Li, H,., Turner, A. P., Ferguson, C., and Bacic, A. (1995). Callose synthesis during the growht of pollen tubes. *In* "Abstract of 7th Cell Wall Meeting" (I. Zarra and G. Revilla, eds.), p. 190. Santiago de Compostela, Spain.

Read, S. M., Li, H., Doblin, M., Turner, A., Ferguson, C., and Bacic, A. (1996). Deposition of callose: The main metabolic preoccupation of the male gametophyte. *In* "Abstract of 14th International Congress of Sexual Plant Reproduction," p. 41. Lorne, Australia.

Reddy, A. S. N., Narasimhulu, S. B., Safadi, F., and Golovkin, M. (1996a). A plant kinesin hevy chain-like protein is a calmodulin-binding protein. *Plant J.* **10,** 9–21.

Reddy, A. S. N., Safadi, F., Narasimhulu, S. B., Golovkin, M., and Hu, X. (1996b). A novel plant calmodulin-binding protein with a kinesin heavy chain motor domain. *J. Biol. Chem.* **271,** 7052–7060.

Reiss, H.-D., and Herth, W. (1985). Nifedipine-sensitive calcium channels are involved in polar growth of lily pollen tubes. *J. Cell Sci.* **76,** 247–254.

Robinson, D. G. (1980). Dictyosome–endoplasmic reticulum associations in higher plant cells? A serial section analysis. *Eur. J. Cell Biol.* **23,** 22–36.

Rosen, W. G., Gawlick, S. R., Dashek, W. V., and Siegesmund, K. A. (1964). Fine structure and cytochemistry of *Lilium* pollen tubes. *Am. J. Bot.* **51,** 61–74.

Rubinstein, A. L., Broadwater, A. H., Lowrey, K. B., and Bedinger, P. A. (1995a). Pex1, a pollen-specific gene with an extensin-like domain. *Proc. Natl. Acad. Sci. USA* **92,** 3086–3090.

Rubinstein, A. L., Màrquez, J., Suèrez-Cervera, M., and Bedinger, P.A. (1995b). Extensin-like glycoproteins in the maize pollen tube wall. *Plant Cell* **7,** 2211–2225.

Rutten, A. L. M. (1993). Ph.D. thesis, Chap. 6. University of Nijmegen, The Netherlands.

Sablin, E. P., Kull, F. J., Cooke, R., Vale, R. D., and Fletterick, R. J. (1996). Crystal structure of the motor domain of the kinesin-related motor ncd. *Nature* **380,** 555–558.

Sanders, L. C., and Lord, E. M. (1989). Directed movement of latex particles in the gynoecia of three species of flowering plants. *Science* **243,** 1606–1608.

Sanders, L. C., and Lord, E. M. (1992). A dynamic role for the stylar matrix in pollen tube extension. *Int. Rev. Cytol.* **140,** 297–318.

Sanders, L. C., Wang, C. S., Walling, L. L., and Lord, E. M. (1991). A homolog of the substrate adhesion molecule vitronectin occurs in four species of flowering plants. *Plant Cell* **3,** 629–635.

Sassen, M. M. A. (1964). Fine structure of *Petunia* pollen grain and pollen tube. *Acta Bot. Neerl.* **13,** 174–181

Scali, M., Cai, G., Del Casino, C., Santucci, A., Tirlapur, U. K., Moscatelli, A., Cresti, M., and Tiezzi, A. (1994). Purification and biochemical characterization of calmodulin from *Corylus avellana* pollen. *Plant Physiol. Biochem.* **32,** 831–838

Schellenbaum, P., Vantard, M., Peter, C.,Fellous, A., and Lambert, A.-M. (1993). Coassembly properties of higher plant microtubule-associated proteins with purified brain and plant tubulins. *Plant J.* **3,** 253–260.

Schindler, M., Meiners, S., and Cherech, D. A. (1989). RGD-dependent linkage between plant cell wall and plasma membrane: Consequences for growth. *J. Cell Biol.* **108,** 1955–1965.

Schlupmann, H., Bacic, A., and Read, S. M. (1993). A novel callose synthase from pollen tubes of *Nicotiana. Planta* **191,** 470–481.

Schroer, T. A., Steuer, E. R., and Sheetz, M. P. (1989). Cytoplasmic dynein is a minus end-directed motor for membranous organelles. *Cell* **56,** 937–946.

Seagull, R. W., Holland, S., and Gibson, D. M. (1990). Isolation of microtubule proteins from cotton (*Gossypium hirsutum*) suspension cells. *J. Cell Biol.* **111,** 294a.

Shimmen, T., and Yokota, E. (1994). Physiological and biochemical aspects of cytoplasmic streaming. *Int. Rev. Cytol.* **155,** 97–139.

Shivanna, K. R., and Rangaswami, N. S. (1992). "Pollen Biology: A Laboratory Manual." Springer-Verlag, Heidelberg.

Showalter, A. M. (1993). Structure and function of plant cell wall properties. *Plant Cell* **5,** 9–23.

Siflow, C. D., Oppenheimer, D. G., Kopczak, S. D., Ploense, S. E., Ludwig, S. R., and Snustad, D. P. (1987). Plant tubulin genes: Structure and differential expression during development. *Dev. Genet.* **8,** 435–460.

Sonesson, A., and Widell, S. (1993). Cytoskeleton components of inside-out and right-side-out plasma membrane vesicles from plants. *Protoplasma* **177,** 45–52.

Staehelin, L. A. (1988). Immunogold localization of the cell-wall-matrix polysaccharides rhamnogalacturonan I and xyloglucan during cell expansion and cytokinesis in *Trifolium pratense* L.: Implications for secretory pathways. *Planta* **174,** 433–445.

Staiger, C. J., Goodbody, K. C., Hussey, P. J., Valenta, R., Drobak, B. K., and Lloyd, C. W. (1993). The profilin multigene family of maize: Differential expression of three isoforms. *Plant J.* **4,** 631–641.

Staiger, C. J., Yuan, M., Valenta, R., Shaw, P. J., Warn, R. M., and Lloyd, C. W. (1994). Microinjected profilin affects cytoplasmic streaming in plant cells by rapidly depolymerizing actin microfilaments. *Curr. Biol.* **4,** 215–219.

Stanley, R. G., and Linskens H. F. (1974). "Pollen Biology, Biochemistry and Management." Springer-Verlag, New York.

Steer, M. W. (1990). Role of actin in tip growth. *In* "Tip Growth in Plant and Fungal Cells" (I. B. Heath, ed.), pp. 110–145. Academic Press, San Diego.

Steer, M. W., and Steer, J. M. (1989). Pollen tube tip growth. *New Phytol.* **111,** 323–358.

Tanchak, M. A., Rennie, P. J., and Fowke, L. C. (1988). Ultrastructure of the partially coated reticulum and dictyosomes during endocytosis by soybean protoplasts. *Planta* **175,** 433–441.

Tang, X., Hepler, P. K., and Scordilis, S. P. (1989b). Immunochemical and immunocytochemical identification of a myosin heavy chain polypeptide in *Nicotiana* pollen tube. *J. Cell Sci.* **92,** 569–574.

Tang, X. L., Lancelle, S. A., and Hepler, P. K. (1989a). Fluorescent microscopic localization of actin in pollen tubes: Comparison of actin antibody and phalloidin staining. *Cell Motil. Cytoskeleton* **12,** 216–224.

Tang, X. W., Liu, G. Q., Yang, Y., Zheng, W. L., Wu, B. C., and Nie, D. T. (1992). Quantitative measurement of pollen tube growth and particle movement. *Acta Bot. Sin.* **34,** 893–898.

Teasdale, R. D., and Richards, D. K. (1990). Boron deficiency in cultured pine cells. *Plant Physiol.* **93,** 1071–1077.

Tester, M. (1990). Plant ion channels: Whole cell and single channel studies. *New Phytol.* **114,** 305–340.

Theriot, J. A., and Mitchison, T. J. (1992). The nucleation-release model of actin filament dynamics in cell motility. *Trends Cell Biol.* **2,** 219–222.

Theriot, J. A., and Mitchison, T. J. (1993). The three faces of profilin. *Cell* **75,** 835–402.

Tiezzi, A., Cresti, M., and Ciampolini, F. (1986). Microtubules in *Nicotiana* pollen tubes: Ultrastructural, immunofluorescence and biochemical data. *In* "Biology of the Reproduction and Cell Motility in Plants and Animals" (M. Cresti and R. Dallai, eds.), pp. 87–94. Siena Univ. Press, Siena, Italy.

Tiezzi, A., Moscatelli, A., Milanesi, C., Ciampolini, F., and Cresti, M. (1987). Taxol-induced structures derived from cytoskeletal elements of the *Nicotiana pollen* tube. *J. Cell Sci.* **88,** 657–661.

Tiezzi, A., Moscatelli, A., and Cresti, M. (1988). Taxol-induced MTs from different sources: An ultrastructural comparison. *J. Submicrosc. Cytol. Morph.* **20,** 613–617.

Tiezzi, A., Moscatelli, A., Cai, G., Bartalesi, A., and Cresti, M. (1992). An immunoreactive homolog of mammalian kinesin in *Nicotiana tabacum* pollen tubes. *Cell Motil. Cytoskeleton* **21,** 132–137.

Tirlapur, U., Cai, G., Faleri, C., Moscatelli, A., Scali, M., Del Casino, C., Tiezzi, A., and Cresti, M. (1995). Confocal imaging and immunogold electron microscopy of changes in distribution of myosin during pollen hydration, germination and pollen tube growth in *Nicotiana tabacum* L. *Eur. J. Cell Biol.* **67,** 209–217.

Tirlapur, U. K., Scali, M., Moscatelli, A., Del Casino, C., Cai, G., Tiezzi, A., and Cresti, M. (1994). Confocal image analysis of spatial variation in immunocytochemically identified

calmodulin during pollen hydration, germination and pollen tube tip growth in *Nicotiana tabacum* L. *Zygote* **2,** 63–68.

Tirlapur, U. K., Faleri, C., and Cresti, M. (1996). Immunoelectron microscopy of myosin associated with the generative cells in pollen tubes of *Nicotiana tabacum* L. *Sex. Plant Reprod.* **9,** 233–237.

Titus, M. A. (1993). Myosins. *Curr. Opin. Cell Biol.* **5,** 7–81.

Tiwari, S. C., and Polito, V. S. (1990a). An analysis of the role of actin during pollen activation leading to germination in pear (*Pyrus communis* L.): Treatment with cytochalasin D. *Sex. Plant Reprod.* **3,** 121–129.

Tiwari, S. C., and Polito, V. S. (1990b). The initiation and organization of MTs in germinating pear (*Pyrus communis*) pollen. *Eur. J. Cell Biol.* **53,** 384–389.

Trave, G., Lacombe, P. J., Pfuhl, M., Saraste, M., and Pastore, A. (1995a). Molecular mechanism of the calcium-induced conformational change in the spectrin EF-hands. *EMBO J.* **14,** 4922–4931.

Trave, G., Pastore, A., Hyvonen, M., and Saraste, M. (1995b). The C-terminal domain of α-spectrin is structurally related to calmodulin. *Eur. J. Biochem.* **227,** 35–42.

Vahey, M., Titus, M., Tratweiu, R., and Scordilis, S. (1982). Tomato actin and myosin: Contractile proteins from higher land plant. *Cell Motil. 2,* 131–147.

Vale, R., and Goldstein, L. S. B. (1990). One motor, many tails: An expanding repertoire of force generating enzymes. *Cell* **60,** 883–885.

Vale, R. D., Reese, T. S., and Sheetz, M. P. (1985). Identification of a novel force-generating protein, kinesin, involved in microtubule-based motility. *Cell* **42,** 39–50.

Valenta, R., Duchene, M., Pettenburger, K., Sillaber, C., Valent, P., Bettelheim, P., Breitenbach, M., Kraft, D., and Scheiner, O. (1991). Identification of profilin as a novel pollen allergen: IgE autoreactivity in sensitized individuals. *Science* **253,** 557–560.

Valenta, R., Duchene, M., Ebner, C., Valent, P., Sillaber, C., Deviller, P., Ferreira, F., Tejkl, M., Edelmann, H., Kraft, D., and Scheiner, O. (1993). Identification of profilin as actin binding protein in higher plants. *J. Biol. Chem.* **268,** 22777–22781.

Valenta, R., Ball, T., Virtala, S., Duchene, M., and Scheiner, O. (1994). cDNA cloning and expression of timoty grass (*Phleum pratense*) pollen profilin in *Escherichia coli*: Comparison with birch pollen profilin. *Biochem. Biophys. Res. Commun.* **199,** 106–118.

Vallee, R. (1993). Molecular analysis of the microtubule motor dynein. *Proc. Natl. Acad. Sci. USA* **90,** 8769–8772.

Vallier, P., Dechamp, C., Valenta, R., Vial, O., and Deviller, P. (1992). Purification and characterization of an allergen from celery immunochemically related to an allergen present in several other plant species. Identification as a profilin. *Clin. Exp. Allergy* **22,** 774–782.

Van Aelst, A. C., and Van Went, J. L. (1992). Ultrastructural immunolocalization of pectins and glycoproteins in *Arabidopsis thaliana* pollen grains. *Protoplasma* **168,** 14–19.

Van Amstel, T. (1994). "Construction of Plant Cell Walls." Ph.D. thesis, Catholic University Nijmegen, The Netherlands.

Van Cutsem, P., and Messiaen, J. (1994). Biological effects of pectic fragments in plant cells. *Acta Bot. Neerl.* **43,** 231–245.

Vantard, M., Schellenbaum, P., Fellous, A., and Lambert, A.-M. (1991). Characterization of maize MT-associated proteins, one of which is immunologically related to tau. *Biochemistry* **30,** 9334–9340.

Vantard, M., Peter, C., Fellous, A., Schellenbaum, P., and Lambert, A.-M. (1994). Characterization of a 100 kDa heat-stable microtubule-associated protein from higher plants. *Eur. J. Biochem.* **220,** 847–853.

Vennigerholz, F., Walles, B., and Geitmann, A. (1992). Immunoctyochemical localization of pectin in stylar tissues. *Micron. Microsc. Acta* **23,** 125–126.

Vidali, L., Perez, H. E., Lopez, V. V., Noguez, R., Zamudio, F., and Sanchez, F. (1995). Purification, characterization, and cDNA cloning of profilin from *Phaseolus vulgaris. Plant Physiol.* **108,** 115–123.

Villanueva, M. A., Ho, S. C., and Wang, J. L. (1990). Isolation and characterization of one isoform actin from cultured soybean cells. *Arch. Biochem. Biophys.* **277,** 35–49.

Wacker, I., and Schnepf, E. (1990). Effects of nifedipine, verapamil, and diltiazen on tip growth in *Funaria hygrometrica. Planta* **180,** 492–501.

Wagner, V. T., and Matthysse, A. G. (1992). Involvement of a vitronectin-like protein in attachment of *Agrobacterium tumefaciens* to the surface of suspension culture cells. *J. Bacteriol.* **174,** 5999–6003.

Wang, C. S., Walling, L. L., Gu, Y. Q., Ware, C. F., and Lord, E. M. (1994). Two classes of proteins and mRNAs in *Lilium longiflorum* L. identified by human vitronectin probes. *Plant Physiol.* **104,** 711–717.

Wang, S. Z., and Adler, R. (1995). Chromokinesin: A DNA-binding, kinesin-like nuclear protein. *J. Cell Biol.* **128,** 761–768.

Wang, W., Takezawa, D., Narasimhulu, S. B., Reddy, A. S. N., and Poovaiah, B. W. (1996). A novel kinesin-like protein with a calmodulin-binding domain. *Plant Mol. Biol.* **31,** 87–100.

Webster, D. R., and Borisy, G. G. (1989). Microtubules are acetylated in domains that turn over slowly. *J. Cell Sci.* **92,** 57–65.

Wehland, J., Schroeder, M., and Weber, K. (1984). Organization of microtubules in stabilized meristematic plant cells revealed by a rat monoclonal antibody reacting only with the tyrosinated form of α-tubulin. *Cell Biol. Int. Rep.* **8,** 147–150.

Weisenseel, M. H., and Jaffe, L. F. (1976). The major growth current through lily pollen tubes enters as K^+ and leaves as H^+. *Planta* **133,** 1–7.

Williamson, R. E. (1993). Organelle movements. *Annu. Rev. Plant Physiol. Plant Mol. Biol.* **44,** 181–202.

Wittink, R.A., Schrauwen, J., and Wullems, G.J. (1996). The pollen specific NTP303 gene encodes a pollen tube specific protein. *In* "Abstract of 14th International Congress of Sexual Plant Reproduction," p. 98. Lorne, Australia.

Wordeman, L., and Mitchison, T. J. (1995). Identification and partial characterization of mitotic centromere-associated kinesin, a kinesin-related protein that associates with centromeres during mitosis. *J. Cell Biol.* **128,** 95–105.

Wu, H. M., Wang, H., and Cheung, A. (1995). A pollen tube growth stimulatory glycoprotein is deglycosylated by pollen tubes and displays a glycosylation gradient in the flower. *Cell* **82,** 395–403.

Wyatt, S. E., and Carpita, N. C. (1993). The plant cytoskeleton-cell-wall continuum. *Trends Cell Biol.* **3,** 413–417.

Wymer, C., and Lloyd, C. (1996). Dynamic microtubules: Implications for cell wall patterns. *Trends Plant Sci.* **1,** 222–228 .

Yang, Z., and Watson, J. C. (1993). Molecular cloning and characterization of Rho, a ras-related small GTP-binding protein from the garden pea. *Proc. Natl. Acad. Sci. USA* **90,** 8732–8736.

Yen, L.-F., Liu, X., and Cai, S. (1995). Purification of actin from maize pollen. *Plant Physiol.* **107,** 73–76.

Ylstra B. (1995). "Molecular Control of Fertilization in Plants," Ph.D. thesis, Vrije Universiteit Amsterdam, Amsterdam, The Netherlands.

Ylstra, B., Turaev, A., Benito Moreno, R. M., St'Ger, E., Van Tunen, A. J., Vicente, O., Mol, J. N. M., and Heberle-Bors, E. (1992). "Molecular Control of Fertilization in Plants," Chap. II. Ph.D. thesis, Vrijs Universiteitamsterdam, Amsterdam, The Netherlands.

Ylstra, B., Busscher, J., Franken, J., Hollman, P. C. H., Mol, J. N. M., and Van Tunen, A. J. (1994a). Flavonols and fertilization in *Petunia* hybrida: Localization and mode of action during pollen tube growth. *Plant J.* **6,** 201–212.

Ylstra, B., Bussher, J., Franken, J., Hollman, P. C. H., Mol, J. N. M., and Van Tunen, A. J. (1994b). "Molecular Control of Fertilization in Plants," Chap. IV. Ph.D. thesis, Vrijs Universiteit Amsterdam, Amsterdam, The Netherlands.

Ylstra, B., Turaev, A., Brinkmann, A. O., Heberle-Bors, E., and Van Tunen, A. J. (1995a). "Molecular Control of Fertilization in Plants," Chap. III. Ph.D. thesis, Vrijs Universiteit Amsterdam, Amsterdam, The Netherlands.

Ylstra, B., Garrido, D., Busscher, J., and Van Tunen, A. J. (1995b). "Molecular Control of Fertilization in Plants," Chap. VI. Ph.D. thesis, Vrijsuniversiteit Amsterdam, Amsterdam, The Netherlands.

Yokota, E., and Shimmen, T. (1994). Isolation and characterization of plant myosin from pollen tubes of lily. *Protoplasma* **177,** 153–162.

Yokota, E., McDonald, A. R., Liu, B., Shimmen, T., and Palevitz, B. A. (1995). Localization of a 170 kDa myosin heavy chain in plant cells. *Protoplasma* **185,** 178–187.

Zhang, G. F., and Staehelin, L. A. (1992). Functional compartmentation of the Golgi apparatus of plant cells. *Plant Physiol.* **99,** 1070–1083

Zhu, J. K., Shi, J., Singh, U., Wyatt, S. E., Bressan, R. A., Hasegawa, P. M., and Carpita, N. C. (1993). Enrichment of vitronectin- and fibronectin-like proteins in NaCl-adapted plant cells and evidences for their involvement in plasma membrane-cell wall adhesion. *Plant J.* **3,** 637–646.

Zhu, J. K., Damsz, B., Kononowicz, A. K., Bressan, R. A., and Hasegawa, P. M. (1994). A higher plant extracellular vitronectin-like adhesion protein is related to the translation elongation factor-1α. *Plant Cell* **6,** 393–404.

This Page Intentionally Left Blank

Biology of the Postsynaptic Glycine Receptor

Christian Vannier[1] and Antoine Triller
Laboratoire de Biologie Cellulaire de la Synapse, INSERM CJF 94-10, Ecole Normale Supérieure, 75005 Paris, France

Glycine is one of the major inhibitory neurotransmitters, and upon binding to its receptor it activates chloride conductances. Receptors are accumulated immediately opposite release sites, at the postsynaptic differentiations, where they form functional microdomains. This review describes recent advances in our understanding of the structure–function relationships of the glycine receptor, a member of the ligand-gated ion channel superfamily. Following purification of the receptor complex and identification of its integral and peripheral membrane protein components, molecular cloning has revealed the existence of several subtypes of the ligand-binding subunit. This heterogeneity is responsible for the distinct pharmacological and functional properties displayed by the various receptor configurations that are differentially expressed and assembled during development. This review also focuses on the molecular aspects of glycinergic synaptogenesis, highlighting gephyrin, the peripheral component of the receptor. The role of this cytoplasmic protein in anchoring and maintaining the channel complex in postsynaptic clusters is discussed. The glycine receptor recently moved into the spotlight as a paradigm in the approach to cell biology of the formation of the postsynaptic membrane.

KEY WORDS: Glycine receptor, Gephyrin, Synaptogenesis, Receptor clustering.

I. Introduction

Synaptic transmission involving small molecules such as amino acids is used by neurons for fast communication. It conveys both excitatory and inhibitory information regulating membrane potentials. In the vertebrate

[1] To whom correspondence should be addressed. Fax: 44 32 36 54.

Copyright © 1997 by Academic Press.
All rights of reproduction in any form reserved.

central nervous system, inhibition is mainly induced by glycine and γ-aminobutyric acid (GABA), but whereas GABAergic transmission is used in all areas of the CNS, glycine-mediated inhibition has a more limited distribution and predominates in the brain stem and spinal cord (Aprison and Daly, 1978).

The action of both neurotransmitters is mediated by distinct receptors which, as documented by numerous structural investigations, belong to the canonical superfamily of fast-acting, ligand-gated ion channels (ionotropic receptors) encompassing glycine, $GABA_A$, serotonin, nicotinic acetylcholine (ACh) receptors, and related glutamate receptors (Unwin, 1989; Betz, 1990; Nakanishi, 1992). ACh and serotonin open sodium channels intrinsic to their receptors and hence are excitatory, while glycine and GABA are generally responsible for the increase in chloride conductance which counteracts membrane depolarization associated with the opening of sodium channels. In contrast to other neurotransmitters, it has not yet been shown that glycine could activate any member of the slower-acting, G-protein-coupled, seven-transmembrane domain (metabotropic) receptor family.

One of the great achievements of molecular biology in recent years has been the revelation of the structural diversity of subunits that combine to build up heteromeric ionotropic receptors. This led to the concept, initially substantiated by numerous studies on ACh and $GABA_A$ receptors, that their electrophysiological and pharmacological diversity largely arises from multiple combinations of heterogeneous subunits, very often occurring in the same cell (Betz, 1990; Sargent, 1993; Burt and Kamatchi, 1991; Seeburg, 1993). Such diversity implies that (i) a neuron will display different responses to a given neurotransmitter, and (ii) the response would result from the presence of given subunits in front of defined presynaptic afferences. This situation is complicated by regulatory mechanisms, by the location of receptors with respect to presynaptic release sites, and by their position relative to each other.

A feature of neurons, essential for neuronal function, is the segregation of different types of receptors and ion channels in discrete microdomains over the cell surface. Such segregation and arrangement of pre- and postsynaptic structural elements determine the interactions between the various inputs and their effects on the firing pattern of the cell. This topographical complexity endows neurons with the ability, first, to select genes encoding given subunits, second, to assemble these subunits in various combinations, and third, to elaborate a complex mosaic surface on their somatic and neuritic compartments. The biological processes governing the molecular structuring and maintenance of the plasma membrane composition are therefore those of neuronal integration as defined by Sherrington (1906).

The puzzle as to how postsynaptic components can be assigned specific localizations and stabilized opposite a specific presynaptic neurotransmitter

release site has been highlighted by extensive study of the peripheral nicotinic ACh receptor. This has provided an explanation for synaptogenesis which combines differential gene expression and local specialization of the cytoskeleton (Cartaud and Changeux, 1993). However, if comparable basic mechanisms are expected to operate in some aspects of neuronal synaptogenesis, one may anticipitate that a more complex situation prevails in central neurons because of the large diversity and number of synapses impinging on them. Another level of complexity arises from the fact that distinct neurotransmitters can be released from the same synaptic bouton (Hökfelt, 1991). A good example can be found in the Mauthner cell of teleosts where afferent boutons containing glycine, GABA, or both amino acids have specific locations on the somatodendritic surface (Triller *et al.,* 1993a). This implies that the corresponding receptors are located in the postsynaptic area facing given amino-acid-containing boutons. Furthermore, there are examples of a differential distribution of the various isoforms of a given receptor in the postsynaptic membrane facing the afferent active zone. This is the case for the $GABA_A$ receptor, some of its subunit isotypes being either restricted to or excluded from postsynaptic differentiation, other subunits being evenly distributed on the dendritic plasma membrane (Baude *et al.,* 1992; Nusser *et al.,* 1995; Somogyi *et al.,* 1989). This situation holds for the ionotropic AMPA and NMDA classes of the glutamate receptors and gains in complexity when the metabotropic receptors are considered (Jones and Baughman, 1991; Baude *et al.,* 1993; Nusser *et al.,* 1994).

Thus, in order to understand glycinergic transmission in the CNS it is of critical importance to elucidate where and how glycine receptors are located in neuronal networks as well as at specific postsynaptic sites in neurons receiving glycinergic inputs. Recent advances in the study of structure–function relationships, and of the biology of the glycine receptor with respect to neuronal differentiation, cell–cell contact formation, and neurologic disorders, will be presented in this review. The aim is to document and discuss the view that this receptor constitutes a new paradigm of neuronal synaptogenesis. Dissection of this process in the case of glycinergic synapses may help address the fundamental questions as to how neuronal proteins are sorted, transported, docked, and maintained at the appropriate compartment and how microdomains are elaborated (Craig and Banker, 1994), which constitutes a major challenge in neuron cell biology.

II. Identification of the Glycine Receptor

The notion that glycine is a postsynaptic inhibitory transmitter arose from pioneer experiments carried out 30 years ago, which showed that the amino

acid and stimulated presynaptic cells evoked identical ionic responses in the neuron membrane: an increase in chloride conductance (Werman *et al.*, 1967, 1968; Aprison, 1990). Glycine is now established as a major neurotransmitter in the CNS with high levels present in the spinal cord (Aprison and Daly, 1978). It is involved in both mutual and feedback inhibition by recurrent axon collaterals of spinal motoneurons (Young and MacDonald, 1983), in brain stem nuclei (Aprison *et al.*, 1975), and in the retina (Pourcho *et al.*,1992). The glycine receptor (GlyR) was originally identified by ligand binding studies and shown to differ from the $GABA_A$ receptor in terms of both pharmacology and localization (Young and Snyder, 1973, 1974). Other amino acids are also agonists and selectively bind to GlyR to elicit a chloride current with the relative efficiency being glycine > β-alanine > taurine > L-alanine (Betz and Becker, 1988; Langosch *et al.*, 1990). The channel activity of the receptor, but not that of the $GABA_A$ receptor, is blocked by strychnine at low concentration ($< 1\ \mu M$). This well-known convulsant plant alkaloid is the most studied high-affinity antagonist of glycine function. Strychnine intoxication not only perturbs the motor system, causing muscular convulsions or generalized hypertonia, but also induces, at subconvulsive doses, alterations of sensory centers, leading in turn to increased startle responses (Young and Snyder, 1973, 1974; Becker, 1992). Equilibrium binding and cross-linking experiments using [^{3}H]strychnine performed on rat spinal cord membranes indicated that the specific interaction between strychnine and GlyR involves a site for competitive binding closely related to, but distinct from, the agonist binding site (Young and Snyder, 1974). This interaction is characterized by a dissociation constant in the nanomolar range ($K_D \approx 1$–$10nM$) (Marvizon *et al.*, 1986). This specific recognition was further exploited in topographical studies to localize abundant [^{3}H]strychnine high-affinity binding sites in rat CNS, thus referred to as glycine receptors. As shown by light microscopy autoradiography, the density of glycine receptors is highest in the gray matter of the lower brain stem and of the spinal cord. It decreases gradually along the neuraxis from the caudal to the rostral regions. Glycine receptors are abundant in areas of primary sensory and acoustic processing (spinal dorsal horn, dorsal column nuclei, dorsal cochlear nucleus) and particularly on motoneurons of the spinal and cranial motor nuclei. Such a distribution is in fair agreement with the clinical symptoms of strychnine poisoning. These pioneer studies thus validated the utilization of the antagonist molecule as a probe to identify and map the sites of glycinergic inhibition in the CNS (Young and Snyder, 1973; Zarbin *et al.*, 1981; Probst *et al.*, 1986; Bristow *et al.*, 1986). Glycine also acts as an allosteric activator of the excitatory NMDA receptor. However, this function involves distinct binding sites since this effect is insensitive to strychnine (Johnson and Ascher, 1987; Bristow *et al.*, 1986).

III. Molecular Biology of the Glycine Receptor

A. Purification of the Receptor and Associated Gephyrin: Specificity of Antibodies

GlyR was the first neurotransmitter receptor to be isolated from the brain. The high affinity of the strychnine–GlyR interaction provided a tool for purifying the native molecule. Purification from a rat spinal cord membrane fraction, after detergent extraction, was successfully achieved in a single step by affinity chromatography on a 2-aminostrychnine-derivatized agarose gel (Pfeiffer and Betz, 1981; Pfeiffer *et al.*, 1982). The homogeneous, native receptor therefore appeared to be a complex of three proteins of 48 (α), 58 (β), and 93 kDa, a composition which is shared by various vertebrate species (Pfeiffer *et al.*, 1982; Graham *et al.*, 1985; Becker *et al.*, 1986). The smallest α and β components are integral transmembrane glycoproteins. Biochemical studies of purified and membrane-anchored receptors, including controlled membrane disruption, intramolecular cross-linking experiments, and sedimentation analysis, have shown that these proteins represent the constitutive subunits of the receptor. They assemble to build up the channel-containing transmembrane core referred to herein as GlyR and form a 250-kDa pentameric complex of $\alpha_3\beta_2$ stoichiometry (Fig. 1A) which is able to reconstitute a functional anion channel in lipid bilayers (Schmitt *et al.*, 1987; Langosch *et al.*, 1988; Garcia-Calvo *et al.*, 1989). The first experiments of covalent affinity labeling using photoreactive [^{3}H]strychnine, controlled proteolysis, and peptide mapping analysis had clearly demonstrated that (i) only the α subunit, of either membrane-bound or purified receptor, could specifically incorporate strychnine and (ii) the antagonist binding site of the receptor was located in the extracellular N-terminal domain of the a subunit (Graham *et al.*, 1981, 1983, 1985). It was then proposed, in view of the available protein sequence of the a subunit, that a segment spanning residues 170 to 220 (in the vicinity of the first transmembrane region), contained the ligand binding site (Grenningloh *et al.*, 1987). Later, a mutagenesis-based approach led to a more precise localization (see below).

In contrast to α and β subunits, the 93-kDa copurifying protein gephyrin is a nonglycosylated polypeptide which reversibly interacts with the α/β pentamer. Being extracted from the synaptic membrane by high-pH treatment, gephyrin is a peripheral membrane protein. It was shown to bind tubulin dimers *in vitro* with a high affinity in the nanomolar range, in a $\approx$1:4 stoichiometry. It was able to link the GlyR to brain microtubules in a copolymerization assay (Schmitt *et al.*, 1987; Kirsch *et al.*, 1991). These initial biochemical studies thus favored the idea of selective association

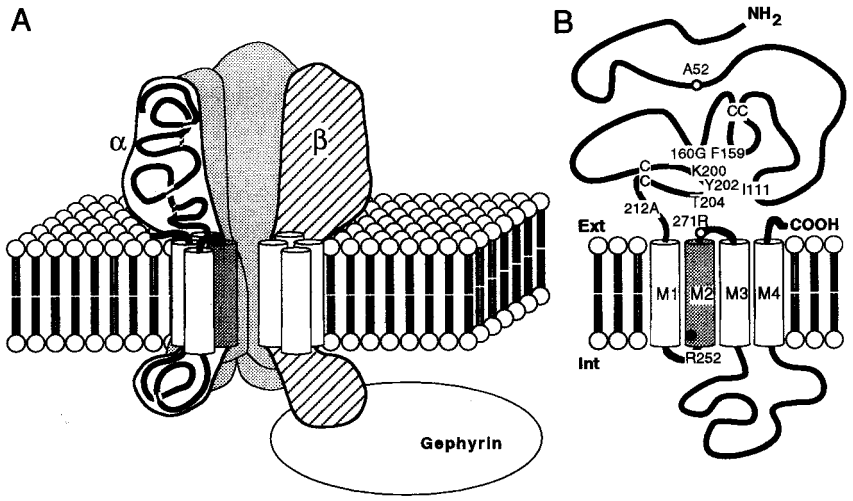

FIG. 1 Structure of the glycine receptor. (A) Arrangement of α and β subunits and of gephyrin. A section is drawn and one subunit is omitted to show the four packed transmembrane regions (cylindres). The pore-forming domain M2 of the α subunit is in gray. (B) Membrane topology of the α subunit indicating the position of disulfide bridges and of functionnally important amino acid residues. See text for details. The dot in M2 indicates the position of glycine254 (modified from Kuhse *et al.*, 1995).

of gephyrin with cytoplasmic domains of the strychnine-sensitive glycine receptor in various areas of the brain (Becker *et al.*, 1989). This conclusion was also based on clear immunohistochemical evidence that the protein was localized on the cytoplasmic face of α-subunit-containing individual synapses (Triller *et al.*, 1985, 1987; Altschuler *et al.*, 1986).

Studies of the glycine receptor have been facilitated by several monoclonal antibodies (mAbs) raised against affinity-purified rat spinal cord glycine receptor (Pfeiffer *et al.*, 1984). They were selected for their ability to bind to the iodinated receptor in an immunoprecipitation assay. Western blot analysis revealed that some of them could be used to probe antigenic sites specific to either the α subunit (GlyR1a, GlyR2b mAbs) or gephyrin (GlyR5a, 7a, 9b mAbs), or to identify both α and β subunits due to a conserved or close antigenic site on each protein (GlyR4a mAb). A combination of bacterially expressed fusion proteins and of synthetic peptides was used to map the various epitopes on the α subunit (Schröder *et al.*, 1991). The 10 N-terminal residues of the mature α subunit (e.g., α1, see below) form the antigenic site recognized by mAb 2b, whereas mAb4a binds to a domain encompassing residues 96 to 105. The mAb 2b antibody is specific to the α1 subunit because its target sequence is highly variable

among the various GlyR subunits (see references herein). In contrast, the epitope bound by mAb 4a is strictly conserved in all α sequences and differs by a single amino acid residue between α and β subunits. Some of these antibodies have been of considerable value in biochemical, cell biology, and immunohistochemical investigations of the receptor.

B. The Glycine Receptor as a Member of the Ligand-Gated Ionotropic Receptor Family

The primary structures of the α and β subunits have been deduced from cDNAs isolated from rat spinal cord libraries screened on the basis of partial amino acid sequence data (Grenningloh *et al.*, 1987, 1990a). Analysis of the sequences revealed that α and β subunits are highly homologous polypeptides. Their overall amino acid sequence identity is close to 50% and their domain organization exhibits remarkable similarity (Betz, 1990). Aside from a cleavable signal peptide which differs between individual subunits, hydropathy analysis predicts a highly conserved region of four hydrophobic segments (M1 to M4) able to cross the membrane bilayer (Fig. 1B). They occupy positions almost identical to that of the transmembrane segment of the ACh and $GABA_A$ receptor subunits. The transmembrane domains M1 to M3, compared to M4, are highly conserved among the various subunits of the glycine and $GABA_A$ receptors (Betz, 1990). In addition, they possess an extended N-terminal domain bearing potential glycosylation sites, consistent with their glycoprotein nature. This domain, as confirmed by immunocytochemistry (Triller *et al.*, 1985), protrudes into the synaptic cleft. It contains a pair of cysteine residues that are known to be conserved in the aforementioned $GABA_A$ and ACh receptor subunits and are thought to stabilize the subunit tertiary structure. A second pair of cysteine residues (shared with human α subunits) that does not exist in $GABA_A$ receptor subunits is located close to the M1 domain (Grenningloh *et al.*, 1990b). A region of significantly lower homology is represented by a large hydrophilic loop between the M3 and M4 segments. The presence of several consensus sites for protein phosphorylation on this loop is consistent with its assumed cytoplasmic orientation.

These features of α and β subunits are shared with the various subunits of the ligand-gated channels of the ACh receptor family. It can be assumed that the glycine receptor thus exhibits the largely documented overall molecular design and transmembrane topology (Fig. 1), based on four membrane-spanning domains able to form α-helices (M2) or β-sheet strands (M1, M3, M4), and therefore may function as an allosteric protein (Betz, 1990; Unwin, 1993). It is conceivable that all the receptor subunits belonging to this family arose from a common ancestor gene as a result of combined

duplications and divergences. From an evolutionary point of view, an interesting fact suggested by a recent analysis of phylogenetic distribution is that GlyRs were derived from $GABA_ARs$ when compartimentalization provided the very common glycine molecule with an informational meaning (Ortells and Lunt, 1995). Such a concept is quite at variance with what is often accepted: glycine neurotransmission precedes that using GABA since the former predominates in phylogenetically older parts of the brain.

C. Diversity of Subunit Isoforms

The initial discovery of glycine receptor subtypes followed a biochemical and immunochemical study of the development of the rat spinal cord (Becker *et al.,* 1988). In these experiments, comparison of the immunoreactivities toward mAb4a and mAb2b antibodies of membrane extracts from neonatal and adult spinal cord led to the notion that an isoform of GlyR predominates around birth. This neonatal receptor ($GlyR_N$) displays a relatively low strychnine binding affinity and only contains a 49-kDa subunit, which differs in antigenicity from the adult 48-kDa polypeptide. As shown by selective immunoprecipitation or even chromatography on a 2-aminostrychnine gel, gephyrin is significantly associated with $GlyR_N$. The expression of this early subtype in the spinal cord receptor is transient. It is gradually and completely replaced within 2 weeks after birth by that of the adult form, $GlyR_A$, containing the 48kDa subunit (Fig. 2A). Coincident with this postnatal disappearance, the marked increase in antagonist binding sites in the spinal cord not only accompanies that of adult-type characteristic epitopes for a subunit and gephyrin, but also a switch from short to long messenger RNA (Akagi and Miledi, 1988; Akagi *et al.,* 1989).

Diversity of the glycine receptor has been further established by the cloning, from rat libraries screened under low-stringency conditions, of variants of the original α subunit cDNA. In contrast, no diversity was found for the β subunit. The four ligand-binding subunits, $\alpha 1$ to $\alpha 4$ ($\alpha 1$ being the originally cloned subunit), now characterized in rat, mouse, and human, reflect a structural complexity which had not been inferred from previous biochemical studies and which is greater than that anticipated from pharmacological analysis. Screening of human fetal and rat brain cDNA libraries with a rat $\alpha 1$ probe led to the identification of the $\alpha 2$, $\alpha 3$, and $\alpha 2^*$ subunits, respectively. More recently, exons of a murine $\alpha 4$ subunit have been identified by screening genomic libraries (Grenningloh *et al.,* 1990b; Kuhse *et al.,* 1990a,b; Matzenbach *et al.,* 1994). The α subunits display a very low degree of interspecies variation since their identity is close to 99%. Moreover, the α subunit variants remain highly homologous with amino acid sequence identities on the order of 80%.

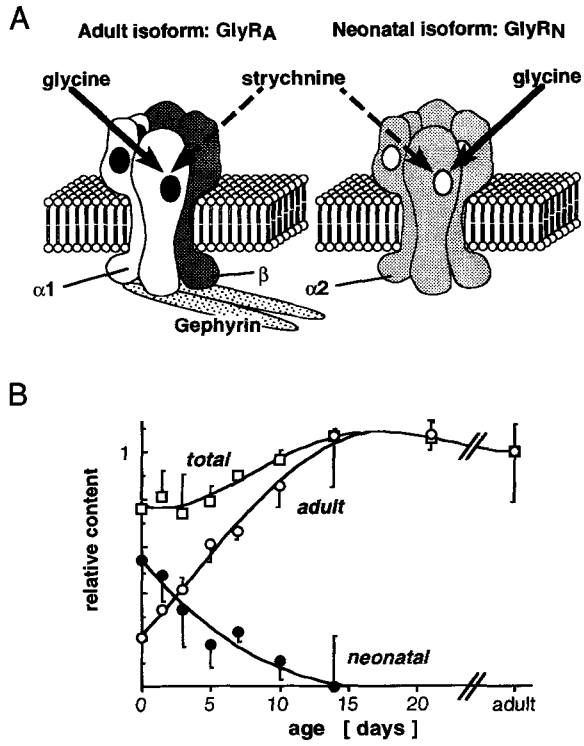

FIG. 2 Postnatal expression of GlyR isoforms in rodent spinal cord. (A) Structure of the adult ($GlyR_A$) and neonatal ($GlyR_N$) receptors. Glycine binding to its site on the $\alpha 1$ subunit is strongly antagonized by strychnine. The antagonist binds to $\alpha 2$ with a lower affinity (dashed arrow). Gephyrin is associated with the β subunit, and therefore with $GlyR_A$ and not with $GlyR_N$. (B) Developmental change in content of isoforms and total receptor protein as measured by immunoassay (modified from Becker, 1995, with permission).

As shown by heterologous expression in *Xenopus laevis* oocytes, the various isoforms can form glycine-gated chloride channels of comparable strychnine sensitivity (albeit lower in $\alpha 3$- than in $\alpha 1$- or $\alpha 2$-containing receptors). Such observations seem to preclude assignment of the aforementioned $GlyR_N$ receptor to any of these subunits. In this respect, the pharmacological properties of the chloride channel-forming $\alpha 2^*$ subunit, which is more than 99% identical to human $\alpha 2$ but exhibits a $\approx$500-fold lower strychnine sensitivity, have attracted much attention (Kuhse *et al.*, 1990a). Site-directed mutagenesis of $\alpha 2^*$ cDNA at position 167 allowed the single exchange of a glutamic acid (rat $\alpha 2^*$) for a glycine (human $\alpha 2$) residue. Such an exchange in the extracellular ligand-binding domain demonstrated

that the altered pharmacology could be attributed to this structural change alone. This illustrates the functional impact of minute sequence alterations between homologous subunits and was thought to account for the particular strychnine resistance of the rodent neonates.

Another important mechanism for the generation of diversity resides in alternative exon usage. For the $\alpha 1$ subunit, alternative splice acceptor site selection generates a variant mRNA that encodes the $\alpha 1^{ins}$ subunit containing eight additional amino acids (Malosio *et al.,* 1991a). This sequence, which includes a serine residue, is inserted in the large cytoplasmic domain and represents a potential phosphorylation site which may allow further functional modulation of the $\alpha 1$ subunit. In the case of the $\alpha 2$ subunit, screening of rat cDNA libraries with an $\alpha 2$* probe revealed two variants, $\alpha 2A$ and $\alpha 2B$, resulting from alternative splicing of the third exon (Kuhse *et al.,* 1991). These subunits differ only by two conservative substitutions in the N-terminal extracellular domain (positions 58 and 59), and both possess a glycine residue at position 167. A strychnine-sensitive chloride channel is also elicited in the oocyte system upon injection of *in vitro* transcribed $\alpha 2A$ mRNA. This is expected from the presence of Gly^{167} in the human subunit (see above).

D. Relationships between Isoforms and Physiology

Analysis of structure–function relationships in recombinant GlyR synthesized in heterologous expression systems such as *X. laevis* oocyte or mammalian cells reveals the peculiar ability of recombinant α subunits to assemble into chloride channels. These reproduce most (but not all) of the electrophysiological and pharmacological properties of native receptors. Interestingly enough, glycine-evoked currents recorded after injection of $\alpha 1$, $\alpha 2$., or $\alpha 3$ *in vitro* transcripts into oocytes resemble those elicited by injected spinal cord or brain poly(A)$^+$ mRNAs (Akagi and Miledi, 1988; Schmieden *et al.,* 1989, Grenningloh *et al.,* 1990b; Kuhse *et al.,* 1990b). Moreover, transient expression of $\alpha 1$ subunits obtained by transfection of cultured mammalian cells also results in channels with properties similar to those observed in cultured spinal neurons (Bormann *et al.,* 1987; Sontheimer *et al.,* 1989; Grenningloh *et al.,* 1990b). These studies have shown that while receptors constructed with the $\alpha 1$ subunit respond to the glycine-like amino acid agonists (glycine $>$ β-alanine $>$ taurine being most effective), $\alpha 2$ receptors are selective for glycine. All α-subunit-based channels are strongly antagonized by strychnine, further demonstrating, in agreement with biochemical data, that the binding sites for both agonists and antagonists reside on the α polypeptides (Betz, 1992; Vandenberg *et al.,* 1992b). Recording of single-channel currents from recombinant homo-oligomeric receptors

allowed monitoring of channel conductances and kinetics. These studies showed that the higher main-state conductances of $\alpha 2$ and $\alpha 3$, compared to those of $\alpha 1$ homo-oligomers, are due to the presence of an alanine residue instead of a glycine (position 254 in the $\alpha 1$ polypeptide) in transmembrane domain M2. Moreover, the $\alpha 1$ subunit is responsible for short channel lifetimes compared to those with $\alpha 2$. Consistent with a $GlyR_N$ to $GlyR_A$ developmental switch, recordings of spinal cord neurons during ontogeny show that the mean open time of the glycine-elicited receptor channel decreases with time after birth (Takahashi *et al.*, 1992; Bormann *et al.*, 1993). This finding indicates that, like the nicotinic receptor, GlyR undergoes a functional maturation via switching from the $\alpha 1$ to the $\alpha 2$ subunit (Fig. 2B). All together, these heterologous expression studies have shown that agonist-gated, strychnine-sensitive glycine receptors can form upon self-assembly into homo-oligomeric complexes of α subunits, a property that is shared with few other members of the ionotropic receptor superfamily (i.e., the NMDA receptor subunit 1). This also suggests that such homo-oligomeric receptors could have functional significance *in vivo* (see references in Bormann *et al.*, 1993).

These properties of the α subunit oligomers contrast with the very weak glycine-activated chloride currents generated in *X. laevis* oocytes when expressing the β protein alone. In this case, responses display no cooperativity for agonist activation (Hill coefficient $n = 1$, compared to $n \approx 3$ for α subunit receptors), and, since agonist gating could not be shown to be significantly altered in cells expressing both α and β subunits compared to the α subunit, the β protein was initially thought to have only a structural role in native Gly receptors (Grenningloh *et al.*, 1990a). However, cotransfection experiments of mammalian cells have shown that the functional homology of recombinant and native receptor channels depends on the presence of the β subunit. A first key observation lies in the differential resistance of expressed glycine receptors toward picrotoxinin, an inhibitor of the $GABA_A$ receptor chloride channel. Whereas receptors built up with both $\alpha 1$ and β subunits are unaffected, $\alpha 1$ homo-oligomers are blocked by picrotoxinin. Consistent with the striking divergence of the M2 domain of α and $GABA_A$ receptor subunits from that of β, site-directed mutagenesis established that this domain in β does contain residues determining inhibitor binding (Pribilla *et al.*, 1992). The presence of the β subunit also affects channel chloride conductances (Bormann *et al.*, 1993): coexpression of α and β subunits diminishes single-channel chloride conductance (compared to $\alpha 1$-3 homomeric receptors) to levels comparable to those recorded from adult neurons. Furthermore, analysis of the consequences of sequence variations imposed in the β subunit–M2 domain by site-directed mutagenesis revealed that negatively charged residues within its carboxy-terminal half were responsible for the different single-channel conductances of recombi-

nant α homo-oligomeric and $\alpha 1/\beta$ hetero-oligomeric receptors. Therefore, the non-ligand-binding β subunit has a crucial role in modulating channel functional properties in heteromeric receptors.

Although the β subunit is involved in regulating properties of recombinant GlyR channels, the heterogeneity of these receptors primarily results from that of the α subunit. This is well illustrated by the $GlyR_N$ to $GlyR_A$ developmental switch of the spinal cord receptors biochemically and functionally characterized both *in vivo* and *in vitro* (Becker *et al.*, 1988; Hoch *et al.*, 1989; Takahashi *et al.*, 1992): the $\alpha 2$ homo-oligomer ($GlyR_N$), giving rise to slow inhibitory postsynaptic currents (IPSC), is progressively replaced after birth by an $\alpha 1/\beta$ hetero-oligomer displaying lower conductances and faster IPSC. Whether such maturation always occurs by combination of α and β subunits is still unknown (Pribilla *et al.*, 1992; Bormann *et al.*, 1993).

E. Molecular Determinants of Ligand Binding and Channel Properties

A comparison of the efficacy profiles and pharmacology of wild-type and site-directed-mutagenized or hereditary-mutated (from human and mouse) $\alpha 1$ and $\alpha 2$ subunits favors a multisite model of the GlyR ligand-binding domain (Fig. 1B; Betz, 1992; Kuhse *et al.*, 1995). As summarized below, distinct structural motifs within the extracytoplasmic N-terminal domain are engaged in ligand binding and discrimination. Two conserved cysteine residues at positions 138 and 152, forming a disulfide loop, are required for subunit tertiary structure. They are found in all $GABA_A$ and nicotinic ACh receptor subunit primary structures known. The site of strychnine binding, as deduced from photoaffinity labeling with [^{3}H]strychnine of the $\alpha 1$ subunit and peptide mapping, has been localized to the N-terminal domain. The reduction of strychnine inhibition after substitution of glycine 160 (homologous to glycine 167 in the $\alpha 2$ subunit) and tyrosine 161, as well as lysine 200 and tyrosine 202, demonstrated that two domains form the antagonist-binding site (Ruiz-Gomez *et al.*, 1990; Vandenberg *et al.*, 1992a). In addition, binding of agonists (including high- and low-affinity agonists) involves several subsites overlapping with the antagonist-binding sites. Alanine 52 determines agonist affinity and a substitution of this residue by a serine reduces glycine affinity, but has no effect on strychnine binding (Ryan *et al.*, 1994; Saul *et al.*, 1994). The response of $\alpha 1$ receptors to β-alanine and taurine depends on the isoleucine and alanine residues at positions 111 and 212, respectively. Phenylalanine, glycine, and tyrosine residues found at positions 159, 160, and 161, respectively, in the $\alpha 1$ subunit represent important determinants for both agonist and high-affinity antago-

nist binding (Schmieden *et al.*, 1992). A glycine residue is conserved in position 160 of most α subunit variants. As mentioned earlier, the $\alpha 2^*$ variant substitution of this glycine results in a very low affinity for strychnine but also for glycine (Kuhse *et al.*, 1990a). Phenylalanine 159 is responsible for selective activation by small amino acids. It has a key role in determining agonist recognition by GlyR, because if it is replaced by tyrosine, a residue common to $GABA_A$ receptor polypeptides, the agonist selectivity is greatly diminished and an $\alpha 1$ channel is generated which responds to GABA, indicating close architectures of ligand-binding sites in GlyR and $GABA_AR$ (Schmieden *et al.*, 1993). Finally, a loop (also considered to be a β-sheet–β-turn motif belonging to a domain encompassing residues 200–212) formed by a disulfide bridge between cysteines 198 and 209 was shown to confer agonist–antagonist discrimination on the $\alpha 1$ subunit because substitution of threonine 204 totally abolishes glycine affinity but leaves strychnine binding unchanged. Mutation of tyrosine 202, however, demonstrates that the aromatic group is crucial for both agonist and antagonist binding (Schmieden *et al.*, 1992; Vandenberg *et al.*, 1992b; Rajendra *et al.*, 1995b). Interestingly, the fact that the positions occupied by all these residues in the GlyR α subunit are homologous to the positions of essential residues in nicotinic ACh and $GABA_A$ receptors suggests that the overall folding pattern of the extracellular region is general and that the ligand-binding pockets in ionotropic receptors have a common architecture referred to as the three-loop model in the ionotropic receptor family (Kuhse *et al.*, 1995; Galzi and Changeux, 1994; Devillers-Thiéry *et al.*, 1993).

A common structural determinant of channel function in the members of the ACh receptor family is found in the M2 transmembrane segment. Like its homologous domains in this family it provides the pore with an environment sufficiently polar to allow ion flow. The M2 region is highly conserved between the $GABA_A$ receptor and the GlyR α subunits and is involved in ion selectivity. It crosses the membrane bilayer as an 18-residue α-helix with uncharged polar amino acids lining the ion channel of the receptor (Betz, 1990; Unwin, 1993). The ion selectivity of the channel is thought to be based on the steric arrangement of transmembrane segment M2. Here, the turn-inducing, proline residues are conserved at either end of M2 in all GlyR and $GABA_AR$ ligand-binding subunits. Evidence that the channel activity in these receptors is linked to the structural constraints thus imposed is inferred from the observation that, in the $\alpha 7$ subunit of nicotinic AChR, if a proline is inserted N-terminal to M2, the cationic selectivity is changed to an anionic one (Grenningloh *et al.*, 1987; Galzi *et al.*, 1992). This M2 segment plays a pivotal role not only as the pore-forming domain but also as a determinant of ligand binding. Two arginine residues at positions 252 and 271 flanking the M2 sequence at its intra- and extracytoplasmic extremities, respectively, have key roles in normal receptor expres-

sion. One of these, arginine 271, is an important residue for receptor activation as its substitutions occurring in the human hereditary hyperexplexia (Shiang *et al.,* 1993), which have no effect on strychnine binding affinity, dramatically reduce the ability of agonists to open the GlyR channel, which also exhibits lower chloride conductance, as shown by recombinant cDNA expression (Langosch *et al.,* 1994; Rajendra *et al.,* 1994). These mutations also result in a very interesting change: the normally glycinergic agonist β amino acids are no longer able to elicit chloride currents and instead acquire antagonistic activities, revealing that they bind competitively to an inhibitory subsite. Therefore, arginine 271 is a critical transducing element which couples channel activation to agonist binding (Rajendra *et al.,* 1995a; Laube *et al.,* 1995). The M2 segment was recently shown to be responsible for the selective, noncompetitive blockade of homomeric α1 open channels by cyanotriphenylborate, a chloride analog which has no effect on recombinant α2 homo-oligomers. This variant-specific block is due to the presence at position 254 inside the α1 pore of a glycine in place of an alanine (Rundström *et al.,* 1994).

Protein phosphorylation also plays an important role in transient receptor modulation. Most of the ligand-gated receptor channels can be phosphorylated since they possess consensus sites for protein phosphorylation within the cytoplasmic loop between the M3 and the M4 domains. Three different protein kinases, cyclic AMP (cAMP)-dependent protein kinase A (PKA), protein kinase C (PKC), and an endogenous tyrosine kinase, phosphorylate the nicotinic AChR. Such covalent modification can either regulate the rate of desensitization of receptors or determine their response to agonists as demonstrated for the ACh and GABA (or glutamate) receptors, respectively (Wagner *et al.,* 1991; Moss *et al.,* 1992; Raymond *et al.,* 1993; Wang *et al.,* 1993). Consistent with the presence on GlyR α subunits of cytoplasmically oriented consensus sequences for phosphorylation by PKC, isolated spinal cord neurons can phosphorylate the α subunit upon exposure to the phorbol ester TPA, which activates the endogenous kinase (Vaello *et al.,* 1994). This is in good agreement with the ability of the kinase to phosphorylate *in vitro* the purified receptor on a single serine at position 391 on the α1 subunit (Ruiz-Gomez *et al.,* 1991). The α subunit is also phosphorylated when adult spinal cord neurons are incubated with forskolin, indicating that activation of adenylyl cyclase can lead to a cyclic AMP-dependent action of PKA on GlyR. Indeed, a phosphorylation is also observed *in vitro* with the purified PKA catalytic subunit. The phosphorylation state of GlyR subunits has functional consequences. More precisely, *Xenopus* oocytes injected with either adult rat brain poly(A)$^+$ mRNAs or α1 subunit transcripts display a time-dependent decrease in glycine-elicited currents upon exposure to the phorbol esters TPA or βPMA which activates the endogenous PKC (Vaello *et al.,* 1994; Uchiyama *et al.,* 1994). In contrast,

PKA, which increases glycine responses in cultured brain stem neurons, also enhances glycine-elicited currents in *Xenopus* oocytes expressing adult rat brain poly(A)$^+$ mRNAs as suggested by the stimulating effect of dibutyryl cAMP (Song and Huang, 1990; Vaello *et al.,* 1994). Further studies will have to determine which subunits are substrates for the various kinases, depending on localization and developmental stage. For instance, α1 subunit phosphorylation by PKA is surprising, unless α1 is present in receptors in its alternatively spliced form, $\alpha 1^{ins}$, which is the only one to bear a PKA phosphorylation consensus site. Moreover, it will be interesting to determine which effects are direct or indirect in homologous systems, since a PKC-dependent up-regulation of glycine receptor channels was reported in rat hippocampal neurons, with no involvement of PKA and tyrosine kinase, contrasting with the observed effect in injected *Xenopus* oocytes (Schonrock and Bormann,1995).

These data indicate that various trimeric G protein-coupled receptors inducing changes in the levels of cyclic AMP or diacylglycerol are most likely able to modulate the glycine sensitivity of neurons in response to neural or hormonal stimulation.

IV. Spatial and Temporal Mapping of Glycine Receptor Complex Expression

A. *In Situ* Hybridization Studies

In situ hybridization investigations (Fig. 3) revealed that, as observed for other ionotropic receptors, each of the various subunit genes has a specific transcription profile in mammalian brain (Malosio *et al.,* 1991b; Sato *et al.,* 1991, 1992; Fujita *et al.,* 1991).

In adults, α1 transcripts (Figs. 3A, and 3E) are present throughout the spinal cord segments and in nuclei of the brain stem belonging to the general motor and somatosensory systems as well as to the auditory, vestibular, and reticular formations (Malosio *et al.,* 1991b). With the exception of $\alpha 1^{ins}$, which represents 25–30% of the total α subunit mRNA, they are also found to a lesser extent in midbrain sites such as the cerebellar deep nuclei, and in the hypothalamus and the colliculi. Both variants represent postnatal isoforms of GlyR as transcription of both α1 and $\alpha 1^{ins}$ subunits, which is barely detectable in embryos, increases gradually during the first 2 weeks after birth and until adulthood, respectively (Malosio *et al.,* 1991a,b). A close developmental increase in α3 transcription, albeit moderate, seems to be restricted to the infralimbic system and in the adult to the hippocampal complex and cerebellar granular layer (Fig. 3C). Only very weak expression

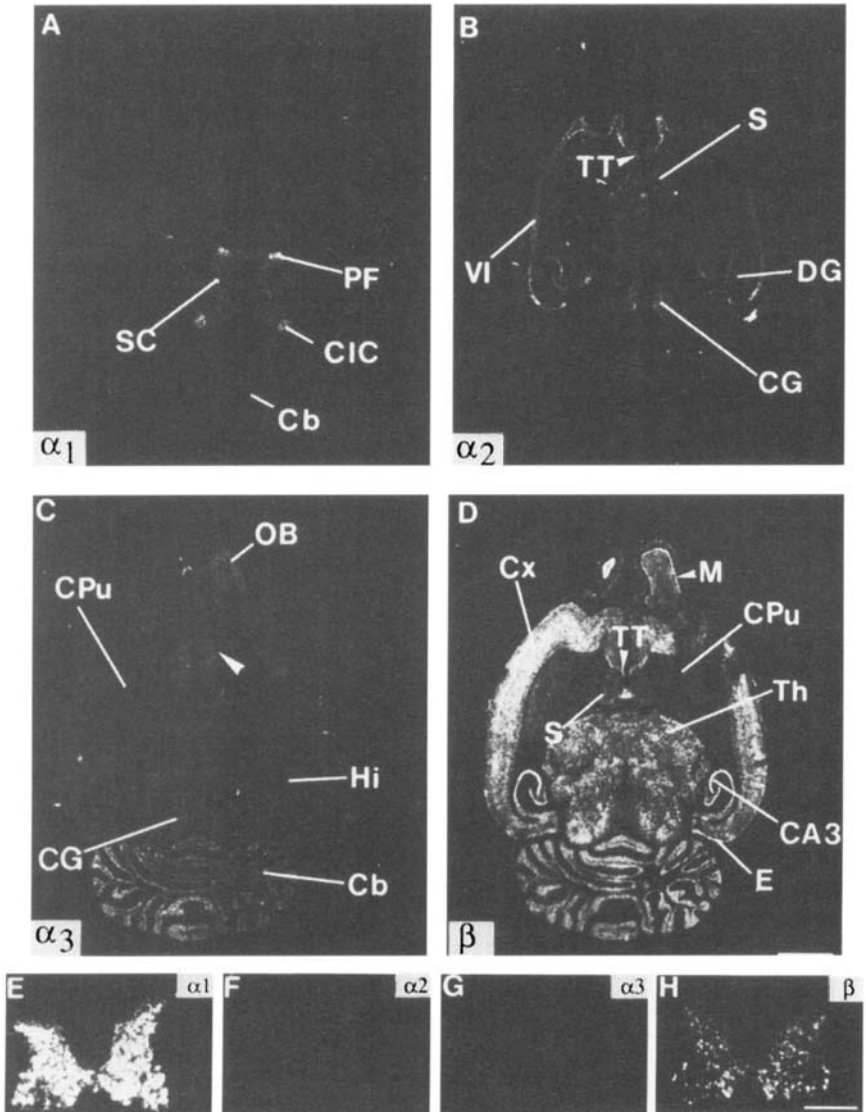

FIG. 3 *In situ* hybridization of GlyR subunit mRNA in horizontal brain sections (A–D) and coronal cord sections (E–H) from adult (P40) rats. CA3, CA3 region of the hippocampus; Cb, cerebellum; CG, central gray; CIC, central nucleus of the inferior colliculus; CPu, caudate putamen; Cx, cortex; DG, dentate gyrus; E, entorhinal cortex; Hi, hippocampus; OB, olfactory bulb; PF, parafascicular nucleus; S, septum; Th, thalamus; TT, tenia tecta; VI, sixth layer of cortex. Arrowhead indicates supposed internal layers of the infralimbic cortex. (A, E) α1; (B, F) α2; (C, G) α3; and (D, H) β; subunit mRNA distributions. Scale bars: 4 mm (D); 1 mm (H) (from Malosio *et al.*, 1991b by permission of Oxford University Press).

could be detected in the spinal cord (Fig. 3G; Kuhse *et al.,* 1990b; Malosio *et al.,* 1991b). In contrast, a very early onset of $\alpha 2$ transcription is observed in most brain areas such as the telencephalon, the diencephalon, the midbrain, and in the spinal cord, which all already contain fair amounts of mRNAs during embryonic life. This transcriptional activity of all $\alpha 2$ splice variants is transient, and the high prenatal levels are maintained only during a few days after birth. As a result, the $\alpha 2$ isoform (mainly $\alpha 2A$) persists in the adult in several brain regions at significant levels (Fig. 3B) and disappears, with the exception of a few neurons, from the spinal cord (Fig. 3F; Malosio *et al.,* 1991b; Kuhse *et al.,* 1991; Sato *et al.,* 1992). This replacement of the $\alpha 2$ by the $\alpha 1$ subunit does not apparently take place in areas such as the deep cortical layers or some other brain regions where significant levels of $\alpha 2$ mRNA persist into adulthood (Fig. 3B).

While the transcription of α subunits is restricted to specific regions in the brain, the mRNAs of the glycine receptor β subunit have a widespread distribution (Figs. 3D and 3H) and appear early in the embryo. The hybridization signals of β mRNA displayed by some formations such as the cortical layer VI, the thalamus, and the colliculi or some neurons such as the olfactory bulb mitral cells and Purkinje cells clearly are relatively strong compared, respectively, to the moderate or even nil signals of α transcripts (Grenningloh *et al.,* 1990a; Malosio *et al.,* 1991b; Fujita *et al.,* 1991). Therefore, the overall distribution of β transcripts is much wider than that corresponding to all α transcripts, and high levels of expression are displayed by many brain regions that are apparently immunohistologically silent (see below) or devoid of [^{3}H]strychnine-binding sites. To date, the functional significance of the ubiquity of β messenger RNAs in the central nervous system is not understood. As the involvement of the GlyR β subunit as a functional component of other neurotransmitter receptors can be ruled out, according to available data, an alternative hypothesis which has not been excluded is that it might merely be associated with unknown strychnine-insensitive α subunits of the glycine receptor (Béchade *et al.,* 1994).

Identification and localization of glycinergic receptors in the CNS have long relied upon the use of strychnine or ligand-binding assays. The distribution of GlyR transcripts appears much wider than expected from biochemical studies and, as no two mRNAs exhibit identical spatial and temporal patterns, overlapping mRNA expression profiles suggest that several combinations could be formed during developmental stages. Taking into account the fact that *in situ* hybridization only predicts the distribution of potentially glycine-responsive neurons, on the one hand, the topographic mapping of the various subunit mRNAs of GlyR using this approach is in rough agreement with data obtained by autoradiography of [^{3}H]strychnine. On the other hand, the finding that mRNAs encoding certain GlyR subunits are

expressed in the higher brain regions, such as the cortex, where high-affinity strychnine binding of the $GlyR_A$ type is barely detectable, nevertheless agrees with reports of the presence of receptors identical to $GlyR_N$ (no β subunit, $\alpha 2$ oligomer) of the neonatal spinal cord at this site (Naas *et al.,* 1991; Becker *et al.,* 1993). However, a few discrepancies exist since the presence of $\alpha 1$ transcripts, for example, in several hypothalamic nuclei, may not be correlated with a superimposed presence of high-affinity antagonist-binding sites (Zarbin *et al.,* 1981; Frostholm and Rotter, 1985). Such mismatches cannot unambiguously be interpreted as no detailed analysis has so far been carried out at the cellular level, but they may be accounted for by at least two distinct phenomena. Interestingly enough, a spatial mismatch between mRNA and binding sites has been encountered in other systems, as exemplified by the glutamate and $GABA_A$ receptors in the spinal cord. In the latter case, while motor neurons receiving GABAergic inhibition from Renshaw cells are consistently predicted by *in situ* hybridization analysis to express a defined receptor subtype, ligand binding is predominantly observed in dorsal horn-located sites where the motor neuron dendrites extend (Persohn *et al.,* 1991). Furthermore, with respect to protein expression, there are various reasons why cells expressing mRNAs do not produce detectable functional channels. These include the lack of messenger translation, incorrect subunit combinations, assembly or transport/targeting defects, low mRNA levels, and defective mRNAs (see references in Tyndale *et al.,* 1994). Although these factors might be thought to operate in cloned cell lines, the absence of functional NMDA receptor-gated channels in adult rat Purkinje and dorsal root ganglion cells which do express NMDAR1 mRNA suggests that *in situ* hybridization detection does not necessarily indicate that a functional protein is made (Moriyoshi *et al.,* 1991; Audinat *et al.,* 1990; Shigemoto *et al.,* 1992; Huettner, 1990). At any rate, these observations call for further analysis of the expression of both GlyR mRNAs and proteins at the cellular level.

In the context of sensory and motor processing in the brain, particularly in regions where GABAergic inhibition has long been thought to be the rule, the widespread expression of GlyR subunits raises questions. Currently, the association of $GABA_A$ receptor and GlyR subunit mRNAs in the same cells may be interpreted either in phylogenetic terms, hypothesizing that GABA substitutes for glycine, or as indicative of a refinement of neuron activity (see Malosio *et al.,* 1991b).

In situ hybridization studies have provided evidence for, as well as confirmation of, control of expression of genes encoding GlyR subunits and point to the problem of the molecular variability that can potentially be achieved *in vivo* via subunit combination in several brain areas. In this respect, the recently described diversity of GlyR in the rat retina, where all the subunit mRNAs are simultaneously transcribed in some neurons,

illustrates the puzzling (but not peculiar to this receptor) feature that a given receptor may take on (Greferath *et al.,* 1994).

B. Immunohistochemical Studies

As in the case of other receptors, it is fundamental to know the subunit stoichiometry within GlyR complexes and to discriminate between receptors present on the neuron cell body and those located on dendrites. As a first step to address these issues, the immunological approach to GlyR protein distribution gives much information.

Morphological studies have so far benefited from the availability of the various monoclonal antibodies that specifically recognize the α1 subunit of the channel (GlyR2b), associated gephyrin (GlyR5a and 7a), or both the adult and embryonic α isoforms and the β subunit (GlyR4a).

Immunohistochemical investigations on GlyR localization in rodent central nervous system using GlyR2b and/or GlyR7a mAbs revealed that, besides the spinal cord, several regions of the brain displayed receptor antigenic sites, including the hypothalamus, the hippocampus, the olfactory bulb (Van den Pol and Gorcs, 1988), the cochlear nuclei (Altschuler *et al.,* 1986; Araki *et al.,* 1988), the cerebellum (Triller *et al.,* 1987; Van den Pol and Gorcs, 1988; Araki *et al.,* 1988; Chen and Hillman, 1993), and the retina (Sassoè-Pognetto *et al.,* 1994; Grünert and Wässle, 1993; Greferath *et al.,* 1994). Most of these studies were carried out using both light and electron microscopy with an anti-gephyrin antibody (GlyR7a mAb). Taken together, they suggested that in rostral brain regions GlyR had a rather restricted distribution, at variance with *in situ* hybridization-based predictions of a much wider expression of some subunits. In all instances, however, except for the cerebellum, as exemplified in the various laminae of the spinal cord gray matter, a characteristic pattern of discontinuous patches in close, but not perfect, relation to punctate glycine immunoreactivity was observed. Evidence was thus obtained for a localization of GlyR in axodendritic, axosomatic, and dendrodendritic postsynaptic membrane areas in numerous neuronal types (Araki *et al.,* 1988; Van den Pol and Gorcs, 1988; Todd, 1990; Basbaum, 1988; Todd and Sullivan, 1990; Mitchell *et al.,* 1993).

V. Cell Biology of the Glycine Receptor

A. Subcellular Localization of Transmembrane Components and Gephyrin

1. GlyR-Rich Postsynaptic Microdomains

The pioneer experiments analyzing the subcellular distribution of the GlyR complex revealed the mosaic organization of the neuronal membrane (Tril-

ler *et al.*, 1985) in rat spinal cord. The visualization of GlyR components using GlyR2b, GlyR4a, GlyR5a, and 7a antibodies in immunofluorescence microscopy revealed an exquisite punctate distribution of epitopes at the neuronal cell surface and demonstrated the cytoplasmic localization of gephyrin (Fig. 4). Also found in the Mauthner cell of the goldfish brain, this pattern was shown by immunoelectron microscopy to result from the restricted colocalization of both transmembrane subunits and gephyrin within postsynaptic membrane areas apposed to presynaptic terminals. These observations thus demonstrated that the postsynaptic plasma membrane of target neurons thought to receive glycinergic inputs (see below) was organized as a mosaic of specialized GlyR-containing, differentiated domains of the membrane whose distribution was superimposable on that of presynaptic elements containing flattened vesicles (Triller *et al.*, 1985, 1987; Seitanidou *et al.*, 1988).

The fine spatial organization of GlyR at the neuronal cell surface *in situ* has been examined at the single-cell level on the Mauthner neuron of the goldfish. This provided a fair model which circumvented the problem of simultaneously and unambiguously recognizing the dendritic and somatic compartments of the same cell (Triller *et al.*, 1990). A quantitative confocal microscopic analysis showed that the area of receptor clusters on dendrites, as visualized with the GlyR 4a mAb directed against the channel-forming glycoproteins, increases according to a somatodendritic gradient, whereas the number of clusters per surface unit decreases. Furthermore, combination of microfluorimetric analysis and 3-D reconstruction indicated that the density of GlyR was comparable in all postsynaptic domains (Triller *et al.*, 1990; Franksson and Triller, 1993). Such size and number variability, which also exists in motoneurons, applies to the release site of the corresponding glycinergic inhibitory terminals. A parallel gradient of the presynaptic grid area computed with confocal microscopy was also found, thus disclosing a principle of structural organization, the functional meaning of which may lie either in a compensation of the dendritic length constant or in an adaptative means for controlling distally delivered excitatory inputs (Alvarez *et al.*, 1993; Sur *et al.*, 1995; Béchade *et al.*, 1994).

In agreement with these results, immunofluorescence studies have also shown that gephyrin localization in the rat higher brain structures is postsynaptic, being mainly somatic in neurons of the diencephalon and the cerebellum. However, comparison of immunoreactivities toward mAb 2b and mAb 4a antibodies suggested that, in some neurons, whereas the α1 subunit was strictly postsynaptic, the other forms of GlyR could exhibit extrasynaptic and/or intracellular localization (Kirsch and Betz, 1993).

2. Assembly of GlyR

Substantial progress has been made in understanding the biosynthesis, assembly, and membrane insertion of GlyR. Although functional homo-

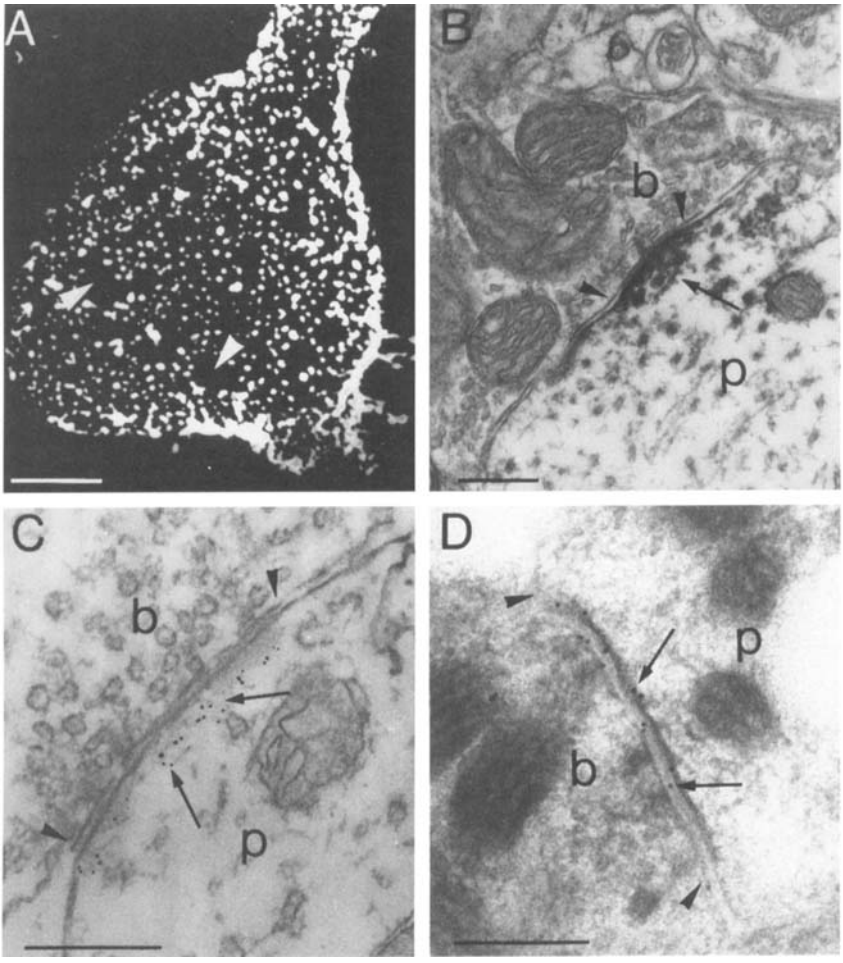

FIG. 4 Cellular and subcellular organization of the glycine receptor and associated gephyrin. (A) View through projection of stacks of confocal sections showing the uneven distribution of the immunofluorescent GlyR (mAbGlyR4a) at the surface of a large neuron. Nonlabeled patches (arrowheads) of the neuronal surface are contacted by nonglycinergic axons. Calibration bar: 10 μm. (B, C) Accumulation (arrows) at postsynaptic densities of peroxidase electron-dense product (B) and gold particles (C) associated with gephyrin immunoreactivities (mAb GlyR 7a) at the level of synaptic complexes (between arrowheads) established between presynaptic boutons (b) containing pleomorphic vesicles and the postsynaptic (p) element. (D) Accumulation of the glycine receptor-associated gold particles (arrows) within the synaptic cleft (between arrowheads). Calibration bars for B, C, and D: 0.25 μm. (A, goldfish brain stem; B, C, and D, rat ventral horn.)

oligomeric chloride channels can be inserted in the plasma membrane of mammalian cells transfected with GlyR α subunits, their formation seems to proceed rather inefficiently, at variance with the situation encountered, for example, in cultured spinal cord neurons. In these cells, $\alpha 2$ subunits are assembled as stable homopentamers ($GlyR_N$) predominantly expressed at the cell surface (Hoch *et al.*, 1989; Sontheimer *et al.*, 1989). Whether this difference is due to differential capabilities of homologous versus heterologous systems in protein processing has not been investigated. Instead, the observation of the marked increase in glycine-elicited whole-cell currents upon coexpression of α and β subunits in comparison with α subunits alone, which suggested that a more efficient assembly and/or transport of receptors could be favored by the β subunit (Pribilla *et al.*, 1992; Bormann *et al.*, 1993), has been exploited in order to analyze channel formation by expressing mutated and chimeric subunits in *Xenopus* oocytes (Kuhse *et al.*, 1993). The results, interpreted on the basis of the predictable defined pharmacologies of the expected hetero-oligomers, clearly showed that whereas $\alpha 1/\alpha 2$ oligomers assemble in variable subunit ratios, α/β oligomers are formed with a fixed 3/2 stoichiometry. Short amino acid sequences (assembly boxes) all located in the N-terminal extracytoplasmic domain and corresponding to three diverging motifs in both subunits were identified which precisely govern receptor assembly. Replacement of these motifs in the β subunit by the corresponding $\alpha 1$ motifs results in the loss of the strict 3/2 subunit ratio in α/β oligomers, suggesting that different amino acid positions are determinants in the early step of subunit–subunit interaction rather than in oligomeric structure stabilizing events. Importantly, these residues impose a mutually exclusive mode of assembly, either in homo-oligomers or in stoichiometric complexes (Kuhse *et al.*, 1993). In line with the fact that their location is homologous to that of residues governing AChR assembly in the ε subunit (Gu *et al.*, 1991), the plausible ability of these residues in the β subunit to impose the order of assembly and the quaternary structure of GlyR is a hypothesis yet to be tested. Additional domains are very likely involved in stabilization and/or transport to the plasma membrane. In favor of this assumption, arginine 252 at the cytoplasmic extremity of the M2 segment was found to be essential for cell surface expression since its mutation results in intracellular retention and aggregation of the $\alpha 1$ subunit (Langosch *et al.*, 1993). As a general rule for cell surface glycoprotein oligomers, only those assembled according to a proper stoichiometry in the endoplasmic reticulum have access to the Golgi complex, to be sorted and subsequently delivered to the plasma membrane. Among several examples, such quality control of newly synthesized proteins has been clearly established for the AChR since only $\alpha 2\beta\gamma$(or ε)δ oligomers are allowed to undergo maturation in the Golgi complex (Sumikawa and Miledi, 1989; Merlie and Smith, 1986). A similar control of proper subunit assembly has

also been described for the T cell antigen receptor where either retention in the ER or degradation operates on misassembled complexes (Klausner *et al.,* 1990). Whether the β subunit, in the case of GlyR, is also responsible for a more efficient transport of the α subunits has not been determined. Again, in view of the ability of α subunits to form cell surface receptors, the requirements for correct transport encountered in other systems may not strictly apply to α homo-oligomeric GlyRs.

B. Gephyrin and Glycine Receptor Clustering

1. Gephyrin Diversity

Isolation of several cDNAs from rat brain and spinal cord libraries revealed the rather high degree of variability of gephyrin structure, as at least five variants are known which arise by alternative splicing of a single pre-mRNA. Differences correspond to four cassettes occurring in the N-terminal region of the protein. Northern blot analysis and PCR amplification showed that variant transcripts are differentially expressed in nervous as well as in nonnervous tissues, such as liver, kidney, or lung, indicating that gephyrin molecules are specific neither for GlyR nor for CNS (Prior *et al.,* 1992). Interestingly, *in situ* hybridization mapping of the various mRNAs in adult and developing rat brain revealed that each variant has a specific spatial and temporal expression profile but that their general distribution, wider than that reported for any GlyR α subunit, closely resembles that of the β subunit mRNA (Kirsch *et al.,* 1993a). Accordingly, a widespread expression of gephyrin was also disclosed by careful immunolabeling experiments showing that, being virtually in all brain areas containing synapses, it can in fact be synthesized independent of the currently detectable α subunits (Kirsch and Betz, 1993). The hypothesis that, in some neurons, gephyrin and the β protein might be associated with channel complexes other than GlyR cannot be ruled out. $GABA_AR$ would be a good candidate (see below). However, further investigations need to delineate more precisely the distribution and behavior of this protein, whose unusual and versatile primary structure may confer as yet uninvestigated membrane interactions and/or turnover features (Kirsch and Betz, 1993).

2. Formation of GlyR Clusters

The data reported above demonstrate the fine localization of GlyR in front of presynaptic endings. How these microdomains are formed during neuron differentiation and innervation is not well understood. Denervation experiments carried out on the Mauthner cell have shown that the presence of

GlyR clusters is dependent on the integrity of afferent axons but not on synaptic activity (Seitanidou *et al.,* 1992). This suggests that different mechanisms are involved in maintenance and/or establishment of focal clustering of GlyR in the postsynaptic membrane, and of the nicotinic acetylcholine receptor at the motor endplate (Changeux, 1991; Hall and Sanes, 1993). Neurons able to acquire a polarized phenotype upon differentiation in culture represent a good model for study of the epigenesis of postsynaptic domains. Cultured fetal spinal cord neurons which possess functional glycine-gated channels (Bormann *et al.,* 1987) predominantly express the $\alpha 2$ homo-oligomer, but GlyR matures with time in culture since a mature isotype, $\alpha 1$, can be biochemically detected (Hoch *et al.,* 1989, 1992; St John and Stephens, 1993). PCR amplification analyses have confirmed that these neurons to some extent reproduce the fetal to adult transition of their *in situ* counterpart (Hoch *et al.,* 1992; Béchade *et al.,* 1995). Moreover, within 1 week, they are able to form plasma membrane GlyR clusters that react with anti-$\alpha 1$, α/β, and gephyrin mAbs. Fluorescence microscopy studies of the development of GlyR clusters in differentiating cells showed that it can be described as a two-step process (Nicola *et al.,* 1992; Kirsch *et al.,* 1993b; Béchade *et al.,* 1995). This process is characterized by an asynchronous clustering of GlyR and gephyrin, with the aggregation of gephyrin under the cell surface being observed first. Subsequently, the number of GlyR clusters increases to match that of gephyrin. As seen at the ultrastructural level, the first detectable gephyrin patches form at sites of cell–cell and cell–substratum contact. Upon culture maturation, they become restricted to the postsynaptic membrane where GlyR is also located. Throughout this process, extrasynaptic distribution of GlyR was not detected (Colin *et al.,* 1996). In contrast to the temporal sequence, the causal sequence of GlyR specific clustering is not established. However, the key role of gephyrin in this process has been demonstrated by inhibiting gephyrin production in cultured neurons with antisense oligonucleotides able to hybridize with all known gephyrin transcripts (Kirsch *et al.,* 1993b). Neurons unable to synthesize gephyrin failed to position GlyR in plasma membrane domains: GlyR remained trapped intracellularly (Fig. 5). Whether this mislocalization results from a targeting defect or from an instability of GlyR clusters at the plasma membrane and subsequent endocytosis is not known.

There is biochemical evidence that gephyrin specifically binds to purified adult GlyR via the β subunit (Meyer *et al.,* 1995): heterologous expression and overlay assay of recombinant proteins have shown that the gephyrin binding site is localized in a stretch of 49 amino acid residues in the cytoplasmic loop between transmembrane segments M3 and M4 of the β subunit. Furthermore, while none of the wild-type β subunits of $GABA_AR$ bind gephyrin *in vitro* or in transfected cells, an 18-residue domain within this stretch has been identified which confers on a chimeric $\beta 1$ subunit of

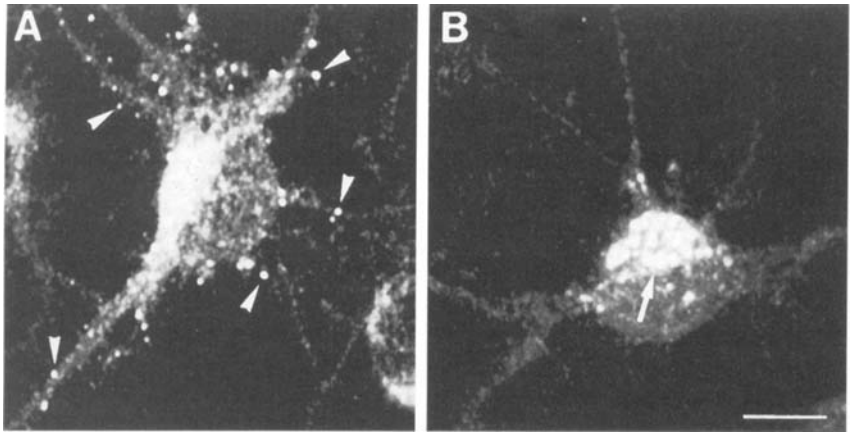

FIG. 5 Absence of glycine receptor clusters in spinal cord neurons treated with antisense oligonucleotides inhibiting the synthesis of gephyrin. (A) Control cultured neuron treated with a sense oligonucleotide displaying GlyR clusters (arrowheads) at the periphery of the neuron. (B) Neuron treated with antisense oligonucleotides lacking peripheral GlyR clutsers; note that the GlyR antigene remained confined within the soma (arrow). Calibration bar: 10 μm. Reprinted with permission from *Nature* (Kirsch *et al.*, 1993b) Copyright (1993) Macmillan Magazines Limited.

$GABA_AR$ the ability to bind gephyrin. On the other hand, the involvement of microtubules in localizing GlyR in the postsynaptic membrane has been suspected in view of the high-affinity cooperative interaction between gephyrin and tubulin dimers *in vitro* (Kirsch *et al.*, 1991). This notion is now favored by recent work (Kirsch and Betz,1995) showing that, in cultured differentiated cells, selective depolymerization of microtubules by nocodazole or demecolcine leads to lateral diffusion of postsynaptic gephyrin–GlyR clusters in the plasma membrane. It was also shown that microfilaments could act as regulatory factors since they antagonize, directly or indirectly, the concentrating and/or stabilizing effect of microtubules on gephyrin clusters. Therefore, the action of gephyrin on GlyR could be dual in preventing its mobility out of the postsynaptic membrane domain and in controlling its density in the membrane via an interaction with both microtubules and microfilaments. This last function could be relevant for synaptic plasticity since, as suggested by heterologous $\alpha 1$ or $\alpha 2$ subunit expression experiments (Takagi *et al.*, 1992; Taleb and Betz, 1994), the denser the receptor packing, the higher the agonist affinity for GlyR. Antagonistic effects of microtubules and microfilaments on local GlyR concentration would provide a mechanism whereby cooperative receptor interactions could be modulated. This proposed regulation of GlyR by the cytoskeleton is in line with the recent idea that a regulatory protein mediates the actin

filament dependence of NMDA receptor activity (Rosenmund and Westbrook, 1993).

Somehow, the ability of gephyrin to copurify with GlyR under mild conditions reflects a reversible interaction that may exist *in vivo* (Schmitt *et al.*, 1987). In view of the available data it cannot be excluded that gephyrin, which is able to self-aggregate, is in a dynamic equilibrium with GlyR and binds with increased affinity to plasma membrane receptors, a hypothesis consistent with the temporal sequence of microdomain formation. The receptor–microtubule linking function of gephyrin would represent a particular role of this family of molecules (Prior *et al.*, 1992). On the basis of the above observations on cytoskeleton–gephyrin–GlyR interactions and the sequence of events in the formation of GlyR-rich domains, a model was proposed to account for the biogenesis of membrane heterogeneity (Fig. 6; Béchade *et al.*, 1994). In this model, gephyrin in its condensed form would act as a nucleating site able to organize newly inserted GlyR channels into clusters. Thus, with regard to synaptogenesis, gephyrin subserves a role comparable to that of the unrelated cytoplasmic 43K protein (rapsyn), which is thought to initiate nicotinic AChR aggregation at the neuromuscular junction. Although the temporal sequence of AChR and 43K clustering may vary from one cell to another and is still disputed, 43K mediation likely occurs via its double interaction with the receptor β subunit and proteins of the submembranous cytoskeleton web. Like gephyrin, rapsyn forms clusters in the absence of AChR (Cartaud and Changeux, 1993; Froehner, 1993). Although they have no sequence homology, some features are shared by gephyrin and rapsyn. First, both proteins can be myristoylated on their N terminus, albeit after proteolytic processing in the case of gephyrin. Such posttranslational modification which helps modulate the protein to membrane anchoring has been shown, in quail fibroblasts using site-directed mutagenesis, to control partially the frequency of rapsyn-enriched plasma membrane domains to which AChRs can still concentrate (Phillips *et al.*, 1991). Second, they both possess consensus sequences for phosphorylation by either protein kinase C or cyclic nucleotide-dependent kinase (Prior *et al.*, 1992; Froehner, 1991). Gephyrin, as well as tubulin, is phosphorylated by a still unknown kinase, associated with isolated GlyR (Langosch *et al.*, 1992). It is then conceivable that local phosphorylation–dephosphorylation interplays alter its interaction with tubulin, as observed for various microtubule-associated proteins such as MAP2 and tau (Brugg and Matus, 1991; Kanai and Hirokawa, 1995). Together with phosphorylation-dependent differential turnover, this could determine gephyrin subcompartimentalization which in turn would lead to the assignment of GlyR to a specific insertion locus.

As a phosphoprotein, gephyrin could also regulate the availability of GlyR for membrane insertion, in a way similar to the control of the respec-

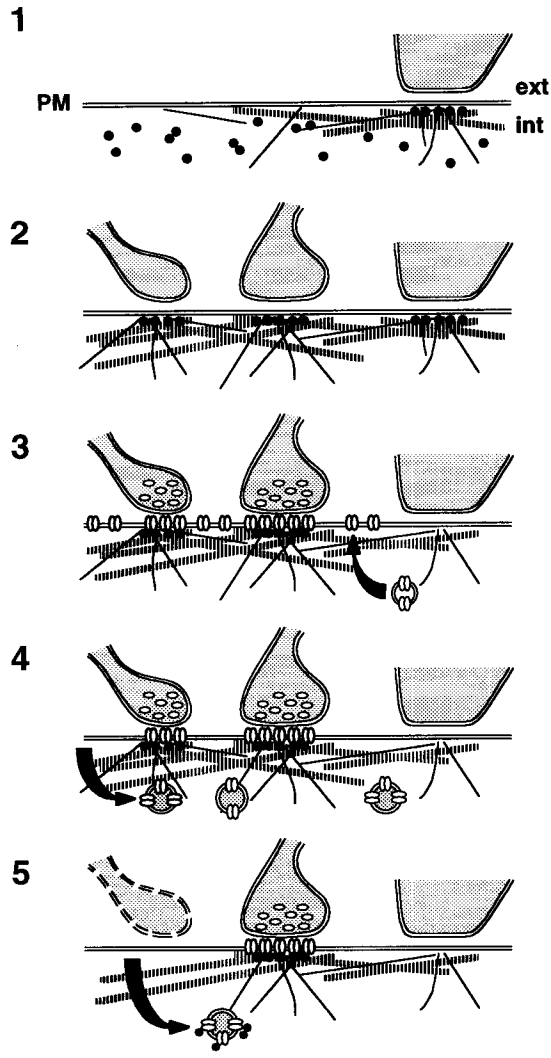

FIG. 6 Postulated temporal sequence of glycine receptor clustering in the postsynaptic membrane. (1) Diffuse cytoplasmic gephyrine first accumulates at sites of cell–cell contacts. (2) Innervation place; gephyrin clusters become restricted to these contacts. At this step, a putative local reorganization of the cytoskeleton makes it able to interact with gephyrin. (3) Plasma membrane insertion of receptor and gephyrin-mediated retention in front of forming terminals. (4) Internalization of extrasynaptic receptor resulting in exclusive localization in postsynaptic domains. (5) Selective stabilization of receptor present in active domains after elimination of nonfunctional clusters.

tive sizes of reserve and releasable pools of synaptic vesicles by synapsins (Greengard *et al.,* 1993). In this case, gephyrin would be involved in determining the size of GlyR clusters, at a given site and depending on its phosphorylation state, by controlling the exocytotic fusion of transport vesicles. On the other hand, it cannot be excluded that a particular phosphorylation state of GlyR β subunit (or even α subunits) is also required for the receptor to bind to already clustered gephyrin. In fact, although nothing is known about the signaling mechanisms involved in proper insertion of the receptor, phosphorylation might be a key modulatory factor accounting for proper clustering of the receptor.

It is beyond the scope of this review to consider how the site of GlyR localization is determined in relation to presynaptic glycinergic innervation, how it is targeted to this site, and what the underlying mechanisms that locally modify the cytoskeleton network for its postsynaptic stabilization are. However, two basic mechanisms whereby receptor postsynaptic localization is achieved and controlled can be proposed (Craig *et al.,* 1994). A first possibility is that before their exit from the TGN, receptors are sorted into specific transport vesicles that are directly targeted to, and only fuse at, the appropriate postsynaptic site. A second possibility is that exocytotic fusion of post-Golgi vesicles is not site-specified and that receptors are randomly inserted into the plasma membrane and are free to diffuse toward postsynaptic sites where they are eventually retained specifically. Data reported herein, showing that GlyR is only detectable as patches at the time of insertion, seem to favor the former mechanism. This, therefore, would confer on cytoskeleton-bound, aggregated gephyrin the function of a multiple-site receptor to which GlyR transport vesicles are docked. In this case, the molecular basis of the selective delivery of transport vesicles to a defined cell surface area remains to be explained (Kelly and Grote, 1993).

Since the turnover rates of free and immobilized receptor are unknown, it cannot be excluded, however, that according to the second mechanism gephyrin acts as an anchor, capturing GlyRs diffusing in the plasma membrane. At any rate, the biochemical specificity of postsynaptic insertion of the receptor may plausibly reside in the gephyrin–β subunit interaction. Working hypotheses would thus confer on the gephyrin binding domain of the β subunit the status either of a docking and retention signal or of a retention signal only, in the first and second models, respectively.

C. Gephyrin at Nonglycinergic Synapses

The distribution of gephyrin antigenic sites in the CNS is much wider than that of GlyR. Such an observation supports the view that gephyrin is not specific for this receptor (Kirsch and Betz, 1993). This raises questions as

to whether gephyrin can associate with other neurotransmitter receptors in nonglycinergic synapses and participate in their clustering (Grünert and Wässle, 1993; Sassoè-Pognetto *et al.*, 1994; Todd *et al.*, 1995). In view of the similar distributions of gephyrin and $GABA_A$ receptor subunit transcripts in most regions of the brain, $GABA_AR$ is seen as a good candidate for an alternative association of gephyrin (Malosio *et al.*, 1991b; Laurie *et al.*, 1992a,b; Wisden *et al.*, 1992). There is to date no direct biochemical demonstration of such an association. However, gephyrin aggregated in the cytoplasm of transfected cells is able to retain intracellularly the cotransfected $GABA_A$ receptor $\beta 3$ subunit (Kirsch *et al.*, 1995).

There is also evidence that gephyrin could be associated with $GABA_AR$ in some instances *in vivo*. Many neurons in the spinal gray matter or the cerebellum are now known to use GABA and glycine as neurotransmitters, both being colocalized in the same presynaptic elements (Ottersen *et al.*, 1988; Todd and Sullivan, 1990; Chen and Hillman, 1993; Triller *et al.*, 1993b; Todd *et al.*, 1995). The hypothesis of the coexistence of gephyrin and $GABA_A$ receptor $\alpha 1$ subunits in the same GABAergic synapses arose from confocal microscopy analyses in neurons of the spinal cord dorsal and ventral horns (Bohlhalter *et al.*, 1994). An ultrastructural study combining double labeling and serial sectioning (Todd *et al.*, 1996) allowed the simultaneous detection of glycine and GABA in the presynaptic bouton and of gephyrin and the $GABA_A$ receptor $\beta 3$ subunit at the postsynaptic receptive membrane of the same synapse. This study also provided evidence that a perfect match of the GlyR $\alpha 1$ subunit and gephyrin was always obtained, in agreement with previous observations (Triller *et al.*, 1987). These data, which also confirm earlier demonstrations of gephyrin in synapses involving axons containing GAD or GABA (Triller *et al.*, 1987; Mitchell *et al.*, 1993), strongly suggest that a postsynaptic colocalization of the $GABA_A$ receptor $\beta 3$ subunit and glycine receptors and of gephyrin may occur in the spinal cord. However, the partial or total segregation of the $\beta 3$ subunit and gephyrin within a single postsynaptic patch was observed, the latter protein being denser at the periphery. Such micro-organization within the postsynaptic domain therefore makes the direct interaction of these proteins, as well as gephyrin-dependent $GABA_A$ receptor clustering, unlikely in spinal cord neurons. Analysis of the distribution of gephyrin in the rat spinal cord dorsal horn also showed that the same presynaptic axonal endings, potentially GABA- and glycinergic, were apposed to gephyrin immunoreactivity at axo-dendritic and axo-somatic but not axo-axonic synapses (Mitchell *et al.*, 1993; Todd *et al.*, 1995). This last situation is reminiscent of the glycinergic synapses formed by AII-amacrine cells in the inner plexiform layer of the retina. These cells have the ability to form the same types of contact containing the GlyR $\alpha 1$ subunit with both the ganglion cell dendrites and the cone bipolar cell axons. Since gephyrin is absent in front of axons of

bipolar cells (Grünert and Wässle, 1993; SassoèPognetto *et al.,* 1994), but is found at postsynaptic membranes of ganglion cells, it has been hypothesized that the association of gephyrin with GlyR selectively occurs in dendrites and not in axons (Yazulla and Studholme, 1991). Therefore, different, but not mutually exclusive, explanations may account for various observations: (a) gephyrin is present at glycinergic synapses expressing undetectable or unknown GlyR subunits, (b) gephyrin is not specific for GlyR and is also associated with nonglycinergic receptors such as GABAR, and (c) some glycine receptors are not bound to gephyrin or are bound to a gephyrin form or other molecules not recognized by the antibodies used. None of these possibilities can so far be excluded.

On the other hand, the notion that gephyrin could be involved in anchoring of the $GABA_A$ receptor is reinforced by the observation that, in the inner plexiform layer of the retina, gephyrin coexists in the same postsynaptic membrane with $GABA_A$ receptor $\alpha 2$ subunits which themselves do not colocalize with the GlyR $\alpha 1$ subunit (Sassoè-Pognetto *et al.,* 1995). It is interesting to note that, in the retina, morphological studies coupled to *in situ* hybridization and immunohistochemistry have shown that $GABA_A$ receptors composed of $\alpha 2$ subunits very likely contain at least $\beta 2/3$ subunits (Greferath *et al.,* 1995). Moreover, in sympathetic preganglionic neurons, which do not receive glycinergic inputs, GABAergic endings are apposed to gephyrin (Cabot *et al.,* 1995), thus confirming the notion of an association of $GABA_AR$ with gephyrin. This notion has also received support in cultured hippocampal neurons where it was shown (i) that gephyrin and $GABA_A$ receptor $\beta 2/3$ subunits have similar distribution patterns and (ii) that gephyrin clustering selectively occurs at GABAergic synapses (Craig *et al.,* 1996).

VI. Pathology—Molecular Basis of Spastic Syndromes

Glycine is the main inhibitory neurotransmitter in the spinal cord and defects in glycinergic transmission lead to motor disorders which include exaggerated startle reflex, spasticity, hypertonia, and tremor. Some hereditary motor disorders in human and mouse are the consequence of the expression of mutated glycine receptor genes. The hallmark of these inherited disorders is an exaggerated startle reflex in response to a sudden stimulus, giving rise to a rapid generalized motor response in the form of hypertonia (see references in Rajendra and Schofield, 1995).

A. Human Hyperexplexia

Hyperexplexia denotes a movement disorder in which there are exaggerated startle reflexes to unexpected sensory stimuli. Hereditary hyperexplexia,

Kok's disease, or familial startle disease (STHE) is a rare autosomal dominant neurologic disorder characterized by marked and continuous, sometimes fatal, muscle rigidity in infancy which progressively evolves in startle-induced, transient massive muscle contractions, a reaction that persists throughout adulthood.

The defective gene in STHE, initially localized on chromosome 5q, was identified by genomic mapping studies as being GLRA1, coding for the α1 subunit of GlyR (Shiang *et al.,* 1993). This identification was consistent first with results of electrophysiological studies of audiogenic startle attacks, which implicate the neurons of the pontomedullary reticular formation, and second with the well-established mediation by glycine of the recurrent inhibition of spinal motoneurons by Renshaw cells and Ia inhibitory interneurons. There, a defect in the glycine receptor leads to disinhibition of the motoneurons and accounts for some clinical characteristics of hyperexplexia. These symptoms are comparable to those of subconvulsive strychnine poisoning, which are due to reduced glycinergic inhibition (Floeter and Hallet, 1993).

Two different point mutations (missense mutations) at the same position in exon 6 have been identified in patients of several families with hereditary hyperexplexia (Shiang *et al.,* 1993; Schorderet *et al.,* 1994). These mutations replace arginine 271 in the polypeptide with an uncharged amino acid, leucine, or glutamine. As indicated earlier, this mutation alone likely accounts for the defective phenotype since recombinant homomeric α1 receptors bearing the same substitutions exhibit dramatically decreased sensitivities of glycine-activated currents (Langosch *et al.,* 1994; Rajendra *et al.,* 1994).

B. Startle Syndromes in the Mouse

Studies of neurologic mutants in the mouse have revealed that at least two genes can cause recessive disorders with clinical and pharmacological features reminiscent of STHE (see Fig. 7). *Spasmodic* and *spastic* phenotypes are inherited as autosomal diseases characterized by muscle tremor, hypertonia, and pronounced startle reactions (Rajendra and Schofield, 1995). Except for the *oscillator* phenotype, startle diseases are rarely lethal, and all homozygous mutant mice are phenotypically normal during the first 2 weeks after birth.

1. *Spasmodic* and *Oscillator* Mice

The phenotypic similarity of the *spasmodic* (*spd*) phenotype and STHE, together with the assignment of *spd* to a small region of mouse chromosome 11, prompted the identification of *Glra1,* encoding the mouse α1 subunit

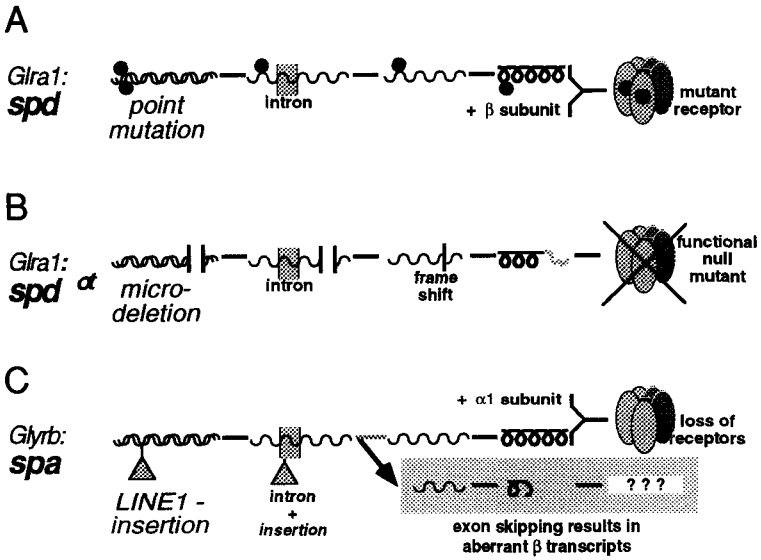

FIG. 7 Murine mutations affecting glycine receptor expression. Position of the different mutations leading to production of abnormal glycine receptor and/or assembly in spasmodic (A), oscillator (B), and spastic (C) mutants (modified from Becker, 1995, with permission).

of GlyR, as the defective gene (Ryan *et al.*, 1994). A missense mutation converting an alanine residue into a serine was found close to the protein N terminus at position 52 (Fig. 7A). Heterologous expression of the mutated protein showed a decrease in glycine sensitivity by one order of magnitude only, without significantly changing the affinity of the α1 subunit for strychnine. This is in agreement with the normal binding of the antagonist found in the *spd* spinal cord. To date, the mechanism of action of this mutation is not known since this region is not involved in ligand binding, receptor assembly, or gating.

The phenotype of the mutant mouse *oscillator* (*spd*^{ot}) is characterized by fine motor tremor and muscle spasms beginning at 2 weeks of age. Oscillator is allelic with spasmodic but corresponds to a much more dramatic alteration of the *Glra1* structure. A microdeletion coincident with the cytoplasmic extremity of the transmembrane segment M3 results in a translational frameshift which generates a truncated form of the α1 subunit which lacks both the cytoplasmic loop between the M3 and M4 domains, and the M4 domain (Fig. 7B; Buckwalter *et al.*, 1994). In homozygotes, this is accompanied by a 10-fold reduction in strychnine binding in spinal cord membranes, indicating that *spd*^{ot} is a functional null allele (Becker, 1995).

2. The *Spastic* Mouse

The highly penetrant recessive *spastic* mutation, which is mapped on chromosome 3 (Eicher and Lane, 1980), does not produce visible phenotypic alterations before 2 weeks of age in *spa/spa* homozygous mice. The disease is associated with a dramatic reduction in the number of expressed GlyRs in the CNS of the adult mutant, but corresponds neither to abnormal subunit structure nor to altered function of residual receptors (White, 1985; Heller and Hallet, 1982; Becker *et al.,* 1986; Becker, 1990). The delayed onset of the spasticity is coincident with the developmental switch from $GlyR_N$ to $GlyR_A$ and suggests a selective lack of accumulation of the adult isoform, in spite of a normal transcription level of $\alpha 1$ subunit mRNA (Becker *et al.,* 1992).

Actually, an insertional mutation affects the β subunit gene *Glrb,* which results in the aberrant splicing of pre-mRNA. This loss of gene function arises from the intronic insertion of a LINE-1 transposable element (Fig. 7C; Mülhardt *et al.,* 1994; Kingsmore *et al.,* 1994). The LINE-1 element is a retrotransposon relatively abundant in mammalian genomes, where it is essentially inactive, but which may cause abnormal splicing and premature termination of transcription in the host gene (see references in Kingsmore *et al.,* 1994). This mutation of *Glrb* results in skipping of either exon 5 or exons 4 and 5. As a consequence, full-length β mRNAs are barely detectable by *in situ* hybridization in mutant mice, and truncated peptides from the extracytoplasmic N-terminal domain are generated by the creation of premature stop codons (Mülhardt *et al.,* 1994).

It has been shown in the retina that this syndrome corresponds to a morphological alteration of synapses containing GlyR (Pinto *et al.,* 1994). The general loss of surface receptors in *spastic* animals is well explained by the putative role of the β subunit in mediating the association of GlyR with gephyrin and may result from the lack of a gephyrin binding site in hetero-oligomers (Kuhse *et al.,* 1993). However, it must be noted that a reduction in transport to, and insertion in, specific membrane areas may alternatively arise from an altered quaternary structure that does not allow exit from the endoplasmic reticulum and leads to degradation.

Startle syndromes related to distinct genetic defects in glycine-mediated neurotransmission correspond either to impairment of GlyR agonist binding function or to reduced expression of functional channels, both mechanisms leading to inefficient glycinergic inhibition and increased muscle tone. Although STHE and spasmodic disease are related to the production of an abnormal $\alpha 1$ subunit, there is an intriguing difference between human and mouse expression patterns of the disease. Human muscle hypertonia, visible at birth, is attenuated in adulthood and this cannot be explained by the accepted developmental maturation described in rodents. This raises

the question as to whether improvements in muscle tone in human could be explained by compensating mechanisms involving other inhibitory systems such as those using GABA (Floeter and Hallet, 1993).

VII. Concluding Remarks

Substantial progress has been made in understanding the relationships between the molecular properties of GlyR and the (patho)physiology of glycinergic synapses. These advances will undoubtedly constitute a springboard to further insights into crucial processes such as the development of inhibitory circuitry in the CNS and of the control of movement. Since an important line of research is concerned with fundamental mechanisms operating in neuronal differentiation or synaptic plasticity, some benefit would also be gained from dissecting the biogenesis of GlyR.

It will be important to establish how the genetic mechanisms governing the expression of GlyR channels are regulated during development and the establishment of intercellular interactions, and also to determine whether neuronal functions are able to modulate these mechanisms. In the context of the elaboration of circuitry during development and adaptative changes upon stimulation, synaptogenesis becomes an intriguing process which is underpinned by precise sorting events, specifying ion channels and receptor targeting in a highly differentiated membrane.

One important issue is to understand posttranslationnal processing, targeting to specific sites, restriction of mobility, and changes in metabolic stability during development and eventually neuronal activity that apply to this receptor. To this end, a promising step was to identify gephyrin as a crucial partner for membrane insertion. Proteins with putative anchoring and/or clustering functions are being actively sought. Besides rapsyn, or neuronal ankyrin, which is supposed to anchor sodium channels at nodes of Ranvier (Froehner, 1993), a major protein of the postsynaptic density, PSD-95, is currently attracting much attention. It interacts with the cytoplasmic domain of NMDA receptor 2A and 2B subunits and is involved in the cell-surface clustering of Shaker-type potassium channels (Kornau *et al.*, 1995; Niethammer *et al.*, 1996; Kim *et al.*, 1995). PSD-95 belongs to a growing family of multimodular proteins associated with intercellular junctions having a highly organized membrane cytoskeleton and thought to control the nucleation of multiprotein signaling complexes in the vicinity of junctions. Among these proteins, the *Drosophila* septate junction protein encoded by the dlg-A gene is essential for normal organization of synaptic structure, which is consistent with binding of this protein to integral mem-

brane proteins and with the idea that members of this family may locally organize the cytoskeleton.

The neuron evolved from simpler eukaryotic cells. On one hand, these have enabled biosynthetic membrane traffic to be understood in molecular terms, revealing a general and fair conservation and analogy of sorting and targeting events from yeast to higher metazoans. On the other hand, genetic manipulation of eukaryotic cells confirms that many cell components of exogenous origin can function in various mechanisms, as do their endogenous, or often homologous, counterparts. Therefore, there is no reason why neuron cell biology should not benefit from the accumulated knowledge of reconstituted systems, including nonneuronal ones, since only variations on the same theme account for conserved basic mechanisms of membrane dynamics.

References

Akagi, H., and Miledi, R. (1988). Heterogeneity of glycine receptors and their messengers RNAs in rat brain and spinal cord. *Science* **242,** 270–273.

Akagi, H., Patton, E., and Miledi, R. (1989). Discrimination of heterogeneous mRNAs encoding strychnine-sensitive glycine receptors in *Xenopus* oocytes by antisense oligonucleotides. *Proc. Natl. Acad. Sci. USA* **86,** 8103–8107.

Altschuler, R., Betz, H., Parakkal, M. H., Reeks, K. A., and Wenthold, R. J. (1986). Identification of glycinergic synapses in the cochlear nucleus through immunocytochemical localization of the postsynaptic receptor. *Brain Res.* **369,** 316–320.

Alvarez, F. J., Harrington, D., Dewey, D. E., and Fyffe, R. (1993). Distribution of glycine receptors on single intracellularly labeled motoneurons of the cat lumbar spinal cord. *Soc. Neurosci. Abstract* **19,** 983.

Aprison, M. H. (1990). The discovery of the neurotransmitter role of glycine. *In* Glycine Neurotransmission" (O. P. Ottersen and J. Storm-Mathisen, eds.), pp. 1–23. Wiley, New York.

Aprison, M. H., and Daly, E. C. (1978). Biochemicals aspects of transmission at inhibitory synapses: The role of glycine. *In* "Advances in Neurochemistry 3" (B. W. Agranoff and M. H. Aprison, eds.), pp. 203–294. Plenum, New York.

Aprison, M. H., Daly, E. C., Shank, R. P., and McBride, W. J. (1975). Neurochemical evidence for glycine as a transmitter and a model for its intrasynaptosomal compartimentation. *In* "Metabolic Compartmentation and Neurotransmission" (S. Berl, D. D. Clarke, and D. Schneider, eds.), pp. 37–63. Plenum, New York.

Araki, T., Yamano, M., Murakami, T., Wanaka, A., Betz, H., and Tohyama, M. (1988). Localization of glycine receptors in the rat central nervous system: An immunocytochemical analysis using monoclonal antibody. *Neuroscience* **2,** 613–624.

Audinat, E., Knöpfel, T., and Gähwiler, B. H. (1990). Responses to excitatory amino acids of Purkinje cells and neurones of the deep nuclei in cerebellar slice cultures. *J. Physiol.* **430,** 297–313.

Basbaum, A. (1988). Distribution of glycine receptor immunoreactivity in the spinal cord of the rat: Cytochemical evidence for a differential glycinergic control of lamina I and V nociceptive neurons. *J. Comp. Neurol.* **278,** 330–336.

Baude, A., Sequier, J. M., McKernan, R. M., Olivier, K. R., and Somogyi, P. (1992). Differential subcellular distribution of the $\alpha 6$ subunit versus the $\alpha 1$ and $\beta 2/3$ subunits of the $GABA_A$/benzodiazepine receptor complex in granule cells of the cerebellar cortex. *Neuroscience* **51,** 739–748.

Baude, A., Nusser, Z., Roberts, J. D. B., Mulvihill, E., McIlhinney, R. A. J., and Somogyi, P. (1993). The 1α form of metabotropic glutamate receptor (mGluR1α) is concentrated at extra- and peri-synaptic membrane of discrete sub-population of neurons as detected by immunogolg reaction in the brain. *Neuron* **11,** 771–787.

Béchade, C., Sur, C., and Triller, A. (1994). The inhibitory neuronal glycine receptor. *BioEssays* **16,** 735–744.

Béchade, C., Colin, I., Kirsch, J., Betz, H., and Triller, A. (1995). Expression of glycine receptor α subunits and gephyrin in cultured spinal neurons. *Eur. J. Neurosci.* **8,** 429–435.

Becker, C.-M. (1990). Disorders of the inhibitory glycine receptor: The spastic mouse. *FASEB J.* **4,** 2767–2774.

Becker, C.-M. (1992). Selective neurotoxicity: Convulsants acting at the inhibitory glycine receptor. *In* "Handbook of Experimental Pharmacology" (H.F. Herken and F. Hucho, eds.), pp. 539-575. Springer-Verlag, Heidelberg.

Becker, C.-M. (1995). Glycine receptors: Molecular heterogeneity and implications for disease. *Neuroscientist* **1,** 130–141.

Becker, C.-M., Hermans-Borgmeyer, I., Schmitt, B., and Betz, H. (1986). The glycine receptor deficiency of the mutant mouse spastic: Evidence for normal glycine receptor structure and localization. *J. Neurosci.* **6,** 1358–1364.

Becker, C.-M., Hoch, W., and Betz, H. (1988). Glycine receptor heterogeneity in rat spinal cord during postnatal development. *EMBO J.* **7,** 3717–3726.

Becker, C.-M., Hoch, W., and Betz, H. (1989). Sensitive immunoassay shows selective association of peripheral and integral membrane proteins of the inhibitory glycine receptor complex. *J. Neurochem.* **53,** 124–131.

Becker, C.-M., Schmieden, V., Tarroni, P., Strasser, U., and Betz H. (1992). Isoform-selective deficit of glycine receptors in the mouse mutant *spastic*. *Neuron* **8,** 283–289.

Becker, C.-M., Betz, H., and Schroder, H. (1993). Expression of inhibitory glycine receptors in postnatal rat cerebral cortex. *Brain Res.* **606,** 220–226.

Betz, H. (1990). Ligand-gated ion channels in the brain: The amino acid receptor superfamily. *Neuron* **5,** 383–392.

Betz, H. (1992). Structure and function of inhibitory glycine receptors. *Q. Rev. Biophys.* **25,** 381–394.

Betz, H., and Becker, C.-M. (1988). The mammalian glycine recptor: Biology and structure of a neuronal chloride channel protein. *Neurochem. Int.* **13,** 137–146.

Bohlhalter, S., Mohler, H., and Fritschy, J.-M. (1994). Inhibitory neurotransmission in rat spinal cord: Co-localization of glycine- and $GABA_A$-receptors at GABAergic synaptic contacts demonstrated by triple immunofluorescence staining. *Brain Res.* **642,** 59–69.

Bormann, J., Hamill, O. P., and Sakman, B. (1987). Mechanism of anion permeation through channels gated by glycine and γ-aminobutyric acid in mouse cultured spinal neurones. *J. Physiol. (London)* **385,** 243–286.

Bormann, J., Rundstrom, N., Betz, H., and Langosch, D. (1993). Residues within transmembrane segment M2 determine chloride conductance of glycine receptor homo- and hetero-oligomers. *EMBO J.* **12,** 3729–3737.

Bristow, D. R., Bowery, N. G., and Woodruff, G. N. (1986). Light microscopic autoradiographic localization of [^{3}H]glycine and [^{3}H]strychnine binding sites in rat brain. *Eur. J. Pharmacol.* **126,** 303–307.

Brugg, B., and Matus, A. (1991). Phosphorylation determines the binding of microtubule-associated protein 2 (MAP2) to microtubules in living cells. *J. Cell Biol.* **114,** 735–743.

Buckwalter, M. S., Cook, S. A., Davisson, M. T., White, W. F., and Camper, S. (1994). A frameshift mutation in the mouse α1 glycine receptor *gene* (Glra1) results in progressive neurological symptoms and juvenile death. *Hum. Mol. Genet.* **3,** 2025–2030.

Burt, D. R., and Kamatchi, G. L. (1991). $GABA_A$ receptor subtypes: From pharmacology to molecular biology. *FASEB J.* **5,** 2916–2923.

Cabot, J. B., Bushnell, A., Alessi, V., and Mendell, N. R. (1995). Postsynaptic gephyrin immunoreactivity exhibits a nearly one-to-one correspondence with gamma-aminobutyric acid-like immunogold-labeled synaptic inputs to sympathetic preganglionic neurons. *J. Comp. Neurol.* **356,** 418–432.

Cartaud, J., and Changeux, J.-P. (1993). Post-transcriptional compartimentalization of acetylcholine receptor biosynthesis in the subneural domain of muscle and electrolyte junctions. *Eur. J. Neurosci.* **5,** 191–202.

Changeux, J.-P. (1991). Compartimentalized transcription of acetylcholine receptor genes during motor endplate epigenesis. *New Biol.* **3,** 413–429.

Chen, S., and Hillman, D. E. (1993). Colocalization of neurotransmitters in the deep cerebellar nuclei. *J. Neurocytol.* **22,** 81–91.

Colin, I., Rostaing, P., and Triller, A. (1996).Gephyrin accumulates at specific plasmalemma loci during neuronal maturation in vitro. *J. Comp. Neurol.* **374,** 467–479.

Craig, A. M., and Banker, G. (1994). Neuronal polarity. *Annu. Rev. Neurosci.* **17,** 267–310.

Craig, A. M., Blackstone, C. D., Huganir, R. L., and Banker, G. (1994). Selective clustering of glutamate and γ-aminobutyric acid receptors opposite terminals releasing the corresponding neurotransmitters. *Proc. Natl. Acad. Sci. USA* **91,** 12373–12377.

Craig, A. M., Banker, G., Chang, W., McGrath, M. E., and Serpinskaya, A. S. (1996). Clustering of gephyrin at GABAergic but not glutamatergic synapses in cultured rat hippocampal neurons. *J. Neurosci.* **16,** 3166–3177.

Devillers-Thiéry, A., Galzi, J. L., Eiselé, J. L., Bertrand, S., Bertrand D., and Changeux, J.P. (1993). Fuctional architecture of the nicotinic acetylcholine receptor: A prototype of ligang-gated ion channels. *J. Membr. Biol.* **136,** 97–112.

Eicher, E. M.,and Lane, P. W. (1980). Assignment of LG XVI to chromosome 3 in the mouse. *J. Hered.* **71,** 315–318.

Floeter, M. K., and Hallet, M. (1993). Glycine receptors: A startling connection. *Nature Genet.* **5,** 319–320.

Franksson, O., and Triller, A. (1993). Confocal microscopy and three-dimensional image analysis methods for recognition and fluorometric measurements: An application to inhibitory glycine receptor. *Neuroprotocols* **2,** 92–100.

Froehner, S. C. (1991). The submembrane machinery for nicotinic acetylcholine receptor cludtering. *J. Cell Biol.* **114,** 1–7.

Froehner, S. C. (1993). Regulation of ion channel distribution at synapses. *Annu. Rev. Neurosci.* **16,** 347–368.

Frostholm, A., and Rotter, A. (1985). Glycine receptor distribution in mouse CNS: Autoradiographic localization of [^{3}H]strychnine binding sites. *Brain Res. Bull.* **15,** 473–486.

Fujita, M., Sato, K., Sato, M., Inoue, T., Tozuka, T., and Tohyama, M. (1991). Regional distribution of the cells expressing glycine receptor β subunit mRNA in the rat brain. *Brain Res.* **560,** 23–37.

Galzi, J. L., and Changeux, J. P. (1994). Neurotransmitter-gated ion channels as unconventional allosteric proteins. *Curr. Opin. Struct. Biol.* **4,** 554–565.

Galzi, J. L., Devillers, T. A., Hussy, N., Bertrand, S., Changeux, J. P., and Bertrand D. (1992). Mutations in the channel domain of a neuronal nicotinic receptor convert ion selectivity from cationic to anionic. *Nature* **359,** 500–505.

Garcia-Calvo, M., Ruiz-Gomez, A., Vazquez, J., Morato, E., Valdivieso, F., and Major, F., Jr. (1989). Functional reconstitution of the glycine receptor. *Biochemistry* **28,** 6405–6409.

Graham, D., Pfeiffer, F., and Betz, H. (1981). UV light-induced crosslinking of strychnine to the glycine receptor of rat spinal cord membranes. *Biochem. Biophys. Res. Commun.* **102,** 1330–1335.

Graham, D., Pfeiffer, F., and Betz, H. (1983). Photoaffinity labeling of the glycine receptor of rat spinal cord. *Eur. J. Biochem.* **131,** 519–525.

Graham, D., Pfeiffer, F., Simler, R., and Betz, H. (1985). Purification and characterization of the glycine receptor of pig spinal cord. *Biochemistry* **24,** 990–994.

Greengard, P., Valtorta, F., Czernik, A. J., and Benfenati, F. (1993). Synaptic vesicle phosphoproteins and regulation of synaptic function. *Science* **259,** 780–785.

Greferath, U., Brandstatter, J. H., Wassle, H., Kirsch, J., Kuhse, J., and Grünert, U. (1994). Differential expression of glycine receptor subunits in the retina of the rat: A study using immunohistochemistry and in situ hybridization. *Visual Neurosci.* **11,** 721–729.

Greferath, U., Grünert, U., Fritschy, J. M., Stephenson, A., Möhler, H., and Wässle, H. (1995). $GABA_A$ receptor subunits have differential distributions in the rat retina: *In situ* hybridization and immunohistochemistry. *J. Comp. Neurol.* **353,** 553–571.

Grenningloh, G., Rienitz, A., Schmitt, B., Methfessel, C., Zensen, M., Beyreuther, K., Gundelfinger, E. D., and Betz, H. (1987). The strychnine-binding subunit of the glycine receptor shows homology with nicotinic acetylcholine receptors. *Nature* **328,** 215–220.

Grenningloh, G., Pribilla, I., Prior, P., Multhaup, G., Beyreuther, K., Taleb, O., and Betz, H. (1990a). Cloning and expression of the 58 kd β subunit of the inhibitory glycine receptor. *Neuron* **4,** 963–970.

Grenningloh, G., Schmieden, V., Schofield. P. R., Seeburg, P. H., Siddique, T., Mohandas, T.K., Becker, C.-M., and Betz, H. (1990b). Alpha subunit variants of the human glycine receptor: Primary structures, functional expression and chromosomal localization of the corresponding genes. *EMBO J.* **9,** 771–776.

Grünert, U., and Wässle, H. (1993). Immunocytochemical localization of glycine receptors in the mammalian retina. *J. Comp. Neurol.* **335,** 523–537.

Gu, Y., Forsayeth, J. R., Verrall, S., Yu, X. M., and Hall, Z. W. (1991). Assembly of the mammalian muscle acetylcholine receptor in transfected COS cells. *J. Cell Biol.* **114,** 799–807.

Hall, Z. W., and Sanes, J. R. (1993). Synaptic structure and development: The neuromuscular junction. *Cell/Neuron* Rev. Suppl. **72/10,** 99–121.

Heller, A. H., and Hallet, M. (1982). Electrophysiological studies with the *spastic* mutant mouse. *Brain Res.* **234,** 299–308.

Hoch, W., Betz, H., and Becker, C. M. (1989). Primary cultures of mouse spinal cord express the neonatal isoform of the inhibitory glycine receptor. *Neuron* **3,** 339–348.

Hoch, W., Betz, H., Schramm, M., Wolters, I., and Becker, C.-M. (1992). Modulation by NMDA receptor antagonists of glycine receptor isoform expression in cultured spinal cord neurons. *Eur. J. Neurosci.* **4,** 389–395.

Hökfelt, T. (1991). Neuropeptides in perspective: The last ten years. *Neuron* **7,** 867–879.

Huettner, J. E. (1990). Glutamate receptor channels in the rat DRG neurons: Activation by kainate and quisqualate and blockade of desensitization by ConA. *Neuron* **5,** 255–286.

Johnson, J. W., and Ascher, P. (1987). Glycine potentiates the NMDA response in cultured mouse brain neurons. *Nature* **325,** 529–531.

Jones, K. A., and Baughman, R. W. (1991). Both NMDA and non-NMDA subtypes of glutamate receptors are concentrated at synapses on cerebral cortical neurons in culture. *Neuron* **7,** 593–603.

Kanai, Y., and Hirokawa, N. (1995). Sorting machanisms of Tau and MAP2 in neurons: Suppressed axonal transit of MAP2 and locally regulated microtubule binding. *Neuron* **14,** 421–432.

Kelly, R. B., and Grote, E. (1993). Protein targeting in the neuron. *Annu. Rev. Neurosci.* **16,** 95–127.

Kim, E., Niethammer, M., Rothschild, A., Jan, Y. N., and Sheng, M. (1995). Clustering of Shaker-type K^+ channels by interaction with a family of membrane-associated guanylate kinases. *Nature* **378,** 85–88.

Kingsmore, S. F., Giros, B., Suh, D., Bieniarz, M., Caron, M. G., and Seldin, M. F. (1994). Glycine receptor β-subunit gene mutation in *spastic* mouse associated with LINE-1 element insertion. *Nature Genet.* **7,** 136–142.

Kirsch, J., and Betz, H. (1993). Widespread expression of gephyrin, a putative receptor-tubulin linker protein, in rat brain. *Brain Res.* **621,** 301–310.

Kirsch, J., and Betz, H. (1995). The postsynaptic localization of the glycine receptor-associated protein gephyrin is regulated by the cytoskeleton. *J. Neurosci.* **15,** 4148–4156.

Kirsch, J., Langosch, D., Prior, P., Littauer, U. Z., and Betz, H. (1991). The 93-kDa glycine receptor-associated protein binds to tubulin. *J. Biol. Chem.* **266,** 22242–22245.

Kirsch, J., Malosio, M.-L., Wolters, I., and Betz, H. (1993a). Distribution of gephyrin transcripts in the adult and developing rat brain. *Eur. J. Neurosci.* **5,** 1109–1117.

Kirsch, J., Wolters, I., Triller, A., and Betz, H. (1993b). Gephyrin antisense oligonucleotides prevent glycine receptor clustering in spinal cord. *Nature* **366,** 745–748.

Kirsch, J., Kuhse, J., and Betz, H. (1995). Targeting of glycine receptor subunits to gephyrin-rich domains in transfected human embryonic kidney cells. *Mol. Cell. Neurosci.* **6,** 450–461.

Klausner, R. D., Lippincott-Schwartz, J., and Bonifacino, J. S. (1990). The T cell antigen receptor: Insights into organelle biology. *Annu. Rev. Cell Biol.* **6,** 403–431.

Kornau, H. C., Schenker, L. T., Kennedy, M. B., and Seeburg, P. H. (1995). Domain interaction between NMDA receptor subunits and the postsynaptic density protein PSD-95. *Science* **269,** 1737–1740.

Koulen, P., Sassoè-Pognetto, M., Grünert, U., and Wässle, H. (1995). Selective clustering of $GABA_A$ and glycine receptors in the mammalian retina. *J. Neurosci.* **16,** 2127–2140.

Kuhse, J., Schmieden, V., and Betz, H. (1990a). A single amino acid exchange alters the pharmacology of neonatal rat glycine receptor subunit. *Neuron* **5,** 867–873.

Kuhse, J., Schmieden, V., and Betz, H. (1990b). Identification and functional expression of a novel ligand binding subunit of the inhibitory glycine receptor. *J. Biol. Chem.* **265,** 22317–22320.

Kuhse, J., Kuryatov, A., Maulet, Y., Malosio, M. L., Schmieden, V., and Betz, H. (1991). Alternative splicing generates two isoforms of the α2 subunit of the inhibitory glycine receptor. *FEBS Lett.* **283,** 73–77.

Kuhse, J., Laube, B., Magalei, D., and Betz, H. (1993). Assembly of the inhibitory glycine receptor: Identification of amino acid sequence motifs governing subunit stoichiometry. *Neuron* **11,** 1049–1056.

Kuhse, J., Betz, H., and Kirsch, J. (1995). The inhibitory glycine receptor: Architecture, synaptic localization and molecular pathology of a postsynaptic ion channel complex. *Curr. Opin. Neurobiol.* **5,** 318–323.

Langosch, D., Thomas, L., and Betz, H. (1988). Conserved quaternary structure of ligand-gated ion channels: The postsynaptic glycine receptor is a pentamer. *Proc. Natl. Acad. Sci. USA* **85,** 7394–7398.

Langosch, D., Becker, C.-M., and Betz, H. (1990). The inhibitory glycine receptor: A ligand-gated chloride channel of the central nervous system. *Eur. J. Biochem.* **194,** 1–8.

Langosch, D., Hoch, W., and Betz, H. (1992). The 93 kDa protein gephyrin and tubulin associated with the inhibitory glycine receptor are phosphorylated by an endogenous protein kinase. *FEBS Lett.* **298,** 113–117.

Langosch, D., Herbold, A., Schmieden, V., Bormann, J., and Kirsch, J. (1993). Importance of Arg-219 for correct biogenesis of alpha 1 homooligomeric glycine receptors. *FEBS Lett.* **336,** 540–544.

Langosch, D., Laube, B., Rundström, N., Schmieden, V., Bormann, J., and Betz, H. (1994). Decreased agonist affinity and chloride conductance of mutant glycine receptors associated with human hereditary hyperekplexia. *EMBO J.* **13,** 4223–4228.

Laube, B., Langosch, D., Betz, H., and Schmieden, V. (1995). Hyperekplexia mutations of the glycine receptor unmask the inhibitory subsite for β-amino-acids. *NeuroReport* **6,** 897–900.

Laurie, D. J., Seeburg, P. H., and Wisden, W. (1992a). The distribution of 13 GAABA receptor subunit mRNAs in the rat brain. II. Olfactory bulb and cerebellum. *J. Neurosci.* **12,** 1063–1076.

Laurie, D. J., Wisden, W., and Seeburg, P. H. (1992b). The distribution of thirteen $GABA_A$ receptor subunit mRNAs in the rat brain. III. Embryonic and postnatal development. *J. Neurosci.* **12,** 4151–4172.

Malosio, M. L., Grenningloh, G., Kuhse, J., Schmieden, V., Schmitt, B., Prior, P., and Betz, H. (1991a). Alternative splicing generates two variants of the α1 subunit of the inhibitory glycine receptor. *J. Biol. Chem.* **266,** 2048–2053.

Malosio, M. L., Marquèze-Pouey, B., Kuhse, J., and Betz, H. (1991b). Widespread expression of glycine receptor subunit mRNAs in the adult and developing rat brain. *EMBO J.* **10,** 2401–2409.

Marvizon, J. C., Vazquez, J., Garcia-Calvo, M., Major, F.,Jr., Ruiz-Gòmez, A., Valdivieso, F., and Benavides, J. (1986). The glycine receptor: Pharmacological studies and mathematical modeling of the allosteric interaction between glycine- and strychnine-binding sites. *Mol. Pharmacol.* **30,** 590–597.

Matzenbach, B., Maulet, Y., Sefton, L., Courtier, B., Avner, P., Guénet, J.-L., and Betz, H. (1994). Structural analysis of mouse glycine receptor a subunit genes. Identification and chromosomal localization of a novel variant α4. *J. Biol. Chem.* **269,** 2607–2612.

Merlie, J. P., and Smith, M. M. (1986). Synthesis and assemply of acetylcholine receptor, a multisubunit membrane glycoprotein. *J. Membr. Biol.* **91,** 1–10.

Meyer, G., Kirsch, J., Betz, H., and Langosch, D. (1995). Identification of a gephyrin binding motif on the glycine receptor β subunit. *Neuron* **15,** 563–572.

Mitchell, K., Spike, R. C., and Todd, A. J. (1993). An immunocytochemical study of glycine receptor and GABA in lamina I–III of rat spinal dorsal horn. *J. Neurosci.* **13,** 2371–2381.

Moriyoshi, K., Masu, M., Ishii, T., Shigemoto, R., Mizuno, N., and Nakanishi, S. (1991). Molecular cloning and characterization of the rat NMDA receptor. *Nature* **354,** 31–37.

Moss, S. J., Smart, T. G., Blackstone, C. D., and Huganir, R. L. (1992). Functional modulation of $GABA_A$ receptor by cAMP-dependent protein phosphorylation. *Science* **257,** 661–665.

Mülhardt, C, Fischer, M, Gass, P, Simon-Chazottes, D., Guénet, J.L., Kuhse, J., Betz, H., and Becker, C.M. (1994). The *spastic* mouse: Aberrant splicing of glycine receptor β subunit mRNA caused by intronic insertion of L1 element. *Neuron* **13,** 1003–1015.

Naas, E., Zilles, K., Gnahn, H., Betz, H., Becker, C. M., and Schroder, H. (1991). Glycine receptor immunoreactivity in rat and human cerebral cortex. *Brain Res.* **561,** 139–146.

Nakanishi, S. (1992). Molecular diversity of glutamate receptors and implications for brain function. *Science* **258,** 597–603.

Nicola, M. A., Becker, C. M., and Triller, A. (1992). Development of glycine receptor alpha subunit in cultivated rat spinal neurons: An immunocytochemical study. *Neurosci. Lett.* **138,** 173–178.

Niethammer, M., Kim, E., and Sheng, M. (1996). Interactions between the C terminus of NMDA receptor subunits and multiple members of the PSD-95 family of membrane-associated guanylate kinases. *J. Neurosci.* **16,** 2157–2163.

Nusser, Z., Mulvihill, E., Streit, P., and Somogyi, P. (1994). Subunit segregation of metabotropic and ionotropic glutamate receptors as revealed by immunogold localization. *Neuroscience* **61,** 421–427.

Nusser, Z., Roberts, J. D. B., Baude, A., Richards, J. G., Sieghart, W., and Somogyi, P. (1995). Immunocytochemical localization of the α1 and β2/3 subunit of the $GABA_A$ receptor in relation to specific GABAergic synapses in the dentate gyrus. *Eur. J. Neurosci.* **7,** 630–646.

Ortells, M. O., and Lunt, G. G. (1995). Evolutionary history of the ligand-gated ion-channel superfamily of receptors. *Trends Neurosci.* **18,** 121–127.

Ottersen, O. P., Storm-Mathisen, J., and Somogyi, P. (1988). Colocalization of glycine-like and GABA-like immunoreactivities in Golgi cell terminals in the rat cerebellum: A postembedding light and electron microscopic study. *Brain Res.* **450,** 342–353.

Persohn, E., Malherbe, P., and Richards, J. G. (1991). *In situ* hybridization histochemistry reveals a diversity of $GABA_A$ receptor subunit mRNAs in neurons of the rat spinal cord and dorsal root ganglia. *Neuroscience* **42,** 497–507.

Pfeiffer, F., and Betz, H. (1981). Solubilization of the glycine receptor from rat spinal cord. *Brain Res.* **226,** 273–279.

Pfeiffer, F., Graham, D., and Betz, H. (1982). Purification by affinity chromatography of the glycine receptor of rat spinal cord. *J. Biol. Chem.* **257,** 9389–9393.

Pfeiffer, F., Simler, R., Grenningloh, G., and Betz, H. (1984). Monoclonal antibodies and peptide mapping reveal structural similarities between the subunits of the glycine receptor of rat spinal cord. *Proc. Natl. Acad. Sci.* USA **81,** 7224–7227.

Phillips, W. D., Maimone, M. M., and Merlie, J. P. (1991). Mutagenesis of the 43-kD postsynaptic protein defines domains involved in plasma membrane targeting and AChR clustering. *J. Cell Biol.* **115,** 1713–1723.

Pinto, L. H., Grünert, U., Studholme, K. M., Yazull, S., Kirsch, J., and Becker, C. M. (1994). Glycine receptors in the retinas of normal and *spastic* mutant mice. *Invest. Ophtalmol. Visual Sci.* **35,** 3633–3639.

Pourcho, R. G., Goebel, D. J., Jojich, L., and Hazlett, J. C. (1992). Immunocytochemical evidence for the involvement of glycine in sensory centers of the rat brain. *Neuroscience* **46,** 643–656.

Pribilla, I., Takagi, T., Langosch, D., Bormann, J., and Betz, H. (1992). The atypical M2 segment of the beta subunit confers picrotoxinin resistance to inhibitory glycine receptor channels. *EMBO J.* **11,** 4305–4311.

Prior, P., Schmitt, B., Grenningloh, G., Pribilla, I., Multaup, G., Beyreuther, K., Maulet, Y., Werner, P., Langosch, D., Kirsch, J., and Betz, H. (1992). Primary structure and alternative splice variants of gephyrin, a putative glycine receptor-tubulin linker protein. *Neuron* **8,** 1161–1170.

Probst, A., Cortes, R., and Palacios, J. M. (1986). The distribution of glycine receptors in the human brain. A light microscopic autoradiographic study using [^{3}H]strychnine. *Neuroscience* **17,** 11–35.

Rajendra, S., and Schofield, P. R. (1995). Molecular mechanisms of inherited startle syndromes. *Trends Neurosci.* **18,** 80–82.

Rajendra, S., Lynch, J. W., Pierce, K. D., French, C. R., Barry, P. H., and Schofield, P. R. (1994). Startle disease mutations reduce the agonist sensitivity of the human inhibitory glycine receptor. *J. Biol. Chem.* **269,** 18739–18742.

Rajendra, S., Lynch, J. W., Pierce, K. D., French, C. R., Barry, P. H., and Schofield, P. R. (1995a). Mutations of an arginine residue in the human glycine receptor transforms beta-alanine and taurine from agonists into competitive antagonists. *Neuron* **14,** 169–175.

Rajendra, S., Vandenberg, R. J., Pierce, K. D., Cunningham, A. M., French, P. W., Barry, P. H., and Schofield, P. R. (1995b). The unique extracellular disulfide loop of the glycine receptor is a principal ligand binding element. *EMBO J.* **14,** 2987–2998.

Raymond, L. A., Blackstone, C. D., and Huganir, R. L. (1993). Phosphorylation of amino acid neurotransmitter receptors in synaptic plasticity. *Trends Neurosci.* **16,** 147–153.

Rosenmund, C., and Westbrook, G. L. (1993). Calcium-induced actin depolymerization reduces NMDA channel activity. *Neuron* **10,** 805–814.

Ruiz-Gomez, A., Morato, E., Garcia, C. M., Valdivieso, F., and Mayor, F. J. (1990). Localization of the strychnine binding site on the 48-kilodalton subunit of the glycine receptor. *Biochemistry* **29,** 7033–7040.

Ruiz-Gomez, A., Vaello, M.-L., Valdivieso, F., and Major, F., Jr. (1991). Phosphorylation of the 48-kDa subunit of the glycine receptor by protein kinase C. *J. Biol. Chem.* **266,** 559–566.

Rundström, N., Schmieden, V., Betz, H., Bormann, J., and Langosch, D. (1994). Cyanotriphenylborate: Subtype-specific blocker of glycine receptor chloride channels. *Proc. Natl. Acad. Sci. USA* **91,** 8950–8954.

Ryan, S. G., Buckwalter, M. S., Lynch, J. W., Handford, C. A., Segura, L., Shiang, R., Wasmuth, J. J., Camper, S. A., Schofield, P., and O'Connel, P. A. (1994). A missense mutation in the gene encoding the α1 subunit of the inhibitory glycine receptor in the *spasmodic* mouse. *Nature Genet.* **7,** 131–135.

Sargent, P. B. (1993). The diversity of neuronal nicotinic acetylcholine receptor. *Annu. Rev. Neurosci.* **16,** 403–443.

Sassoè-Pognetto, M., Wässle, H., and Grünert, U. (1994). Glycinergic synapses in the rod pathway of the rat retina: Cone bipolar cells express the α1 subunit of the glycine receptor. *J. Neurosci.* **14,** 5131–5146.

Sassoè-Pognetto, M., Kirsch, J., Grünert, U., Grefferath, U., Fritschy, J. M., Möhler, H. Betz, H., and Wässle, H. (1995). Colocalization of gephyrin and $GABA_A$-receptor subunits in the rat retina. *J. Comp. Neurol.* **357,** 1–14.

Sato, K., Zhang, J. H., Saika, T., Sato, M., Tada, K., and Tohyama, M. (1991). Localization of glycine receptor α1 subunit mRNA-containing neurons in the brain: An analysis using in situ hybridization histochemistry. *Neuroscience* **43,** 381–395.

Sato, K., Kiyama, H., and Tohyama, M. (1992). Regional distribution of cells expressing glycine receptor α2 subunit mRNA in the rat brain. *Brain Res.* **590,** 95–108.

Saul, B., Schmieden, V., Kling, C., Mülhardt, C., Gass, P., Kuhse, J., and Becker, C. M. (1994). Point mutation of glycine receptor alpha 1 subunit in the spasmodic mouse affects agonist responses. *FEBS Lett.* **350,** 71–76.

Schmieden, V., Grenningloh, G., Schofield, P. R., and Betz H. (1989). Functional expression in *Xenopus* oocytes of the strychnine binding 48 kd subunit of the glycine receptor. *EMBO J.* **8,** 695–700.

Schmieden, V., Kuhse, J., and Betz, H. (1992). Agonist pharmacology of neonatal and adult glycine receptor alpha subunits: Identification of amino acid residues involved in taurine activation. *EMBO J.* **11,** 2025–2032.

Schmieden, V., Kuhse, J., and Betz, H. (1993). Mutation of glycine receptor subunit creates beta-alanine receptor responsive to GABA. *Science* **262,** 256–258.

Schmitt, B., Knaus, P., Becker, C.-M., and Betz, H. (1987). The Mr 93,000 polypeptide of the glycine receptor is a peripheral membrane protein. *Biochemistry* **26,** 805–811.

Schonrock, B., and Bormann, J. (1995). Modulation of hippocampal glycine receptor channels by protein kinase C. *NeuroReport* **6,** 301–304.

Schorderet, D. F., Pescia, G., Bernasconi, A., and Regli, F. (1994). An additional family with startle disease and a G1192A mutation at the alpha1 subunit of the inhibitory glycine receptor gene. *Hum. Mol. Genet.* **3,** 1201.

Schröder, S., Hoch, W., Becker, C.-M., Grenningloh, G., and Betz, H. (1991). Mapping of antigenic epitopes on the α1 subunit of the inhibitory glycine receptor. *Biochemistry* **30,** 42–47.

Seeburg, P. H. (1993). The molecular biology of mammalian glutamate receptor channels. *Trends Neurosci.* **16,** 359–365.

Seitanidou, T., Triller, A., and Korn, H. (1988). Distribution of glycine receptors on the membrane of a central neuron: An immunoelectron microscopy study. *J. Neurosci.* **8,** 4319–4333.

Seitanidou, T., Nicola, M.-A., Triller, A., and Korn, H. (1992). Partial glycinergic denervation induces changes in the distribution of a glycine receptor-associated protein in a central neuron. *J. Neurosci.* **12,** 116–131.

Sherrington, C. (1906). "The Integrative Action of the Nervous System." Cambridge Univ. Press, Cambridge, UK.

Shiang, R., Ryan, S. G., Zhu, Y. Z., Hahn, A. F., O'Connell, P., and Wasmuth, J. J. (1993). Mutations in the alpha 1 subunit of the inhibitory glycine receptor cause the dominant neurologic disorder, hyperekplexia. *Nature Genet.* **5,** 351–358.

Shigemoto, R., Ohishi, H., Nakanishi, S., and Mizuno, N. (1992). Expression of the mRNA for the rat NMDA receptor (NMDAR1) in the sensory and autonomic ganglion neurons. *Neurosci. Lett.* **144,** 229–232.

Somogyi, P., Takagi, H., Richards, J. G., and Möhler, H. (1989).Subcellular localization of benzodiazepine/$GABA_A$ receptors in the cerebellum of rat, cat, and monkey using monoclonal antibodies. *J. Neurosci.* **9,** 2197–2209.

Song, Y., and Huang, L. Y. M. (1990). Modulation of glycine receptor channels by cAMP-dependent protein kinase in spinal trigeminal neurons. *Nature* **348,** 242–245.

Sontheimer, H., Becker, C. M., Pritchett, D. B., Schofield, P. R., Grenningloh, G., Kettenmann, H., Betz, H., and Seeburg, P. H. (1989). Functional chloride channels by mammalian cell expression of rat glycine receptor subunit. *Neuron* **2,** 1491–1497.

St John, P., and Stephens, S. (1993). Adult-type glycine receptor form clusters on embryonic rat spinal cord neurons developing in vitro. *J. Neurosci.* **13,** 2749–2757.

Sumikawa, K., and Miledi, R. (1989). Change in desensitization of cat muscle acetylcholine receptor caused by coexpression of torpedo acetylcholine receptor subunits in Xenopus oocytes. *Proc. Natl. Acad. Sci. USA* **86,** 367–371.

Sur, C., Triller, A., and Korn, H. (1995). Morphology of the release site of inhibitory synapses on the soma and dendrite of an identified neuron. *J. Comp. Neurol.* **351,** 247–260.

Takagi, T., Pribilla, I., Kirsch, J., and Betz, H. (1992). Coexpression of the receptor-associated protein gephyrin changes the ligand binding affinities of $\alpha 2$ glycine receptors. *FEBS Lett.* **303,** 178–180.

Takahashi, T., Momiyama, A., Hirai, K., Hishinuma, F., and Akagi, H. (1992). Functional correlation of fetal and adult forms of glycine receptors with developmental changes in inhibitory synaptic receptor channels. *Neuron* **9,** 1155–1161.

Taleb, O., and Betz, H. (1994). Expression of the human glycine receptor $\alpha 1$ subunit in Xenopus oocytes: Apparent affinities of agonists increase at high receptor density. *EMBO J.* **13,** 1318–1324.

Todd, A. J. (1990). An electron microscope study of glycine-like immunoreactivity in laminae I–III of the spinal dorsal horn of the rat. *Neuroscience* **39,** 387–394.

Todd, A. J., and Sullivan, A. C. (1990). Light microscope study of the coexistence of GABA-like and glycine-like immunoreactivities in the spinal cord of the rat. *J. Comp. Neurol.* **296,** 496–505.

Todd, A. J., Spike, R. C., Chong, D., and Neilson, M. (1995). The relationship between glycine and gephyrin in synapses of the rat spinal cord. *J. Neurosci.* **16,** 974–982.

Todd, A. J., Watt, C., Spike, R. C., and Sieghart, W. (1996). Colocalization of GABA, glycine, and their receptors at synapses in the rat spinal cord. *Eur. J. Neurosci.* **7,** 1–11.

Triller, A., Cluzeaud, F., Pfeiffer, F., Betz, H., and Korn, H. (1985). Distribution of glycine receptors at central synapses: an immunoelectron microscopy study. *J. Cell Biol.* **101,** 683–688.

Triller, A., Cluzeaud, F., and Korn, H. (1987). Gamma-aminobutyric acid-containing terminals can be apposed to glycine receptors at central synapses. *J. Cell Biol.* **104,** 947–956.

Triller, A., Seitanidou, T., Franksson, O., and Korn, H. (1990). Size and shape of glycine receptor clusters in a central neuron exhibit a somato-dendritic gradient. *New Biol.* **2,** 637–641.

Triller, A., C., Sur, C., and Korn, H. (1993a). Different distribution of glycinergic and GABAergic innervation on an identified neuron. *J. Comp. Neurol.* **338,** 83–96.

Triller, A., Sur, C., Storm-Mathisen, J., Ottersen, O.P., and Korn, H. (1993b). Glycine and GABA coexist in the same presynaptic boutons of the rat spinal cord. *Eur. J. Neurosci.* **Suppl. 6,** 729.

Tyndale, R. F., Hales, T. G., Olsen, R. W., and Tobin, A. J. (1994). Distinctive patterns of $GABA_A$ receptor subunits mRNAs in 13 cell lines. *J. Neurosci.* **14,** 5417–5428.

Uchiyama, M., Hirai, K., Hishinuma, F., and Akagi, H. (1994). Down-regulation of glycine receptor channels by protein kinase C in Xenopus oocytes injected with synthetic RNA. *Mol. Brain Res.* **24,** 295–300.

Unwin, N. (1989). The structure of ion channels in membranes of excitable cells. *Neuron* **3,** 665–676.

Unwin, N. (1993). Neurotransmitter action: Opening of ligand-gated ion channels. *Cell* **72/** *Neuron* **10** (Suppl.), 31–41.

Vaello, M. L., Ruiz, G. A., Lerma, J., and Mayor, F. J. (1994). Modulation of inhibitory glycine receptors by phosphorylation by protein kinase C and cAMP-dependent protein kinase. *J. Biol. Chem.* **269,** 2002–2008.

Vandenberg, R. J., French, C. R., Barry, P. H., Shine, J., and Schofield, P. R. (1992a). Antagonism of ligand-gated ion channel receptors: Two domains of the glycine receptor alpha subunit form the strychnine-binding site. *Proc. Natl. Acad. Sci. USA* **89,** 1765–1769.

Vandenberg, R. J., Handford, C. A., and Schofield, P. R. (1992b). Distinct agonist- and antagonist-binding sites on the glycine receptor. *Neuron* **9,** 491–496.

Van den Pol, A. N., and Gorcs, T. (1988). Glycine and glycine receptor immunoreactivity in brain and spinal cord. *J. Neurosci.* **8,** 472–492.

Wagner, K., Edson, K., Heginbotham, L., Post, M., Huganir, R. L., and Czernick, A. (1991). Determination of the tyrosine phosphorylation sites of the nicotinic acetylcholine receptor. *J. Biol. Chem.* **266,** 23784-23789.

Wang, L.-Y., Taverna, F. A., Huang, X. P., MacDonald, J. F., and Hampson, D. R. (1993). Phosphorylation and modulation of a kainate receptor (Glu-R6) by cAMP-dependent protein kinase. *Science* **259,** 1173–1175.

Werman, R., Davidoff, R. A., and Aprison, M. H. (1967). Inhibition of motoneurons by iontophoresis of glycine. *Nature* **214,** 681–683.

Werman, R., Davidoff, R. A., and Aprison, M. H. (1968). Inhibitory action of glycine on spinal neurons in the cat. *J. Neurophysiol.* **31,** 81–95.

White, W. F. (1985). The glycine receptor in the mutant mouse spastic (spa): Strychnine binding characteristics and pharmacology. *Brain Res.* **329,** 1–6.

Wisden, W., Laurie, D. J., Monyer, H., and Seeburg, P. H. (1992). The distribution of 13 $GABA_A$ receptor subunit mRNAs in the rat brain. I. Telencephalon, diencephalon, mesencephalon. *J. Neurosci.* **12,** 1040–1062.

Yazulla, S., and Studholme, K.M. (1991). Glycine-receptor immunoreactivity in retinal bipolar cells is postsynaptic to glycinergic and BABAergic amacrine cell synapses. *J. Comp. Neurol.* **310,** 11–20.

Young, A. B., and MacDonald, R. L. (1983). Glycine as a spinal cord neurotransmitter. *In* "Handbook of the Spinal Cord" (R. A. Davidoff ed.), Vol. 1, pp. 1–43. Dekker, New York.

Young, A. B., and Snyder, S. H. (1973). Strychnine binding associated with glycine receptors of the central nervous system. *Proc. Natl. Acad. Sci. USA* **70,** 2832–2836.

Young, A. B., and Snyder, S. H. (1974). Strychnine binding in rat spinal cord membranes associated with the synaptic glycine recptor: Cooperativity of glycine interactions. *Mol. Pharmacol.* **10,** 790–809.

Zarbin, M. A., Wamsley, J. K., and Kuhar, M. J. (1981). Glycine receptor: Light microscopic autoradiographic localization with [^{3}H]strychnine. *J. Neurosci.* **1,** 532–547.

Cell Fate Specification by Localized Cytoplasmic Determinants and Cell Interactions in Ascidian Embryos

Hiroki Nishida
Department of Life Science, Tokyo Institute of Technology, Nagatsuta, Midori-ku, Yokohama 226, Japan

Tadpole larvae of ascidians show the basic body plan of chordates. An ascidian larva consists of only a few types of cells and has a relatively small number of cells. Cell lineages are invariant among individuals and have been described in detail. These advantages facilitate the analysis of how the fate of each blastomere becomes specified during development. Over a century of research on ascidian embryogenesis has uncovered many interesting features concerning cellular mechanisms responsible for the fate specification. During embryogenesis, the developmental fate of a blastomere is specified by one of three different mechanisms: localized maternal cytoplasmic determinants, inductive interactions, or lateral inhibition in an equivalence cell group.

KEY WORDS: Ascidian embryogenesis, Developmental fates, Cell lineages, Cytoplasmic determinants, Induction, Equivalence group, Lateral inhibition, Embryonic axes.

I. Introduction

Fertilized eggs cleave many times to give rise to multicellular organisms. Within a multicellular embryo, some embryonic blastomeres develop into one type of tissue, whereas other blastomeres develop into another type of tissue. Each cell of an early embryo becomes restricted to a particular developmental fate by developing along one of several developmental pathways. A central question in developmental biology is how developmental fates of embryonic cells are specified. This is an important question in embryology that many researchers have been interested in since the end of the 19th century. Experimental embryology of ascidians began over a

Copyright © 1997 by Academic Press.
All rights of reproduction in any form reserved.

century ago. Chabry (1887) was the first investigator to destroy particular blastomeres of ascidian embryos and observe the effect on development. Chabry's experiments marked the beginning of experimental embryology of animal development. The present chapter will focus on recent advances in the experimental embryology of ascidians and on various cellular mechanisms proposed to date that are thought to be responsible for the specification of each cell type comprising the ascidian larva.

The phylum Chordata includes ascidians as well as all vertebrates. Ascidians are simple marine invertebrate chordates. Until the studies of Kowalevsky (1866, 1871), ascidians were considered to be mollusks. Kowalevsky described the structure of the ascidian larva and the morphological aspects of how ascidians develop. His findings caused great excitement because the anatomy of the short-lived ascidian larve, unlike that in any other invertebrate, closely exhibits the basic morphology of a vertebrate. Ascidian larvae have a dorsal nerve cord and notochord. While tadpole larvae exhibit the basic body plan of a vertebrate, the ascidian larval body plan is relatively simple, consisting of only a few kinds of tissue and of a relatively small number of cells. This less complex body plan allows us to analyze the various mechanisms of cellular specification for each cell type more easily. Indeed, it is now possible to understand the cellular basis of how the tadpole larva is formed during development. The study of ascidian embryogenesis made exciting new contributions toward understanding the development of higher vertebrates as well as helping our understanding of the basic developmental processes that are shared by all chordates.

II. General Aspects of Ascidian Embryogenesis

A. Larval Structure

Most ascidian species produce eggs that develop into tadpole larvae. Tadpole larvae settle on a suitable benthic substrate and are transformed into adults by way of complex metamorphic processes. This type of developmental strategy is termed "indirect development" or "urodele development." However, in approximately 3000 ascidian species, there are 20 or so species that exhibit "direct" or "anural" development in which the development of a tailed larvae is absent (Berrill, 1931; Jeffery and Swalla, 1990, 1992). In this section, we will discuss the basic features of the ascidian tadpole larvae.

Fertilized eggs of hermaphrodite ascidians quickly develop into bilaterally symmetrical tadpole larvae consisting of a head or trunk region and a

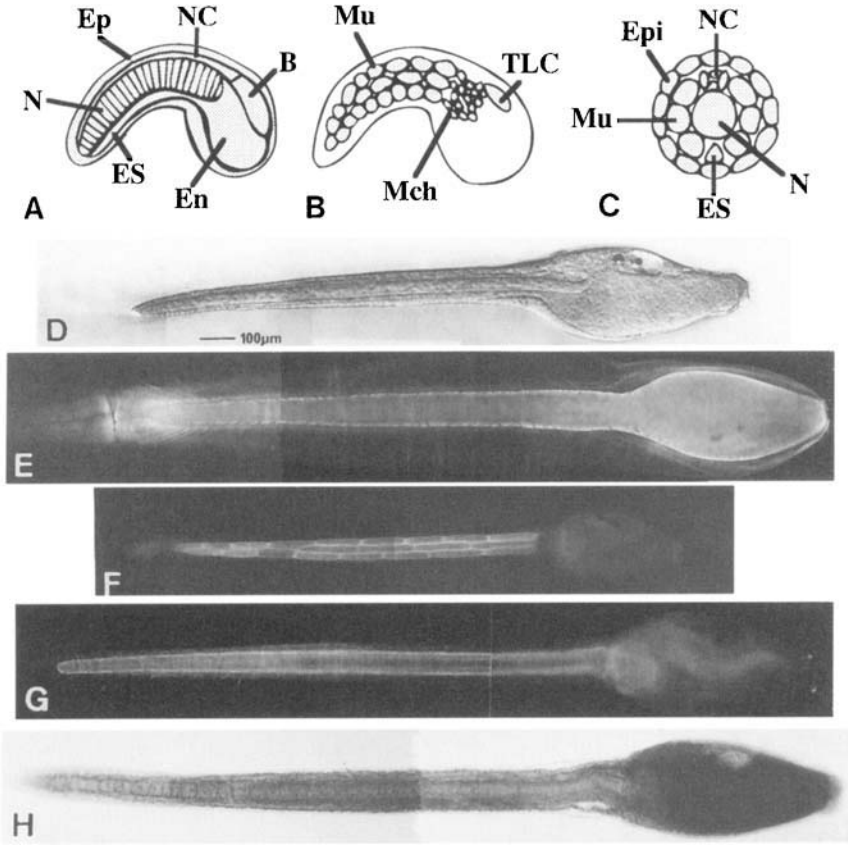

FIG. 1 (A–C) Structures of ascidian embryos at the tailbud stage. (A) Mid-sagittal section; (B) sagittal section; (C) cross section through the tail. N, notochord; Ep, epidermis; NC, nerve cord; B, brain; ES, endodermal strand; En, endoderm; Mu, muscle; Mch, mesenchyme; TLC, trunk lateral cells. (D) A hatched swimming larva of *Halocynthia roretzi*. (E–H) Various tissues of the larvae were stained with markers of tissue differentiation. (E) Epidermis was stained with epidermis-specific antibody. (F) Muscle was stained with NBD–phallacidin, which binds to filamentous actin. (G) Notochord was stained with notochord-specific monoclonal antibody. (H) Endoderm was histochemically stained for alkaline phosphatase. From Nishida (1993, 1994a).

tail region (Fig. 1). The basic anatomy of an ascidian larva resembles that of the amphibian tadpole, but ascidian larvae are about 1.5 mm long, for example, in *Halocynthia roretzi*. They have a notochord in the central region of the tail and a central nervous system situated on the dorsal side. Pharyngeal gill slits are present in larvae of some species. These features are common to all chordates. The structure of a tadpole larva is simple

compared to that of the vertebrate body. Essentially, major components of the larvae are the epidermis, notochord, muscle, mesenchyme, endoderm, and nervous system (Katz, 1983). Among these cell types, only the nervous system is most complex and contains several cell types (Nicol and Meinertzhagen, 1991). The other larval tissues consist of morphologically homogeneous populations of cells. Each larval tissue is bilaterally arranged except for the brain, a vesicle structure that shows an invariant left–right asymmetry. The total number of larval cells is relatively few, approximately 2500 (Monroy, 1979).

Approximately 800 epidermis cells surround a whole larva (Figs. 1A, 1D, and 1E). The epidermis of the anterior tip is specialized to three palps, adhesive organs used to attach to substratum at the time of settlement. Epidermis cells secrete materials for the larval tunic (Mancuso, 1974; Lübbering *et al.*, 1992). In the median plane, some cells of the peripheral nervous system are present in the epidermal layer, close to the surface of the larvae (Torrence and Cloney, 1982; Crowther and Whittaker, 1994). These cells are thought to be mechanosensory cells.

The central nervous system is positioned on the dorsal side. The so-called brain is located in the dorsal region of the trunk (see Fig. 18B). The brain is also called the sensory vesicle, as it may not be a genuine brain. In this article, I used "brain," which has been traditionally used by ascidian researchers. An otolith protrudes into the brain vesicle and senses gravity. Posterior to the brain vesicle are an ocellus, which senses light, and visceral ganglion. These structures are important in controlling larval behavior during settlement. A hollow nerve cord is present in the dorsal region of the tail, which is made up of ependimal glial cells and axon bundles. The structures of the central nervous system of the ascidian larva have been described in detail by Nicol and Meinertzhagen (1991).

The major mesodermal tissues are muscle, notochord, and mesenchyme. On either side of the notochord in the tail region, there are 21 muscle cells that are aligned in three rows in *H. roretzi* (Figs. 1B, 1C, and 1F). In *Ciona intestinalis,* the number of muscle cells on each side is 18. These muscle cells are striated, but they never fuse with each other and therefore remain mononucleated. In the center of the tail, there are precisely 40 notochord cells in most solitary ascidian species (Figs. 1A and 1G). Notochord cells are vacuolated cells that are initially disc-shaped and undergo elongation along the anterior–posterior axis. This change in cell shape results in tail elongation (Cloney, 1964; Miyamoto and Crowther, 1985). There are clusters of mesenchyme cells bilaterally situated in the trunk region (Fig. 1B). In addition to these major types of mesodermal tissue, two minor types of mesodermal tissue have been identified. On either side of the visceral ganglion, there are trunk lateral cells (TLCs) (Nishida, 1987), while trunk ventral cells (TVCs) are present ventrolaterally to the endoderm (Whit-

taker, 1990). These three larval cell types, mesenchyme, TLC, and TVC, are maintained in larvae as stem cells that undergo terminal differentiation after metamorphosis and give rise to adult cells. For example, mesenchyme cells give rise to tunic cells. TLCs give rise to coelomic blood cells and body wall muscle cells. TVCs give rise to heart and body wall muscle cells (Hirano and Nishida, unpublished observation).

Tadpole larvae of *Halocynthia* do not feed until completion of metamorphosis. They do not have a mouth. Endodermal cells look homogeneous and are preserved for formation of the branchial suck and digestive organs in adults. Thus, the structure of the tadpole larvae is simple. Ascidian embryogenesis provides a simple model system for investigating mechanisms of fate specification.

B. Embryogenesis

The time that is required for embryogenesis of *H. roretzi, C. intestinalis,* and *Ascidia ahodori* is shown in Table I. Fertilized eggs quickly develop into tadpole larvae. In *Halocynthia,* the first cleavage occurs at 1 hr 45 min, and the embryos continue to divide every 50 min until the 8-cell stage at 13°C. Asynchronous cleavages occur three times, resulting in a 64-cell embryo that corresponds to the late blastula stage. Cleavages occur bilaterally. The pattern is complicated, but is invariant among individuals (Conklin, 1905b; Satoh, 1979; Nishida, 1986). Each blastomere is designated by a unique letter and number code (see Fig. 4).

Gastrulation begins at the 110-cell stage (Figs. 2A, 2B, and 4). Ascidian embryos do not have a blastocoel. A single layer of endoderm and mesoderm cells invaginates into the interior of the blastula, pushing against a

TABLE I
Time Table of Ascidian Embryogenesis

	Halocynthia roretzi (Maboya)[a] at 13°C	*Ciona intestinalis* (Katayuureiboya) at 18°C	*Ascidia ahodori* (Natsumeboya) at 25°C
First cleavage	1.8 hr	1 hr	0.7 hr
Late blastula	8 hr	4.5 hr	2.8 hr
Gastrula	9–12 hr	5–6 hr	3–4 hr
Neurula	13–17 hr	7–8 hr	4–6 hr
Early tailbud	18 hr	9 hr	6 hr
Hatch (swimming larva)	35 hr	18 hr	11 hr

[a] Japanese name of each species is indicated in parentheses.

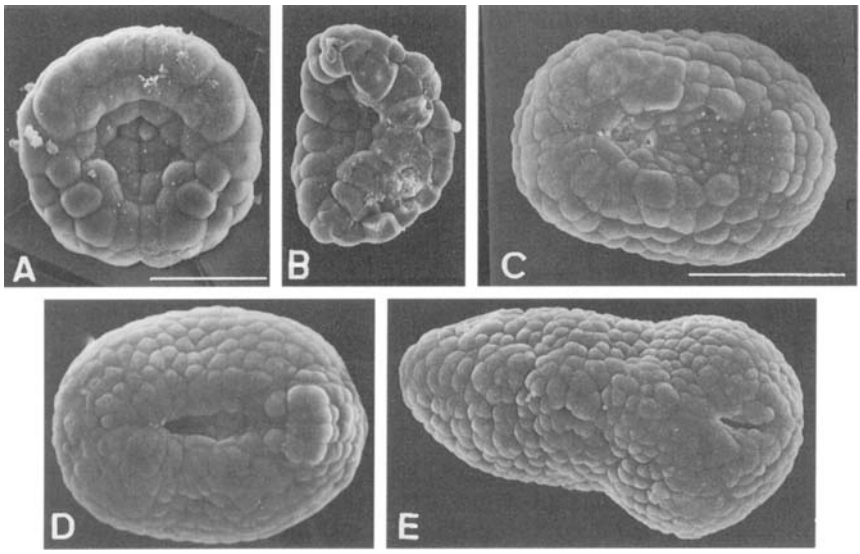

FIG. 2 Scanning electron micrographs of developing *Halocynthia* embryos. (A) Gastrula at the 118-cell stage. Vegetal view. Anterior is up. (B) Embryo dissected in the median plane at the 188-cell stage. Archenteron is invaginating. (C) Early neurula, dorsal view. Anterior is to the right. Blastopore is closing. (D) Middle neurula. Neural tube is closing. (E) Initial tailbud at 18 hr of development. Scale bar, 100 μm. From Nishida (1986).

single layer of ectoderm cells. During the neurula stage, the dorsal neural tube closes from posterior to anterior (Figs. 2C, 2D, and 2E). The mechanism of neural tube formation demonstrates the close relationship of the ascidian and vertebrates. The head and tail region can be distinguished at 18 hr of development and embryos are at the tailbud stage (Fig. 2E). Following elongation of the tail, the almost completely formed larvae hatches from the vitelline membrane at 35 hr. Larvae swim for about 1 day and then attach to an appropriate substrate and begin metamorphosis (Willey, 1893a,b; Ishikawa *et al.*, 1972; Cloney, 1978).

C. Cell Lineages

During every cell division of a fertilized ascidian egg, cell fates become progressively restricted in a highly determinate manner. The mechanism responsible for restriction of cell fate is one of the most interesting subjects in developmental biology. Detailed descriptions of cell lineages of ascidian embryos have provided a basis for experimental studies of cell fate specification.

The ascidian cell lineages were first described in detail by Conklin (1905b), whose observations were later confirmed and amended by Ortolani (1955, 1957, 1962). Recently, cell lineages was reexamined using modern cell labeling techniques by Nishida (1987). The developmental fate of each blastomere was investigated by labeling individual blastomeres by intracellular injection of horse radish peroxidase (HRP) and following the fates of HRP-containing descendant clones. Most of the previous descriptions were reconfirmed and some were amended. Tracing cell lineages using HRP has provided detailed information on the clonal organization of the larvae. Nicol and Meinertzhagen (1988a,b) described the cell lineage of the central nervous system in detail using scanning electron microscopy and by observation of serial sections of developing embryos. The cell lineages of the ascidian embryo have now been well established.

Ascidian cell lineages exhibit the following features (Fig. 3): (1) The cleavage pattern is bilaterally symmetrical. Cleavage patterns are complicated, but are invariant among individual embryos and among all indirect developing species examined to date. Embryonic cells are designated according to the naming system of Conklin (1905b) (Fig. 4). (2) The developmental fate of each blastomere is also invariant. Developmental fates are rigidly determinate as to the type of tissue, the position, and probably even the cellular number of the derived clones. For example, the B7.4 blastomere

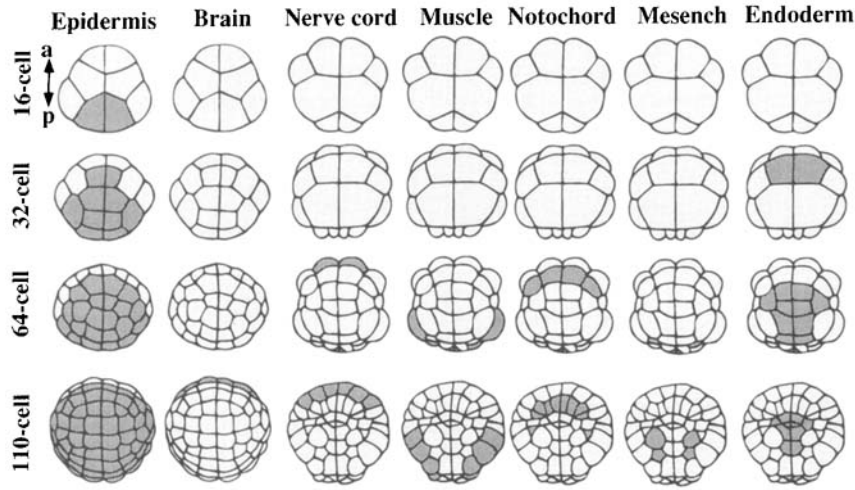

FIG. 3 Restriction of developmental fate during cleavage stages. Blastomeres are shaded when the developmental fate is restricted to give rise to cells of a single type of tissue, indicated above. Stages are shown to the left. For epidermis and brain, embryos are viewed from the animal pole. For nerve cord, muscle, notochord, mesenchyme (Mesench), and endoderm, embryos are viewed from the vegetal pole.

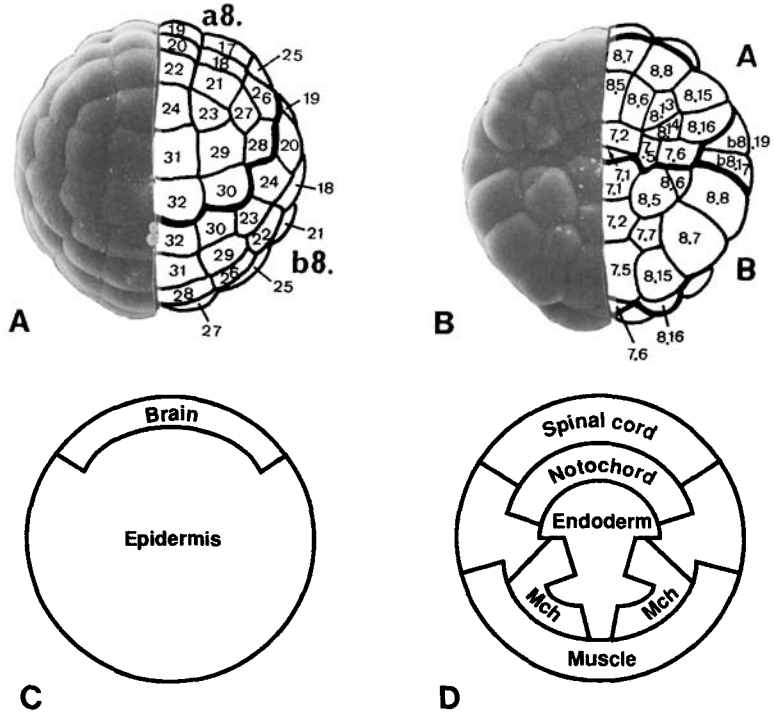

FIG. 4 (A and B) Animal and vegetal hemispheres at the 110-cell stage, respectively. Anterior is up, and posterior is down. Embryo is bilaterally symmetrical. In the right halves of embryos, the name of each blastomere is indicated. For example, a right–anterior blastomere in the animal hemisphere is a8.25. Boundaries between the a, b, A, and B-line cells are indicated by thick lines. (C and D) Fate maps of animal and vegetal hemispheres, respectively. Lateral portion of the vegetal hemisphere is not shown because it is somewhat complicated.

of the 64-cell embryo divides three times, giving rise to 8 muscle cells in the middle part of the tail. (3) Tissues are generated by a relatively small number of cell divisions. Most cells of the larva are formed 9–12 cell divisions after the first cleavage. For example, most of the 42 muscle cells of a swimming larva of *Halocynthia* differentiate after 9 cell divisions. Similarly, the 40 notochord cells are generated by 9 cell divisions after fertilization. (4) The clonal restriction of developmental fates takes place relatively early in development. The fates of blastomeres are gradually restricted and blastomeres arise which are destined to form a single type of tissue. Cells whose descendants contribute exclusively to the formation of a single cell type are designated primordial cells. Figure 3 summarizes when fates are restricted during embryonic cleavage. The fate of the two blastomeres of the animal hemisphere is first restricted to exclusively form

the epidermis at the 16-cell stage. Then, a pair of vegetal cells are restricted to become endoderm at the 32-cell stage. At the 64-cell stage, blastomeres appear that are restricted to form nerve cord, muscle, notochord, mesenchyme, and trunk lateral cells. At the 110-cell stage, the brain lineage separates from the epidermis lineage in the anterior region of the embryos. The number of blastomeres which generate a single type of tissue is 48 at the 64-cell stage and 102 at the 110-cell stage. Thus, by the initiation of gastrulation, most blastomeres of the 110-cell embryo are fated to give rise to a single cell type. This is a unique feature of ascidian embryogenesis and is not found in the development of other animals. (5) The fate map of the ascidian embryo closely resembles that of the amphibian embryo. The fate map of an ascidian blastula is shown in Fig. 4. Cells of the animal hemisphere give rise to the epidermis and brain. Various mesodermal tissues are derived from the marginal zone. Vegetal pole cells develop into endoderm. Comparison between the ascidian fate map and that of the amphibian reveals that the so-called anterior region of the ascidian embryo corresponds to the dorsal region of the amphibian embryo. The notochord and neural rudiment are located in these regions.

III. Localized Cytoplasmic Determinants in Eggs and Embryos

A. Ooplasmic Segregation

Eggs of many kinds of animals show the movement of egg cytoplasm just after fertilization (Sardet *et al.,* 1994). The ooplasm of oscidian eggs undergoes dramatic movement between fertilization and the beginning of the first cleavage, and this process is known as ooplasmic segregation (Conklin, 1905b). Movement of the ooplasm that is inherited by muscle-lineage blastomeres during cleavage and ultimately by muscle cells of larva has been especially well described in several ascidians (Conklin, 1905b; Sawada and Osanai, 1981; Jeffery and Meier, 1983; Bates and Jeffery, 1988; Sardet *et al.,* 1989). This ooplasm is referred to as the myoplasm (Conklin, 1905c). In some species, pigment granules (e.g., the yellow pigment in *Styela*) are concentrated in the myoplasm, making this portion of the embryonic cytoplasm easily distinguishable from other embryonic regions (Conklin, 1905b; Bates and Jeffery, 1988).

Figure 5 shows ooplasmic segregation in eggs of *H. roretzi* (Hirai, 1941; Nishida, 1994b). In *Halocynthia* eggs, the myoplasm is recognizable as a transparent region of egg cytoplasm and is located in the cortex of unfertilized eggs except for the animal pole region (Fig. 5A). The first meiotic

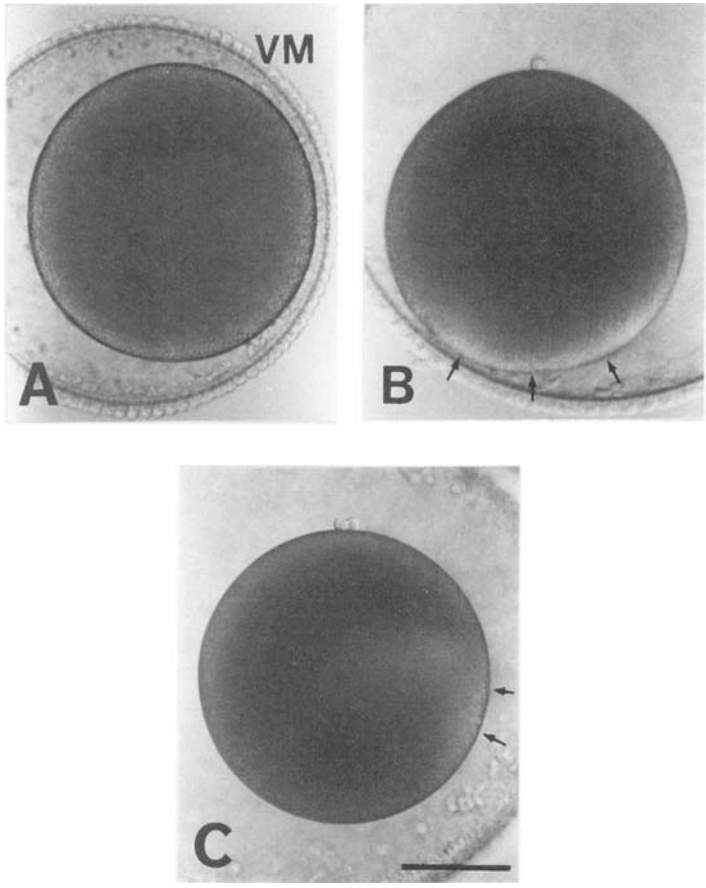

FIG. 5 Ooplasmic segregation in *Halocynthia* eggs. (A) Unfertilized egg. VM, vitelline membrane. (B) A fertilized egg after the first phase of segregation. The transparent myoplasm (arrows) has moved toward the vegetal pole. The first polar body is visible at the animal pole. (C) An egg after the second phase of segregation. The myoplasm (arrows) has moved toward the future posterior pole. The second polar body is visible. Scale bar, 100 μm. For color photographs of the sectioned eggs, see Fig. 1 of Nishida (1994b). From Nishida (1994b).

spindle is located at the animal pole. Movement of the ooplasm occurs in two phases between fertilization and first cleavage. The first phase of ooplasmic segregation (0–10 min after insemination at 9°C) is immediately accompanied by a rapid contraction of the egg cortex and plasma membrane, resulting in a segregation of myoplasm to the vegetal pole (Fig. 5B). Eggs show radial symmetry along the animal–vegetal axis. During the second phase of segregation (85–110 min), the myoplasm moves toward the future posterior pole together with the sperm aster and forms a crescent-

shaped domain just vegetal of the equator (Fig. 5C). After the male pronucleus has encountered the female pronucleus at the posterior pole, they move together to the center of the egg. At the second stage of ooplasmic segregation, the myoplasm situated in the posterior egg region can be used to orient eggs. During the second phase of ooplasmic segregation, the bilateral symmetry of the egg is established. First cleavage occurs at 160 min at 9°C.

Mechanisms of ooplasmic segregation have been investigated (Sawada, 1988; Jeffery and Bates, 1989; Jeffery, 1995). During the first phase of ooplasmic segregation, an actin network situated just beneath the plasma membrane contracts toward the vegetal pole. A drug that depolymerizes microfilament, cytochalasin E, inhibits the movement of cytoplasm, but microtubule inhibitors such as colcemid and nocodazole do not (Sawada and Schatten, 1989). The contraction of the actin network is triggered by fertilization following the release of free calcium into the cytoplasm (Jeffery, 1982; Speksnijder *et al.*, 1990; Roegiers *et al.*, 1995). Contraction of the actin network toward the vegetal pole is accompanied by movement of the cortical cytoplasm (myoplasm) and plasma membrane toward the vegetal pole. The cortical cytoplasm is anchored to the actin network by an interior filamentous lattice that is likely made of intermediate filaments (Jeffery and Meier, 1983). The actin network is linked to the plasma membrane by ankryin-like protein (Jeffery and Swalla, 1993). After the first phase of ooplasmic segregation, a plasma membrane lamina is formed at the vegetal pole where the myoplasm is present (Jeffery and Meier, 1983). The plasma membrane lamina and interior filamentous lattice may serve as a cytoskeletal framework for the positioning of morphogenetic determinants, which will be discussed in the next section.

The second phase of ooplasmic segregation involves sperm aster. The vegetally located myoplasm moves toward the equatorial region into the future posterior pole of the egg together with sperm aster (Sawada and Schatten, 1988). Much less is known about the mechanism responsible for coordinating ooplasmic movements of the second phase of ooplasmic segregation than that of the first phase. In contrast to the first phase of segregation, the second phase is sensitive to microtubule inhibitors and is not inhibited by drugs that disrupt microfilament (Sawada and Schatten, 1989).

B. Cytoplasmic Determinants Responsible for Tissue Differentiation

1. Autonomy of Tissue Differentiation

Ascidians have been the subject of experimental embryology for more than 100 years and are classic organisms to study what is known as "mosaic

development" (Conklin, 1905a). In mosaic embryos, isolated blastomeres develop autonomously according to their normal fate in the intact embryo. A number of studies on the developmental capacities of isolated blastomeres have demonstrated the strict developmental autonomy of blastomeres of the ascidian embryo (reviewed by Venuti and Jeffery, 1986; Meedel, 1992; Nishida, 1992a; Satoh, 1993). Isolated blastomeres develop into partial embryos in which tissue differentiation occurs exactly according to the normal fates of the individual blastomeres. Isolated ascidian blastomeres, when cultured in seawater, and not in a complex culture medium, can divide and differentiate into various larval tissues. This fact facilitates the interpretation of experiments. The cell-autonomous differentiation of blastomeres indicates that cellular interactions during ascidian embryogenesis are rare. The mosaic behavior of isolated blastomeres has been taken as evidence that prelocalized ooplasmic factors (cytoplasmic determinants) specify tissue precursor cells during embryogenesis (Conklin, 1905c). Cell fates are fixed by cytoplasmic determinants that are differentially partitioned into specific blastomeres during cleavage.

Using various kinds of tissue-specific morphological and molecular markers, a number of studies that have examined the developmental potentials of isolated blastomeres from 8- and 16-cell embryos have indicated that epidermis, muscle, notochord, mesenchyme, and endoderm autonomously differentiate. In contrast, the development of brain and sensory pigment cells is nonautonomous (a reference list is cited in Nishida, 1992a). Whereas these studies have provided a basic understanding of the cellular mechanisms responsible for the specification of cell fates in ascidian embryos, single blastomeres isolated from 8- and 16-cell embryos give rise to more than one type of larval tissue. As a consequence, partial embryos are made up of several kinds of larval tissue. These results do not exclude the possibility that cell to cell signaling may be occurring between the different types of cells that comprise a partial embryo.

A precise way to analyze the autonomy of tissue differentiation is to continuously dissociate embryonic cells each time they divide from the beginning of development until fate restriction has occurred. If the differentiation of a particular tissues has occurred in a dissociated cell, then the possibility has been excluded both that differentiation requires cell to cell signaling prior to blastomere isolation and that cell interaction occurs between different types of cells within partial embryos. For example, Nishida (1992b) continuously dissociated embryonic cells from the first cleavage to the 110-cell stage and allowed the cells to develop into partial embryos. the results of this study showed how extremely autonomous the expression of epidermis, muscle, and endoderm-specific markers is in the ascidian. In this experiment, cells after the 110-cell stage were not dissociated but they were allowed to develop as partial embryos. By the 110-cell stage the

developmental fates of most blastomeres are restricted to give rise to a single cell type in intact embryos. Indeed, in the dissociation experiments, most of the resulting partial embryos derived from dissociated cells consisted of one type of larval cell. Therefore, in these experiments the differentiated cells did not have the opportunity to interact with progenitor cells of other cell types. In summary, these results demonstrate that fate specification and the initial events of differentiation of epidermis, muscle, and endoderm cells are executed autonomously, without the involvement of any cell–cell signaling.

In striking contrast, notochord cells failed to differentiate when embryonic cells were dissociated, suggesting that cell interactions are required for notochord development. The result of recent experiments pertaining to the specification of epidermal, muscle, and endodermal cell fates will be discussed further in the following sections and recent results pertaining to notochord development will be discussed in more detail in a later section.

2. Muscle

The developmental fate of each blastomere of an 8-cell ascidian embryo is shown in Fig. 6A. Larval muscle cells are derived from three different progenitor cells: B, A, and b-line blastomeres. Each cell of the B4.1 (posterior–vegetal) cell pair produces 14 of 21 muscle cells along the anterior–middle region of one side of the tail in *Halocynthia* (Fig. 1B). Each A4.1 (anterior–vegetal) and each b4.2 (posterior–animal) cell produces 2 and 5 muscle cells located at the caudal tip of the tail, respectively (Nishida and Satoh, 1983; Nishida, 1987). Muscle cells that arise from B-line cells are designated primary muscle cells and those that arise from the A and b-line cells are designated secondary muscle cells. Secondary muscle cell development is nonautonomous and is thought to require cellular interactions with cells of other tissues (Meedel *et al.,* 1987; Nishida, 1990).

Development of the primary muscle cells during ascidian embryogenesis has been intensively investigated (Satoh *et al.,* 1990). The hypothesis that localized cytoplasmic determinants in the egg play a crucial role in the determination of the fate of primary muscle cells was derived from the following observations: (1) Colored pigment granules associated with myoplasm are inherited by muscle-lineage cells by an invariant cleavage (Conklin, 1905b,c); (2) Isolated and dissociated muscle-precursor blastomeres exhibit autonomous differentiation (Nishida, 1992a); (3) Muscle differentiation occurs in cleavage-arrested embryos (Whittaker, 1973a). These observations are consistent with Conklin's idea (1905c) that factors present in the egg cytoplasm mediate the differentiation of primary muscle cells. However, the most convincing proof of this idea would require that the

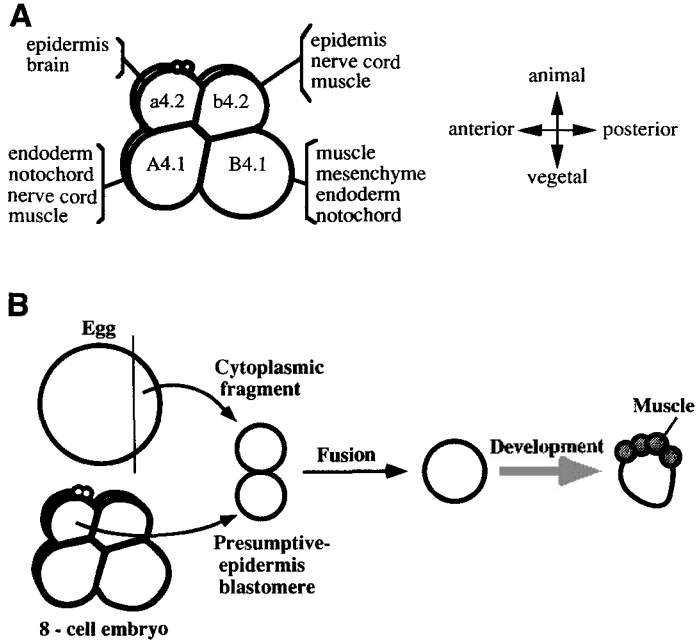

FIG. 6 (A) Lateral view of a bilaterally symmetrical 8-cell embryo, demonstrating the orientation of the blastomeres and the major descendant tissues. (B) Experiments of cytoplasmic transfer involving fusion of blastomere and egg fragment.

transfer of particular cytoplasm into nonmuscle cells converts these cells into muscle cells.

Cytoplasmic redistribution was achieved by Whittaker (1980) who altered the position of the third cleavage furrow by compressing four-celled embryos, and in another experiment Whittaker (1982) used a microsurgical method to alter the partitioning of myoplasm. Transfer of cytoplasm from muscle-precursor blastomeres into nonmuscle precursors using microinjection techniques has been performed by Deno and Satoh (1984). These studies suggested that the cytoplasm, rather than the nucleus, is important in the determination of muscle cells and that cytoplasmic determinants for muscle are present in the muscle-progenitor blastomeres. However, the number of cases in which the microinjected cells expressed muscle-cell features was low (2% of injected cells).

Recently, a new technique involving polyethylene glycol-mediated electrofusion was developed to transfer ascidian cytoplasm. Details of this recent method are shown in Fig. 6B. Isolated blastomeres were fused with cytoplasmic fragments from various regions of eggs and embryos (Nishida,

1992c). For example, presumptive-epidermis blastomeres (a4.2 in Fig. 6A) were fused to cytoplasmic fragments produced from various egg regions, and the development of muscle cells is monitored by examining the expression of myosin, actin (Fig. 1F), and acetylcholinesterase. Isolated presumptive-epidermis blastomeres develop into spherical clusters of epidermal cells and these cell clusters never develop muscle cells. If introduction of cytoplasm to the recipient epidermal lineage cells results in the development of muscle features, then muscle determinants must exist in the introduced cytoplasm.

Cytoplasmic fragments were produced from various regions of unfertilized eggs, fertilized eggs after the first and second phase of ooplasmic segregation, and 8-cell embryos, and fused with epidermis-precursor blastomeres (Nishida, 1992c; Yamada and Nishida, 1997). For example, the fusion of nonnucleated blastomere fragments containing B4.1 cytoplasm with epidermis progenitor cells resulted in the development of muscle features in nearly 100% of tested specimens (Fig. 8A). The deduced spatial distributions of cytoplasmic determinants is summarized in Fig. 7. Muscle determinants are present in the cytoplasm of unfertilized eggs and they are widely distributed along a gradient, with maximum activity at the vegetal pole. Muscle determinants are segregated by movements of the ooplasm triggered by fertilization. During the first phase of ooplasmic segregation, these determinants are moved into the vegetal pole region of the egg. Just prior to first cleavage, the muscle determinants are secondarily shifted into the future posterior egg region from where the future muscle-lineage blastomeres will form. Interestingly, the distribution of cytoplasm that promotes muscle differentiation appears to correspond to that of myoplasm, a microscopically visible portion of the egg cytoplasm that is inherited by muscle-lineage cells during development.

Myosin heavy chains (Makabe and Satoh, 1989; Makabe *et al.*, 1990), muscle actin (Tomlinson *et al.*, 1987; Kusakabe *et al.* 1991), and acetylcholinesterase (Perry and Melton, 1983; Meedel and Whittaker, 1983a) genes are expressed at the gastrula stage, suggesting that muscle determinants may be regulatory molecules, responsible for activation of a cascade of specific genes that ultimately results in synthesis of muscle-specific proteins. These determinants might be localized molecules or localized active forms of widely distributed molecules.

Various kinds of organelles and molecules are reported to be concentrated in myoplasm. Mitochondria (Zalokar and Sardet, 1984), endoplasmic reticulum (Speksnijder *et al.*, 1993), and pigment granules (Conklin, 1905b; Jeffery and Meier, 1983) are enriched in myoplasm. It has been shown that muscle determinants are not associated with mitochondria (Conklin, 1931; Whittaker, 1979) or pigment granules (Conklin, 1931; Bates, 1988). Conklin (1931) centrifuged ascidian eggs. Displacement of mitochondria and pig-

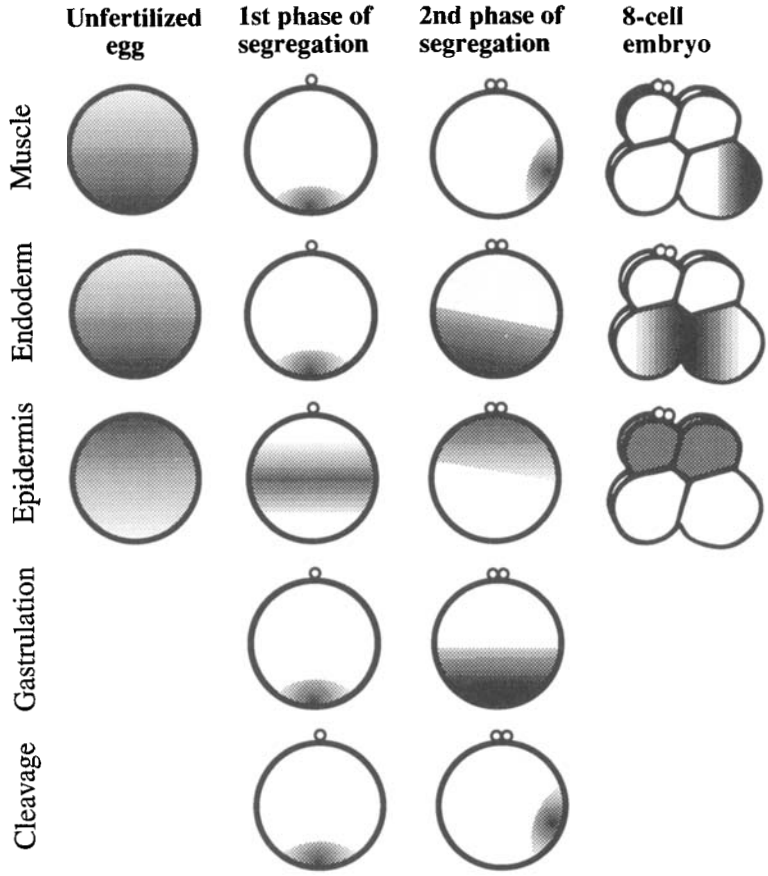

FIG. 7 (Top to third rows) Distribution of cytoplasmic determinants of three kinds of tissues, namely, muscle, endoderm, and epidermis, during ooplasmic segregation and at the 8-cell stage. Shaded areas represent locations of cytoplasmic determinants. Animal pole is up and vegetal pole is down. Anterior is to the left and posterior is to the right. (Fourth row) Distribution of cytoplasmic determinants for gastrulation movement. (Bottom row) Distribution of cytoplasmic determinants for generation of unique cleavage pattern.

ment granules did not affect muscle development. Bates (1988) used a microsurgical method to alter the normal partitioning of myoplasm. Myoplasm-enriched egg fragments produced after the first stage of ooplasmic segregation from the vegetal egg region developed into normal larvae with pigment granules in both the head the the tail regions. The role of endoplasmic reticulum in muscle specification is not yet known. The cytoskeletal elements, actin (Jeffery and Meier, 1983), ankryin (Jeffery and Swalla, 1993), and p58, which is the antigen for an antibody against

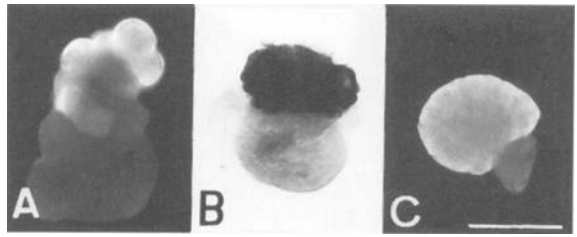

FIG. 8 Examples of fusion-mediated cytoplasmic transfer experiments. (A) A partial embryo that was derived from fusion of a presumptive-epidermis blastomere and a cytoplasmic fragment of a presumptive-muscle blastomere. The embryo was stained with anti-ascidian myosin antibody. Muscle differentiation is evident in the upper region of the embryo. In the other region, epidermis is formed because the recipient of cytoplasm was an epidermis precursor cell. (B) A partial embryo that was derived from fusion of a presumptive-epidermis blastomere and a cytoplasmic fragment of a presumptive-endoderm blastomere. The embryo was histochemically stained for endoderm-specific alkaline phosphatase. Endoderm was formed. (C) A partial embryo that was derived from fusion of a presumptive-nonepidermis blastomere and a cytoplasmic fragment of a presumptive-epidermis blastomere. The embryo was stained with epidermis-specific antibody. Differentiated epidermis almost covers the embryo. Scale bar, 100 μm. From Nishida (1992c, 1993, 1994a).

vertebrate neurofilaments (Swalla *et al.*, 1991), are also enriched in myoplasm. These cytoskeletal elements are likely to be involved in generating the motive force of ooplasmic segregation and to anchor muscle determinants to the myoplasmic domain.

Several antigens are reported to be localized in myoplasm (Nishikata *et al.*, 1987a; Bates and Bishop, 1996), and several maternal RNAs are localized in myoplasm (Swalla and Jeffery, 1995, 1996a). Among them, some are mitochondrial components and others are not. It is not yet known if these molecules are involved in muscle-cell specification. A myoplasmic protein termed myoplasmin-C1, which is recognized by a monoclonal antibody, may be involved in muscle specification. Myoplasmin-C1 is localized in egg myoplasm (Figs. 9A–C) and it is inherited by larval muscle cells. The protein is not a mitochondrial protein. When the monoclonal antibody that binds to myoplasmin-C1 was injected into eggs, the development of muscle-specific acetylcholinesterase was suppressed (Nishikata *et al.*, 1987a). The cDNA of myoplasmin-C1 has been cloned, and its deduced amino acid sequence suggests that myoplasmin-C1 is a cytoskeletal protein (Nishikata and Wada, 1996). Myoplasmin-C1 may play a role in anchoring and segregating muscle determinants, as does p58 (Swalla *et al.*, 1991).

Marikawa *et al.* (1994) separated unfertilized eggs into various fragments exhibiting different colors by centrifugation. Fertilized red fragments developed into permanent blastulae, in which only the differentiation of epidermis was observed. When black fragments were fused with red fragment and these fused egg fragments were fertilized, formation of muscle cells

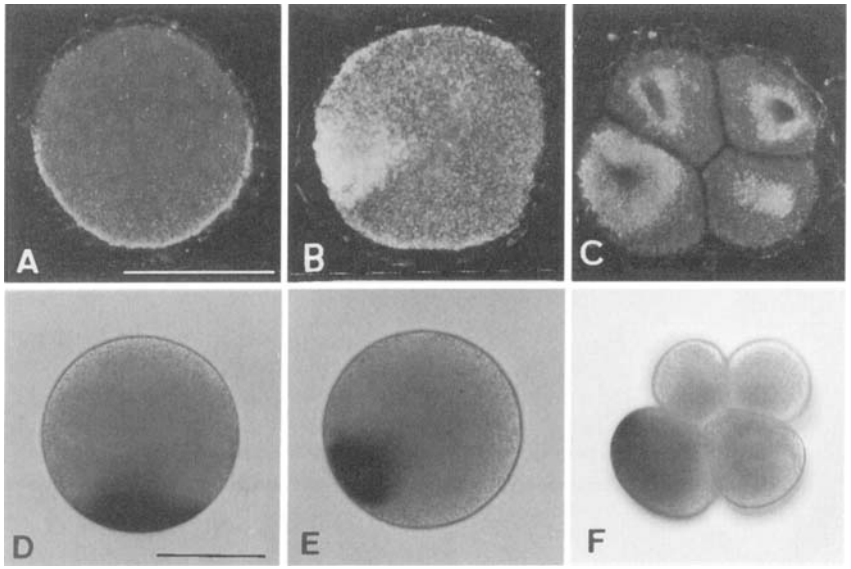

FIG. 9 (A–C) Preferential distribution of myoplasmin-C1 protein that is recognized by a monoclonal antibody in the myoplasm of a section of an unfertilized egg (A), an egg after the second phase of ooplasmic segregation (B), and an 8-cell embryo (C) of *Ciona intestinalis*. Posterior is to the left. (D–F) Strictly restricted distribution of *pem* mRNA in the myoplasm of an egg after the first phase of segregation (D), an egg after the second phase of segregation (E), and an 8-cell embryo (F) of *Ciona savignyi*. Scale bar, 100 μm. From Nishikata *et al.* (1987a) and Yoshida *et al.* (1996).

was observed. These results indicate that muscle determinants are concentrated in the black fragments and they are absent in the red fragments. UV irradiation inactivated the ability of the black fragments to develop muscle-cell features. Injection of mRNA isolated from unirradiated black fragments into UV-irradiated black fragments restored their ability to promote muscle formation when fused to red fragments (Marikawa *et al.*, 1995), although the injection of the same mRNA directly into red fragments or presumptive-epidermis blastomeres did not result in muscle formation. Therefore, it was suggested that mRNA in black fragments is necessary but not sufficient for muscle formation.

Black-fragment-specific cDNAs have been cloned by subtracting the mRNA of the red fragment from that of the black fragment (Yoshida *et al.*, 1996). One of the mRNAs, termed posterior end mark (*pem*), was shown to be strictly localized to the myoplasmic region of the egg (Figs. 9D–F). The deduced amino acid sequence of *pem* did not show any similarity to other known proteins. Overexpression of this gene by the injection of synthesized *pem* mRNA into eggs resulted in development of tadpole

larvae with deficiencies in the anteriormost region including the palps, brain, and sensory pigment cells. This abnormality was caused by the translocation of the anterior epidermis and dorsal neuronal cells into a more posterior position. Injection of *pem* mRNA into irradiated black fragments did not restore their ability to promote muscle formation and the injection of *pem* mRNA directly into red fragments and presumptive-epidermis blastomeres did not result in muscle formation. To elucidate the role of this gene product further, loss-of-function experiments such as experiments using antisense RNA or DNA should be carried out.

Recently, several genes that are expressed in muscle-lineage cells have been cloned in *Halocynthia.* Expression of the muscle actin gene and myosin genes starts as early as the 32-cell stage (Satou *et al.,* 1995). The upstream element that is required for lineage-specific expression of a muscle actin gene is as short as 38 base pairs (Satou and Satoh, 1996). These results suggest that the spatial regulation of this lineage-specific gene may be relatively simple in ascidian embryos. A homologue of a myogenic factor has been cloned. The expression of AMD1, a gene for a MyoD-related factor, begins at the 64-cell stage (Araki *et al.,* 1994). It is not yet known whether the protein products of this gene are maternally present in eggs.

3. Endoderm

Endoderm cells are present in the central part of the trunk region of tadpole larvae (Figs. 1A, 1D, and 1H). These cells are homogeneous in appearance, rich in yolk granules, and likely provide the embryos with nutrients. Endoderm cells in *Halocynthia* do not undergo terminal differentiation during larval development because *Halocynthia* tadpoles are nonfeeding. However, during embryogenesis, endoderm cells start to express endoderm-specific alkaline phosphatase (ALP) (Minganti, 1954; Whittaker, 1977) (Fig. 1H). Although the role of ALP in the endoderm is not yet known, ALP has often been used as a molecular marker of endoderm differentiation (e.g., Whittaker, 1977). All of the endoderm cells of a larva are derived from the vegetal blastomeres of an eight-cell embryo, namely, the anterior A4.1 cell pair and the posterior B4.1 cell pair (Fig. 6A). The A4.1 cells give rise to anterior endoderm and the B4.1 cells develop into posterior endoderm. In contrast, blastomeres of the animal hemisphere (a4.2 and b4.2 cell pairs) do not produce endoderm.

To examine the presence and localization of endoderm determinants, experiments involving transfer of cytoplasm have been carried out by fusing isolated blastomeres with cytoplasmic fragments that were prepared from various regions of eggs and embryos. Again, the recipient cells were isolated presumptive-epidermis blastomeres (a4.2 in Fig. 6A). The formation of endoderm was monitored by examining embryos for the expression of

ALP (Fig. 8B). The deduced distribution of endodermal determinants that promote expression of ALP is shown in Fig. 7 (Nishida, 1993; Yamada and Nishida, 1997). Endoderm determinants reside in the unfertilized egg and they appear to be widely distributed in the form of a gradient, with maximum activity at the vegetal pole. Endoderm determinants move toward the vegetal pole of the egg during the first phase of segregation, as do the muscle determinants. Prior to first cleavage, the distribution extends in the equatorial direction. These determinants are present within the entire vegetal hemisphere from which the future endoderm-lineage blastomeres are formed. During cleavages, these determinants are partitioned into endoderm-lineage cells.

Marikawa and Satoh (1995) showed that, similar to muscle determinants, endoderm determinants are concentrated in black fragments by centrifugation and they are absent in red fragments of unfertilized eggs. UV irradiation of black fragments destroys the ability of these fragments to promote the expression of ALP when they are fused with red fragments.

In *C. intestinalis,* inhibitors of transcription, such as actinomycin D, did not prevent the appearance of ALP activity even when the treatment is started before fertilization (Whittaker, 1977). In contrast, actinomycin D suppressed the appearance of markers of muscle, epidermis, notochord, and sensory pigment cells. Actinomycin D results suggest that a maternal mRNA that encodes ALP may be present in the cytoplasm of an unfertilized *Ciona* egg. The cytoplasmic factor responsible for the activity of ALP may be maternal mRNA that encodes ALP. However, the results of more recent experiments suggest that nuclear activity is required for expression of ALP activity. Nonnucleated fragments produced from fertilized eggs do not develop ALP activity, suggesting that there is a nuclear requirement for expression of ALP activity (Bates and Jeffery, 1987a; Meedel and Whittaker, 1983b). In contrast, the expression of ALP activity in *H. roretzi* is sensitive to actinomycin D treatment. This study suggests that ALP genes are first transcribed at the gastrula stage (Nishida and Kumano, 1997). An experiment involving cytoplasmic transfer, as described above, was performed using *Halocynthia* embryos. Therefore, at least in *Halocynthia* embryos, it is likely that there are cytoplasmic factors that are responsible for the activation of ALP gene expression.

Recently, endoderm-specific ALP protein has been isolated from *Halocynthia* and the N-terminal amino acid sequence was determined (Kumano and Nishida, 1996). Cloning of the gene that encodes endoderm-specific ALP is required to determine if there are maternal ALP mRNA molecules in the cytoplasm of ascidian eggs.

4. Epidermis

The epidermis covers the entire ascidian larva (Figs. 1A and 1C–E). The epidermis consists of approximately 800 cells that are arranged in a single

layer, which secrete transparent larval tunic materials (Fig. 1E). The epidermis of a larva originates exclusively from the four animal blastomeres of the bilaterally symmetrical 8-cell embryo, namely, the anterior a4.2 cell pair and the posterior b4.2 cell pair (Fig. 6A). The a4.2 cells give rise to the epidermis of the head and trunk regions while the b4.2 cells give rise to the epidermis of the tail region of the tadpole larva. In contrast, blastomeres of the vegetal hemisphere (A4.1 and B4.1 cell pairs) do not produce epidermis.

Fusion of blastomeres and cytoplasmic fragments was carried out to examine the presence and distribution of epidermis determinants (Nishida, 1994a; Yamada and Nishida, 1997). In these experiments, the recipient cells were isolated vegetal blastomeres. Ectopic formation of epidermis was estimated by observing the expression of an epidermis-specific antigen (Figs. 1E and 8C), the secretion of larval tunic materials, and epithelial morphology. The deduced distribution of epidermis determinants is shown in Fig. 7. Epidermis determinants appear to be present in the unfertilized egg and they are widely distributed in the egg cytoplasm along a gradient, concentrated in the animal pole region. After the first phase of ooplasmic segregation, these determinants are still widely distributed, but now the highest concentration is in the equatorial region. After the second phase of ooplasmic segregation, prior to the first cleavage, epidermis determinants are moved into the animal hemisphere where the future epidermis-lineage blastomeres will form. During cleavages, epidermis determinants are inherited by cells located in the animal hemisphere. It is noteworthy that the inferred movements of epidermis determinants during ooplasmic segregation appear to coincide closely with the movements of a light-colored cytoplasm, termed the "ectoplasm," in the pigmented eggs of *Styela* (Conklin, 1905b,c; Jeffery *et al.*, 1983).

The epidermis-specific antigen that was used in fusion experiments first appeared at the early tailbud stage during embryogenesis. Expression of this antigen was blocked by treatment with an inhibitor of transcription, if the treatment was initiated before the late gastrula stage. It has been suggested that the gene which encodes the antigen is activated at the gastrula stage (Nishikata *et al.*, 1987b). Thus, the epidermis determinants in the egg cytoplasm may be regulatory molecules that are responsible for the activation of epidermal genes at the time of gastrulation.

Recently, eight epidermis-specific cDNAs, HrEpiA–H, were cloned (Ueki *et al.*, 1991; Ishida *et al.*, 1996). The expression of most of these genes is initiated during gastrulation and is restricted to only epidermis-lineage cells. The 5′ upstream regions of the HrEpiB and HrEpiD genes were investigated in detail (Ueki and Satoh, 1995). The 5′ flanking region from −345 of the HrEpiB gene, taking the transcription initiation site as +1, was found to be sufficient for epidermis-specific expression, whereas the 5′ upstream region from −166 of the HrEpiD gene regulated the expression

of the HrEpiD gene. A comparison of the sequences of these two regions demonstrated the presence of several conserved sequences for DNA-binding regulatory proteins, some of which were shared by both genes. It will be important to look for *trans*-acting factors that bind to these sequences.

A feature that was common to all three kinds of cytoplasmic determinants responsible for muscle, endoderm, and epidermis development was that the cytoplasm introduced by fusion never suppressed the formation of tissues derived from recipient blastomeres. A single cluster of ectopically formed tissue cells that probably contained transferred cytoplasm developed within the embryo (Fig. 8). Therefore, the transferred determinants do not likely diffuse throughout the recipient and are likely inherited by a subset of the descendant cells of the fused cell. Cytoplasmic determinants are likely bound to various components of the cytoplasmic skeleton, as suggested by Conklin (1931) and Jeffery and Meier (1983). A second possibility is that determinants may be anchored to the plasma membrane. The binding of determinants to cytoskeletons and membranes would explain why determinants are difficult to transfer with micropipettes (Deno and Satoh, 1984).

During the first phase of ooplasmic segregation, all three kinds of determinants move in the vegetal direction (Fig. 7). This movement coincides with the visible movements of the cortical cytoplasm and plasma membrane during the first phase (Fig. 5). Therefore, at least during the first phase, the determinants are likely to be present in the cortical cytoplasm or plasma membrane. The three kinds of cytoplasmic determinants move in different directions during the second phase of ooplasmic segregation. It will be of great interest to determine the way in which the egg segregates these cytoplasmic factors. Prior to the onset of first cleavage, three kinds of determinants reside in egg regions that correspond to the future fate map of the embryo.

Results of experiments with isolated and dissociated blastomeres indicate that fate determination and initial events of muscle, endoderm, and epidermis cell differentiation are autonomous. These processes do not require communication with cells from other lineages. Cytoplasmic transfer experiments unambiguously demonstrate the presence of localized cytoplasmic factors in ascidian eggs that promote formation of the three kinds of larval tissue. Therefore, each of the determinants, which are segregated into each lineage cell, appears to be sufficient for the determination of muscle, endoderm, and epidermis cell fates. As the expression of zygotic genes is required for tissue differentiation, these determinants likely function as regulatory molecules that activate tissue-specific genes. As yet, the identity and mode of action of ascidian cytoplasmic determinants are unknown.

Determinants will be localized molecules or localized active forms of widely distributed molecules.

C. Determinants for Gastrulation Movements

In addition to tissue-specific determinants, there is evidence suggesting that ascidian eggs contain cytoplasmic factors that are responsible for controlling morphogenetic movements. In ascidians, gastrulation starts at the 110-cell stage. During gastrulation, endoderm and mesoderm precursor cells invaginate into embryos (Figs. 2A and 2B).

Ortolani (1958) pioneered the bisection of ascidian eggs and discovered that when fertilized eggs were bisected near the equator, animal fragments developed into permanent blastulae. More recently, it was shown that when a small region of vegetal pole cytoplasm is removed from *Styela* zygotes at the first stage of ooplasmic segregation, the operated embryos failed to gastrulate (Bates and Jeffery, 1987b). Cytoplasmic deletions of other egg regions had no effect on larval development. The removal of cytoplasm from the vegetal pole region can be mimicked by UV irradiation of the fertilized egg at the vegetal pole (Jeffery, 1990a). These results suggest that cytoplasmic factors that are required for gastrulation are localized in the vegetal pole region at the first stage of ooplasmic segregation (Fig. 7). In these experiments, the differentiation of endoderm and muscle cells occurred in spite of a deficiency in morphogenesis, suggesting the presence of maternal factors which are specifically involved in morphogenetic movements. When vegetal pole cytoplasm was transplanted by cell fusion methods to the animal pole or equatorial position of *Halocynthia* eggs, ectopic gastrulation occurred at the site of transplantation (Nishida, 1996a). This experiment supports the idea that vegetal pole cytoplasm specifies the site of gastrulation. Vegetal pole cytoplasm is required for and is sufficient to promote gastrulation.

After completion of the second phase of ooplasmic segregation, most of the vegetal hemisphere had to be removed to suppress gastrulation. It was suggested that, during the second phase of ooplasmic segregation, cytoplasmic factors responsible for gastrulation spread throughout the entire vegetal hemisphere (Fig. 7), where vegetal cells invaginate during gastrulation (Bates and Jeffery, 1987b; Nishida, 1996a).

As mentioned above, the effect of removal of vegetal pole cytoplasm can be mimicked by UV-irradiating eggs at the vegetal pole (Jeffery, 1990a). By comparing maternal messages of normal and UV-irradiated eggs using an *in vitro* translation system, Jeffery (1990b) suggested that a UV-sensitive maternal mRNA that encodes a cytoskeletal protein (p30) is involved in gastrulation.

D. Determinants for Generation of a Unique Cleavage Pattern

The cleavage pattern of an ascidian embryo is unique and invariant (Conklin, 1905b; Satoh, 1979). Cleavages progress in a bilaterally symmetrical manner; however, the cleavage pattern differs significantly between the anterior half and the posterior half of the embryo. Only the most posterior blastomeres in the vegetal hemisphere undergo unequal cleavage. As cell lineages and cleavage patterns have been well described, the ascidian embryo offers a good experimental system for analyzing the mechanism of unequal cleavage.

Figure 10 shows the pattern of cleavage up to the 64-cell stage. The third cleavage is horizontal, separating the embryo into an animal and a vegetal quartet of cells. But the cleavage planes in the two posterior (B3) blastomeres are slightly oblique and, consequently, the B4.1 cell pair protrudes posteriorly from the embryo (Fig. 10B). After the 8-cell stage, three succes-

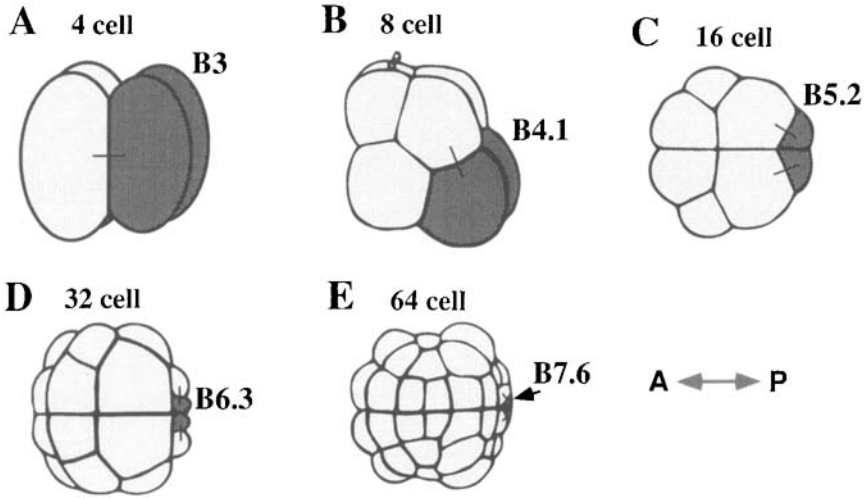

FIG. 10 Cleavage pattern of an ascidian embryo. (A) 4-cell stage. (B) 8-cell stage. (C) 16-cell stage. (D) 32-cell stage. (E) 64-cell stage. (A and B) Lateral view. (C–E) Vegetal view. Cleavage pattern shows bilateral symmetry. Posteriormost vegetal blastomere pair at each stage is shaded and labeled. Only the posteriormost blastomeres (B4.1, B5.2, and B6.3) at each stage divide unequally, producing a small blastomere pair posteriorly. Lines between two blastomeres indicate sister blastomeres of previous cleavage. The lines in C, D, and E represent three successive unequal cleavages. In these figures, it appears that many blastomeres cleave unequally. However, only the B4.1, B5.2, and B6.3 cells divide unequally up to the 64-cell stage (late blastula stage), and these three cleavages are the only unequal cleavages that occur during the cleavage stages in ascidian embryos.

sive, unequal cleavages occur in the vegetal hemisphere such that only the cells of the most posterior blastomere pair at each stage undergo unequal cleavage, always producing smaller cells posteriorly (the B5.2, B6.3, and B7.6 blastomeres in Figs. 10C–F). All the other cleavages are equal in terms of cell size. The smallest and most posterior blastomere of a 64-cell embryo, B7.6, does not divide during embryogenesis. It gives rise to a single cell situated in the endodermal strand (Nishida, 1987). In general, a cleavage furrow forms perpendicular to the axis of a mitotic apparatus and at the equatorial region of the spindle (Rappaport, 1969). Therefore, cleavage patterns depend upon the mechanism that determines the position of the mitotic apparatus (Freeman, 1983). One possibility is that unequal cell division in ascidian embryos may involve the posterior pole cytoplasm attracting the spindle pole. This would result in the production of smaller cells at the posterior pole.

In *Halocynthia* eggs, the vegetal pole egg cytoplasm after the first phase of ooplasmic segregation and the posterior–vegetal cytoplasm after the second phase of ooplasmic segregation are required for generation of a posterior cleavage pattern. When the vegetal pole cytoplasm or the posterior–vegetal cytoplasm at each stage was removed from *Halocynthia* eggs, the cleavage pattern was radialized along the animal–vegetal axis. No unequal cleavage occurs in such embryos (Figs. 11 and 21D) (Nishida, 1994b, 1996a). However, in *Styela* eggs removal of the posterior pole cytoplasm at the second stage of segregation did not affect normal cleavages (Bates and Jeffery, 1987b). Transplantation of posterior–vegetal cytoplasm to an anterior–vegetal position after the second phase in *Halocynthia* eggs caused a reversal of the anterior–posterior polarity of the cleavage pattern, resulting in successive unequal cleavages at the anterior region (Nishida, 1994b). These results using *Halocynthia* suggest that a localized cytoplasmic factor in the vegetal pole after the first phase of segregation, and then in the posterior–vegetal region after the second phase, may be involved in the generation of unequal cleavage (Fig. 7).

Recently, a novel structure, designated the centrosome-attracting body (CAB), present in the unequally cleaving blastomeres has been reported (Hibino *et al.,* 1997). During unequal cleavage, a thick microtubule bundle appears between the CAB and one of the centrosomes (Fig. 12). Then, as the shortening of the microtubule bundle occurred, the nucleus together with the centrosomes was drawn toward the CAB, which was situated at the posterior cortex of the blastomere. Finally, a cleavage furrow formed in the middle of the asymmetrically located mitotic apparatus and produced two blastomeres of different size. The smaller cell inherited the CAB. Therefore, the CAB seems to play an essential role in generating unequal cleavages in *Halocynthia* embryos. Formation of CAB starts at the two-cell stage in the posterior–vegetal region. Therefore, factors in the poste-

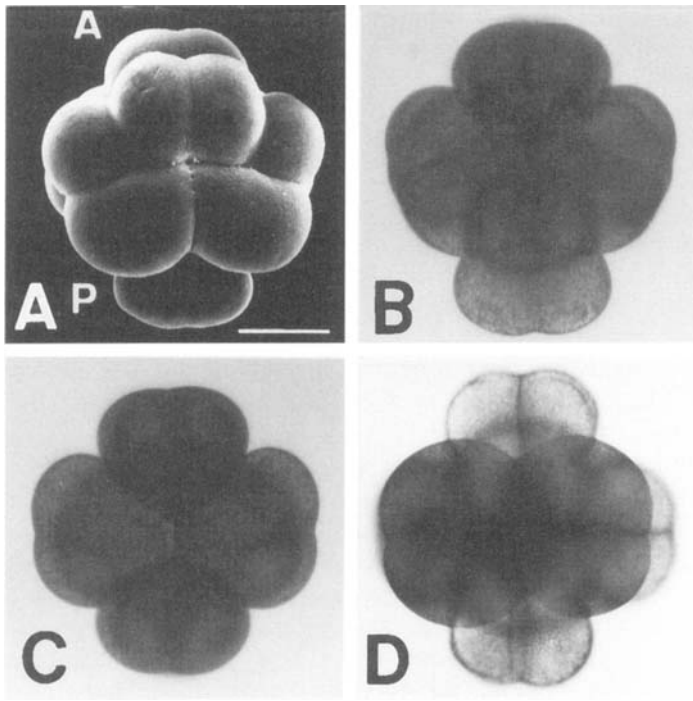

FIG. 11 (A) Scanning electron microscope image of a 16-cell embryo. Vegetal view. Anterior (A) is up, and posterior (P) is down. Two pairs of posterior blastomere have unequally divided. (B) Photomicrograph of a 16-cell embryo as in (A). (C) Posterior–vegetal cytoplasm was removed from the egg after the second phase of ooplasmic segregation (see Fig. 21A). Cleavage pattern is radialized. (D) Posterior–vegetal cytoplasm was transplanted to the anterior position of a normal egg. Such embryos have posterior cytoplasm in both sides. Unequal cleavages occur in both sides of the embryo, generating miller-image duplication of the posterior cleavage pattern.

rior–vegetal region in egg cytoplasm may be responsible for CAB formation and subsequent unequal cleavages.

Figure 7 summarizes the postulated movements of known cytoplasmic determinants in *Halocynthia* eggs. Most of the determinants, except for the determinant of epidermis, are temporarily segregated into the vegetal pole region during the first phase of segregation. Then, once the second phase of segregation begins, various cytoplasmic determinants move in two ways. First, muscle determinants and cleavage pattern determinants move to the future posterior pole. These movements appear to coincide with visible movements of the cytoplasm. Second, endoderm determinants and determinants for gastrulation are distributed over the entire vegetal half, although there is no information concerning the distribution of determinants within the egg interior. Such a movement does not coincide with the visible move-

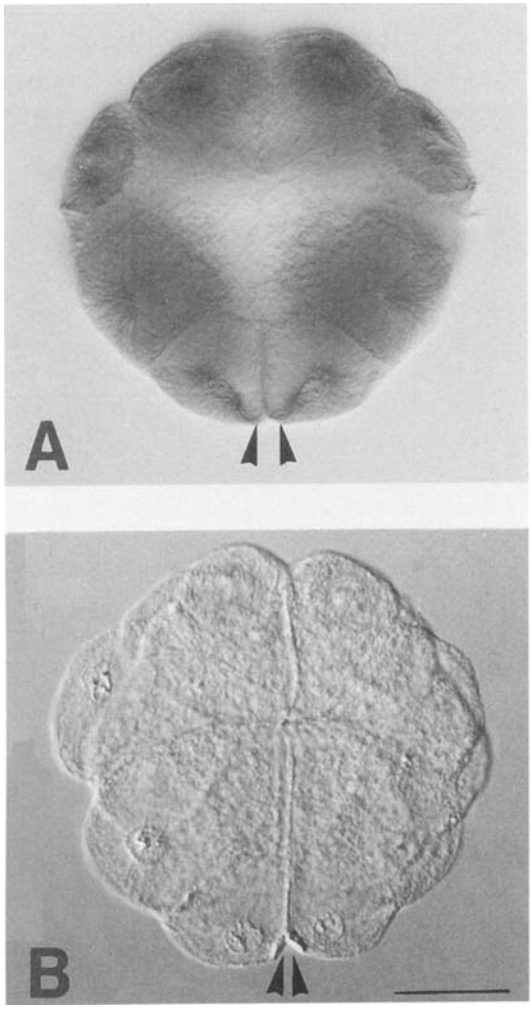

FIG. 12 Microtubule array and CAB (centrosome-attracting body) in the 16-cell-stage embryo. (A) A 16-cell-stage embryo extracted with extraction buffer was stained with anti-α-tubulin antibody. Anterior is up, and posterior is down. Interphase. Nuclei are visible. A bundle of microtubules is present between one of the centrosomes and the position of the CAB (arrowheads) in the posteriormost blastomere (B5.2). (B) An extracted but unstained embryo was observed with a Nomarsky microscope. A pair of CAB was observed at the posterior pole of the embryo (arrowheads). Scale bar, 100 μm. From Hibino *et al.* (1997).

ment of ooplasm. Endoderm and gastrulation determinants are likely bound to the cytoskeleton during the first phase of segregation. Then, these determinants may be released from the cytoskeleton and diffuse within the cytoplasm of the vegetal hemisphere. Alternatively, mRNAs encoding these

factors may be segregated to the vegetal pole. After translation of these mRNAs, the proteins may spread throughout the vegetal hemisphere. This has been observed in the case of bicoid mRNA and protein in *Drosophila* eggs (Driever and Nüsslein-Volhard, 1988).

IV. Inductive Interactions

A great deal of experimental evidence has accumulated over the years demonstrating the important role of intercellular interactions in the development of certain kinds of tissues, even in animals that have determinate and invariant cell lineages. Ascidian embryogenesis has been regarded as a typical example of "mosaic development," in which isolated blastomeres exhibit developmental autonomy. However, recent results have revealed that cellular interactions also play important roles in fate determination in ascidian embryos, as will be discussed in the following sections. Therefore, ascidians are developmental systems that exhibit a highly stereotyped cell lineage, yet also utilize cell interactions like aspects of *Caenorhabditis elegans*. Embryonic induction is a classic example of cell–cell signaling involving the interaction between "inducing" cells and "responding" cells (Spemann and Mangold, 1924; Spemann, 1938). The result of induction is the cell fate determination of the responding cells. In this process, the fate of the responding cell is controlled by a signal(s) emitted from the inducing cells (Gurdon, 1987; Slack, 1993).

A. Inductive Interactions in Tissue Formation

1. Notochord Induction

In vertebrates, it is well known that the notochord arises as a result of inductive interactions with vegetal cells (Nieuwkoop, 1969, 1973). As ascidians are chordates, it is of great interest from an evolutionary perspective to see if the induction of the ascidian notochord occurs in the same way as it does in vertebrates.

The ascidian notochord consists of a single row of 40 cells, aligned along the center of the tail of the tadpole larva (Figs. 13A–C). The developmental fate of notochord-lineage cells is restricted exclusively to the notochord at the 64-cell stage in A-line and at the 110-cell stage in B-line blastomeres (Fig. 3). Among the 40 notochord cells, 32 cells (primary notochord cells) in the anterior and middle part of the tail are derived from the four precursor blastomeres of the A-line of the 64-cell embryo (left and right A7.3 and

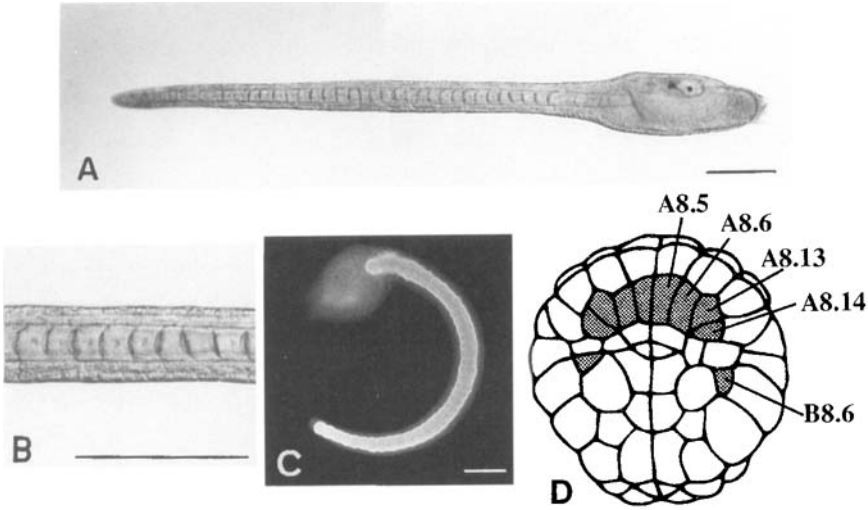

FIG. 13 (A) A *Halocynthia* larva which has 40 notochord cells in the center of the tail. (B) Higher magnification of the tail. (C) Expression of the notochord-specific antigen in the middle-tailbud embryo. The staining is strictly restricted to the outer surfaces of notochord cells. (D) Vegetal view of the 110-cell-stage embryo. Blastomeres whose fate is restricted to form notochord are shaded. Names of the blastomeres are shown. Scale bar, 100 μm. From Nakatani and Nishida (1994).

A7.7 cells, which divide into A8.5, A8.6, A8.13, and A8.14 cell pairs in Fig. 13D) after three subsequent divisions (see Fig. 19A), while the posterior 8 cells (secondary notochord cells) originate from the two precursor blastomeres of the B-line (left and right B8.6 cells) of the 110-cell embryo after two subsequent divisions (Fig. 13D, see also Fig. 19D). Thus, in the notochord lineage, every differentiated notochord cell is formed as a result of nine divisions after fertilization. Notochord cells are disc-shaped and a vacuole forms at one end of each cell (Cloney, 1964; Mancuso and Dolcemascolo, 1977; Katz, 1983; Miyamoto and Crowther, 1985) (Fig. 13B). During metamorphosis, when the larval tail is retracted into the trunk, the notochord cells degenerate and disappear.

The results of earlier experiments involving isolation of blastomeres at the 8- and 16-cell stages have suggested that notochord cells develop autonomously, indicating that differentiation of the notochord does not require cellular interactions (Reverberi and Minganti, 1946; Crowther and Whittaker, 1986; Nishikata and Satoh, 1990). However, notochord-lineage blastomeres isolated at an early stage, such as the 8- or the 16-cell stage, also gave rise to cells other than notochord. Therefore, nonnotochord cells may be inducing the differentiation of notochord cells within the partial

embryos. Manual isolation of presumptive-notochord blastomeres from 110-cell embryos resulted in autonomous differentiation of notochord cells. However, continuous dissociation of cells from the first cleavage to the 110-cell stage abolished differentiation of notochord cells (Nishida, 1992b). These results suggest that cellular communication during cleavage may be required for differentiation of notochord cells.

Taking advantage of the simplicity of ascidian embryos, cellular mechanisms involved in the formation of primary notochord cells were analyzed at the single-cell level. Detailed analysis of notochord development that involved isolation and recombination of blastomeres at various stages was carried out (Nakatani and Nishida, 1994). At first, when notochord formations are sensitive to cell dissociation was examined. Dissociation of embryonic cells during the 32-cell stage abolished notochord differentiation. By isolating notochord-lineage cells at various stages, it was shown that the presumptive-notochord blastomeres, manually isolated from 32-cell embryos, do not develop any notochord-specific features (specific morphologies and a specific antigen) (Fig. 14). However, the isolation of cells after the 64-cell stage resulted in notochord differentiation. Therefore, presumptive-notochord cells acquire the capacity for autonomous development at the 64-cell stage.

Although the involvement of inductive interactions is assumed by the failure of differentiation of isolated blastomeres, the role of cell interactions must be further tested by experiments involving the recombination of isolated blastomeres. To confirm the involvement of induction in the determination of notochord and to identify the inducer blastomeres, the

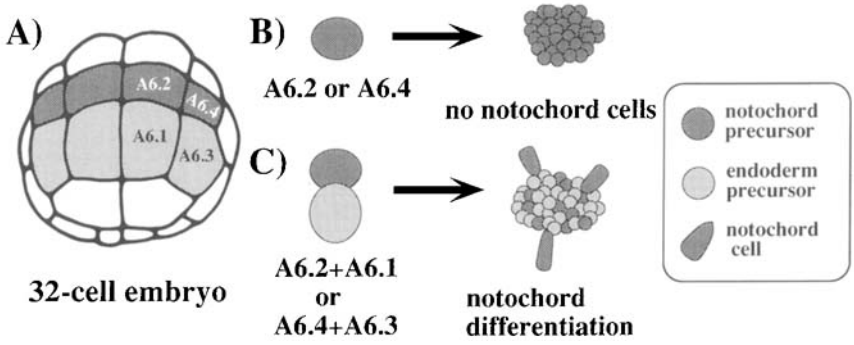

FIG. 14 Experiments that involve isolation and recombination of blastomeres to reveal the requirement of induction for notochord formation. (A) Vegetal view of a 32-cell embryo. (B) Isolation of presumptive-notochord blastomeres. Partial embryos do not differentiate into notochord. (C) Recombination of presumptive-notochord blastomeres and inducer blastomeres. Notochord forms.

presumptive-notochord blastomeres at the 32-cell stage were recombined with one of the surrounding blastomeres. When the presumptive-notochord blastomeres were recombined with presumptive-endoderm blastomeres, notochord differentiation occurred (Fig. 14C). Interestingly, when two presumptive-notochord blastomeres were recombined, notochord also formed. It is suggested that, for the primary notochord lineage, notochord formation occurs as the result of an inductive influence from vegetal blastomeres that include the presumptive-endoderm blastomeres and the presumptive-notochord blastomeres themselves. However, an isolated single notochord precursor cell cannot induce itself in an autocrine manner.

Recombination at various times after isolation of presumptive-notochord blastomeres and inducer blastomeres suggested that inductive interactions must be initiated before the decompaction of blastomeres during the 32-cell stage. Furthermore, the recombination of animal hemisphere cells (epidermis precursors) with endoderm cells did not result in notochord formation. This result differs from how mesoderm is induced in amphibian embryos. Animal hemisphere cells do not have the competence to form notochord in ascidians. In conclusion, ascidians as well as vertebrates utilize inductive interactions that play a crucial role in the determination of notochord. However, there are significant differences in how notochord cells are induced in ascidians compared to amphibians. Ascidian animal hemisphere cells do not have the competence to form notochord cells, whereas in amphibian embryos animal cells do respond to inductive signals.

It has been believed that notochord is autonomously specified in ascidian embryos. This is because isolated blastomeres from 8- and 16-cell embryos develop autonomously into partial embryos that contain differentiated notochord. Now it is assumed that notochord induction occurs within partial embryos that were derived from blastomeres isolated at the early stages, because isolated blastomeres can give rise to both inducing and responding cells. Paradoxically, under such conditions, blastomeres develop autonomously, but notochord formation is not an autonomous process. We should note that although studies with isolated blastomeres can serve to demonstrate the developmental autonomy of blastomeres and the inability of blastomeres to undergo regulative development, autonomous development of early blastomeres does not always mean autonomy of tissue differentiation.

In *Xenopus,* activin and basic fibroblast growth factor (bFGF) are mesoderm-inducing factors (Smith, 1989; Asashima, 1994). To examine if these growth factors are effective on ascidian notochord induction, presumptive-notochord blastomeres of ascidian embryos were isolated at the 32-cell stage and treated with activin and bFGF (Nakatani *et al.,* 1996). Activin up to 500 ng/ml did not induce notochord, whereas 0.02 ng/ml

bFGF was found to be an efficient inducer of the notochord in *Halocynthia* (Fig. 15). Pulse treatments of cells with bFGF indicated that the period of competence in which cells could be induced to develop into notochord was short. Isolated blastomeres treated only at the 32-cell stage responded to bFGF. This result is consistent with results obtained from blastomere recombination experiments. Treatment of cells isolated from the animal hemisphere with bFGF did not develop into notochord. Therefore, only notochord-lineage blastomeres are competent to be induced to develop into differentiated notochord cells.

The *Brachyury (T)* gene plays an important role in the formation of mesoderm in the mouse (Herrmann *et al.,* 1990). This gene is expressed from early gastrulation in mesoderm and primitive ectoderm and then becomes restricted to notochord (Wilkinson *et al.,* 1990). Homologs of the mouse T gene have been cloned in *Xenopus* (Smith *et al.,* 1991) and in the zebrafish (Schulte-Merker *et al.,* 1992). Similar to the mouse *T* gene, these genes are expressed in the mesoderm and especially in notochord-progenitor cells. Recently, an ascidian homolog of *Brachyury,As-T,* was cloned and its pattern of expression was analyzed by *in situ* hybridization (Yasuo and Satoh, 1993, 1994). During ascidian embryogenesis, transcripts of the *As-T* gene are first detected at the 64-cell stage, immediately after notochord induction, and these transcripts appear exclusively in the presumptive-notochord blastomeres of the primary lineage (Fig. 16). Expression of *As-T* begins in the secondary notochord lineage at the 110-cell stage. *As-T* transcripts were not detected in other mesodermal precursor cells. The expression of these transcripts continues until the late tailbud stage in notochord-progenitor cells.

Experimental results showed that the notochord precursor cells when isolated at the 32-cell stage do not express *As-T.* Recombination of notochord precursors with inducer blastomeres results in *As-T* expression. When

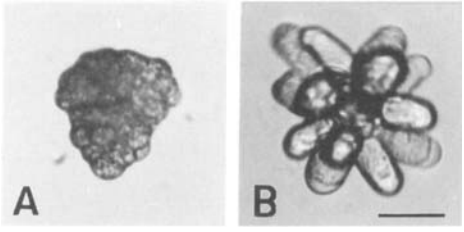

FIG. 15 Treatment of presumptive-notochord blastomeres isolated at the 32-cell stage with basic fibroblast growth factor (bFGF). (A) Nontreated embryo. (B) Embryos treated with 0.2 ng/ml bFGF. Notochord cells elongate and a vacuole forms at one end of each cell. Cells expressed notochord-specific antigens when immunostained. Scale bar, 50 μm. From Nakatani *et al.* (1996).

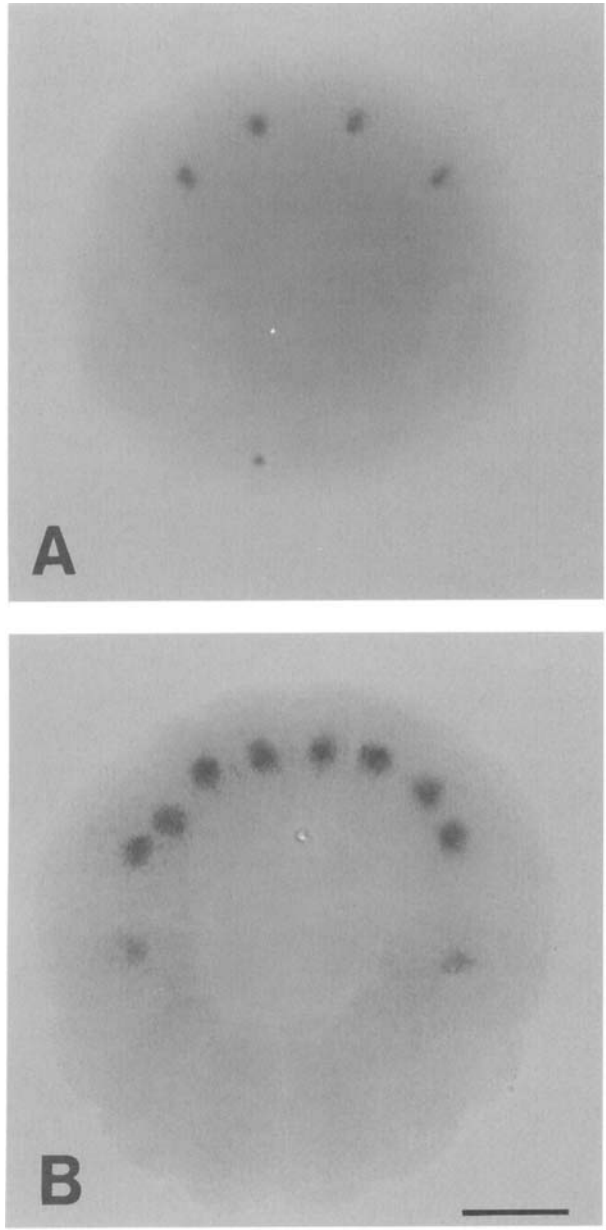

FIG. 16 (A and B) Expression of *brachyury* homologue, *As-T,* in the 64- and 110-cell embryos, respectively. Transcripts were detected by *in situ* hybridization. The signal is visible in the nuclei of notochord precursor cells. Scale bar, 100 μm. From Yasuo and Satoh (1993, 1994) and Nakatani *et al.* (1996).

presumptive-notochord blastomeres were treated with bFGF, the expression of the *As-T* gene was also detected (Nakatani *et al.,* 1996). Therefore, inductive interactions that mediate notochord determination are required for the expression of *As-T.* The expression of *As-T* is closely correlated with the determined state of notochord precursor cells. The major role of inductive interactions may be to cause expression of the *As-T* gene in the presumptive-notochord cells. These findings indicate that the molecular mechanism of notochord induction in ascidians is similar to that of other chordates.

2. Brain Induction

The so-called brain (sensory vesicle) of ascidian larvae is located in the dorsal region of the trunk. The central nervous system is formed by the folding of the neural plate (Figs. 2C–F) and, as in vertebrates, neural induction is involved. The brain is derived from six blastomeres of the anterior–animal region (the a-line blastomeres) of the 110-cell embryo (Fig. 3, 4, 6, and 18). Isolated a-line cells from 8-cell embryos do not develop brain structures. Experiments involving the ablation and recombination of blastomeres indicate that the anterior–vegetal (A-line) cells have an inductive influence on brain development (Rose, 1939; Reverberi and Minganti, 1946).

Recently, the differentiation of neural tissues was monitored by examining the development of neural-type membrane excitability (Okado and Takahashi, 1988; reviewed by Okamura *et al.,* 1993; Takahashi and Okamura, 1995). When the a-line animal blastomeres of 8-cell embryos, which are fated to give rise to brain and epidermis (Fig. 6A), were isolated and cleavage-arrested using cytochalasin B, they developed membrane excitability typical of epidermis cells. However, when they were cultured in contact with cleavage-arrested A-line vegetal cells, they showed a neural type of differentiation. Therefore, inductive interactions with the vegetal cells are essential for neural development. Effective recombination of the a- and A-line cells for neural-type differentiation is estimated to occur during the gastrula stage (Okado and Takahashi, 1990). Interestingly, isolated a-line cells can be induced to develop neural features when they are treated with protease (Okado and Takahashi, 1993). The proteolysis of the extracellular domain of a putative receptor molecule may activate the intracellular domain of the receptor.

Okamura *et al.* (1994) cloned a cDNA that encodes a neuron-specific sodium channel. Expression of this gene begins in the late gastrula embryo. Experiments involving the recombination of blastomeres consistently demonstrate that the expression of this sodium channel gene in brain-lineage

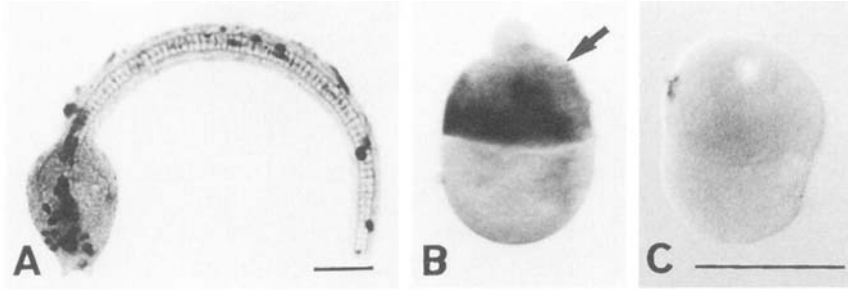

FIG. 17 (A) The expression of TuNa1, a gene that encodes a neuron-specific sodium channel, is detected in cells of central nervous system as well as peripheral nervous system. Transcripts were detected by *in situ* hybridization. (B) TuNa1 expression is induced in the a-line cell by cell iteration with the A-line cell. An a-line brain-lineage blastomere was isolated (arrow) and recombined to an A-line cell of the vegetal hemisphere at the 8-cell stage. Their cleavages were arrested by cytochalasin B and they were cultured until larval stage. Signal is evident in the cleavage-arrested a-line cell. (C) An a-line cell was cultured with another cell of the animal hemisphere. No signal is observed. Scale bar, 50 μm. From Okamura *et al.* (1994).

cells requires contact with the A-line cells of the vegetal hemisphere (Fig. 17). These results indicate that neural induction in ascidian embryos is similar to neural induction in vertebrates.

3. Induction of Sensory Pigment Cells

The brain of an ascidian larva is composed of two pigment cells, termed the ocellus melanocyte and the otolith melanocyte (Figs. 18A and 18B). The ocellus responds to light, whereas the otolith is sensitive to gravity (Dilly, 1962, 1964). Each sensory organ contains a single melanocyte. The ocellus melanocyte and the otolith melanocyte are easily distinguished by their morphology. These pigment cells originate from two blastomeres (a8.25 cell) that are bilaterally positioned in the animal hemisphere of the 110-cell embryo (Fig. 18C). The a8.25 cell also gives rise to part of the brain.

Formation of these pigment cells requires the inductive influence from vegetal blastomeres of the A-line. When a-line melanocyte-lineage cells are isolated during the cleavage stage, they do not develop into melanocytes. When they are recombined with A-line vegetal blastomeres, melanocyte differentiation occurs (Rose, 1939; Reverberi and Minganti, 1946; Riverberi *et al.*, 1960). In *Halocynthia,* the time of melanocyte determination was studied by Nishida and Satoh (1989). When embryonic cells were dissociated at 9 hr (the 110-cell stage, beginning of gastrulation) and cultured until the hatching stage, pigment cell development did not occur. However, dissociation of cells after 10 hr (the 180-cell stage, middle gastrula) resulted

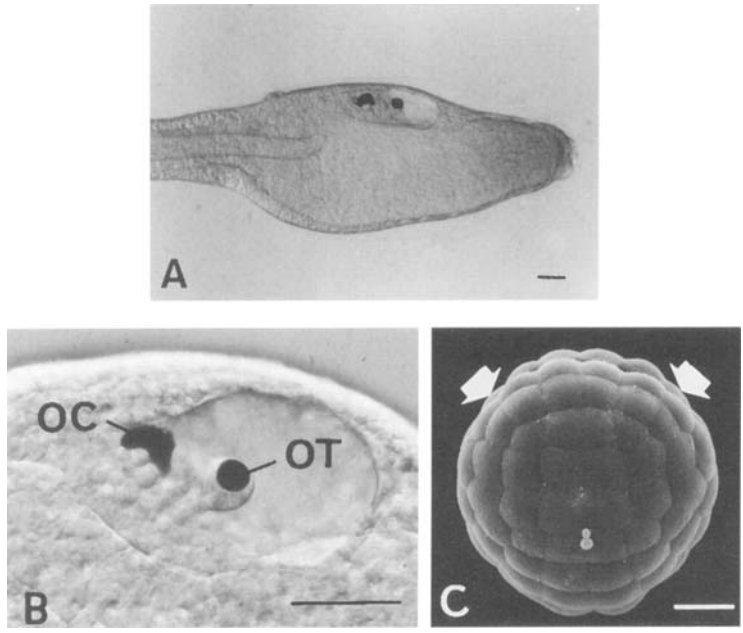

FIG. 18 (A) A tadpole larva with two sensory pigmented spots in the brain (sensory vesicle). (B) Higher magnification of the brain of a larva. OC, ocellus melanocyte; OT, otolith melanocyte. (C) An SEM image of the animal hemisphere of a 110-cell embryo, showing bilateral melanocyte-lineage cells, a8.25 (arrows). Anterior is at the top of the photomicrograph. Scale bar, 50 μm. From Nishida and Satoh (1989).

in development of pigment cells. The timing of melanocyte determination will be discussed further in a later section.

To identify which precursor cell is the inducer of sensory pigment cells, various sets of blastomeres were coisolated together with the presumptive melanocyte of the 110-cell embryos (Nishida, 1991). As previously mentioned, the fates of most of the blastomeres are restricted to a single type of tissue by the 110-cell stage. The results of these studies suggest that the nerve cord (previously this was designated as spinal cord) precursor blastomeres, which are vegetal cells of the A-line, can induce the a-line cells to form pigment cells. In addition, embryos from which all nerve cord precursors had been ablated failed to form sensory pigment cells. Therefore, it is probable that the inducers of ascidian sensory pigment cells are nerve cord precursor cells. However, the induction of sensory pigment cells in ascidian embryos is not comparable to the induction of sensory organs in vertebrate embryos, because sensory pigment cells are induced at about the 180-cell stage during gastrulation in ascidians, but not induced from

the neural tube of neurula or tailbud as in vertebrates. Similar to neuronal cells, isolated a-line cells can be induced to differentiate into melanocytes by treatment with protease (Ortolani *et al.*, 1979). Tyrosinase is an essential enzyme for melanin synthesis (Whittaker, 1966, 1973b). Recently, a gene of tyrosinase was cloned (Sato *et al.*, 1997). Study of trancriptional control elements of this gene may help to elucidate the molecular mechanisms responsible for pigment cell induction.

4. Induction of Trunk Lateral Cells

TLCs were first described as larval cells situated dorsally to mesenchyme cell clusters at the tailbud stage in *Halocynthia* (Nishida and Satoh, 1985). TLCs originate exclusively from A7.6 blastomeres of the 110-cell embryo. Mita-Miyazawa *et al.* (1987) produced a monoclonal antibody that recognizes larval TLCs. After metamorphosis, this TLC-specific antigen was expressed in the coelomic cells of juveniles and in adult basophilic blood cells. It has been suggested that TLCs may be the precursors of some types of adult blood cells (Nishide *et al.*, 1989). Although TLCs do not play a role in the larva, they initiate some steps of differentiation before metamorphosis, as indicated by the expression of the TLC-specific antigen.

When prospective TLC blastomeres were isolated from embryos before the 16-cell stage, they did not express TLC-specific antigen. Isolates after the 32-cell stage, however, autonomously expressed the antigen. Results of experiments involving recombination of blastomeres at the 16-cell stage showed that inductive influences emanating from animal hemisphere cells (presumptive epidermis blastomeres) are required for TLC formation. The inducing activity is distributed widely in the animal hemisphere. In contrast, only presumptive TLC blastomeres have the competence to be induced to form TLCs (Kawaminami and Nishida, 1997).

B. Stage of Determination and Fate Restriction

The determinative state of cells can be operationally defined only by isolation and grafting experiments. A determined cell continues to develop autonomously according to its development fate after isolation from the embryo or after grafting to any other region of an embryo. A series of such isolation and grafting experiments, carried out at different stages, usually reveals the time at which the fate of particular embryonic cells is unequivocally determined (Slack, 1991).

In classical embryology, most studies of embryonic induction were performed in vertebrates, for example, studies of mesoderm induction (Nieuwkoop, 1969, 1973) and neural induction (Spemann and Mangold, 1924;

Spemann, 1938) in amphibian embryos. Embryos of vertebrates consist of a large number of cells compared with those of invertebrates. The inductive interactions are generally assumed to determine the fates of large groups of cells, with all descendants of the induced cells following a single common developmental pathway.

Inductive interactions and the timing of determination have recently been investigated in detail in invertebrate embryos, namely, those of ascidians and a nematode. In these animals, embryogenesis involves a relatively small number of cells. The determination and induction of certain cell types in *Halocynthia* have been analyzed at the single-cell level, and it has been shown that inductive interactions occur during the cell cycle immediately prior to asymmetric cell division, during which the developmental fate is restricted to a single type of cell (Nishida, 1996b). These studies serve to emphasize the importance of the events that occur in the last cell cycle prior to fate restriction.

Figure 19 summarizes the temporal relationships between the stage of fate restriction and the time of determination or period of inductive interaction in four examples in *Halocynthia* embryos. In the case of notochord induction (Fig. 19A), inductive interactions take place during the 32-cell stage, as mentioned before. However, the developmental fate of the presumptive-notochord blastomeres of the 32-cell embryo (A6.2 cells, for example) have not yet been restricted to exclusively produce notochord cells at this stage. These cells also produce nerve cord cells. During the next cell division, the developmental fates that give rise to notochord and nerve cord are separated into two daughter cells. So the fate of one daughter blastomere (A7.3 cell) is restricted to produce notochord and the other daughter cell (A7.4 cell) is restricted to produce nerve cord cells. This being the case, inductive interactions occur just prior to fate restriction (Nakatani and Nishida, 1994).

In the case of the induction of otolith and ocellus melanocyte precursors (Fig. 19B), presumptive melanocyte cells acquire the ability to develop

FIG. 19 Four examples illustrating the timing of cell determination and fate restriction during ascidian embryogenesis. The timing of determination was inferred by experiments involving dissociation, isolation, and recombination of embryonic cells. (A) Timing of induction and fate determination in the primary notochord lineage during ascidian embryogenesis. (B) Events during the development of the sensory pigment cell lineage. (C) Events during development of the secondary muscle lineage. (D) Events during development of the secondary notochord lineage. Numbers in circles indicate the rounds of cell division in the relevant lineage up to the final cell division. In each figure, a lineage tree is shown. Letters with numbers, such as A6.2, designate a particular blastomere. The relevant lineage is indicated by thick lines. Nonrelevant lineages are indicated by broken lines and cell divisions are omitted. From Nishida (1996b).

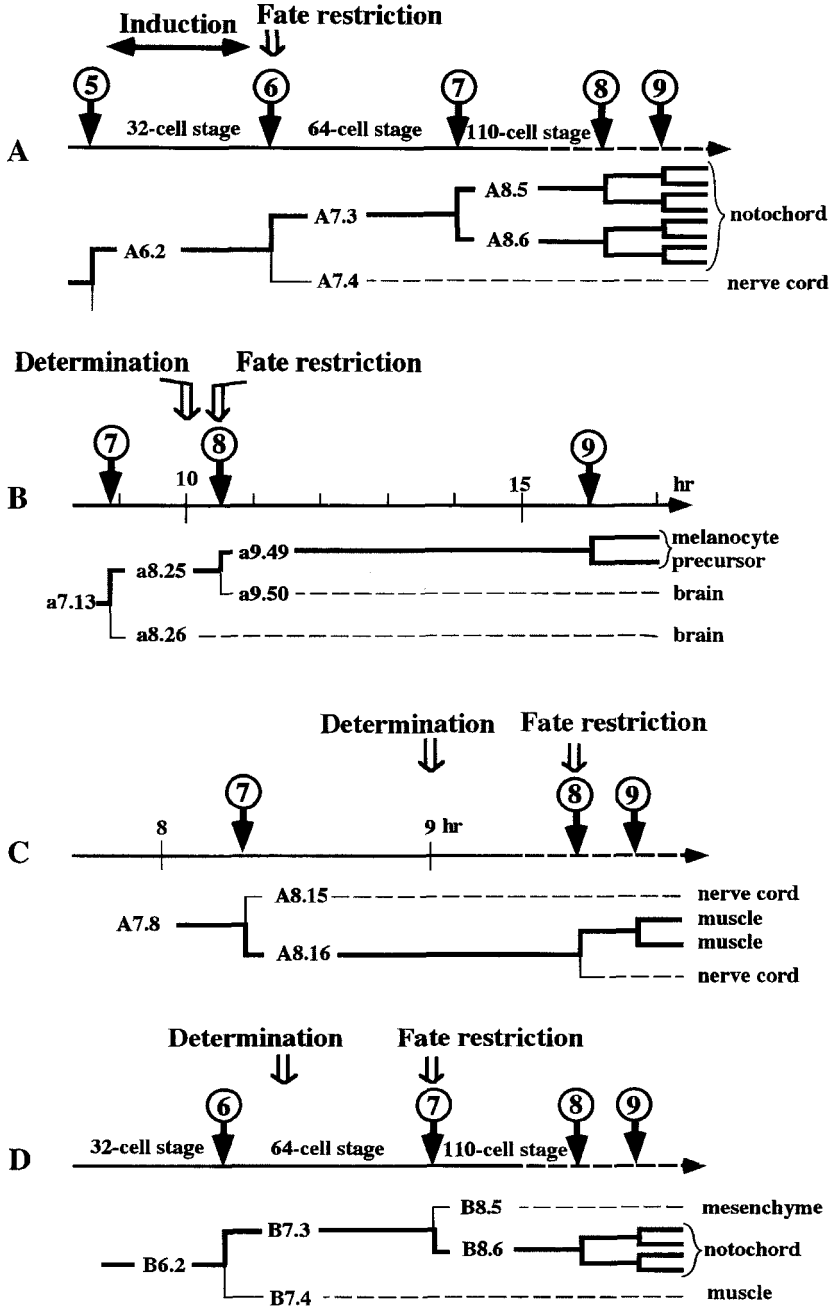
Induction
Fate restriction
A
5
6
7
8
9
32-cell stage
64-cell stage
110-cell stage
A8.5
A7.3
A8.6
notochord
A6.2
A7.4
nerve cord
Determination
Fate restriction
B
7
8
9
10
15
hr
melanocyte
precursor
a9.49
a8.25
a7.13
a9.50
brain
a8.26
brain
Determination
Fate restriction
C
7
8
9
8
9 hr
A8.15
nerve cord
A7.8
muscle
muscle
A8.16
nerve cord
Determination
Fate restriction
D
6
7
8
9
32-cell stage
64-cell stage
110-cell stage
B8.5
mesenchyme
B7.3
B8.6
notochord
B6.2
B7.4
muscle

autonomously in isolation before their developmental fate is restricted to formation of melanocytes (Nishida and Satoh, 1989). Figure 19C presents the case for secondary muscle cells. As mentioned before, there are 21 muscle cells on each side of the tail of the tadpole larva of the ascidian *Halocynthia.* The 14 cells of the anterior and middle parts of the tail are designated primary muscle cells, while the 7 cells in the posterior part are called the secondary muscle cells. The fates of primary muscle cells are specified by localized ooplasmic factors. Therefore, blastomeres of the primary muscle lineage show developmental autonomy even at early cleavage stages. In contrast, the secondary muscle lineage does not. To define the stage at which cells acquire the capacity for autonomous development, secondary muscle lineage blastomeres were isolated at various stages (Nishida, 1990). The results suggest that the determination of secondary muscle cell fates occur part of the way through the cell cycle, immediately before the eighth cell division, at which time the fate of one daughter cell is restricted to muscle.

Figure 19D presents the case for secondary notochord cells. The tadpole larvae of ascidians have 40 notochord cells in the tail. Of these cells, 32 in the anterior and middle parts of the tail are derived from the primary lineage, while 8 in the posterior part originate from the secondary lineage. The inductive interactions that occur in the primary notochord precursor cells have been studied in detail and described before (Fig. 19A). In studies of the secondary notochord lineage, experiments involving the isolation of blastomeres at various stages were carried out. The results suggest that determination precedes the restriction of the developmental fate to produce notochord cells (Nakatani and Nishida, 1994).

Similar examples can be found in the embryogenesis of other animals. A recent study has shown that induction is required for establishment of gut cells in *C. elegans* (Goldstein, 1992, 1993, 1995). Determination of gut fate is accomplished by a contact-dependent inductive interaction prior to fate restriction, and only one daughter cell of the induced mother cell inherits the capacity to form gut.

In each case, determination seems to occur during the last cell cycle, immediately before fate restriction. These studies were carried out with invertebrate embryos that contain a small number of cells. Cellular interactions and determination occur within a small number of cells and could, therefore, be analyzed at the single-cell level. The results reveal novel aspects of induction that are different from those observed in vertebrates. In vertebrates, it has been postulated that inductive interactions which are mediated by diffusible factors generally determine the fate of large groups of cells, with all descendants of the induced cells assuming a single common developmental pathway (Fig. 20). Nonequivalent or asymmetric cell divisions that produce two distinct cells play a fundamental role in generating

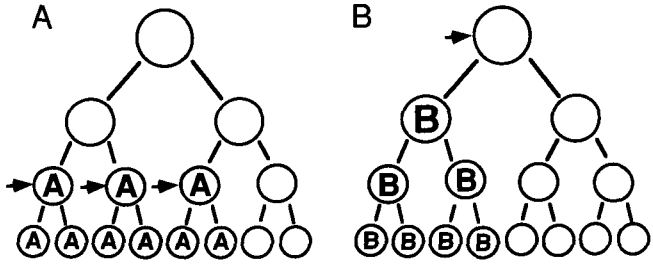

FIG. 20 (A) Inductive influences (arrows) determine the fate of groups of cells usually depending on the position of the responding cells rather than on their lineage. All the progeny of the induced cells assume a common developmental fate, which is represented by A. (B) The mother cell is subject to an inductive influence (arrow). Consequently, one daughter cell assumes a fate, B, that is different from the fate of the other daughter cell. From Nishida (1996b).

different types of cells in embryos with a small cell number, such as ascidian embryos. In the cases discussed herein, only one daughter cell of a mother cell that was subject to an inductive influence became fated to give rise to a certain cell type (Fig. 20B). The number of cases studied so far in invertebrates is too small to allow us to postulate the general significance of determination prior to fate restriction. It is now important to study the timing of induction in cases where induction occurs within a small number of cells and in a contact-dependent manner.

In the examples discussed herein, inductive interaction and determination occur at the last cell cycle before asymmetric cell division that results in fate restriction. The phenomenon has several important implications for understanding how developmental fates are determined. Presumably, inductive influences cause some localized change in the mother cell and polarize the mother cell, resulting in asymmetric division. An obvious hypothesis is that particular cytoplasmic factors are captured at the site of contact with the inducer cell, as suggested by Goldstein (1995) in the induction of gut in *C. elegans*. Alternatively, factors may be activated near the contact site, causing one daughter to differentiate differently. Recently, the Numb and Prospero proteins involved in *Drosophila* neurogenesis (Rhyu *et al.*, 1994; Knoblich *et al.*, 1995; Hirata *et al.*, 1995) and Notch protein involved in vertebrate neurogenesis (Chenn and McConnell, 1995) have been shown to be inherited by one daughter cell in nonequivalent cell divisions. Asymmetrically segregated Numb and Prospero proteins are required for asymmetric fates. Although it is unknown whether cellular interactions are involved in these processes, the translocation of the Numb and Prospero proteins in a particular direction occurs during the cell cycle just before asymmetric cell division. Another likely possibility is that only

one of the daughter chromosomes or DNA that will be inherited by one daughter cell is modified in the mother cell, although there is no evidence to support this. The necessary involvement of DNA replication and critical nuclear events in the quantal cell cycle prior to cell differentiation have long been postulated (Holtzer *et al.,* 1975). In future studies, it will be important to examine the events that occur during the last cell cycle in mother cells.

C. Instructive and Permissive Induction

Notochord-lineage and brain-lineage blastomeres that are isolated before inductive interactions take place do not develop into epidermis cells or other kinds of tissue as far as has been examined (Nishida, 1991; Nakatani and Nishida, 1994). This indicates an important difference in the process of induction of notochord and brain in ascidian embryos compared to mesodermal and neural induction in amphibian embryos. It is possible that intrinsic differences may already exist between precursors of notochord and brain and those of epidermis before induction. Inductive influences may be required for the expression of features of differentiation, rather than choosing a particular cell fate among the repertoire of possible developmental pathways. In this regard, these interactions may be considered an example of a "permissive" type of induction (Wessells, 1977; Gurdon, 1987). Inherited maternal cytoplasmic factors could be responsible for the differences observed between precursors of notochord and brain and precursors of epidermis. In ascidians, epidermis formation appears to be mediated by maternal epidermis determinants, and there does not appear to be a "default fate" such as epidermis in animal-hemisphere cells of amphibian embryos. This will be discussed again in a later section.

D. Competence

The distribution of the competence to be induced to form notochord cells and TLCs in *Halocynthia* embryos was analyzed. The results indicated that the competence to be induced to make notochord is restricted to the presumptive-notochord blastomeres. Likewise, the competence to be induced to form TLCs is restricted to the presumptive-TLC blastomeres. Again, it seems that there are intrinsic differences between responding blastomeres and other blastomeres.

V. Specification of the Anterior–Posterior Axis

A. Cytoplasmic Determinants vs Induction

The definition of the axis of eggs and early embryos as a whole is somewhat difficult, because embryonic cells show complicated movements during morphogenesis, and the definition depends on what parts of the embryo one stresses. Conklin (1905b) assigned the animal–vegetal axis of ascidian eggs to the ventral–dorsal axis. Only in the animal hemisphere does the animal–vegetal axis of eggs and early embryos correspond precisely to the ventral–dorsal axis of larvae. The central region of the ventral epidermis of larvae originates from the animal pole region, whereas equatorial blastomeres in the animal hemisphere develop into dorsal epidermis. However, in the vegetal hemisphere, it is difficult to define the dorsal–ventral axis. Blastomeres in the vegetal pole region of early embryos do not give rise to the dorsal tissues of larvae, as they give rise to endoderm (Fig. 4).

The anterior–posterior axis has been defined as roughly perpendicular to the animal–vegetal axis in ascidians eggs (Conklin, 1905b). The anterior–posterior axis (A-P axis) of eggs and early embryos does not correspond precisely to the A-P axis of larvae because cells do not remain stationary during morphogenetic movements. Again, in the animal hemisphere, the A-P axis of eggs and early embryos corresponds precisely to the A-P axis of larvae because positional rearrangement does not take place in the animal hemisphere. Anterior–animal blastomeres give rise to head epidermis of larvae and posterior–animal blastomeres develop into tail epidermis. In the vegetal hemisphere, anterior blastomeres, which are designated A-line cells, mainly give rise to anterior endoderm, notochord, and nerve cord (Figs. 4 and 6A). Notochord and nerve cord cells are located in the larval tail. Posterior–vegetal blastomeres, which are designated B-line cells, mainly develop into posterior endoderm, mesenhyme, and muscle. Muscle cells are found in the tail, while posterior endoderm and mesenchyme cells are found in the trunk region (Conklin, 1905b; Nishida, 1987). In the present paper, "anterior" and "posterior" are used in the way that these adjectives have been traditionally applied to ascidian eggs and early embryos according to Conklin (1905b). Thus, in the present context, "anterior fate" refers to the fate that gives rise to the anterior part of the fate map of blastulae (Fig. 4) and does not mean the fate that gives rise to the anterior structures of larvae.

How is the anterior–posterior axis of the embryo specified in an ascidian? The fate map of the animal hemisphere is straightforward (Fig. 4). In contrast, that of the vegetal hemisphere is more complicated. Among the various tissues comprising the fate map, epidermis and endoderm fates are determined by cytoplasmic determinants. Inductive interactions occurring

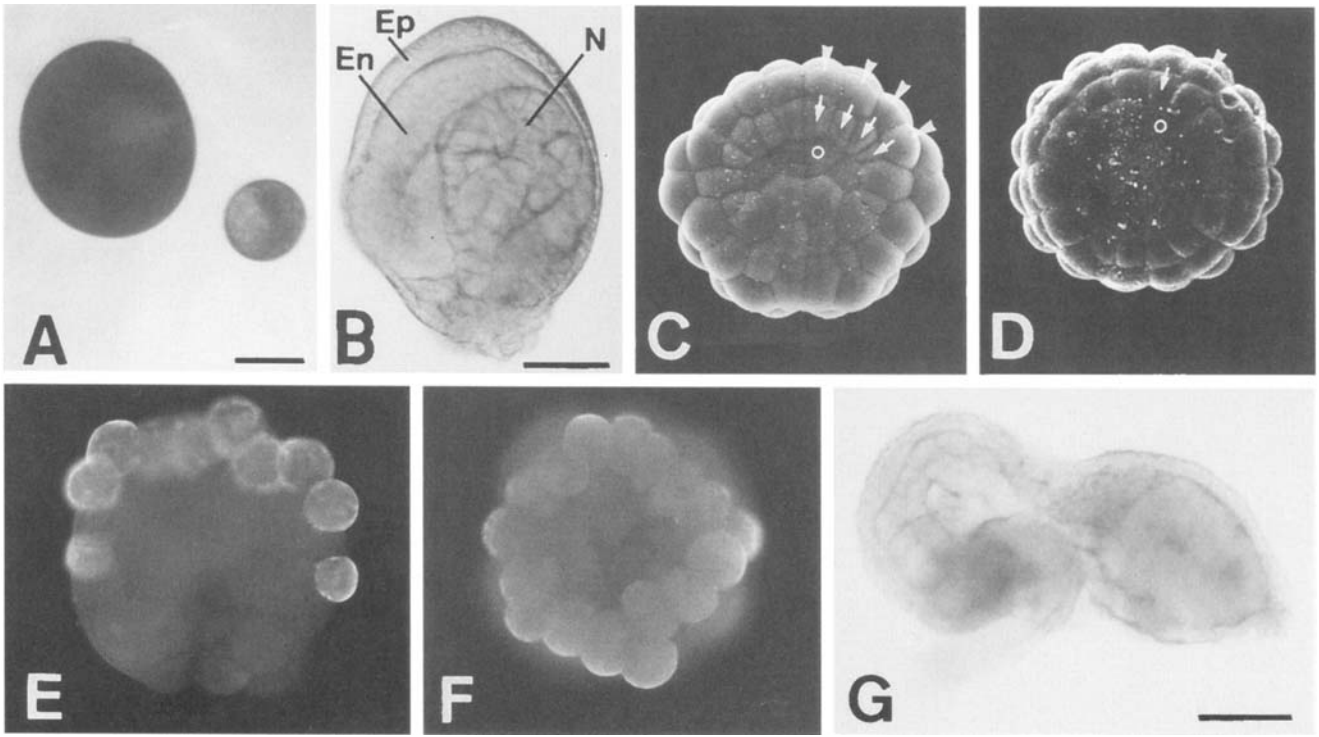
A
B
Ep
En
N
C
D
E
F
G

at the 32-cell stage are involved in the formation of notochord. Anterior to the notochord precursors, there are nerve cord precursors. It is not yet known whether nerve cord is induced by notochord. Anterior to the nerve cord precursors, there are precursors of brain and sensory pigment cells. These cells are induced during gastrulation. As notochord and brain are formed by induction, it is likely that anterior components of ascidian embryos are induced sequentially during embryogenesis. By contrast, primary muscle precursors in the posterior region are determined by cytoplasmic factors in eggs. The determinative mechanism of mesenchyme formation is not yet known. Here, I would like to propose that in the equatorial region of the vegetal hemisphere, posterior fate is determined by cytoplasmic factors in the egg and anterior fate is determined by sequential induction during embryogenesis. There is evidence to support this idea using *Halocynthia* eggs.

Posterior–vegetal cytoplasm was removed from *Halocynthia* eggs at the second stage of ooplasmic segregation by cutting off egg fragments with a fine glass needle. The egg volume removed was 8–15% of the total volume (Figs. 21A and 22, Exp. A). The larvae derived from these operated eggs did not have a normal tadpole morphology (Fig. 21B). These larvae consisted of epidermis, endoderm, and notochord but they lacked muscle. There were tissues that are derived only from the anterior hemisphere of the fate map (Fig. 4). Also, they showed radial symmetry along the animal–vegetal axis. There was no indication of an anterior–posterior axis. Removal of egg cytoplasm from the other regions did not affect normal embryogenesis (Nishida 1994b). In contrast, in *Styela* eggs, Bates and Jeffery (1987b) reported that removal of the posterior–vegetal cytoplasm at the second stage of segregation did not affect normal development.

FIG. 21 (A) A posterior–vegetal cytoplasmic fragment has been removed from a *Halocynthia* egg after the second phase of ooplasmic segregation. (B) A larva derived from an egg from which posterior–vegetal cytoplasm had been removed. Ep, epidermis; En, endoderm; N, notochord. (C) SEM image of vegetal view of a normal embryo at the 76-cell stage. Arrowheads show blastomeres that are precursors of nerve cord. Arrows indicate notochord precursors, and an open circle shows an endoderm precursor. (D) SEM image of vegetal view of a posterior–vegetal cytoplasm-deficient embryo. Cleavage pattern is radialized. (E) Cell division of a normal embryo had been inhibited from progressing beyond the 110-cell stage. Expression of the notochord-specific antigen was detected. There is a row of eight positive cells, in addition to two smaller positive cells. Refer to the 110-cell embryo in Fig. 13D. (F) Posterior-vegetal cytoplasm deficient embryo was treated similarly to the embryo in E. In this specimen, stained cells encircled the embryo. (G) Posterior cytoplasm is transplanted to the anterior position. The fate of introduced cytoplasm was traced. It was shown that tadpole larvae developed with their anterior–posterior axis reversed with regard to developmental fate. Scale bar, 100 μm. From Nishida (1994b).

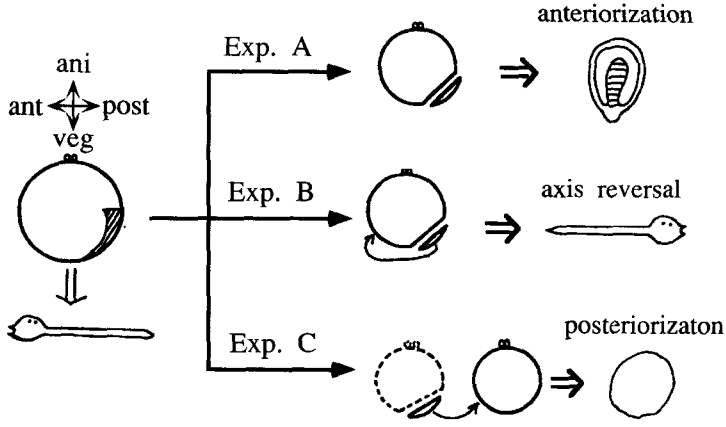

FIG. 22 Summary of experiments that involve removal and transplantation of the posterior–vegetal cytoplasm (PVC) from *Halocynthia* eggs after the second phase of ooplasmic segregation. (Exp. A) Removal of PVC. (Exp. B) Transplantation of PVC to the anterior–vegetal position of PVC-removed eggs. (Exp. C) Transplantation of PVC to the anterior–vegetal position of normal eggs. Embryos have PVC in both sides in this case.

Figure 21C shows a vegetal view of normal *Halocynthia* embryos at the 76-cell stage, while Fig. 21D shows an embryo lacking posterior cytoplasm. The cleavage pattern was radially symmetrical in these deficient embryos. Mirror-image duplication of the anterior half of a normal embryo can be recognized. In normal and deficient embryos, notochord precursors are indicated by arrows. In deficient embryos, it looks like notochord precursors encircle the embryos. This was confirmed taking advantage of ascidian development. Nishikata and Satoh (1990) reported that when cleavages were continuously inhibited by treatment with cytochalasin B after the 110-cell stage, eventually, some of the notochord precursor cells expressed the notochord-specific antigen. The maximal number and arrangement of positive cells coincided with those of the notochord-lineage cells (Fig. 21E). The radialized embryos were treated similarly. The number of positive cells exceeded that of normal embryos, and positive cells encircled the embryos (Fig. 21F) (Nishida, 1994b). These results suggest that without posterior ooplasm, induction proceeds in the posterior direction. Consequently, mirror-image duplication of the anterior half occurs. Removal of anterior cytoplasm had no effect on normal embryogenesis.

In the second series of experiments, posterior cytoplasm was transplanted to the anterior position by electrofusion of egg fragments (Fig. 22, Exp. B). A posterior egg fragment was cut off, stained with Nile blue, and then fused to the anterior position. The fate of introduced cytoplasm was traced

by monitoring the color. In a significant number of cases, tadpole larvae developed with their anterior–posterior axis reversed in terms of the cleavage pattern as well as the developmental fate (Fig. 21G). In such cases, sequential induction is likely to proceed in the posterior direction. In addition, formation of the anterior components from the original anterior part must be inhibited by the introduced posterior cytoplasm. In contrast, transplantation of anterior cytoplasm to the posterior position had no effect.

In the third series of experiments, posterior cytoplasm was transplanted to the anterior position of normal eggs (Fig. 22, Exp. C). In this case, the eggs operated had posterior cytoplasm on both sides. The number of notochord cells was significantly reduced, and in 7% of cases, embryos had no notochord. These results suggest that posterior cytoplasm suppresses the formation of the anterior components.

By looking at the fate map again in Fig. 4, the removal of posterior cytoplasm causes the posterior blastomeres to adopt the fates of anterior blastomeres. When posterior cytoplasm was transplanted to an anterior position, posterior fate overcame anterior fates. In contrast, transplantation of anterior cytoplasm to a posterior position did not affect development. Therefore, posterior fates were dominant over anterior fates in these cytoplasmic transfer experiments using *Halocynthia* embryos. The presence of posterior cytoplasm specifies posterior fate, while anterior fate is directed by the absence of posterior cytoplasm. Provided that posterior fate is determined by cytoplasmic factors present in the egg and, in addition, that anterior fate is determined by sequential inductions during embryogenesis, it is easy to explain the posterior dominance that was observed in cytoplasmic transfer experiments. Without posterior cytoplasm, sequential inductions also proceed in the posterior direction, with formation of anterior components. Removal or transplantation of anterior cytoplasm does not affect normal development. There may be no maternal determinants unique to the anterior part of the zygote. When posterior cytoplasm is present, sequential inductions cannot occur because the developmental fate of these cells has already been determined by maternal cytoplasmic factors and the blastomeres do not have the competence to be induced.

B. Comparison with Amphibian Development

In unfertilized eggs of many kinds of animals, there is an animal–vegetal axis. The second axis of bilateral embryos that is perpendicular to the animal–vegetal axis is specified just after fertilization or during early embryogenesis. These two axes are the basis for the bilateral body plan. There are important and significant differences between ascidians and amphibians in the processes involved in establishment of the second axis of the egg.

The second axis is the so-called anterior–posterior axis in ascidian eggs and the so-called dorsal–ventral axis in amphibian eggs. The anterior region of the ascidian fate map at the blastula stage (Fig. 4) is comparable to the dorsal region of the amphibian fate map; this is where the notochord and central nervous system rudiments exist and both cell types are induced during embryogenesis.

In *Xenopus,* the specification of the dorsal–ventral axis begins after fertilization with a shift of vegetal–cortical cytoplasm to the future dorsal side (Scharf and Gerhart, 1980). In *Xenopus,* it was recently shown that transplantation of dorsal cytoplasm to a ventral position causes the formation of a secondary axis (Yuge *et al.,* 1990). Dominance of the dorsal fate was observed. Hainski and Moody (1992) reported that mRNA from dorsal blastomeres can alter ventral blastomeres and yield a secondary axis. This is the most important and significant difference from ascidian development, because cytoplasmic transfer experiments in *Xenopus* eggs indicate that there exist dorsal determinants rather than ventral determinants in egg cytoplasm. The dorsal determinants are thought to be involved in the formation of the Nieuwkoop center of *Xenopus* embryos.

In contrast, in ascidian, transfer of egg cytoplasm showed that posterior determinants are present and that there may be no maternal determinants unique to the anterior part, which corresponds to the dorsal part of amphibian. It is likely that there is no Nieuwkoop center in the ascidian embryo. In the animal hemisphere, epidermis determinants exist. In the vegetal pole region, endoderm determinants exist. And in the posterior region, posterior determinants are present. Therefore, the competence to be induced to notochord and brain might be restricted to the anterior marginal region of the embryo. Inductive influence automatically progresses in the anterior direction.

As mentioned before, induction of notochord and brain in ascidian may be regarded as permissive type, because presumptive notochord and brain blastomeres that are isolated before induction do not differentiate into epidermis or other cell types. However, as indicated above, in ascidian, there may be no maternal determinants to specify anterior fate. Therefore, anterior blastomeres that were isolated before induction may indeed be neutral cells that have no default fate, such as epidermis in amphibian embryos. If this is correct, the fate of these cells is determined by inductive interactions. In this regard, these inductions can be regarded as "instructive." The distinction between instructive and permissive induction is easily applicable to vertebrate development (Wessells, 1977; Gurdon, 1987). However, if there is no default fate, such as is the case in ascidian embryos, the distinction is not clear because there is no way to know whether a cell is neutral or its fate is already specified to some extent.

C. Evolutionary Modifications of Ascidian Development

The idea of induction of notochord and sensory pigment cells is supported by interesting observations and experiments using anural ascidian embryos, which show an alternate mode of development. Most ascidian species produce tadpole (urodele) larva. However, in fewer than 20 of approximately 3000 ascidian species, fertilized eggs develop into tailless (anural) larvae that develop directly into adults (Berrill, 1931; Jeffery and Swalla, 1990, 1992). Urodele development is thought to be the ancestral mode of development in the ascidian. *Molgula oculata* and *Molgula occulta* are closely related species (Swalla and Jeffery, 1990). *M. oculata* shows urodele development, whereas *M. occulta* shows anural development (Fig. 23). The anural embryo lacks some of the typical urodele features. In *M. occulta* embryos, the pattern of early cleavage is similar to that of urodele species. The embryos exhibit typical gastrulation and neural tube formation. However, they do not contain a sensory pigment cell in their brain and they have no tail. Although notochord and muscle-lineage cells are present in the posterior region of the neurula, they do not differentiate into notochord and muscle cells.

The mechanisms underlying the transition from urodele to anural development have been investigated. When eggs of *M. occulta* (anural species) are fertilized with sperm of *M. oculata* (urodele species), the interspecific hybrids develop some of the urodele features, including a sensory pigment cell and a short tail containing notochord, but there are no muscle cells (Fig. 23) (Swalla and Jeffery, 1990). In the reciprocal cross, embryos develop into tailed tadpole larvae. The results of interspecific hybridization suggest that zygotic expression of the urodele genome in the anural zygote is responsible for differentiation of sensory pigment cells and notochord and that zygotic events play a crucial role in the formation of these tissues. This supports the idea that pigment cells and notochord are induced during urodele embryogenesis. In contrast, muscle does not differentiate in the hybrids. This result supports the idea that ascidian muscle formation involves maternal ooplasmic factors. Swalla *et al.* (1991) and Bates (1995) reported that p58, a cytoskeletal protein recognized by an antibody against vertebrate neurofilaments that is concentrated in myoplasm of urodele eggs, is missing or reduced in eggs of anural species.

Recently, cDNA clones encoding genes that are expressed differentially in anural (*M. occulta*) and urodele (*M. oculata*) eggs were isolated using a subtractive procedure (Swalla *et al.*, 1993). *Manx (Uro-11)* mRNA is present in oocytes of urodele species but it is absent from anural oocytes. In the urodele embryos, zygotic expression of *Manx* occurs in the posterior epidermis and neural and tail muscle cells. *Manx* encodes a DNA-binding protein with zinc fingers. It was very exciting to discover that when interspecific

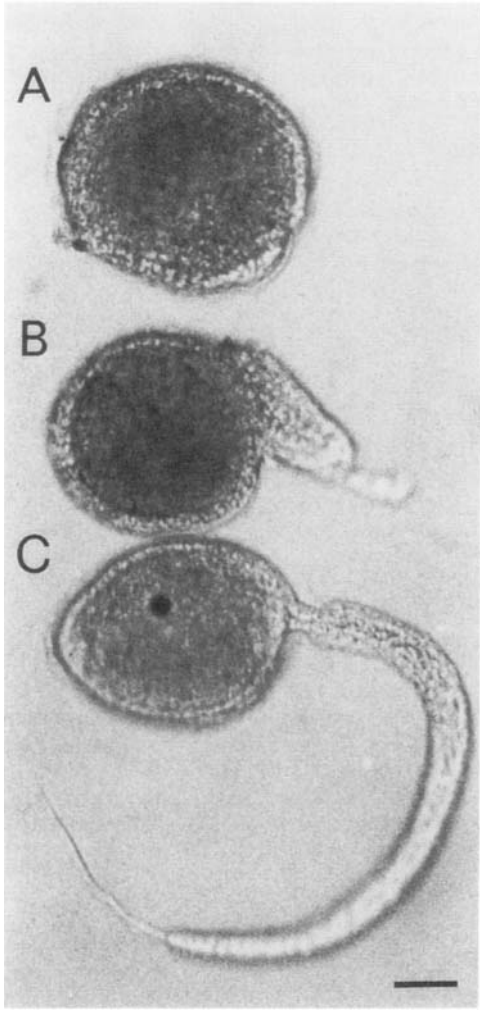

FIG. 23 (A) *Molgula occulta* larvae do not have sensory pigment cells or tails. (B) A larva derived from an interspecific hybrid between eggs of *M. occulta* and sperm of *M. oculata* develops a sensory pigment cell and a short tail. (C) An *M. oculata* tadpole larva. Scale bar, 20 μm. From Swalla and Jeffery (1990).

hybrid embryos are treated with an antisense phosphorothioate oligodeoxynucleotide of *Manx,* tail formation in the hybrid embryo is inhibited (Swalla and Jeffery, 1996b). *Manx* was suggested to be involved in expression of chordate features in the urodele ascidian, and a modification of the *Manx* gene may be involved in the evolutionary transition from urodele to anural development.

VI. Lateral Inhibition in the Equivalence Group

A developmental equivalence group, which was first reported in the nematode *C. elegans,* is defined as a group of cells having equivalent developmental potential which ultimately assume different fates through a lateral inhibition among members of the group (Kimble *et al.,* 1979). In addition to the nematode, the existence of equivalence groups has been reported in the grasshopper and *Drosophila* embryo (Doe and Goodman, 1985), in the leech embryo (Weisblat and Blair, 1984), and in the ascidian embryo (Nishida and Satoh, 1989). It was recently suggested that similar mechanisms may operate in vertebrate neurogenesis (Coffman *et al.,* 1993).

In the brain of ascidian larva, there are two unique pigment cells, termed the ocellus melanocyte and the otolith melanocyte (Figs. 17A and 17B). The ocellus melanocyte and the otolith melanocyte are easily distinguished by their morphology, and each consists of a single cell. These pigment cells originate from two blastomeres that are bilaterally positioned but are separate in the cleavage-stage embryo (Fig. 17C). How are these single unique cells formed in the bilaterally symmetrical embryo?

There are nine cell divisions in both the right and the left melanocyte lineages from the zygote to terminally differentiated melanocyte. At each cell division only one daughter cell remains as the melanocyte lineage cell. The two postmitotic melanocyte precursors meet at the midline of the embryo during neural tube closure (Figs. 2C–F), and one cell develops into an ocellus pigment cell and the other cell into an otolith pigment cell. Cell lineage studies showed that there was no relationship between the right–left position of the melanocyte lineage blastomere and its derivatives (Nishida and Satoh, 1985).

How do these precursor cells choose mutually exclusive fates? The fates of two pigment cell precursors can be predicted once both cells meet at the midline and align along the antero–posterior axis as the neural tube closes. The anterior cell develops into the otolith and the posterior cell into the ocellus (Whittaker, 1973b). This observation suggests that the cue for choosing one of the alternative developmental pathways is positional information. Experimental studies suggest that the bilateral pigment cell precursors constitute an equivalence group (Nishida and Satoh, 1989). When one of two pigment cells derived from the right or left side is destroyed before the middle tailbud stage, the other precursor cell predominantly differentiates into an ocellus (Fig. 24A), and the otolith disappears. Therefore, the two pigment cell precursors are still equipotent before the middle tailbud stage. These two precursors are the members of an equivalence group. Destruction of one precursor after the middle tailbud stage results in the development of either an ocellus or an otolith (Fig. 24B). It is suggested that cell interactions may play a role in determination of

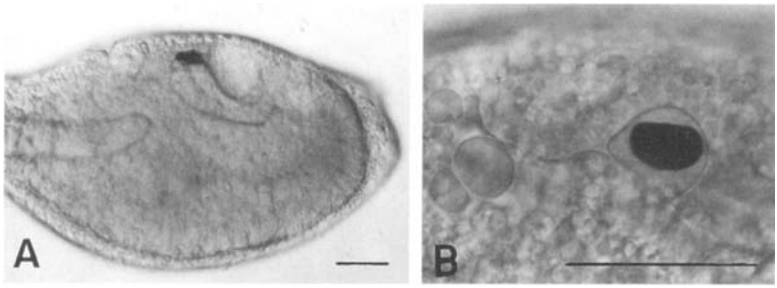

FIG. 24 (A) One of two melanocyte precursor cells derived from the right or the left side is destroyed before the middle tailbud stage. Only the ocellus formed. (B) Destruction of one precursor after the middle tailbud stage. In this case only the otolith formed. Scale bar, 50 μm. From Nishida and Satoh (1989).

mutually exclusive fates and that if the interactions do not occur, the pigment cell precursor automatically chooses an ocellus pathway (referred to as the dominant fate in the equivalence group). This idea is supported by evidence that both bilateral precursors develop into ocelli when morphogenetic movements are inhibited before neural tube closure.

It may be assumed that two kinds of interactions are involved in the specification of fates within the equivalence group. One kind of interaction is an external influence on the equivalence group and is thought to be positional information existing along the anterior–posterior axis. The other kind of interaction is that between members within the equivalence group and is thought to be responsible for the choice of mutually exclusive fates. The posterior-positioned ocellus precursor cell laterally inhibits the anterior-positioned cell to assume the dominant fate, forcing the latter to choose the alternative otolith fate.

In summary, equivalent precursors lie bilaterally during the cleavage stages and then align along the antero–posterior axis at the initial tailbud stage 18 hr after fertilization. Then, from 18 to 21 hr, cellular interactions occur in a position-dependent manner. The melanocyte precursor that is positioned posteriorly by chance is biased to choose the pathway of the dominant fate (i.e., ocellus fate) and laterally inhibits the anterior precursor, forcing the anterior cell to develop into an otolith. Thus, cell fates are irreversibly determined at the middle tailbud stage (21 hr).

VII. Concluding Remarks

The tadpole larvae of the ascidian consist of only a few different kinds of tissue. Proposed mechanisms responsible for cell fate specification for each

TABLE II

Summary of Cellular Mechanisms of Fate Specification

Ectoderm	
Epidermis	Cytoplasmic determinants
Brain (sensory vesicle)	Induction
Nerve cord (spinal cord)	?
Sensory pigment cells	Induction and lateral inhibition
Mesoderm	
Primary muscle	Cytoplasmic determinants
Secondary muscle	Cell interaction?
Primary notochord	Induction
Secondary notochord	Cell interaction?
Mesenchyme	?
Trunk lateral cell	Induction
Endoderm	Cytoplasmic determinants

Note. ?: Not known. Cell interaction?: Cell interaction is suggested by the results of isolation of blastomeres, but is yet to be proved by recombination experiments.

tissue are summarized in Table II. So far, three kinds of cellular mechanisms have been proposed to be involved in fate specification during ascidian embryogenesis: cytoplasmic determinants, inductive interaction, and lateral inhibition (Fig. 25). As mentioned in the section on anterior–posterior axis specification, it can now be envisaged at the cellular level how developmental fates are determined in most cell types and how larval tissues are generated. A more complete understanding of ascidian development is required if we are to elucidate exactly how many mechanisms are involved and how often these mechanisms are used during ascidian embryogenesis. Up to now, there has been uncertainty concerning the cellular mechanisms of fate specification of mesenchyme and nerve cord cells. To achieve a total understanding, the mechanisms responsible for specification of these cell types await future studies.

When examining the unique features of ascidian embryogenesis, namely, the mosaic manner of development, it is important to identify cytoplasmic determinants. It is not known how many maternal molecules are involved in the fate specification of a single cell type. Nor is it known whether the determinants are proteins, maternal mRNAs, or some other molecule, or whether they are localized molecules or localized active forms of widely distributed molecules.

Molecular techniques such as differential cloning, subtraction, and differential display will help to the identify ascidian determinants. These tech-

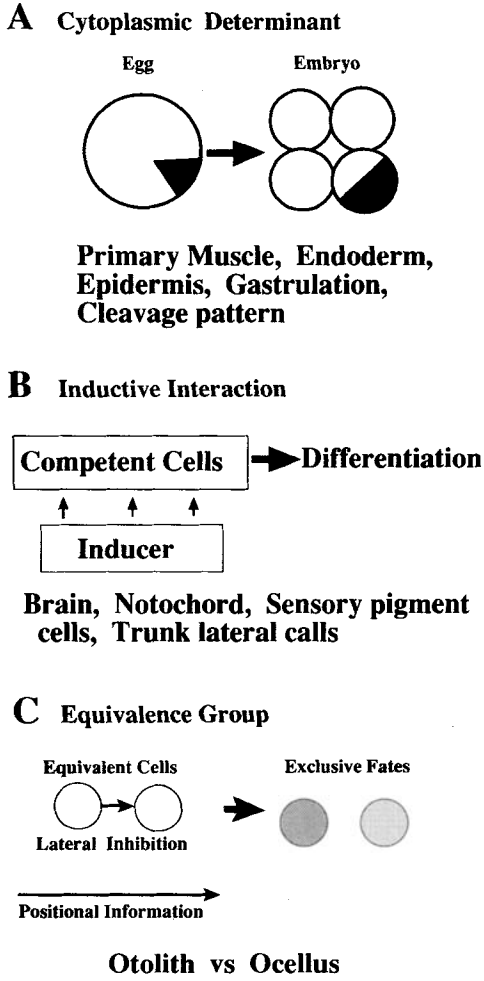

FIG. 25 Three kinds of cellular mechanism (A–C) are involved in cell fate specification during ascidian embryogenesis.

niques were used to identify localized messages in egg cytoplasm (Swalla and Jeffery, 1995, 1996a; Yoshida *et al.*, 1996) and to detect differences in messages between species that show different developmental characteristics such as anural and urodele species (Swalla *et al.*, 1993). Analysis of the upstream *cis*-element of genes that show lineage-specific expression as well as analysis of the *trans*-acting factors will also contribute to the identification of determinants. Expression of the muscle actin gene and myosin genes

starts as early as the 32-cell stage (Satou *et al.*, 1995). The upstream element required for lineage-specific expression of the muscle actin gene is as short as 38 bp (Satou and Satoh, 1996), suggesting that the control mechanisms responsible for lineage-specific expression may be simple in ascidian embryos.

Over the years, many researchers of ascidian development have concentrated on the study of embryogenesis. During ascidian embryogenesis, cell lineages are invariant. Ascidian embryos lack a capacity for compensatory regulation. Are adult cell lineages also invariant? Do ascidians exhibit compensatory regulation during metamorphosis? Nakauchi and Takeshita (1983) showed that isolated blastomeres at the two-cell stage develop into left- or right-half larvae; however, the half larvae can metamorphose into normal whole juveniles. It will be interesting to compare the developmental mechanisms utilized at two different phases of development, namely, embryogenesis and metamorphosis, in a single kind of animal.

Acknowledgments

I express cordial thanks to Dr. W. R. Bates for his critical reading of the manuscript. Our studies included in this review were supported by grants-in-aid from the Ministry of Education, Science and Culture, Japan, and by the "Research for the Future" program from the Japanese Society of the Promotion of Science.

References

Araki, I., Saiga, H., Makabe, K. W., and Satoh, N. (1994). Expression of a AMD1, a gene for a MyoD1-related factor in the ascidian *Halocynthia roretzi*. *Roux's Arch. Dev. Biol.* **203,** 320–327.

Asashima, M. (1994). Mesoderm induction during early amphibian development. *Dev. Growth Differ.* **36,** 343–355.

Bates, W. R. (1988). Development of myoplasm-enriched ascidian embryos. *Dev. Biol.* **129,** 241–252.

Bates, W. R. (1995). Direct development in the ascidian *Molgula retortiformis* (Berrill, 1871). *Biol. Bull.* **188,** 16–22.

Bates, W. R., and Bishop, C. (1996). Localization of constitutive heat shock proteins in developing ascidians. *Dev. Growth Differ.* **38,** 307–314.

Bates, W. R., and Jeffery, W. R. (1987a). Alkaline phosphatase expression in ascidian egg fragments and andromerogons. *Dev. Biol.* **119,** 382–389.

Bates, W. R., and Jeffery, W. R. (1987b). Localization of axial determinants in the vegetal pole region of ascidian eggs. *Dev. Biol.* **124,** 65–76.

Bates, W. R., and Jeffery, W. R. (1988). Polarization of ooplasmic segregation and dorsoventral axis determination in ascidian embryos. *Dev. Biol.* **130,** 98–107.

Berrill, N. J. (1931). Studies in tunicate development. Part II. abbraviation of development in the Molgulidae. *Philos. Trans. R. Soc. London, Ser. B* **219,** 281–346.

Chabry, L. (1887). Contribution à l'embryologie normale et teratologique des Ascidies simples. *J. Anat. Physiol. (Paris)* **23,** 167–319.

Chenn, A., and McConnell, S. K. (1995). Cleavage orientation and the asymmetric inheritance of Notch 1 immunoreactivity in mammalian neurogenesis. *Cell* **82,** 631–641.

Cloney, R. A. (1964). Development of the ascidian notochord. *Acta Embryol. Morphol. Exp.* **7,** 111–130.

Cloney, R. A. (1978). Ascidian metamorphosis: Review and analysis. *In* "Settlement and Metamorphosis of Marine Invertebrate Larvae" (F. S. Chia and M. E. Rice, eds.), pp. 255–282. Elsevier, Amsterdam.

Coffman, C. R., Skoglund, P., Harris, W. A., and Kintner, C. R. (1993). Expression of an extracellular deletion of *Xotch* diverts cell fate in *Xenopus* embryos. *Cell* **73,** 659–671.

Conklin, E. G. (1905a). Mosaic development in ascidian eggs. *J. Exp. Zool.* **2,** 145–223.

Conklin, E. G. (1905b). The organization and cell lineage of the ascidian egg. *J. Acad. Nat. Sci. (Philadelphia)* **13,** 1–119.

Conklin, E. G. (1905c). Organ-forming substances in the eggs of ascidians. *Biol. Bull.* **8,** 205–230.

Conklin, E. G. (1931). The development of centrifuged eggs of ascidian. *J. Exp. Zool.* **60,** 1–119.

Crowther, R. J., and Whittaker, J. R. (1986). Developmental autonomy of presumptive notochord cells in partial embryos of an ascidian. *Int. J. Invertebr. Reprod. Dev.* **9,** 253–261.

Crowther, R. J., and Whittaker, J. R. (1994). Serial repetition of cilia pairs along the tail surface of an ascidian larva. *J. Exp. Zool.* **268,** 9–16.

Deno, T., and Satoh, N. (1984). Studies on the cytoplasmic determinant for muscle cell differentiation in ascidian embryos: An attempt at transplantation of the myoplasm. *Dev. Growth Differ.* **26,** 43–48.

Dilly, P. N. (1962). Studies on the receptors in the cerebral vesicle of the ascidian tadpole. I. The otolith. *Q. J. Microsc. Sci.* **103,** 393–398.

Dilly, P. N. (1964). Studies on the receptors in the cerebral vesicle of the ascidian tadpole. 2. The ocellus. *Q. J. Microsc. Sci.* **105,** 13–20.

Doe, C. Q., and Goodman, C. S. (1985). Neurogensis in grasshopper and *fushi tarazu Drosophila* embryos. *Cold Spring Harbor Symp. Quant. Biol.* **50,** 891–903.

Driever, W., and Nüsslein-Volhard, C. (1988). The bicoid protein determines position in the *Drosophila* embryo in a concentration-dependent manner. *Cell* **54,** 95–104.

Freeman, G. (1983). The role of egg organization in the generation of cleavage patterns. *In* "Time, Space, and Pattern in Embryonic Development" (W. R. Jeffery and R. A. Raff, eds.), pp. 171–196. A. R. Liss, New York.

Goldstein, B. (1992). Induction of gut in *Caenorhabditis elegans* embryos. *Nature (London)* **357,** 255–257.

Goldstein, B. (1993). Establishment of gut fate in the E lineage of *C. elegans:* The role of lineage-dependent mechanisms and cell interaction. *Development* **118,** 1267–1277.

Goldstein, B. (1995). An analysis of the response to gut induction in the *C. elegans* embryo. *Development* **121,** 1227–1236.

Gurdon, J. B. (1987). Embryonic induction—molecular prospects. *Development* **99,** 285–306.

Hainski, A. M., and Moody, A. S. (1992). *Xenopus* maternal RNAs from dorsal animal blastomere induce a secondary axis in host embryos. *Development* **116,** 347–355.

Herrmann, B. G., Labeit, S., Poustka, A., King, T. R., and Lehrach, H. (1990). Cloning of the T gene required in mesoderm formation in the mouse. *Nature (London)* **343,** 617–622.

Hibino, T., Nishikata, T., and Nishida, H. (1997). CAB (Centrosome Attracting Body): A novel structure closely related to unequal cleavages in the ascidian embryo. Submitted for publication.

Hirai, E. (1941). The early development of *Cynthia roretzi. Sci. Rep. Tohoku Imp. Univ., Ser. 4* **16,** 217–232.

Hirata, J., Nakagoshi, H., Nabeshima, Y., and Matsuzaki, F. (1995). Asymmetric segregation of the homeodomain protein Prospero during *Drosophila* development. *Nature* (*London*) **337,** 627–630.

Holtzer, H., Rubinstein, N., Fellini, S., Yeoh, G., Chi, J., Birnbaum, J., and Okayama, M. (1975). Lineages, quantal cell cycle, and the generation of cell diversity. *Q. Rev. Biophys.* **8,** 523–557.

Ishida, T., Ueki, T., and Satoh, N. (1996). Spatio-temporal expression patterns of eight epidermis-specific genes in the ascidian embryo. *Zool. Sci.* **13,** 699–709.

Ishikawa, M., Numakunai, T., De Vincentis, M., and Lancieri, M. (1972). Enzymatic activities relating to the respiration and the onset of metamorphosis of the ascidian tadpole. *Dev. Growth Differ.* **14,** 229–236.

Jeffery, W. R. (1982). Calcium ionophore polarizes ooplasmic segregation in ascidian eggs. *Science* **216,** 545–547.

Jeffery, W. R. (1990a). Ultraviolet irradiation during ooplasmic segregation prevents gastrulation, sensory cell induction, and axis formation in the ascidian embryo. *Dev. Biol.* **140,** 388–400.

Jeffery, W. R. (1990b). An ultraviolet-sensitive maternal mRNA encoding a cytoskeletal protein may be involved in axis formation in the ascidian embryo. *Dev. Biol.* **141,** 141–148.

Jeffery, W. R. (1995). Development and evolution of an egg cytoskeletal domain in ascidian. *Curr. Top. Dev. Biol.* **31,** 243–276.

Jeffery, W. R., and Bates, W. R. (1989). Ooplasmic segregation in the ascidian *Styela. In* "The Molecular Biology of Fertilization" (H. Schatten and G. Schatten, eds.), pp. 341–367. Academic Press, New York.

Jeffery, W. R., and Meier, S. (1983). A yellow crescent cytoskeletal domain in ascidian eggs and its role in early development. *Dev. Biol.* **96,** 125–143.

Jeffery, W. R., and Swalla, B. J. (1990). Anural development in ascidians: Evolutionary modification and elimination of the tadpole larva. *Semin. Dev. Biol.* **1,** 253–261.

Jeffery, W. R., and Swalla, B. J. (1992). Evolution of alternate modes of development in ascidians. *BioEssays* **14,** 219–226.

Jeffery, W. R., and Swalla, B. J. (1993). An ankryin-like protein in ascidian eggs and its role in the evolution of direct development. *Zygote* **1,** 197–208.

Jeffery, W. R., Tomlinson, C. G., and Brodeur, R. D. (1983). Localization of actin messenger RNA during early ascidian development. *Dev. Biol.* **99,** 408–417.

Katz, M. J. (1983). Comparative anatomy of the tunicate tadpole. *Ciona intestinalis. Biol. Bull.* **164,** 1–27.

Kawaminami, T., and Nishida, H. (1997). Induction of trunk lateral cells, the blood cell precursors, during ascidian embryogenesis. *Dev. Biol.* **181,** 14–20.

Kimble, J., Sulston, J., and White, J. (1979). Regulative development in the post-embryonic lineage of *Caenorhabditis elegans. In* "Cell Lineage, Stem Cells and Cell Differentiation" (N. le Douarin, ed.), INSERM Symp. No. 10, pp. 59–68. Elsevier, Amsterdam/New York.

Knoblich, J. A., Jan, L. Y., and Jan, Y. N. (1995). Asymmetric segregation of Numb and Prospero during cell division. *Nature* (*London*) **337,** 624–627.

Kowalevsky, A. (1866). Entwicklungsgeschichte der einfachen Ascidien. *Mém. Acad. Imp. Sci. St. Pétersbourg* **10** (Ser. 7), 1–19.

Kowalevsky, A. (1871). Weitere Studien uber die Entwicklung der einfachen Ascidien. *Arch. Mirkosk. Anat.* **7,** 101–130.

Kumano, G., and Nishida, H. (1996). Biochemical evidence for membrane-bound endoderm-specific alkaline phosphatase in larvae of the ascidian, *Halocynthia roretzi. Eur. J. Biochem.* **240,** 485–489.

Kusakabe, T., Suzuki, J., Saiga, H., Jeffery, W. R., Makabe, K. W., and Satoh, N. (1991). Temporal and spatial expression of a muscle actin gene during embryogensis of the ascidian *Halocynthia roretzi. Dev. Growth Differ.* **33,** 227–234.

Lübbering, B., Nishikata, T., and Goffinet, G. (1992). Initial stages of tunic morphogenesis in the ascidian *Halocynthia:* A fine structural study. *Tissue Cell* **24,** 121–130.

Makabe, K. W., and Satoh, N. (1989). Temporal expression of myosin heavy chain gene during ascidian embryogenesis. *Dev. Growth Differ.* **31,** 71–77.

Makabe, K. W., Fujiwara, S., Saiga, H., and Satoh, N. (1990). Specific expression of myosin heavy chain gene in muscle lineage cells of the ascidian embryo. *Roux's Arch. Dev. Biol.* **199,** 307–313.

Mancuso, V. (1974). Formation of the ultrastructural components of *Ciona intestinalis* tadpole test by the animal embryo. *Experientia* **30,** 1078.

Mancusco, V., and Dolcemascolo, G. (1977). Aspetti ultrastrutturali della corda della larvae di *Ciona intestinalis* durante l'allungamento della corda. *Acta Embryol. Exp.* 207–220.

Marikawa, Y., and Satoh, N. (1995). Ultraviolet-sensitive ooplasmic factors are responsible for the development of an endoderm-specific alkaline phosphatase in the ascidian embryos. *Dev. Growth Differ.* **38,** 167–173.

Marikawa, Y., Yoshida, S., and Satoh, N. (1994). Development of egg fragments of the ascidian *Ciona savignyi:* The cytoplasmic factors responsible for muscle differentiation are separated into specific fragment. *Dev. Biol.* **162,** 134–142.

Marikawa, Y., Yoshida, S., and Satoh, N. (1995). Muscle determinants in the ascidian egg are inactivated by UV irradiation and the inactivation is partially rescued by injection of maternal mRNAs. *Roux's Arch. Dev. Biol.* **204,** 180–186.

Meedel, T. H. (1992). Development of the ascidian embryo: Cell fate specification by autonomous and inductive processes. *In* "Morphogenesis: An Analysis of the Development of Biological Form" (E. F. Rossomand and S. Alexander, eds.), pp. 263–317. Dekker, New York.

Meedel, T. H., and Whittaker, J. R. (1983a). Development of translationally active mRNA for larval muscle acetylcholinesterase during ascidian embryogenesis. *Proc. Natl. Acad. Sci. USA* **80,** 4761–4765.

Meedel, T. H., and Whittaker, J. R. (1983b). Two histospecific enzyme expression in the same cleavage-arrested one-celled ascidian embryos. *J. Exp. Zool.* **250,** 168–175.

Meedel, T. H., Crowther, R. J., and Whittaker, J. R. (1987). Determinative properties of muscle lineage in ascidian embryos. *Development* **100,** 245–260.

Minganti, A. (1954). Fosfatasi alcaline nello siviluppo delle ascidie. *Pubbl. Stn. Zool. Napoli* **25,** 9.

Mita-Miyazawa, I., Nishikata, T., and Satoh, N. (1987). Cell- and tissue-specific monoclonal antibodies in eggs and embryos of the ascidian *Halocynthia roretzi. Development* **99,** 115–162.

Miyamoto, D. M., and Crowther, R. J. (1985). Formation of the notochord in living ascidian embryos. *J. Embryol. Exp. Morphol.* **86,** 1–17.

Monroy, A. (1979). Introductory remarks on the segregation of cell lines in the embryo. *In* "Cell Lineage, Stem Cells and Cell Determination" (N. le Douarin, ed.), INSERM Symp. No. 10, pp. 3–13. Elsevier, Amsterdam/New York.

Nakatani, Y., and Nishida, H. (1994). Induction of notochord during ascidian embryogenesis. *Dev. Biol.* **166,** 289–299.

Nakatani, Y., Yasuo, H., Satoh, N., and Nishida, H. (1996). Basic fibroblast growth factor induces notochord formation and the expression of *As-T,* a brachyury homolog, during ascidian embryogenesis. *Development* **122,** 2023–2031.

Nakauchi, M., and Takeshita, T. (1983). Ascidian one-half embryos can develop into functional adult ascidians. *J. Exp. Zool.* **227,** 155–158.

Nicol, D., and Meinertzhagen, I. A. (1988a). Development of the central nervous system of the larva of the ascidian, *Ciona intestinalis* L. I. The early lineages of the neural plate. *Dev. Biol.* **130,** 721–736.

Nicol, D., and Meinertzhagen, I. A. (1988b). Development of the central nervous system of the larva of the ascidian, *Ciona intestinalis* L. II. Neural plate morphogenesis and cell lineages during neurulation. *Dev. Biol.* **130,** 737–766.

Nicol, D., and Meinertzhagen, I. A. (1991). Cell counts and maps in the larval central nervous system of the ascidian *Ciona intestinalis* (L.), *J. Comp. Neurol.* **309,** 415–429.

Nieuwkoop, P. D. (1969). The formation of mesoderm in Urodelean amphibians. I. Induction by the endoderm. *Wilhelm Roux's Arch. Entwicklungsmech. Org.* **162,** 341–373.

Nieuwkoop, P. D. (1973). The "organization centre" of the amphibian embryo, its origin, spatial organization and morphogenetic action. *Adv. Morphol.* **10,** 1–39.

Nishida, H. (1986). Cell division pattern during gastrulation of the ascidian, *Halocynthia roretzi. Dev. Growth Diff.* **28,** 191–201.

Nishida, H. (1987). Cell lineage analysis in ascidian embryos by intracellular injection of a tracer enzyme. III. Up to the tissue-restricted stage. *Dev. Biol.* **121,** 526–541.

Nishida, H. (1990). Determinative mechanisms in secondary muscle lineages of ascidian embryos: Development of muscle-specific features in isolated muscle progenitor cells. *Development* **108,** 559–568.

Nishida, H. (1991). Induction of brain and sensory pigment cells in the ascidian embryo analyzed by experiments with isolated blastomeres. *Development* **112** 389–395.

Nishida, H. (1992a). Determination of developmental fates of blastomeres in ascidian embryos. *Dev. Growth Differ.* **34,** 253–262.

Nishida, H. (1992b). Developmental potenetial for tissue differentiation of fully dissociated cells of the ascidian embryo. *Roux's Arch. Dev. Biol.* **201,** 81–87.

Nishida, H. (1992c). Regionality of egg cytoplasm that promotes muscle differentiation in embryo of the ascidian, *Halocynthia roretzi. Development* **116,** 521–529.

Nishida, H. (1993). Localized regions of egg cytoplasm that promote expression of endoderm-specific alkaline phosphatase in embryos of the ascidian *Halocynthia roretzi. Development* **118,** 1–7.

Nishida, H. (1994a). Localization of egg cytoplasm that promotes differentiation to epidermis in embryos of othe ascidian *Halocynthia roretzi. Development* **120,** 235–243.

Nishida, H. (1994b). Localization of determinants for the formation of the anterior-posterior axis in the eggs of the ascidian *Halocynthia roretzi. Development* **120,** 3093–3104.

Nishida, H. (1996a). Vegetal egg cytoplasm promotes gastrulation and is responsible for specification of vegetal blastomeres in embryos of the ascidian *Halocynthia roretzi. Development* **122,** 1271–1279.

Nishida, H. (1996b). Determination at the last cell cycle before fate restriction. *Zool. Sci.* **13,** 15–20.

Nishida, H., and Kumano, G. (1997). Analysis of temporal expression of the endoderm-specific alkaline phosphatase during development of the ascidian, *Halocynthia roretzi. Dev. Growth Differ.* **39,** 199–205.

Nishida, H., and Satoh, N. (1983). Cell lineage analysis in ascidian embryos by intracellular injection of a tracer enzyme. I. Up to 8-cell stages. *Dev. Biol.* **99,** 382–394.

Nishida, H., and Satoh, N. (1985). Cell lineage analysis in ascidian embryos by intracellular injection of a tracer enzyme. II. The 16- and 32-cell stages. *Dev. Biol.* **110,** 440–454.

Nishida, H., and Satoh, N. (1989). Determination and regulation in the pigment cell lineage of the ascidian embryo. *Dev. Biol.* **132,** 355–367.

Nishide, K., Nishikata, T., and Satoh, N. (1989). A monoclonal antibody specific to embryonic trunk-lateral cells of the ascidian *Halocynthia roretzi* stains coelomic cells of juvenile and adult basophilic blood cells. *Dev. Growth Differ.* **31,** 595–600.

Nishikata, T., and Satoh, N. (1990). Specification of notochord cells in the ascidian embryos analyzed with a specific monoclonal antibody. *Cell Differ. Dev.* **30,** 43–53.

Nishikata, T., and Wada, M. (1996). Molecular characterization of myoplasmic-C1: A cytoskeletal component localized in the myoplasm of the ascidian egg. *Dev. Genes Evol.* **206,** 72–79.

Nishikata, T., Mita-Miyazawa, I., Deno, T., and Satoh, N. (1987a). Monoclonal antibodies against components of the myoplasm of eggs of the ascidian *Ciona intestinalis* partially block the development of muscle-specific acetylcholinesterase. *Development* **100,** 577–586.

Nishikata, T., Mita-Miyazawa, I., Deno, T., Takamura, K., and Satoh, N. (1987b). Expression of epidermis-specific antigens during embryogensis of the ascidian. *Halocynthia roretzi. Dev. Biol.* **121,** 408–416.

Okado, H., and Takahashi, K. (1988). A simple 'neural induction' model with two interacting cleavage-arrested ascidian blastomeres. *Proc. Natl. Acad. Sci. USA* **85,** 6197–6201.

Okado, H., and Takahashi, K. (1990). Induced neural-type differentiation in the cleavage-arrested blastomere isolated from early ascidian embryos. *J. Physiol. (London)* **427,** 603–623.

Okado, H., and Takahashi, K. (1993). Neural differentiation in cleavage-arrested ascidian blastomeres induced by a proteolytic enzyme. *J. Physiol. (London)* **463,** 269–290.

Okamura, Y., Okado, H., and Takahashi, K. (1993). The ascidian embryo as a prototype of vertebrate neurogenesis. *BioEssays* **15,** 723–730.

Okamura, Y., Ono, F., Okagaki, R., Chong, J. A., and Mandel, G. (1994). Neural expression of a sodium channel gene requires cell-specific interactions. *Neuron* **13,** 937–948.

Ortolani, G. (1955). The presumptive territory of the mesoderm in the ascidian germ. *Experientia* **11,** 445–446.

Ortolani, G. (1957). Il territorio precoce della corda nelle Ascidie. *Acta Embryol. Morphol. Exp.* **1,** 33–36.

Ortolani, G. (1958). Cleavage and development of egg fragments in ascidians. *Acta Embryol. Morphol. Exp.* **1,** 247–272.

Ortolani, G. (1962). Territorio presuntivo del sistema nervoso nelle larve di Ascidie. *Acta Embryol. Morphol. Exp.* **5,** 189–198.

Ortolani, G., Patricolo, E., and Mansueto, C. (1979). Trypsin-induced cell surface changes in ascidian embryonic cells. *Exp. Cell Res.* **122,** 137–147.

Perry, H. E., and Melton, D. A. (1983). A rapid increase in acetylcholinesterase mRNA during ascidian embryogenesis as demonstrated by microinjection into *Xenopus laevis* oocyte. *Cell Differ.* **13,** 233–238.

Rappaport, R. (1969). Aster-equatorial surface relations and furrow establishment. *J. Exp. Zool.* **171,** 59–68.

Reverberi, G., and Minganti, A. (1946). Fenomeni di evocatione nelle sviluppo dell'uovo di ascidie. *Pubbl. Stn. Zool. Napoli* **20,** 199–252.

Reverberi, G., Ortolani, G., and Farinella-Ferruzza, N. (1960). The causal formation of the brain in the ascidian larva. *Acta Embryol. Morphol. Exp.* **3,** 296–336.

Rhyu, M. S., Jan, L. Y., and Jan, Y. N. (1994). Asymmetric distribution of Numb protein during division of the sensory organ precursor cell confers distinct fates to daughter cells. *Cell* **76,** 477–491.

Roegiers, F., McDougall, A., and Sardet, C. (1995). The sperm entry point defines the orientation of the calcium-induced contraction wave that directs the first phase of cytoplasmic reorganization in the ascidian egg. *Development* **121,** 3457–3466.

Rose, S. M. (1939). Embryonic induction in the ascidia. *Biol. Bull.* **155,** 608–614.

Sardet, C., McDougall, A., and Houliston, E. (1994). Cytoplasmic domains in eggs. *Trends Cell Biol.* **4,** 166–172.

Sardet, C., Speksnijder, J., Inoue, S., and Jaffe, L. (1989). Fertilization and ooplasmic movements in the ascidian egg. *Development* **105,** 237–249.

Sato, S., Masuya H., Numakunai, T., Satoh, N., Ikeo, K., Gojobori, T., Tamura, K., Ide, H., Takeuchi, T., and Yamamoto, H. (1997). An ascidian tyrosinase gene: Its unique structure and expression in the developing brain. *Dev. Dyn.* **208,** 363–374.

Satoh, N. (1979). Visualization with scanning electron microscopy of cleavage pattern of the ascidian eggs. *Bull. Mar. Biol. Stn. Asamushi Tohoku Univ.* **16,** 169–178.

Satoh, N. (1993). "Developmental Biology of Ascidians." Cambridge Univ. Press, Cambridge, UK.

Satoh, N., Deno, T., Nishida, H., Nishikata, T., and Makabe, K. (1990). Cellular and molecular mechanisms of muscle cell differentiation in ascidian embryos. *Int. Rev. Cytol.* **122,** 221–258.

Satou, Y., and Satoh, N. (1996). Two cis-regulatory elements are essential for the muscle-specific expression of an actin gene in the ascidian embryo. *Dev. Growth Differ.* **38,** 565–573.

Satou, Y., Kusakabe, K., Araki, I., and Satoh, N. (1995). Timing of initiation of muscle-specific gene expression in the ascidian embryo precedes that of developmental fate restriction in lineage cells. *Dev. Growth Differ.* **37,** 319–327.

Sawada, T. (1988). The mechanism of ooplasmic segregation in the ascidian eggs. *Zool. Sci.* **5,** 667–675.

Sawada, T., and Osanai, K. (1981). The cortical contraction related to the ooplasmic segregation in *Ciona intestinalis* eggs. *Wilhelm Roux's Arch. Dev. Biol.* **190,** 208–214.

Sawada, T., and Schatten, G. (1988). Microtubules in ascidian eggs during meiosis, fertilization, and mitosis. *Cell Motil. Cytoskeleton* **9,** 219–230.

Sawada, T., and Schatten, G. (1989). Effects of cytoskeletal inhibitors on ooplasmic segregation and microtubule organization during fertilization and early development in the ascidian *Molgula occidentalis. Dev. Biol.* **132,** 331–342.

Scharf, S. R., and Gerhart, J. C. (1980). Determination of the dorsal-ventral axis in eggs of *Xenopus laevis:* Complete rescue of UV-impaired eggs by oblique orientation before first cleavage. *Dev. Biol.* **79,** 181–198.

Schulte-Merker, S., Ho, R. K., Herrmann, B. G., and Nüsslein-Volhard, C. (1992). The protein product of the zebrafish homologue of the mouse *T* gene is expressed in nuclei of the germ ring and the notochord of the early embryo. *Development* **116,** 1021–1032.

Slack, J. M. W. (1991). "From Egg to Embryo." 2nd Ed. Cambridge, Univ. Press, Cambridge, UK.

Slack, J. M. W. (1993). Embryonic induction. *Mech. Dev.* **41,** 91–107.

Smith, J. C. (1989). Mesoderm induction and mesoderm-inducing factors in early amphibian development. *Development* **105,** 665–667.

Smith, J. C., Price, B. M. J., Green, J. B. A., Weigel, D., and Herrmann, B. G. (1991). Expression of a *Xenopus* homolog of *Brachyury (T)* is an immediate-early response to mesoderm induction. *Cell* **67,** 79–87.

Speksnijder, J. E., Sardet, C., and Jaffe, L. F. (1990). The activation wave of calcium in the ascidian egg and its role in ooplasmic segregation. *J. Cell Biol.* **110,** 1589–1598.

Speksnijder, J. E., Terasaki, M., Hage, W. J., Jaffe, L. F., and Sardet, C. (1993). Polarity and reorganization of the endoplasmic reticulum during fertilization and ooplasmic segregation in the ascidian egg. *J. Cell Biol.* **120,** 1337–1346.

Spemann, H. (1938). "Embryonic Development and Induction." Yale Univ. Press, New Haven, CT.

Spemann, H., and Mangold, H. (1924). Über Induktion von Embryonalanlagen durch Implantation artfremder Organisatoren. *Arch. Mikrosk. Anat. Entwicklungs Mech.* **100,** 599–638.

Swalla, B. J., and Jeffery, W. R. (1990). Interspecific hybridization between an anural and urodele ascidian: Differential expression of urodele features suggests multiple mechanisms control anural development. *Dev. Biol.* **142,** 319–334.

Swalla, B. J., and Jeffery, W. R. (1995). A maternal RNA localized in the yellow crescent is segregated to the larval muscle cells during ascidian development. *Dev. Biol.* **170,** 353–364.

Swalla, B. J., and Jeffery, W. R. (1996a). PCNA mRNA has a 3′ UTR antisense to yellow crescent RNA and is localized in ascidian eggs and embryos. *Dev. Biol.* **178,** 23–43.

Swalla, B. J., and Jeffery, W. R. (1996b). Requirement of the *Manx* gene for expression of Chordate features in a tailless ascidian larva. *Science* **274,** 1205–1208.

Swalla, B. J., Badgett, M. R., and Jeffery, W. R. (1991). Identification of a cytoskeletal protein localized in the myoplasm of ascidian eggs: Localization is modified during anural development. *Development* **111,** 425–436.

Swalla, B. J., Makabe, K. M., Satoh, N., and Jeffery, W. R. (1993). Novel genes expressed differentially in ascidians with alternate modes of development. *Development* **119,** 307–318.

Takahashi, K., and Okamura, Y. (1995). Neural excitability is induced by cell–cell interactions during early embryogenesis. *Perspect. Dev. Neurobiol.* **2,** 317–325.

Tomlinson, C. R., Beach, R. L., and Jeffery, W. R. (1987). Differential expression of a muscle actin gene in muscle cell lineages of ascidian embryos. *Development* **101,** 751–765.

Torrence, S. A., and Cloney, R. A. (1982). Nervous system of ascidian larvae: Caudal primary sensory neurons. *Zoomorphology* **99,** 103–115.

Ueki, T., and Satoh, N. (1995). Sequence motifs shared by the 5′ flanking regions of two epidermis-specific genes in the ascidian embryo. *Dev. Growth Differ.* **37,** 597–604.

Ueki, T., Makabe, K. W., and Satoh, N. (1991). Isolation of cDNA clones for epidermis-specific genes of the ascidian embryo. *Dev. Growth Differ.* **33,** 579–586.

Venuti, J. M., and Jeffery, W. R. (1986). Cell lineage and determination of cell fate in ascidian embryos. *Int. J. Dev. Biol.* **33,** 197–212.

Weisblat, D. A., and Blair, S. S. (1984). Developmental interdeterminacy in embryos of the leech *Helobdella triserialis. Dev. Biol.* **78,** 577–597.

Wessells, N. K. (1977). "Tissue Interactions and Development." Benjamin, Menlo Park, CA.

Whittaker, J. R. (1966). An analysis of melanogenesis in differentiating pigment cells of ascidian embryos. *Dev. Biol.* **14,** 1–39.

Whittaker, J. R. (1973a). Segregation during ascidian embryogenesis of egg cytoplasmic information for tissue-specific enzyme development. *Proc. Natl. Acad. Sci. USA* **70,** 2096–2100.

Whittaker, J. R. (1973b). Tyrosinase in the presumptive pigment cells of ascidian embryos: Tyrosine accessibility may initiate melanin synthesis. *Dev. Biol.* **30,** 441–454.

Whittaker, J. R. (1977). Segregation during cleavage of a factor determining endodermal alkaline phosphatase development in ascidian embryos. *J. Exp. Zool.* **202,** 139–153.

Whittaker, J. R. (1979). Development of tail muscle acetylcholinesterase in ascidian embryos lacking mitochondrial localization and segregation. *Biol. Bull.* **157,** 344–355.

Whittaker, J. R. (1980). Acetylcholinesterase development in extra cells caused by changing the distribution of myoplasm in ascidian embryos. *J. Embryol. Exp. Morphol.* **55,** 343–354.

Whittaker, J. R. (1982). Muscle lineage cytoplasm can change the developmental expression in epidermal lineage cells of ascidian embryos. *Dev. Biol.* **93,** 463–470.

Whittaker, J. R. (1990). Determination of alkaline phosphatase expression in endodermal cell lineages of an ascidian embryo. *Biol. Bull.* **178,** 222–230.

Wilkinson, D. G., Bhatt, S., and Herrmann, B. G. (1990). Expression pattern of the mouse *T* gene and its role in mesoderm formation. *Nature (London)* **343,** 657–659.

Willey, A. (1893a). Studies on the Protochordata. I. On the origin of the branchial stigmata, praeoral lobe, endostyle, atrial cavities, etc. in *Ciona intestinalis,* Linn., with remarks on *Clavelina lepadiformis. Q. J. Microsc. Sci.* **34,** 317–360.

Willey, A. (1893b). Studies on the Protochordata. II. The development of the neuro-hypophysial system in *Ciona intestinalis* and *Clavelina lepadiformis,* with an account of the origin of the sense-organs in *Ascidia mentula. Q. J. Microsc. Sci.* **35,** 295–334.

Yamada, A., and Nishida, H. (1997). Distribution of cytoplasmic determinants in unfertilized eggs of the ascidian *Halocynthia roretzi. Dev. Genes Evol.* **206,** 297–304.

Yasuo, H., and Satoh, N. (1993). Function of vertebrate *T* gene. *Nature (London)* **364,** 582–583.

Yasuo, H., and Satoh, N. (1994). An ascidian homolog of the mouse *Brachyury (T)* gene is expressed exclusively in notochord cells at the fate restricted stage. *Dev. Growth Differ.* **36,** 9–18.

Yoshida, S., Marikawa, Y., and Satoh, N. (1996). posterior end mark, a novel gene encoding a localized factor in the ascidian embryo. *Development* **122,** 2005–2012.

Yuge, M., Kobayakawa, Y., Fujisue, M., and Yamana, K. (1990). A cytoplasmic determinant for dorsal axis formation in an early embryo of *Xenopus laevis. Development* **110,** 1051–1056.

Zalokar, M., and Sardet, C. (1984). Tracing of cell lineage in embryonic development of *Phallusia mammillata* (Ascidia) by vital staining of mitochondria. *Dev. Biol.* **102,** 195–205.

Distribution of Na^+,K^+-ATPase in Photoreceptor Cells of Insects

Otto Baumann
Institut für Zoophysiologie und Zellbiologie, Universität Potsdam, D-14471 Potsdam, Germany

Light stimulation of insect photoreceptors causes opening of cation channels and an inward current that is partially carried by Na^+ ions. There is also an efflux of K^+ ions upon photostimulation. Na^+ and K^+ gradients across the photoreceptor membrane are reestablished by the activity of the enzyme Na^+,K^+-ATPase. About two-thirds of the total amount of ATP consumed in response to a light stimulus is attributed to the activity of this ion pump, demonstrating the importance of this enzyme for photoreceptor function. Insect photoreceptor cells are polarized epithelial cells; their plasma membrane is organized into two domains having a distinct morphology, molecular composition, and function. The visual pigment rhodopsin and the molecular components of the transduction machinery are localized in the rhabdomere, an array of densely packed microvilli, whereas Na^+,K^+-ATPase resides in the nonrhabdomeric membrane. Comparative immunolocalization studies on compound eyes of diverse insect species have demonstrated subtle variations in the distribution patterns of Na^+,K^+-ATPase. These may be accounted for by differences in the mechanisms responsible for Na^+,K^+-ATPase positioning.

KEY WORDS: Na^+,K^+-ATPase, Ion homeostasis, Signal transduction, Photoreceptor, Insect, Cell polarity, Cell–cell interaction.

I. Introduction

The ability to sense and to react to environmental stimuli is pivotal for life. To serve this function, multicellular organisms have evolved sensory cells that are physiologically and morphologically specialized to perceive a stimulus of a defined modality and to transmit the information to secondary

International Review of Cytology, Vol. 176
0074-7696/97 $25.00

Copyright © 1997 by Academic Press.
All rights of reproduction in any form reserved.

neurons. In order to achieve high sensitivity to the stimulus, the molecular machinery that transduces the external signal into an electrical response is typically gathered in a subcompartment of the sensory cell, a transduction compartment; "household functions," such as protein and ATP synthesis, are confined to the remaining cell body. This concept of compartmentalization of sensory cells is well documented in the vertebrate photoreceptor cells, the rods and cones. Vertebrate photoreceptors are composed of an outer and an inner segment that are connected by a ciliar remnant. The outer segment is filled with stacks of membrane discs carrying the visual receptor molecule rhodopsin and contains the molecular components of visual transduction. Metabolic functions, in contrast, are restricted to the inner segment.

The photoreceptor cells of insects differ significantly from vertebrate rods in both their morphology and their physiology. The visual receptor molecule of insect photoreceptors, which is also termed rhodopsin, shares structural homology with vertebrate rhodopsin (O'Tousa *et al.,* 1985; Zuker *et al.,* 1985; Schwemer, 1989; Gartner and Towner, 1995) but is localized in the rhabdomere, a dense array of microvilli that represent the transduction compartment (Carlson and Chi, 1979). In vertebrate photoreceptors, photon absorption by rhodopsin causes an activation of a phosphodiesterase that hydrolyzes cGMP, leading to a decrease in the concentration of cGMP, a closure of cGMP-dependent cation channels, and, ultimately, in a hyperpolarization of the cell (Yau and Baylor, 1989). Activation of insect rhodopsin, in contrast, stimulates a phosphoinositide cascade and finally leads to opening of cation-selective ion channels and a depolarizing receptor potential (Hardie and Minke, 1993, 1995; Ranganathan *et al.,* 1995; Zuker, 1996).

This review focuses on the role of Na^+,K^+-ATPase in the physiology of insect photoreceptors. This ion pump is crucial for the excitability of photoreceptors and all other cells as it establishes and maintains Na^+ and K^+ concentration gradients across the plasma membrane. It transports three Na^+ ions out of the cell and two K^+ ions into the cell for each ATP molecule hydrolyzed (Horisberger *et al.,* 1991; Vasilets and Schwarz, 1994; Kotyk and Amler, 1995). The transport cycle is driven by phosphorylation–dephosphorylation steps that cause cyclic transitions between two conformational states of the enzyme, one of them (E_1) with a high affinity for intracellular Na^+, the other (E_2) with a high affinity for extracellular K^+.

In the vertebrate photoreceptor, Na^+,K^+-ATPase is spatially restricted to the plasma membrane of the inner segment (Ueno *et al.,* 1980; Stahl and Baskin, 1984; Schneider, 1992), supporting the concept of compartmentalization. The main purpose of this chapter is to explore recent data that deal with the distribution of Na^+,K^+-ATPase in photoreceptors of diverse insect species and that may contribute to our understanding of the organization and functioning of these sensory cells.

II. Structural and Functional Organization of the Insect Retina

The compound eye of insects is composed of several hundred to several thousand individual units, the ommatidia, that are arranged in a hexagonal pattern. The cellular organization of the ommatidia shows a large variation among different species (Nilsson, 1989). In the following, I will focus on the ommatidium in the compound eye of the honeybee drone (*Apis mellifera*). My choice of the ommatidium of the honeybee is not arbitrary but is based on its being of the simple apposition type, viz., the archetype of compound eye design (Nilsson, 1989). Moreover, more is known about the anatomy and physiology of the compound eye of the honeybee drone than of that of any other insect spieces, except Brachyceran flies (e.g., *Drosophila, Calliphora*). The anatomy of the latter has been covered in detail by other reviews (Carlson and Chi, 1979; Hardie, 1986). Structural differences between the ommatidia of honeybees and those of other species will be discussed where relevant.

A. Organization of an Ommatidium in the Honeybee Compound Eye

Each ommatidium comprises a dioptric apparatus composed of the corneal facet and the crystalline cone, the photoreceptor cells, and a sheath of pigmented glial cells (Fig. 1a; Varela and Porter, 1969; Perrelet, 1970). The corneal facet, a specialized part of the cuticule, forms a lens that focuses the incident light on the distal tip of photoreceptor cells (Varela and Wiitanen, 1970). The crystalline cone consists of four cone cells, surrounded by two primary pigment cells, and functions as a transparent spacer between the corneal lens and the photoreceptor cells (Varela and Wiitanen, 1970). The latter are arranged in a rosette known as the retinula and extend for approximately 400 μm to the basal lamina, which delimits the retina toward the optic ganglia. In the honeybee compound eye, each retinula is composed of nine (six large and three small) photoreceptors (Fig. 1b). However, only eight photoreceptor cells are observed in any cross section of a retinula as the cell bodies of two small photoreceptor cells are aligned in tandem, each extending just one-half of the thickness of the retina. The axons of the photoreceptors pierce the basal lamina and synapse with secondary neurons within the optic ganglia (Ribi, 1981). The cluster of crystalline cone and retinula cells is surrounded by approximately 30 pigmented glial cells (=secondary pigment cells) that act as an optic screen between the ommatidia, provide metabolic substrate to the photoreceptor cells (Tsacopoulos *et al.*,

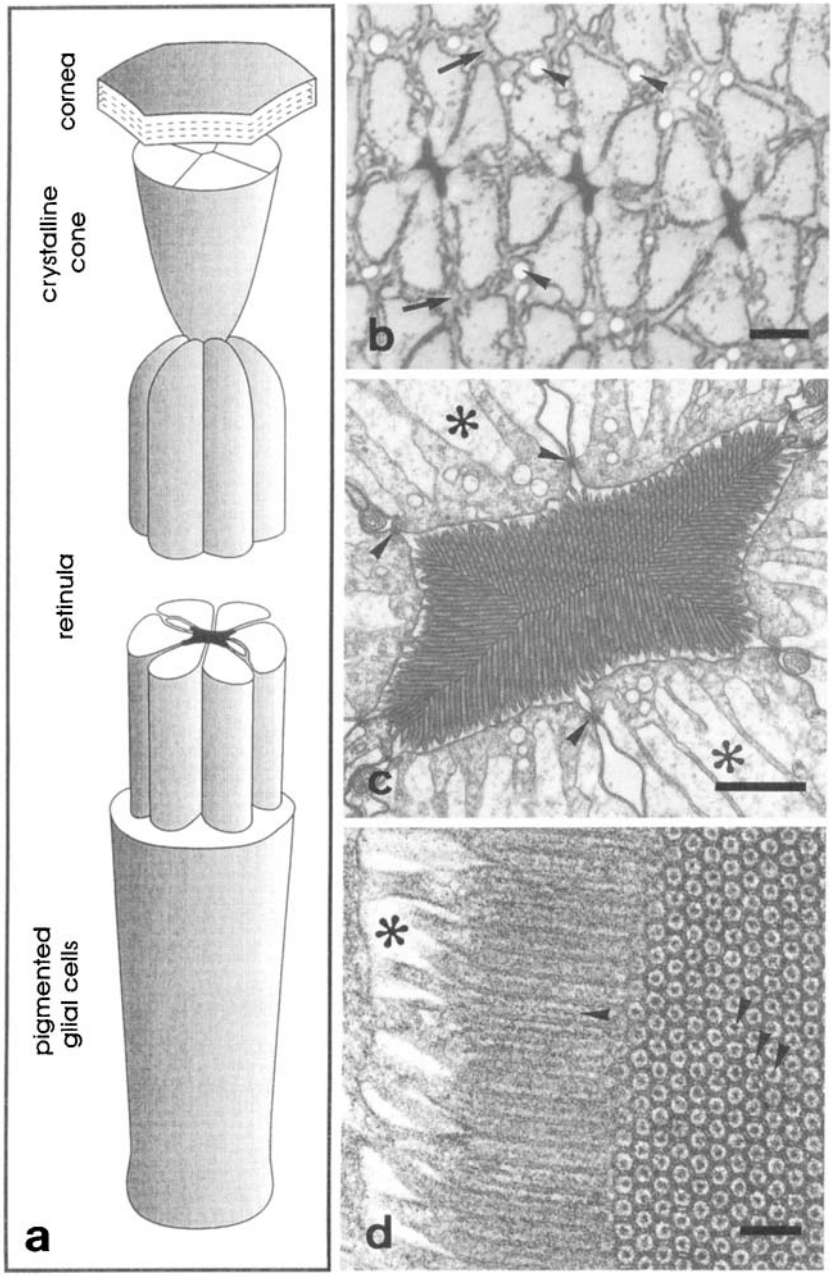
a
cornea
crystalline cone
retinula
pigmented glial cells
b
c
d

1988, 1994), and participate in ion homeostasis within the retina (Coles and Tsacopoulos, 1981; Coles *et al.,* 1986). The pigmented glial cells are tightly coupled by numerous gap junctions, thereby forming a functional syncytium (Perrelet, 1970; Baumann, 1992). Tracheoles emerge from large air sacs beneath the basal lamina and penetrate the retina. The tracheoles extend alongside the ommatidia and are embedded between the pigmented glial cells.

B. Organization of the Plasma Membrane of Photoreceptor Cells

Insect photoreceptors are polarized epithelial cells. Their plasma membrane is organized into two distinct domains with differences in morphology, molecular composition, and functional properties. The rhabdomere, which is the site of photon absorption and visual transduction, is structurally most impressive. It is a rod-like structure that extends alongside the photoreceptor all the way from the distal end of the cell to the basal lamina and is composed of microvilli, i.e., cylindrical foldings of the plasma membrane

FIG. 1 Organization of the honeybee ommatidium. (a) Schematic view of a single ommatidium. The corneal facet focuses the incident light through the crystalline cone onto the distal tip of the photoreceptors. The latter are up to 400 μm long and arranged in a rosette called the retinula. The photoreceptive compartment of the photoreceptors, the rhabdomeres, form a rod-like structure, the rhabdom, in the center of the retinula. Light entering the rhabdom at its distal tip is trapped within it and absorbed by the visual pigment rhodopsin that is incorporated in the microvillar membranes of the rhabdomeres. Pigmented glial cells ensheath the retinula and provide optical isolation between adjacent ommatidia. Note that the primary pigment cells surrounding the crystalline cone, the distal half of the pigmented glial cells, and the axons of the photoreceptors have been omitted for simplicity. (b) Light micrograph of three ommatidia in a transverse section, demonstrating the rosette-like arrangement of the photoreceptor cells. The rhabdoms are seen as dark trapezoids in the center of the retinulae. The outline of each photoreceptor is visualized by relatively dark staining, representing numerous mitochondria that reside below and closely juxtaposed to the nonrhabdomeric part of the plasma membrane. Tracheoles (arrowheads) are embedded between pigmented glial cells (arrows) that are very narrow in this plane of the section. (c) Electron micrograph of a cross-sectioned rhabdom. Belt desmosomes (arrowheads) separate the rhabdomeric part of the plasma membrane from the smooth nonrhabdomeric surface. The vacuole-like organelles in the submicrovillar cytoplasm are cisternae of the smooth endoplasmic reticulum (asterisks). (d) A high-magnification view of a longitudinal section through the rhabdom. The microvilli are densely packed in a hexagonal pattern. They are oriented parallel to the section plane at the left and are seen in the cross section at the right. A single actin filament (arrowheads) is located in the center of each microvillus. The microvilli are fused and constricted at their base, giving rise to a relatively large extracellular compartment (asterisk). Bars: (b) 10 μm; (c) 1 μm; (d) 250 nm.

that are stacked in a honeycomb-like pattern (Fig. 1d). The microvillar long axis is aligned perpendicularly to the visual axis of the ommatidium. In the compound eye of the honeybee drone, the rhabdomere of a large photoreceptor is composed of approximately 1×10^5 microvilli, each measuring 60–80 nm in diameter and 0.5–1 μm in length (Perrelet, 1970; O. Baumann, unpublished results). The extracellular space (ECS) between the microvilli is only a few nanometers wide and is bridged by regular ridges. These may contain chaoptin, a photoreceptor-specific cell adhesion molecule that is required for the maintenance of rhabdomere structure (Van Vactor *et al.,* 1988; Krantz and Zipursky, 1990). Each microvillus is stabilized by a single actin filament at its center (Arikawa *et al.,* 1990). This actin filament is linked to the microvillar membrane by crossbridge components, one of which may be an unconventional myosin (Porter and Montell, 1993; Hicks *et al.,* 1996). The microvilli are constricted at their bases, thus creating a relatively large volume of ECS at the base of the rhabdomere (Perrelet and Baumann, 1969; Boschek, 1971; Kumar and Ready, 1995).

Freeze-fracture studies of various insect photoreceptors have demonstrated that the microvillar membrane is tightly packed with membrane proteins (Perrelet *et al.,* 1972; Nickel and Menzel, 1976; Boschek and Hamdorf, 1976). Intramembrane particle densities of up to 10,000/μm^2 have been reported for some insect photoreceptors (Nickel and Menzel, 1976; Bennett and White, 1989); up to 90% of these particles may represent the visual pigment rhodopsin (Boschek and Hamdorf, 1976; Schinz *et al.,* 1982; Suzuki *et al.,* 1993). Components of the visual transduction cascade, ion channels, and structural proteins may account for the remaining intramembrane particles.

The rhabdomeres of all photoreceptors within a retinula of the honeybee appear to be compacted into a single structure, the rhabdom, positioned on the optical axis of the ommatidium (Figs. 1a–c). Because of the large amount of proteins and lipids in the microvilli, the refractive index of the rhabdom is higher than that of the surrounding cytoplasm. Consequently, the rhabdom functions as a waveguide, and light entering at its distal tip travels within it and is gradually absorbed by the rhodopsin (Warrant and McIntyre, 1993).

Although the rhabdomere covers less than 10% of the outline of a honeybee photoreceptor, it accounts for about two-thirds of the total plasma membrane area (exempting the axonal part of the plasma membrane; Perrelet, 1970). The remaining part of the plasma membrane is delimited from the rhabdomeric domain by *zonulae adherentes* (belt desmosomes) located alongside the rhabdomere and linking the adjacent photoreceptors (Fig. 1c). This nonrhabdomeric part of the plasma membrane is smooth and has a lower density of intramembrane particles in freeze-fracture replicas (Chi

and Carlson, 1979; Suzuki *et al.*, 1993; O. Baumann and B. Walz, unpublished results). In the honeybee retina, numerous mitochondria are aligned below the nonrhabdomeric surface (Fig. 1b; Perrelet, 1970), indicating that this membrane domain is involved with functions that require large amounts of ATP.

Developmentally, insect photoreceptors are derived from simple epithelial cells possessing an apical surface covered by short microvilli, a circumferential band of belt desmosomes, and a smooth basolateral domain. A recent study of the morphogenesis of *Drosophila* photoreceptors has demonstrated that the belt demosomes are preserved during ommatidial development and that the rhabdomere is derived by an involution of the apical surface into the retinal epithelium (Longley and Ready, 1995). The rhabdomere must thus be regarded as the equivalent of the apical membrane domain of epithelial cells, and the nonrhabdomeric part the equivalent of the basolateral membrane domain.

C. Mobility of Membrane Proteins in the Photoreceptor Plasma Membrane

When we discuss the organization of the plasma membrane into distinct domains, the rate of lateral and rotational diffusion of membrane components and their ability to move between membrane domains is of special relevance. Unfortunately, no direct measurements are available on the mobility of membrane proteins and lipids in insect photoreceptors. Several lines of evidence suggest, however, that the mobility of membrane proteins is restricted within the microvillar membrane. Freeze-fracture studies of various insect photoreceptors have visualized a regular, almost crystalline, particle arrangement within the microvillar membrane (Nickel and Menzel, 1976; Chi and Carlson, 1979; Bennett and White, 1989; Suzuki *et al.*, 1993). Analysis of the lipid composition of rhabdomeric membranes has further demonstrated that their cholesterol content is two to three times higher than that in the photoreceptive disc membranes of vertebrate rods, probably resulting in a stiffer membrane and reduced lateral diffusion (Zinkler, 1975). Moreover, the high sensitivity of some insect photoreceptors to polarized light can only be explained by an alignment and restricted rotational diffusion of rhodopsin (Rossel, 1989). Finally, the mobility of rhodopsin has been directly analyzed by electron spin resonance spectroscopy on isolated membranes of squid photoreceptors in which the visual pigment rhodopsin is also located in the membrane of microvilli (Venien-Bryan *et al.*, 1995). These measurements have demonstrated that the rotational mobility of rhodopsin is lower in the microvillar membrane than in disc membranes of vertebrate rods.

Several lines of evidence indicate, furthermore, that the exchange of protein between the microvillar membrane and the remaining membrane areas, including the membrane loops at the microvillar bases, is limited. First, freeze-fracture studies have demonstrated that the particle density in the membrane loops at the microvillar bases is lower than that on the microvilli themselves (O. Baumann and B. Walz, unpublished results). Similarly, antirhodopsin immunoreactivity appears to be lower at the microvillar bases than on the microvilli (see Figs. 1 and 2 in Suzuki and Hirosawa, 1992). Second, studies of developing *Drosophila* photoreceptors have shown that rhodopsin molecules are concentrated at the base of the rhabdomere during the first day of adult life and only later become incorporated into the entire microvillar membrane (Kumar and Ready, 1995; Niemeyer *et al.,* 1996). Finally, Na^+,K^+-ATPase does not move between the microvilli proper and the remaining cell surface, even when it has access to the membrane loops at the microvillar bases (Baumann and Takeyasu, 1993; Baumann, 1997). The microvillar membrane may thus be regarded as a microdomain with a distinct protein composition and restricted diffusion of membrane proteins.

III. Phototransduction in Insect Photoreceptors

Insect photoreceptors respond to a light stimulus by an increase in membrane conductance, resulting in a light-induced inward current and graded depolarization. The biochemistry linking photon absorption by rhodopsin and channel activation, however, is not yet completely understood. Moreover, the majority of the literature on phototransduction in insect photoreceptors is based on research on the compound eye of *Drosophila* or related flies, and the extent to which these findings apply to other insect orders is unknown. In the following, I will give a brief overview of what is known about signal transduction in *Drosophila* photoreceptors. For more detailed information, the reader is referred to recent reviews on this topic (Hardie and Minke, 1993, 1995; Ranganathan *et al.,* 1995; Zuker, 1996).

A diagrammatic simplified view of the visual transduction cascade in *Drosophila* photoreceptors is shown in Fig. 2. Light-activated rhodopsin, metarhodopsin, stimulates a heterotrimeric G protein of the G_q-family (Lee *et al.,* 1990, 1994; Scott *et al.,* 1995). The G protein in turn activates a phospholipase C (PLC) encoded by the *norpA* (no receptor potential) gene (Bloomquist *et al.,* 1988; Toyoshima *et al.,* 1990; Schneuwly *et al.,* 1991). Activation of PLC is an obligatory step in visual exitation, as demonstrated by the complete absence of a photoresponse in *norpA* mutants (Minke and Selinger, 1992; Peretz *et al.,* 1994). PLC catalyzes the breakdown of the

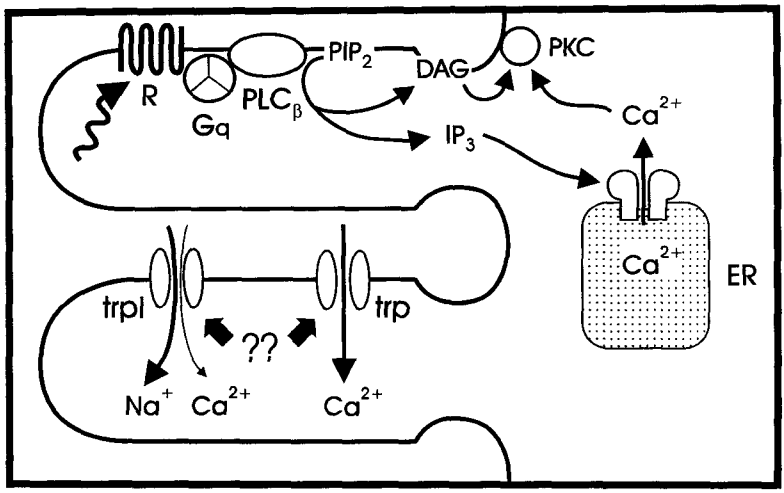

FIG. 2 Simplified view of phototransduction in *Drosophila* photoreceptor cells. On absorption of a photon, the visual receptor protein rhodopsin (R) activates a heterotrimeric G protein (G_q). On exchange of GDP for GTP, the G protein releases its $\beta\gamma$ subunits. The G_q α subunit then activates a phospholipase C (PLCβ) which hydrolyzes the membrane phospholipid phosphatidylinositol 4,5-biphosphate (PIP_2) into inositol 1,4,5-triphosphate (IP_3) and diacylglycerol (DAG). IP_3 opens the IP_3-dependent Ca^{2+} channel localized at the endoplasmic reticulum beneath the microvillar bases, thus releasing Ca^{2+} from the Ca^{2+} store. Ca^{2+} has been implicated as an intracellular messenger for light adaptation. Two classes of light-activated channels reside in the microvillar membrane. One of them is probably encoded by the *trpl* gene and is relatively nonselective for cations. The other is at least partially encoded by the *trp* gene and highly selective for Ca^{2+}. Upon the opening of these channels, extracellular Na^+ and Ca^{2+} enter the cell and cause a depolarizing receptor potential. DAG, together with Ca^{2+}, activates a protein kinase C (PKC) that regulates deactivation and desensitization of the photoresponse.

minor membrane component phosphatidylinositol 4,5-bisphosphate (PIP_2) into the intracellular messengers inositol 1,4,5-triphosphate (IP_3) and diacylglycerol (DAG) (Devary *et al.*, 1987). The latter compound activates a photoreceptor-specific protein kinase C (PKC) and thus regulates deactivation and desensitization of the light response (Ranganathan *et al.*, 1991; Smith *et al.*, 1991; Hardie *et al.*, 1993). IP_3, on the other hand, has been demonstrated to stimulate the release of Ca^{2+} from the endoplasmic reticulum in a variety of systems (Berridge, 1993). In microvillar photoreceptors, a specialized compartment of the smooth endoplasmic reticulum abutting the microvillar bases (Walz, 1982; Baumann and Walz, 1989a; Matsumoto-Suzuki *et al.*, 1989) represents a Ca^{2+} store and IP_3-sensitive Ca^{2+} source (Baumann and Walz, 1989b; Baumann *et al.*, 1991; Walz and Baumann, 1995). By the use of fluorescent Ca^{2+}-sensitive dyes in the photoreceptors

of the honeybee (Walz *et al.*, 1994) and *Drosophila* (Peretz *et al.*, 1994; Ranganathan *et al.*, 1994; Hardie, 1996), a light-induced increase in cytosolic free Ca^{2+} has been measured that may result from Ca^{2+} influx across the plasma membrane (Ziegler and Walz, 1989; Peretz *et al.*, 1994; Ranganathan *et al.*, 1994; Hardie, 1996) or, at least in drone photoreceptors, also from a Ca^{2+} release from intracellular stores (Ziegler and Walz, 1990; Baumann *et al.*, 1991). Cytosolic Ca^{2+} modulates the light sensitivity of the cell via positive and negative feedback loops on the transduction machinery and light-activated conductances (Hardie, 1991a, 1995; Ranganathan *et al.*, 1991; Hardie and Minke, 1992, 1994; Walz, 1992). However, it is still a matter of debate whether the Ca^{2+} rise directly or indirectly leads to an increase in membrane conductance.

Recent genetic and electrophysiological experiments have provided evidence that the light-activated conductance in *Drosophila* photoreceptors is actually composed of two distinct ion channels (Hardie and Minke, 1992, 1993, 1995; Peretz *et al.*, 1994; Niemeyer *et al.*, 1996). One of them is highly selective for Ca^{2+} ($P_{Ca} : P_{Na} \sim 40:1$) and is encoded by the *trp* (transient receptor potential) gene (Hardie and Minke, 1992). The other conductance represents a nonselective cation channel encoded by the *trpl* (*trp*-like) gene (Hardie and Minke, 1992; Niemeyer *et al.*, 1996). Both the trp and trpl protein share significant structural homology with the vertebrate voltage-dependent Ca^{2+} channel (Phillips *et al.*, 1992; Hardie and Minke, 1993) and are localized at the rhabdomere (Pollock *et al.*, 1995; Niemeyer *et al.*, 1996). However, the way in which PLC activation is linked to the opening of these channels remains unclear.

IV. Ion Concentrations and Light-Induced Ion Movements in the Insect Retina

The resting concentrations of the major physiologically relevant ions Na^+, K^+, and Cl^- and the light-induced movements of these ions have been studied in the honeybee drone retina in great detail (Fig. 3). This model permits measurements with ion-selective electrodes in all retinal compartments, viz., the photoreceptor cells, the pigmented glial cells, and the ECS. In the dark-adapted retina, the mean $[Na^+]$ is 6 m*M* in the photoreceptors (Coles *et al.*, 1986), 196 m*M* in the ECS (Cardinaud *et al.*, 1994), and 53 m*M* in pigmented glial cells (Coles and Orkand, 1985; Coles *et al.*, 1986). Although $[Na^+]$ in glial cells seems high, similar values have been obtained with a different method, viz., by electron probe X-ray microanalysis on cryofixed retina (Coles and Rick, 1985). Measurements of resting free $[K^+]$ with ion-selective electrodes give a value of 127 m*M* in photoreceptor cells

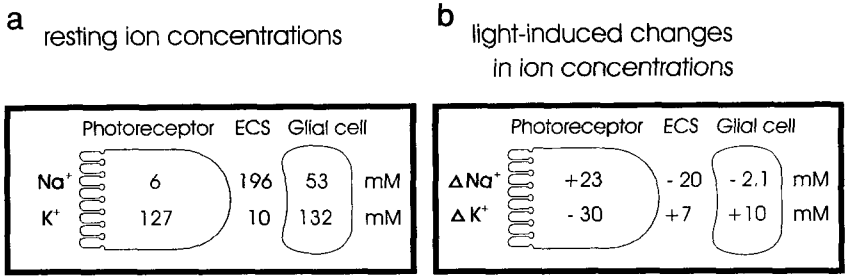

FIG. 3 Resting concentrations and light-induced changes in Na^+ and K^+ within the photoreceptor cells, the pigmented glial cells, and the extracellular space (ECS) of the honeybee drone retina (data combined from Coles *et al.*, 1986; Cardinaud *et al.*, 1994). Light stimulation results in an influx of Na^+ into the photoreceptors. Moreover, K^+ is released from the photoreceptors and enters the pigmented glial cells.

(Coles and Orkand, 1985; Coles *et al.*, 1986), 10.2 m*M* in the ECS (Cardinaud *et al.*, 1994), and 132 m*M* in pigmented glial cells (Coles and Orkand, 1985; Coles *et al.*, 1986). For resting [Cl^-], values of 24 m*M* have been obtained for photoreceptor cells and 18 m*M* for pigmented glial cells (Coles *et al.*, 1986, 1989).

Light stimulation of insect photoreceptors leads to an increase in intracellular free Na^+ within the photoreceptors and a concomitant decrease in Na^+ in the ECS (Fig. 3b). The increase in Na^+ concentration within the photoreceptors can amount to tens of m*M*, as demonstrated by Coles and Orkand (1985), and results from Na^+ influx via the light-activated cation-selective conductances (Fulpius and Baumann, 1969; Hardie and Minke, 1992). In photoreceptor cells of the honeybee drone, but not of the worker bee or other insect species, there is also Na^+ influx through voltage-gated Na^+ channels (Coles and Schneider-Picard, 1989; Vallet *et al.*, 1992). Moreover, secondary transport mechanisms that utilize the electrochemical Na^+ gradient to translocate other molecules in or out of the cell may be activated during a light stimulus and contribute to the light-induced Na^+ movements. Among these the electrogenic Na^+/Ca^{2+} exchanger (Minke and Armon, 1984; Minke and Tsacopoulos, 1986; Ziegler and Walz, 1989; Hardie, 1995) is turned on by the massive light-induced rise in cytosolic Ca^{2+} and, together with the Ca^{2+}-ATPase of the endoplasmic reticulum (Walz, 1982; Baumann and Walz, 1989a,b; Walz and Baumann, 1995), brings intracellular [Ca^{2+}] back to baseline values after a light stimulus. Experiments on the honeybee retina further indicate that the uptake of alanine, which is the metabolic substrate that is used by photoreceptors and that is provided by glial cells, occurs via a Na^+-dependent transport mechanism (Tsacopoulos and Veuthey, 1993; Tsacopoulos *et al.*, 1994).

Photostimulation also causes an increase in K^+ conductance of the photoreceptor plasma membrane and an efflux of K^+ ions from the photoreceptor cells (Fig. 3b). Quantitative analysis of the light-induced K^+ movements in honeybee drone photoreceptors has demonstrated that the light-induced decrease in intracellular K^+ concentration can be rather large, amounting to tens of m*M* (Coles and Tsacopoulos, 1979; Coles *et al.,* 1986). Several voltage-gated K^+ conductances with various operating ranges and activation/inactivation kinetics have been identified in insect photoreceptor cells (Hardie, 1991b; Hardie *et al.,* 1991; Weckström *et al.,* 1991; Laughlin and Weckström, 1993; Cuttle *et al.,* 1995). The distribution of these conductances among the photoreceptor cells of different spieces is correlated with the visual ecology of the animals (reviewed by Weckström and Laughlin, 1995). Delayed-rectifier conductances are found in photoreceptor cells of fast-flying insects and lead to a low membrane resistance when the photoreceptors are depolarized by bright light, thus permitting the transduction of fast-voltage changes (Weckström *et al.,* 1991; Laughlin and Weckström, 1993). Slow-moving insects, in contrast, contain an inactivating K^+ conductance (Laughlin and Weckström, 1993; Cuttle *et al.,* 1995).

If all the K^+ that is extruded from the photoreceptor cells during light stimulation accumulates in the narrow ECS, extracellular $[K^+]$ should rise to about 200 m*M* (Coles *et al.,* 1986). Quantitative analysis of K^+ movements in the drone retina has demonstrated, however, that only a small amount of the K^+ released from the photoreceptor cells remains in the ECS, whereas the majority of K^+ enters the pigmented glial cells (Coles and Tsacopulos, 1979, 1981; Coles and Orkand, 1983). The pigmented glial cells thus maintain extracellular $[K^+]$ within strict limits and prevent the photoreceptors from becoming depolarized by high extracellular $[K^+]$. Several mechanisms may be involved in K^+ clearance from the ECS: (1) spatial buffering, in which K^+ ions enter the glial cell syncytium at regions where the plasma membrane faces an elevated extracellular $[K^+]$, and other K^+ ions leave the syncytium in regions within the eye where extracellular $[K^+]$ is less elevated (Coles and Orkand, 1983; Coles *et al.,* 1986); (2) passive uptake of KCl and H_2O (Coles and Orkand, 1983; Coles *et al.,* 1986); (3) active uptake by a Na^+,K^+-ATPase (Coles and Orkand, 1985; Coles *et al.,* 1986). Immunolocalization of Na^+,K^+-ATPase in honeybee drone retina has confirmed the presence of this pump on the plasma membrane of glial cells (Baumann and Takeyasu, 1993). The density of the pump molecules, however, appears to be far lower on the glial cell than on the photoreceptor surface. Moreover, if a Na^+,K^+-ATPase contributes to extracellular K^+ clearance, it should have quite unique properties: the high resting $[Na^+]$ in glial cells and uptake of K^+ in response to an increase in extracellular $[K^+]$ suggest that the pump may be regulated by extracellular $[K^+]$ rather than by intracellular $[Na^+]$ (Coles and Orkand, 1985).

After photostimulation, Na^+ and K^+ gradients are reestablished across the plasma membrane of the photoreceptor by the activity of the Na^+,K^+-ATPase. As the Na^+,K^+-ATPase exchanges three Na^+ for two K^+ ions during each transport cycle (Jansonius, 1990), there is an imbalance of transported charges and the activity of the Na^+,K^+-ATPase has a hyperpolarizing effect on the membrane potential. Such a transient hyperpolarization can be directly observed after a bright light stimulus (Baumann and Hadjilazaro, 1971; Hardie, 1983; Jansonius, 1990). This after-hyperpolarization is abolished by cardiac glycosides (Tsacopoulos *et al.,* 1983), which are specific inhibitors of Na^+,K^+-ATPase.

Manometric measurements on compound eyes and direct recordings of local O_2 changes with O_2-selective electrodes have demonstrated a rapid light-induced increase in O_2 consumption (Hamdorf *et al.,* 1988; Tsacopoulos and Poitry, 1982; Tsacopoulos *et al.,* 1983). In blowfly retina, O_2 consumption during light exposure may transiently rise up to 20× the resting value in darkness (Hamdorf *et al.,* 1988). This light-activated O_2 consumption indicates an increase in aerobic metabolism within the retina, particularly within the photoreceptor cells, as these contain the vast majority of mitochondria within the retina (Perrelet, 1970; Baumann and Takeyasu, 1993). Since the respiratory quotient of insect photoreceptors is one (Langer, 1960; Hamdorf and Kaschef, 1964), O_2 consumption is caused by carbohydrate oxidation and can be directly correlated with the amount of ATP produced (6 ATP/O_2 molecule). Based on this relationship and on parallel measurements of O_2 consumption and ion movements in drone retina, Tsacopoulos *et al.* (1983) have calculated that at least 60% of the ATP consumed in response to a light stimulus is used by Na^+,K^+-ATPase. This result is in accordance with the finding that light-induced O_2 consumption of retinal tissue is reduced by as much as 80% during incubation with cardiac glycosides (Tsacopoulos and Poitry, 1982). Na^+,K^+-ATPase must thus be regarded as the main consumer of ATP in insect retina (Tsacopoulos and Poitry, 1982; Tsacopoulos *et al.,* 1983).

It has been proposed that stimulus-induced ATP hydrolysis by Na^+,K^+-ATPase and other metabolic processes leads to a decrease in the ATP/ADP ratio, which in turn activates the oxidative metabolism (Tsacopoulos and Poitry, 1982). However, the absence of a measurable ATP decrease after a light stimulus (Tsacopoulos and Coles, 1984) and the finding that light-induced O_2 consumption precedes Na^+,K^+-ATPase activity in the drone retina (Tsacopulos *et al.,* 1983) argue against this notion. Instead, light stimulation may directly activate the oxidative metabolism by a second messenger system downstream of rhodopsin, perhaps Ca^{2+} (Fein and Tsacopoulos, 1988), thus preparing the cells for the large amount of ATP needed by Na^+,K^+-ATPase.

V. Molecular Analysis of Na^+,K^+-ATPase

Na^+,K^+-ATPase belongs to the P-type ATPases, a large family of membrane proteins that also includes the Ca^{2+}-ATPases of the plasma membrane and of the sarcoplasmic/endoplasmic reticulum, the mammalian H^+,K^+-ATPase found in gastric tissue, and H^+-ATPases found in a diverse range of species (reviewed by Lutsenko and Kaplan, 1995; Møller *et al.,* 1996). These enzymes utilize the energy of ATP hydrolysis to translocate cations across cellular membranes. During the catalytic cycle, the enzymes are transiently phosphorylated by the γ phosphate of ATP. Phosphorylation occurs on an aspartyl residue in the conserved sequence DKTG, which is characteristic for P-type ATPases and distinguishes them from V-type ATPases and F_0F_1-ATPases.

The structural and functional organization of Na^+,K^+-ATPase has been described in detail in several recent reviews (Horisberger *et al.,* 1991; Vasilets and Schwarz, 1994; Kotyk and Amler, 1995). Na^+,K^+-ATPase is a heterodimer with an α subunit of about 110 kDa and a glycosylated β subunit of about 35 kDa (excluding carbohydrate). The α subunit has an even number of α-helical transmembrane segments (either 8 or 10, depending on the interpretation of the hydropathy plots) and its N and C terminals are located on the cytoplasmic side of the plasma membrane. The α subunit is regarded as the catalytic subunit of Na^+,K^+-ATPase, because it contains the binding sites for the transported ions, and the binding pocket and the phosphorylation site for ATP. Moreover, the binding site for cardiac glycosides (e.g., ouabain), putative phosphorylation sites for PKC and protein kinase A (PKA) (Chibalin *et al.,* 1992), and an ankyrin-binding motif (Jordan *et al.,* 1995) are located on the α subunit. The β subunit, in contrast, traverses the membrane only once and has a short cytoplasmic N-terminal domain and a large C-terminal ectodomain. Although the β subunit is not directly involved with transport functions (Blanco *et al.,* 1994), it may play a role in modulating transport activity, in particular the K^+ activation of Na^+,K^+-ATPase (Schmalzing *et al.,* 1992; Jaisser *et al.,* 1992, 1994; Jaunin *et al.,* 1993; Eakle *et al.,* 1994; Geering *et al.,* 1996). Moreover, association of the β subunit with a newly synthesized α subunit is necessary for the delivery of functional Na^+,K^+-ATPase to the cell surface (Takeyasu *et al.,* 1988; Renaud *et al.,* 1991; Jaunin *et al.,* 1992, 1993).

The α subunit of Na^+,K^+-ATPase has been cloned and sequenced from a variety of species. Of particular interest for this review is the Na^+,K^+-ATPase α subunit of *Drosophila,* the only insect α subunit that has been sequenced so far. Comparison of the *Drosophila* α subunit with vertebrate α subunits demonstrates a high conservation through evolution (Lebovitz *et al.,* 1989). Its deduced sequence of 1038 amino acids shows about 80%

identity with vertebrate α subunits. In particular, regions of structural or functional interest are conserved (Fig. 4). The 10 putative membrane-spanning segments (H1–H10) show 63% sequence similarity (H10) to 100% sequence identity (H4, H6) between *Drosophila* and vertebrates. The aspartyl residue, which is phosphorylated during ATP hydrolysis, is present at position 391 and located on the third, large intracellular domain amidst a conserved sequence of 44 amino acids (Lebovitz *et al.,* 1989). Regions that are suggested to form the ATP-binding pocket, e.g., the fluorescein isothiocyanate-binding site and the CIR-ATP (an alkylating ATP analogue) reactive site, are also conserved and distributed over the third cytoplasmic domain (Lebovitz *et al.,* 1989). Moreover, the third cytoplasmic domain contains the ankyrin-binding motif $ALLK_{473}$ (Jordan *et al.,* 1995). In the 10-transmembrane-segment model, a consensus sequence ($RRNS_{958}$) for PKA is located on the short intracellular loop that connects the membrane-spanning domains H8 and H9 (Chibalin *et al.,* 1992; Beguin *et al.,* 1994; Feschenko and Sweadner, 1994). A sequence of 26 amino acids (N_{911}–A_{936} on the extracellular domain linking transmembrane segments H7 and H8 is 65% identical to the region which is involved with the binding of the β subunit in vertebrate Na^+,K^+-ATPase (Lemas *et al.,* 1994). However, the N-terminal domain exhibits little sequence similarity to vertebrate Na^+,K^+-ATPase α subunits (Lebovitz *et al.,* 1989) and lacks the PKC phosphorylation sites (Feschenko and Sweadner, 1995).

Only one gene encoding for the α subunit has been identified in *Drosophila;* it has been localized to position 93B on the right arm of the third chromosome (Lebovitz *et al.,* 1989). Immunofluorescent localization in adult flies has demonstrated that the Na^+,K^+-ATPase α subunit is expressed in abundance in neural tissues, including the retina, muscle, and Malpighian tubules (Lebovitz *et al.,* 1989). Mutations in the α subunit gene lead to a "bang-sensitive" behavior of the flies, i.e., the flies are shortly paralyzed after vigorous agitation (Schubiger *et al.,* 1994). In vertebrates, however, there are at least three unlinked genes (α1, α2, α3) encoding Na^+,K^+-ATPase α subunits which exhibit a tissue-specific and developmental pattern of expression (see, for example, Takeyasu *et al.,* 1989; Schneider, 1992). α1 is the predominant form in kidney and other Na^+-transporting epithelia, whereas α2 is prominent in skeletal muscle and brain, and α3 in brain.

The β subunit of *Drosophila* Na^+,K^+-ATPase has only recently been cloned and sequenced (Sun and Salvaterra, 1995). Two genes encoding for β subunits have been identified and termed *Nervana* (nerve antigen, *Nrv*) 1 and 2. Both genes are located on the right arm of the third chromosome near position 92C–D. The encoded proteins exhibit 55% similarity to each other and approximately 46% homology to vertebrate Na^+,K^+-ATPase β subunits. The encoded proteins have a single putative transmembrane do-

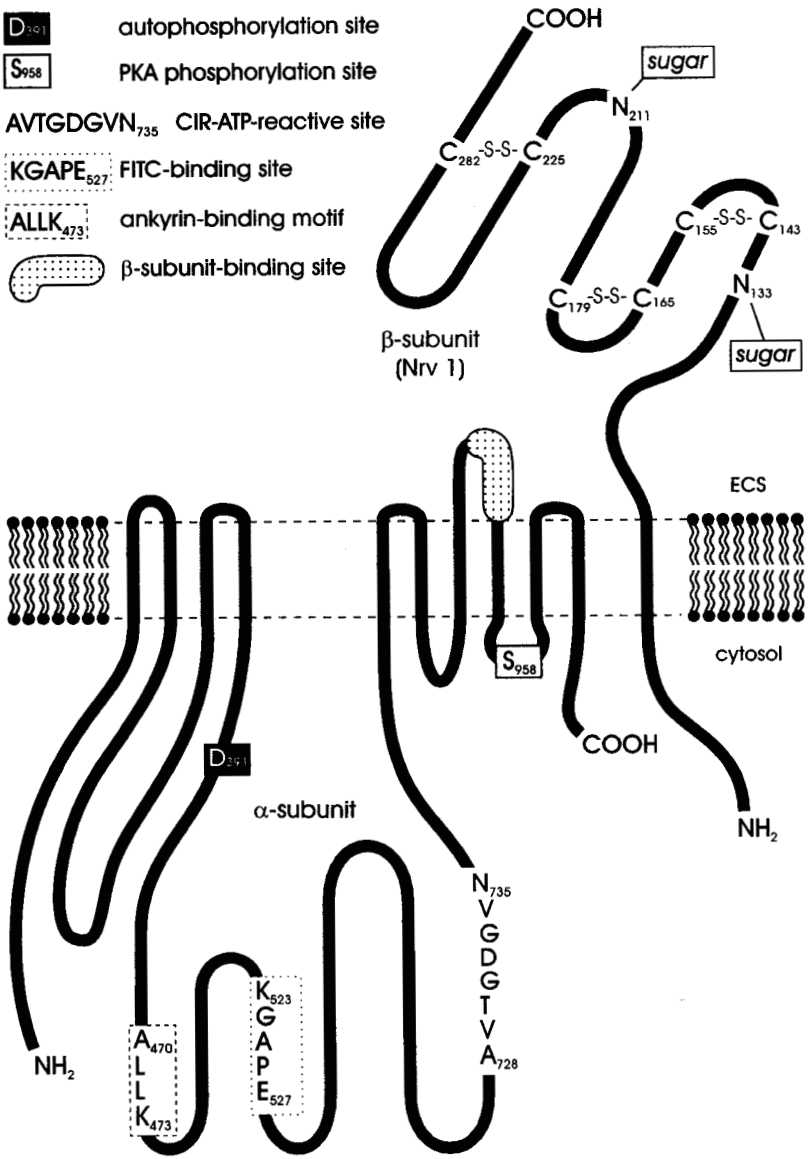

FIG. 4 Structural model of *Drosophila* Na^+,K^+-ATPase, based on the sequence of the α subunit (Lebovitz *et al.*, 1989) and the Nrv 1 β subunit (Sun and Salvaterra, 1995). Amino acyl residues that have been identified to be of functional relevance are highlighted. The α subunit is shown with 10 transmembrane segments, because the putative protein kinase A (PKA) phosphorylation site would be located on the extracellular side in the 8-transmembrane-segment model (Vasilets and Schwartz, 1994).

main near the N terminus and six cysteines that lie in the extracellular domain, which correspond to those involved in disulfide bond formation in the vertebrate Na^+,K^+-ATPase β subunit (Fig. 4). Copurification with the Na^+,K^+-ATPase α subunit directly demonstrates that Nrv proteins represent the β subunit of the pump. *Nrv1* has an open reading frame of 309 amino acids, whereas *Nrv2* encodes for two transcripts by alternative splicing, with 322 and 323 amino acids, respectively. Similarly, the vertebrate Na^+,K^+-ATPase β subunit occurs in several isoforms ($\beta 1$, $\beta 2$, $\beta 3$) (Malik *et al.*, 1996). Since Nrv proteins are only observed in neurons, Sun and Salvaterra (1995) speculate that there may be even more β subunit isoforms in *Drosophila* and that these are expressed in nonneural tissues.

VI. Localization of Na^+,K^+-ATPase in Photoreceptors

Initial presumptions concerning the localization of Na^+,K^+-ATPase in insect photoreceptors have been based on structural and/or physiological data:

- Jansonius (1990) has argued that Na^+,K^+-ATPase must reside predominantly on the nonrhabdomeric part of the plasma membrane, because rhodopsin accounts for the majority of the microvillar membrane proteins and there is not enough space left on the microvillar membrane to house a large number of pump molecules.
- Dimitracos and Tsacopoulos (1985) have studied the recovery of ion transport and photoresponse after a transient inhibition of oxidative metabolism. They have reported that Na^+,K^+-ATPase activity is the first function to recover after anoxia and have concluded that, for anatomical reasons, Na^+,K^+-ATPase can use the first ATP molecules produced by mitochondria after the onset of oxidative metabolism. Since most mitochondria in honeybee photoreceptors are positioned at the periphery of the cell, close to the nonrhabdomeric part of the plasma membrane (see Fig. 1b), the authors have further concluded that Na^+,K^+-ATPase is localized to this membrane area.
- The hypothesis that Na^+,K^+-ATPase is localized on the nonrhabdomeric surface domain of insect photoreceptors is in agreement with the results of Walz (1985) on the microvillar photoreceptor cells in the leech *Hirudo medicinalis*. Because of their unique morphology, leech photoreceptors are suitable for selectively analyzing ion transport across the microvillar and the nonmicrovillar domains of the plasma membrane. Measurements with K^+-sensitive electrodes demonstrate a light-induced increase of $[K^+]$ in the entire ECS. After the light stimulus, extracellular $[K^+]$ returns to its resting

level. K^+ clearance from the extracellular compartment next to the nonrhabdomeric photoreceptor surface is sensitive to ouabain or temperature, indicating a reuptake by Na^+,K^+-ATPase located in this membrane domain. K^+ clearance from the extracellular compartment next to the rhabdomeric surface, in contrast, is insensitive to these treatments, indicating a diffusional process.

Recently, the distribution of Na^+,K^+-ATPase in insect photoreceptors has been directly analyzed by immunofluorescence microscopy and immunogold electron microscopy. These studies have been performed with monoclonal antibody α5-IgG raised against the chicken kidney Na^+,K^+-ATPase α subunit; this antibody recognizes all known chicken Na^+,K^+-ATPase α subunit isoforms (Takeyasu *et al.,* 1989; Kone *et al.,* 1991). Several lines of evidence strongly suggest that this antibody is a reliable probe for the immunolocalization of the α subunit of insect Na^+,K^+-ATPase: (1) The antibody cross-reacts with the product of the gene for the *Drosophila* Na^+,K^+-ATPase α subunit expressed in mouse L cells (Lebovitz *et al.,* 1989). (2) In several different insect species, the antibody identifies a single polypeptide of approximately 110 kDa on immunoblots of homogenized retina (Fig. 5).[1] (3) Immunolabeling experiments demonstrate that the antigen is located at the plasma membrane as it is expected for Na^+,K^+-ATPase (Baumann and Takeyasu, 1993; Lee *et al.,* 1993; Baumann *et al.,* 1994; Just and Walz, 1994; Schubiger *et al.,* 1994; Baumann and Lautenschläger, 1995; Stürmer *et al.,* 1995; Baumann, 1997). (4) When α5-IgG binding is detected with gold-coupled secondary antibodies, gold grains are predominantly localized on the cytoplasmic side of the plasma membrane (Baumann and Takeyasu, 1993; Baumann *et al.,* 1994), in accordance with the topology of the α5-IgG-binding epitope on the chicken Na^+,K^+-ATPase α subunit (Lemas *et al.,* 1992).

Immunolocalization studies with α5-IgG have confirmed the above notion that the Na^+,K^+-ATPase is located predominantly on the nonrhabdomeric surface domain of photoreceptor cells (Baumann and Takeyasu, 1993; Baumann *et al.,* 1994; Baumann and Lautenschläger, 1995). Unexpectedly, these studies have demonstrated that the distribution of Na^+,K^+-ATPase on the surface of insect photoreceptors is far more complex than previously assumed and that subtle differences in the localization pattern exist among photoreceptor cells of different insect species (Figs. 6–8).

[1] A molecular weight of approximately 130 kDa has been reported for the blowfly Na^+,K^+-ATPase α subunit (Baumann *et al.,* 1994). However, this has been the result of crosslinking of the Na^+, K^+-ATPase α- and β subunits by boiling of the samples. Samples were heated to only 60°C in the experiment shown in Fig. 4, resulting in a mobility of 110 kDa for the Na^+,K^+-ATPase α subunit.

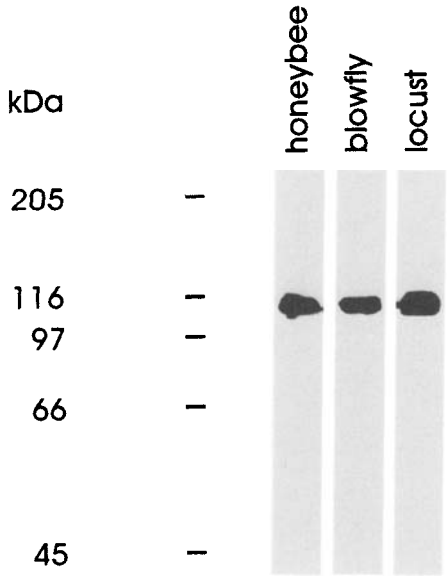

FIG. 5 Monoclonal antibody against the chicken Na^+,K^+-ATPase α subunit applied to immunoblots of honeybee, blowfly, and locust retina. The antibody identifies a 110-kDa protein in the retina of each species.

A. Honeybee

In the honeybee drone photoreceptor, Na^+,K^+-ATPase is localized on the nonrhabdomeric smooth surface but is absent from the microvillar membrane domain (Baumann and Takeyasu, 1993). However, Na^+,K^+-ATPase is not homogeneously distributed over the nonrhabdomeric surface but is concentrated only on those membrane areas that face the adjacent pigmented glial cells. As shown in Fig. 6a, the pigmented glial cells send finlike processes between the photoreceptor cells toward the rhabdom but do not reach the belt desmosomes. A strip with a width of approximately 1 μm lying next to the belt desmosome is uncovered by glial cells and has no detectable Na^+,K^+-ATPase (Figs. 6b and 8a). Moreover, several patches of surface scattered over the entire nonrhabdomeric membrane domain are not apposed to pigmented glial cells and are negative for Na^+,K^+-ATPase.

B. Locust and Cockroach

The compound eyes of the locust *Schistocerca gregaria* and the cockroach *Periplaneta americana* are of the closed apposition type and their morphol-

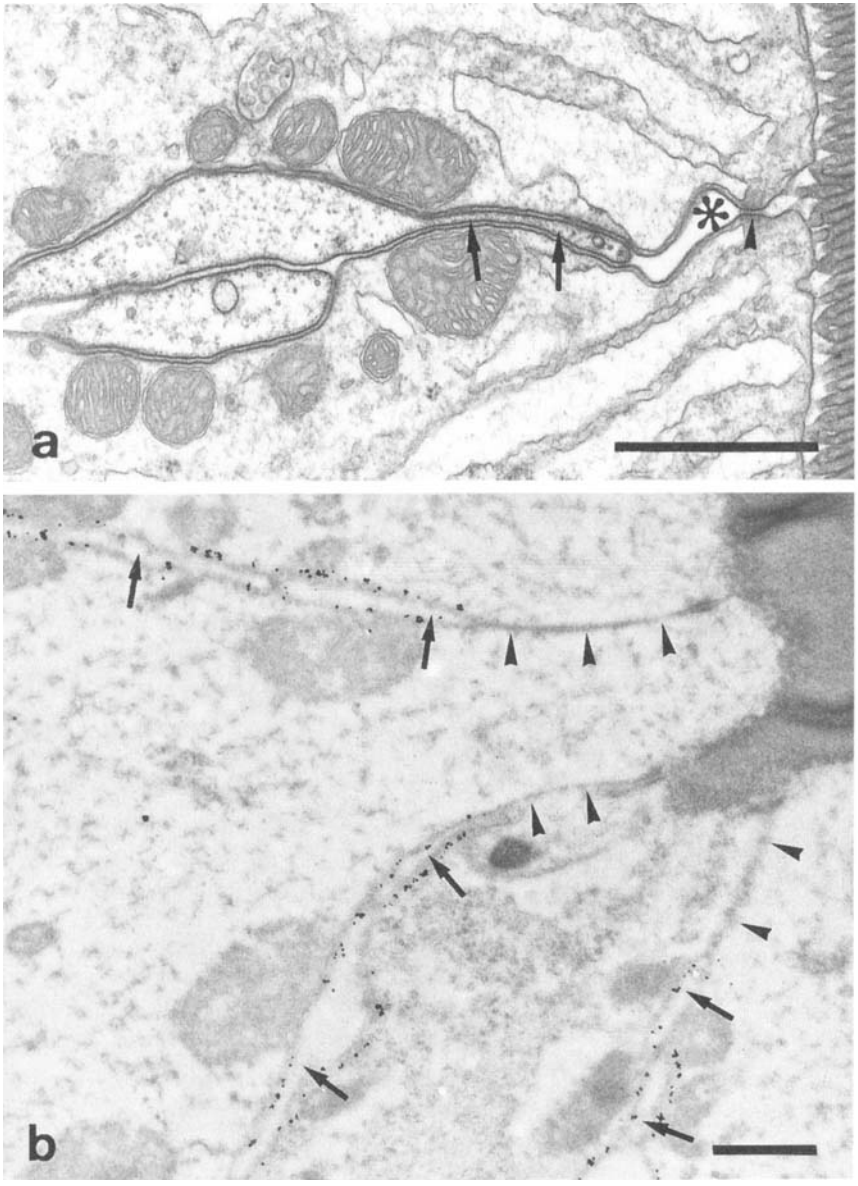

FIG. 6 Immunogold localization of Na^+,K^+-ATPase in the honeybee drone photoreceptor. (a) Electron micrograph of drone photoreceptors. A belt desmosome (arrowhead) delimits the rhabdomeric surface from the smooth nonrhabdomeric surface domain. Narrow processes of pigmented glial cells (arrows) are wedged between the photoreceptors. The majority of the nonrhabdomeric surface is tightly apposed to pigmented glial cells. Only a small area next to the belt desmosome is free of glia and exposed to an ECS (asterisk). (b) Na^+,K^+-

ogy is similar to that of the honeybee compound eye. However, in both the locust and the cockroach retina, the pigmented glial cells are confined to the periphery of the ommatidium (Butler, 1973; Wilson *et al.*, 1978). At their lateral side, the photoreceptor cells have no contact with the glial cells but are closely apposed to the adjacent photoreceptor (Fig. 8b).

Immunolocalization of the Na^+,K^+-ATPase α subunit in locust and cockroach retina (Stürmer *et al.*, 1995; O. Baumann, unpublished results) has demonstrated that Na^+,K^+-ATPase is homogeneously distributed over the entire nonrhabdomeric surface of photoreceptor cells but is absent from the microvillar membrane (Figs. 7a and 8b). The boundary between the Na^+,K^+-ATPase-positive and the Na^+,K^+-ATPase-negative surfaces is marked by belt desmosomes.

The distribution of Na^+,K^+-ATPase in locust retina has also been assayed by Polyanovsky *et al.* (1993) with the K^+-dependent *p*-nitrophenylphosphatase method (Ernst and Hootman, 1981). In this cytochemical assay, lead citrate is used to detect the sites at which phosphate is produced by Na^+,K^+-ATPase-mediated hydrolysis of *p*-nitrophenylphosphate. The specificity of this method is demonstrated by the inhibition of the reaction with oubain. In the locust retina, a lead phosphate precipitate is observed all along the nonrhabdomeric part of the plasma membrane, but not on the rhabdom.

C. Moth

The compound eye of moths is of the optical superposition type, and the fused-type rhabdom extends from the basal lamina only halfway up the dioptric apparatus. Since the zone between the rhabdom and the dioptric apparatus is transparent, light can pass between the ommatidia, and each rhabdom gathers light from several lenses (Nilsson, 1989). A major difference between the ommatidia of moths and the apposition-type compound eyes is the size of the rhabdom; it has a fan-like cross section and extends over almost the entire ommatidial diameter in moth ommatidia (Fig. 7d; Meinecke, 1981; Anton-Erxleben and Langer, 1988). More than half of the outline of a photoreceptor is thus covered by microvilli (Fig. 8c), and the

---

ATPase detected by the anti-α-subunit antibody and secondary, gold-coupled antibody. The Na^+,K^+-ATPase is strictly localized to sites of photoreceptor–glia contact. The narrow processes of pigmented glial cells are indicated by arrows. Note the absence of label at the glia-free areas of the nonrhabdomeric surface (arrowheads). Bars: 0.5 μm.

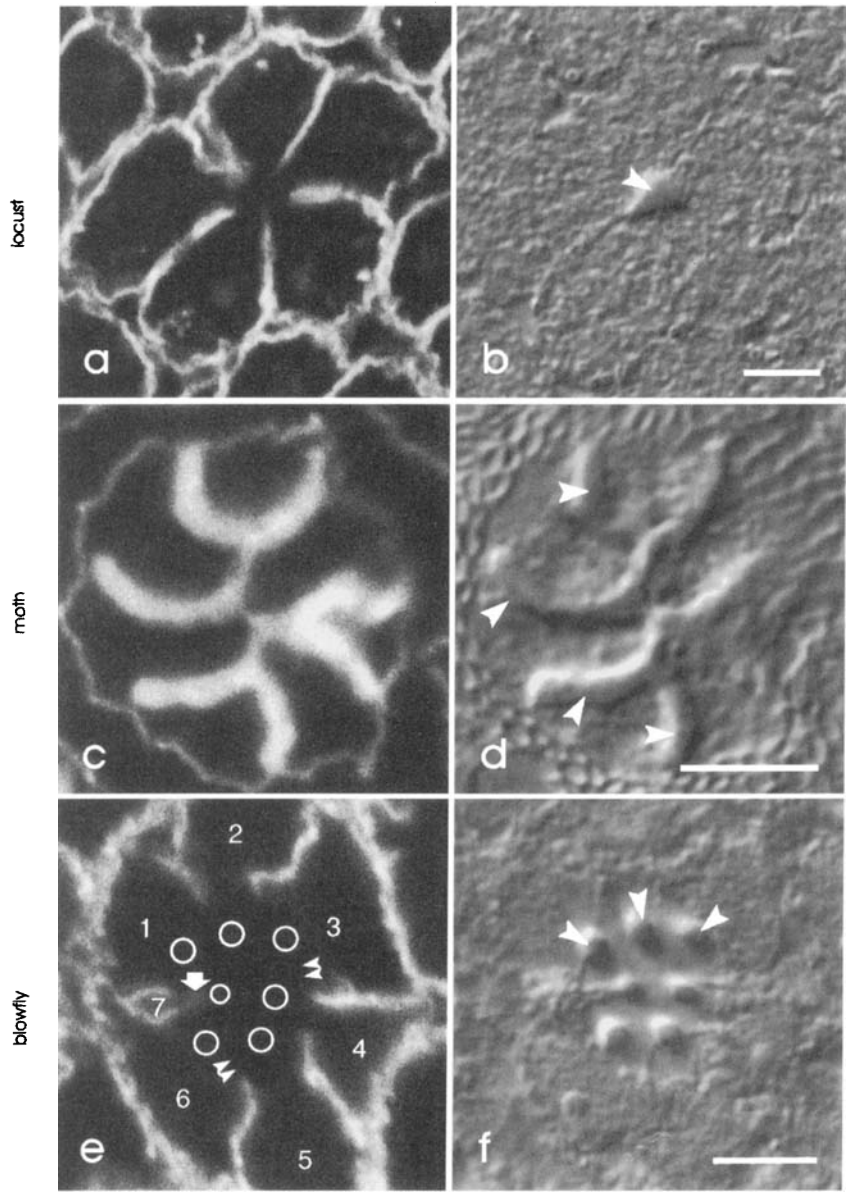

FIG. 7 Immunofluorescence localization of the Na^+,K^+-ATPase α subunit in diverse insect retinae (a,c,e). Nomarski contrast images (b,d,f) demonstrate the position of the rhabdoms and rhabdomeres, respectively (arrowheads). (a) In the locust *Schistocerca gregaria,* Na^+,K^+-ATPase is located over the entire nonrhabdomeric surface of the photoreceptor cells. (c) In the moth *Manduca sexta,* both the nonrhabdomeric surface and the rhabdom are labeled with anti-Na^+,K^+-ATPase. (e) A complex pattern of anti-Na^+,K^+-ATPase labeling is seen in the retina of the blowfly *Calliphora erythrocephala.* The positions of the rhabdomeres, as deduced

nonrhabdomeric surface apparently accounts for a very small fraction of the total cell surface (exempting the axonal surface).

In the moth *Manduca sexta,* Na^+,K^+-ATPase has been detected on both the nonrhabdomeric domain of the plasma membrane and the microvillar membrane (Figs. 7c and 8c; Baumann and Lautenschläger, 1995). Nevertheless, the distribution of Na^+,K^+-ATPase is also polarized in moth photoreceptors, because less than half of the total amount of immunogold labeling resides over the rhabdomere, indicating a far lower density of pump molecules on this membrane domain.

D. Fly

The fruitfly *Drosophila melanogaster* and the blowfly *Calliphora erythrocephala* belong to higher dipteran flies, and the anatomy of their compound eyes is almost identical. Their compound eyes are of the neuronal superposition type, i.e., individual photoreceptor cells within adjacent ommatidia have the same visual field and their electrical responses converge on the same neuron within the optic ganglia (Carlson and Chi, 1979; Hardie, 1986). The retinulae have an open-type rhabdom with a large ECS, known as the intraommatidial space, separating the rhabdomeres (Fig. 7f). This results in an additional smooth surface domain between the microvillar rhabdomere and the belt desmosomes (Fig. 8d) called either the juxtarhabdomeric (Baumann *et al.,* 1994) or the stalk domain (Longley and Ready, 1995). There are eight photoreceptor cells within an ommatidium, with the rhabdomeres of the six large cells (R1–R6) being grouped in an assymetric trapezoid around the intraommatidial space (Figs. 7e and 7f). The rhabdomeres of the two small cells (R7 and R8) are positioned in the center of the intraommatidial space and are connected by a narrow stalk to the cell body. Only one of the R7/R8 rhabdomeres is seen in cross sections of the retina, because the rhabdomere of R8 is contiguous with that of R7 and forms an extension of it in the proximal part of the ommatidium. R1–6 and

---

from the Nomarski-contrast image (f), are superimposed on the fluoresence image (white circles). The blowfly ommatidium has an open-type rhabdom, with the rhabdomeres being separated by an extensive extracellular space, the intraommatidial space. There is an additional smooth surface domain (juxtarhabdomeric surface) that faces the intraommatidial space and that is interposed between the rhabdomere and the belt desmosomes. Na^+,K^+-ATPase resides at the smooth surface domain that faces either adjacent photoreceptors or pigment cells. No Na^+,K^+-ATPase can be detected at the juxtarhabdomeric domain of photoreceptors R1–6 (double arrowheads), whereas weak labeling is seen at the juxtarhabdomeric surface of R7 (arrow). The rhabdomere is negative in all cells. Bars: 5 μm.

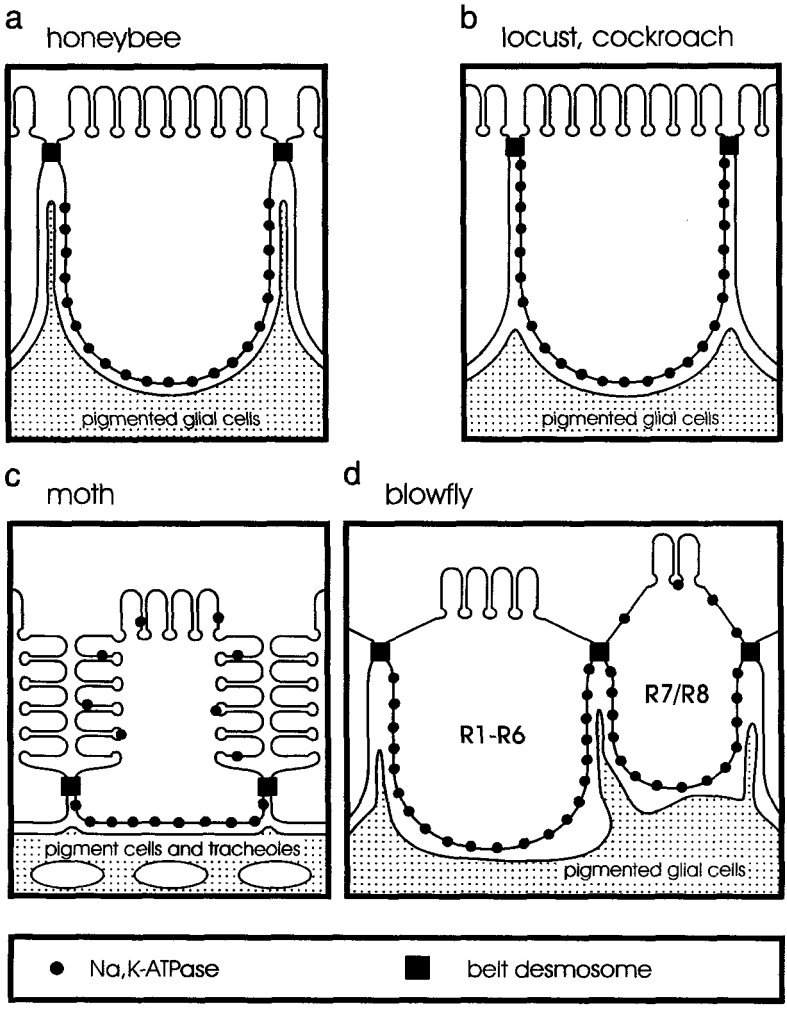

FIG. 8 Patterns of Na^+,K^+-ATPase distribution in insect photoreceptor cells. (a) In honeybee drone photoreceptors, Na^+,K^+-ATPase is localized exclusively to the sites of photoreceptor–glia contact. Finlike processes of the pigmented glial cells are wedged between the photoreceptors, leaving only a narrow strip of the nonrhabdomeric surface next to the belt desmosomes uncovered. (b) In locust and cockroach photoreceptors, the nonrhabdomeric surface closely adheres to the surface of either the adjacent photoreceptor or the pigmented glial cells. In these species, Na^+,K^+-ATPase is homogeneously distributed over the entire nonrhabdomeric surface. (c) In photoreceptor cells of the moth *Manduca sexta,* Na^+,K^+-ATPase is located on both the rhabdomeric and the rhabdomeric surface. However, the density of pump molecules is higher on the nonrhabdomeric surface. (d) In the retina of the blowfly *Calliphora erythrocephala,* photoreceptor cells R1–6 and R7/R8 represent distinct retinal subsystems. In R1–6, Na^+,K^+-ATPase is restricted to the smooth surface areas that face either the adjacent photore-

R7/R8 represent distinct retinal subsystems that express different rhodopsin genes and that are characterized by differences in spectral sensitivity, polarization sensitivity, gain of transduction machinery, and neuronal projection (Hardie, 1979, 1986).

Immunofluorescence and immunogold labeling of the blowfly retina have demonstrated that R1–6 and R7/8 also differ with respect to their positioning of Na^+,K^+-ATPase on the cell surface (Baumann *et al.,* 1994). In photoreceptors R1–R6, Na^+,K^+-ATPase is localized on the nonrhabdomeric surface that corresponds to the basolateral domain. No Na^+,K^+-ATPase is detectable on the juxtarhabdomeric surface area or on the microvillar membrane (Figs. 7e and 8d). In R7 and R8, however, Na^+,K^+-ATPase has additionally been localized to the juxtarhabdomeric surface area and to the membrane loops at the microvillar bases. Quantitative analysis of immunogold labeling has demonstrated that the relative density of pump molecules on the juxtarhabdomeric domain is only about 20% of that on the remaining smooth surface (Baumann *et al.,* 1994; Baumann, 1997). Comparative immunofluorescence studies indicate an identical pattern of Na^+,K^+-ATPase localization in the retina of *D. melanogaster* (O. Baumann, unpublished results).

In summary, Na^+,K^+-ATPase distribution is polarized in all the insect photoreceptor cells that have been examined to date (Fig. 8). Na^+,K^+-ATPase is localized either exclusively on the entire nonrhabdomeric surface, as in locust, cockroach, and blowfly R7/8, or on a subdomain of the nonmicrovillar surface, as in honeybee and blowfly R1–R6. Moreover, Na^+,K^+-ATPase can reside at low density in the microvillar membrane, as in the case of the moth *M. sexta.*

The localization of some Na^+,K^+-ATPase on the microvilli is curious. In most epithelial cells, Na^+,K^+-ATPase is restricted to the basolateral domain (Simons and Fuller, 1985). Na^+,K^+-ATPase has been found on the microvillar membrane domain only in the vertebrate retinal pigment epithelium (Cauldwell and McLaughlin, 1984; Gundersen *et al.,* 1991; Rizzolo and Zhou, 1995), in the vertebrate choroid plexus (Masuzawa *et al.,* 1984; Seigel *et al.,* 1984; Marrs *et al.,* 1993), and in ion-transporting cells of the cockroach salivary gland (Just and Walz, 1994). However, in these cell types, Na^+,K^+-ATPase is predominantly localized at the microvilli-bearing apical surface.

What are the reasons for these differences in the distribution pattern of Na^+,K^+-ATPase on insect photoreceptors? Do these subtle differences arise

---

ceptor or the pigmented glial cells. In R7 and R8, however, some Na^+,K^+-ATPase also resides on the smooth surface domain that faces the intraommatidial space and the microvillar bases, although at lower density. Note that photoreceptors and pigmented glial cells do not seem to adhere as tightly as in other species.

because of functional requirements or are they side effects of various mechanisms involved in maintaining protein distribution? These questions cannot be answered at present. However, it is plausible that, in the moth, the relatively small nonrhabdomeric surface provides insufficient space to house the total number of pump molecules required for proper functioning of the cell.

VII. Developmental Redistribution of Na^+,K^+-ATPase

The localization of Na^+,K^+-ATPase during photoreceptor development has been examined only in blowfly retina (Baumann, 1997) and is presented in schematic form in Fig. 9.

Development of the fly compound eye occurs in the eye imaginal disc, a monolayer of pluripotent epithelial cells that arises by invagination of the head ectoderm (Ready *et al.*, 1976; Cagan and Ready, 1989). During the third instar larval stage and the first third of pupal life, the progenitor cells become determined to their future fate by a series of cell–cell interactions. Simultaneously, the cells are arranged in a repetitive array of cell clusters that prefigures the organization of adult ommatidia (reviewed in Tomlinson, 1988; Banerjee and Zipursky, 1990; Zipursky and Rubin, 1994). At this stage, the photoreceptor precursors have short irregular microvilli on their apical surface and a subapical circumferential band of belt desmosomes connecting them to neighboring prospective cone cells (Longley and Ready, 1995). The apical membrane domain and the belt desmosomes then move toward the lateral side of the photoreceptor cell body and are involuted into the retinal epithelium until they reach the basal lamina at about 67% of pupal life (Longley and Ready, 1995). During the second half of pupal development, the microvilli grow in length and are arranged in a tight hexagonal pattern (Longley and Ready, 1995; Baumann, 1997). Simultaneously, the juxtarhabdomeric domain is established between the rhabdomere and the belt desmosomes and enlarges to its final extent. At the time of eclosion, the photoreceptors are completely differentiated as judged by morphological criteria.

Until 44% of pupal life, Na^+,K^+-ATPase is present at low density on the entire photoreceptor surface, including the microvillar bases but exempting the microvillar membrane proper (Baumann, 1997). Between mid-pupal life and eclosion, Na^+,K^+-ATPase distribution becomes polarized by a complex spatiotemporal pattern. At between 44 and 67% of pupal development, large amounts of Na^+,K^+-ATPase are synthesized and delivered to the surface that corresponds to the basolateral domain, resulting in an increase in labeling density on this membrane domain. Although the density of

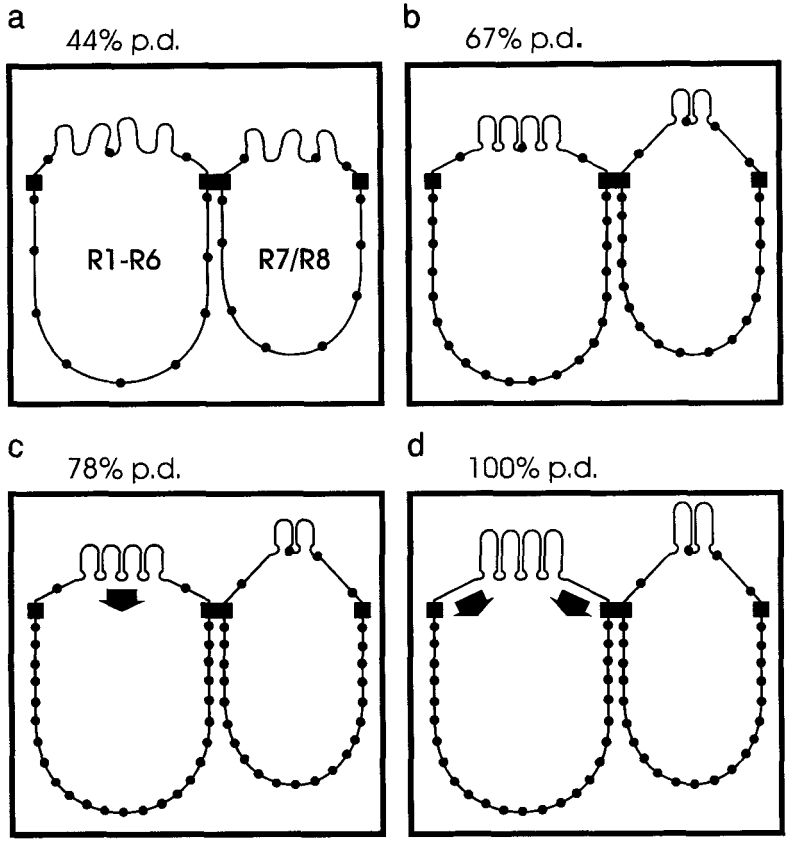

FIG. 9 Developmental changes in the distribution of Na^+,K^+-ATPase during the differentiation of blowfly photoreceptor cells. (a) At 44% of pupal development, the photoreceptor cells have short irregular microvilli. Na^+,K^+-ATPase is homogeneously distributed over the entire cell surface, including the microvillar bases but exempting the microvillar membrane proper. (b) At between 44 and 67% of pupal life, the microvilli become tightly packed and the juxtarhabdomeric surface area is established between the rhabdomere and the belt desmosomes. The density of Na^+,K^+-ATPase increases on the lateral/peripheral surface. (c) At about 78% of pupal life, the microvillar bases of photoreceptors R1–6 lack Na^+,K^+-ATPase (arrow). (d) At the time of eclosion, microvilli have reached their final length and the juxtarhabdomeric surface of R1–6 has been cleared of Na^+,K^+-ATPase (arrows).

Na^+,K^+-ATPase molecules remains constant at the microvillar bases and at the developing juxtarhabdomeric domain (as far as can be determined by immunofluorescence microscopy), the total amount of Na^+,K^+-ATPase molecules must also increase on these domains as they become enlarged. At between 67% of pupal life and eclosion, the microvillar bases and the

juxtarhabdomeric surface of R1–6 but not of R7/8 become sequentially cleared of Na^+,K^+-ATPase, and the final Na^+,K^+-ATPase distribution is established. This developmental process seems to occur according to a strict timetable, which is specific for each photoreceptor, R1 to R6.

VIII. Development and Maintenance of a Restricted Distribution of Na^+,K^+-ATPase on the Plasma Membrane

Studies on vertebrate epithelial cells have suggested several distinct mechanisms that might be engaged in the development and maintenance of the polarized distribution of Na^+,K^+-ATPase: (1) Newly synthesized Na^+,K^+-ATPase might be sorted at the *trans*-Golgi network and specifically delivered to a distinct membrane domain (Zurzolo and Rodriguez-Boulan, 1993; Gottardi and Caplan, 1993; Mays *et al.*, 1995). (2) Na^+,K^+-ATPase could be delivered to the entire cell surface, but surface domains may differ in their rate of Na^+,K^+-ATPase turnover (Hammerton *et al.*, 1991; Mays *et al.*, 1995). (3) Tight junctions may provide a barrier that prevents diffusion of membrane proteins between membrane domains (Cereijido *et al.*, 1989). (4) Na^+,K^+-ATPase might be linked to a submembranous network of spectrin, short actin filaments, and ankyrin and thus be restricted in its distribution, lateral diffusion, and turnover rate (Morrow *et al.*, 1989; Nelson and Hammerton, 1989; Koob *et al.*, 1990; Nelson *et al.*, 1990; Hammerton *et al.*, 1991). (5) Na^+,K^+-ATPase might be linked to cell adhesion molecules and specifically retained at sites of cell–cell contact (Gloor *et al.*, 1990; McNeill *et al.*, 1990; Schmalzing *et al.*, 1992). These various mechanisms may work together within a cell, although the relative contribution of each may vary between cell types (Mays *et al.*, 1995).

Unfortunately, only limited information is available regarding whether and in which manner these mechanisms are involved in the establishment and maintenance of Na^+,K^+-ATPase distribution in insect photoreceptors. Indeed, the extent to which mechanisms (1)–(3) contribute, or whether they act at all, remains unknown.

A. Maintenance of the Distribution of Na^+,K^+-ATPase in Honeybee Photoreceptors

The finding that the distribution of Na^+,K^+-ATPase in honeybee photoreceptors is strictly correlated with the sites of photoreceptor–glia contact

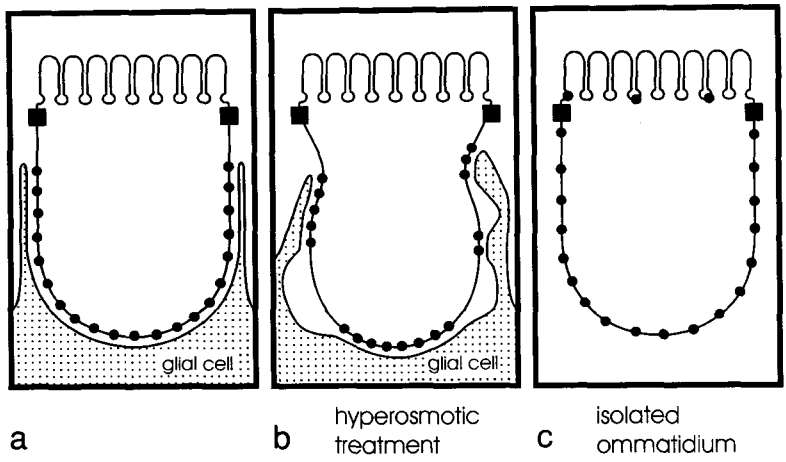

FIG. 10 Effects of disturbances in photoreceptor–glia contact on the localization of Na^+,K^+-ATPase in honeybee drone photoreceptors. (a) In control tissue, the distribution of Na^+,K^+-ATPase is correlated with the sites of photoreceptor–glia contact. (b) Incubation of retinal tissue in Ringer solution supplemented with 400 m*M* sucrose leads to a shrinkage of the cells, a rearrangement of photoreceptor–glia contact sites, and a corresponding redistribution of Na^+,K^+-ATPase on the photoreceptor surface. (c) In isolated retinulae, in the absence of glial cells, Na^+,K^+-ATPase is localized over the entire photoreceptor surface, including the microvillar bases but exempting the microvillar membrane. Note that the neighboring photoreceptors have been omitted for simplicity.

(Fig. 10a) has led to the suggestion that the adhesion of glial cells to the surface of photoreceptors plays a crucial role in maintaining the Na^+,K^+-ATPase position in this system (Baumann and Takeyasu, 1993). Further support for this concept has been provided by the results of two experiments that have examined the effects of a disturbance in photoreceptor–glia contact on Na^+,K^+-ATPase distribution (Baumann and Takeyasu, 1993). First, remodeling of the sites of photoreceptor–glia contact by incubation of retinal tissue in hyperosmotic saline results in a corresponding redistribution of Na^+,K^+-ATPase on the photoreceptor surface (Fig. 10b). Second, following isolation of single retinulae by dissociating the retina by proteolytic and mechanical procedures (Tsacopoulos *et al.,* 1994), Na^+,K^+-ATPase is dispersed over the entire nonrhabdomeric cell surface and is also localized at the bases of the microvilli (Fig. 10c). The finding that Na^+,K^+-ATPase is excluded from the microvillar membrane, even in isolated retinulae, supports the view that this membrane area represents a microdomain with limited lateral diffusion of membrane proteins.

The restriction of Na^+,K^+-ATPase, on the photoreceptor surface, to the sites of contact with pigmented glial cells could be mediated by barriers

that limit diffusion between Na^+,K^+-ATPase-positive and Na^+,K^+-ATPase-negative membrane domains. Fine-structured analyses of the honeybee retina, however, have not visualized any junctional structures that could serve this purpose (Baumann and Takeyasu, 1993). Alternatively, Na^+,K^+-ATPase molecules may be directly or indirectly linked to cell adhesion molecules mediating photoreceptor–glia adhesion and could thus be trapped at contact sites (Baumann and Takeyasu, 1993). This view is supported by the observation of a relatively electron-dense material that fills the narrow intercellular space between photoreceptors and glial cells, indicating a tight molecular interaction over the entire extent of the contact sites. Staining with wheat germ agglutinin, a marker for glycoproteins, has further demonstrated that not all glycoproteins of the nonrhabdomeric surface of photoreceptors are concentrated at contact sites with pigmented glial cells, suggesting that the mechanism maintaining Na^+,K^+-ATPase distribution is specific (Baumann and Takeyasu, 1993).

The molecules that mediate photoreceptor–glia adhesion in the honeybee retina and that are possible involved in maintaining the Na^+,K^+-ATPase position have not yet been identified. However, there are some minimal requirements for the functional properties of the adhesion mechanism. Cell–cell contact and the distribution of Na^+,K^+-ATPase are not disturbed by nominally Ca^{2+}-free media (Baumann and Takeyasu, 1993), indicating the involvement of Ca^{2+}-independent cell adhesion molecules. Moreover, cell–cell adhesion should be mediated by a heterophilic mechanism, because it occurs between photoreceptors and glial cells, but not among photoreceptors.

Cell–cell contact may also play a prominent role in determining the distribution of Na^+,K^+-ATPase in locust and cockroach photoreceptor cells. However, whereas the honeybee photoreceptor has only intimate contact with pigmented glial cells, cockroach and locust photoreceptors also adhere tightly to the adjacent photoreceptors, and Na^+,K^+-ATPase is localized at both photoreceptor–glia and photoreceptor–photoreceptor contact sites. In order to adapt the model for Na^+,K^+-ATPase localization in honeybee photoreceptors to locust and cockroach photoreceptors, the cell adhesion molecules involved in maintaining Na^+,K^+-ATPase distribution must be postulated as being expressed on the surface of both cell types, viz., pigmented glial cells and photoreceptors.

Studies on vertebrate systems have demonstrated that cell adhesion molecules interact with Na^+,K^+-ATPase via the submembranous spectrin/ankyrin network (McNeill *et al.*, 1990; Nelson *et al.*, 1990). An isoform of spectrin, α-spectrin, has been identified and localized in the retina of the honeybee drone (Baumann, 1992), of the cockroach, and of the locust (O. Baumann, unpublished results) by use of a polyclonal antibody against *Drosophila* α-spectrin (Byers *et al.*, 1987); α-spectrin has only been localized

to the plasma membrane of pigmented glial cells. However, spectrin is known to occur in several isoforms (Byers *et al.,* 1987, 1992; Dubreuil *et al.,* 1990; Volk, 1992; Thomas and Kiehart, 1994), and spectrin isoforms distinct from α-spectrin may be expressed in photoreceptors. The role of the spectrin/ankyrin system in maintaining the distribution of Na^+,K^+-ATPase in the photoreceptors of the honeybee thus awaits further clarification.

B. Maintenance of the Distribution of Na^+,K^+-ATPase in Fly Photoreceptors

In blowfly retina, cell–cell adhesion may play a less prominent role in the establishment and maintenance of a polarized Na^+,K^+-ATPase distribution. Here, Na^+,K^+-ATPase is also localized to the juxtarhabdomeric surface area, a cell domain that does not face an adjacent cell. Moreover, cell–cell adhesion appears to be less tight in the fly retina, because there are often large gaps between the cells (Baumann, 1997), and retinulae can be easily isolated from the blowfly retina without proteolytic methods, by simple mechanical procedures (Hardie, 1991b; Ranganathan *et al.,* 1991). Finally, Na^+,K^+-ATPase is not redistributed in isolated blowfly retinulae, indicating that the maintenance of the distribution of Na^+,K^+-ATPase does not require interaction with pigmented glial cells (Baumann, 1997).

The immunolocalization of α-spectrin in adult blowfly retina has demonstrated an almost perfect match in its distribution with the localization of Na^+,K^+-ATPase, indicating that these proteins are interlinked (Baumann *et al.,* 1994). Most impressively, the juxtarhabdomeric membrane domain of R7/8, but not R1–6, has a large amount of α-spectrin underneath it. Analysis of the localization of Na^+,K^+-ATPase and α-spectrin during photoreceptor differentiation has demonstrated, however, that the redistribution of α-spectrin lags several days behind that of Na^+,K^+-ATPase. If α-spectrin is directly involved with the establishment of Na^+,K^+-ATPase localization, then changes in the α-spectrin pattern should precede or at least coincide with the redistribution of Na^+,K^+-ATPase (Baumann, 1997). Moreover, Na^+,K^+-ATPase can be easily and almost completely extracted from isolated retinal membranes of adult blowfly retina by 0.5% Triton X-100, but no α-spectrin can be detected in the solubilized fraction (Baumann, 1997). In other systems, in which an association of Na^+,K^+-ATPase with the submembraneous spectrin network has been demonstrated, detergent treatment results in only a limited extraction of Na^+,K^+-ATPase from cellular membranes (Madreperla *et al.,* 1989; Marrs *et al.,* 1993; Rizzolo and Zhou, 1995) or extraction of a macromolecular complex containing Na^+,K^+-ATPase and spectrin (Nelson and Hammerton, 1989; Nelson *et al.,* 1990;

Marrs *et al.*, 1993). Although these negative results provide no evidence that Na^+,K^+-ATPase localization is independent of the spectrin/ankyrin system in blowfly photoreceptors, they at least suggest that Na^+,K^+-ATPase is not intimately linked to α-spectrin. The involvement of other spectrin isoforms in the development and stabilization of a polarized Na^+,K^+-ATPase distribution, however, cannot be excluded.

Recent experiments on midgut epithelial cells of *Drosophila* embryos have also provided evidence for an independence of the distribution of Na^+,K^+-ATPase from α-spectrin. In these cells, Na^+,K^+-ATPase, α-spectrin, β-spectrin, and ankyrin are restricted to the basolateral domain of the plasma membrane (Lee *et al.*, 1993; Dubreuil, 1996). Biochemical and immunocytochemical experiments on α-spectrin mutants have revealed that the protein level and the distribution of Na^+,K^+-ATPase, two spectrin isoforms (β-spectrin and β_{Heavy}-spectrin), and ankyrin are unaffected by the absence of α-spectrin (Lee *et al.*, 1993; Dubreuil and Yu, 1994; Dubreuil, 1996). However, the surface morphology of epithelial cells is altered in α-spectrin mutants, indicating that this molecule contributes to the shaping of cells (Lee *et al.*, 1993).

IX. Concluding Remarks

In insect photoreceptors, light stimulation leads to an increase of intracellular Na^+ concentration and a decrease of intracellular K^+ concentration by up to tens of m*M*. Ion concentrations are reestablished by the activity of Na^+,K^+-ATPase, and the majority of energy used upon light stimulation is utilized for this function. The Na^+,K^+-ATPase is concentrated on the surface of the cell body, whereas light reception, the signal transduction machinery, and light-activated channels are restricted to the microvillar rhabdomere. The functional compartmentalization of insect photoreceptors thus compares well with that of vertebrate photoreceptors, which also have a specialized transduction compartment, the outer segment, and a cell body undertaking "household functions," among them the establishment of Na^+ and K^+ gradients across the plasma membrane.

Although Na^+,K^+-ATPase is enriched on the nonrhabdomeric part of the plasma membrane in all insect photoreceptors examined to date, there are species-specific differences in localization patterns, and Na^+,K^+-ATPase may even occur at a relatively low density on the microvillar membrane. These subtle variations in Na^+,K^+-ATPase location may result from differences in the molecular mechanisms that establish and maintain the distribution of Na^+,K^+-ATPase molecules. Two species appear to be particularly attractive for analyzing these mechanisms, but for different reasons. In the

honeybee drone retina, the pattern of Na^+,K^+-ATPase is directly correlated with the sites of photoreceptor–glia contact, and this tissue thus provides an attractive model for analyzing the role of glial cells in maintaining the distribution of membrane proteins on the surface of neuronal cells. Because the honeybee drone retina is relatively large, enough tissue can be obtained for biochemical experiments. The retina of Brachyceran flies (*Drosophila, Calliphora*), on the other hand, represents an attractive model for studying variations of Na^+,K^+-ATPase localization between different cell types within a single tissue. Moreover, *Drosophila* has the advantage of permitting genetic manipulations that may provide insights into the role of individual components of, e.g., the submembrane cytoskeleton in the localization of Na^+,K^+-ATPase.

Acknowledgments

I am grateful to Drs. Bernd Walz and Kunio Takeyasu for their critical comments on the manuscript, and to Dr. Theresa Jones for linguistic corrections.

References

Anton-Erxleben, F., and Langer, H. (1988). Functional morphology of the ommatidia in the compound eye of the moth, *Antheraea polyphemus* (Insecta, Saturniidae). *Cell Tissue Res.* **252,** 385–396.

Arikawa, K., Hicks, J. L., and Williams, D. S. (1990). Identification of actin filaments in the rhabdomeral microvilli of *Drosophila* photoreceptors. *J. Cell Biol.* **110,** 1993–1998.

Banerjee, U., and Zipursky, S. L. (1990). The role of cell–cell interaction in the development of the *Drosophila* visual system. *Neuron* **4,** 177–187.

Baumann, F., and Hadjilazaro, B. (1971). Afterpotentials in retinula cells of the drone. *Vision Res.* **11,** 1198.

Baumann, O. (1992). The submembrane cytoskeleton of pigmented glial cells, primary pigment cells and crystalline cone cells in the honeybee compound eye. *Cell Tissue Res.* **270,** 353–363.

Baumann, O. (1997). Biogenesis of plasma membrane domains in fly photoreceptor cells: Fine-structural analysis of the cell surface and immunolocalization of Na^+,K^+-ATPase and α-spectrin during cell differentiation. *J. Comp. Neurol.* (in press).

Baumann, O., and Lautenschläger, B. (1995). Immunulocalization of the Na,K-ATPase in photoreceptor cells of the moth *Manduca sexta*—Evidence for Na,K-ATPase on both the nonmicrovillar and the microvillar domains of the plasma membrane. *Cell Tissue Res.* **281,** 119–126.

Baumann, O., and Takeyasu, K. (1993). Polarized distribution of Na,K-ATPase in honeybee photoreceptors is maintained by interaction with glial cells. *J. Cell Sci.* **105,** 287–301.

Baumann, O., and Walz, B. (1989a). Topography of the Ca^{2+}-sequestering endoplasmic reticulum in photoreceptors and pigmented glial cells in the compound eye of the honeybee drone. *Cell Tissue Res.* **255,** 511–522.

Baumann, O., and Walz, B. (1989b). Calcium- and inositol polyphosphate-sensitivity of the calcium-sequestering endoplasmic reticulum in the photoreceptor cells of the honeybee drone. *J. Comp. Physiol. A* **165,** 627–636.

Baumann, O., Walz, B., Somlyo, A. V., and Somlyo, A. P. (1991). Electron probe microanalysis of calcium release and magnesium uptake by endoplasmic reticulum in bee photoreceptors. *Proc. Natl. Acad. Sci. USA* **88,** 741–744.

Baumann, O., Lautenschläger, B., and Takeyasu, K. (1994). Immunolocalization of Na,K-ATPase in blowfly photoreceptor cells. *Cell Tissue Res.* **275,** 225–234.

Beguin, P., Beggah, A. T., Chibalin, A. V., Burgener-Kairuz, P., Jaisser, F., Mathews, P. M., Rossier, B. C., Cotecchia, S., and Geering, K. (1994). Phosphorylation of the Na,K-ATPase α-subunit by protein kinase A and C in vitro and in intact cells. *J. Biol. Chem.* **269,** 24437–24445.

Bennett, R. R., and White, R. H. (1989). Influence of carotenoid deficiency on the visual sensitivity, visual pigment and P-face particles of photoreceptor membrane in the moth *Manduca sexta*. *J. Comp. Physiol. A* **164,** 321–331.

Berridge, M. J. (1993). Inositol trisphosphate and calcium signalling. *Nature* (*London*) **361,** 315–361.

Blanco, G., Detomaso, A. W., Koster, J., Xie, Z. J., and Mercer, R. W. (1994). The α-subunit of the Na,K-ATPase has catalytic activity independent of the β-subunit. *J. Biol. Chem.* **269,** 23420–23425.

Bloomquist, B., Shortridge, R., Schneuwly, S., Perdew, M., Montell, C., Steller, H., Rubin, G., and Pak, W. (1988). Isolation of a putative phospholipase C gene of Drosophila, *norpA,* and its role in phototransduction. *Cell* **54,** 723–733.

Boschek, C. B. (1971). On the fine structure of the peripheral retina and lamina ganglionaris of the fly, *Musca domestica*. *Z. Zellforsch. Mikrosk. Anat.* **118,** 369–409.

Boschek, C. B., and Hamdorf, K. (1976). Rhodopsin particles in the photoreceptor membrane of an insect. *Z. Naturforsch. C. Bioscii* **31,** 762–763.

Butler, R. (1973). The anatomy of the compound eye of *Periplaneta americana* L. *J. Comp. Physiol.* **83,** 239–262.

Byers, T. J., Dubreuil, R., Branton, D., Kiehart, D. P., and Goldstein, L. S. B. (1987). *Drosophila* spectrin. II. Conserved features of the alpha-subunit are revealed by analysis of cDNA clones and fusion proteins. *J. Cell Biol.* **105,** 2103–2110.

Byers, T. J., Brandin, E., Lue, R. A., Winograd, E., and Branton, D. (1992). The complete sequence of *Drosophila* β-spectrin reveals supra-motifs comprising eight 106-residue segments. *Proc. Natl. Acad. Sci. USA* **89,** 6187–6191.

Cagan, R. L., and Ready, D. F. (1989). The emergence of order in the *Drosophila* pupal retina. *Dev. Biol.* **136,** 346–362.

Cardinaud, B., Coles, J. A., Perrottet, P., Spencer, A. J., Osborne, M. P., and Tsacopoulos, M. (1994). The composition of the interstitial fluid in the retina of the honeybee drone: Implications for the supply of substrates of energy metabolism from blood to neurons. *Proc. R. Soc. London Ser. B* **257,** 49–58.

Carlson, S. D., and Chi, C. (1979). The functional morphology of the insect photoreceptor. *Annu. Rev. Entomol.* **24,** 379–416.

Cauldwell, R., and McLaughlin, J. (1984). Redistribution of Na,K-ATPase in the dystrophic rat retinal epithelium. *J. Neurocytol.* **13,** 895–910.

Cereijido, M., Ponce, A., and Gonzalez-Mariscal, M. (1989). Tight junctions and apical/basolateral polarity. *J. Membr. Biol.* **110,** 1–9.

Chi, C., and Carlson, S. D. (1979). Ordered membrane particles in the rhabdomeric microvilli of the house fly (*Musca domestica* L.). *J. Morphol.* **161,** 309–322.

Chibalin, A. V., Vasilets, L. A., Hennekes, H., Pralong, D., and Geering, K. (1992). Phosphorylation of Na,K-ATPase α-subunits in microsomes and in homogenates of *Xenopus* oocytes resulting from stimulation of protein kinase A and protein kinase C. *J. Biol. Chem.* **267,** 22378–22384.

Coles, J. A., and Orkand, R. K. (1983). Modification of potassium movement through the retina of the drone (*Apis mellifera*) by glial uptake. *J. Physiol. (London)* **340,** 157–174.

Coles, J. A., and Orkand, R. K. (1985). Changes in sodium activity during light stimulation in photoreceptors, glia and extracellular space in drone retina. *J. Physiol. (London)* **362,** 415–435.

Coles, J. A., and Rick, R. (1985). An electron microprobe analysis of photoreceptors and outer pigment cells in the retina of the honeybee drone. *J. Comp. Physiol. A* **156,** 213–222.

Coles, J. A., and Schneider-Picard, G. (1989). Amplification of small signals by voltage-gated sodium channels in drone photoreceptors. *J. Comp. Physiol. A* **165,** 109–118.

Coles, J. A., and Tsacopoulos, M. (1979). Potassium activity in photoreceptors, glial cells and extracellular space in the drone retina: Changes during photostimulation. *J. Comp. Physiol.* **290,** 525–549.

Coles, J. A., and Tsacopoulos, M. (1981). Ionic and possible metabolic interactions between sensory neurones and glial cells in the retina of the honeybee drone. *J. Exp. Biol.* **95,** 75–92.

Coles, J. A., Orkand, R. K., Yamate, C. L., and Tsacopoulos, M. (1986). Free concentrations of Na, K, and Cl in the retina of the honeybee drone: Stimulus-induced redistribution and homeostasis. *Ann. NY Acad. Sci.* **481,** 303–317.

Coles, J. A., Orkand, R. K., and Yamate, C. L. (1989). Chloride enters glial cells and photoreceptors in response to light stimulation in the retina of the honey bee drone. *Glia* **2,** 287–297.

Cuttle, M. F., Hevers, W., Laughlin, S. B., and Hardie, R. C. (1995). Diurnal modulation of photoreceptor potassium conductance in the locust. *J. Comp. Physiol. A* **176,** 307–316.

Devary, O., Heichal, O., Blumenfeld, A., Cassel, D., Suss, E., Barash, S., Rubinstein, C. T., Minke, B., and Selinger, Z. (1987). Coupling of photoexited rhodopsin to inositol phospholipid hydrolysis in fly photoreceptors. *Proc. Natl. Acad. Sci. USA* **84,** 6939–6943.

Dimitracos, S. A., and Tsacopoulos, M. (1985). The recovery from a transient inhibition of the oxidative metabolism of the photoreceptors of the drone (*Apis mellifera*). *J. Exp. Biol.* **119,** 165–181.

Dubreuil, R. R. (1996). Molecular and genetic dissection of the membrane cytoskeleton in *Drosophila. Curr. Top. Membr.* **43,** 147–167.

Dubreuil, R. R., and Yu, J. (1994). Ankyrin and β-spectrin accumulate independently of α-spectrin in *Drosophila. Proc. Natl. Acad. Sci. USA* **91,** 10285–10289.

Dubreuil, R. R., Byers, T. J., Stewart, C. T., and Kiehart, D. P. (1990). A β-spectrin isoform from Drosophila (β_H) is similar in size to vertebrate dystrophin. *J. Cell Biol.* **111,** 1849–1858.

Eakle, K. A., Kabalin, M. A., Wang, S. G., and Farley, R. A. (1994). The influence of β subunit structure on the stability of Na^+/K^+-ATPase complexes and interaction with K^+. *J. Biol. Chem.* **269,** 6550–6557.

Ernst, S. A., and Hootman, S. R. (1981). Microscopical methods for the localization of Na^+,K^+-ATPase. *Histochem. J.* **13,** 397–418.

Fein, A., and Tsacopoulos, M. (1988). Activation of mitochondrial oxidative metabolism by calcium ions in *Limulus* ventral photoreceptor. *Nature (London)* **331,** 437–440.

Feschenko, M. S., and Sweadner, K. J. (1994). Conformation-dependent phosphorylation of Na,K-ATPase by protein kinase A and protein kinase C. *J. Biol. Chem.* **269,** 30436–30444.

Feschenko, M. S., and Sweadner, K. J. (1995). Structural basis for species-specific differences in the phosphorylation of Na,K-ATPase by protein kinase C. *J. Biol. Chem.* **270,** 14072–14077.

Fulpius, B., and Baumann, F. (1969). Effects of sodium, potassium, and calcium ions on slow and spike potentials in single photoreceptor cells. *J. Gen. Physiol.* **53,** 541–561.

Gartner, W., and Towner, P. (1995). Invertebrate visual pigments. *Photochem. Photobiol.* **62,** 1–16.

Geering, K., Beggah, A., Good, P., Girardet, S., Roy, S., Schaer, D., and Jaunin, P. (1996). Oligomerization and maturation of Na,K-ATPase: Functional interaction of the cytoplasmic NH_2 terminus of the β-subunit with the α-subunit. *J. Cell Biol.* **133,** 1193–1204.

Gloor, S., Antonicek, H., Sweadner, K. J., Pagliusi, S., Frank, R., Moos, M., and Schachner, M. (1990). The adhesion molecule on glia (AMOG) is a homologue of the β subunit of the Na,K-ATPase. *J. Cell Biol.* **110,** 165–174.

Gottardi, C. J., and Caplan, M. J. (1993). Delivery of Na^+,K^+-ATPase in polarized epithelial cells. *Science* **260,** 552–554.

Gundersen, D., Orlowski, J., and Rodriguez-Boulan, E. (1991). Apical polarity of Na,K-ATPase in retinal pigment epithelium is linked to a reversal of the ankyrin-fodrin submembrane cytoskeleton. *J. Cell Biol.* **112,** 863–872.

Hamdorf, K., and Kaschef, A. H. (1964). Der Sauerstoffverbrauch des Facettenauges von *Calliphora erythrocephala* in Abhängigkeit von der Temperatur und dem Ionenmilieu. *Z. Vergl. Physiol.* **48,** 251–265.

Hamdorf, K. Hochstrate, P., Höglund, G., Burbach, B., and Wiegand, U. (1988). Light activation of the sodium pump in blowfly photoreceptors. *J. Comp. Physiol. A* **162,** 285–300.

Hammerton, R. W., Krzeminski, K. A., Mays, R. W., Ryan, T. A., Wollner, D. A., and Nelson, W. J. (1991). Mechanism for regulating cell surface distribution of Na^+,K^+-ATPase in polarized epithelial cells. *Science* **254,** 847–850.

Hardie, R. C. (1979). Electrophysiological analysis of fly retina. I. Comparative properties of R1-6 and R7 and 8. *J. Comp. Physiol.* **129,** 19–33.

Hardie, R. C. (1983). Functional organization of the fly retina. *Prog. Sens. Physiol.* **5,** 1–79.

Hardie, R. C. (1986). The photoreceptor array of the dipteran retina. *Trends Neurosci.* **9,** 419–423.

Hardie, R. C. (1991a). Whole-cell recordings of the light induced current in dissociated *Drosophila* photoreceptors: Evidence for feedback by calcium permeating the light-sensitive channels. *Proc. R. Soc. London Ser. B* **245,** 203–210.

Hardie, R. C. (1991b). Voltage-sensitive potassium channels in *Drosophila* photoreceptors. *J. Neurosci.* **11,** 3079–3095.

Hardie, R. C. (1995). Photolysis of caged Ca^{2+} facilitates and inactivates but does not directly excite light-sensitive channels in *Drosophila* photoreceptors. *J. Neurosci.* **15,** 889–902.

Hardie, R. C. (1996). INDO-1 measurements of absolute resting and light-induced Ca^{2+} concentration in *Drosophila* photoreceptors. *J. Neurosci.* **16,** 2924–2933.

Hardie, R. C., and Minke, B. (1992). The *trp* gene is essential for a light-activated Ca^{2+} channel in *Drosophila* photoreceptors. *Neuron* **8,** 643–651.

Hardie, R. C., and Minke, B. (1993). Novel Ca^{2+} channels underlying transduction in *Drosophila* photoreceptors—Implications for phosphoinositide-mediated Ca^{2+} mobilization. *Trends Neurosci.* **16,** 371–376.

Hardie, R. C., and Minke, B. (1994). Calcium-dependent inactivation of light-sensitive channels in *Drosophila* photoreceptors. *J. Gen. Physiol.* **103,** 409–427.

Hardie, R. C., and Minke, B. (1995). Phosphoinositide-mediated phototransduction in *Drosophila* photoreceptors: The role of Ca^{2+} and trp. *Cell Calcium* **18,** 256–274.

Hardie, R. C., Voss, D., Pongs, O., and Laughlin, S. B. (1991). Novel potassium channels encoded by the *shaker* locus in *Drosophila* photoreceptors. *Neuron* **6,** 477–486.

Hardie, R. C., Peretz, A., Suss-Toby, S., Rom-Glas, A., Bishop, S. A., Selinger, Z., and Minke, B. (1993). Protein kinase C is required for light adaptation in *Drosophila* photoreceptors. *Nature (London)* **363,** 634–637.

Hicks, J. L., Liu, X., and Williams, D. S. (1996). Role of ninaC proteins in photoreceptor cell structure: Ultrastructure of *ninaC* deletion mutants and binding to actin filaments. *Cell Motil. Cytoskeleton* **35,** 367–379.

Horisberger, J.-D., Lemas, V., Kraehenbühl, J.-P., and Rossier, B. C. (1991). Structure–function relationship of Na,K-ATPase. *Annu. Rev. Physiol.* **53,** 365–384.

Jaisser, F., Canessa, C. M., Horisberger, J. D., and Rossier, B. C. (1992). Primary sequence and functional expression of a novel ouabain-resistant Na,K-ATPase: The β-subunit modulates potassium activation of the Na,K-pump. *J. Biol. Chem.* **267,** 16895–16903.

Jaisser, F., Jaunin, P., Geering, K., Rossier, B. C., and Horisberger, J. D. (1994). Modulation of the Na,K-pump function by β subunit isoforms. *J. Gen. Physiol.* **103,** 605–623.

Jansonius, N. M. (1990). Properties of sodium pump in the blowfly photoreceptor cell. *J. Comp. Physiol. A* **167,** 461–467.

Jaunin, P., Horisberger, J. D., Richter, K., Good, P. J., Rossier, B. C., and Geering, K. (1992). Processing, intracellular transport, and functional expression of endogenous and exogenous α-β3, Na,K-ATPase complexes in *Xenopus* oocytes. *J. Biol. Chem.* **267,** 577–585.

Jaunin, P., Jaisser, F., Beggah, A. T., Takeyasu, K., Mangeat, P., Rossier, B. C., Horisberger, J. D., and Geering, K. (1993). Role of the transmembrane and extracytoplasmic domain of β-subunits in subunit assembly, intracellular transport, and functional expression of Na,K-pumps. *J. Cell Biol.* **123,** 1751–1759.

Jordan, C., Puschel, B., Koob, R., and Drenckhahn, D. (1995). Identification of a binding motif for ankyrin on the α-subunit of Na^+,K^+-ATPase. *J. Biol. Chem.* **270,** 29971–29975.

Just, F., and Walz, B. (1994). Immunocytochemical localization of Na^+/K^+-ATPase and V-H^+-ATPase in the salivary glands of the cockroach, *Periplaneta americana*. *Cell Tissue Res.* **278,** 161–170.

Kone, B. C., Takeyasu, K., and Fambrough, D. M. (1991). Structure–function studies of the Na/K-ATPase isozymes. *Soc. Gen. Physiol. Ser.* **46,** 265–269.

Koob, R., Kraemer, D., Trippe, G., Aebi, U., and Drenckhahn, D. (1990). Association of kidney and parotid Na^+,K^+-ATPase microsomes with actin and analogs of spectrin and ankyrin. *Eur. J. Cell Biol.* **53,** 93–100.

Kotyk, A., and Amler, E. (1995). Na,K-adenosinetriphosphatase: The paradigm of a membrane transport protein. *Physiol. Res.* **44,** 261–274.

Krantz, D. E., and Zipursky, S. L. (1990). *Drosophila* chaoptin, a member of the leucine-rich repeat family, is a photoreceptor cell-specific adhesion molecule. *EMBO J.* **9,** 1969–1977.

Kumar, J. P., and Ready, D. F. (1995). Rhodopsin plays an essential structural role in *Drosophila* photoreceptor development. *Development* **121,** 4359–4370.

Langer, H. (1960). Über den chemischen Aufbau des Facettenauges von *Calliphora erythrocephala* Meig. und seine Veränderungen mit dem Imaginalalter. *Z. Vergl. Physiol.* **42,** 595–626.

Laughlin, S. B., and Weckström, M. (1993). Fast and slow photoreceptors—A comparative study of the functional diversity of coding and conductances in the Diptera. *J. Comp. Physiol. A* **172,** 593–609.

Lebovitz, R. M., Takeyasu, K., and Fambrough, D. M. (1989). Molecular characterization and expression of the $(Na^+ + K^+)$-ATPase alpha-subunit in the *Drosophila melanogaster*. *EMBO J.* **8,** 193–202.

Lee, J. K., Coyne, R. S., Dubreuil, R. R., Goldstein, L. S. B., and Branton, D. (1993). Cell shape and interaction defects in α-spectrin mutants of *Drosophila melanogaster*. *J. Cell Biol.* **23,** 1797–1809.

Lee, Y-J., Dobbs, M. B., Verardi, M. L., and Hyde, D. R. (1990). *dgq: A Drosophila* gene encoding a visual system-specific G_α molecule. *Neuron* **5,** 889–898.

Lee, Y.-J., Shah, S., Suzuki, E., Zars, T., O'Day, P. M., and Hyde, D. R. (1994). The *Drosophila dgq* gene encodes a G_α protein that mediates phototransduction. *Neuron* **13,** 1143–1157.

Lemas, M. V., Takeyasu, K., and Fambrough, D. M. (1992). The carboxyl-terminal 161 amino acids of the Na,K-ATPase α-subunit are sufficient for assembly with the β-subunit. *J. Biol. Chem.* **267,** 20987–20991.

Lemas, M. V., Hamrick, M., Takeyasu, K., and Fambrough, D. M. (1994). 26 amino acids of an extracellular domain of the Na,K-ATPase α-subunit are sufficient for assembly with the Na,K-ATPase β-subunit. *J. Biol. Chem.* **269,** 8255–8259.

Longley, R. L., and Ready, D. F. (1995). Integrins and the development of three-dimensional structure in the *Drosophila* compound eye. *Dev. Biol.* **171,** 415–433.

Lutsenko, S., and Kaplan, J. H. (1995). Organization of P-type ATPases: Significance of structural diversity. *Biochemistry* **34,** 15607–15613.

Madreperla, S. A., Edidin, M., and Adler, R. (1989). Na^+,K^+-adenosine trisphosphatase polarity in retinal photoreceptors: A role for cytoskeletal attachments. *J. Cell Biol.* **109,** 1483–1493.

Malik, N., Canfield, V. A., Beckers, M. C., Gros, P., and Levenson, R. (1996). Identification of the mammalian Na,K-ATPase $\beta 3$ subunit. *J. Biol. Chem.* **271,** 22754–22758.

Marrs, J. A., Napolitano, E. W., Murphy-Erdosh, C., Mays, R. W., Reichardt, L. F., and Nelson, W. J. (1993). Distinguishing roles of the membrane-cytoskeleton and cadherin mediated cell–cell adhesion in generating different Na+,K^+-ATPase distributions in polarized epithelia. *J. Cell Biol.* **123,** 149–164.

Masuzawa, T., Ohta, T., Kawamura, M., Nakahara, N., and Sato, F. (1984). Immunohistochemical localization of Na^+,K^+-ATPase in the choroid plexus. *Brain Res.* **302,** 357–362.

Matsumoto-Suzuki, E., Hirosawa, K., and Hotta, Y. (1989). Structure of the subrhabdomeric cisternae in the photoreceptor cells of *Drosophila melanogaster. J. Neurocytol.* **18,** 87–93.

Mays, R. W., Siemers, K. A., Fritz, B. A., Lowe, A. W., Vanmeer, G., and Nelson, W. J. (1995). Hierarchy of mechanisms involved in generating Na/K-ATPase polarity in MDCK epithelial cells. *J. Cell Biol.* **130,** 1105–1115.

McNeill, H., Ozawa, M., Kemler, R., and Nelson, W. J. (1990). Novel function of the cell adhesion molecule uvomorulin as an inducer of cell surface polarity. *Cell* **62,** 309–316.

Meinecke, C. C. (1981). The fine structure of the compound eye of the African armyworm moth, *Spodoptera exempta* Walk (Lepidoptera, Noctuidae). *Cell Tissue Res.* **216,** 333–347.

Minke, B., and Armon, E. (1984). Activation of electrogenic Na-Ca exchange by light in fly photoreceptors. *Vision Res.* **24,** 109–115.

Minke, B., and Selinger, Z. (1992). The inositol–lipid pathway is necessary for light excitation in fly photoreceptors. *In* "Sensory Transduction" (D. Corey and S. D. Roper, eds.), pp. 201–217. Rockefeller Univ. Press, New York.

Minke, B., and Tsacopoulos, M. (1986). Light induced sodium dependent accumulation of calcium and potassium in the extracellular space of bee retina. *Vision Res.* **26,** 679–690.

Møller, J. V., Juul, B., and Lemaire, M. (1996). Structural organization, ion transport, and energy transduction of P-type ATPases. *Biochim. Biophys. Acta* **1286,** 1–51.

Morrow, J. S., Cianci, C. D., Ardito, T., Mann, A. S., and Kashgarian, M. (1989). Ankyrin links fodrin to the alpha subunit of the Na,K-ATPase in Madin–Darby canine kidney cells and in intact renal tubule cells. *J. Cell Biol.* **108,** 455–465.

Nelson, W. J., and Hammerton, R. W. (1989). A membrane-cytoskeletal complex containing Na^+,K^+-ATPase, ankyrin and fodrin in Mandin-Darby canine kidney (MDCK) cells: Implications for the biogenesis of epithelial cell polarity. *J. Cell Biol.* **108,** 893–902.

Nelson, W. J., Shore, E. M., Wang, A. Z., and Hammerton, R. W. (1990). Identification of a membrane-cytoskeletal complex containing the cell adhesion molecule uvomorulin (E-cadherin), ankyrin, and fodrin in Madin-Darby canine kidney epithelial cells. *J. Cell Biol.* **110,** 349–357.

Nickel, E., and Menzel, R. (1976). Insect UV-, and green-photoreceptor membranes studied by the freeze-fracture technique. *Cell Tissue Res.* **175,** 357–368.

Niemeyer, B. A., Suzuki, E., Scott, K., Jalink, K., and Zuker, C. S. (1996). The *Drosophila* light-activated conductance is composed of the two channels TRP and TRPL. *Cell* **85,** 651–659.

Nilsson, D.-E. (1989). Optics and evolution of the compound eye. *In* "Facets of Vision" (D. G. Stavenga and R. C. Hardie, eds.), pp. 30–73. Springer-Verlag, Berlin/Heidelberg.

O'Tousa, J. E., Baehr, W., Martin, R. L., Hirsh, J., Pak, W. L., and Applebury, M. L. (1985). The *Drosophila ninaE* gene encodes an opsin. *Cell* **40,** 839–850.

Peretz, A., Suss-Toby, E., Rom-Glas, A., Arnon, A., Payne, R., and Minke, B. (1994). The light response of *Drosophila* photoreceptors is accompanied by an increase in cellular calcium: Effects of specific mutations. *Neuron* **12,** 1257–1267.

Perrelet, A. (1970). The fine structure of the retina of the honey bee drone. *Z. Zellforsch. Mikrosk. Anat.* **108,** 530–562.

Perrelet, A., and Baumann, F. (1969). Evidence for extracellular space in the rhabdome of the honeybee drone eye. *J. Cell Biol.* **40,** 825–830.

Perrelet, A., Bauer, H., and Fryder, V. (1972). Fracture faces of an insect rhabdom. *J. Microsc.* **13,** 97–106.

Phillips, A., Bull, A., and Kelly, L. (1992). Identification of a *Drosophila* gene encoding a calmodulin-binding protein with homology to the *trp* phototransduction gene. *Neuron* **8,** 631–642.

Pollock, J. A., Assaf, A., Peretz, A., Nichols, C. D., Mojet, M. H., Hardie, R. C., and Minke, B. (1995). TRP, a protein essential for inositide-mediated Ca^{2+} influx is localized adjacent to the calcium stores in *Drosophila* photoreceptors. *J. Neurosci.* **15,** 3747–3760.

Polyanovsky, A. D., Schraermeyer, U., Gribakin, F. G., and Stieve, H. (1993). Functional regionalization of plasma membrane in the photoreceptor cells of arthropods: An electron microscopic approach. *In* "Sensory Systems of Arthropods" (K. Wiese, F. G. Gribakin, A. V. Popov, and G. Renninger, eds.), pp. 34–41. Birkhäuser, Basel.

Porter, J. A., and Montell, C. (1993). Distinct roles of the *Drosophila* ninaC kinase and myosin domains revealed by systematic mutagenesis. *J. Cell Biol.* **122,** 601–612.

Ranganathan, R., Harris, G. L., Stevens, C. F., and Zuker, C. S. (1991). A *Drosophila* mutant defective in extracellular calcium dependent photoreceptor inactivation and rapid desensitization. *Nature (London)* **354,** 230–235.

Ranganathan, R., Bacskai, B. J., Tsien, R. Y., and Zuker, C. S. (1994). Cytosolic calcium transients: Spatial localization and role in *Drosophila* photoreceptor cell function. *Neuron* **13,** 837–848.

Ranganathan, R., Malicki, D. M., and Zuker, C. S. (1995). Signal transduction in *Drosophila* photoreceptors. *Annu. Rev. Neurosci.* **18,** 283–317.

Ready, D. F., Hanson, T. E., and Benzer, S. (1976). Development of the *Drosophila* retina, a neurocrystalline lattice. *Development* **53,** 217–240.

Renaud, K. J., Inman, E. M., and Fambrough, D. M. (1991). Cytoplasmic and transmembrane domain deletions of Na^+,K^+-ATPase β-subunit: Effects on subunit assembly and intracellular transport. *J. Biol. Chem.* **266,** 20491–20497.

Ribi, W. A. (1981). The first optic ganglion of the bee. IV. Synaptic fine structure and connectivity patterns of receptor cell axons and first order interneurones. *Cell Tissue Res.* **215,** 443–464.

Rizzolo, L. J., and Zhou, S. (1995). The distribution of Na^+,K^+-ATPase and 5A11 antigen in apical microvilli of the retinal pigment epithelium is unrelated to α-spectrin. *J. Cell Sci.* **108,** 3623–3633.

Rossel, S. (1989). Polarization sensitivity in compound eyes. *In* "Facets of Vision" (D. G. Stavenga and R. C. Hardie, eds.), pp. 298–316. Springer-Verlag, Berlin/Heidelberg/New York.

Schinz, R. H., Lo, M-V. C., Larrivee, D. C., and Pak, W. L. (1982). Freeze-fracture study of the *Drosophila* photoreceptor membrane: Mutations affecting membrane particle density. *J. Cell Biol.* **93,** 961–969.

Schmalzing, G., Kröner, S., Schachner, M., and Gloor, S. (1992). The adhesion molecule on glia (AMOG/β2) and α1 subunits assemble to functional sodium pumps in *Xenopus* oocytes. *J. Biol. Chem.* **28,** 20212–20216.

Schneider, B. (1992). Na^+,K^+-ATPase isoforms in the retina. *Int. Rev. Cytol.* **133,** 151–185.

Schneuwly, S., Burg, M. G., Lending, C., Perdew, M. H., and Pak, W. L. (1991). Properties of photoreceptor-specific phospholipase-C encoded by the *norpA* gene of *Drosophila melanogaster. J. Biol. Chem.* **266,** 24314–24319.

Schubiger, M., Feng, Y., Fambrough, D. M., and Palka, J. (1994). A mutation in the *Drosophila* sodium pump α subunit gene results in bang-sensitive paralysis. *Neuron* **12,** 373–381.

Schwemer, J. (1989). Visual pigments of compound eyes—Structure, photochemistry, and regeneration. *In* "Facets of Vision" (D. G. Stavenga and R. C. Hardie, eds.), pp. 112–133. Springer-Verlag, Berlin/Heidelberg/New York.

Scott, K., Becker, A., Sun, Y. M., Hardy, R., and Zuker, C. (1995). $G_{q\alpha}$ protein function in vivo: Genetic dissection of its role in photoreceptor cell physiology. *Neuron* **15,** 919–927.

Seigel, G. J., Holm, C., Schreiber, J. H., Desmond, T., and Ernst, S. A. (1984). Purification of mouse brain ($Na^+ + K^+$)-ATPase catalytic subunit, characterization of antiserum, and immunocytochemical localization on cerebellum, choroid plexus, and kidney. *J. Histochem. Cytochem.* **32,** 1309–1318.

Simons, K., and Fuller, S. D. (1985). Cell surface polarity in epithelia. *Annu. Rev. Cell Biol.* **1,** 243–288.

Smith, D. P., Ranganathan, R., Hardy, R. W., Marx, J., Tsuchida, T., and Zuker, C. S. (1991). Photoreceptor deactivation and retinal degeneration mediated by a photoreceptor-specific protein kinase C. *Science* **254,** 1478–1484.

Stahl, W. L., and Baskin, D. G. (1984). Immunocytochemical localization of Na^+,K^+ adenosine trisphosphatase in the rat retina. *J. Histochem. Cytochem.* **32,** 248–250.

Stürmer, K., Baumann, O., and Walz, B. (1995). Actin-dependent light-induced translocation of mitochondria and ER cisternae in the photoreceptor cells of the locust. *Schistocerca gregaria. J. Cell Sci.* **108,** 2273–2283.

Sun, B., and Salvaterra, P. M. (1995). Two *Drosophila* nervous system antigens, Nervana 1 and 2, are homologous to the β subunit of Na^+,K^+-ATPase. *Proc. Natl. Acad. Sci. USA* **92,** 5396–5400.

Suzuki, E., and Hirosawa, K. (1991). Immunoelectron microscopic study of the opsin distribution in the photoreceptor cells of *Drosophila melanogaster. J. Electron Microsc.* **40,** 187–192.

Suzuki, E., Katayama, E., and Hirosawa, K. (1993). Structure of photoreceptive membranes of *Drosophila* compound eyes as studied by quick-freezing electron microscopy. *J. Electron Microsc.* **42,** 178–184.

Takeyasu, K. Tamkun, M. M., Renaud, K. J., and Fambrough, D. M. (1988). Ouabain-sensitive ($Na^+ + K^+$)-ATPase activity expressed in mouse L cells by transfection with DNA encoding the α-subunit of an avian sodium pump. *J. Biol. Chem.* **263,** 4347–4354.

Takeyasu, K., Renaud, K. J., Taormino, J., Wolitzky, B. A., Barnstein, A. M., Tamkun, M. M., and Fambrough, D. M. (1989). Differential subunit and isoform expression involved in regulation of sodium pump in skeletal muscle. *Curr. Top. Membr. Transport.* **34,** 143–165.

Thomas, G. H., and Kiehart, D. P. (1994). β_{Heavy}-spectrin has a restricted tissue and subcellular distribution during *Drosophila* embryogenesis. *Development* **120,** 2039–2050.

Tomlinson, A. (1988). Cellular interactions in the developing *Drosophila* eye. *Development* **104,** 183–193.

Toyoshima S., Matsumoto, N., Wang, P., Inoue, H., Yoshioka, T., Hotta, Y., and Osawa, T. (1990). Purification and partial amino-acid sequence of phosphoinositide-specific phospholipase C of *Drosophila* eye. *J. Biol. Chem.* **265,** 14842–14848.

Tsacopoulos, M., and Coles, J. A. (1984). Stimulation causes an increase in [ATP] in honeybee drone retina. *Experientia* **40,** 600.

Tsacopoulos, M., and Poitry, S. (1982). Kinetics of oxygen consumption after a single flash of light in photoreceptors of the drone (*Apis mellifera*). *J. Gen. Physiol.* **80,** 19–55.

Tsacopoulos, M., and Veuthey, A.-L. (1993). The nutritive function of glia in a crystal-like nervous tissue: The retina of the honeybee drone. *Dev. Neurosci.* **15,** 336–342.

Tsacopoulos, M., Orkand, R. K., Coles, J. A., Levy, S., and Poitry, S. (1983). Oxygen uptake occurs faster than sodium pumping in bee retina after a light flash. *Nature* (*London*) **301,** 604–606.

Tsacopoulos, M., Evêquoz-Mercier, V., Perrottet, P., and Buchner, E. (1988). Honeybee retinal glial cells transform glucose and supply the neurons with metabolic substrate. *Proc. Natl. Acad. Sci. USA* **85,** 8727–8731.

Tsacopoulos, M., Veuthey, A.-L., Saravelos, S. G., Perrottet, P., and Tsoupras, G. (1994). Glial cell transform glucose to alanine, which fuels the neurons in the honeybee retina. *J. Neurosci.* **14,** 1339–1351.

Ueno, S., Mayahara, H., Tsukahara, I., and Ogawa, K. (1980). Ultracytochemical localization of ouabain-sensitive, potassium-dependent *p*-nitrophenyl phosphate activity in the guinea pig retina. II. Neurons and Müller cells. *Acta Histochem. Cytochem.* **14,** 186–206.

Vallet, A. M., Coles, J. A., Eilbeck, J. C., and Scott, A. C. (1992). Membrane conductances involved in ampliflication of small signal by sodium channels in photoreceptors of drone honey bee. *J. Physiol. (London)* **456,** 303–324.

Van Vactor, D., Krantz, D. E. J., Reinke, R., and Zipursky, S. L. (1988). Analysis of mutants in chaoptin, a photoreceptor cell-specific glycoprotein in *Drosophila,* reveals its role in cellular morphogenesis. *Cell* **52,** 281–290.

Varela, F. G., and Porter, K. R. (1969). Fine structure of the visual system of the honeybee *(Apis mellifera). J. Ultrastruct. Res.* **29,** 236–259.

Varela, F. G., and Wiitanen, W. (1970). The optics of the compound eye of the honeybee *(Apis mellifera). J. Gen. Physiol.* **55,** 336–358.

Vasilets, L. A., and Schwarz, W. (1994). The Na^+/K^+pump—Structure and function of the alpha-subunit. *Cell. Physiol. Biochem.* **4,** 81–95.

Venien-Bryan, C., Davies, A., Langmack, K., Baverstock, J., Watts, A., Marsh, D., and Saibil, H. (1995). Effect of the C-terminal proline repeats on ordered packing of squid rhodopsin and its mobility in membranes. *FEBS Lett.* **359,** 45–49.

Volk, T. (1992). A new member of the spectrin superfamily may participate in the formation of embryonic muscle attachments in *Drosophila. Development* **116,** 721–730.

Walz, B. (1982). Calcium-sequestering smooth endoplasmic reticulum in retinula cells of the blowfly. *J. Ultrastruct. Res.* **81,** 240–248.

Walz, B. (1985). Light-induced changes of extra- and intracellular potassium concentration in the photoreceptors of the leech, *Hirudo medicinalis. J. Comp. Physiol. A* **157,** 199–210.

Walz, B. (1992). Enhancement of sensitivity in photoreceptors of the honey bee drone by light and by Ca^{2+}. *J. Comp. Physiol A* **170,** 605–613.

Walz, B., and Baumann, O. (1995). Structure and cellular physiology of Ca^{2+} stores in invertebrate photoreceptors. *Cell Calcium* **18,** 342–351.

Walz, B., Zimmermann, B., and Seidl, S. (1994). Intracellular Ca^{2+} concentration and latency of the light-induced Ca^{2+} changes in photoreceptors of the honeybee drone. *J. Comp. Physiol A* **174,** 421–431.

Warrant, E. J., and McIntyre, P. D. (1993). Arthropod eye design and the physical limits to spatial resolving power. *Prog. Neurobiol.* **40,** 413–461.

Weckström, M., and Laughlin, S. B. (1995). Visual ecology and voltage-gated ion channels in insect photoreceptors. *Trends Neurosci.* **18,** 17–21.

Weckström, M., Hardie, R. C., and Laughlin, S. B. (1991). Voltage-activated potassium channels in blowfly photoreceptors and their role in light adaptation. *J. Physiol. (London)* **440,** 635–657.

Wilson, M., Garrard, P., and McGinness, S. (1978). The unit structure of the locust compound eye. *Cell Tissue Res.* **195,** 205–226.

Yau, K.-W., and Baylor, D. A. (1989). Cyclic GMP-activated conductance of retinal photoreceptor cells. *Annu. Rev. Neurosci.* **12,** 289–327.

Ziegler, A., and Walz, B. (1989). Analysis of extracellular calcium and volume changes in the compound eye of the honeybee drone, *Apis mellifera. J. Comp. Physiol. A* **165,** 697–709.

Ziegler, A., and Walz, B. (1990). Evidence for light-induced release of Ca^{2+} from intracellular stores in bee photoreceptors. *Neurosci. Lett.* **111,** 87–91.

Zinkler, D. (1975). Zum Lipidmuster der Photorezeptoren von Insekten. *Verh. Dtsch. Zool. Ges.* **67,** 28–32.

Zipursky, S. L., and Rubin, G. M. (1994). Determination of neuronal cell fate: lessons from the R7 neuron of *Drosophila. Annu. Rev. Neurosci.* **17,** 373–397.

Zuker, C. S. (1996). The biology of vision in *Drosophila. Proc. Natl. Acad. Sci. USA* **93,** 571–576.

Zuker, C. S., Cowman, A. F., and Rubin, G. M. (1985). Isolation and structure of a rhodopsin gene from *Drosophila melanogaster. Cell* **40,** 851–858.

Zurzolo, C., and Rodriguez-Boulan, E. (1993). Delivery of Na^+,K^+-ATPase in polarized epithelial cells. *Science* **260,** 550–552.

INDEX

A

B

C

D

E

F

G

H

I

K

L

M

N

O

P

R

S

T

V

X